Arthritis & Rheumatology

An Official Journal of the American College of Rheumatology
www.arthritisrheum.org and wileyonlinelibrary.com

GENERAL INFORMATION

TO SUBSCRIBE

Institutions and Non-Members

Email: wileyonlinelibrary.com
Phone: (201) 748-6645
Write: Wiley Periodicals LLC
Attn: Journals Admin Dept UK
111 River Street
Hoboken, NJ 07030

Volumes 74, 2022:
Institutional Print Only: **Arthritis & Rheumatology and Arthritis Care & Research:** $2,603 in US, Canada, and Mexico; $2,603 outside North America
Institutional Online Only: $2,495 in US, Canada, Mexico, and outside North America
Institutional Print and Online Only: $2,802 in US, Canada, and Mexico; $2,802 outside North America

For submission instructions, subscription, and all other information visit: wileyonlinelibrary.com.

Arthritis & Rheumatology accepts articles for Open Access publication. Please visit https://authorservices.wiley.com/author-resources/Journal-Authors/open-access/hybrid-open-access.html for further information about OnlineOpen.

Wiley's Corporate Citizenship initiative seeks to address the environmental, social, economic, and ethical challenges faced in our business and which are important to our diverse stakeholder groups. Since launching the initiative, we have focused on sharing our content with those in need, enhancing community philanthropy, reducing our carbon impact, creating global guidelines and best practices for paper use, establishing a vendor code of ethics, and engaging our colleagues and other stakeholders in our efforts.
Follow our progress at www.wiley.com/go/citizenship.

Access to this journal is available free online within institutions in the developing world through the HINARI initiative with the WHO. For information, visit www.healthinternetwork.org.

Disclaimer

The Publisher, the American College of Rheumatology, and Editors cannot be held responsible for errors or any consequences arising from the use of information contained in this journal; the views and opinions expressed do not necessarily reflect those of the Publisher, the American College of Rheumatology and Editors, neither does the publication of advertisements constitute any endorsement by the Publisher, the American College of Rheumatology and Editors of the products advertised.

Members:

American College of Rheumatology/Association of Rheumatology Professionals

For membership rates, journal subscription information, and change of address, please write:
American College of Rheumatology
2200 Lake Boulevard
Atlanta, GA 30319-5312
(404) 633-3777

ADVERTISING SALES AND COMMERCIAL REPRINTS

Sales: Kathleen Malseed, National Account Manager
E-mail: kmalseed@pminy.com
Phone: (215) 852-9824
Pharmaceutical Media, Inc.
30 East 33rd Street, New York, NY 10016

Production: Patti McCormack
E-mail: pmccormack@pminy.com
Phone: (212) 904-0376
Pharmaceutical Media, Inc.
30 East 33rd Street, New York, NY 10016

Publisher: Arthritis & Rheumatology is published by Wiley Periodicals LLC, 101 Station Landing, Suite 300, Medford, MA 02155
Production Editor: Ramona Talantor, artprod@wiley.com

ARTHRITIS & RHEUMATOLOGY (Print ISSN 2326-5191; Online ISSN 2326-5205 at Wiley Online Library, wileyonlinelibrary.com) is published monthly on behalf of the American College of Rheumatology by Wiley Periodicals LLC, a Wiley Company, 111 River Street, Hoboken, NJ 07030-5774. Periodicals postage paid at Hoboken, NJ and additional offices. POSTMASTER: Send all address changes to Arthritis & Rheumatology, Wiley Periodicals LLC, c/o The Sheridan Press, PO Box 465, Hanover, PA 17331. **Send subscription inquiries care of** Wiley Periodicals LLC, Attn: Journals Admin Dept UK, 111 River Street, Hoboken, NJ 07030, (201) 748-6645 (nonmember subscribers only; American College of Rheumatology/Association of Rheumatology Health Professionals members should contact the American College of Rheumatology). **Subscription Price:** (Volumes 74, 2022: Arthritis & Rheumatology and Arthritis Care & Research) Print only: $2,603.00 in U.S., Canada and Mexico, $2,603.00 rest of world. For all other prices please consult the journal's website at wileyonlinelibrary.com. All subscriptions containing a print element, shipped outside U.S., will be sent by air. Payment must be made in U.S. dollars drawn on U.S. bank. Prices are exclusive of tax. Asia-Pacific GST, Canadian GST and European VAT will be applied at the appropriate rates. For more information on current tax rates, please go to www.wileyonlinelibrary.com/tax-vat. The price includes online access to the current and all online backfiles to January 1st 2018, where available. For other pricing options including access information and terms and conditions, please visit https://onlinelibrary.wiley.com/library-info/products/price-lists. Terms of use can be found here: https://onlinelibrary.wiley.com/terms-and-conditions. **Delivery Terms and Legal Title:** Where the subscription price includes print issues and delivery is to the recipient's address, delivery terms are Delivered at Place (DAP); the recipient is responsible for paying any import duty or taxes. Title to all issues transfers Free of Board (FOB) our shipping point, freight prepaid. We will endeavor to fulfill claims for missing or damaged copies within six months of publication, within our reasonable discretion and subject to availability. **Change of Address:** Please forward to the subscriptions address listed above 6 weeks prior to move; enclose present mailing label with change of address. **Claims** for undelivered copies will be accepted only after the following issue has been received. Please enclose a copy of the mailing label or cite your subscriber reference number in order to expedite handling. Missing copies will be supplied when losses have been sustained intransit and where reserve stock permits. Send claims care of Wiley Periodicals LLC, Attn: Journals Admin Dept UK, 111 River Street, Hoboken, NJ 07030. If claims are not resolved satisfactorily, please write to Subscription Distribution c/o Wiley Periodicals LLC, 111 River Street, Hoboken, NJ 07030. **Cancellations:** Subscription cancellations will not be accepted after the first issue has been mailed. **Journal Customer Services:** For ordering information, claims and any enquiry concerning your journal subscription please go to https://wolsupport.wiley.com/s/contactsupport?tabset-a7d10=2 or contact your nearest office. **Americas:** Email: cs-journals@wiley.com; Tel: +1 877 762 2974. **Europe, Middle East and Africa:** Email: cs-journals@wiley.com; Tel: +44 (0) 1865 778315; 0800 1800 536 (Germany). **Asia Pacific:** Email: cs-journals@wiley.com; Tel: +65 6511 8000. **Japan:** For Japanese speaking support, Email: cs-japan@wiley.com. **Visit our Online Customer Help** at https://wolsupport.wiley.com/s/contactsupport?tabset-a7d10=2. **Back Issues:** Single issues from current and prior year volumes are available at the current single issue price from csjournals@wiley.com. Earlier issues may be obtained from Periodicals Service Company, 351 Fairview Avenue-Ste 300, Hudson, NY 12534, USA. Tel: + 1 518 822-9300, Fax: +1 518 822-9305, Email: psc@periodicals.com. Printed in the USA by The Sheridan Group.

Arthritis & Rheumatology

An Official Journal of the American College of Rheumatology
www.arthritisrheum.org and wileyonlinelibrary.com

Cover design: Todd Machen

This journal is printed on acid-free paper.

Arthritis & Rheumatology

An Official Journal of the American College of Rheumatology
www.arthritisrheum.org and wileyonlinelibrary.com

VOLUME 74 • May 2022 • NO. 5

Cover image: The figure on the cover (from Zhou et al, pages 871–881) shows electron microscopy images of mitochondria in dermal fibroblasts from healthy donors (top) and systemic sclerosis patients (bottom). Mitochondria in systemic sclerosis fibroblasts commonly exhibit significant damage with associated functional impairment.

In this Issue

Highlights from this issue of *A&R* | By Lara C. Pullen, PhD

Impaired Mitochondrial Transcription Factor TFAM Drives Fibrosis in Systemic Sclerosis

In this issue, Zhou et al (p. 871) report data that demonstrate, on multiple experimental levels, that severe mitochondrial damage is a cardinal feature of fibroblasts from patients with systemic sclerosis (SSc). The investigators describe how prolonged activation of transforming growth factor β (TGFβ) promotes mitochondrial damage that alters the key mitochondrial transcription factor A (TFAM), and they propose that the impaired TFAM signaling and associated mitochondrial damage that occurs in SSc fibroblasts activates profibrotic transcriptional programs with enhanced Smad3 signaling. This induction of transcriptional programs promotes fibroblast-to-myofibroblast transition, thus driving tissue fibrosis.

p. 871

The researchers questioned whether mitochondrial damage in SSc fibroblasts might be precipitated by deregulation of the transcription factor TFAM. They found that not only was TFAM expression down-regulated in fibroblasts in SSc skin and in cultured SSc fibroblasts, but that this down-regulation was associated with decreased mitochondrial number. Moreover, the SSc cells exhibited accumulation of damaged mitochondria characterized by release of mitochondrial DNA (mtDNA), accumulations of deletions in mtDNA, metabolic alterations with impaired oxidative phosphorylation, and release of the mitokine GDF15.

The authors present several lines of evidence that the down-regulation of TFAM, as well as the damage and ultimate loss of mitochondria, might be mediated by the persistent, but not transient, activation of TGFβ signaling. For example, they found that normal fibroblasts subjected to long-term, but not acute, exposure to TGFβ mimicked SSc fibroblasts, with down-regulation of TFAM and accumulation of mitochondrial damage. Moreover, down-regulation of TFAM promoted fibroblast activation with up-regulation of fibrosis-relevant Gene Ontology terms in RNA-Seq, partially in a reactive oxygen species–dependent manner. In addition, mice with fibroblast-specific knockout of TFAM were prone to fibrotic tissue remodeling, with fibrotic responses even to NaCl instillation. The TFAM-knockdown fibroblasts thus demonstrated enhanced sensitivity to profibrotic stimuli, which the authors propose is the result of enhanced Smad3 signaling.

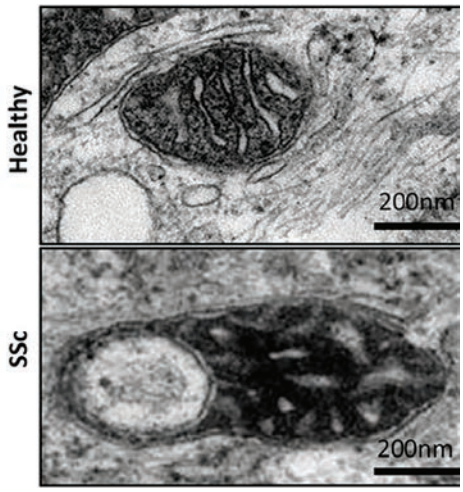

Figure 1. Representative electron microscopy images of mitochondria in dermal fibroblasts from a healthy control and an SSc patient.

Mediating Role of Inflammatory Biomarkers Between BMI and Pain Associations in Individuals with Hand OA

Leptin is a proinflammatory adipokine that is primarily secreted by adipose tissue. Multiple studies have indicated that leptin may influence pain and pain sensitivity. In this issue, Gløersen et al (p. 810) report the results of their Nor-Hand study. They found that, in people with hand osteoarthritis (OA), a higher body mass index (BMI) was associated with greater pain severity in the hands, feet, and knees/hips.

p. 810

The study included 281 OA patients undergoing secondary care, and its cross-sectional design allowed for documentation of only associations. The investigators found that the participants with a higher BMI reported greater pain severity in their hands, feet, and knees/hips, as well as a higher painful total body joint count, a more frequent presence of widespread pain, and more central pain sensitization. The researchers identified 2 inflammatory biomarkers in the serum (leptin in plasma and high-sensitivity C-reactive protein [hsCRP] in serum) that mediated the association between BMI and pain. The effect sizes for mediation by leptin were larger for the hands than for the lower extremities. Low-grade inflammation, as reflected by increased levels of hsCRP, appeared to contribute to generalized pain. The authors call for longitudinal studies to confirm the mediating role of inflammatory biomarkers on pain.

Impact of Cytokine Inhibitor Therapy on Response to SARS–CoV-2

In this issue, Simon et al (p. 783) report the results of their study revealing that patients with immune-mediated inflammatory diseases (IMIDs) treated with biologic disease-modifying antirheumatic drugs (bDMARDs) have a lower prevalence of SARS–CoV-2 antibodies, seroconvert less frequently after SARS–CoV-2 infection, and may exhibit a reduced longevity of their humoral immune response when compared to IMID patients who receive no treatment.

p. 783

The investigators measured anti–SARS–CoV-2 IgG antibodies in a prospective cohort of health care professional controls and non–health care controls and IMID patients receiving no treatment or receiving treatment with conventional or biologic DMARDs during the first and second COVID-19 waves. The study included 4,508 participants (2,869 IMID patients and 1,639 controls: >1,300 patients treated with bDMARDs and targeted synthetic DMARDs). The cohort size allowed the researchers to assess the influence of different agents on the SARS–CoV-2 immune response. They note, however, that as most of the IMID patients receiving bDMARDS were treated with cytokine inhibitors, their findings are most robust for cytokine blockers.

The unadjusted relative risk (RR) and adjusted RR for SARS–CoV-2 IgG antibodies were significantly lower in IMID patients treated with bDMARDS as compared to non–health care controls. This difference was primarily driven by treatment with tumor necrosis factor inhibitors, interleukin-17 (IL-17) inhibitors, and IL-23 inhibitors. Adjusted RRs for untreated IMID patients and IMID patients receiving conventional synthetic DMARDs did not significantly differ from non–health care controls. Lack of seroconversion in PCR–positive participants was more common among bDMARD-treated patients (38.7%) than among non–health care controls (16%).

The researchers then reassessed patients during the second COVID-19 wave who had been assessed in the first wave. Overall, 44% of positive participants lost SARS–CoV-2 antibodies by follow-up, with higher rates in IMID patients treated with bDMARDS. The authors conclude that, although it is highly unlikely that cytokine inhibitors lower the susceptibility to SARS–CoV-2 infection, the bDMARDs may mitigate the overshooting inflammatory response to the virus and, consequently, the severity of SARS–CoV-2 infection.

Journal Club

A monthly feature designed to facilitate discussion on research methods in rheumatology.

Association of Polygenic Risk Scores with Radiographic Progression in RA Patients

Honda et al, *Arthritis Rheumatol* 2022;74:791–800

Despite advances in therapeutic agents, some RA patients still experience progressive joint destruction. There are several predictors of joint destruction, including the presence of anti–citrullinated protein antibodies (ACPAs), but their predictive accuracy is insufficient. More reliable predictors that can accurately identify patients who will experience progressive disease are needed. Genetic factors identified by genome-wide association studies for RA may be such candidates, but each individual factor has a limited effect on disease. Honda et al (p. XXX) examined whether polygenic risk score, which can estimate the accumulation of genetic factors as a whole, could be a predictor.

Japanese patients with RA were stratified into 2 groups according to their Sharp/van der Heijde score (SHS): the severe progressive group in the top quartile of SHS (score change of >35 points) and the nonsevere progressive group (the remainder of the patients). Polygenic risk score was constructed by linkage disequilibrium clumping and the *P* value threshold method in the training set (n = 500) to predict SHS status, and it was validated in a testing set (n = 740). The best polygenic risk score model consisted of 43,784 single-nucleotide polymorphisms (SNPs) selected with a *P* value threshold of 0.13 and r^2 value threshold of 0.1. Patients in the top quintile for polygenic risk score had ~2× the risk of severe progression compared to those in the bottom quintile, which was higher when restricted to patients with younger age (<40 years) at RA onset. Discriminatory power of polygenic risk scores for SHS status was comparable/superior to that of ACPAs. Multivariable logistic regression analysis using polygenic risk scores and other clinical information showed significant and independent associations of polygenic risk score, ACPA, female sex, and BMI with SHS status. Classification accuracy of the multivariable model for the SHS status as evaluated by area under curve was 0.648 for all patients and 0.711 for the patients with younger age at RA onset.

Questions

1. **Is the classification accuracy of the multivariable model sufficient for clinical practice?**
2. **Why did polygenic risk scores have better predictive ability in the patients with younger age at RA onset?**
3. **Can polygenic risk scores be applied to other populations?**
4. **Can polygenic risk scores be used to predict disease progression in ACPA-negative patients?**
5. **Which approaches can be taken to improve the polygenic risk score model in the future?**

In this Issue

Highlights from this issue of *A&R* | By Lara C. Pullen, PhD

Impaired Mitochondrial Transcription Factor TFAM Drives Fibrosis in Systemic Sclerosis

In this issue, Zhou et al (p. 871) report data that demonstrate, on multiple experimental levels, that severe mitochondrial damage is a cardinal feature of fibroblasts from patients with systemic sclerosis (SSc). The investigators describe how prolonged activation of transforming growth factor β (TGFβ) promotes mitochondrial damage that alters the key mitochondrial transcription factor A (TFAM), and they propose that the impaired TFAM signaling and associated mitochondrial damage that occurs in SSc fibroblasts activates profibrotic transcriptional programs with enhanced Smad3 signaling. This induction of transcriptional programs promotes fibroblast-to-myofibroblast transition, thus driving tissue fibrosis.

p. 871

The researchers questioned whether mitochondrial damage in SSc fibroblasts might be precipitated by deregulation of the transcription factor TFAM. They found that not only was TFAM expression down-regulated in fibroblasts in SSc skin and in cultured SSc fibroblasts, but that this down-regulation was associated with decreased mitochondrial number. Moreover, the SSc cells exhibited accumulation of damaged mitochondria characterized by release of mitochondrial DNA (mtDNA), accumulations of deletions in mtDNA, metabolic alterations with impaired oxidative phosphorylation, and release of the mitokine GDF15.

The authors present several lines of evidence that the down-regulation of TFAM, as well as the damage and ultimate loss of mitochondria, might be mediated by the persistent, but not transient, activation of TGFβ signaling. For example, they found that normal fibroblasts subjected to long-term, but not acute, exposure to TGFβ mimicked SSc fibroblasts, with down-regulation of TFAM and accumulation of mitochondrial damage. Moreover, down-regulation of TFAM promoted fibroblast activation with up-regulation of fibrosis-relevant Gene Ontology terms in RNA-Seq, partially in a reactive oxygen species–dependent manner. In addition, mice with fibroblast-specific knockout of TFAM were prone to fibrotic tissue remodeling, with fibrotic responses even to NaCl instillation. The TFAM-knockdown fibroblasts thus demonstrated enhanced sensitivity to profibrotic stimuli, which the authors propose is the result of enhanced Smad3 signaling.

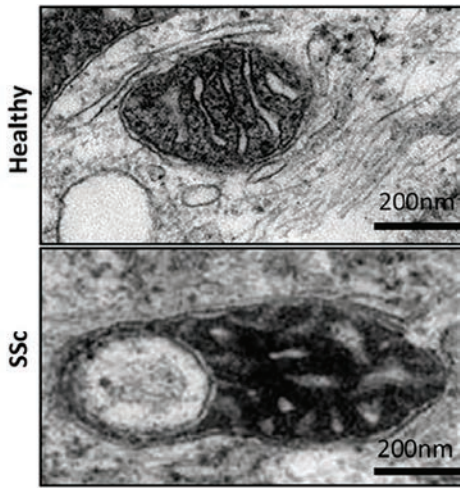

Figure 1. Representative electron microscopy images of mitochondria in dermal fibroblasts from a healthy control and an SSc patient.

Mediating Role of Inflammatory Biomarkers Between BMI and Pain Associations in Individuals with Hand OA

Leptin is a proinflammatory adipokine that is primarily secreted by adipose tissue. Multiple studies have indicated that leptin may influence pain and pain sensitivity. In this issue, Gløersen et al (p. 810) report the results of their Nor-Hand study. They found that, in people with hand osteoarthritis (OA), a higher body mass index (BMI) was associated with greater pain severity in the hands, feet, and knees/hips.

p. 810

The study included 281 OA patients undergoing secondary care, and its cross-sectional design allowed for documentation of only associations. The investigators found that the participants with a higher BMI reported greater pain severity in their hands, feet, and knees/hips, as well as a higher painful total body joint count, a more frequent presence of widespread pain, and more central pain sensitization. The researchers identified 2 inflammatory biomarkers in the serum (leptin in plasma and high-sensitivity C-reactive protein [hsCRP] in serum) that mediated the association between BMI and pain. The effect sizes for mediation by leptin were larger for the hands than for the lower extremities. Low-grade inflammation, as reflected by increased levels of hsCRP, appeared to contribute to generalized pain. The authors call for longitudinal studies to confirm the mediating role of inflammatory biomarkers on pain.

Impact of Cytokine Inhibitor Therapy on Response to SARS–CoV-2

In this issue, Simon et al (p. 783) report the results of their study revealing that patients with immune-mediated inflammatory diseases (IMIDs) treated with biologic disease-modifying antirheumatic drugs (bDMARDs) have a lower prevalence of SARS–CoV-2 antibodies, seroconvert less frequently after SARS–CoV-2 infection, and may exhibit a reduced longevity of their humoral immune response when compared to IMID patients who receive no treatment.

p. 783

The investigators measured anti–SARS–CoV-2 IgG antibodies in a prospective cohort of health care professional controls and non–health care controls and IMID patients receiving no treatment or receiving treatment with conventional or biologic DMARDs during the first and second COVID-19 waves. The study included 4,508 participants (2,869 IMID patients and 1,639 controls: >1,300 patients treated with bDMARDs and targeted synthetic DMARDs). The cohort size allowed the researchers to assess the influence of different agents on the SARS–CoV-2 immune response. They note, however, that as most of the IMID patients receiving bDMARDS were treated with cytokine inhibitors, their findings are most robust for cytokine blockers.

The unadjusted relative risk (RR) and adjusted RR for SARS–CoV-2 IgG antibodies were significantly lower in IMID patients treated with bDMARDS as compared to non–health care controls. This difference was primarily driven by treatment with tumor necrosis factor inhibitors, interleukin-17 (IL-17) inhibitors, and IL-23 inhibitors. Adjusted RRs for untreated IMID patients and IMID patients receiving conventional synthetic DMARDs did not significantly differ from non–health care controls. Lack of seroconversion in PCR–positive participants was more common among bDMARD-treated patients (38.7%) than among non–health care controls (16%).

The researchers then reassessed patients during the second COVID-19 wave who had been assessed in the first wave. Overall, 44% of positive participants lost SARS–CoV-2 antibodies by follow-up, with higher rates in IMID patients treated with bDMARDS. The authors conclude that, although it is highly unlikely that cytokine inhibitors lower the susceptibility to SARS–CoV-2 infection, the bDMARDs may mitigate the overshooting inflammatory response to the virus and, consequently, the severity of SARS–CoV-2 infection.

Journal Club

A monthly feature designed to facilitate discussion on research methods in rheumatology.

Association of Polygenic Risk Scores with Radiographic Progression in RA Patients

Honda et al, *Arthritis Rheumatol* 2022;74:791–800

Despite advances in therapeutic agents, some RA patients still experience progressive joint destruction. There are several predictors of joint destruction, including the presence of anti–citrullinated protein antibodies (ACPAs), but their predictive accuracy is insufficient. More reliable predictors that can accurately identify patients who will experience progressive disease are needed. Genetic factors identified by genome-wide association studies for RA may be such candidates, but each individual factor has a limited effect on disease. Honda et al (p. XXX) examined whether polygenic risk score, which can estimate the accumulation of genetic factors as a whole, could be a predictor.

Japanese patients with RA were stratified into 2 groups according to their Sharp/van der Heijde score (SHS): the severe progressive group in the top quartile of SHS (score change of >35 points) and the nonsevere progressive group (the remainder of the patients). Polygenic risk score was constructed by linkage disequilibrium clumping and the *P* value threshold method in the training set (n = 500) to predict SHS status, and it was validated in a testing set (n = 740). The best polygenic risk score model consisted of 43,784 single-nucleotide polymorphisms (SNPs) selected with a *P* value threshold of 0.13 and r^2 value threshold of 0.1. Patients in the top quintile for polygenic risk score had ~2× the risk of severe progression compared to those in the bottom quintile, which was higher when restricted to patients with younger age (<40 years) at RA onset. Discriminatory power of polygenic risk scores for SHS status was comparable/superior to that of ACPAs. Multivariable logistic regression analysis using polygenic risk scores and other clinical information showed significant and independent associations of polygenic risk score, ACPA, female sex, and BMI with SHS status. Classification accuracy of the multivariable model for the SHS status as evaluated by area under curve was 0.648 for all patients and 0.711 for the patients with younger age at RA onset.

Questions

1. **Is the classification accuracy of the multivariable model sufficient for clinical practice?**
2. **Why did polygenic risk scores have better predictive ability in the patients with younger age at RA onset?**
3. **Can polygenic risk scores be applied to other populations?**
4. **Can polygenic risk scores be used to predict disease progression in ACPA-negative patients?**
5. **Which approaches can be taken to improve the polygenic risk score model in the future?**

Clinical Connections

Extramucosal Formation and Prognostic Value of Secretory Antibodies in Rheumatoid Arthritis

Martinsson et al, *Arthritis Rheumatol* 2022;74:801–809

CORRESPONDENCE
Klara Martinsson, PhD: klara.martinsson@liu.se
Alf Kastbom, MD, PhD: alf.kastbom@liu.se

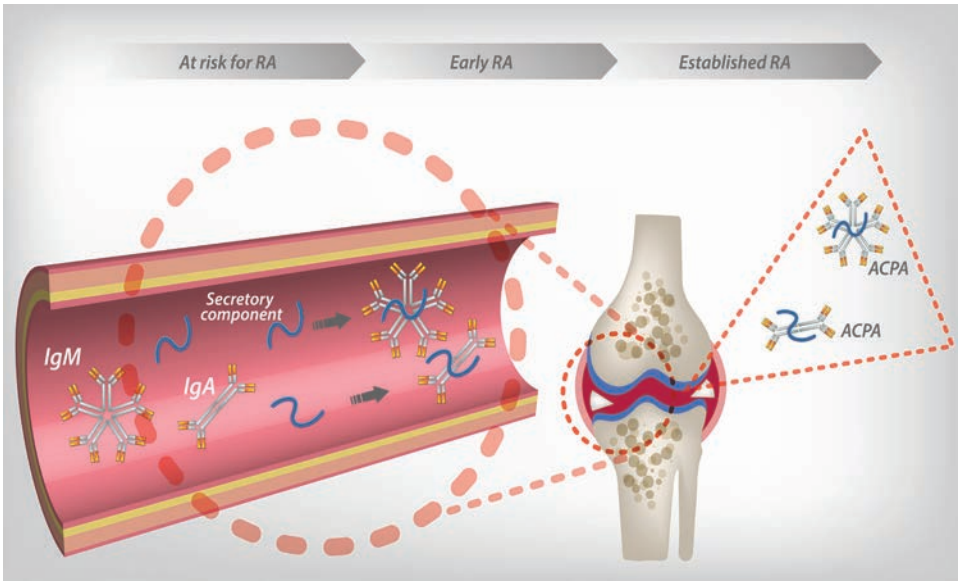

KEY POINTS

- Levels of secretory IgA and IgM in serum are increased in patients with early RA and at-risk patients.
- Disease activity is higher in patients with early RA with elevated secretory IgA and IgM levels.
- At-risk patients progressing to arthritis show higher secretory IgA levels relative to nonprogressors.
- Secretory ACPA can be formed in the presence of free SC and IgA/IgM ACPA, potentially outside the mucosa.

SUMMARY

Recent advances suggest that mucosal surfaces are important early in the development of rheumatoid arthritis (RA), particularly in anti–citrullinated protein antibody (ACPA)–positive disease. Martinsson et al studied patients in different phases of RA—from at-risk to established disease—and investigated levels and possible extramucosal formation of secretory Ig, including ACPA.

Serum levels of secretory IgA and secretory IgM were increased in both patients with early RA and at-risk patients compared to healthy controls. In addition, disease activity was higher in patients with early RA with elevated total secretory Ig compared to those without increased levels. At-risk patients who were developing arthritis during the follow-up period (39 of 82 patients) had higher baseline secretory IgA levels compared to those who did not. In established RA, secretory IgA and IgM levels were higher in serum than in synovial fluid, but interestingly secretory component (SC)–containing ACPAs adjusted for total secretory Ig concentrations were higher in synovial fluid. The authors also present evidence that secretory autoantibodies can be formed in vitro in the presence of free SC, evident in both IgA/IgM ACPA–positive sera and affinity-purified IgA/IgM ACPA preparations.

Taken together, these data suggest the following: circulating secretory Ig are elevated before and at RA onset, SC ACPAs are enriched in RA joints, and, in the presence of free SC, secretory Ig may form outside the mucosa. These findings shed new light on the potential mucosal connection in RA development.

Urine Proteomics and Renal Single-Cell Transcriptomics Implicate IL-16 in Lupus Nephritis

Fava et al, *Arthritis Rheumatol* 2022;74:829–839

CORRESPONDENCE
Andrea Fava, MD: afava1@jhu.edu

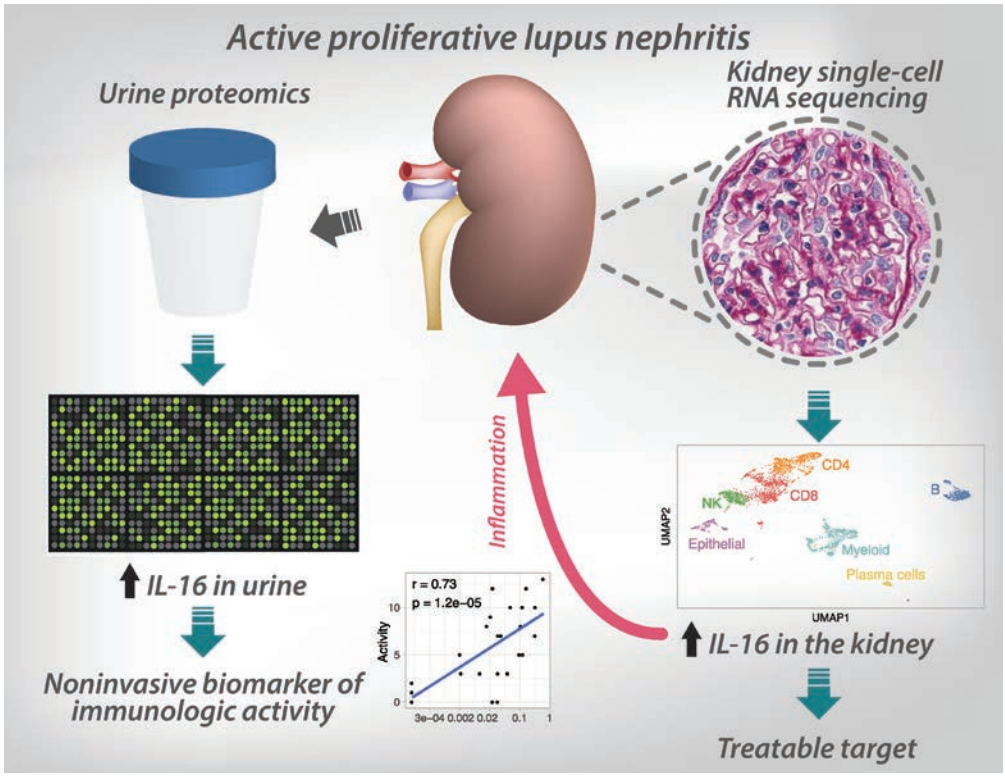

KEY POINTS

- Urinary IL-16 correlates with LN histologic activity.
- IL-16, a proinflammatory chemokine, is one of the most abundant cytokines in proliferative LN kidneys.
- IL-16 is a novel urinary biomarker and potentially treatable target.

SUMMARY

Urine collects the byproducts of intrarenal biologic processes, including inflammation, tubular damage, and tissue remodeling. To discover novel treatable targets and noninvasive biomarkers, Fava et al quantified 1,000 proteins in the urine of patients with lupus nephritis (LN). They found that urine studies can measure intrarenal increased immune activation, neutrophil and platelet degranulation, and extracellular matrix disruption among other pathways. Upon concurrent kidney biopsy, the immunologic activity (according to the National Institutes of Health Activity Index) of proliferative LN, the most aggressive form of LN, was most strongly associated with the urinary levels of interleukin-16 (IL-16), along with CD163 and transforming growth factor β. These biomarkers decreased in patients who were responding to treatment.

IL-16 is a proinflammatory chemokine that can recruit CD4+ immune cells, such as neutrophils and T cells, to the kidney. Kidney single-cell transcriptomics revealed that *IL16* was expressed by most immune cells, and it was the second most expressed cytokine in LN. IL-16 was found a key sites of kidney inflammation within the glomerulus and in the periglomerular space. Importantly, the abundance of IL-16–positive cells in LN kidney correlated with LN activity and urinary IL-16 levels. These findings implicate IL-16 in LN pathogenesis, nominating IL-16 as a noninvasive biomarker and a potentially treatable target.

Arthritis & Rheumatology
Vol. 74, No. 5, May 2022, pp 735–751
DOI 10.1002/art.42087

American College of Rheumatology
Empowering Rheumatology Professionals

The 2021 European Alliance of Associations for Rheumatology/American College of Rheumatology Points to Consider for Diagnosis and Management of Autoinflammatory Type I Interferonopathies: CANDLE/PRAAS, SAVI, and AGS

Kader Cetin Gedik,[1] Lovro Lamot,[2] Micol Romano,[3] Erkan Demirkaya,[3] David Piskin,[4] Sofia Torreggiani,[5] Laura A. Adang,[6] Thais Armangue,[7] Kathe Barchus,[8] Devon R. Cordova,[9] Yanick J. Crow,[10] Russell C. Dale,[11] Karen L. Durrant,[12] Despina Eleftheriou,[13] Elisa M. Fazzi,[14] Marco Gattorno,[15] Francesco Gavazzi,[16] Eric P. Hanson,[17] Min Ae Lee-Kirsch,[18] Gina A. Montealegre Sanchez,[1] Bénédicte Neven,[19] Simona Orcesi,[20] Seza Ozen,[21] M. Cecilia Poli,[22] Elliot Schumacher,[8] Davide Tonduti,[23] Katsiaryna Uss,[1] Daniel Aletaha,[24] Brian M. Feldman,[25] Adeline Vanderver,[26] Paul A. Brogan,[13] and Raphaela Goldbach-Mansky[1]

Objective. Autoinflammatory type I interferonopathies, chronic atypical neutrophilic dermatosis with lipodystrophy and elevated temperature/proteasome-associated autoinflammatory syndrome (CANDLE/PRAAS), stimulator of interferon genes (STING)–associated vasculopathy with onset in infancy (SAVI), and Aicardi-Goutières syndrome (AGS) are rare and clinically complex immunodysregulatory diseases. With emerging knowledge of genetic causes and targeted treatments, a Task Force was charged with the development of "points to consider" to improve diagnosis, treatment, and long-term monitoring of patients with these rare diseases.

Methods. Members of a Task Force consisting of rheumatologists, neurologists, an immunologist, geneticists, patient advocates, and an allied health care professional formulated research questions for a systematic literature review. Then, based on literature, Delphi questionnaires, and consensus methodology, "points to consider" to guide patient management were developed.

Results. The Task Force devised consensus and evidence-based guidance of 4 overarching principles and 17 points to consider regarding the diagnosis, treatment, and long-term monitoring of patients with the autoinflammatory interferonopathies, CANDLE/PRAAS, SAVI, and AGS.

Conclusion. These points to consider represent state-of-the-art knowledge to guide diagnostic evaluation, treatment, and management of patients with CANDLE/PRAAS, SAVI, and AGS and aim to standardize and improve care, quality of life, and disease outcomes.

This article is published simultaneously in *Annals of the Rheumatic Diseases*.

Supported by the European Alliance of Associations for Rheumatology/American College of Rheumatology, and supported in part by the intramural research program of the NIH (National Institute of Allergy and Infectious Diseases [Drs. Cetin Gedik and Goldbach-Mansky], National Human Genome Research Institute, and National Institute of Arthritis and Musculoskeletal and Skin Diseases), the Deutsche Forschungsgemeinschaft (grant CRC237 369799452/B21 to Dr. Lee-Kirsch), the Autoinflammatory Alliance, and the Systemic JIA Foundation.

[1]Kader Cetin Gedik, MD, Gina A. Montealegre Sanchez, MD, Katsiaryna Uss, Raphaela Goldbach-Mansky, MD: National Institute of Allergy and Infectious Diseases, NIH, Bethesda, Maryland; [2]Lovro Lamot, MD, PhD: University of Zagreb School of Medicine, Zagreb, Croatia; [3]Micol Romano, MD, Erkan Demirkaya, MD: University of Western Ontario, London, Ontario, Canada; [4]David Piskin, MD: University of Western Ontario, London Health Sciences Center, and Lawson Health Research Institute, London, Ontario, Canada; [5]Sofia Torreggiani: National Institute of Allergy and Infectious Diseases, NIH, Bethesda, Maryland, and UOC Pediatria a Media Intensità di Cura, Fondazione IRCCS Ca' Granda Ospedale Maggiore Policlinico, Milan, Italy; [6]Laura A. Adang, MD, PhD: Children's Hospital of Philadelphia, Philadelphia, Pennsylvania; [7]Thais Armangue, MD, PhD: Sant Joan de Deu Children's Hospital and IDIBAPS–Hospital Clinic; University of Barcelona, Barcelona, Spain; [8]Kathe Barchus, Elliot Schumacher: Autoinflammatory Alliance, San Francisco, California; [9]Devon R. Cordova: Aicardi-Goutieres Syndrome Americas Association, Manhattan Beach, California; [10]Yanick J. Crow, PhD: University of Edinburgh, Edinburgh, UK, and Laboratory of Neurogenetics and Neuroinflammation, Institut Imagine, University of Paris, Paris, France; [11]Russell C. Dale, MD: University of Sydney, Sydney, New South Wales, Australia;

INTRODUCTION

Autoinflammatory type I interferonopathies are genetically defined (monogenic or digenic) immunodysregulatory disorders characterized by the presence of a type I interferon (IFN) signature in peripheral blood and variable systemic inflammation (1–3). In this expanding group of ultra-rare diseases, chronic atypical neutrophilic dermatosis with lipodystrophy and elevated temperature/proteasome-associated autoinflammatory syndrome (CANDLE/PRAAS), stimulator of interferon genes (STING)–associated vasculopathy with onset in infancy (SAVI), and Aicardi-Goutières syndrome (AGS) are the most common.

Patients with type I interferonopathies present early in life often within the first week of life; prenatal onset has been reported in patients with AGS. However, late-onset cases presenting at ages 14, 18, and 5.6 years with CANDLE/PRAAS, SAVI, and AGS, respectively, have been reported (4–11). Despite CANDLE/PRAAS, SAVI, and AGS having distinct clinical phenotypes of varying disease severity, the individual clinical manifestations of these diseases can overlap, and all are associated with high morbidity and mortality if untreated (4–12). Recent advances in the genetic description of these disorders permit better characterization of disease-specific clinical manifestations, and provide evidence supporting the pathogenic role of type I IFN signaling (1,2,12,13). These developments prompted the Task Force led by the steering committee (2 convenors [PAB, RG-M], a neurologist [AV], 2 methodologists [BMF, ED], and 3 pediatric rheumatologists/European Alliance of Associations for Rheumatology [EULAR] fellows [KCG, LL, MR] and a rheumatologist [ST]) to review the existing data and develop consensus statements, with the aim of formulating state-of-the-art guidance on the diagnosis, treatment, and long-term monitoring of patients with these rare diseases.

Thus, the objective of this project was to develop points to consider for the diagnosis, treatment, and long-term monitoring of patients with CANDLE/PRAAS, SAVI, and AGS.

The Task Force targets its guidance to pediatricians, internists, and subspecialists involved in the care of patients with autoinflammatory type I interferonopathies and to patients and caregivers. These points to consider were developed not only to provide a resource for physicians to facilitate management but also for policy makers governing who has a role in authorizing patients' access to various diagnostic tools and treatment options, all with the ultimate goal to harmonize the level of care and to improve quality of life and disease outcomes in this patient population.

METHODS

The EULAR (14) and the American College of Rheumatology (ACR) standardized operating procedures were followed during the project period (see Supplementary Methods, on the *Arthritis & Rheumatology* website at https://onlinelibrary.wiley.com/doi/10.1002/art.42027). With approval from the EULAR and ACR Executive Committees, an international Task Force consisting of worldwide recognized experts from North America, South America, Europe, and Australia convened to develop points to consider for the diagnosis, treatment, and long-term monitoring of 3 type I interferonopathies: CANDLE/PRAAS, SAVI, and AGS. The Task Force members were selected based on expertise in treatment and care of these patients.

A face-to-face meeting in August 2019 defined the goal of the project and the target population. Then, the Task Force developed research questions related to diagnosis, treatment, and long-term monitoring of these diseases using the Population, Intervention, Comparison, Outcome (PICO) format. Search terms were derived from PICO questions and a systematic literature review (SLR) was performed by 3 research fellows (KCG, MR, LL), with support from a librarian (Darren Hamilton, London Health Sciences Center, London, Ontario, Canada), an epidemiologist (DP), and a senior methodologist (ED) to identify relevant literature published before September 2020.

Two rounds of pre–consensus meeting questionnaires, using the Delphi technique (15), including questions pertaining to diagnosis, treatment, and long-term monitoring, were sent to all Task Force members to indicate their agreement with each question or statement with yes/no using the Delphi technique; the Delphi questionnaire was sent to 28 Task Force members, of whom 22 were voting members. The Task Force members were asked to indicate their agreement with each statement, and a free text option was provided to capture every member's comment for each statement. Draft statements and items in questions with 80% or higher agreement were retained for voting at the

[12]Karen L. Durrant, RN: Autoinflammatory Alliance and Kaiser San Francisco Hospital, San Francisco, California; [13]Despina Eleftheriou, PhD, Paul A. Brogan, PhD: University College London, London, UK; [14]Elisa M Fazzi, PhD: ASST Civil Hospital and University of Brescia, Brescia, Italy; [15]Marco Gattorno, MD: IRCCS Istituto Giannina Gaslini, Genoa, Italy; [16]Francesco Gavazzi, MD, PhD: Children's Hospital of Philadelphia, Philadelphia, Pennsylvania, and University of Brescia, Brescia, Italy; [17]Eric P. Hanson, MD: Riley Hospital for Children and Indiana University School of Medicine, Indianapolis; [18]Min Ae Lee-Kirsch, PhD: Technische Universität Dresden, Dresden, Germany; [19]Bénédicte Neven, MD: Necker Children's Hospital, AP-HP, Institut Imagine Institut des Maladies Genetiques, University of Paris, Paris, France; [20]Simona Orcesi, MD: IRCCS Mondino Foundation and University of Pavia, Pavia, Italy; [21]Seza Ozen, MD: Hacettepe University, Ankara, Turkey; [22]M. Cecilia Poli, MD, PhD: Universidad del Desarrollo, Santiago, Chile; [23]Davide Tonduti, MD: V. Buzzi Children's Hospital, Milan, Italy; [24]Daniel Aletaha, MD: Medical University of Vienna, Vienna, Austria; [25]Brian M. Feldman, MD: Hospital for Sick Children and University of Toronto Institute of Health Policy Management and Evaluation, Toronto, Ontario, Canada; [26]Adeline Vanderver, MD: Children's Hospital of Philadelphia and University of Pennsylvania, Philadelphia.

Drs. Cetin Gedik, Lamot, and Romano contributed equally to this work.

Address correspondence to Raphaela Goldbach-Mansky, MD, Translational Autoinflammatory Diseases Section, Laboratory of Clinical Immunology and Microbiology, National Institute of Allergy and Infectious Diseases, NIH, Bethesda, Maryland. Email: goldbacr@mail.nih.gov.

Submitted for publication November 7, 2021; accepted in revised form January 11, 2022.

consensus meetings. Statements and items in questions that did not reach a greater than 80% consensus were reviewed and reworded and sent out in a second round of the Delphi questionnaire. The original and the revised/modified draft statements with the previously achieved level of agreement and the participants' comments were included in the second survey. A free text option to capture comments and additional items was again included. Draft statements with 80% or higher agreement were retained for voting at the consensus meetings, and statements which did not achieve 80% agreement were marked for further discussion and refinement at the 2 consensus meetings. Responses were anonymous.

Based on the SLR findings and 2 pre–consensus meeting Delphi questionnaires, draft statements were refined by the steering group and were sent to the voting members prior to the consensus meetings. These draft statements were reviewed, discussed, revised, and voted on in 2 consensus meetings that were held online in October 2020 due to the COVID-19 pandemic, one for CANDLE/PRAAS and SAVI, and one for AGS.

Two conveners (RG-M, PAB), 3 methodologists (BMF, ED, DA), 3 fellows, an allied health professional, and 3 disease experts attended both consensus meetings and, otherwise, participation was based on disease-specific expertise. The voting panel included 19 experts, 1 allied health professional, and 1 patient representative for each disease. The joint statements addressing all 3 interferonopathies were voted on by the entire voting panel; CANDLE/SAVI-specific statements were voted on by 10 experts, 1 allied health professional, 1 SAVI, and 1 CANDLE/PRAAS patient presentative, and AGS-specific statements were voted on by 14 experts, 1 allied health professional, and 1 AGS patient representative. During the meetings, statements that achieved at least 80% agreement were accepted; statements with <80% were discussed a final time in a Nominal Groups round robin discussion (https://www.cdc.gov/healthyyouth/evaluation/pdf/brief7.pdf) and were only accepted if the revised statement reached an 80% agreement.

The Oxford Levels of Evidence (LoE) were applied to each point to consider (16). The strength of each statement ranged from A (directly based on level I evidence) to D (directly based on level IV evidence or extrapolated recommendations from level I, II, or III evidence) (16). Finally, the finalized statements were circulated in a post–consensus meeting Delphi questionnaire to determine level of agreement (LoA). Members of the Task Force were asked to provide their final LoA for each point to consider using a scale of 0 (completely disagree) to 10 (completely agree), which is reported in the tables below.

RESULTS

Systematic literature review

A summary of the literature search strategy and results is provided in the Supplementary Methods (https://onlinelibrary.wiley.com/doi/10.1002/art.42027). Based on SLR and consensus conferences, 4 overarching principles and 17 disease-specific points to consider pertaining to the genetically defined interferonopathies (Table 1) with their respective LoE, grade of recommendation, and LoA were generated (17).

Overarching principles guiding the management of patients with CANDLE/PRAAS, SAVI, and AGS

The systemic inflammatory multiorgan involvement in patients with CANDLE/PRAAS, SAVI, or AGS can ultimately result in progressive organ injury and early mortality (4). Damage accrues over time, often manifesting later in life, thus highlighting the importance of early diagnosis and treatment (1,12).

Autoinflammatory syndromes may present with phenotypic overlap early in life, which poses diagnostic challenges (12). In addition, mutations in individual genes may be associated with considerable phenotypic heterogeneity and variable disease severity (18,19). Genetic confirmation is thus essential for making a precise diagnosis which then facilitates targeted therapy and initiation of genetic counseling with the goal of achieving better clinical outcomes. Patients, their parents, and siblings should have access to formal genetic counseling. Genetic counseling can initiate the risk assessment process depending on the type of inheritance for specific disease-causing mutations and help patients understand their test results, including the medical implications for themselves, their reproductive health concerns, and impact on their relatives. Patients with clinical symptoms of CANDLE/PRAAS, SAVI, or AGS who do not harbor any of the disease-causing mutations described here should be referred to specialty/research centers that can guide further workup and treatment. There is no cure for type I interferonopathies. Current treatment options therefore aim to prevent development or progression of end organ damage by controlling systemic and organ inflammation (20,21), to improve quality of life, and to improve disease outcomes (1). Given the paucity of long-term outcome data on newly available treatments, monitoring of disease activity and development of organ-specific and treatment-related complications is essential (1,22,23). A multidisciplinary team is required to provide optimal care in the context of multiorgan system involvement (24,25).

Points to consider 1–8: diagnostic evaluation focuses on raising an early suspicion and on facilitating genetic testing, appropriate clinical and laboratory workup, and early treatment

Diagnostic evaluation. The presence of a chronically elevated peripheral blood IFN signature is a common finding in patients with the type I interferonopathies CANDLE/PRAAS, SAVI, and AGS. In contrast, traditional inflammatory markers such as C-reactive protein and erythrocyte sedimentation rate are

Table 1. Points to consider for the diagnosis, treatment, and long-term monitoring of patients with type I interferonopathies, CANDLE/PRAAS, SAVI, and AGS*

	LoE and GoR, C/S/AGS†	LoA (0–10), mean ± SD
Overarching principles		
A. Patients with autoinflammatory interferonopathies CANDLE/PRAAS, SAVI, or AGS present with chronic systemic and organ-specific inflammation; when untreated, chronic inflammation results in progressive organ damage, early morbidity, and increased mortality.	4C/4C/4C	9.8 ± 0.7
B. A confirmed genetic diagnosis is required to make the diagnosis of CANDLE/PRAAS, SAVI, and AGS, which facilitates initiation of targeted treatments, genetic counseling, screening for complications, and informs prognosis.	5D/5D/4C	9.5 ± 1.0
C. The goal of treatment of type I interferonopathies is to reduce systemic and organ inflammation to prevent or limit the development of and/or the progression of organ injury and damage, and to improve quality of life.	2B/2B/2B	9.8 ± 0.5
D. In CANDLE/PRAAS, SAVI, or AGS, long-term monitoring of disease activity, organ-specific injury/damage and of treatment related complications is required and involves a multidisciplinary team.	5D/5D/4C	9.9 ± 0.3
Individual points to consider		
I. Points to consider for diagnostic evaluation		
1. Patients presenting with unexplained systemic inflammation (including elevations of CRP, ESR, and/or an IFN signature) and clinical features‡ that include rashes, lipodystrophy, musculoskeletal, neurologic, pulmonary, and metabolic findings should receive a prompt diagnostic workup for CANDLE/PRAAS, SAVI, and AGS comprising: • Genetic evaluation. • Clinical evaluation focusing on the extent of inflammatory organ involvement. • Screening for disease-related comorbidities.	4C/4C/4C	9.8 ± 0.7
2. Patients with clinical symptoms of CANDLE/PRAAS, SAVI, or AGS who do not carry any of the disease-causing mutations described here should be referred to specialty/research centers that can guide further workup and treatment.	5D/5D/5D	9.8 ± 0.5
Genetic evaluation		
3. Mutations in the following disease-causing genes should be included in the genetic analyses: • CANDLE/PRAAS: *PSMB8*, *PSMA3, PSMB4*, *PSMB9*, *PSMB10*, *POMP*, and *PSMG2*. • SAVI: *STING1* (previously *TMEM173*). • AGS: *TREX1*, *RNASEH2A, RNASEH2B*, *RNASEH2C*, *SAMHD1*, *ADAR1*, *IFIH1, LSM11*§, and *RNU7-1*§.	4C/4C/4C	9.8 ± 0.6
4. Genetic mimics of CANDLE/PRAAS, SAVI, and AGS are recognized and should be included in the diagnostic workup (a non-exhaustive list is below for reference): • For CANDLE-like conditions: splice variants in *IKBKG*, frameshift mutations in *SAMD9L*, and recessive mutations in *RNASEH2* (*A*, *B*, *C*). • For SAVI-like conditions: *TREX1*, *ADA2*, and *COPA*. • For AGS-like conditions: *RNASET2*.	4C/4C/4C	9.4 ± 0.9
Clinical evaluation (see also Tables 3 and 4)		
5. In patients with suspected CANDLE/PRAAS, SAVI, or AGS, assessment for disease- and treatment-related comorbidities should include screening for: • *Skin manifestations*: nodular rashes, violaceous annular rashes, panniculitis, lipodystrophy, or vasculopathic skin lesions. • *Neurologic manifestations*: intracerebral calcifications, leukoencephalopathy, progressive microcephaly, or cerebral atrophy. • *Pulmonary manifestations*: interstitial lung disease/pulmonary hypertension. • *Hepatic manifestations*: hepatic steatosis, hepatitis, hepatosplenomegaly. • *Metabolic manifestations*: hypertension, hyperlipidemia, glucose intolerance (=metabolic syndrome). • *Musculoskeletal manifestations*: arthritis, contractures, and myositis. • *Growth and development*: growth retardation, osteoporosis, bone development delay, pubertal delay. • *Hematologic manifestations*: cytopenias (e.g., more specifically lymphopenia, thrombocytopenia). • *Ophthalmologic manifestations*: episcleritis, keratitis, retinopathy, glaucoma. • *Cardiac manifestations*: cardiomyopathy.	4C/4C/4C	9.7 ± 0.6
6. Neuroimaging should be performed in individuals with suspected neurologic symptoms. • MRI best identifies white and grey matter changes. • CT is generally more sensitive for detecting cerebral calcification and can be considered when calcium-sensitive modalities on MRI are not available or do not detect calcifications.	4C/4C/4C	9.8 ± 0.4
7. In patients with presumed CANDLE/PRAAS, SAVI, or AGS, tissue sampling as appropriate (e.g., CSF if neurologic involvement is suspected, or lesional skin biopsies) may support the diagnosis.	4C/4C/4C	9.4 ± 1.1
8. All patients should undergo a basic immunodeficiency workup that includes a history of infections, lymphocyte subsets, and immunoglobulin levels, as a minimum.	4C/4C/4C	9.3 ± 1.5

(Continued)

Table 1. (*Cont'd*)

	LoE and GoR, C/S/AGS†	LoA (0–10), mean ± SD
II. Points to consider for treatment		
9. Treatment of patients with CANDLE/PRAAS, SAVI, and AGS should be aimed at achieving disease control or low disease activity to prevent progression of organ damage.	2B/2B/2B	9.4 ± 1.2
For patients with SAVI and CANDLE/PRAAS, disease control should be maintained with the lowest possible dose of glucocorticoids.	4C/4C/NA	
10. JAKIs are of benefit for improving symptoms¶ in CANDLE/PRAAS, SAVI, and AGS.	2B/2B/2B	9.3 ± 0.9
11. In patients with CANDLE/PRAAS, SAVI, or AGS on JAKI, screening for treatment-related comorbidities is important. We currently recommend monitoring for BK viral loads in urine and blood to prevent viral organ injury such as nephropathy.	4C/4C/5D	9.3 ± 1.6
12. Glucocorticoids are of benefit for improving symptoms¶ in CANDLE/PRAAS or SAVI. Chronic glucocorticoids do not improve the neurologic features of AGS although acute courses of glucocorticoids may be useful for the treatment of non-CNS inflammatory conditions.	4C/4C/5D	9.0 ± 1.3
III. Points to consider for long-term monitoring and management		
Disease related comorbidities and disease progression		
13. A multidisciplinary management team is required for optimal care of patients with CANDLE/PRAAS, SAVI, and AGS, that is customized based on patient's disease manifestations.	5D/5D/5D	9.9 ± 0.3
14. Disease activity and burden of disease should be monitored regularly depending on disease activity and severity (see Table 4).	5D/5D/5D	9.3 ± 1.8
• Symptom control can be monitored by assessing disease-specific symptoms¶ using validated patient reported outcome and quality of life assessments, and by recording missing school or workdays.	5D/5D/5D	
15. Disease and development of children should be monitored at each visit.	5D/5D/5D	9.8 ± 0.4
Risk of COVID-19		
16. At the time of writing, there is no evidence to suggest that risks to patients with CANDLE/PRAAS, SAVI, or AGS of COVID-19 are any different from the healthy population. Therefore, treatment for interferonopathy should not be stopped unless a specific contraindication to ongoing treatment arises.	5D/5D/5D	9.5 ± 0.8
Vaccinations		
17. Generally, for CANDLE/PRAAS and SAVI all routine vaccines (live and killed) are indicated when not receiving immunosuppressive treatments or glucocorticoids, although this should be considered on a case-by-case basis.	5D/5D/5D	9.4 ± 0.9

* CANDLE/PRAAS = chronic atypical neutrophilic dermatosis with lipodystrophy and elevated temperature/proteasome-associated autoinflammatory syndrome; SAVI = STING-associated vasculopathy with onset in infancy; AGS = Aicardi-Goutières syndrome; LoA = level of agreement; CRP = C-reactive protein; ESR = erythrocyte sedimentation rate; IFN = interferon; MRI = magnetic resonance imaging; CT = computed tomography; CSF = cerebrospinal fluid; NA = not applicable; JAKIs = Janus kinase inhibitors; CNS = central nervous system.
† Level of evidence (LoE) is classified as follows: 1a = systematic review of randomized controlled trials (RCTs); 1b = individual RCT; 2a = systematic review of cohort studies; 2b = individual cohort study (including low-quality RCT); 3a = systematic review of case–control studies; 3b = individual case–control study; 4 = case-series (and poor-quality cohort and case–control studies); 5 = expert opinion without explicit critical appraisal, or based on physiology, bench research, or "first principles." Grade of recommendation (GoR) is classified as follows: A = based on consistent level 1 studies; B = based on consistent level 2 or 3 studies or extrapolations from level 1 studies; C = based on level 4 studies or extrapolations from level 2 or 3 studies; D = based on level 5 studies or on troublingly inconsistent or inconclusive studies of any level. LoE and GoR are reported separately for CANDLE/PRAAS (C), SAVI (S), and AGS (A).
‡ Disease-characteristic clinical features are listed in Table 3.
§ These 2 genes were published after the consensus meeting occurred.
¶ Clinical symptoms are listed in Table 3 and Table 4.

typically elevated in CANDLE/PRAAS and SAVI but rarely in patients with AGS (2,7,12,18,26–30). A peripheral blood IFN signature may be measured using different methodologies, including a 28-gene IFN scoring system using NanoString technology or by quantitative reverse transcriptase polymerase chain reaction methods. Gene subsets should be measured repeatedly to establish chronic elevation (13). Scores may be negative in the diagnostic phase in patients with milder disease, or in response to glucocorticoid treatment. In addition, patients with AGS with *RNASEH2B* mutations may have a negative IFN signature even with active disease (31). A practical barrier is the limited number of centers with the ability to check an IFN signature. Thus, a chronically elevated peripheral blood IFN signature is not required for diagnosis but can be very useful in raising the suspicion of an interferonopathy. For most IFN signatures, sensitivity and specificity data are not available. However, in a retrospective study, the IFN signature at a set cut-off score was helpful in differentiating patients with an interferonopathy from healthy controls and from patients with cryopyrin-associated periodic syndrome (an interleukin-1–mediated autoinflammatory disease). The IFN signature demonstrated an area under the receiver operator characteristic curve of 0.98, with sensitivity and specificity exceeding 0.8 (12). Currently, the IFN signature should be interpreted in the context of normal values of the laboratory that conducts the test, since no internationally standardized methodologies or reference ranges are currently available.

Genetic evaluation. As there can be significant overlap of clinical features across several autoinflammatory disorders, a confirmed genetic diagnosis is critical to facilitating a precision medicine approach and targeted therapy. Next-generation sequencing (e.g., targeted gene panel, whole exome or whole genome sequencing) to screen for pathogenic variants rather than single-gene Sanger sequencing is recommended. Sanger sequencing of individual genes may still be cost effective in patients with known familial disease, and may be the only available option if next-generation sequencing is not yet available to the patient. However, this increasingly outdated "gene by gene" approach ultimately may result in diagnostic delay and may not be cost-effective (32). In addition to the known disease-causing genes (1,2,5,7,12,18,31,33–39) (Table 1), screening should be considered for diseases that can mimic one of these disorders; their genetic causes (8,12,40–45) are listed in Table 2. Allelic, monogenic or digenic, double heterozygous mutations in genes encoding proteasome or immunoproteasome subunits are the cause for CANDLE/PRAAS, with biallelic pathogenic *PSMB8* variants being the most common cause. Digenic disease-causing mutations including *PSMB8*, *PSMA3*, *PSMB4*, and *PSMB9* (1,2,26), compound heterozygous mutations including *PSMB4*, *PSMB8i*, and *PSMG2* (2,12), and autosomal dominant loss-of-function mutations in *POMP* (2) also cause CANDLE/PRAAS but are rarer. However, novel disease-causing genes are being added as causes for CANDLE/PRAAS. All proteasome genes should be specifically assessed in a patient with a suggestive clinical phenotype. Both parents may need to be tested to confirm digenic inheritance. The inheritance of SAVI is mostly autosomal dominant, and most patients harbor a de novo heterozygous missense mutation in the *STING1* gene that confers a gain-of-function by increasing TANK-binding kinase 1–mediated IRF3 phosphorylation and *IFNB1* transcription (7,46). Liu et al also reported somatic mosaic mutations in one patient (OMIM-615934). So far only additive *STING1* gain-of-function mutations in p.R284W require homozygosity to confer disease (47). Furthermore, mostly loss-of-function mutations in genes encoding proteins that regulate nucleic acid metabolism or signaling cause AGS (34). These include biallelic null mutations in *TREX1* and *SAMHD1*; biallelic null mutations in the disease-causing genes, *RNASEH2A*, *RNASEH2B*, *RNASEH2C*, or *ADAR1* have not been reported. Disease-causing *IFIH1* variants are all heterozygous gain-of-function mutations that increase type I IFN signaling (34). Recently, biallelic mutations in *LSM11* and *RNU7-1*, which encode components of the replication-dependent histone pre-mRNA–processing complex, extend defects in nucleic acid metabolism to histone mRNAs (48). It is important to note that large deletions, such as deletions in AGS-related genes including *SAMHD1*, may be missed on exome sequencing and need to be reviewed using other testing modalities (31,49,50). If, following routine genetic workup, a molecular diagnosis is not established in a patient with suggestive phenotypic features, referral to a research center of excellence for further evaluation should be considered.

Table 2. List of genetically defined diseases and genes that should be considered in the differential diagnosis of CANDLE/PRAAS, SAVI, and AGS*

Genetically defined diseases	Genes
CANDLE/PRAAS mimics/overlaps	
Differential diagnoses:	
• NEMO deleted exon 5 autoinflammatory syndrome (NEMO-NDAS)	*IKBKG* (exon 5 deletion/splice variant)
• SAMD9L associated autoinflammatory disease (SAAD)	*SAMD9L* (frameshift mutations)
• Other	*RNASEH2B*
SAVI mimics/overlaps	
Differential diagnoses:	
• Deficiency of the enzyme adenosine deaminase 2 (DADA2)	*ADA2*
• Familial chilblain lupus (CHBL)	*TREX1*, *SAMHD1*
• COPA syndrome	*COPA*
AGS mimics/overlaps	
Differential diagnoses:	
• Other	*RNASET2*
Other disorders with partially overlapping phenotypes	
Differential diagnoses:	
• Spondyloenchondrodysplasia (SPENCD)	*ACP5*
• Singleton Merten syndromes	*IFIH1*, *DDX58*
• Retinal vasculopathy with cerebral leukodystrophy (RVCL)	*TREX1*
• Trichohepatoenteric syndrome (THES)	*TTC37*, *SKIV2L*
• Lipopolysaccharide responsive and beige-like anchor protein (LRBA) deficiency	*LRBA*
• Monogenic early onset lupus	e.g., *C1Q* (*A*, *B*, *C*), several others

* Based on current evidence, all type I interferonopathies, including but not limited to the genetically defined diseases listed in the table, should be considered in the differential diagnosis of chronic atypical neutrophilic dermatosis with lipodystrophy and elevated temperature/proteasome-associated autoinflammatory syndrome (CANDLE/PRAAS), STING-associated vasculopathy with onset in infancy (SAVI), or Aicardi-Goutières syndrome (AGS) because of overlapping clinical and laboratory features.

Table 3. Clinical features suggestive of CANDLE/PRAAS, SAVI, and AGS*

Systemic inflammation	
CANDLE/PRAAS, SAVI, AGS	*Clinical features*: Recurrent fever, hepatosplenomegaly *Laboratory features*: Elevated CRP, ESR, and IFN signature
Skin manifestations	
CANDLE/PRAAS	Neutrophilic panniculitis, nodular rashes, violaceous annular rashes, lipodystrophy
SAVI	Vasculopathy (i.e., chilblain lesions, acral ischemia ranging from Raynaud's phenomenon to gangrene), loss of digits
AGS	Chilblain lesions, acral lesions (including Raynaud's phenomenon), panniculitis
Neurologic manifestations	
CANDLE/PRAAS	*Clinical features*: Headache, cognitive impairment *Lumbar puncture*: Sterile pleocytosis *Neuroimaging*: Basal ganglia calcifications
SAVI	*Neuroimaging*: Basal ganglia calcifications (rare)
AGS	*Clinical features*: Subacute or acute onset of neurologic symptoms including developmental delay, irritability, neurologic impairment or regression, dystonia and spasticity, focal motor findings, progressive microcephaly, seizures *Lumbar puncture*: Sterile pleocytosis, elevated CSF neopterin and tetrahydrobiopterin, elevated IFNα *Neuroimaging*: leukoencephalopathy, cerebral calcifications, early and rapid cerebral atrophy with or without calcification, Moyamoya disease†
Pulmonary manifestations	
CANDLE/PRAAS	Pulmonary hypertension without fibrosis
SAVI	Interstitial lung disease with or without secondary pulmonary hypertension
AGS	Pulmonary hypertension
Hepatic manifestations	
CANDLE/PRAAS	Elevated transaminases, hepatic steatosis
AGS	Elevated transaminases, autoimmune hepatitis
Metabolic and endocrine manifestations	
CANDLE/PRAAS	Hypertension, hyperlipidemia, glucose intolerance (=metabolic syndrome)
AGS	Hypothyroidism, diabetes insipidus, diabetes
Musculoskeletal manifestations	
CANDLE/PRAAS, SAVI, AGS	Myositis
CANDLE/PRAAS, SAVI, AGS	Arthritis, joint contractures
Growth and development	
CANDLE/PRAAS, SAVI, AGS	Growth retardation, osteoporosis, bone development delay, pubertal delay
Hematologic manifestations	
CANDLE/PRAAS, SAVI, AGS	Anemia, leukopenia, lymphopenia, and/or thrombocytopenia
Ophthalmologic manifestations	
CANDLE/PRAAS	Episcleritis and keratitis
SAVI, AGS	Retinopathy, glaucoma
Cardiac manifestations	
AGS	Cardiomyopathy, valve calcifications

* CANDLE/PRAAS = chronic atypical neutrophilic dermatosis with lipodystrophy and elevated temperature/proteasome-associated autoinflammatory syndrome; SAVI = STING-associated vasculopathy with onset in infancy; AGS = Aicardi-Goutières syndrome; CRP = C-reactive protein; ESR = erythrocyte sedimentation rate; IFN = interferon; CSF = cerebrospinal fluid.
† Vasculopathy characterized by progressive narrowing of the terminal intracranial portion of the internal carotid artery and circle of Willis.

Clinical evaluation. In patients with undifferentiated autoinflammatory diseases or otherwise unexplained systemic inflammation, certain clinical features are suggestive of CANDLE/PRAAS, SAVI, or AGS (Tables 1 and 3).

The following clinical features are relevant to the workup of patients with suspected interferonopathies:

Cutaneous manifestations. Inflammatory skin lesions are present in all 3 diseases; however, the nature of the rash differs. Nodular rashes or violaceous annular rashes should prompt a diagnostic workup for CANDLE/PRAAS. Another specific cutaneous finding for CANDLE/PRAAS is panniculitis (particularly neutrophilic panniculitis) and panniculitis-induced lipodystrophy, which are hallmarks of the disease (1,2,9,12, 18,36,37,51).

The presence of vasculopathic skin lesions such as pernio ("chilblain lesions") or acral ischemia presenting as Raynaud's phenomenon, and/or "purple toes" is suggestive of SAVI (7,44,47) and AGS (33,52–55); the development of gangrene with prolonged ischemic attacks is a feature of SAVI (1,7,44) (Table 3). Skin involvement is the most common symptom in patients with SAVI at presentation (1,7,56–59) but some patients can present with severe lung disease and only minimal skin involvement (8,46,60,61).

In addition to chilblain-like lesions and acrocyanosis, other skin manifestations, such as periungual erythema, or necrotic lesions of the toes, fingers, and outer helix, can be seen in patients with AGS (33,52–55). Moreover, some patients with AGS can have panniculitis as well (34). Finally, some patients with AGS have recurrent oral ulcers (50,62).

Table 4. Evaluation of inflammatory disease manifestations and organ involvement with proposed interval monitoring*

		Follow-up frequency
A. Monitoring of systemic inflammation and development		
	ESR, CRP, CBC with differential (cytopenias), IFN signature when available	At each visit†
	Urinalysis (proteinuria, renal disease)	At each visit†
	Renal ultrasound	To consider at baseline
	Hepatosplenomegaly and lymphadenopathy	At each visit†
	Height and weight	At each visit†
	DEXA scan‡ (BMD)	As clinically indicated
	Sexual development	As clinically indicated
B. Monitoring of clinical disease signs and symptoms		
CANDLE/PRAAS		
	Fever, rash, progressive lipodystrophy, headache, musculoskeletal symptoms (joint pain, contractures, weakness), shortness of breath, weight changes, developmental assessment, fatigue	At each visit†
SAVI		
	Fever, rash, peripheral acral vasculitis and dystrophic changes, respiratory symptoms (shortness of breath, tachypnea, digital clubbing), fatigue	At each visit†
AGS		
	Developmental assessment, changes in neurologic tone affecting joint integrity, skin findings, musculoskeletal findings, clinical evidence of cytopenias, endocrine disturbance, ocular abnormalities, or cardiomyopathy	At each visit†
C. Monitoring of organ manifestations		
CANDLE/PRAAS		
Skin disease	Skin exam, assessment of lipodystrophy	Every 3–6 months till stable then every 6–12 months
	Lesional skin biopsy (neutrophilic panniculitis)	Baseline only
Musculoskeletal disease	Arthritis, contractures, weakness	Every 6-12 months
	CK, aldolase, LDH for myositis	
Endocrine, metabolic disease‡	Metabolic syndrome	Every 12–36 months depending on symptoms
	Lipid profile (dyslipidemia), fasting glucose, hemoglobin A1C, serum insulin (insulin resistance)	At each visit†
	BP measurement (systemic hypertension)	At each visit†
Hepatic disease‡	ALT, AST, GGT, liver elastography, or screening for hepatic steatosis with the best available method	Every 6–12 months
Pulmonary arterial hypertension‡	Echocardiography, cardiology and/or pulmonology referral if signs of PAH	Every 6–12 months, if PAH then as clinically indicated
CNS disease‡	Lumbar puncture (if headaches), brain MRI	Every 12–36 months depending on symptoms
Eye disease‡	Scleritis, episcleritis, keratitis	Yearly or based on clinical need
Dental disease	Tooth abnormalities (tooth agenesis, hypodontia), delayed tooth eruption	Yearly or based on clinical need
SAVI		
Skin disease	Wound care (including wound culture as necessary)	As needed
Pulmonary disease‡	Low radiation chest CT	At baseline and then as needed
	PFTs	Every 3–6 months
	Pulmonology referral	If signs of ILD: as needed
AGS		
Neurologic damage/ progression‡	Brain MRI (cerebral white and grey matter changes)	At baseline and then as needed
	MRI/MRA in patients with *SAMHD1*-associated AGS (intracerebral vasculitis)	At baseline and then as needed
	Electroencephalogram (epilepsy)	Yearly
	Muscle MRI or ultrasound (myositis)	As needed
Hepatic disease‡	ALT, AST, GGT, bilirubin total and direct, albumin, and INR (autoimmune hepatitis)	Every 6–12 months

(Continued)

Table 4. (*Cont'd*)

		Follow-up frequency
Endocrinopathies	TSH (hypothyroidism)	Yearly
	GH testing and glucose tolerance test	As needed based on symptoms
Renal disease	Urinalysis	Every 6–12 months
Eye disease‡	Ophthalmologic evaluation (glaucoma)	Yearly
Cardiorespiratory	Echocardiogram (cardiomyopathy and PAH)	Every 1–2 years
Scoliosis, hip dislocation‡	Hip x-rays and spine screening in non-ambulatory patients (hip dislocation)	Every 6–12 months
D. Monitoring of autoimmunity, cytopenias, immunodeficiency, and JAKI-related complications		
Autoimmunity and cytopenias and immunodeficiency	Screening for autoimmunity (autoantibodies as indicated), CBC with differential (screening for anemia, thrombocytopenia, leukopenias)	Every 6–12 months and when indicated
	History of infections, lymphocyte subsets, immunoglobulin levels	At baseline and then every 3–6 months
	Consider immunology or hematology referral	
Infections	Clinical history, viral reactivation (on JAKIs), opportunistic infections	At each visit
JAKI monitoring	CBC with differential, LFTs, urinalysis, renal function, creatinine clearance, BK viral loads in urine and blood, urine β_2-microglobulin	At each visit

* ESR = erythrocyte sedimentation rate; CRP = C-reactive protein; CBC = complete blood count; IFN = interferon; DEXA = dual-energy x-ray absorptiometry; BMD = bone mineral density; CANDLE/PRAAS = chronic atypical neutrophilic dermatosis with lipodystrophy and elevated temperature/proteasome-associated autoinflammatory syndrome; SAVI = STING-associated vasculopathy with onset in infancy; AGS = Aicardi-Goutières syndrome; CK = creatinine kinase; LDH = lactate dehydrogenase; BP = blood pressure; ALT = alanine aminotransferase; AST = aspartate aminotransferase; GGT = gamma glutamyl transferase; PAH = pulmonary arterial hypertension; MRI = magnetic resonance imaging; CT = computed tomography; PFTs = pulmonary function tests; ILD = interstitial lung disease; MRA = magnetic resonance angiography; INR = international normalized ratio; TSH = thyroid-stimulating hormone; GH = growth hormone; JAKI = Janus kinase inhibitor; LFTs = liver function tests.
† The visit frequency is set according to clinical need and the patient's disease activity. If there is no active disease, then patients should be followed every 3 months to assess disease activity and monitor drug toxicity.
‡ Requires subspecialty evaluation.

Lesional skin biopsies in areas that can safely be biopsied can be beneficial in revealing the neutrophilic dermatosis, small vessel vasculitis (from necrotic area), fasciitis (57), and granulomatous nodular dermatitis (59), thus supporting the diagnosis of SAVI while in AGS specifically, a lesional biopsy can demonstrate deposition of immunoglobulin and complement in the walls of small vessels (63).

Neurologic manifestations. Although CANDLE/PRAAS-affected patients present with headaches and may develop aseptic meningitis (24), neurologic findings are most common and severe in AGS and include subacute or acute neurologic decline, unexplained developmental delay, progressive microcephaly, dystonia, spasticity, encephalopathy, irritability, and focal motor findings. A lumbar puncture typically shows sterile cerebrospinal fluid (CSF) pleocytosis (11,64,65).

Neuroimaging should be performed in individuals with a suspected diagnosis of an interferonopathy in the presence of neurologic symptoms. The initial workup may include magnetic resonance imaging (MRI) of the brain which identifies best white and grey matter changes (41). Head computed tomography (CT) should be considered when calcium-sensitive modalities on MRI are not available or not able to detect calcifications, since it is more sensitive for the detection of cerebral calcification (66). Risks and benefits of sedating a child for brain MRI should be considered (67). It is useful to have a baseline brain MRI to assess the severity and to monitor disease-associated complications; however, this is not a diagnostic prerequisite, especially for SAVI and CANDLE/PRAAS. Neuroimaging may be particularly helpful in patients with suspected AGS due to the dominant neurologic phenotype which should be differentiated from mimickers of interferonopathies.

Basal ganglia or other intracerebral calcifications are overlapping neuroimaging findings for all 3 diseases (68); they are more common, more severe, and typically start earlier in life in patients with AGS compared with CANDLE/PRAAS, while calcifications are rare in SAVI (8,41,68,69). In addition, the presence of leukoencephalopathy is suggestive of AGS and typically starts early in life in AGS patients with severe disease; it is unusual in CANDLE/PRAAS or SAVI (11,70,71). Other supportive neuroimaging characteristics for AGS are early and rapid cerebral atrophy with or without calcifications, cerebral white and grey matter changes, and Moyamoya disease (12,41,69,70,72–74). Intracerebral large vessel vasculitis or Moyamoya can be seen and is associated with *SAMHD1* mutations (49,74–77).

Additional workup for neurodegenerative diseases in patients with suspected AGS may also be considered. Lumbar punctures are not required to make the diagnosis of AGS but may support the diagnosis (72) and characterize the immunologic features of the central nervous system (CNS) inflammation, including the presence of lymphocytosis and raised levels of IFNα, CXCL10, and CCL2 in the CSF (31,54,69). The CSF studies are most beneficial if a molecular diagnosis of AGS is not confirmed by genetic testing and provide support for additional molecular testing (72).

Pulmonary manifestations. The presence of early onset interstitial lung disease (ILD) raises suspicion for SAVI, in particular in the context of unexplained systemic inflammation (1,7,46,56,61). Many patients with SAVI are reported to have lung involvement, mostly manifested as ILD, ranging from mild ILD with no respiratory symptoms to lung fibrosis. Also, alveolar hemorrhage is reported as the presenting feature in a few cases with SAVI (47,60). Although ILD is a major concern for patients with SAVI, it is rarely present in patients with CANDLE/PRAAS (1,18,51) and not reported in AGS. Low radiation chest CT and pulmonary function tests are recommended modalities to screen for ILD (8). Lung biopsies may distinguish infectious from inflammatory disease but are not required to make the diagnosis of SAVI (7,46,60,61).

Another significant pulmonary manifestation is pulmonary hypertension, which is a potentially life threatening and possibly underdiagnosed complication of CANDLE/PRAAS and AGS (1,12,78). While CANDLE/PRAAS and AGS are known to affect the vascular system, the full impact of systemic vasculopathy is currently undercharacterized. All patients with suspected CANDLE/PRAAS and AGS should undergo regular evaluation for pulmonary hypertension; echocardiography is recommended as a screening and monitoring tool.

Hepatic manifestations. Forty to eighty percent of patients with CANDLE/PRAAS develop metabolic syndrome and hepatic steatosis, often in the first decade of life (1). In addition, patients may develop hepatosplenomegaly which could be due to extensive metabolic disturbance in fat processing (2,5,9,36,37,39,51). In an open-label trial in CANDLE/PRAAS, it is reported that baricitinib did not significantly improve hepatic steatosis in 2 patients with hepatic steatosis prior to baricitinib treatment nor prevent it in 3 patients with hyperlipidemia at baseline, pointing to the role of proteasome dysfunction in the etiology of hepatic steatosis (1).

In AGS, hepatosplenomegaly and/or transaminitis can be an initial presentation in the neonatal period when it resembles congenital viral infection (31,33,72,79). Patients can develop autoimmune hepatitis; the presence of liver-specific antibodies has been described (34,62,80).

Transaminases should be evaluated at presentation and may be monitored as a marker for hepatic disease activity in patients with type I interferonopathies, although it should be noted they can also be elevated in CANDLE/PRAAS and AGS due to myositis (12).

Information about the clinical features of hepatic involvement in patients with SAVI is limited. However, case reports of patients with SAVI presenting with hepatic disease, such as necrotizing granulomatous hepatitis, cholestatic hepatitis, and cholangitis and multiple biliary cysts, are presented (58,81).

Metabolic manifestations. Metabolic abnormalities are significant concerns in patients with CANDLE/PRAAS and patients can develop metabolic syndrome defined by Ford et al (presence of at least 3 of the following 5 criteria: hypertriglyceridemia ≥110 mg/dl, low high-density lipoprotein cholesterol ≤40 mg/dl, abdominal obesity with waist circumference ≥90th percentile [sex specific], hyperglycemia ≥110 mg/dl, systolic or diastolic blood pressure ≥90th percentile [age, height, sex specific]) (82). In addition, these patients can have increased abdominal girth secondary to intra-abdominal fat deposition (1,51). The workup in CANDLE/PRAAS should include screening for metabolic abnormalities.

Patients with AGS may have hypothyroidism, often requiring replacement therapy, and insulin-dependent diabetes mellitus is reported (34,49,53,54,77,83–85). Other endocrine manifestations include central diabetes insipidus, growth hormone deficiency, and adrenal insufficiency (34,83).

Musculoskeletal manifestations. Myositis is a common feature of patients with CANDLE/PRAAS. It is usually patchy in distribution and can be demonstrated by muscle MRI (1,39,51). In addition, most patients with CANDLE/PRAAS will develop variable degrees of joint contractures in the hands and feet; these can be severely disabling (1,2,9,37,51). Myopathy is described in individual case reports in AGS (86). In AGS-affected patients, joint involvement can include a lupus-like arthritis, or progressive arthropathy with joint contractures (50,87,88). Articular involvement in SAVI is seen in one-third of the patients (8). Rheumatoid factor (RF) positivity was reported in a majority of cases (57%) (8) while anti–cyclic citrullinated peptide (anti-CCP) was not common in patients with SAVI but systematic testing has not been performed. Interestingly, the course of the arthritis in SAVI can be destructive, especially in childhood, when associated with RF and anti-CCP antibodies (7,43).

Growth and development. Many children with chronic inflammation, including patients with type I interferonopathies, have lengths/heights and bone mineral density (BMD) that are below that of age-matched controls. Height and BMD are further decreased in the context of treatment with glucocorticoids. Weight percentiles can increase sharply with high doses of glucocorticoids, and this should be taken into consideration when evaluating weight (1).

In addition to abnormalities in stature, patients with AGS can have significant developmental delay; after a subacute onset most individuals develop profound neurologic regression and present with severe impairment in psychomotor development (22,23,34). Patients with AGS and CANDLE/PRAAS may also present with mild developmental delay (5,22,51); these delays are not reported in patients with SAVI (8).

Hematologic manifestations. Cytopenias can occur in all 3 diseases due to temporary bone marrow suppression or homing changes and may correlate with disease activity (1,12). Cytopenias including autoimmune cytopenias occur more frequently in patients with CANDLE/PRAAS and AGS but are also seen in patients with SAVI (1,8,18,33,50,52,54,60,79,83,89). Thrombocytopenia in patients with AGS can be present during the neonatal period mimicking congenital infection, but also later during the course of the disease associated with other hematologic abnormalities such as anemia and leukopenia (19,79). Complete blood count with differential should be evaluated at presentation and may be monitored as a marker for disease activity in patients with type I interferonopathies.

Ophthalmologic manifestations. Patients with type I interferonopathies can develop different types of ophthalmologic manifestations. While patients with CANDLE/PRAAS can present with keratitis and/or episcleritis (2,18,51), patients with SAVI and AGS can develop glaucoma (8,54,76). Glaucoma has been reported in 6.3% of patients with AGS (up to 20.8% of patients with *SAMHD1* mutations), with most cases presenting in the first 6 months of life, in patients who were not receiving glucocorticoids (34,76). Retinopathy has been described in AGS and SAVI but it remains unclear whether this occurs in the context of secondary mutations (90).

Cardiac manifestations. Patients with AGS, especially those with mutations in *TREX1*, are prone to develop infantile-onset hypertrophic cardiomyopathy (31,34). There is an important risk of cardiac valve calcification in disease related to mutations in *IFIH1* and *ADAR* (91).

Other considerations

Immunodeficiency workup. Patients with known type I interferonopathies may have some degree of immunodeficiency, either due to chronic disease and cytopenias or due to treatment with immunosuppressants (92). Early manifestations may overlap with non–type I interferonopathy immunodeficiencies. Therefore, a basic immunologic workup should be considered even in the context of a confirmed diagnosis. The workup should include a history of infections and assessment of lymphocyte subsets and immunoglobulin levels, as a minimum (1,12,93).

Infections in patients with CANDLE/PRAAS can be associated with the development of macrophage activation syndrome. Opportunistic infections in patients with other CANDLE/PRAAS mutations or SAVI and AGS are rare, although pneumocystis infection has been reported in a patient with SAVI who was not on any immunosuppressive treatment (89). Furthermore, defects in maturation of CD8+ cells are identified in patients with CANDLE/PRAAS (2,94), and in some patients with SAVI (8,57,89). Severe infections are reported in 2 patients with *POMP* mutations (94), which may be modified by additional genetic variants.

Points to consider 9–12: treatment focus on optimizing inflammatory disease control

The goal of treatment is the control of the systemic and organ-specific disease manifestations and to manage complications of existing organ damage that are consequences of untreated disease.

Pharmacologic treatment with Janus kinase inhibitors (JAKI), particularly baricitinib, is widely used to treat patients with type I interferonopathies (1,95–98). The JAKIs are reported to be beneficial in controlling inflammatory symptoms and in preventing progression of end organ damage. Specifically, treatment with baricitinib resulted in a significantly lower daily diary score as well as significant reduction in glucocorticoid use in patients with type I interferonopathies in different open-label trials (1,95). In the study by Sanchez et al, none of the patients had achieved remission before initiating baricitinib treatment, and 50% of patients with CANDLE/PRAAS achieved lasting remission with no clinical symptoms and normalization of inflammatory markers on baricitinib; all discontinued glucocorticoids. In addition, patients with CANDLE/PRAAS had improvement in myositis and cytopenias (hemoglobin, lymphocytes, and platelets). Moreover, significant clinical improvement, including fewer vasculitis flares, prevention of skin involvement/progression of spontaneous amputations/the development of gangrene, and stabilization of ILD by preserving pulmonary function, was achieved in patients with SAVI (1). However, to date, no patient with SAVI treated with JAKI achieved complete remission. Furthermore, JAKIs reduce IFNα-mediated STAT-1 phosphorylation in a dose-dependent manner in patients with interferonopathy (26,56), thus demonstrating an in vivo effect of the JAKIs on type I IFN signaling. The JAKIs ruxolitinib and tofacitinib are also reported as potential treatment options (44,56,59,98). Population pharmacokinetics and pharmacodynamic analyses in children treated with baricitinib showed a substantially shorter half-life in pediatric than in adult populations requiring more frequent dosing, and led to a proposed weight-based and estimated glomerular filtration rate–based dosing regimen to guide dose adjustments in the growing child (26). Doses of JAKI used to treat these conditions that were published are summarized in Supplementary Table 4, on the *Arthritis & Rheumatology* website at https://onlinelibrary.wiley.com/doi/10.1002/art.42027. A beneficial effect of JAKI on inflammatory disease manifestations is also observed in patients with AGS, including in an open-label trial. The treatment led to a decrease in interferon signaling gene expression scores and improvement of AGS-related symptoms, including neurologic disability, crying, sleep disturbances, irritability, seizures, fever, and skin inflammation of the trunk, arms, and legs (95–97). In all instances, preexisting organ damage is irreparable (e.g., the neurologic manifestations), stressing the need for early treatment. In patients with AGS, treatment with HIV-1 reverse-transcriptase inhibitors reduced IFN scores; however, clinical benefit was not demonstrated (99) and thus it is unclear if these drugs can be recommended.

Viral reactivation including BK viral reactivation has been reported in type I interferonopathy patients treated with JAKI (1,59). BK polyomavirus reactivation caused by therapeutic immunosuppression is a commonly reported complication in renal transplant patients that can result in nephropathy and renal allograft loss. There is no proven treatment for BK nephropathy and management is limited to early detection and to controlling BK viral load by reducing the dose of immunosuppressive medications (100,101). Monitoring for BK viral load in blood and urine and renal function prior to initiation of JAKI, at baseline, and then routinely at each visit is recommended.

Other viral reactivations, such as herpes, are reported in CANDLE/PRAAS and SAVI (1); however, there are insufficient data to routinely recommend anti-viral drug prophylaxis for patients with CANDLE/PRAAS and SAVI treated with JAKI. Similarly, in AGS, viral prophylaxis for patients on JAKI is not currently recommended.

Finally, the data from an open-label trial indicated that patients with AGS who are receiving baricitinib should be monitored closely for thrombocytosis, leukopenia, and infection, especially those with underlying thrombotic risk factors or those who are receiving systemic glucocorticoids or immunosuppressive regimens (95), while no such events were reported in 2 other reports (96,97).

Glucocorticoids are generally considered useful in CANDLE/PRAAS and SAVI patients with systemic inflammation, although their use is limited by toxicity (1). When used for a prolonged time, glucocorticoids cause serious side effects including growth arrest, truncal obesity, hypertension, glucose intolerance, and osteopenia (102). Therefore, the lowest possible dose of glucocorticoids should be targeted for disease control.

There is generally no role for chronic glucocorticoids in AGS, as glucocorticoids do not improve the long-term neurologic features nor outcome of AGS. However, short courses of glucocorticoids to treat acute CNS and non-CNS inflammatory manifestations, such as cytopenias and hepatitis, may be beneficial.

Points to consider 13–17: long-term monitoring and management focus on assessing inflammatory organ manifestations, minimizing treatment-related toxicities, and encouraging general health measures, including vaccines, and fostering of self-management skills and medical decision-making

A multidisciplinary team approach to regular clinical follow-up is recommended and may include access to medical subspecialists, including a rheumatologist, geneticist, neurologist, ophthalmologist, pulmonologist, cardiologist, hepatologist, gastroenterologist, hematologist, immunologist, dermatologist, endocrinologist, nephrologist, and access to supportive services including a physiatrist, wound care specialist, psychologist, bone health specialist, physical therapist, dental/oral surgeon, dietitian, psychiatrist, rehabilitation care, orthopedic care, and social support services. With current treatment strategies the ultimate treatment goal in inflammatory diseases, namely inflammatory remission, can only be achieved in a subset of patients. Remission is mainly described in patients with CANDLE/PRAAS (1). The current treatment goal is therefore to reduce systemic and organ inflammation and to prevent or limit the development or progression of organ injury/damage. This requires treatment adjustments and close monitoring of disease progression. Table 4 provides general and disease-specific guidance for the monitoring of disease activity and assessment of organ damage. The monitoring should include 1) assessment of the level of systemic inflammation, and of growth and sexual development, 2) the assessment of general and disease-specific clinical signs and symptoms including the use of validated instruments when available (1,22,23), 3) monitoring of disease-specific organ manifestations, and 4) monitoring of the development of autoimmune features (see Supplementary Table 5 [https://onlinelibrary.wiley.com/doi/10.1002/art.42027] for autoantibody associations with organ-specific autoimmune manifestations in CANDLE/PRAAS, SAVI, and AGS), cytopenias, treatment-related complications, and infections (immunodeficiencies). Preliminary guidance regarding the monitoring of JAKI treatment (Table 4) is provided but may need to be adjusted as experience with treatment of interferonopathies grows.

All patients should be evaluated at each visit for the presence of disease-specific symptoms and presence of systemic inflammation (Table 4).

Chronic inflammation and chronic glucocorticoid treatment negatively affect bone health (e.g., osteoporosis), growth (stunting), and development (1). These parameters should be monitored regularly, as well as cardiac (e.g., hypertension) and ophthalmologic complications of chronic glucocorticoid use.

Patients with CANDLE/PRAAS should also be monitored for headaches, skin and musculoskeletal disease, development of metabolic syndrome (hypertension, hyperglycemic and hepatic steatosis), and for development of primary pulmonary hypertension. Pulmonary hypertension can be insidious in onset. Although ILD is rare, it should be screened for at baseline and monitored as indicated by pulmonary function tests and low radiation chest CT. Ophthalmologic and dental assessment may be required in patients with eye inflammation and hypodontia and tooth eruption problems (1,2,5,9,18,36,37,39,51).

Patients with SAVI may require wound care (including wound culture as necessary) and close assessment of ILD and the development of secondary pulmonary hypertension. Patients should be screened for systemic hypertension, otolaryngology, ophthalmology, and dental disease at baseline and be followed as indicated. Patients should be instructed in self-care, including keeping peripheries warm, and in emergency management of acute ischemic digits (e.g., with, but not limited to, intravenous fluids, pentoxyphylline, or intravenous vasodilators), prompt use of antibiotics if infection is suspected, and meticulous wound care (1,8,103).

Patients with AGS are monitored for progression of neurologic disease including gross and fine motor function and cognitive function using validated scales when available (22,23). Patients with *SAMHD1* mutations require yearly MRI and MR angiography studies to screen for intracerebral artery disease (e.g., Moyamoya) (49,74,77). Patients should be monitored for the development of systemic hypertension, pulmonary hypertension, and cardiomyopathy (78). Other complications include autoimmune hepatitis

(25,83) and autoimmune endocrinopathies, most frequently hypothyroidism (34). Other manifestations that can develop insidiously include glaucoma and epilepsy, and should be monitored as clinically indicated (76,104). Neurologic tone abnormalities in nonambulatory patients can lead to joint dislocation and scoliosis and should be monitored. Families should be instructed in prevention of skin complications, physical therapy, management of disturbed sleep–wake patterns, and irritability commonly seen in AGS. Families can also participate in home stretching programs, and appropriate positioning of children with tone abnormalities.

The heightened type I interferon–mediated autoimmune response contributes to the development of autoantibodies and autoimmune diseases (105) (see Supplementary Table 5, https://onlinelibrary.wiley.com/doi/10.1002/art.42027). Antinuclear antibodies are seen in up to 62.5% of patients with SAVI (8), in up to 42% of patients with CANDLE/PRAAS (1,2,5,9,18,39,51,93), and 23% of patients with AGS (62). Moreover, antiphospholipid antibodies are present in patients with CANDLE/PRAAS, SAVI, and AGS (1,7,62). Antineutrophil cytoplasmic antibodies are, intermittently, elevated in up to 71% of patients with SAVI and 18% of patients with AGS (8,62), and RF positivity is reported in patients with SAVI (see above). Urinalysis for kidney dysfunction and screening for autoimmunity based on the disease symptoms are recommended as kidney disease is reported mostly in patients with AGS (50,62,79) and SAVI (8,106,107). Antibodies associated with specific autoimmune diseases including autoimmune arthritis, pauci-immune glomerulonephritis, autoimmune cytopenias, thyroiditis, and/or hepatitis have been described in CANDLE/PRAAS, SAVI, or AGS with variable frequencies (Supplementary Table 5). As it remains difficult to diagnose these diseases based on clinical symptoms, regular screening for autoantibodies as outlined in Table 4 is currently recommended. Renal pathology prior to treatment with JAKI should be assessed by a baseline renal ultrasound and urine protein/creatinine ratio (or albumin/creatinine ratio).

All patients and families should have access to formal genetic counseling and may require social and other support. Supportive care, including adaptive equipment (e.g., orthoses, walkers, wheelchairs, seating equipment), may be required.

Treatment during infections including COVID-19. Disease flares and progression can occur if immunosuppressive treatment is held (108) and disease can flare in the context of an infection. Thus, any patient who develops an acute infection (or other complications) may require adjustment of immunosuppressive treatment (and/or institution of other supportive treatment), which should be conducted only under expert supervision. In line with these suggestions, recently published ACR guidance recommends continuing or initiating immunosuppressants when indicated in patients with pediatric rheumatic diseases in the context of exposure to SARS–CoV-2 or if experiencing asymptomatic SARS–CoV-2 infection. Immunosuppressants may be temporarily delayed or withheld if a patient has symptomatic COVID-19 (109).

Box 1: Research agenda

To define autoinflammatory disease outcomes, including:
- Develop validated remission criteria for each disease including patient reported outcome measures.
- Develop minimal disease activity criteria.
- Identify sensitive biomarkers of progression of organ disease (including central nervous system).

To further assess efficacy of Janus kinase inhibitors (JAKI) and other type I IFN targeted therapies.

To assess long-term safety with treatment of JAKI.
- Assess long-term effect of chronic BK viral reactivation.
- Recommend monitoring guidance including frequency of BK viral load measurements and management of BK viremia.

To assess requirement of viral prophylaxis on JAKI.

To identify novel therapeutic targets and better treatments.

To validate an interferon signature to diagnose and monitor patients (e.g., number of interferon response genes to include, sensitivity and specificity of score).

To evaluate the effect of vaccination in triggering or exacerbating disease activity in patients with type I interferonopathies while on or off treatments with immunosuppressive medications and/or glucocorticoids.

To identify new genetic causes for interferonopathies.

Vaccination. Whether vaccination may trigger disease flares in interferonopathies is an important and currently unanswered question. There are no data suggesting that patients with CANDLE/PRAAS and SAVI develop disease flares with routine childhood vaccinations and the Task Force therefore recommended compliance with local regulations when patients are not treated with immunosuppressive treatments or glucocorticoids. No such consensus was achieved for AGS: the safety of vaccines in this population is not fully evaluated, and anecdotal reports of vaccine-induced neurologic regression were concerns debated by the Task Force. No specific recommendation on vaccination for AGS was therefore possible. In line with the general EULAR guidance, the Task Force recommends avoiding live vaccines in patients with CANDLE/PRAAS, SAVI, and AGS while on treatment with JAKI or other immunosuppressive medications (110). Treatment discontinuation can result in withdrawal flares. In general, we suggest following recommendations for other autoimmune and inflammatory rheumatic diseases (110,111); we however currently do not advise treatment adjustments for treatments recommended for the type I interferonopathies including JAKI.

RNA-based SARS–CoV-2 vaccines are not live vaccines, suggesting that they may be safe for immunosuppressed patients. Whether vaccines against COVID-19 have the potential to provoke

a disease flare is unknown; theoretical concerns about disease flare in type I interferonopathies caused by RNA vaccines exist. There are currently no data to back specific recommendations.

CONCLUSION

The aim of these points to consider is to address the unmet need to provide guidance for health care professionals involved in the care of patients with the recently characterized type I interferonopathies, CANDLE/PRAAS, SAVI, and AGS. A lack of high-level evidence is a limitation to these points to consider and reflects the challenges of studying novel, ultra-rare diseases. To address these challenges, the Task Force generated guidance statements based on results from a thorough SLR and on specialists'/experts' opinions where evidence was lacking or was insufficient. The Task Force included various specialists with broad expertise in relevant clinical areas and representing different regions, disease interests, and practice environments.

Important areas of future research are outlined in Box 1. The cost and availability of genetic testing, interferon signature assays, and JAKI treatment are substantial barriers that currently prevent optimized care for patients with interferonopathies. Furthermore, patients with the autoinflammatory interferonopathies CANDLE/PRAAS, SAVI, and AGS live in many different countries and are managed in different health care systems. These points to consider address the multiple challenges of managing patients with these ultra-rare diseases, by providing guidance on improving clinical recognition, support for decision-making on genetic testing, as well as treatment and long-term management. These points to consider were developed to increase awareness of these diseases, and to standardize the level of care by characterizing the diagnostic and therapeutic tools that can improve care.

ACKNOWLEDGMENTS

The Task Force gratefully thanks the librarian Darren Hamilton (London Health Sciences Center, London, Ontario, Canada) for his contribution to the systematic literature search, Hayyah Clairman and Natasha Naraidoo for their support in conducting the Delphi questionnaires using the REDCap platform, and the European Alliance of Associations for Rheumatology and the American College of Rheumatology for financial and logistical support. This project is part of a series of "points to consider" consensus efforts to standardize the diagnosis, treatment, and long-term monitoring of patients with the 3 major groups of known autoinflammatory diseases including 1) the interleukin-1–mediated diseases cryopyrin-associated periodic syndrome, tumor necrosis factor receptor–associated periodic syndrome, mevalonate kinase deficiency, and deficiency of the interleukin-1 receptor antagonist, 2) the autoinflammatory interferonopathies CANDLE/PRAAS, SAVI, and AGS, and 3) the early diagnosis, treatment, and long-term monitoring of inflammatory conditions with potential progression to hemophagocytic lymphohistiocytosis/macrophage activation syndrome. We would like to acknowledge and are grateful for the generous and invaluable financial and organizational support from the Autoinflammatory Alliance and the Systemic JIA Foundation. The Autoinflammatory Alliance substantially contributed to an international meeting and workgroup organization in August 2019 that developed the outline of the points to consider project. The funds for this preceding international meeting were largely due to patient fundraisers, online fundraising, and the work of countless volunteers who made this project possible.

AUTHOR CONTRIBUTIONS

All authors contributed to the formulation of the points to consider. In details, the steering committee of the Task Force (Drs. Goldbach-Mansky, Brogan, Vanderver, Feldman, and Demirkaya) defined the research questions for the SLR. A systematic literature review was conducted by Drs. Cetin Gedik, Romano, and Lamot with support from a librarian (nonauthor Darren Hamilton) and epidemiologist (Dr. Piskin) under supervision of a senior methodologist (Dr. Demirkaya). Drs. Cetin Gedik, Lamot, and Romano extracted the data. Drs. Goldbach-Mansky, Brogan, and Vanderver synthesized the results from SLR and Delphi questionnaires and generated draft statements. The manuscript was drafted by Drs. Cetin Gedik, Lamot, and Romano and revised by Drs. Goldbach-Mansky, Brogan, and Vanderver, Demirkaya, and Feldman. Dr. Aletaha oversaw the proceedings and provided advice on the points to consider project as EULAR methodologist. All other authors participated in the Task Force meetings, in 2 pre-meeting Delphi questionnaires, suggested and agreed upon the research questions, read the final statements prior to the manuscript, discussed results, and made contributions to the text. All authors approved the final version of the manuscript.

REFERENCES

1. Sanchez GA, Reinhardt A, Ramsey S, Wittkowski H, Hashkes PJ, Berkun Y, et al. JAK1/2 inhibition with baricitinib in the treatment of autoinflammatory interferonopathies. J Clin Invest 2018;128:3041–52.
2. Brehm A, Liu Y, Sheikh A, Marrero B, Omoyinmi E, Zhou Q, et al. Additive loss-of-function proteasome subunit mutations in CANDLE/PRAAS patients promote type I IFN production. J Clin Invest 2015;125:4196–211.
3. Crow YJ, Manel N. Aicardi-Goutières syndrome and the type I interferonopathies [review]. Nat Rev Immunol 2015;15:429–40.
4. Kim H, Sanchez GA, Goldbach-Mansky R. Insights from Mendelian interferonopathies: comparison of CANDLE, SAVI with AGS, monogenic lupus. J Mol Med 2016;94:1111–27.
5. Arima K, Kinoshita A, Mishima H, Kanazawa N, Kaneko T, Mizushima T, et al. Proteasome assembly defect due to a proteasome subunit β type 8 (PSMB8) mutation causes the autoinflammatory disorder, Nakajo-Nishimura syndrome. Proc Natl Acad Sci U S A 2011;108:14914–9.
6. Piccoli C, Bronner N, Gavazzi F, Dubbs H, De Simone M, De Giorgis V, et al. Late-onset Aicardi-Goutières syndrome: a characterization of presenting clinical features. Pediatr Neurol 2021;115:1–6.
7. Liu Y, Jesus AA, Marrero B, Yang D, Ramsey SE, Sanchez GA, et al. Activated STING in a vascular and pulmonary syndrome. N Engl J Med 2014;371:507–18.
8. Frémond ML, Hadchouel A, Berteloot L, Melki I, Bresson V, Barnabei L, et al. Overview of STING-associated vasculopathy with onset in infancy (SAVI) among 21 patients. J Allergy Clin Immunol Pract 2021;9:e11:803–18.
9. Garg A, Hernandez MD, Sousa AB, Subramanyam L, de Villareal LM, dos Santos HG, et al. An autosomal recessive syndrome of joint contractures, muscular atrophy, microcytic anemia, and panniculitis-associated lipodystrophy. J Clin Endocrinol Metab 2010;95:E58–63.
10. Li J, An S, Du Z. Familial interstitial lung disease caused by mutation of the STING1 gene. Front Pediatr 2020;8:543.
11. Stellitano LA, Winstone AM, van der Knaap MS, Verity CM. Leukodystrophies and genetic leukoencephalopathies in childhood: a

national epidemiological study. Dev Med Child Neurol 2016;58: 680–9.

12. De Jesus AA, Hou Y, Brooks S, Malle L, Biancotto A, Huang Y, et al. Distinct interferon signatures and cytokine patterns define additional systemic autoinflammatory diseases. J Clin Invest 2020;130:1669–82.
13. Kim H, de Jesus AA, Brooks SR, Liu Y, Huang Y, VanTries R, et al. Development of a validated interferon score using NanoString technology. J Interferon Cytokine Res 2018;38:171–85.
14. Van der Heijde D, Aletaha D, Carmona L, Edwards CJ, Kvien TK, Kouloumas M, et al. 2014 update of the EULAR standardised operating procedures for EULAR-endorsed recommendations. Ann Rheum Dis 2015;74:8–13.
15. Niederberger M, Spranger J. Delphi technique in health sciences: a Map. Front Public Health 2020;8:457.
16. OCEBM Levels of Evidence Working Group. Oxford Centre for Evidence-Based Medicine: levels of evidence (March 2009). URL: https://www.cebm.net/2009/06/oxford-centre-evidence-based-medicine-levels-evidence-march-2009/.
17. Fleiss JL. Statistical methods for rates and proportions. 2nd ed. New York: Wiley; 1981.
18. Liu Y, Ramot Y, Torrelo A, Paller AS, Si N, Babay S, et al. Mutations in proteasome subunit β type 8 cause chronic atypical neutrophilic dermatosis with lipodystrophy and elevated temperature with evidence of genetic and phenotypic heterogeneity. Arthritis Rheum 2012;64: 895–907.
19. Crow YJ, Jackson AP, Roberts E, van Beusekom E, Barth P, Corry P, et al. Aicardi-Goutières syndrome displays genetic heterogeneity with one locus (AGS1) on chromosome 3p21. Am J Hum Genet 2000;67:213–21.
20. Psarras A, Emery P, Vital EM. Type I interferon-mediated autoimmune diseases: pathogenesis, diagnosis and targeted therapy. Rheumatology (Oxford) 2017;56:1662–75.
21. Crow YJ, Shetty J, Livingston JH. Treatments in Aicardi-Goutières syndrome. Dev Med Child Neurol 2020;62:42–7.
22. Adang L, Gavazzi F, De Simone M, Fazi E, Galli J, Koh J, et al. Developmental outcomes of Aicardi Goutières syndrome. J Child Neurol 2020;35:7–16.
23. Adang LA, Gavazzi F, Jawad AF, Cusack SV, Kopin K, Peer K, et al. Development of a neurologic severity scale for Aicardi Goutières syndrome. Mol Genet Metab 2020;130:153–60.
24. Torrelo A. CANDLE syndrome as a paradigm of proteasome-related autoinflammation. Front Immunol 2017;8:927.
25. Lanzi G, Fazzi E, D'Arrigo S, Orcesi S, Maraucci I, Bertini E, et al. The natural history of Aicardi-Goutières syndrome: follow-up of 11 Italian patients. Neurology 2005;64:1621–4.
26. Kim H, Brooks KM, Tang CC, Wakim P, Blake M, Brooks SR, et al. Pharmacokinetics, pharmacodynamics, and proposed dosing of the oral JAK1 and JAK2 inhibitor baricitinib in pediatric and young adult CANDLE and SAVI patients. Clin Pharmacol Ther 2018;104: 364–73.
27. Wang BX, Grover SA, Kannu P, Loon G, Laxer RM, Yeh EA, et al. Interferon-stimulated gene expression as a preferred biomarker for disease activity in Aicardi-Goutières syndrome. J Interferon Cytokine Res 2017;37:147–52.
28. Rice GI, Duany YD, Jenkinson EM, Forte GM, Anderson BH, Ariaudo G, et al. Gain-of-function mutations in IFIH1 cause a spectrum of human disease phenotypes associated with upregulated type I interferon signaling. Nat Genet 2014;46:503–9.
29. Livingston JH, Lin JP, Dale RC, Gill D, Brogan P, Munnich A, et al. A type I interferon signature identifies bilateral striatal necrosis due to mutations in ADAR1. J Med Genet 2014;51:76–82.
30. Armangue T, Orsini JJ, Takanohashi A, Gavazzi F, Conant A, Ulrick N, et al. Neonatal detection of Aicardi Goutières syndrome by increased C26:0 lysophosphatidylcholine and interferon signature on newborn screening blood spots. Mol Genet Metab 2017;122: 134–9.
31. Garau J, Cavallera V, Valente M, Tonduti D, Sproviero D, Zucca S, et al. Molecular genetics and interferon signature in the Italian Aicardi Goutières syndrome cohort: report of 12 new cases and literature review. J Clin Med 2019;8:750.
32. Omoyinmi E, Standing A, Keylock A, Price-Kuehne F, Gomes SM, Rowcxenio D, et al. Clinical impact of a targeted next-generation sequencing gene panel for autoinflammation and vasculitis. PLoS One 2017;12:e0181874.
33. Al Mutairi F, Alfadhel M, Nashabat M, El-Hattab AW, Ben-Omran T, Hertecant J, et al. Phenotypic and molecular spectrum of Aicardi-Goutières syndrome: a study of 24 patients. Pediatr Neurol 2018; 78:35–40.
34. Crow YJ, Chase DS, Schmidt JL, Szynkiewicz M, Forte GM, Gornall HL, et al. Characterization of human disease phenotypes associated with mutations in TREX1, RNASEH2A, RNASEH2B, RNASEH2C, SAMHD1, ADAR, and IFIH1. Am J Med Genet A 2015;167A: 296–312.
35. De Jesus AA, Brehm A, VanTries R, Pillet P, Parentelli AS, Sanchez GA, et al. Novel proteasome assembly chaperone mutations in PSMG2/PAC2 cause the autoinflammatory interferonopathy CANDLE/PRAAS4. J Allergy Clin Immunol 2019;143:1939–43.
36. Kitamura A, Maekawa Y, Uehara H, Izumi K, Kawachi I, Nishizaea M, et al. A mutation in the immunoproteasome subunit PSMB8 causes autoinflammation and lipodystrophy in humans. J Clin Invest 2011; 121:4150–60.
37. Agarwal AK, Xing C, DeMartino GN, Mizrachi D, Hernandez MD, Sousa AB, et al. PSMB8 encoding the β5i proteasome subunit is mutated in joint contractures, muscle atrophy, microcytic anemia, and panniculitis-induced lipodystrophy syndrome. Am J Hum Genet 2010;87:866–72.
38. Sarrabay G, Méchin D, Salhi A, Boursier G, Rittore C, Crow Y, et al. PSMB10, the last immunoproteasome gene missing for PRAAS. J Allergy Clin Immunol 2020;145:1015–7.
39. Ayaki T, Murata K, Kanazawa N, Uruha A, Ohmura K, Sugie K, et al. Myositis with sarcoplasmic inclusions in Nakajo-Nishimura syndrome: a genetic inflammatory myopathy. Neuropathol Appl Neurobiol 2020;46:579–87.
40. Sönmez HE, Karaaslan C, de Jesus AA, Batu ED, Anlar B, Sözeri B, et al. A clinical score to guide in decision making for monogenic type I IFNopathies. Pediatr Res 2020;87:745–52.
41. Vanderver A, Prust M, Kadom N, Demarest S, Crow YJ, Helman G, et al. Early-onset Aicardi-Goutières syndrome: magnetic resonance imaging (MRI) pattern recognition. J Child Neurol 2015;30:1343–8.
42. Tonduti D, Izzo G, D'Arrigo S, Riva D, Moroni I, Zorzi G, et al. Spontaneous MRI improvement and absence of cerebral calcification in Aicardi-Goutières syndrome: diagnostic and disease-monitoring implications. Mol Genet Metab 2019;126:489–94.
43. Clarke SL, Robertson L, Rice GI, Seabra L, Hilliard TN, Crow YJ, et al. Type 1 interferonopathy presenting as juvenile idiopathic arthritis with interstitial lung disease: report of a new phenotype. Pediatr Rheumatol Online J 2020;18:37.
44. König N, Fiehn C, Wolf C, Schuster M, Costa EC, Tüngler V, et al. Familial chilblain lupus due to a gain-of-function mutation in STING. Ann Rheum Dis 2017;76:468–72.
45. Jain A, Misra DP, Sharma A, Wakhlu A, Agarwal V, Negi VS. Vasculitis and vasculitis-like manifestations in monogenic autoinflammatory syndromes [review]. Rheumatol Int 2018;38:13–24.
46. Jeremiah N, Neven B, Gentili M, Callebaut I, Maschalidi S, Stolzenberg MC, et al. Inherited STING-activating mutation underlies a familial inflammatory syndrome with lupus-like manifestations. J Clin Invest 2014;124:5516–20.

47. Lin B, Berard R, Al Rasheed A, Aladba B, Kranzusch PJ, Henderlight M, et al. A novel STING1 variant causes a recessive form of STING-associated vasculopathy with onset in infancy (SAVI). J Allergy Clin Immunol 2020;146:1204–8.
48. Uggenti C, Lepelley A, Depp M, Badrock AP, Rodero MP, El-Daher MT, et al. cGAS-mediated induction of type I interferon due to inborn errors of histone pre-mRNA processing. Nat Genet 2020;52: 1364–72.
49. Xin B, Jones S, Puffenberger EG, Hinze C, Bright A, Tan H, et al. Homozygous mutation in SAMHD1 gene causes cerebral vasculopathy and early onset stroke. Proc Natl Acad Sci U S A 2011;108: 5372–7.
50. Ramantani G, Kohlhase J, Hertzberg C, Innes AM, Engel K, Hunger S, et al. Expanding the phenotypic spectrum of lupus erythematosus in Aicardi-Goutières syndrome. Arthritis Rheum 2010;62:1469–77.
51. Torrelo A, Patel S, Colmenero I, Gurbindo D, Lendínez F, Hernández A, et al. Chronic atypical neutrophilic dermatosis with lipodystrophy and elevated temperature (CANDLE) syndrome. J Am Acad Dermatol 2010;62:489–95.
52. Medinilla EE, García MV, Ramírez MD, Medina RC, Antón JL. Aicardi-Goutières syndrome: phenotypic and genetic spectrum in a series of three cases. An Pediatr 2019;90:312–4. In Spanish.
53. Videira G, Malaquias MJ, Laranjinha I, Martins R, Taipa R, Magalhães M. Diagnosis of Aicardi-Goutières syndrome in adults: a case series. Mov Disord Clin Pract 2020;7:303–7.
54. Abe J, Nakamura K, Nishikomori R, Kato M, Mitsuiki N, Izawa K, et al. A nationwide survey of Aicardi-Goutières syndrome patients identifies a strong association between dominant TREX1 mutations and chilblain lesions: Japanese cohort study. Rheumatology (Oxford) 2014;53:448–58.
55. Yarbrough K, Danko C, Krol A, Zonana J, Leitenberger S. The importance of chilblains as a diagnostic clue for mild Aicardi-Goutières syndrome. Am J Med Genet A 2016;170:3308–12.
56. Frémond ML, Rodero MP, Jeremiah N, Belot A, Jeziorski E, Duffy D, et al. Efficacy of the Janus kinase 1/2 inhibitor ruxolitinib in the treatment of vasculopathy associated with TMEM173-activating mutations in 3 children. J Allergy Clin Immunol 2016;138:1752–5.
57. Keskitalo S, Haapaniemi E, Einarsdottir E, Rajamäki K, Heikkilä H, Ilander M, et al. Novel TMEM173 mutation and the role of disease modifying alleles. Front Immunol 2019;10:2770.
58. Melki I, Rose Y, Uggenti C, Van Eyck L, Frémond ML, Kitabayashi N, et al. Disease-associated mutations identify a novel region in human sting necessary for the control of type I interferon signaling. J Allergy Clin Immunol 2017;140:543–52.
59. Volpi S, Insalaco A, Caorsi R, Santori E, Messia V, Sacco O, et al. Efficacy and adverse events during Janus kinase inhibitor treatment of SAVI syndrome. J Clin Immunol 2019;39:476–85.
60. Tang X, Xu H, Zhou C, Peng Y, Liu H, Liu J et al. STING-associated vasculopathy with onset in infancy in three children with new clinical aspect and unsatisfactory therapeutic responses to tofacitinib. J Clin Immunol 2020;40:114–22.
61. Picard C, Thouvenin G, Kannengiesser C, Dubus JC, Jeremiah N, Rieux-Laucat F, et al. Severe pulmonary fibrosis as the first manifestation of Interferonopathy (TMEM173 mutation). Chest 2016;150: e65–71.
62. Cattalini M, Galli J, Andreoli L, Olivieri I, Ariaudo G, Fredi M, et al. Exploring autoimmunity in a cohort of children with genetically confirmed Aicardi-Goutières syndrome. J Clin Immunol 2016;36:693–9.
63. Kolivras A, Aeby A, Crow YJ, Rice GI, Sass U, André J, et al. Cutaneous histopathological findings of Aicardi-Goutières syndrome, overlap with chilblain lupus. J Cutan Pathol 2008;35:774–8.
64. Crow YJ, Zaki MS, Abdel-Hamid MS, Abdel-Salam G, Boespflug-Tanguy O, Cordiero NJ, et al. Mutations in ADAR1, IFIH1, and RNASEH2B presenting as spastic paraplegia. Neuropediatrics 2014;45:386–91.
65. Izzotti A, Pulliero A, Orcesi S, Cartiglia C, Longobardi MG, Capra V, et al. Interferon-related transcriptome alterations in the cerebrospinal fluid cells of Aicardi-Goutières patients. Brain Pathol 2009;19: 650–60.
66. La Piana R, Uggetti C, Roncarolo F, Vanderver A, Olivieri I, Tonduti D, et al. Neuroradiologic patterns and novel imaging findings in Aicardi-Goutières syndrome. Neurology 2016;86:28–35.
67. Salerno S, Granata C, Trapenese M, Cannata V, Curione D, Espagnet MC, et al. Is MRI imaging in pediatric age totally safe? A critical reprisal [review]. Radiol Med 2018;123:695–702.
68. Livingston JH, Stivaros S, van der Knaap MS, Crow YH. Recognizable phenotypes associated with intracranial calcification. Dev Med Child Neurol 2013;55:46–57.
69. Abdel-Salam GM, Zaki MS, Lebon P, Meguid NA. Aicardi-Goutières syndrome: clinical and neuroradiological findings of 10 new cases. Acta Paediatr 2004;93:929–36.
70. Uggetti C, La Piana R, Orcesi S, Egitto MG, Crow YJ, Fazzi E. Aicardi-Goutieres syndrome: neuroradiologic findings and follow-up. AJNR Am J Neuroradiol 2009;30:1971–6.
71. Uyur-Yalcin E, Maras-Genc H, Kara B. Clinical and neuroradiologic variability of Aicardi-Goutieres syndrome: two siblings with RNASEH2C mutation and a boy with TREX1 mutation. Turk J Pediatr 2015;57:504–8.
72. Goutières F, Aicardi J, Barth PG, Lebon P. Aicardi-Goutières syndrome: an update and results of interferon-α studies. Ann Neurol 1998;44:900–7.
73. Lanzi G, Fazzi E, D'Arrigo S. Aicardi-Goutières syndrome: a description of 21 new cases and a comparison with the literature. Eur J Paediatr Neurol 2002;6 Suppl:A9–22.
74. Ramesh V, Bernardi B, Stafa A, Garone C, Franzoni E, Abinum M, et al. Intracerebral large artery disease in Aicardi-Goutières syndrome implicates SAMHD1 in vascular homeostasis. Dev Med Child Neurol 2010;52:725–32.
75. Rossler L, Ludwig-Seibold C, Thiels C, Schaper J. Aicardi-Goutières syndrome with emphasis on sonographic features in infancy. Pediatr Radiol 2012;42:932–40.
76. Crow YJ, Massey RF, Innes JR, Pairaudeau PW, Hills CA, Woods CG, et al. Congenital glaucoma and brain stem atrophy as features of Aicardi-Goutières syndrome. Am J Med Genet A 2004;129A:303–7.
77. Thiele H, du Moulin M, Barczyk K, George C, Schwindt W, Nürnberg G, et al. Cerebral arterial stenoses and stroke: novel features of Aicardi-Goutières syndrome caused by the Arg164X mutation in SAMHD1 are associated with altered cytokine expression. Hum Mutat 2010;31:E1836–50.
78. Adang LA, Frank DB, Gilani A, Takanohashi A, Ulrick N, Collins A, et al. Aicardi Gières syndrome is associated with pulmonary hypertension. Mol Genet Metab 2018;125:351–8.
79. Samanta D, Ramakrishnaiah R, Crary SE, Sukumaran S, Burrow TA. Multiple autoimmune disorders in Aicardi-Goutières syndrome. Pediatr Neurol 2019;96:37–9.
80. Cross Z, Kriegermeier A, McMann J, Rand E, Takanohashi A, Ulrick N, et al. Autoimmune hepatitis in Aicardi-Goutieres syndrome. Neurology 2019;92 Suppl 15:4.6–045.
81. Ishikawa T, Tamura E, Kasahara M, Uchida H, Higuchi M, Kobayashi H, et al. Severe liver disorder following liver transplantation in STING-associated vasculopathy with onset in infancy. J Clin Immunol 2021; 41:967–74.
82. Ford ES, Ajani UA, Mokdad AH, on behalf of the National Health and Nutrition Examination Survey. The metabolic syndrome and concentrations of C-reactive protein among U.S. youth. Diabetes Care 2005;28:878–81.

83. Rice G, Patrick T, Parmar R, Taylor CF, Aeby A, Aicardi J, et al. Clinical and molecular phenotype of Aicardi-Goutieres syndrome. Am J Hum Genet 2007;81:713–25.
84. Abe J, Izawa K, Nishikomori R, Awaya T, Kawai T, Yasumi T, et al. Heterozygous TREX1 p.Asp18Asn mutation can cause variable neurological symptoms in a family with Aicardi-Goutieres syndrome/familial chilblain lupus. Rheumatology (Oxford) 2013;52:406–8.
85. Hebbar M, Kanthi A, Shrikiran A, Patil S, Muranjan M, Francis F, et al. p.Arg69Trp in RNASEH2C is a founder variant in three Indian families with Aicardi-Goutières syndrome. Am J Med Genet A 2018;176:156–60.
86. Tumienė B, Voisin N, Preikšaitienė E, Petroška D, Grinkinienė J, Samaitienė R, et al. Inflammatory myopathy in a patient with Aicardi-Goutières syndrome. Eur J Med Genet 2017;60:154–8.
87. Dale RC, Gornall H, Singh-Grewal D, Alcausin M, Rice GI, Crow YJ. Familial Aicardi-Goutières syndrome due to SAMHD1 mutations is associated with chronic arthropathy and contractures. Am J Med Genet A 2010;152A:938–42.
88. Buers I, Rice GI, Crow YJ, Rutsch F. MDA5-associated neuroinflammation and the Singleton-Merten syndrome: two faces of the same type I Interferonopathy spectrum [review]. J Interferon Cytokine Res 2017;37:214–9.
89. Saldanha RG, Balka KR, Davidson S, Wainstein BK, Wong M, Macintosh R, et al. A mutation outside the dimerization domain causing atypical STING-associated vasculopathy with onset in infancy. Front Immunol 2018;9:1535.
90. Cooray S, Henderson R, Solebo AL, Ancliffe P, Eleftheriou D, Brogan PA. Retinal vasculopathy in STING-associated vasculitis of infancy (SAVI). Rheumatology (Oxford) 2021;60:e351–3.
91. Crow Y, Keshavan N, Barbet JP, Bercu G, Bondet V, Boussard C, et al. Cardiac valve involvement in ADAR-related type I interferonopathy. J Med Genet 2020;57:475–8.
92. Lee-Kirsch MA. The type I interferonopathies. Annu Rev Med 2017;68:297–315.
93. Al-Mayouf SM, AlSaleem A, AlMutairi N, AlSonbul A, Alzaid T, Alazami AM, et al. Monogenic interferonopathies: phenotypic and genotypic findings of CANDLE syndrome and its overlap with C1q deficient SLE. Int J Rheum Dis 2018;21:208–13.
94. Poli MC, Ebstein F, Nicholas SK, de Guzman MM, Forbes LR, Chinn IK, et al. Heterozygous truncating variants in POMP escape nonsense-mediated decay and cause a unique immune dysregulatory syndrome. Am J Hum Genet 2018;102:1126–42.
95. Vanderver A, Adang L, Gavazzi F, McDonald K, Helman G, Frank DB, et al. Janus kinase inhibition in the Aicardi-Goutières syndrome. N Engl J Med 2020;383:986–9.
96. Meesilpavikkai K, Dik WA, Schrijver B, van Helden-Meeuwsen CG, Versnel MA, van Hagen PM, et al. Efficacy of baricitinib in the treatment of chilblains associated with Aicardi-Goutières syndrome, a type I interferonopathy. Arthritis Rheumatol 2019;71:829–31.
97. Zimmermann N, Wolf C, Schwenke R, Lüth A, Schmidt F. Engel K, et al. Assessment of clinical response to Janus kinase inhibition in patients with familial chilblain lupus and TREX1 mutation. JAMA Dermatol 2019;155:342–6.
98. Patel PN, Hunt R, Pettigrew ZJ, Shirley JB, Vogel TP, de Guzman MM. Successful treatment of chronic atypical neutrophilic dermatosis with lipodystrophy and elevated temperature (CANDLE) syndrome with tofacitinib. Pediatr Dermatol 2021;38:528–9.
99. Rice GI, Meyzer C, Bouazza N, Hully M, Boddaert N, Semeraro M. et al. Reverse-transcriptase inhibitors in the Aicardi–Goutières syndrome. N Engl J Med 2018;379:2275–7.
100. Kasiske BL, Zeier MG, Chapman JR, Craig JC, Ekberg H, Garvey CA, et al. KDIGO clinical practice guideline for the care of kidney transplant recipients: a summary. Kidney Int 2010;77:299–311.
101. Smith JM, McDonald RA, Finn LS, Healey PJ, Davis CL, Limaye AP, et al. Polyomavirus nephropathy in pediatric kidney transplant recipients. Am J Transplant 2004;4:2109–17.
102. Buchman AL. Side effects of corticosteroid therapy. J Clin Gastroenterol 2001;33:289–94.
103. Frémond ML, Crow YJ. Sting-mediated lung inflammation and beyond. J Clin Immunol 2021;41:501–14.
104. Ramantani G, Maillard LG, Bast T, Husain RA, Niggeman P, Kohlhase K, et al. Epilepsy in Aicardi-Goutières syndrome. Eur J Paediatr Neurol 2014;18:30–7.
105. Theofilopoulos AN, Baccala R, Beutler B, Kono DH. Type I interferons (α/β) in immunity and autoimmunity [review]. Annu Rev Immunol 2005;23:307–35.
106. Ma M, Mazumder S, Kwak H, Adams M, Gregory M. Case report: acute thrombotic microangiopathy in a patient with STING-associated vasculopathy with onset in infancy (SAVI). J Clin Immunol 2020;40:1111–5.
107. Abid Q, Best Rocha A, Larsen CP, Schulert G, Marsh R, Yasin S, et al. APOL1-associated collapsing focal segmental glomerulosclerosis in a patient with stimulator of interferon genes (STING)-associated vasculopathy with onset in infancy (SAVI). Am J Kidney Dis 2020;75:287–90.
108. Adang L, Goldbach-Mansky R, Vanderver A. JAK inhibition in the Aicardi-Goutières syndrome. N Engl J Med 2020;383:2191–3.
109. Wahezi DM, Lo MS, Rubinstein TB, Ringold S. Ardoin SP, Downes KJ, et al. American College of Rheumatology guidance for the management of pediatric rheumatic disease during the COVID-19 pandemic: version 1. Arthritis Rheumatol 2020;72:1809–19.
110. Furer V, Rondaan C, Heijstek MW, Agmon-Levin N, van Assen S, Bijl M, et al. 2019 update of EULAR recommendations for vaccination in adult patients with autoimmune inflammatory rheumatic diseases. Ann Rheum Dis 2020;79:39–52.
111. Curtis JR, Johnson SR, Anthony DD, Arasaratnam RJ, Baden LR, Bass AR, et al. American College of rheumatology guidance for COVID-19 vaccination in patients with rheumatic and musculoskeletal diseases: version 3. Arthritis Rheumatol 2021;73:e60–75.

American College of Rheumatology
Empowering Rheumatology Professionals

Arthritis & Rheumatology
Vol. 74, No. 5, May 2022, pp 752–765
DOI 10.1002/art.42081

REVIEW

Safety and Efficacy of Mesenchymal Stromal Cells and Other Cellular Therapeutics in Rheumatic Diseases in 2022: A Review of What We Know So Far

Gary S. Gilkeson

Although a number of new immunosuppressive agents and biologics have been approved for treating various autoimmune inflammatory rheumatic diseases, there remains a substantial number of patients who have no clinical response or limited clinical response to these available treatments. Use of cellular therapies is a novel approach for the treatment of autoimmune inflammatory rheumatic diseases, with perhaps enhanced efficacy and less toxicity than current therapies. Autologous hematopoietic stem cell transplants were the first foray into cellular therapies, with proven efficacy in scleroderma and multiple sclerosis. Newer, yet unproven, cellular therapies include allogeneic mesenchymal stromal cells, which have been shown to be effective in graft-versus-host disease and in healing Crohn's fistulas. Chimeric antigen receptor T cells are effective in various malignancies, with possible application in rheumatic diseases, as shown in preclinical studies in murine lupus and recently in human lupus. Treg cells are one of the master controllers of the immune response and are decreased in number and/or effectiveness in specific autoimmune diseases. Expansion of autologous Treg cells is an attractive approach to controlling autoimmunity. There are a number of other regulatory cells in the immune system, including Breg cells, dendritic cells, macrophages, and other T cell types, that are in early stages of development as treatments. In this review, the current evidence for the efficacy and mechanisms of actions of cellular therapies already in use or in clinical trials in human autoimmune diseases will be discussed, including the limitations of these therapies and potential side effects.

Introduction

A number of therapeutic agents were recently approved for treating autoimmune diseases, including biologics and immunosuppressive agents (1). Even with the availability of these new drugs, a number of patients do not adequately respond, or experience significant side effects from the medications. Thus, new treatment modalities in autoimmune diseases are needed.

A novel approach to treating autoimmune diseases is cell-based therapies, both autologous and allogeneic (2). Autologous hematopoietic stem cell transplantation (HSCT) resets the bone marrow, establishing a non-autoimmune immune system (3). Chimeric antigen receptor T cells (CAR T cells), which utilize the patient's T cells, adding targeting and therapeutic molecules to the cells, constitute an expanding method of treatment in cancer, with potential applications in autoimmunity (4,5). Allogeneic mesenchymal stromal cells (MSCs), due to their immunomodulatory effects and repair abilities, are of increasing interest in autoimmunity (6). Enhancing Treg cell function may improve autoimmunity by expanding Treg cells to keep autoreactivity in check (7,8). There is therapeutic potential for the use of Breg cells, T follicular cells, dendritic cells, induced pluripotent stem cells, and monocytes as therapeutics. The development of potential treatments using these cell types is in the very early stages. This review is focused on cellular therapies that are already in human trials or being used in practice. Table 1 contains an overview of the different cellular therapies discussed.

This review is focused primarily on lupus, scleroderma, and rheumatoid arthritis (RA), where there is the most human experience in cellular therapies. Cellular therapies are being pilot tested in other autoimmune diseases, such as myositis, vasculitis, Sjögren's syndrome, ankylosing spondylitis, and psoriatic arthritis; however, there are very limited data in humans (9–11). Autologous cellular therapies are currently used for reparative purposes

Gary S. Gilkeson, MD: Medical University of South Carolina and Medical Research Service, Ralph H. Johnson VAMC, Charleston.

Author disclosures are available at https://onlinelibrary.wiley.com/action/downloadSupplement?doi=10.1002%2Fart.42081&file=art42081-sup-0001-Disclosureform.pdf.

Address correspondence to Gary S. Gilkeson, MD, 96 Jonathan Lucas Street Suite 822, MSC637, Charleston, SC 29425. Email: gilkeson@musc.edu.

Submitted for publication August 2, 2021; accepted in revised form February 1, 2022.

Table 1. Comparison of cellular therapies in inflammatory rheumatic diseases*

	HSCT	MSCs	Treg cells†	CAR T cells
Cell type	Autologous	Allogeneic	Autologous	Autologous
HLA matching	NA	NA	NA	NA
Preconditioning	Yes	No	No	No
Treatment mortality	Yes (3–5%)	No	No	Rare, though cytokine storm is common
Relapse	Yes, but with milder disease	Yes, in most, though not all, patients	Unknown	Unknown
Hospitalization	Yes	No	No	In some cases
Approved for use in humans	Yes, for scleroderma	Yes, for GVHD and refractory Crohn's disease	No	Yes, for lymphomas
Stage of development	Approved for scleroderma	Phase II studies	Phase I studies	Preclinical phase
Advantages	Proven efficacy	No preconditioning	Autologous/no preconditioning	Experience in cancer therapy
Disadvantages	Morbidity and mortality	Suggestive, but not proven, efficacy	Difficult to derive	Cytokine storm
Side effects	Infection	Minimal	Minimal experience	Cytokine storm

* HSCT = hematopoietic stem cell transplantation; MSCs = mesenchymal stromal cells; CAR T cells = chimeric antigen receptor T cells; NA = not applicable; GVHD = graft-versus-host disease.
† CD4+CD25+ Treg cells.

Table 2. Trials of autologous HSCT for treating lupus*

Author, year (ref.)	No. of patients	Conditioning	Mortality, no. (%)	Transplant-related mortality, no. (%)	SLE-related mortality, no. (%)	Overall survival, %	Relapse-free survival, % (no. of years of follow-up)	Country
Farge et al, 2010 (78)	85	Multiple	18 (21)	11 (13)	5 (6)	79†	44 (5)	Europe
Burt et al, 2006 (79)	50	CYC + ATG	8 (16)	2 (4)	4 (8)	84	50 (5)	US
Song et al, 2011 (80)	18	TLI + CYC + ATG	Unknown	0 (0)	Unknown	Unknown	72 (1)	China
Rosen et al, 2000 (81)	7	CYC + ATG	2 (29)	1 (14)	1 (14)	71	72 (5)	Germany
Goklemez et al, 2021 (82)	8	CYC + FL + RTX	2 (25)	0 (0)	2 (25)	75	75 (4)	US

* HSCT = hematopoietic stem cell transplantation; SLE = systemic lupus erythematosus; CYC = cyclophosphamide; ATG = antithymocyte globulin; TLI = total lymphoid irradiation; FL = fludarabine; RTX = rituximab.
† After 5 years of follow-up.

in wound healing, fracture healing, and osteoarthritis, but discussion of these uses is outside the intent of this review.

Hematopoietic stem cell transplantation

The initial foray into cellular therapies in rheumatic diseases involved allogeneic HSCT in cancer patients with preexisting autoimmune diseases (12). It was noted that patients who survived the cancer and transplantation often had remission of their rheumatic disease (13). The morbidity and mortality associated with allogeneic transplantation in autoimmunity, however, precluded its use unless there was a coexisting malignancy (12). Autologous HSCT was first used for treating solid tumors, allowing more aggressive chemotherapy. The morbidity and mortality associated with autologous HSCT is significantly less than that associated with allogeneic HSCT, and with experience, outcomes have improved, with the risk/benefit ratio being acceptable in life/organ-threatening autoimmune diseases such as scleroderma and lupus (13).

There are a number of case reports and series describing successful suppression of autoimmunity with autologous transplants. There are 3 published randomized controlled trials (though not blinded for ethical reasons) comparing standard of care with cyclophosphamide to autologous HSCT in scleroderma (Autologous Stem Cell Transplantation International Scleroderma [ASTIS], Autologous Stem Cell Systemic Sclerosis Immune Suppression Trial [ASSIST], and Scleroderma Cytoxan or Transplant [SCOT]) and a recent retrospective review of 80 patients undergoing HSCT (Non-interventional Systemic Sclerosis 1 [NISSCI]) (14,15). Although conditioning regimens varied, with later trials using non–marrow ablative conditioning, each trial demonstrated that the patients who underwent transplantation had significantly improved survival compared to those who received standard of care (14–16). Skin disease improved the most, with notable improvements 1 month after transplantation. Lung function also either stabilized or improved in more patients undergoing autologous bone marrow transplantation (BMT) than in those receiving standard of care (14). Meta-analyses indicate that autologous HSCT is superior to standard of care in patients with progressive life-threatening disease, and it is recommended as an intervention by the European HSCT group (15). In Europe, more autologous HSCTs are performed for multiple sclerosis and scleroderma than other autoimmune indications (15). A recent review by Snowden et al (17) described the primarily European 20-year experience with HSCT in autoimmune disease from 1995–2015. There was a chronological increase in progression-free survival through the 5-year time intervals. Overall, there is an increase in the number of autologous HSCTs being done for multiple sclerosis, scleroderma, and Crohn's disease. The number of HSCTs performed in patients with lupus or RA have fallen significantly, to only 1–2 per year, perhaps due to the availability of other therapies. Overall, HSCT survival was the worst in scleroderma, but this preceded prescreening for cardiac disease (17).

The primary difficulty with regard to HSCT is choosing the right time and the right patient for this aggressive, expensive, and potentially fatal treatment. Patients with advanced disease, especially those with scleroderma heart involvement, do poorly (18). An in-depth cardiac evaluation prior to transplantation (magnetic resonance imaging, volume loading) to prove lack of cardiac involvement in scleroderma is recommended, as most deaths were due to cardiac toxicity of the conditioning regimen (19). The European HSCT group recently published guidelines for determining which scleroderma patients are candidates for HSCT, with cardiac testing being a primary recommendation (19). There are a few published uncontrolled trials of allogeneic HSCT in lupus. None of the lupus trials were placebo-controlled or included a comparison with standard of care; thus, the efficacy of allogeneic HSCT compared to standard of care is unknown (20) (Table 2). Patient selection is also a major hurdle in lupus. As conditioning regimens evolve, with less morbidity and mortality, allogeneic HSCT will likely become more widely used in select patients with severe disease. It is clear that HSCT for autoimmune diseases should only be done in select centers of excellence where HSCT experts work together with rheumatologists to enhance patient outcomes.

Mesenchymal stromal cells

Mesenchymal stem cells were first described by Friedenstein in 1966 (21). They were called "mesenchymal stem cells" based

on their ability to differentiate into chondrocytes, adipocytes, and osteoblasts. The nomenclature was recently changed, when it was acknowledged that MSCs were not truly stem cells, as their differentiation potential is limited. "Mesenchymal stromal cells" is proposed as a more applicable name, though others use the term "medicinal signaling cells" based on their therapeutic potential, while maintaining the MSC abbreviation (22).

There are 3 criteria for classifying cells as MSCs according to the International Society of Stem Cell Therapeutics (23). First, they must be plate adherent in culture. Second, they must have the capacity to differentiate into osteoblasts, chondrocytes, and adipocytes in culture. Third, they must not express endothelial cell, hematopoietic cell, or class II antigen–presenting cell markers (CD31, CD45, and HLA–DR), while expressing stromal cell markers (CD73, CD90, and CD105). MSCs express major histocompatibility complex (MHC) class I molecules and can present MHC class I epitopes to CD8+ T lymphocytes. CD80, CD86, CD28, and inducible costimulator ligand, key costimulatory molecules in T cell activation, are not expressed on MSCs; however, MSCs do express low levels of other costimulators, which can lead to T cell costimulation (24).

Allogeneic MSCs are not approved for any disease in the US. Allogeneic MSCs are approved for childhood acute graft-versus-host disease (GVHD) resistant to steroids in Japan, New Zealand, and Canada (25). A US Food and Drug Administration application for the use of MSCs in childhood acute steroid-resistant GVHD is under review. MSCs are approved for refractory anal/rectal fistulas in patients with Crohn's disease in the European Union and South Korea (26). The route of administration for the treatment of fistulas in Crohn's disease is local injection and not intravenous (IV) administration.

MSCs are a heterogeneous group of cells. Although MSCs can be derived from most human tissues, MSCs from 3 sources are used most in human therapeutics: allogeneic bone marrow–derived MSCs (BM-MSCs), adipose tissue–derived MSCs (AD-MSCs), and umbilical cord–derived MSCs (UC-MSCs). Bone marrow, though obtainable, requires a painful procedure and yields limited numbers of cells. MSCs do not circulate in the peripheral blood so cannot be harvested by apheresis. Large numbers of MSCs can be derived from adipose tissue or umbilical cords. There are conflicting reports regarding the immunosuppressive ability of MSCs from the 3 sources. Available data suggest that AD-MSCs and UC-MSCs are more immunosuppressive, both in vitro and in vivo, than BM-MSCs (27,28). In our experience in murine lupus, UC-MSCs and BM-MSCs had similar in vivo efficacy in suppressing lupus nephritis and in in vitro T cell and B cell suppression assays (29). Most MSC trials at this point are using either UC-MSCs or AD-MSCs due to the ease of obtaining a large number of cells derived from a single source.

Screening of donors is required to ensure that no infectious vectors are present in the donor cells. Cytomegalovirus (CMV) and herpes simplex virus (HSV) can infect MSCs, though MSCs from healthy CMV/HSV-seropositive donors do not contain virus detectable by polymerase chain reaction, unless the viral disease is active (30). Epstein–Barr virus (EBV) cannot infect MSCs due to their lacking the EBV receptor (30). An unanswered question is the difference in effectiveness between MSCs from one individual and those derived from another individual. It is assumed such differences exist, but the proper validating procedures have not yet been determined. Given that women are more prone than men to most autoimmune diseases, could MSCs derived from men be more immune effective? There are reports of global gene expression differences in UC-MSCs derived from men versus those derived from women, but there is no evidence these differences are clinically relevant (31).

Early studies found that MSCs derived from autoimmune patients are ineffective and dysfunctional. BM-MSCs from lupus patients are not as effective as allogeneic BM-MSCs in suppressing murine models of lupus and inflammatory arthritis. MSCs derived from lupus patient bone marrow have an altered endoskeleton, slow growth, poor migration, and early loss of viability and do not protect against the development of disease in animal models or in humans (32). They also have altered microRNA (miRNA) expression, altered RNA-Seq profiles, and enhanced type I interferon (IFN) production, all resulting in decreased efficacy in in vitro suppression assays and in vivo animal and human trials (33). Similar defects are found in BM-MSCs from patients with other autoimmune diseases.

A multitude of mechanisms of action for MSCs have been proposed from in vitro experiments and in vivo animal models. Increased Treg cell numbers and altered T cell and B cell subsets are repeat findings. MSC effects can be divided into 6 different mechanisms (34–36) (Figure 1). First is direct cell-to-cell contact with immune cells or endothelial cells, resulting in functional impacts through cell receptor interactions and/or mitochondrial transfer (37). Second are paracrine effects through the release of mediators with immunomodulatory, antiapoptotic, angiogenic, and antioxidant effects (38) (Figure 2). MSCs produce basal levels of chemokines, cytokines, and antiinflammatory mediators. These include CXCL12, interleukin-6 (IL-6), prostaglandin E_2 (PGE_2), and transforming growth factor β (TGFβ) (35,39,40). CXCL12 is found in sites of inflammation and is an important chemoattractant for MSCs (40). Exposure of MSCs to inflammatory cytokines and Toll-like receptor (TLR) ligands increases production of antiinflammatory mediators (41). MSC-derived TGFβ is a major driver of the differentiation of FoxP3– CD4+ T cells to FoxP3+ Treg cells (42). MSCs express COX-2 and secrete low levels of PGE_2 (35). PGE_2 is important in T cell immunosuppression mediated by MSCs. Human MSCs express other immune effectors, including galectins and nitric oxide (43). Indoleamine dioxygenase is produced by human MSCs and is immunosuppressive by limiting availability of tryptophan to T cells (44) (Table 2).

A third cellular action of MSCs is by impacting the differentiation of monocytes to IL-10–producing alternatively activated (M2)

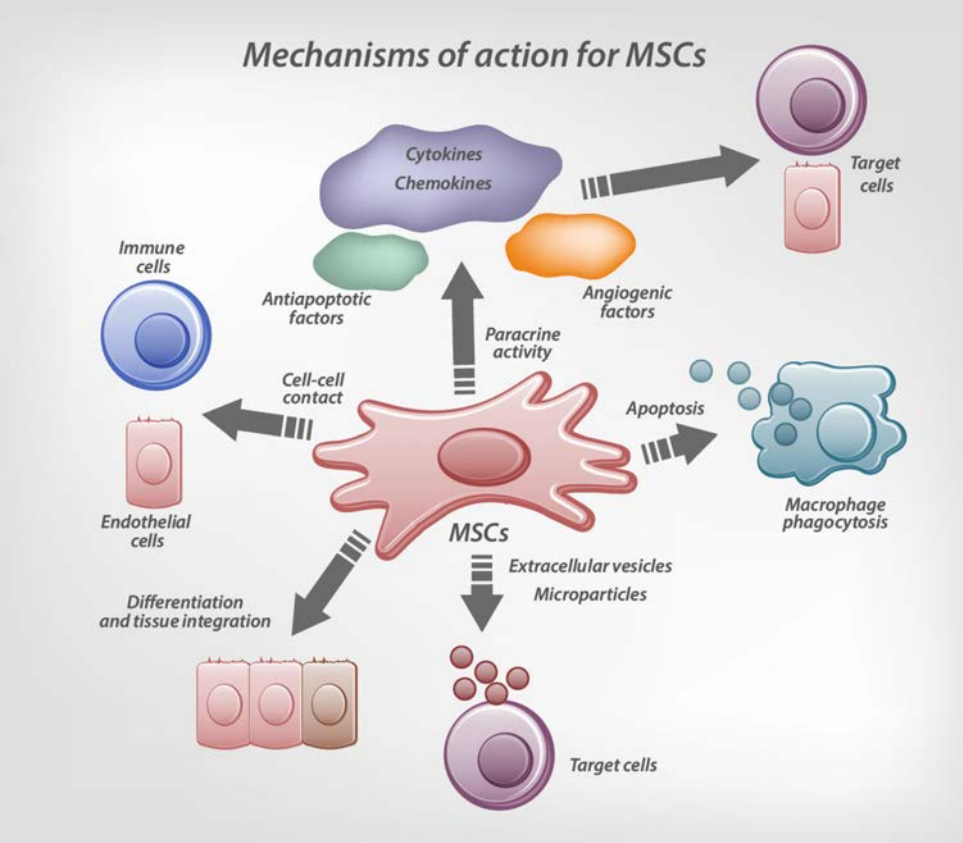

Figure 1. Schematic illustration of mechanisms of action of mesenchymal stromal cells (MSCs). There are multiple proposed mechanisms by which MSCs exert their immune effects. The figure illustrates the following mechanisms of action: 1) MSCs secrete a number of factors, including cytokines, angiogenic factors, and antiapoptotic factors as a paracrine effect. 2) MSCs undergo apoptosis and are engulfed by tissue macrophages, altering macrophage function. 3) MSCs extrude extracellular vesicles that are taken up by target cells and impact cellular function. 4) MSCs can differentiate and integrate into target tissues. 5) MSCs can act by cell-to-cell contact either by intercellular receptor interactions or via transfer of mitochondria. This contact can occur between MSCs and immune cells, MSCs and endothelial cells, and MSCs and other target organ cells.

macrophages (34). Apoptosis of MSCs and engulfment by macrophages leads to a switch in tissue macrophages from inflammatory (classically activated [M1]) to antiinflammatory (M2) (34). Absorption of MSC apoptotic bodies decreases the development of conventional dendritic cells (34). A fourth cellular effect of MSCs is via production of extracellular vesicles and other microparticles (45). The extracellular vesicles are able to fuse to the cell membrane of target cells and release proteins and miRNAs impacting target cell function. Similar to the extracellular vesicle fusion, during cell-to-cell contact, MSCs can transfer mitochondria to target cells, a fifth cellular action (45). The sixth and final cellular action is via MSCs integrating into the target tissue. This is a key feature for tissue repair of MSCs, but it is not clear this is a mechanism for immune modulation.

MSCs are often described as being "immune privileged" since they lack MHC class II, as well as specific costimulatory molecules. Thus, the donor and recipient do not need to be HLA matched. An allogeneic reaction can develop, though not in all patients, and does not appear clinically significant regarding future blood transfusions or pregnancies, but does likely decrease MSC lifespan. It has been postulated that HLA mismatch may be advantageous in that the immune interactions may activate MSCs. How well and how long "immune privilege," if it is present, lasts is an unresolved issue.

What happens to MSCs once they are injected IV is an area of incomplete understanding (46). Upon IV administration, the cells immediately go to the lungs where, due to their size, they cannot traverse lung capillary beds. Most are detained in the lungs, where they presumably undergo apoptosis and are taken up by resident lung macrophages. A small percentage of the cells do get beyond the lungs and migrate to sites of inflammation. This is likely via MSCs adhering to the endothelium and crossing through the vessel wall into the local tissues. Alternatively, the cells may migrate into the lung tissue where they encounter lung resident macrophages or enter the systemic circulation. Cells can be detected in regions of inflammation such as skin and kidneys in mice 2–4 weeks after infusion (29). Others reported finding no cells 2–3 days postinfusion. Other methods of infusion are being tested to bypass the lung, including subcutaneous, intraperitoneal, and intra-organ administration (in the heart, kidney, or joint).

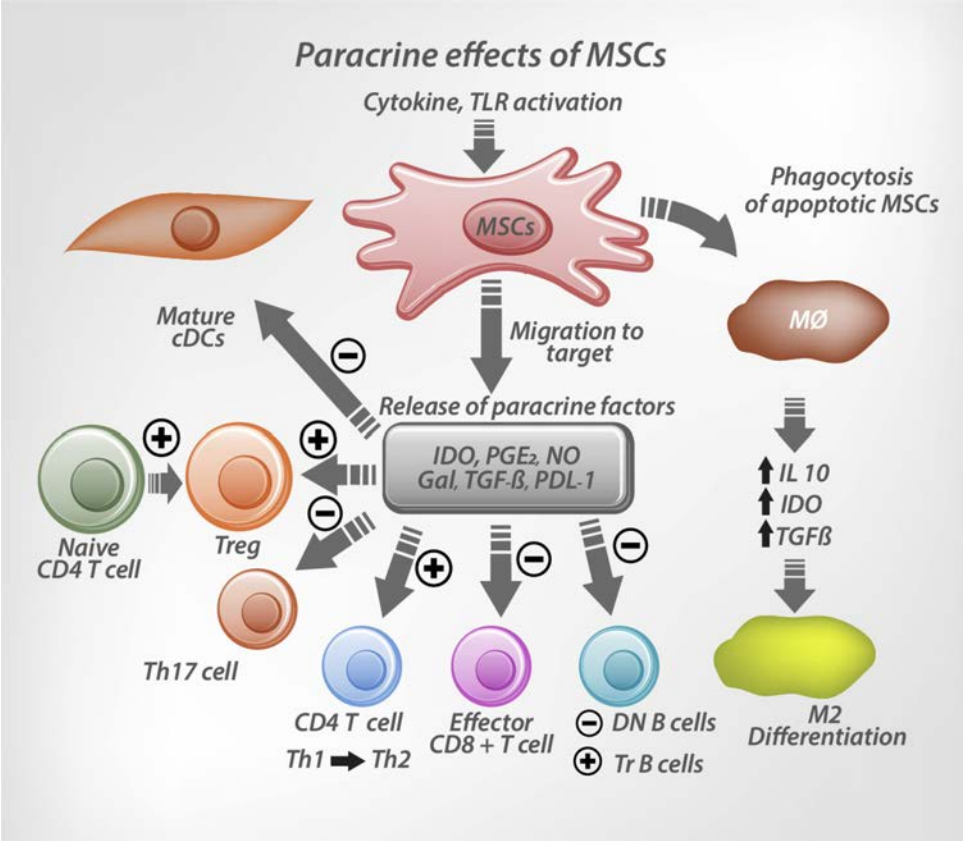

Figure 2. Schematic illustration of the paracrine effects of mesenchymal stromal cells (MSCs). MSCs are activated by cytokines and/or by Toll-like receptor (TLR) activation in the local tissues. They then migrate to target tissue or undergo apoptosis to be phagocytosed by resident macrophages (Mθ), leading to differentiation into alternatively activated (M2) macrophages. The many cytokines and other mediators they excrete have effects on nearly all active immune cells, enhancing Treg cell development and activity, modifying B cell subsets, and decreasing function and differentiation of CD8 effector cells, Th17 cells, and conventional dendritic cells (cDCs). IDO = indoleamine dioxygenase; PGE_2 = prostaglandin E_2; NO = nitric oxide; TGFβ = transforming growth factor β; PDL-1 = programmed death ligand 1; IL-10 = interleukin-10; DN = double negative; Tr = transitional.

MSCs, used in a variety of clinical settings, are well tolerated. There are a minimal number of mild infusion reactions that are short-lived (47). There is a theoretical risk of the cells turning malignant, which is minimized by using low passage number cells (47). MSCs are considered immunosuppressive, but there are no data indicating that patients receiving MSCs have higher infection rates than patients receiving placebo. There are a couple of reports of patients having thromboses develop upstream from the infusion site. Both patients were undergoing hemodialysis, which perhaps contributed to a prothrombotic state (48).

Efficacy of MSCs in lupus

MSCs derived from mice or humans were used to treat murine models of lupus over 15 years ago. A number of different lupus-prone strains were studied, and the majority showed improvement in renal disease and life expectancy in mice pre- or post-development of lupus nephritis (29,49,50). Different infusion methods were used, including IV and intraperitoneal, with similar results. The optimum dose of MSCs is unclear at this time. Multiple dosing does not appear to impact outcomes as much as the total dose of cells given does. The source of the MSCs (bone marrow, adipose tissue, or umbilical cord) was also not a differentiating factor. From the murine studies and prior human studies in non-lupus patients, a dose of 1 million cells per kilogram was selected for the initial human studies by Dr. Sun's group in Nanjing. This is the dose used in most trials in humans to date (51). Some trials used set numbers of cells (70 million or 140 million), while most infused based on weight (1 million cells per kilogram). In trials in pediatric Crohn's disease and in GVHD, doses of up to 10 million cells per kilogram were infused, with no adverse effect (52).

To date, 9 studies on the use of MSCs for the treatment of refractory lupus have been published (51,53–57). There are ongoing trials, though only one in the US (Table 3). The one report describing autologous MSC treatment involved 2 patients who received an infusion of autologous MSCs (58). There was no clinical change in the patients' lupus; however, an increase in the number of peripheral blood Treg cells was found. Early trials used

allogeneic BM-MSCs, including those from first-degree relatives (FDRs). Later trials excluded FDRs from being donors due to questions of their MSC functionality. Most recent trials used UC-MSCs. The majority of the published trials were done at Nanjing Drum Tower Hospital (Table 3).

Patients had disease refractory to 6 months of cyclophosphamide, and their disease activity ranged from moderate to severe (pulmonary hemorrhage, progressive renal failure, or transverse myelitis). Approximately 60% of the patients experienced either clinical remission or significant disease improvement. Some patients have minimal to no disease 5 years after treatment (59). Some patients received 1 infusion, while others received 2 infusions, 1 month apart. There was no difference in efficacy with regard to the number of infusions. None of these trials, unfortunately, were placebo-controlled. In reviewing the data on >400 patients treated in Nanjing, the characteristics defining patients less likely to respond were young age and arthritis as their primary disease manifestation (56). There was a trend toward patients who were receiving hydroxychloroquine being less responsive. These trials included only Asian patients, so examining efficacy in other ethnicities is needed. Patients who experienced a relapse were treated again, many with a repeat response. In these trials, immunosuppressive agents were continued following the MSC infusions.

The one trial of allogeneic MSCs that did not report benefit was a placebo-controlled trial of MSCs in new-onset lupus nephritis (57). Patients received either cyclophosphamide or mycophenolate, with 12 assigned to the MSC group and 6 assigned to the placebo group. The trial was stopped after only 18 patients, since the investigators saw no difference between the patient groups. There was an extremely high 85% response rate (defined as decreased proteinuria) in both arms. The inordinately high response rate and the lack of details regarding cellular origin, passage number, freezing and thawing, or validation of the immune activity of the cells were weaknesses of this trial. It is important to know the methods of derivation of the MSCs. Galipeau et al showed that passaging the cells beyond the fifth passage leads to early differentiation of the cells and lessened efficacy. If the cells are frozen and thawed without culturing for 2–3 days prior to infusion, the cells are also ineffective (60).

In summary, there are suggestive data from uncontrolled trials on the efficacy of MSCs for patients with refractory lupus. There are currently 2 trials listed as ongoing in ClinicalTrials.gov (Table 3). Two are small case series, while the third is the MSC in Systemic Lupus Erythematosus (MiSLE) trial of 81 patients, a multicenter, double-blind, placebo-controlled trial in the US.

MSCs in rheumatoid arthritis

As with lupus, there were preclinical studies of MSCs in animal models of arthritis. These animal trials showed promise, leading to initiation of human trials of MSCs in RA (61). There are 9 published trials of MSCs for the treatment of refractory RA, with 2 being placebo-controlled trials (Table 4). Six of the trials used allogeneic MSCs (5 used UC-MSCs and 1 used AD-MSCs) (62,63). The other 3 trials used bone marrow autologous cells, with one of them being a placebo-controlled trial, though not blinded. In these trials, the patients had failed to respond to standard immunosuppression and most had failed to respond to at least one biologic. The number of cells infused ranged from 1 million to 2 million cells per kilogram. Two of the allogeneic MSC trials were phase I safety trials, though they reported efficacy measures. Full remission was not achieved in any of the patients. Among those who did respond, the length of response varied from a few months to 3 years. In the largest trial of 63 patients (uncontrolled), there was a 53.3% response, as measured by the American College of Rheumatology criteria for 20% improvement in disease activity (ACR20) (64). If the cells were "licensed" by pretreatment with IFNγ, the response increased to 93.3%. In a phase II controlled trial of allogeneic AD-MSCs injected in the knees of RA patients, the ACR20 response was 20% in the placebo group versus 45% in the MSCs group at 1 month and 0% in the placebo group versus 25% in the MSCs group at 3 months (65). Most of the trials, whether of autologous or allogeneic cells, showed decreased erythrocyte sedimentation rate, Health Assessment Questionnaire, and Disease Activity Score in 28 joints. Overall, the response rates were significant, though not seemingly better than those for approved biologics, raising the question as to where MSCs might fit into the current RA treatment landscape. The benefits (ACR20 achieved in 45–53.3% of patients) can be balanced against the very low toxicity in defining the niche for MSCs in RA therapy if further larger trials indicate efficacy.

MSCs in scleroderma

Scleroderma is another autoimmune disease in which MSCs are being investigated, as treatments for digital ulcers, non-healing tissue loss, gastrointestinal (GI) issues, and pulmonary disease (66). Trials of allogeneic MSCs infused systemically in patients with scleroderma are in progress in France and about to begin in Canada. Local application of autologous or allogeneic MSCs has shown impressive efficacy in healing refractory digital ulcers or improving skin ulcers. Effects on skin disease, GI disease, and pulmonary disease will need to be addressed by further controlled trials assessing the best source of MSCs, the need for licensing of the MSCs prior to infusion, and patient groups most likely to respond (67).

MSCs in pediatric rheumatic disease

If MSCs are effective in adult patients with ulcerative colitis, RA, or lupus, then what is their efficacy in pediatric diseases (68)? There is extensive experience using MSCs in pediatric GVHD disease, implying the safety of such an approach in pediatric rheumatic

Table 3. Trials of allogeneic MSCs in lupus and lupus nephritis*

	Study type	MSC source	MSC dose	Patient characteristics (no. of patients)	Length of follow-up	Outcome
Completed studies, by author, year (ref.)						
Sun et al, 2009 (53)†	Open-label pilot	Allogeneic BM	1×10^6 per kg	Refractory LN (4)	12 months	4/4 with clinical response
Sun et al, 2010 (54)†	Open-label phase I	Allogeneic UC	1×10^6 per kg	Refractory SLE (16)	8 months	Improved disease in most
Liang et al, 2010 (51)†	Open-label phase I	Allogeneic BM	1×10^6 per kg	Refractory SLE (15)	12 months	Improved disease in most
Gu et al, 2014 (83)†	Open-label phase I	Allogeneic BM and UC	1×10^6 per kg	Refractory LN (81)	12 months	Response in 50% at 1 year
Deng et al, 2017 (57)	Phase II RCT	Allogeneic UC	2×10^8 MSCs total given in 2 doses	New onset LN (20 [12 receiving MSCs, 8 receiving placebo])	6 months	No difference
Barbado et al, 2018 (84)	Pilot	Allogeneic BM	1.5×10^6 per kg	Refractory LN (3)	9 months	2 CR; 1 PR
Wang et al, 2018 (85)†	Open-label multicenter	Allogeneic BM or UC	1×10^6 per kg	Refractory LN (81)	5 years	42% CR at 5 years
Liang et al, 2018 (86)†	Open-label	Allogeneic BM or UC	1×10^6 per kg	Refractory SLE, SS, SSc, PM/DM, RA, MCTD, ALD (404)	5 years	Improved disease in 60%
Trials proposed or in progress, by country						
US	Phase II RCT	Allogeneic UC	1×10^6 or 5×10^6 per kg	Refractory SLE (81)	1 year	Ongoing Recruiting
Chile	Phase II RCT	Allogeneic UC	1×10^6 per kg	New onset LN (39)	1 year	Unclear
Spain	Phase II RCT	Allogeneic BM	1×10^6 per kg	Refractory LN (36)	1 year	Not started
China	Phase II RCT	Allogeneic UC	1×10^6 per kg	Refractory LN (230)	1 year	Not started
France	Phase I	Allogeneic UC	Escalating dosing	Refractory SLE (10)	1 year	Not started

* There are currently 22 trials of mesenchymal stromal cells (MSCs) for lupus listed on ClinicalTrials.gov. BM = bone marrow; LN = lupus nephritis; UC = umbilical cord; SLE = systemic lupus erythematosus; RCT = randomized controlled trial; CR = complete remission; PR = partial remission; SS = Sjögren's syndrome; SSc = systemic sclerosis; PM/DM = polymyositis/dermatomyositis; RA = rheumatoid arthritis; MCTD = mixed connective tissue disease; ALD = autoimmune liver disease.
† Studies performed at Nanjing Drum Tower Hospital, Nanjing, China.

Table 4. Trials of MSCs in RA*

	Study phase	MSC source	Number of patients with refractory RA	Outcome
Completed studies, by author, year (ref.)				
Liang et al, 2012 (87)	Phase I	Allogeneic UC	4	Improved ESR and DAS28
Yang et al, 2018 (88)	Phase I/II randomized	Allogeneic UC	105	Good response with increased Treg cells
Park et al, 2018 (89)	Phase I	Allogeneic UC	9	Improved ESR and DAS28
He et al, 2020 (64)	Phase I/II	Allogeneic UC	63	53.3% reached ACR20
Wang et al, 2013 (62)	Phase I/II	Allogeneic UC	64	Decrease in HAQ and DAS28
Ghoryani et al, 2019 (90)	Phase I	Autologous BM	9	Decrease in DAS28; increased Treg cells
Ghoryani et al, 2020 (91)	Phase I	Autologous BM	13	Increased Treg cells
Shadmanfar et al, 2018 (65)	Phase I/II randomized	Autologous BM (intraarticular)	30	Improved WOMAC and VAS
Álvaro-Gracia et al, 2017 (92)	Phase I/II randomized	Allogeneic AD	53	ACR20 improved, though short-lived
Studies in progress, by country				
US	Phase I dose escalation	BM (type unknown) vs. UC	20	Ongoing
China	Phase I	Allogeneic UC	9	Ongoing

* There are currently 59 trials of mesenchymal stromal cells (MSCs) for rheumatoid arthritis (RA) listed on ClinicalTrials.gov. UC = umbilical cord; ESR = erythrocyte sedimentation rate; DAS28 = Disease Activity Score in 28 joints; ACR20 = American College of Rheumatology criteria for 20% improvement; HAQ = Health Assessment Questionnaire; BM = bone marrow; WOMAC = Western Ontario and McMaster Universities Osteoarthritis Index; VAS = visual analog scale; AD = adipose tissue.

diseases. A recent publication from a single center in California summarized a case series of 3 patients, each of whom had a different autoimmune disease (68). Each of these individuals received MSCs outside of approved US medical settings. A patient with dermatomyositis did not respond, while a patient with mixed connective tissue disease/lupus and a patient with juvenile idiopathic arthritis (JIA) had significant improvement in their disease activity, and each are continuing to receive the infusions as their only therapy. There is a plan to expand studies done in children with specific types of JIA. There are a few case reports in other rheumatic diseases, but these are insufficient to draw conclusions as to whether they are a reasonable target for MSC therapy (69).

MSC microparticles

It is unclear whether the presumed efficacy of MSCs in autoimmune diseases is mediated by paracrine secretions of MSCs, microparticles of MSCs, or whether cell-to-cell contact is needed (Figure 1). Due to the questions and concerns regarding trapping of MSCs in the lung, use of microparticles is appealing, as their size would allow passage through the lungs. Microparticles from MSCs contain many of the antiinflammatory molecules expressed by MSCs. Microparticles can also fuse in the membranes of other cells or be phagocytosed.

Pretreatment MSC manipulation

Even before knowing if unmanipulated MSCs are effective in treating disease, various methods of manipulating the cells are under investigation. Would preactivating the MSCs via pretreatment with IFNγ enhance efficacy? Priming does enhance in vitro immunosuppressive properties and has enhanced efficacy in animal models of inflammatory bowel disease and in renal ischemia–reperfusion models. There are no reports of priming of MSCs in human trials thus far. Alternatively, using molecular techniques, MSCs can be transfected with different DNA cassettes to enhance MSC homing to sites of inflammation and to express the effector molecule of choice.

Future of MSC therapy

Despite the promising reports of MSC therapy in autoimmune diseases, almost all of the trials were unblinded, and those that were not, were small. It is very important moving forward that investigators and funding agencies work together to develop trials using MSCs with standard operating procedures regarding cell preparation, patient selection, outcome measures, and mechanistic studies. There is significant inherent bias in unblinded trials since both the patient and the investigator want to see improvement, introducing unintentional bias in grading subjective outcomes. The risk of not performing large multicenter placebo-controlled trials is that a potentially useful therapy will be underutilized due to a lack of convincing data showing efficacy.

TREG cell therapy

Many patients with autoimmune disease either have low numbers of CD4+CD25+FoxP3+CD127– Treg cells or the Treg

cells they have are not active in suppressing immune activity (70). The first delineation of Treg cells was between Treg cells that develop in the thymus (natural Treg cells) and those induced in the periphery (induced Treg cells) (71). The natural Treg cells are immune inhibitory and important for maintaining immune balance. Induced Treg cells are in the peripheral tissues and inhibit inflammatory responses by secreting IL-10 and TGFβ. IL-2 is a key cytokine for the induction of Treg cell development and activity. Expression of the molecule Helios by Treg cells inhibits IL-2 activity, thus limiting Treg cell development and inhibitory activity. Helios-negative cells have increased activity due to their IL-2 axis being uninhibited. The identification of different Treg cell groups initiated interest in expanding, manipulating, and genetically modifying Treg cells for use in treating autoimmune diseases.

The first disease in which ex vivo IL-2–expanded Treg cells were investigated was type 1 diabetes mellitus. In the trials published to this point, there was a demonstrated effect on the maintenance of insulin levels and C peptide up to 2 years after treatment in phase I studies (72). The only rheumatic disease studied to this point is lupus. A phase I dose-escalation trial was initiated for the use of expanded Treg cells in patients with lupus. Unfortunately, only 1 patient, a woman with discoid lupus erythematosus, was enrolled. She received a single infusion of autologous Treg cells at a low dose. There was no improvement in her skin disease, though migration of the cells to the skin and a change in the skin T cell profile from Th1 dominant to Th17 dominant was demonstrated (7). At this time, efforts are directed at developing techniques for enhancing Treg cell efficacy. Current results indicate safety of the infusions and long-term (>3 months) effects on immune function, primarily in the target organs. Using CAR T technology as described below may allow more precision targeting of Treg cells.

CAR T cells in autoimmune diseases

CAR T cells, along with immune checkpoint inhibitor therapy, have markedly altered the landscape for treatments of previously difficult-to-treat cancers. An excellent review of CAR T cells in autoimmunity was recently published in this journal, so I will summarize this area briefly (73). CAR T cells express a single-chain antibody for a given cell surface receptor, with initial endeavors targeting CD19 to treat B cell lymphomas and acute lymphoblastic leukemia. The receptor is linked to intracellular domains that activate the T cell into killing the target cells (i.e., B cells). Due to targeting CD19, which is expressed earlier in B cell development than CD20, there is near complete deletion of B cells that lasts for years (74). CAR T cells were used in animal models of lupus and RA with demonstrated efficacy (75). CD19 CAR T cell–directed therapy was completed in a single patient with refractory lupus. She had an impressive response to treatment, with decreased proteinuria and improved serologic features. She had complete B cell depletion with follow-up to 44 weeks (76). More advanced CAR T cells are being developed to enhance their efficacy by secretion of cytokines.

The downside to CAR T cells is that other antigen targeting is not as effective as targeting CD19, although with further development this temporary road bump will be overcome. The other more important downside is the cytokine release syndrome that develops in many patients (4). This syndrome can be serious and life-threatening (77). There is concern that patients with autoimmune diseases may have a higher prevalence and worse outcome from this cytokine release syndrome. Other off-target toxicities occur with CAR T cells as well. Treg cells are also now being used in CAR T cell therapy to suppress the targeted antigen-expressing cell. A further issue with treating autoimmunity with CAR T cells is that the antigen/cells leading to disease are not as clear as in cancer. There are a number of other hurdles to overcome with regard to CAR T cell treatment for autoimmune diseases, including rate of relapse of disease, manufacturing difficulties, lack of data regarding dosage and scheduling, and the high cost of this therapeutic approach. These questions will need to be addressed in clinical trials. As with BMT, CAR T cell therapies should only be performed in centers with extensive CAR T cell experience and a group of multidisciplinarian physicians collaborating to enhance patient outcomes.

Other cellular therapies

There are other potential cellular therapies being evaluated in preclinical in vivo and in vitro experiments. Each of these potential cellular targets are either increased, decreased, or have decreased function in autoimmune diseases. Breg cells, dendritic cells, natural killer (NK) cells, macrophages, and T follicular cells are all of potential use in treating autoimmune diseases. There are "suppressor/regulatory" phenotypes for each of these cell types that can be expanded, or their efficacy enhanced such as the Breg cells and M2 macrophages. Another approach is to enhance targeting and/or effector function of immune cells, including Treg cells, NK cells, and MSCs. Induced pluripotent stem cells offer a more boutique personalized approach; however, there is sparse literature on their use in the treatment of autoimmune diseases.

Comparing cellular therapies

It is difficult to compare the relative efficacy of these cellular therapies given the limited number of placebo-controlled trials at this time. There is proven efficacy of HSCT in severe scleroderma, though the morbidity and mortality associated with BMT is still an issue for most other autoimmune diseases. Newer approaches to marrow ablative therapies may allow expanded use of this

therapy. CAR T cells may lead to cytokine storm, though treatment regimens for it are known and effective. Data on efficacy in human lupus is from one patient. Experience with Treg cells in human trials is limited, though thus far they appear safe. The vast literature on MSCs, though not definitive as to efficacy, clearly demonstrate the safety of this approach. MSCs are by far the easiest to produce and administer. An ongoing multicenter placebo-controlled trial will hopefully provide insight into the efficacy of MSCs compared to standard of care in lupus. The need to derive alternative targets for CAR T cells, other than CD19, remains a limitation of this therapeutic approach. Registries of trials of these cellular therapies should be established, similar to the European BMT registry, that would serve as a repository for all trial results in cellular therapies in autoimmune diseases. This registry would allow for a broader understanding of factors that impact efficacy and toxicity as well as establishing standing operating procedures for future trials to use.

Conclusions

Use of cellular therapies for the treatment of autoimmune diseases is in its infancy and not proven to be of benefit by double-blind placebo-controlled trials thus far, other than trials of HSCT in scleroderma. Case reports of success of HSCT in other autoimmune diseases, primarily lupus, suggest efficacy, but ongoing morbidity/mortality associated with this therapy limits its use. Phase I and limited phase II studies suggest safety, and possible efficacy, of MSCs in scleroderma, RA, lupus, Sjögren's syndrome, ankylosing spondylitis, and childhood dermatomyositis. The major issue is the lack of placebo-controlled trials to definitively prove the efficacy of MSC therapy. MSCs are also being used to engineer extracellular vesicles to transport a given targeted payload to the tissue being targeted. Treg cells and CAR T cells are in early phases of testing in human autoimmune diseases. Placebo-controlled trials of all cellular therapies are needed to establish safety and efficacy.

AUTHOR CONTRIBUTIONS

Dr. Gilkeson drafted the article, revised it critically for important intellectual content, and approved the final version to be published.

REFERENCES

1. Smolen JS, Caporali R, Doerner T, Fautrel B, Benedetti F, Pieper B, et al. Treatment journey in rheumatoid arthritis with biosimilars: from better access to good disease control through cost savings and prevention of nocebo effects [review]. RMD Open 2021;7:e001637.
2. Dazzi F, van Laar JM, Cope A, Tyndall A. Cell therapy for autoimmune diseases. Arthritis Res Ther 2007;9:206.
3. Marmont AM. Will hematopoietic stem cell transplantation cure human autoimmune diseases? J Autoimmun 2008;30:145–50.
4. Freyer CW, Porter DL. Cytokine release syndrome and neurotoxicity following CAR T-cell therapy for hematologic malignancies. J Allergy Clin Immunol 2020;146:940–8.
5. Santamaria-Alza Y, Vasquez G. Are chimeric antigen receptor T cells (CAR-T cells) the future in immunotherapy for autoimmune diseases? Inflamm Res 2021;70:651–63.
6. El-Badri NS, Maheshwari A, Sanberg PR. Mesenchymal stem cells in autoimmune disease. Stem Cells Dev 2004;13:463–72.
7. Dall'Era M, Pauli ML, Remedios K, Taravati K, Sandova PM, Putnam AL, et al. Adoptive Treg cell therapy in a patient with systemic lupus erythematosus. Arthritis Rheumatol 2019;71:431–40.
8. Eggenhuizen PJ, Ng BH, Ooi JD. Treg enhancing therapies to treat autoimmune diseases. Int J Mol Sci 2020;21.
9. Tyndall A, Uccelli A. Multipotent mesenchymal stromal cells for autoimmune diseases: teaching new dogs old tricks. Bone Marrow Transplant 2009;43:821–8.
10. Tyndall A. Application of autologous stem cell transplantation in various adult and pediatric rheumatic diseases. Pediatr Res 2012;71: 433–8.
11. Berthelot JM, Le Goff B, Maugars Y. Bone marrow mesenchymal stem cells in rheumatoid arthritis, spondyloarthritis, and ankylosing spondylitis: problems rather than solutions? Arthritis Res Ther 2019; 21:239.
12. Ikehara S, Good RA, Nakamura T, Sekita K, Inoue S, Oo MM, et al. Rationale for bone marrow transplantation in the treatment of autoimmune diseases. Proc Natl Acad Sci U S A 1985;82:2483–7.
13. Greco R, Labopin M, Badoglio M, Veys P, Silva JM, Abinun M, et al. Allogeneic HSCT for autoimmune diseases: a retrospective study from the EBMT ADWP, IEWP, and PDWP working parties. Front Immunol 2019;10:1570.
14. Sullivan KM, Goldmuntz EA, Keyes-Elstein L, McSweeney PA, Pinckney A, Welch B, et al. Myeloablative autologous stem-cell transplantation for severe scleroderma. N Engl J Med 2018;378: 35–47.
15. Henes J, Oliveira MC, Labopin M, Badoglio M, Scherer HU, Del Papa N, et al. Autologous stem cell transplantation for progressive systemic sclerosis: a prospective non-interventional study from the European Society for Blood and Marrow Transplantation Autoimmune Disease Working Party. Haematologica 2021;106:375–83.
16. Assassi S, Wang X, Chen G, Goldmuntz E, Keyes-Elstein L, Ying J, et al. Myeloablation followed by autologous stem cell transplantation normalises systemic sclerosis molecular signatures. Ann Rheum Dis 2019;78:1371–8.
17. Snowden JA, Badoglio M, Labopin M, Giebel S, McGrath E, Marjanovic Z, et al. Evolution, trends, outcomes, and economics of hematopoietic stem cell transplantation in severe autoimmune diseases. Blood Adv 2017;1:2742–55.
18. Spierings J, Nihtyanova SI, Derrett-Smith E, Clark KE, van Laar JM, Ong V, et al. Outcomes linked to eligibility for stem cell transplantation trials in diffuse cutaneous systemic sclerosis. Rheumatology (Oxford) 2021. E-pub ahead of print.
19. Farge D, Burt RK, Oliveira MC, Mousseaux E, Rovira M, Marjanovic Z, et al. Cardiopulmonary assessment of patients with systemic sclerosis for hematopoietic stem cell transplantation: recommendations from the European Society for Blood and Marrow Transplantation Autoimmune Diseases Working Party and collaborating partners. Bone Marrow Transplant 2017;52:1495–503.
20. Burt RK, Han X, Gozdziak P, Yaung K, Morgan A, Clendenan AM, et al. Five year follow-up after autologous peripheral blood hematopoietic stem cell transplantation for refractory, chronic, corticosteroid-dependent systemic lupus erythematosus: effect of conditioning regimen on outcome. Bone Marrow Transplant 2018;53:692–700.
21. Friedenstein AJ, Chailakhjan RK, Lalykina KS. The development of fibroblast colonies in monolayer cultures of guinea-pig bone marrow and spleen cells. Cell Tissue Kinet 1970;3:393–403.
22. Viswanathan S, Shi Y, Galipeau J, Krampera M, Leblanc K, Martin I, et al. Mesenchymal stem versus stromal cells: International Society

for Cell & Gene Therapy mesenchymal stromal cell committee position statement on nomenclature. Cytotherapy 2019;21:1019–24.

23. Nolta JA, Galipeau J, Phinney DG. Improving mesenchymal stem/stromal cell potency and survival: Proceedings from the International Society of Cell Therapy MSC preconference held in May 2018, Palais des Congrès de Montréal, organized by the ISCT MSC scientific committee. Cytotherapy 2020;22:123–6.
24. Li P, Li SH, Wu J, Zang WF, Dhingra S, Sun L, et al. Interleukin-6 downregulation with mesenchymal stem cell differentiation results in loss of immunoprivilege. J Cell Mol Med 2013;17:1136–45.
25. Xie Q, Liu R, Jiang J, Peng J, Yang C, Zhang W, et al. What is the impact of human umbilical cord mesenchymal stem cell transplantation on clinical treatment? Stem Cell Res Ther 2020;11:519.
26. Barnhoorn MC, Wasser MN, Roelofs H, Maljaars PW, Molendijk I, Bonsing BA, et al. Long-term evaluation of allogeneic bone marrow-derived mesenchymal stromal cell therapy for Crohn's disease perianal fistulas. J Crohns Colitis 2020;14:64–70.
27. Farkhad NK, Mahmoudi A, Mahdipour E. How similar are human mesenchymal stem cells derived from different origins? A review of comparative studies. Curr Stem Cell Res Ther 2021;16:980–93.
28. De Castro LL, Lopes-Pacheco M, Weiss DJ, Cruz FF, Rocco PR. Current understanding of the immunosuppressive properties of mesenchymal stromal cells. J Mol Med (Berl) 2019;97:605–18.
29. Collins E, Gu F, Qi M, Molano I, Ruiz P, Sun L, et al. Differential efficacy of human mesenchymal stem cells based on source of origin. J Immunol 2014;193:4381–90.
30. Sundin M, Orvell C, Rasmusson I, Sundberg B, Ringdén O, Le Blanc K. Mesenchymal stem cells are susceptible to human herpesviruses, but viral DNA cannot be detected in the healthy seropositive individual. Bone Marrow Transplant 2006;37:1051–9.
31. Bianconi E, Casadei R, Frabetti F, Ventura C, Facchin F, Canaider S. Sex-specific transcriptome differences in human adipose mesenchymal stem cells. Genes (Basel) 2020;11.
32. Gao L, Bird AK, Meednu N, Dauenhauer K, Liesveld J, Anolik J, et al. Bone marrow–derived mesenchymal stem cells from patients with systemic lupus erythematosus have a senescence-associated secretory phenotype mediated by a mitochondrial antiviral signaling protein–interferon-β feedback loop. Arthritis Rheumatol 2017;69:1623–35.
33. Gao L, OConnell M, Allen M, Liesveld J, McDavid A, Anolik JH, et al. Bone marrow mesenchymal stem cells from patients with SLE maintain an interferon signature during in vitro culture. Cytokine 2020;132:154725.
34. Ceccariglia S, Cargnoni A, Silini AR, Parolini O. Autophagy: a potential key contributor to the therapeutic action of mesenchymal stem cells. Autophagy 2020;16:28–37.
35. Zhang Z, Huang S, Wu S, Qi J, Li W, Liu S, et al. Clearance of apoptotic cells by mesenchymal stem cells contributes to immunosuppression via PGE2. EBioMedicine 2019;45:341–50.
36. El-Jawhari JJ, El-Sherbiny Y, McGonagle D, Jones E. Multipotent mesenchymal stromal cells in rheumatoid arthritis and systemic lupus erythematosus; from a leading role in pathogenesis to potential therapeutic saviors? Front Immunol 2021;12:643170.
37. Alunno A, Bistoni O, Montanucci P, Basta G, Calafiore R, Gerli R. Umbilical cord mesenchymal stem cells for the treatment of autoimmune diseases: beware of cell-to-cell contact. Ann Rheum Dis 2018;77:e14.
38. Figueroa FE, Cuenca Moreno J, La Cava A. Novel approaches to lupus drug discovery using stem cell therapy. Role of mesenchymal-stem-cell-secreted factors [review]. Expert Opin Drug Discov 2014;9:555–66.
39. Deng W, Chen W, Zhang Z, Huang S, Kong W, Sun Y, et al. Mesenchymal stem cells promote CD206 expression and phagocytic activity of macrophages through IL-6 in systemic lupus erythematosus. Clin Immunol 2015;161:209–16.
40. Wang D, Wang S, Huang S, Zhang Z, Yuan X, Feng X, et al. Serum IFN-γ predicts the therapeutic effect of mesenchymal stem cells transplantation in systemic lupus erythematosus patients. Stem Cells Transl Med 2017;6:1777–85.
41. Delarosa O, Dalemans W, Lombardo E. Toll-like receptors as modulators of mesenchymal stem cells. Front Immunol 2012;3:182.
42. Wang D, Huang S, Yuan X, Liang J, Xu R, Yao G, et al. The regulation of the Treg/Th17 balance by mesenchymal stem cells in human systemic lupus erythematosus. Cell Mol Immunol 2017;14:423–31.
43. Zhang Z, Feng R, Niu L, Huang S, Deng W, Shi B, et al. Human umbilical cord mesenchymal stem cells inhibit T follicular helper cell expansion through the activation of iNOS in lupus-prone B6.MRL^{-} *Fas*^{lpr} mice. Cell Transplant 2017;26:1031–42.
44. François M, Romieu-Mourez R, Li M, Galipeau J. Human MSC suppression correlates with cytokine induction of indoleamine 2,3-dioxygenase and bystander M2 macrophage differentiation. Mol Ther 2012;20:187–95.
45. Chen J, Wang Q, Feng X, Zhang Z, Geng L, Xu T, et al. Umbilical cord-derived mesenchymal stem cells suppress autophagy of T cells in patients with systemic lupus erythematosus via transfer of mitochondria. Stem Cells Int 2016;2016:4062789.
46. Ullah M, Liu DD, Thakor AS. Mesenchymal stromal cell homing: mechanisms and strategies for improvement. iScience 2019;15:421–38.
47. Munir H, McGettrick HM. Mesenchymal stem cell therapy for autoimmune disease: risks and rewards. Stem Cells Dev 2015;24:2091–100.
48. Wu Z, Zhang S, Zhou L, Cai J, Tan J, Gao X, et al. Thromboembolism induced by umbilical cord mesenchymal stem cell infusion: a report of two cases and literature review. Transplant Proc 2017;49:1656–8.
49. Ma X, Che N, Gu Z, Huang J, Wang D, Liang J, et al. Allogenic mesenchymal stem cell transplantation ameliorates nephritis in lupus mice via inhibition of B-cell activation. Cell Transplant 2013;22:2279–90.
50. Park MJ, Kwok SK, Lee SH, Kim EK, Park SH, Cho ML. Adipose tissue-derived mesenchymal stem cells induce expansion of interleukin-10-producing regulatory B cells and ameliorate autoimmunity in a murine model of systemic lupus erythematosus. Cell Transplant 2015;24:2367–77.
51. Liang J, Zhang H, Hua B, Wang H, Lu L, Shi S, et al. Allogenic mesenchymal stem cells transplantation in refractory systemic lupus erythematosus: a pilot clinical study. Ann Rheum Dis 2010;69:1423–9.
52. Boberg E, von Bahr L, Afram G, Lindström C, Ljungman P, Heldring N, et al. Treatment of chronic GvHD with mesenchymal stromal cells induces durable responses: a phase II study. Stem Cells Transl Med 2020;9:1190–202.
53. Sun L, Akiyama K, Zhang H, Yamaza T, Hou Y, Zhao S, et al. Mesenchymal stem cell transplantation reverses multiorgan dysfunction in systemic lupus erythematosus mice and humans. Stem Cells 2009;27:1421–32.
54. Sun L, Wang D, Liang J, Zhang H, Feng X, Wang H, et al. Umbilical cord mesenchymal stem cell transplantation in severe and refractory systemic lupus erythematosus. Arthritis Rheum 2010;62:2467–75.
55. Wang D, Li J, Zhang Y, Zhang M, Chen J, Li X, et al. Umbilical cord mesenchymal stem cell transplantation in active and refractory systemic lupus erythematosus: a multicenter clinical study. Arthritis Res Ther 2014;16:R79.
56. Wen L, Labopin M, Badoglio M, Wang D, Sun L, Farge-Bancel D. Prognostic factors for clinical response in systemic lupus erythematosus patients treated by allogeneic mesenchymal stem cells. Stem Cells Int 2019;2019:7061408.

57. Deng D, Zhang P, Guo Y, Lim TO. A randomised double-blind, placebo-controlled trial of allogeneic umbilical cord-derived mesenchymal stem cell for lupus nephritis. Ann Rheum Dis 2017;76: 1436–9.
58. Carrion F, Nova E, Ruiz C, Diaz F, Inostroza C, Rojo D, et al. Autologous mesenchymal stem cell treatment increased T regulatory cells with no effect on disease activity in two systemic lupus erythematosus patients. Lupus 2010;19:317–22.
59. Li W, Chen W, Sun L. An update for mesenchymal stem cell therapy in lupus nephritis. Kidney Dis (Basel) 2021;7:79–89.
60. Galipeau J, Krampera M, Barrett J, Dazzi F, Deans RJ, DeBruijn J, et al. International Society for Cellular Therapy perspective on immune functional assays for mesenchymal stromal cells as potency release criterion for advanced phase clinical trials. Cytotherapy 2016;18: 151–9.
61. Liu Y, Mu R, Wang S, Long L, Liu X, Li R, et al. Therapeutic potential of human umbilical cord mesenchymal stem cells in the treatment of rheumatoid arthritis. Arthritis Res Ther 2010;12:R210.
62. Wang L, Cong X, Liu G, Zhou J, Bai B, Li Y, et al. Human umbilical cord mesenchymal stem cell therapy for patients with active rheumatoid arthritis: safety and efficacy. Stem Cells Dev 2013;22:3192–202.
63. Luque-Campos N, Contreras-López RA, Jose Paredes-Martínez M, Torres MJ, Bahraoui S, Wei M, et al. Mesenchymal stem cells improve rheumatoid arthritis progression by controlling memory T cell response. Front Immunol 2019;10:798.
64. He X, Yang Y, Yao M, Yang L, Ao L, Hu X, et al. Combination of human umbilical cord mesenchymal stem (stromal) cell transplantation with IFN-γ treatment synergistically improves the clinical outcomes of patients with rheumatoid arthritis. Ann Rheum Dis 2020;79: 1298–304.
65. Shadmanfar S, Labibzadeh N, Emadedin M, Jaroughi N, Azimian V, Mardpour S, et al. Intra-articular knee implantation of autologous bone marrow-derived mesenchymal stromal cells in rheumatoid arthritis patients with knee involvement: results of a randomized, triple-blind, placebo-controlled phase 1/2 clinical trial. Cytotherapy 2018;20:499–506.
66. Peltzer J, Aletti M, Frescaline N, Busson E, Lataillade JJ, Martinaud C. Mesenchymal stromal cells based therapy in systemic sclerosis: rational and challenges [review]. Front Immunol 2018;9:2013.
67. Van Rhijn-Brouwer FC, Gremmels H, Fledderus JO, Schuurman AH, Bonte-Mineur F, Vonk MC, et al. A randomised placebo-controlled double-blind trial to assess the safety of intramuscular administration of allogeneic mesenchymal stromal cells for digital ulcers in systemic sclerosis: the MANUS Trial protocol. BMJ Open 2018;8: e020479.
68. Wong SC, Medrano LC, Hoftman AD, Jones OY, McCurdy DK. Uncharted waters: mesenchymal stem cell treatment for pediatric refractory rheumatic diseases; a single center case series. Pediatr Rheumatol Online J 2021;19:87.
69. Figueroa FE, Carrión F, Villanueva S, Khoury M. Mesenchymal stem cell treatment for autoimmune diseases: a critical review. Biol Res 2012;45:269–77.
70. Alexander T, Sattler A, Templin L, Kohler S, Groß C, Meisel A, et al. Foxp3+ Helios+ regulatory T cells are expanded in active systemic lupus erythematosus. Ann Rheum Dis 2013;72:1549–58.
71. Scheinecker C, Göschl L, Bonelli M. Treg cells in health and autoimmune diseases: new insights from single cell analysis. J Autoimmun 2020;110:102376.
72. Putnam AL, Brusko TM, Lee MR, Liu W, Szot GL, Ghosh T, et al. Expansion of human regulatory T-cells from patients with type 1 diabetes. Diabetes 2009;58:652–62.
73. Orvain C, Boulch M, Bousso P, Allanore Y, Avouac J. Is there a place for CAR–T cells in the treatment of chronic autoimmune rheumatic diseases? Arthritis Rheumatol 2021;73:1954–65.
74. Levin AG, Rivière I, Eshhar Z, Sadelain M. CAR T cells: building on the CD19 paradigm. Eur J Immunol 2021;51:2151–63.
75. Haddadi MH, Hajizadeh-Saffar E, Khosravi-Maharlooei M, Basiri M, Negahdari B, Baharvand H. Autoimmunity as a target for chimeric immune receptor therapy: a new vision to therapeutic potential. Blood Rev 2020;41:100645.
76. Mougiakakos D, Kronke G, Volkl S, Kretschmann S, Aigner M, Kharboutli S, et al. CD19-targeted CAR T cells in refractory systemic lupus erythematosus. N Engl J Med 2021;385:567–9.
77. Schubert ML, Schmitt M, Wang L, Ramos CA, Jordan K, Müller-Tidow C, et al. Side-effect management of chimeric antigen receptor (CAR) T-cell therapy. Ann Oncol 2021;32:34–48.
78. Farge D, Labopin M, Tyndall A, Fassas A, Mancardi GL, Van Laar J, et al. Autologous hematopoietic stem cell transplantation for autoimmune diseases: an observational study on 12 years' experience from the European Group for Blood and Marrow Transplantation Working Party on Autoimmune Diseases. Haematologica 2010;95:284–92.
79. Burt RK, Traynor A, Statkute L, Barr WG, Rosa R, Schroeder J, et al. Nonmyeloablative hematopoietic stem cell transplantation for systemic lupus erythematosus. JAMA 2006;295:527–35.
80. Song XN, Lv HY, Sun LX, Meng JB, Wang JK, Zhang JQ, et al. Autologous stem cell transplantation for systemic lupus erythematosus: report of efficacy and safety at 7 years of follow-up in 17 patients. Transplant Proc 2011;43:1924–27.
81. Rosen O, Thiel A, Massenkeil G, Hiepe F, Häupl T, Radtke H, et al. Autologous stem-cell transplantation in refractory autoimmune diseases after in vivo immunoablation and ex vivo depletion of mononuclear cells. Arthritis Res 2000;2:327–36.
82. Goklemez S, Hasni S, Hakim FT, Muraro PA, Pirsl F, Rose J, et al. Long-term follow-up after lymphodepleting autologous hematopoietic cell transplantation for treatment-resistant systemic lupus erythematosus. Rheumatology (Oxford) 2021. doi: https://doi.org/10.1093/rheumatology/keab877. E-pub ahead of print.
83. Gu F, Wang D, Zhang H, Feng X, Gilkeson GS, Shi S, et al. Allogeneic mesenchymal stem cell transplantation for lupus nephritis patients refractory to conventional therapy. Clin Rheumatol 2014;33: 1611–9.
84. Barbado J, Tabera S, Sánchez A, García-Sancho J. Therapeutic potential of allogeneic mesenchymal stromal cells transplantation for lupus nephritis. Lupus 2018;27:2161–5.
85. Wang D, Zhang H, Liang J, Wang H, Hua B, Feng X, et al. A long-term follow-up study of allogeneic mesenchymal stem/stromal cell transplantation in patients with drug-resistant systemic lupus erythematosus. Stem Cell Reports 2018;10:933–41.
86. Liang J, Zhang H, Kong W, Deng W, Wang D, Feng X, et al. Safety analysis in patients with autoimmune disease receiving allogeneic mesenchymal stem cells infusion: a long-term retrospective study. Stem Cell Res Ther 2018;9:312.
87. Liang J, Li X, Zhang H, Wang D, Feng X, Wang H, et al. Allogeneic mesenchymal stem cells transplantation in patients with refractory RA. Clin Rheumatol 2012;31:157–61.
88. Yang Y, He X, Zhao R, Guo W, Zhu M, Xing W, et al. Serum IFN-γ levels predict the therapeutic effect of mesenchymal stem cell transplantation in active rheumatoid arthritis. J Transl Med 2018; 16:165.
89. Park EH, Lim HS, Lee S, Roh K, Seo KW, Kang KS, et al. Intravenous infusion of umbilical cord blood-derived mesenchymal stem cells in rheumatoid arthritis: a phase Ia clinical trial. Stem Cells Transl Med 2018;7:636–42.
90. Ghoryani M, Shariati-Sarabi Z, Tavakkol-Afshari J, Ghasemi A, Poursamimi J, Mohammadi M. Amelioration of clinical symptoms of patients with refractory rheumatoid arthritis following treatment with autologous bone marrow-derived mesenchymal stem cells: a successful clinical trial in Iran. Biomed Pharmacother 2019;109:1834–40.

91. Ghoryani M, Shariati-Sarabi Z, Tavakkol-Afshari J, Mohammadi M. The sufficient immunoregulatory effect of autologous bone marrow-derived mesenchymal stem cell transplantation on regulatory T cells in patients with refractory rheumatoid arthritis. J Immunol Res 2020; 2020:3562753.

92. Álvaro-Gracia JM, Jover JA, García-Vicuña R, Carreño L, Alonso A, Marsal S, et al. Intravenous administration of expanded allogeneic adipose-derived mesenchymal stem cells in refractory rheumatoid arthritis (Cx611): results of a multicentre, dose escalation, randomised, single-blind, placebo-controlled phase Ib/IIa clinical trial. Ann Rheum Dis 2017;76:196–202.

Arthritis & Rheumatology
Vol. 74, No. 5, May 2022, pp 766–775
DOI 10.1002/art.42030

American College of Rheumatology
Empowering Rheumatology Professionals

SARS–CoV-2 Infection and COVID-19 Outcomes in Rheumatic Diseases: A Systematic Literature Review and Meta-Analysis

Richard Conway,[1] Alyssa A. Grimshaw,[2] Maximilian F. Konig,[3] Michael Putman,[4] Alí Duarte-García,[5] Leslie Yingzhijie Tseng,[6] Diego M. Cabrera,[6] Yu Pei Eugenia Chock,[6] Huseyin Berk Degirmenci,[7] Eimear Duff,[8] Bugra Han Egeli,[9] Elizabeth R. Graef,[10] Akash Gupta,[6] Patricia Harkins,[8] Bimba F. Hoyer,[11] Arundathi Jayatilleke,[12] Shangyi Jin,[13] Christopher Kasia,[4] Aneka Khilnani,[14] Adam Kilian,[15] Alfred H. J. Kim,[16] Chung Mun Alice Lin,[17] Candice Low,[18] Laurie Proulx,[19] Sebastian E. Sattui,[20] Namrata Singh,[21] Jeffrey A. Sparks,[22] Herman Tam,[23] Manuel F. Ugarte-Gil,[24] Natasha Ung,[25] Kaicheng Wang,[26] Leanna M. Wise,[27] Ziyi Yang,[13] Kristen J. Young,[28] Jean W. Liew,[10] Rebecca Grainger,[29] Zachary S. Wallace,[30] and Evelyn Hsieh,[31] on behalf of the COVID-19 Global Rheumatology Alliance

Objective. The relative risk of SARS–CoV-2 infection and COVID-19 disease severity among people with rheumatic and musculoskeletal diseases (RMDs) compared to those without RMDs is unclear. This study was undertaken to quantify the risk of SARS–CoV-2 infection in those with RMDs and describe clinical outcomes of COVID-19 in these patients.

Methods. We conducted a systematic literature review using 14 databases from January 1, 2019 to February 13, 2021. We included observational studies and experimental trials in RMD patients that described comparative rates of SARS–CoV-2 infection, hospitalization, oxygen supplementation/intensive care unit (ICU) admission/mechanical ventilation, or death attributed to COVID-19. Methodologic quality was evaluated using the Joanna Briggs Institute critical appraisal tools or the Newcastle-Ottawa scale. Risk ratios (RRs) and odds ratios (ORs) with 95% confidence intervals (95% CIs) were calculated, as applicable for each outcome, using the Mantel-Haenszel formula with random effects models.

Results. Of the 5,799 abstracts screened, 100 studies met the criteria for inclusion in the systematic review, and 54 of 100 had a low risk of bias. Among the studies included in the meta-analyses, we identified an increased prevalence of SARS–CoV-2 infection in patients with an RMD (RR 1.53 [95% CI 1.16–2.01]) compared to the general population. The odds of hospitalization, ICU admission, and mechanical ventilation were similar in patients with and those without an RMD, whereas the mortality rate was increased in patients with RMDs (OR 1.74 [95% CI 1.08–2.80]). In a smaller number of studies, the adjusted risk of outcomes related to COVID-19 was assessed, and the results varied; some studies demonstrated an increased risk while other studies showed no difference in risk in patients with an RMD compared to those without an RMD.

Conclusion. Patients with RMDs have higher rates of SARS–CoV-2 infection and an increased mortality rate.

PROSPERO registry no.: CRD42020205668.

The views expressed here are those of the authors and participating members of the COVID-19 Global Rheumatology Alliance and do not necessarily represent the views of the American College of Rheumatology (ACR), the European Alliance of Associations for Rheumatology, the UK NHS, the NIHR, the UK Department of Health, or any other organization.

Supported by the ACR. The COVID-19 Global Rheumatology Alliance is supported by Amgen, Janssen, AbbVie, Gilead, Novartis, UCB Pharma, Pfizer, GlaxoSmithKline, and Bristol-Myers Squibb.

[1]Richard Conway, MBBCh BAO, PhD: St. James's Hospital and Trinity College, Dublin, Ireland; [2]Alyssa A. Grimshaw, MSLIS: Yale University, New Haven, Connecticut; [3]Maximilian F. Konig, MD: The Johns Hopkins University School of Medicine, Baltimore, Maryland; [4]Michael Putman, MD, MSci, Christopher Kasia, MD: The Medical College of Wisconsin, Milwaukee; [5]Alí Duarte-García, MD, MSc: Mayo Clinic, Rochester, Minnesota; [6]Leslie Yingzhijie Tseng, MSc, Diego M. Cabrera, MD, Yu Pei Eugenia Chock, MD, MPH, Akash Gupta, MD: Yale School of Medicine, New Haven, Connecticut; [7]Huseyin Berk Degirmenci, MD: Tufts University School of Medicine, Boston, Massachusetts; [8]Eimear Duff, MBBCh BAO, MBA, Patricia Harkins, MBBCh BAO: St. James's Hospital, Dublin, Ireland; [9]Bugra Han Egeli, MD: Boston University School of Medicine, Boston, Massachusetts and University of Southern California, Los Angeles; [10]Elizabeth R. Graef, DO, Jean W. Liew, MD, MS: Boston University School of Medicine, Boston, Massachusetts; [11]Bimba F. Hoyer, MD: University Hospital Schleswig-Holstein, Campus Kiel, Germany; [12]Arundathi Jayatilleke, MD, MS: Temple University, Philadelphia, Pennsylvania; [13]Shangyi Jin, MD, Ziyi Yang, MD: Chinese Academy of Medical Sciences and Peking Union Medical College and National Clinical Research Center for Dermatologic and Immunologic Diseases, Beijing, China; [14]Aneka Khilnani, MD: George Washington University School of Medicine and Health Sciences, Washington DC; [15]Adam Kilian, MD: Saint Louis University School of Medicine, St. Louis, Missouri; [16]Alfred H. J. Kim, MD, PhD: Washington University School of Medicine, St. Louis, Missouri; [17]Chung Mun Alice Lin, BChMBBS: National Institute of Health Research and Newcastle University, Newcastle-upon-Tyne, UK; [18]Candice Low, MBBCh BAO, MD: St. Vincent's University Hospital, Dublin, Ireland; [19]Laurie Proulx, BComm: Canadian Arthritis Patient Alliance, Ottawa,

INTRODUCTION

The SARS–CoV-2 pandemic has resulted in unprecedented morbidity and mortality due to COVID-19. In the general population, risk factors associated with poor COVID-19 outcomes include older age, sex, and chronic diseases (1,2).

Patients with rheumatic diseases may be at an increased risk of infection as a result of underlying disease, associated comorbidities, and use of potentially immunosuppressive treatments (3). Furthermore, concern exists regarding whether individuals with rheumatic diseases potentially experience more severe COVID-19 disease and poorer outcomes. However, 1 year after the first cases of COVID-19 were described, the applicability of this heuristic to SARS–CoV-2 infection, and the magnitude of any such heightened risk in these patients, remains unclear. Data directly addressing these questions are limited and lack clarity because of the rapid publication of many small studies during the pandemic, and these studies are frequently underpowered to show clinically significant effects.

The present systematic review and meta-analysis are aimed at quantifying the risk of contracting SARS–CoV-2 infection and describing COVID-19 outcomes in patients with rheumatic and musculoskeletal diseases (RMDs).

PATIENTS AND METHODS

The Preferred Reporting Items for Systematic Reviews and Meta-Analyses statement for reporting was used in this study (4). The study protocol was registered with PROSPERO a priori (no. CRD42020205668).

Data sources and literature search. A systematic search of the literature was conducted by a medical librarian (AAG and a second librarian) in the BioRxiv, China National Knowledge Infrastructure, Cochrane Library, Disaster Lit, Global Health, Google Scholar, LitCovid, medRxiv, Ovid Embase, Ovid Medline, PubMed, Scopus, Wanfang Data, and Web of Science Core Collection databases to find relevant articles published from January 1, 2019 to February 13, 2021. Databases were searched using a combination of controlled vocabulary and free-text terms for COVID-19 and rheumatic diseases. The search was peer reviewed by a second medical librarian using Peer Review of Electronic Search Strategies (5). Details of the full search strategy are listed in Supplementary Table 1 (available on the *Arthritis & Rheumatology* website at http://onlinelibrary.wiley.com/doi/10.1002/art.42030). Details regarding included RMDs are shown in Supplementary Table 2 (http://onlinelibrary.wiley.com/doi/10.1002/art.42030). The bibliographies of included studies were reviewed to identify additional relevant literature.

Study selection eligibility criteria. Citations from all databases were imported into an EndNote x9 Library (Clarivate Analytics), where duplicates were removed. The unduplicated results were imported into Covidence v2627 for screening and data extraction. Two independent screeners reviewed titles and abstracts, and a third screener resolved disagreements. The full texts of the collected articles were then reviewed for inclusion by 2 independent screeners with a third screener to resolve disagreements.

Observational studies and experimental trials were eligible for inclusion if data regarding adult and/or pediatric patients with rheumatic diseases were reported and SARS–CoV-2 infection or the subsequent clinical course were included as outcomes. Publications were excluded if they did not include quantifiable data regarding patients with rheumatic diseases, did not include original primary data, did not focus on human subjects, did not report data regarding outcomes related to SARS–CoV-2 infection or its associated clinical course, included duplicate or retracted data, were case reports or series, or were not yet published as a full-text study. There were no restrictions regarding language, and individuals fluent in a particular foreign language reviewed the articles in that language. Outcomes of interest included SARS–CoV-2 infection and COVID-19 outcomes (hospitalization, oxygen supplementation, intensive care unit [ICU] admission, mechanical ventilation, or death).

Data collection process. Two reviewers independently extracted data using Qualtrics software version Oct–May 2020–2021. A third reviewer assessed the forms to resolve any conflicts. Extracted data included study characteristics (first author, year of publication, country of origin, study design, sample

Ontario, Canada; [20]Sebastian E. Sattui, MD, MS: University of Pittsburgh Medical Center, Pittsburgh, Pennsylvania; [21]Namrata Singh, MD, MSCI: University of Washington, Seattle; [22]Jeffrey A. Sparks, MD, MMSc: Brigham and Women's Hospital and Harvard Medical School, Boston, Massachusetts; [23]Herman Tam, MBBS, MSc: Stollery Children's Hospital and University of Alberta, Edmonton, Alberta, Canada; [24]Manuel F. Ugarte-Gil, MD, MSc: Universidad Cientifica del Sur and Hospital Guillermo Almenara Irigoyen, Seguro Social de Salud del Peru, Lima, Peru; [25]Natasha Ung, MBBS: Campbelltown Hospital, Campbelltown and University of Western Sydney, New South Wales, Australia; [26]Kaicheng Wang, MD, MPH: Yale School of Medicine and Yale School of Public Health, New Haven, Connecticut; [27]Leanna M. Wise, MD, MPH: University of Southern California, Los Angeles; [28]Kristen J. Young, MD, MEd: University of Texas Southwestern, Dallas; [29]Rebecca Grainger, MB, ChB, BMedSci, PhD: University of Otago, Wellington, New Zealand; [30]Zachary S. Wallace, MD, MSc: Harvard Medical School, Boston, Massachusetts; [31]Evelyn Hsieh, MD, PhD: VA Connecticut Healthcare System, West Haven, Connecticut.

Dr. Conway and Ms. Grimshaw contributed equally to this work.

Request for access to data should be made to the Data Access and Sharing Committee of the COVID-19 Global Rheumatology Alliance.

Author disclosures are available at https://onlinelibrary.wiley.com/action/downloadSupplement?doi=10.1002%2Fart.42030&file=art42030-sup-0001-Disclosureform.pdf.

Address correspondence to Richard Conway, MBBCh BAO, PhD, Department of Rheumatology, St. James's Hospital, Dublin 8, Ireland (email: drrichardconway@gmail.com); or to Evelyn Hsieh, MD, PhD, Section of Rheumatology, Allergy & Immunology, Yale School of Medicine, New Haven, CT (email: evelyn.hsieh@yale.edu).

Submitted for publication July 10, 2021; accepted in revised form November 16, 2021.

size, and study sponsor), baseline demographic and clinical characteristics of the participants (age, sex, race or ethnicity, and comorbidities [each comorbidity individually reported as well as grouped into categories of diabetes, respiratory, cardiovascular, smoking, or other]), SARS–CoV-2 infection status, and COVID-19 outcomes (hospitalization, oxygen supplementation, ICU admission, mechanical ventilation, or death).

Risk of bias in individual studies. Two reviewers independently assessed the risk of bias using the Joanna Briggs Institute (JBI) checklists for prevalence and analytical cross-sectional studies (3–5) and the Newcastle-Ottawa scale for case–control and cohort studies (6–8). The JBI checklists for prevalence and cross-sectional analytical studies are divided into 3 categories for assessment of bias (for prevalence studies, scores 0–3 = high risk of bias, scores 4–6 = some concerns, and scores 7–9 = low risk of bias; for cross-sectional analytical studies, scores 0–3 = high risk of bias, scores 4–6 = some concerns, and scores 7–8 = low risk of bias). In this context, the comparability domain of the Newcastle-Ottawa scale was primarily used to differentiate risk of bias and was used to determine the global risk of bias (global risk of bias on a scale of 0–2, where score 0 = high risk of bias, score 1 = some concerns, and score 2 = low risk of bias) (9,10). Disagreements were resolved by a third reviewer.

Data analysis. Studies included in the systematic review were further evaluated for their suitability in the meta-analyses if comparative data were reported for patients with and those without RMDs. Regarding COVID-19 prevalence, studies were included if the number of COVID-19 cases among patients in the RMD group was reported, and if the number of COVID-19 cases within the overall regional populations was reported. Regarding hospitalization, ICU admission, mechanical ventilation, and death, studies were included if they provided raw data demonstrating the rate of each outcome among patients with RMDs who were clinically diagnosed as having COVID-19 as well as the rate of each outcome among a comparator group of patients without RMDs who were clinically diagnosed as having COVID-19. Data were insufficient to meta-analyze the risk of oxygen supplementation. Studies were excluded if the non-RMD comparator group was selected from a nonrepresentative sample, such as those with similar diseases (e.g., inflammatory bowel disease patients) or family members.

Meta-analyses were performed using R version 4.1.0 and the meta package version 4.18-1. Risk estimates were calculated using the Mantel-Haenszel formula with random effects models. Risk estimates with 95% confidence intervals (95% CIs) are reported as risk ratios (RRs) for prevalence of COVID-19, and as odds ratios (ORs) for risk of hospitalization, oxygen supplementation, ICU admission, mechanical ventilation, or death. Heterogeneity among studies was assessed using I^2 and Cochran's chi-square tests. We performed sensitivity analyses to evaluate the effect of the study design (limited to cohort studies or cross-sectional studies), risk of bias (limited to studies with a low risk of bias), country of origin, and study size (limited to studies with >20 RMD patients). Funnel plots and Egger's regression tests were used to evaluate publication bias. *P* values less than 0.05 were considered significant.

RESULTS

The literature search resulted in identification of 13,076 articles; after duplicates were removed, 5,799 articles remained for title/abstract screening. We undertook a full text review of 534 articles (Figure 1). Of these, 98 articles met the inclusion criteria. Two additional studies were identified via review of the bibliographies of included articles, resulting in the inclusion of 100 studies (see Supplementary Table 3 and Supplementary References 1–100, http://onlinelibrary.wiley.com/doi/10.1002/art.42030). Studies were excluded due to having an incorrect study design, not having original data, having irrelevant outcomes, examining an incorrect study population, being duplicates, including irrelevant exposures, being conference abstracts, and containing duplicate study data (Supplementary Table 4, http://onlinelibrary.wiley.com/doi/10.1002/art.42030). The majority of single region/country studies were from Europe (63%), with the rest from Asia (14%), North America (13%), worldwide (6%), or South America (1%). The majority (75%) focused on adult populations; however, 14% of studies included pediatric and adult populations, and 1% included only pediatric populations. In 10% of studies, the age range was unspecified.

Risk-of-bias assessment. Overall, the majority of studies had a low risk of bias. Of the 4 studies assessed using the Newcastle-Ottawa scale for case–control studies, 2 had a low risk of bias, 1 had some concerns, and 1 had a high risk of bias (Supplementary Table 5, http://onlinelibrary.wiley.com/doi/10.1002/art.42030). Of the 46 studies assessed using the Newcastle-Ottawa scale for cohort studies, 33 had a low risk of bias, 6 had some concerns, and 7 had a high risk of bias (Supplementary Table 6, http://onlinelibrary.wiley.com/doi/10.1002/art.42030). Of the 37 studies assessed using the JBI checklist for prevalence studies, 25 had a low risk of bias, 8 had some concerns, and 4 had a high risk of bias (Supplementary Table 7, http://onlinelibrary.wiley.com/doi/10.1002/art.42030). Of the 13 studies assessed using the JBI checklist for analytical cross-sectional studies, 8 had a low risk of bias, 2 had some concerns, and 3 had a high risk of bias (Supplementary Table 7).

SARS–CoV-2 infection. In 46 studies, comparative rates of SARS–CoV-2 infection in patients with RMDs were reported (Supplementary Table 8, http://onlinelibrary.wiley.com/doi/10.1002/art.42030). A total of 15 studies showed increased rates of SARS–CoV-2 infection, 27 showed no difference, and

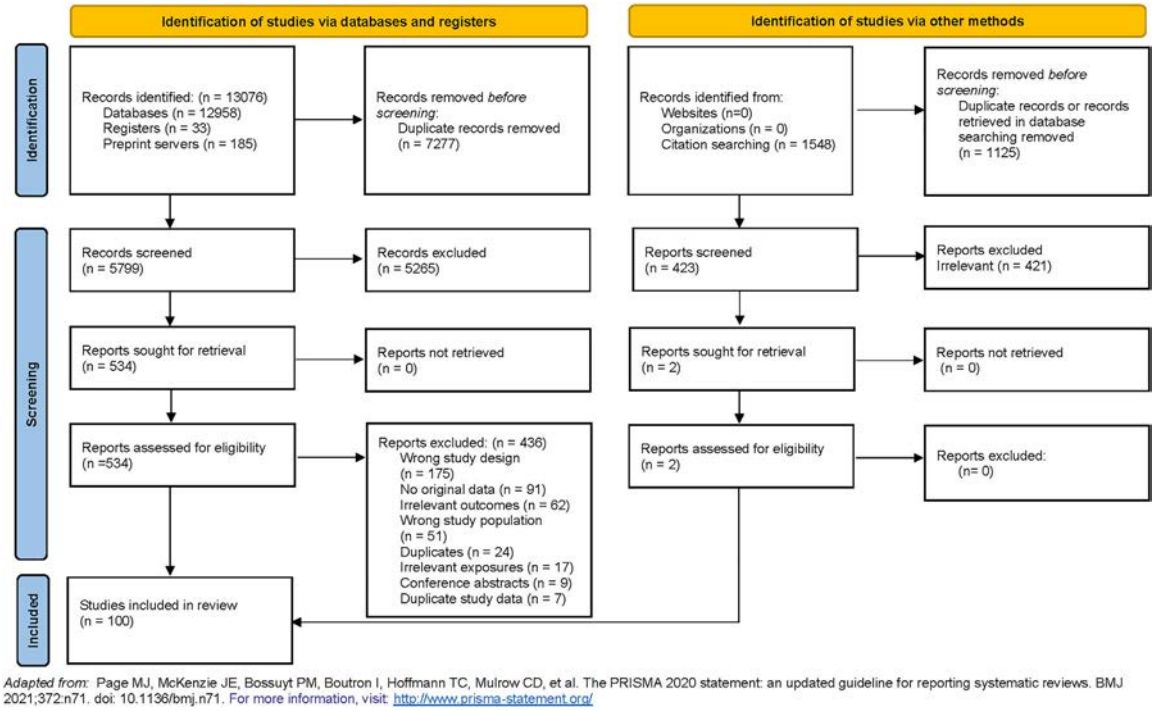

Figure 1. Flow chart of the methods used for identification of studies in patients with rheumatic and musculoskeletal diseases in which comparative rates of SARS–CoV-2 infection, hospitalization, oxygen supplementation, intensive care unit admission, mechanical ventilation, and death attributed to COVID-19 are reported. The flow chart is designed in accordance with the Preferred Reporting Items for Systematic Reviews and Meta-Analyses (PRISMA). Color figure can be viewed in the online issue, which is available at http://onlinelibrary.wiley.com/doi/10.1002/art.42030/abstract.

4 showed decreased rates. A total of 23 studies met the inclusion criteria for the meta-analysis (Supplementary Table 9, http://onlinelibrary.wiley.com/doi/10.1002/art.42030). The pooled relative risk based on unadjusted data demonstrated an increased risk of COVID-19 infection among patients with RMDs (RR 1.53 [95% CI 1.16–2.01]) (Figure 2). We observed moderately high heterogeneity (I^2 = 73% [95% CI 59–82%]; $P < 0.01$) but did not detect evidence of publication bias

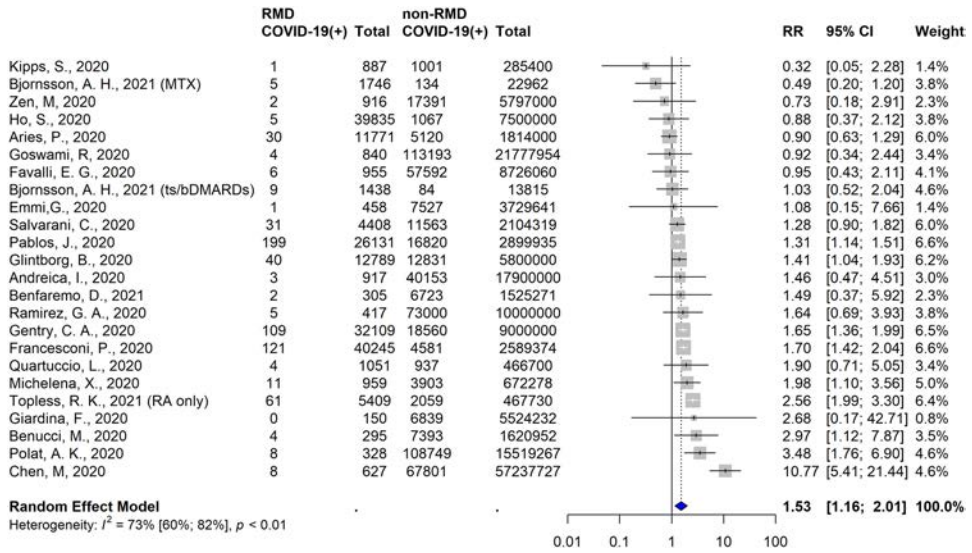

Figure 2. Studies identified in the systematic literature review and meta-analysis in which the risk of COVID-19 among populations of patients with rheumatic and musculoskeletal diseases (RMDs) compared to those without RMDs was reported. The risk of COVID-19 is assessed as risk ratios (RRs) with 95% confidence intervals (95% CIs). Color figure can be viewed in the online issue, which is available at http://onlinelibrary.wiley.com/doi/10.1002/art.42030/abstract.

(Supplementary Figure 1, http://onlinelibrary.wiley.com/doi/10.1002/art.42030).

In 8 studies, adjusted comparative risk measures were reported, with 2 outcomes reported in 2 of these studies. The 5 studies that demonstrated an increased risk of COVID-19 among patients with RMDs were the study by Pablos et al (OR 1.3 [95% CI 1.15–1.52]) (14), the study by Zhong et al (OR 2.68 [95% CI 1.14–6.27]) (13), the study by Francesconi et al in patients with rheumatoid arthritis (RA) (OR 1.64 [95% CI 1.32–2.05]) (12), the study by Topless et al in patients with RA (OR 1.34 [95% CI 1.02–1.77]) (18), and the study by Chen et al in patients with RA (OR 10.90 [95% CI 5.43–21.89]) (11). The 5 studies that showed no difference in risk of COVID-19 were the study by Topless et al in patients with gout (OR 1.01 [95% CI 0.83–1.23]) (18), the study by Jung et al (OR 1.13 [95% CI 0.57–2.24]) (15), the study by Francesconi et al in patients with connective tissue disease (CTD) (OR 1.09 [95% CI 0.72–1.66]) (12), the study by Salvarani et al (OR 0.94 [95% CI 0.66–1.34]) (17), and the study by Kipps et al (RR 0.32 [95% CI 0.05–2.28]) (16). Unless specified otherwise, risk in patients with multiple RMDs was reported as a combined group.

Hospitalization. In 70 studies, hospitalization rates were reported among patients with RMD who were clinically diagnosed as having COVID-19 and/or who were diagnosed as having COVID-19 by polymerase chain reaction (PCR) testing (Supplementary Table 10, http://onlinelibrary.wiley.com/doi/10.1002/art.42030). Among these, 11 studies compared hospitalization rates among patients with RMDs to those among the general population (n = 2) or those among other non-RMD comparator populations (n = 9) (Supplementary Table 11 http://onlinelibrary.wiley.com/doi/10.1002/art.42030). Three studies showed an increased risk of hospitalization among patients with RMDs and 7 showed no significant effect. None of the 70 studies demonstrated a decreased risk of hospitalization among patients with RMDs. In a meta-analysis of 10 comparative studies that included unadjusted hospitalization rates, the risk of hospitalization was not increased among patients with RMDs when

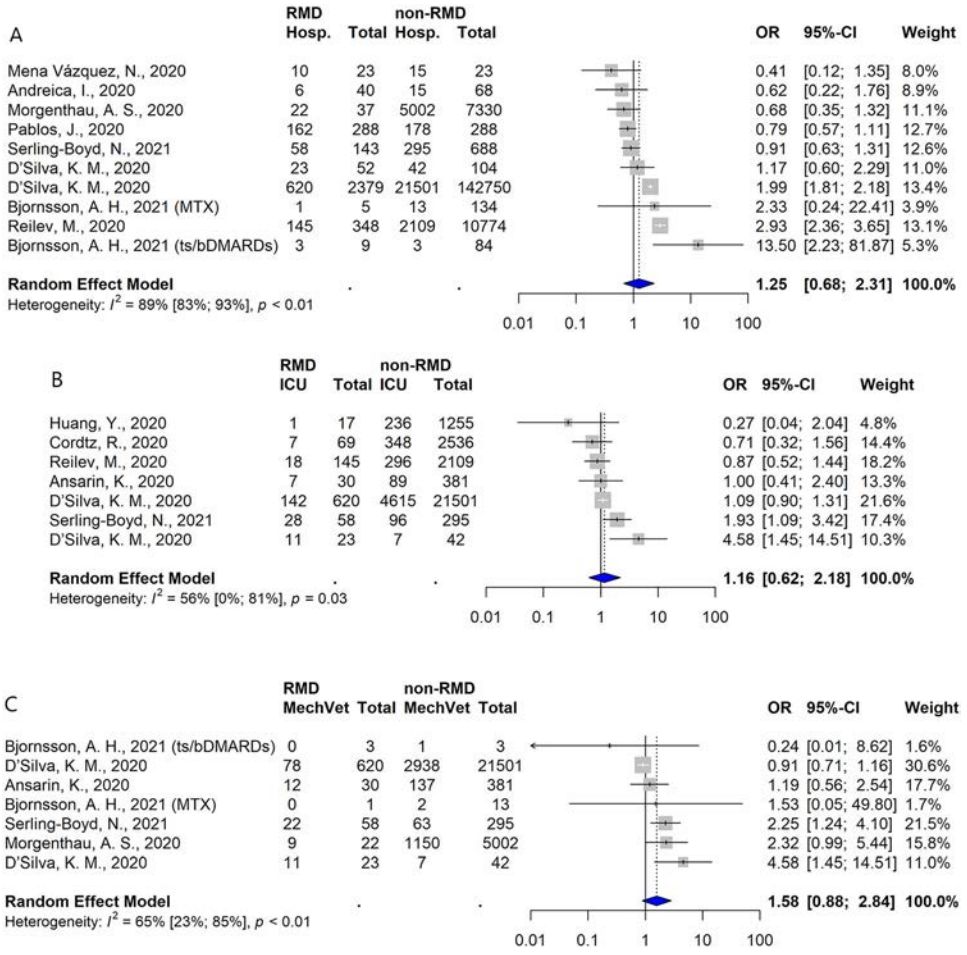

Figure 3. Studies showing the likelihood of hospitalization (Hosp.) (**A**), intensive care unit (ICU) admission (**B**), and mechanical ventilation (MechVet) (**C**) following the development of COVID-19 among populations of patients with RMDs relative to those without RMDs. Values are the odds ratios (ORs) with 95% CIs. See Figure 2 for other definitions. Color figure can be viewed in the online issue, which is available at http://onlinelibrary.wiley.com/doi/10.1002/art.42030/abstract.

compared to non-RMD comparators (OR 1.25 [95% CI 0.68–2.31]) (Figure 3A).

Among the 5 studies in which adjusted risk estimates were reported, 3 of the studies included patients with clinical symptom–based or PCR-confirmed COVID-19 diagnoses, whereas 2 included patients whose COVID-19 diagnosis was confirmed by PCR only. Data from 2 studies demonstrated an increased risk of hospitalization: the study by Cordtz et al (adjusted HR 1.46 [95% CI 1.15–1.86]) (19) and the study by Reilev et al (adjusted OR 1.5 [95% CI 1.1–1.9]) (20). D'Silva et al reported an increased risk of hospitalization in 1 matched model (RR 1.14 [95% CI 1.03–1.26]) and a neutral risk in an extended matched model (RR 1.06 [0.96–1.17]) (21). Finally, in 2 studies, no significant difference in risk of hospitalization was reported: in the study by Serling-Boyd et al, adjusted HR 0.87 (95% CI 0.68–1.11) (23); in and the study by D'Silva et al, adjusted OR 1.27 (95% CI 0.61–2.64) in model 1, adjusted OR 1.22 (95% CI 0.56–2.63) in model 2, and adjusted OR 1.10 (95% CI 0.51–2.38) in model 3 (22).

Oxygen supplementation, ICU, and mechanical ventilation. Sixty-two studies included the proportion of patients requiring new oxygen supplementation (n = 28), ICU admission (n = 52), and mechanical ventilation (n = 42) during hospitalization for COVID-19. In these studies, the diagnosis of COVID-19 was based on clinical symptoms and/or based on the results of PCR testing (for the list of studies, see Supplementary Table 12, http://onlinelibrary.wiley.com/doi/10.1002/art.42030).

In terms of the risk of oxygen supplementation, in 3 studies, comparative findings in patients with and those without an RMD were reported (Supplementary Table 11, http://onlinelibrary.wiley.com/doi/10.1002/art.42030). One of these studies showed an increased risk of oxygen supplementation among patients with RMDs, and the other 2 studies showed no significant difference between the groups. No studies included adjusted analyses.

Regarding ICU admission, 11 studies compared the rates between patients with and those without RMDs (Supplementary Table 11, http://onlinelibrary.wiley.com/doi/10.1002/art.42030), with 2 studies showing evidence of an increased risk among patients with RMDs and the rest showing no statistically significant difference. Adjusted risk estimates were reported in 2 studies, including the study by Serling-Boyd et al (adjusted HR 1.27 [95% CI 0.86–1.86]) (23), which demonstrated no effect, and the study by D'Silva et al (22), in which 3 adjusted models were evaluated, all demonstrating a positive association between RMD status and ICU admission/mechanical ventilation rates (in model 1, adjusted OR 3.26 [95% CI 1.17–9.09]; in model 2, adjusted OR 3.11 [95% CI 1.07–9.05]; in model 3, adjusted OR 2.92 [95% CI 1.002–8.49]).

Finally, 8 studies compared the rates of mechanical ventilation between patients with and those without RMDs (Supplementary Table 11, http://onlinelibrary.wiley.com/doi/10.1002/art.42030). Seven studies showed no significant difference based on RMD status, including the study by Serling-Boyd et al, in which an adjusted HR of 1.51 (95% CI 0.93–2.44) was reported (23). However, D'Silva et al reported that the risk of ICU admission/mechanical ventilation was significantly increased in patients with

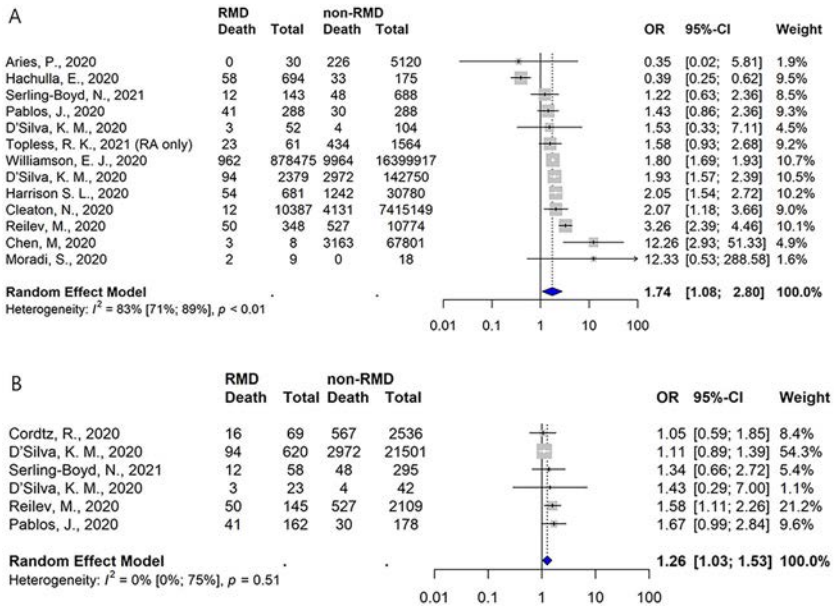

Figure 4. Studies showing the likelihood of death occurring following the development of COVID-19 among populations of patients with RMDs relative to those without RMDs overall (**A**) and among populations limited to hospitalized patients only (**B**). Values are the odds ratios (ORs) with 95% CIs. See Figure 2 for other definitions. Color figure can be viewed in the online issue, which is available at http://onlinelibrary.wiley.com/doi/10.1002/art.42030/abstract.

RMDs, as shown in unadjusted models (OR 3.22 [95% CI 1.16–8.92]) and in adjusted models (as described above) (22).

Pooled risk estimates included those for the reported comparative ICU admission rates in 7 studies, and those for the mechanical ventilation rates in another 7 studies (all determined in unadjusted models), as shown in Figures 3B and C. Overall, the risks of ICU admission or mechanical ventilation were not significantly different between patients with and those without RMDs.

Mortality rate. Mortality rates were reported in 71 studies (Supplementary Table 13, http://onlinelibrary.wiley.com/doi/10.1002/art.42030). Of these, in 16 studies, mortality rates were reported in RMD patents in comparison to the general population (n = 7) or non-RMD comparator populations (n = 9) (Supplementary Table 14, http://onlinelibrary.wiley.com/doi/10.1002/art.42030). For RMD patients, in 5 studies an increased risk of death was reported, in 9 a neutral effect of death was reported, and in 2 a decreased risk of death was reported. A meta-analysis of 13 studies that included comparative mortality rates showed an unadjusted OR of 1.74 (95% CI 1.08–2.80) for the risk of death in those with RMDs (Figure 4A). Moderately high heterogeneity was observed (I^2 = 83% [95% CI 71–89%]), but we did not detect evidence of publication bias (Supplementary Figure 2, http://onlinelibrary.wiley.com/doi/10.1002/art.42030). Among 6 studies focused solely on hospitalized patients, the unadjusted OR for the risk of death among hospitalized RMD patients was 1.26 (95% CI 1.03–1.53) (Figure 4B).

Adjusted risk estimates for the risk of death were reported in 7 studies. Compared to the general population, the adjusted estimates for the risk death in different studies were as follows: in the study by Williamson et al, HR 1.19 (95% CI 1.11–1.27) in patients with RA/systemic lupus erythematosus/psoriasis (24); in the study by Topless et al, OR 1.9 (95% CI 1.2–3.0) in patients with RA, and OR 1.2 (95% CI 0.9–1.7) in patients with gout (18); and in the study by Reilev et al, OR 0.9 (95% CI 0.6–1.3) in patients with RA/CTD (20). In studies assessing the risk of death in RMD patients compared to non-RMD comparators, D'Silva et al reported an RR of 1.08 (95% CI 0.81–1.44) (21), Harrison et al reported an OR of 1.17 (95% CI 0.85–1.60) (25), and Serling-Boyd et al reported an HR of 1.02 (95% CI 0.53–1.95) (23), while in the French RMD COVID-19 cohort (FAI^{2}R/SFR/SNFMI/SOFREMIP/CRI/IMIDIATE Consortium), an OR of 1.45 (95% CI 0.87–2.42) was reported (26).

Sensitivity analyses. Our sensitivity analyses demonstrated overall stability in terms of the pooled estimates for each of the outcomes when we limited the samples based on study design (limited to cohort or cross-sectional studies), risk of bias (limited to studies with a low risk of bias), country of study (excluding Italy, which had a disproportionate number of studies in which the prevalence of SARS–CoV2 infection was reported), or study size (limited to studies with >20 patients diagnosed as having an RMD only). Not unexpectedly, we observed that 95% CIs widened as sample sizes decreased (Supplementary Figures 3–10, http://onlinelibrary.wiley.com/doi/10.1002/art.42030).

DISCUSSION

In this study, we conducted a systematic review and meta-analysis to quantify the risk of COVID-19 and COVID-19 outcomes in patients with RMDs. In an unadjusted meta-analysis, the relative risk of developing SARS–CoV-2 infection was 52% higher in patients with RMDs compared to the general population. Compared to patients without an RMD, those with RMDs were also at a higher risk of having a poor outcome following COVID-19 infection, with a 74% increase in risk of death. Other measures of severity, including rates of hospitalization, rates of oxygen supplementation, rates of ICU admission, and rates of mechanical ventilation, were not significantly higher among patients with RMDs versus non-RMD comparators.

Our study focused on RMDs as a combined group, which limits our ability to extrapolate our findings to any individual patient with an RMD. This group was composed of patients with many different diseases that have different organ manifestations, severity, and treatments. Prior studies have shown differences in COVID-19 outcomes in specific rheumatic diseases (27,28). Some RMDs (e.g., gout) may be associated with increased prevalence of general COVID-19 risk factors, such as cardiovascular disease, but none of the studies included in our meta-analysis included patients with gout (29). Findings from previous studies have also suggested a differential effect of baseline use of rheumatic disease medications on COVID-19 outcomes (30,31). Other factors, such as age, sex, comorbidities, and disease activity, have also been shown to influence COVID-19 outcomes in patients with RMDs (31,32). Due to the heterogeneity of the study designs, it was not possible to statistically combine the results of the included studies to generate additional pooled estimates of the overall influence of these risk factors on COVID-19 outcomes.

The discrepancy between the observed increased risk of COVID-19 infection and associated mortality rate without a corresponding increased risk of hospitalization, ICU admission, and mechanical ventilation may appear surprising. However, these findings may be related to the overall power to detect differences given the smaller number of studies in which these outcomes were reported, which may be more difficult to systematically assess. Our pooled analysis, focusing only on studies of hospitalized patients (Figure 4B), allowed for comparison between RMD and non-RMD groups of subjects whose characteristics may be more similar in terms of risk factor profile (e.g., age, presence of multiple comorbidities) than might be observed between an RMD population and a general population comparator group, and we still found a significantly increased risk of death. However, it is important to take the smaller number of studies and smaller effect size into consideration.

This is not the first systematic literature review and meta-analysis assessing outcomes in patients with immune-mediated diseases. Wang et al performed a meta-analysis of 14 studies assessing RMD patients diagnosed as having COVID-19 that were published through October 2020; their findings showed that RMD patients had a 53% increased risk of SARS–CoV-2 infection with no increased risk of death or other markers of poor outcomes (33). Xu et al conducted a meta-analysis of 31 studies of COVID-19 in rheumatic disease patients published through August 2020 to evaluate the comparative RRs across regions of the world, but comparison to a non-RMD group was not included (34). Akiyama et al performed a meta-analysis of 62 studies in patients with autoimmune diseases and COVID-19 published through July 2020; however, this study included a more heterogeneous group of autoimmune diseases, such as inflammatory bowel disease and multiple sclerosis, which may have different outcomes compared to RMDs (35). Their findings demonstrated an increased risk of SARS–CoV-2 infection in patients with RMDs but no increase in the frequency of severe outcomes in those with autoimmune diseases. Interpretation of the results of these previously conducted meta-analyses is limited by the low number of included studies and patients, as evidenced by the generally wide confidence intervals for the reported risk estimates.

Applying these results in clinical care is complex, but these findings suggest that patients with RMDs are at an increased risk of developing SARS–CoV-2 infection and severe COVID-19 compared to the general population. The reasons for this lie outside the scope of the present study, but 3 plausible explanations should be considered. First, bias resulting from greater baseline contact with the health care system or a lower threshold for seeking care when a patient becomes symptomatic could falsely inflate the rate of COVID-19 among patients with RMDs. Second, patients with RMDs may have a greater burden of comorbidities that are typically associated with worse outcomes. Finally, it may be that immune dysregulation related to RMD treatments or to the RMDs themselves may result in higher rates of symptomatic infections and severe outcomes (21,30,36). All 3 of these explanations may account for prior observations that higher RMD disease activity is associated with worse outcomes in COVID-19, since these patients are more likely to be identified, are more likely to have comorbidities, and are more likely to have immune dysregulation or to be receiving immunosuppressive therapies. Regardless of the cause, patients with RMDs should be encouraged to be vaccinated against SARS–CoV-2 and should be encouraged to employ risk mitigation strategies as much as possible (37,38).

Our study has considerable strengths. We comprehensively identified potential studies from 14 databases through February 2021, making it the most current literature review and meta-analysis of COVID-19 in RMDs. We assembled a geographically diverse study team, enabling the inclusion of studies in all available languages. This is particularly relevant in COVID-19 because it exhibits wide regional variation in outcomes (39). To ensure reliability of the literature search and data extraction process, these tasks were performed manually; machine learning methods are being developed to streamline this process, and these approaches have potential strengths but remain exploratory at this time (40). Despite these strengths, our study had several limitations. The studies we included are significantly heterogenous in design and reporting, as evidenced by the formal testing of heterogeneity performed in the meta-analysis. The study protocol was created a priori; the increased volume of relevant articles rapidly published during the COVID-19 pandemic resulted in an amendment to the protocol to exclude case reports and case series. COVID-19 outcomes have changed and generally improved over time, which may limit comparability between cohorts assembled at different periods during the pandemic (41,42). Due to the small number of studies that include adjusted RRs, our meta-analysis was limited to the analysis of unadjusted numbers. However, we have presented the complementary adjusted RRs from those individual studies in which adjusted RRs were included. Interpretation of the unadjusted RRs is complicated by the potential imbalance of other risk factors between RMD patients and general populations.

In conclusion, we performed the most comprehensive systematic literature review and meta-analysis assessing COVID-19 outcomes in patients with RMDs to date. Our findings show that patients with RMDs have higher rates of SARS–CoV-2 infection and death from COVID-19 in unadjusted analyses. This may be mediated by factors other than the RMD itself.

AUTHOR CONTRIBUTIONS

All authors were involved in drafting the article or revising it critically for important intellectual content, and all authors approved the final version to be published. Dr. Conway had full access to all of the data in the study and takes responsibility for the integrity of the data and the accuracy of the data analysis.

Study conception and design. Conway, Grimshaw, Konig, Putman, Duarte-García, Liew, Grainger, Wallace, Hsieh.

Acquisition of data. Conway, Grimshaw, Konig, Putman, Duarte-García, Tseng, Cabrera, Chock, Degirmenci, Duff, Egeli, Graef, Gupta, Harkins, Hoyer, Jayatilleke, Jin, Kasia, Khilnani, Kilian, Kim, Lin, Low, Proulx, Sattui, Singh, Sparks, Tam, Ugarte-Gil, Ung, Wise, Yang, Young, Liew, Grainger, Wallace, Hsieh.

Analysis and interpretation of data. Conway, Grimshaw, Konig, Putman, Duarte-García, Wang, Liew, Grainger, Wallace, Hsieh.

ACKNOWLEDGMENT

We would like to thank all members of the COVID-19 Global Rheumatology Alliance. Open access funding was provided by IReL.

REFERENCES

1. Petrilli CM, Jones SA, Yang J, Rajagopalan H, O'Donnell L, Chernyak Y, et al. Factors associated with hospital admission and critical illness among 5279 people with coronavirus disease 2019 in New York City: prospective cohort study. BMJ 2020;369:m1966.

2. Guan WJ, Liang WH, Zhao Y, Liang HR, Chen ZS, Li YM, et al. Comorbidity and its impact on 1590 patients with COVID-19 in China: a nationwide analysis. Eur Respir J 2020;55:2000547.
3. Listing J, Gerhold K, Zink A. The risk of infections associated with rheumatoid arthritis, with its comorbidity and treatment. Rheumatology (Oxford) 2013;52:53–61.
4. Liberati A, Altman DG, Tetzlaff J, Mulrow C, Gøtzsche PC, Ioannidis JP, et al. The PRISMA statement for reporting systematic reviews and meta-analyses of studies that evaluate healthcare interventions: explanation and elaboration. BMJ 2009;339:b2700.
5. McGowan J, Sampson M, Salzwedel DM, Cogo E, Foerster V, Lefebvre C. PRESS Peer Review of Electronic Search Strategies: 2015 guideline statement. J Clin Epidemiol 2016;75:40–6.
6. Wells G, Shea B, O'Connell D, Robertson J, Peterson J, Welch V. The Newcastle-Ottawa scale (NOS) for assessing the quality of nonrandomized studies in meta-analysis. URL: http://www.evidencebasedpublichealth.de/download/Newcastle_Ottowa_Scale_Pope_Bruce.pdf.
7. Moola S. Systematic reviews of etiology and risk. In: Joanna Briggs institute reviewer's manual. Adelaide: The Joanna Briggs Institute; 2017. URL: https://jbi-global-wiki.refined.site/space/MANUAL/3283910762/Chapter+7%3A+Systematic+reviews+of+etiology+and+risk.
8. Monteiro F, Canavarro MC, Pereira M. Prevalence and correlates of psychological distress of middle-aged and older women living with HIV. Psychol Health Med 2017;22:1105–17.
9. Viswanathan M, Patnode CD, Berkman ND, Bass EB, Chang S, Hartling L, et al. Recommendations for assessing the risk of bias in systematic reviews of health-care interventions. J Clin Epidemiol 2018;97:26–34.
10. Putman M, Chock YP, Tam H, Kim AH, Sattui SE, Berenbaum F, et al. Antirheumatic disease therapies for the treatment of COVID-19: a systematic review and meta-analysis. Arthritis Rheumatol 2021;73:36–47.
11. Chen M, Wei Y, Zhang Q, Wan Q, Chen X. Epidemiology and clinical characteristics of COVID-19 in rheumatic diseases at a tertiary care hospital in Wuhan, China. Clin Exp Rheumatol 2021;39:442–3.
12. Francesconi P, Cantini F, Profili F, Mannoni A, Bellini B, Benucci M. COVID-19 epidemiology in rheumatic diseases in Tuscany: a case-control study. Joint Bone Spine 2021;88:105131.
13. Zhong J, Shen G, Yang H, Huang A, Chen X, Dong L, et al. COVID-19 in patients with rheumatic disease in Hubei province, China: a multicentre retrospective observational study. Lancet Rheumatol 2020;2:e557–64.
14. Pablos JL, Abasolo L, Alvaro-Gracia JM, Blanco FJ, Blanco R, Castrejon I, et al. Prevalence of hospital PCR-confirmed COVID-19 cases in patients with chronic inflammatory and autoimmune rheumatic diseases. Ann Rheum Dis 2020;79:1170–3.
15. Jung SY, Kim MS, Kim MC, Choi SH, Chung JW, Choi ST. Effect of hydroxychloroquine pre-exposure on infection with SARS-CoV-2 in rheumatic disease patients: a population-based cohort study. Clin Microbiol Infect 2020;27:611–7.
16. Kipps S, Paul A, Vasireddy S. Incidence of COVID-19 in patients with rheumatic disease: is prior health education more important than shielding advice during the pandemic? Clinical Rheumatol 2021;40:1575–9.
17. Salvarani C, Mancuso P, Gradellini F, Viani N, Pandolfi P, Reta M, et al. Susceptibility to COVID-19 in patients treated with antimalarials: a population based study in Emilia-Romagna, Northern Italy. Arthritis Rheumatol 2021;73:48–52.
18. Topless RK, Phipps-Green A, Leask M, Dalbeth N, Stamp LK, Robinson PC, et al. Gout, rheumatoid arthritis, and the risk of death related to coronavirus disease 2019: an analysis of the UK Biobank. ACR Open Rheumatol 2021;3:333–40.
19. Cordtz R, Lindhardsen J, Soussi BG, Vela J, Uhrenholt L, Westermann R, et al. Incidence and severeness of COVID-19 hospitalisation in patients with inflammatory rheumatic disease: a nationwide cohort study from Denmark. Rheumatology (Oxford) 2020;28:SI159–67.
20. Reilev M, Kristensen KB, Pottegård A, Lund LC, Hallas J, Ernst MT, et al. Characteristics and predictors of hospitalization and death in the first 11 122 cases with a positive RT-PCR test for SARS-CoV-2 in Denmark: a nationwide cohort. Int J Epidemiol 2020;49:1468–81.
21. D'Silva KM, Jorge A, Cohen A, McCormick N, Zhang Y, Wallace ZS, et al. COVID-19 outcomes in patients with Systemic Autoimmune Rheumatic Diseases (SARDs) compared to the general population: a US multi-center comparative cohort study. Arthritis Rheumatol 2021;73:914–20.
22. D'Silva KM, Serling-Boyd N, Wallwork R, Hsu T, Fu X, Gravallese EM, et al. Clinical characteristics and outcomes of patients with coronavirus disease 2019 (COVID-19) and rheumatic disease: a comparative cohort study from a US 'hot spot'. Ann Rheum Dis 2020;79:1156–62.
23. Serling-Boyd N, D'Silva KM, Hsu TYT, Wallwork R, Fu X, Gravallese EM, et al. Coronavirus disease 2019 outcomes among patients with rheumatic diseases 6 months into the pandemic. Ann Rheum Dis 2020;80:660–6.
24. Williamson EJ, Walker AJ, Bhaskaran K, Bacon S, Bates C, Morton CE, et al. Factors associated with COVID-19-related death using OpenSAFELY. Nature 2020;584:430–6.
25. Harrison SL, Fazio-Eynullayeva E, Lane DA, Underhill P, Lip GY. Comorbidities associated with mortality in 31,461 adults with COVID-19 in the United States: a federated electronic medical record analysis. PLoS Medicine 2020;17:e1003321.
26. Florence A, Nassim AA, Jean-David A, Didier A, Yannick A, Blanca AB, et al. Severity of COVID-19 and survival in patients with rheumatic and inflammatory diseases: data from the French RMD COVID-19 cohort of 694 patients. Ann Rheum Dis 2020;80:527–38.
27. Conway R, Nikiphorou E, Demetriou C, Low C, Leamy K, Ryan J, et al. POS1162 predictors of hospitalisation in patients with rheumatic disease and COVID-19 in Ireland: data from the COVID-19 Global Rheumatology Alliance physician-reported registry. Ann Rheum Dis 2021;80 suppl:859–60.
28. Pablos JL, Galindo M, Carmona L, Lledo A, Retuerto M, Blanco R, et al. Clinical outcomes of hospitalised patients with COVID-19 and chronic inflammatory and autoimmune rheumatic diseases: a multicentric matched cohort study. Ann Rheum Dis 2020;79:1544–9.
29. Dalbeth N, Robinson PC. Patients with gout: an under-recognised group at high risk of COVID-19. Lancet Rheumatol 2021;3:e317–8.
30. Sparks JA, Wallace ZS, Seet AM, Gianfrancesco MA, Izadi Z, Hyrich KL, et al. Associations of baseline use of biologic or targeted synthetic DMARDs with COVID-19 severity in rheumatoid arthritis: results from the COVID-19 Global Rheumatology Alliance physician registry. Ann Rheum Dis 2021;80:1137–46.
31. Strangfeld A, Schäfer M, Gianfrancesco MA, Lawson-Tovey S, Liew JW, Ljung L, et al. Factors associated with COVID-19-related death in people with rheumatic diseases: results from the COVID-19 Global Rheumatology Alliance physician-reported registry. Ann Rheum Dis 2021;80:930–42.
32. Hasseli R, Mueller-Ladner U, Hoyer BF, Krause A, Lorenz HM, Pfeil A, et al. Older age, comorbidity, glucocorticoid use and disease activity are risk factors for COVID-19 hospitalisation in patients with inflammatory rheumatic and musculoskeletal diseases. RMD Open 2021;7:e001464.
33. Wang Q, Liu J, Shao R, Han X, Su C, Lu W. Risk and clinical outcomes of COVID-19 in patients with rheumatic diseases compared with the general population: a systematic review and meta-analysis. Rheumatol Int 2021;41:851–61.
34. Xu C, Yi Z, Cai R, Chen R, Thong BY, Mu R. Clinical outcomes of COVID-19 in patients with rheumatic diseases: a systematic review and meta-analysis of global data. Autoimmun Rev 2021;20:102778.

35. Akiyama S, Hamdeh S, Micic D, Sakuraba A. Prevalence and clinical outcomes of COVID-19 in patients with autoimmune diseases: a systematic review and meta-analysis. Ann Rheum Dis 2020. DOI: 10.1136/annrheumdis-2020-218946. E-pub ahead of print.
36. Kalil AC, Patterson TF, Mehta AK, Tomashek KM, Wolfe CR, Ghazaryan V, et al. Baricitinib plus remdesivir for hospitalized adults with Covid-19. N Engl J Med 2021;384:795–807.
37. Smolen JS, Landewé RB, Bijlsma JW, Burmester GR, Dougados M, Kerschbaumer A, et al. EULAR recommendations for the management of rheumatoid arthritis with synthetic and biological disease-modifying antirheumatic drugs: 2019 update. Ann Rheum Dis 2020; 79:685–99.
38. Fraenkel L, Bathon JM, England BR, St.Clair EW, Arayssi T, Carandang K, et al. 2021 American College of Rheumatology guideline for the treatment of rheumatoid arthritis. Arthritis Rheumatol 2021;73:1108–23.
39. Mazumder A, Arora M, Sra MS, Gupta A, Behera P, Gupta M, et al. Geographical variation in case fatality rate and doubling time during the COVID-19 pandemic. Epidemiol Infect 2020;148: e163.
40. Van de Schoot R, de Bruin J, Schram R, Zahedi P, de Boer J, Weijdema F, et al. An open source machine learning framework for efficient and transparent systematic reviews. Nat Mach Intell 2021;3: 125–33.
41. Anesi GL, Jablonski J, Harhay MO, Atkins JH, Bajaj J, Baston C, et al. Characteristics, outcomes, and trends of patients with COVID-19-related critical illness at a learning health system in the United States. Ann Intern Med 2021;174:613–21.
42. Roth GA, Emmons-Bell S, Alger HM, Bradley SM, Das SR, de Lemos JA, et al. Trends in patient characteristics and COVID-19 in-hospital mortality in the United States during the COVID-19 pandemic. JAMA Netw Open 2021;4:e218828.

American College of Rheumatology
Empowering Rheumatology Professionals

Arthritis & Rheumatology
Vol. 74, No. 5, May 2022, pp 776–782
DOI 10.1002/art.42034

BRIEF REPORT

B Cell Reconstitution Is Strongly Associated With COVID-19 Vaccine Responsiveness in Rheumatic Disease Patients Who Received Treatment With Rituximab

Sarah Jinich,[1] Kaitlin Schultz,[2] Deanna Jannat-Khah,[3] and Robert Spiera[3]

Objective. To assess the association of a detectable antibody response to COVID-19 vaccination with factors including B cell depletion in patients who received treatment with rituximab (RTX).

Methods. We conducted a retrospective review of the charts of adult patients who received treatment with RTX and completed messenger RNA vaccination for SARS–CoV-2. The primary outcome measure was the presence or absence and strength of the serologic antibody response to vaccination. Comparisons between those with and those without a detectable serologic response were calculated using *t*-tests, Fisher's exact test, and Wilcoxon's rank sum test. The relationship between the serologic response to COVID-19 vaccination and B cell reconstitution status was assessed using negative predictive values and positive predictive values with data reported as percentages with 95% confidence intervals (95% CIs).

Results. In 56 patients being treated with RTX, a significant difference in terms of the level of B cell reconstitution was observed in those with a positive serologic response compared to those with a negative serologic response to vaccination (proportion of B cells reconstituted among total lymphocytes, median 2% [interquartile range (IQR) 0.13–10%] versus median 0% [IQR 0–0%]; $P < 0.001$).There was also a significant difference in the time since the last RTX infusion between patients with a positive serologic response compared to those with a negative serologic response to vaccination (median time since last infusion 594 days [IQR 262–1,163] versus median 138 days [IQR 68–197]; $P < 0.001$). There was no serologic response to COVID-19 vaccination after the last exposure to RTX in 13% of patients (3 of 24) at >12 months after last exposure, 55% of patients (6 of 11) at 6–12 months after last exposure, and 86% of patients (18 of 21) at <6 months after last exposure.

Conclusion. B cell reconstitution and a longer time since a patient's last exposure to RTX are associated with a positive serologic response to the COVID-19 vaccine. Strategies for maximizing vaccine responsiveness in patients who receive treatment with RTX should incorporate assessment of B cell reconstitution.

INTRODUCTION

The SARS–CoV-2 pandemic remains a pressing threat to public health worldwide, and immunosuppressed patients are a particularly high-risk group. Organizations such as the American College of Rheumatology (ACR) and Public Health England have recommended vaccination in this population to mitigate that risk. Current guidance is evolving but suggests modifying vaccination timing according to rituximab (RTX) infusion schedules (1). The ACR recommends receiving COVID-19 vaccination ~4 weeks before the subsequent scheduled RTX infusion, indicating that patients who receive cycles of RTX every 6 months should be vaccinated 5 months after exposure to RTX and that patients who receive RTX every 4 months should be vaccinated 3 months after exposure to RTX (1). The NHS, via the Joint Committee on Vaccination and Immunization, encourages delaying immunosuppressive treatment until at least 2 weeks after vaccination (2). There is also guidance to consider the timing of prior RTX

[1]Sarah Jinich, BA: Albert Einstein College of Medicine, New York, New York; [2]Kaitlin Schultz, BA: Hospital for Special Surgery, New York, New York; [3]Deanna Jannat-Khah, DRPH, MSPH, Robert Spiera, MD: Hospital for Special Surgery and Weill Cornell Medical College, New York, New York.

Author disclosures are available at https://onlinelibrary.wiley.com/action/downloadSupplement?doi=10.1002%2Fart.42034&file=art42034-sup-0001-Disclosureform.pdf.

Address correspondence to Robert Spiera, MD, 535 East 70th Street, New York City, New York 10028. Email spierar@hss.edu.

Submitted for publication August 2, 2021; accepted in revised form November 24, 2021.

treatment in relation to vaccination, but no specific timeline is given (2).

Recent studies evaluating the immunogenicity of the SARS–CoV-2 messenger RNA (mRNA) vaccines in patients with rheumatic and musculoskeletal diseases have demonstrated that patients are able to mount a detectable antibody response against SARS–CoV-2 spike proteins (3–4); however, it has been reported that patients exposed to RTX have a deficient serologic response (3–4).

CD20-depleting agents, like RTX, result in weakened serologic responses to vaccines for *Streptococcus pneumoniae*, tetanus, and seasonal influenza (5). Anti-CD20 therapies deplete B cells for extended periods of time with reconstitution not becoming detectable in peripheral blood for 6–9 months after infusion, resulting in diminished humoral immune responsiveness to recall antigens (6). Studies assessing the immunogenicity of vaccines in patients receiving RTX have demonstrated that those who were more recently treated with RTX showed greater impairment of serologic response to the vaccine when compared to those who were less recently exposed to RTX (5,7). Specifically, diminished SARS–CoV-2 vaccine responsiveness in patients receiving RTX has been reported (4,8–11). In this study, we retrospectively assessed the COVID-19 vaccination response in rheumatic disease patients receiving RTX. We hypothesized that B cell reconstitution would be associated with vaccine responsiveness.

PATIENTS AND METHODS

We retrospectively reviewed the charts of adult patients from a single rheumatology practice who received both doses of a COVID-19 vaccine. The study was approved by the Hospital for Special Surgery Institutional Review Board. Since this was a retrospective review, patients did not provide written consent. Data were collected from patients who visited the clinic from February 24 through May 20, 2021 and who were serologically screened for antibodies to the SARS–CoV-2 spike protein. Adult patients were eligible for inclusion if they received RTX and both doses of a COVID-19 mRNA vaccine (Pfizer or Moderna) and had a recorded assessment indicating the presence of antibodies to the SARS–CoV-2 spike protein.

We collected and evaluated information including demographic characteristics, diagnoses, date of vaccination (first and second doses), date of most recent RTX infusion, type of vaccine, quantitative serologic vaccine response, type of antirheumatic therapy (including dates of infusions if applicable), and percentage of CD19-positive cells in the lymphocyte population. Serologic response to vaccination was assessed using a semiquantitative anti–SARS–CoV-2 enzyme immunoassay (Roche Elecsys Anti–SARS–CoV-2 [specificity 99.8% and sensitivity 99.5%], Siemens Healthineers SARS–CoV-2 Total [COV2T] Assay Atellica IM [specificity 99.82% and sensitivity 100%], or ADVIA Centaur XP/XPT [specificity 99.81% and sensitivity 100%]). In 52 patients (93%), seropositivity was measured using Roche Elecsys Anti–SARS–CoV-2, and in 4 patients (7%), seropositivity was measured using Siemens Healthineers SARS–CoV-2 Total (COV2T) Assay Atellica IM or ADVIA Centaur XP/XPT. In the laboratory assays, serologic responses had an upper limit defined as anti–SARS–CoV-2 antibody levels of >250 units/ml or >2,500 units/ml, which we recorded and analyzed as 251 units/ml and 2,501 units/ml, respectively.

The primary outcome measure was the presence or absence and strength of the serologic response to COVID-19 vaccination. Descriptive statistics, including percentages, medians, and interquartile ranges (IQRs) are reported. Bivariate comparisons between patients with and those without serologic response were performed using Fisher's exact test, Student's *t*-test, and Wilcoxon's rank sum test. We used the Shapiro–Wilk test to assess normality for continuous variables. Box and whisker plots were created to visualize the differences in time between last RTX infusion to first vaccination among patients with and those without a serologic response and to visualize the percentage of CD19-positive cells between patients with and those without a serologic response. The relationship between serologic response to COVID-19 vaccination and B cell reconstitution status was assessed using negative and positive predictive values. *P* values less than or equal to 0.05 were considered significant, and all analyses were performed using Stata version 14.0.

RESULTS

A total of 56 patients met criteria for inclusion in our study. Baseline demographic and clinical characteristics, vaccine type, diagnoses, and medication exposure are shown in Table 1. The majority were women (n = 39 [70%]) and were White (n = 50 [89%]), and the median age was 64 years (IQR 52–72 years) (Table 1). With regard to demographic characteristics (age, sex, race, primary diagnosis), there were no statistically significant differences between those who were seropositive and those who were seronegative for the COVID-19 spike protein. A majority were receiving treatment for antineutrophil cytoplasmic antibody–associated vasculitis (n = 30 [54%]) and rheumatoid arthritis (RA) (n = 6 [11%]). Comorbidities included chronic kidney disease in 6 patients (10.7%) and a history of recurrent infections in 3 patients (5.4%); neither comorbidity was associated with antibody response ($P = 0.24$) or lack thereof ($P = 0.67$). Eleven patients (20%) had IgG levels <700 mg/dl, and 1 patient (2%) had an IgG level <400 mg/dl. Six patients (11%) had lymphopenia. Neither hypogammaglobulinemia ($P = 0.32$) nor lymphopenia ($P = 0.41$) correlated with vaccine response or lack thereof, and no patients had RTX dosing regimens that were altered at any point based on IgG or lymphocyte levels (Table 1).

Of the patients who received treatment with another antirheumatic therapy in addition to RTX, a glucocorticoid was the

Table 1. Demographic and clinical characteristics of patients with a negative serologic response to the COVID-19 vaccine compared to those with a positive serologic response*

	Total (n = 56)	Patients with a negative antibody response (n = 27)	Patients with a positive antibody response (n = 29)
Age, mean ± SD years	62.71 ± 14.70	64.70 ± 15.01	60.90 ± 14.41
Age, median (IQR) years	64 (52–72)	65 (53–74)	60 (52–71)
Sex			
Female	39 (70)	21 (78)	18 (62)
Male	17 (30)	6 (22)	11 (38)
Race			
White	50 (89)	24 (89)	26 (90)
Black	1 (2)	0 (0)	1 (3)
Asian	5 (9)	3 (11)	2 (7)
RA	6 (11)	3 (11)	3 (10)
SLE	3 (5)	2 (7)	1 (3)
Sjögren's syndrome	5 (9)	3 (11)	2 (7)
SSc	4 (7)	3 (11)	1 (3)
PMR	1 (2)	1 (4)	0 (0)
IgG4-related disease	1 (2)	1 (4)	0 (0)
ANCA-associated vasculitis			
MPA	4 (7)	2 (7)	2 (7)
EGPA	1 (2)	0 (0)	1 (3)
GPA	25 (45)	10 (37)	15 (52)
MCTD	1 (2)	0 (0)	1 (3)
PM	1 (2)	0 (0)	1 (3)
RP	2 (4)	2 (7)	0 (0)
Sarcoidosis	1 (2)	0 (0)	1 (3)
DM	1 (2)	0 (0)	1 (3)
Diabetes	0 (0)	0 (0)	0 (0)
Asthma	0 (0)	0 (0)	0 (0)
COPD	0 (0)	0 (0)	0 (0)
Prior COVID-19 infection	0 (0)	0 (0)	0 (0)
Chronic kidney disease	6 (11)	2 (7)	4 (14)
Recurrent infection	3 (5)	0 (0)	3 (10)
IgG level before vaccination, median (IQR) mg/dl	831.5 (702–1,040)	817 (652–997)	868 (736–1,191)
<400 mg/dl	1 (2)	1 (4)	0 (0)
<700 mg/dl	11 (20)	7 (26)	4 (14)
Lymphopenia	6 (11)	4 (15)	2 (7)
Antirheumatic therapies other than RTX			
Any immunosuppressant†	12 (21)	9 (33)	3 (10)
LEF	2 (4)	1 (4)	1 (3)
HCQ	3 (5)	1 (4)	2 (7)
AZA	1 (2)	1 (4)	0 (0)
Upadacitinib	1 (2)	0 (0)	1 (3)
MTX	2 (4)	2 (7)	0 (0)
MMF	5 (9)	4 (15)	1 (3)
TCZ	1 (2)	1 (4)	0 (0)
Glucocorticoids	12 (21)	5 (19)	7 (24)
Prednisone dose, median (IQR) mg	5 (3–5.5)	5 (4.5–6)	5 (2–5)
Vaccine type, Moderna	26 (46)	13 (48)	13 (45)
B cell status‡			
Detectable B cells	23 (41)	2 (7)	21 (72)
Missing	17 (29)	14 (52)	3 (10)
RTX for remission induction	6 (11)	4 (15)	2 (7)

* Except where indicated otherwise, values are the number (%) of patients. IQR = interquartile range; RA = rheumatoid arthritis; SLE = systemic lupus erythematosus; SSc = systemic sclerosis; PMR = polymyalgia rheumatica; ANCA = antineutrophil cytoplasmic antibody; MPA = microscopic polyangiitis; EGPA = eosinophilic granulomatosis; GPA = granulomatosis with polyangiitis; MCTD = mixed connective tissue disease; PM = polymyositis; RP = relapsing polychondritis; DM = dermatomyositis; COPD = chronic obstructive pulmonary disease; RTX = rituximab; HCQ = hydroxychloroquine; MMF = mycophenolate mofetil.

† Any immunosuppressant included leflunomide (LEF), azathioprine (AZA), upadacitinib, methotrexate (MTX), mycophenolate mofetil (MMF), and tocilizumab (TCZ).

‡ $P < 0.001$ by Fisher's exact test.

Table 2. Time since the last exposure to RTX and the degree of B cell reconstitution in patients with a negative serologic response to the COVID-19 vaccine compared to those with a positive response*

	Total (n = 56)	Patients with a negative antibody response (n = 27)	Patients with a positive antibody response (n = 29)	*P*
B cells among the total lymphocyte population, median (IQR) %	0.4 (0–7)	0 (0–0)	2 (0.13–10)	<0.001
SARS–CoV-2 spike antibody concentration, median (IQR) units/ml†	1.565 (0–251)	0 (0–0)	251 (30–1,010)	<0.001
Time from last RTX infusion to completion of vaccination, median (IQR) days	226 (122–677.5)	138 (68–197)	594 (262–1,163)	<0.001
Interval between last RTX exposure and completion of vaccination				<0.001
<6 months	21 (38)	18 (67)	3 (10)	
6–12 months	11 (20)	6 (22)	5 (17)	
>12 months	24 (43)	3 (11)	21 (72)	
Time from completion of vaccination to antibody immunoassay, median (IQR) days	33 (17.5–51.5)	30 (16–44)	35 (20–57)	0.29

* Except where indicated otherwise, values are the number (%) of patients. RTX = rituximab; IQR = interquartile range.
† In 52 patients (93%), seropositivity was measured using the Roche Elecsys Anti–SARS–CoV-2 test (specificity 99.8% and sensitivity 99.5%). In 4 patients (7%), seropositivity was measured using Siemens Healthineers SARS–CoV-2 Total (COV2T) Assay Atellica IM (specificity 99.82% and sensitivity 100%) or ADVIA Centaur XP/XPT (specificity 99.81% and sensitivity 100%) tests.

most common concomitant medication (n = 12 [21%]; median 5 mg [IQR 3–5.5 mg]). No difference in terms of prednisone dosage was observed in patients who had positive antibody responses compared to those who had negative antibody responses to COVID-19 vaccination ($P = 0.32$). Multiple patients also took mycophenolate mofetil (n = 5 [9%]) as well as other immunosuppressants, although a significant antibody response was not observed in patients taking immunosuppressants compared to those not taking immunosuppressants ($P = 0.052$). The majority of patients (50 [89%]) received their most recent RTX infusion for remission maintenance, and only 6 (11%) received their most recent RTX infusion for remission induction. Four patients receiving RTX for remission induction had received their last RTX dose >12 months prior to the date of vaccination and were in remission at the time of inoculation. Additionally, among the 4 patients who had received their last RTX dose <6 months prior to vaccination, a single, reduced dose of 500 mg was given. However, there was not a statistically significant difference in terms of vaccine responsiveness based on the prior dose of RTX ($P = 0.34$). Overall findings did not change when patients taking mycophenolate mofetil and methotrexate were excluded from the analysis (Supplementary Table 1, available on the *Arthritis & Rheumatology* website at http://onlinelibrary.wiley.com/doi/10.1002/art.42034).

In 39 patients (70%) B cell status was measured at the time of antibody immunoassay. The time since last RTX infusion was significantly longer in seropositive patients (median 594 days [IQR 262–1,163 days]) compared to seronegative patients (median 138 days [IQR 68–197 days]) ($P < 0.001$) (Table 2). There was a significant difference in terms of the proportion of B cell reconstitution among total lymphocytes in patients who had positive antibody responses to vaccination compared to those who had negative antibody responses to vaccination (B cells median 2% of total lymphocytes [IQR 0.13–10%]) versus median 0% of total lymphocytes [IQR 0–0%]; $P < 0.001$) (Table 2). Only 13% of patients (3 of 24) did not have a serologic response >12 months after last RTX exposure. Of those who received the vaccine 6–12 months after the last exposure to RTX, 55% (6 of 11) did not have a serologic response to the vaccine. Finally, 86% of patients (18 of 21) did not experience a serologic response when receiving the vaccine <6 months after the last exposure to RTX (Figure 1 and Table 2). Again, when patients taking mycophenolate mofetil and methotrexate were excluded, the findings remained consistent (Supplementary Table 2, http://onlinelibrary.wiley.com/doi/10.1002/art.42034).

The degree of B cell reconstitution and the time between the last exposure to RTX and date of vaccination were both statistically significant indicators of vaccine response (Figure 1). SARS–CoV-2 IgG antibody seropositivity was 74% among those who had received the vaccine >6 months after the last exposure to RTX (including those in the 6–12-month group and those in the >12-month group). In contrast, among those with detectable B cells, the frequency of SARS–CoV-2 IgG antibody seropositivity was 91.3% ($P = 0.006$). Among those who had received the vaccine 6–12 months after last exposure to RTX, only 45% were seropositive for SARS–CoV-2 IgG antibodies, with the frequency of seropositivity increasing to 80% among those with detectable B cells ($P = 0.190$). B cell reconstitution's positive predictive value for COVID-19 serologic response to COVID-19 vaccinations was 91.3% (95% confidence

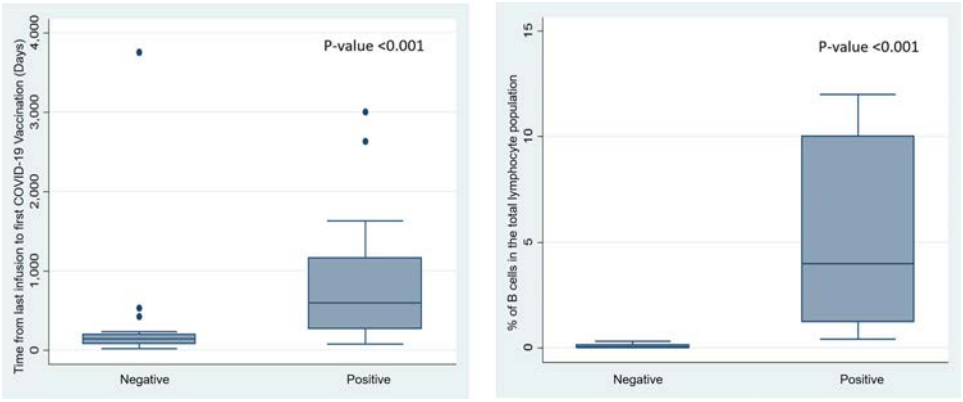

Figure 1. Vaccine response in patients receiving treatment with rituximab (RTX) according to the time since the last RTX infusion and B cell status at the time that the antibody level measurement was collected. Left, Vaccine response and time since the last RTX infusion. Among the 27 patients with a negative serologic response to the vaccine, the time between the last RTX infusion and the first vaccination was a median 138 days (interquartile range [IQR] 68–197). The 29 patients with a positive serologic response received their first vaccine dose a median of 594 days (IQR 262–1,163) after the last RTX infusion. Right, B cell status according to vaccine response. Among 39 patients with available data on percentages of B cells among total lymphocytes in the serum, 13 patients had a negative serologic response to the vaccine and 26 patients had a positive serologic response. Among those in the group who had a negative serologic response, the median percentage of B cells was 0% (IQR 0–0%). In the group with a positive serologic response to the vaccine, the median percentage of B cells was 2% (IQR 0.13–10%). Percentages of B cells in the total lymphocyte population were measured by flow cytometry. Results are shown as box plots, where lines inside the boxes show the median, the boxes represent the interquartile range, and the whiskers represent the minimum and maximum values; symbols represent outliers. *P* values were calculated using Wilcoxon's rank sum test.

interval [95% CI] 72–98.9%), and the negative predictive value was 68.8% (95% CI 41.3–89%).

DISCUSSION

B cell–depleting therapies are used in some of the most serious rheumatic diseases, and there is a need for further data regarding COVID-19 vaccine responsiveness in individuals receiving such therapies to inform decisions regarding the timing of therapy administration, particularly in patients placed on remission maintenance regimens. COVID-19 vaccination guidelines indicate that the time since the last RTX infusion should be taken into consideration in predicting the likelihood of vaccine responsiveness (1). However, findings from a small retrospective study suggested that B cell reconstitution may be a more accurate predictor of vaccine response (8). Another small study found that in 2 rheumatic disease patients in whom B cell repletion took place following treatment with RTX, a humoral immune response to the vaccine was observed, whereas in 3 other rheumatic disease patients who were receiving RTX and whose B cells remained depleted, there was no evidence of a humoral immune response (12). The relevance of B cell depletion in vaccine responsiveness was also demonstrated in a larger study that included 96 patients receiving treatment with anti-CD20 therapies, including both RTX and ocrelizumab, for a variety of indications including nonrheumatic conditions. A positive correlation between CD19 B cell count and serologic response to vaccination was identified and peripheral CD19-positive cells of >27 cells/μl had a positive predictive value of 67% for vaccine responsiveness. A longer time since the last RTX infusion and a higher detectable CD4 cell count were also associated with vaccine responsiveness (9).

Our results support these data while focusing exclusively on rheumatic disease patients who received treatment with RTX (the only B cell–depleting therapy approved for the treatment of rheumatic diseases), with a recognized positive predictive value of 91.3%. Another descriptive study found that of 134 subjects with either systemic lupus erythematosus or RA, only 24% of the 17 subjects who received treatment with RTX had detectable anti–SARS–CoV-2 antibodies measured 8 days after the date of the second vaccination, but a correlation between the time since the last RTX infusion and vaccine response was not identified, and B cell status was not recorded (13). A more recent prospective study of 98 rheumatic disease patients receiving treatment with RTX found that high levels of exposure to RTX over time, low IgG levels prior to the last course of RTX, and a short interval between the last RTX course and the date of BNT162b2 vaccination (Pfizer-BioNTech) were associated with a lack of a humoral response to vaccination in autoimmune rheumatic disease patients. B cell status was not assessed (14).

In our retrospective study, the time since the last RTX infusion was similarly associated with a positive serologic response to the COVID-19 vaccine, but the assessment of B cell reconstitution status provided complementary data that could help predict vaccine responsiveness. Of subjects who received the vaccine 6–12 months after the last exposure to RTX, 55% were seronegative for SARS–CoV-2 antibodies, but among those subjects in whom B cell reconstitution had begun after exposure to RTX, only

1 patient (20%) was seronegative for SARS–CoV-2 antibodies. In patients who were vaccinated >12 months after the last RTX infusion, only 1 patient (6%) who had reconstituted B cells was seronegative. When combined with the 13% of patients who were vaccinated >12 months since the last exposure to RTX in whom no SARS–CoV-2 antibodies were generated in response to the vaccine, ~25% of patients who received the COVID-19 vaccine >6 months after the last exposure to RTX did not show a response to the vaccine.

Six months is often the interval between infusions for the treatment of RA and for remission maintenance regimens in treating antineutrophil cytoplasmic antibody–associated vasculitis (AAV), and this is shorter than the duration from last exposure to RTX often suggested in current vaccination guidelines (1). Those guidelines were developed prior to the emergence of data regarding the likelihood of achieving a serologic response to COVID-19 vaccines in patients receiving treatment with RTX, and recognizing that as many as 50% of patients who receive treatment with RTX may not achieve seropositivity with this strategy could be important to clinicians when making decisions regarding the timing of vaccine or RTX administration. B cell reconstitution increases the likelihood of a serologic response in these groups.

Assessment of B cell reconstitution has been used in other clinical settings, including stratifying the risk of flare in patients with AAV, and is easily accessible even with readily available commercial assays (15). Particularly in communities with limited access to COVID-19 vaccines, confirming B cell reconstitution prior to vaccine administration may be prudent. In patients with well-controlled disease who are receiving RTX as a remission maintenance therapy, delaying vaccination and further RTX administration until peripheral B cell reconstitution begins is a feasible strategy for increasing the likelihood of a serologic response to vaccination. This may also be relevant regarding potential strategies for determining the timing of revaccination in patients receiving treatment with B cell–depleting agents who did not have a serologic response after initial vaccination and may also be relevant to the administration of additional vaccine doses in fully vaccinated patients who are at risk of waning immunity due to immunosuppression and time since initial vaccine administration.

One strength of our study is having a well-characterized cohort of patients with RTX-treated rheumatic disease in whom vaccine responsiveness was assessed. A major limitation is the retrospective nature of the study, since there was no uniformity regarding timing of the measurement of antibodies in relation to the timing of vaccine administration. Antibody titers were measured at the next clinic visit, and in the case of 9 patients, this was <2 weeks after the second vaccine dose. However, only 4 of these patients were negative for SARS–CoV-2 antibodies, and all 3 patients in whom antibody status was checked at subsequent visits remained negative for SARS–CoV-2 antibodies. Furthermore, a study that included 3,099 adults vaccinated with the BNT162b2 vaccine demonstrated that 96% of subjects developed antibodies 4 weeks after their initial vaccine dose, a timeframe that all subjects in this study were within in terms of antibody measurements relative to the date of vaccination (16).

The retrospective design of our study is also a limitation in that B cell reconstitution was not assessed at the time of vaccination or just prior to vaccination, but rather at the next clinic visit after COVID-19 vaccine administration. It is conceivable that some patients were B cell depleted at the time of vaccination and did not demonstrate a serologic response but B cells had reconstituted by the time of the clinic visit and assessment. Potentially, if anything, this could weaken the association between B cell reconstitution and serologic response observed in this study. In our cohort, there were 2 patients who had a negative serologic response but had low levels of B cell reconstitution at the time of the assessment, which was 1–3 months after administration of the first vaccine. This could be better assessed in future prospective studies, but it is unclear if these studies could be ethically performed prospectively, since vaccinating B cell–depleted patients in the context of limited vaccine access may not be feasible. Finally, our analysis only includes patients who received mRNA vaccines, and our findings may not be generalizable to patients receiving other vaccines, such as adenovirus vector vaccines.

One important consideration is that the lack of a detectable antibody response to the COVID-19 vaccine does not imply a lack of improved immunity relative to prior to vaccination, since other facets of immunity are enhanced by vaccination (7,12). Nevertheless, demonstration of a humoral immune response is the most commonly used biomarker of vaccine responsiveness and likely indicates a more robust degree of immunity in seropositive patients than in seronegative patients. Strategies to optimize achieving serologic response in immunosuppressed patients remain a priority, and our findings could inform achieving serologic response in the large groups of patients receiving treatment with RTX and possibly other B cell–depleting therapies.

AUTHOR CONTRIBUTIONS

All authors were involved in drafting the article or revising it critically for important intellectual content, and all authors approved the final version to be published. Dr. Spiera had full access to all of the data in the study and takes responsibility for the integrity of the data and the accuracy of the data analysis.

Study conception and design. Spiera.
Acquisition of data. Jinich, Schultz, Spiera.
Analysis and interpretation of data. Jannat-Khah, Spiera.

REFERENCES

1. Curtis JR, Johnson SR, Anthony DD, Arasaratnam RJ, Baden LR, Bass AR, et al. American College of Rheumatology guidance for COVID-19 vaccination in patients with rheumatic and musculoskeletal diseases: version 1. Arthritis Rheumatol 2021;73:1093–107.
2. UK Health Security Agency. COVID-19: the green book, chapter 14a: coronavirus (COVID-19) vaccination information for public health professionals. 2020.

3. Boyarsky BJ, Ruddy JA, Connolly CM, Ou MT, Werbel WA, Garonzik-Wang JM, et al. Antibody response to a single dose of SARS-CoV-2 mRNA vaccine in patients with rheumatic and musculoskeletal diseases. Ann Rheum Dis 2021;80:1098–99.
4. Deepak P, Kim W, Paley MA, Yang M, Carvidi AB, El-Qunni AA, et al. Glucocorticoids and B cell depleting agents substantially impair immunogenicity of mRNA vaccines to SARS-CoV-2 [preprint]. medRxiv 2021.
5. Arnold J, Winthrop K, Emery P. COVID-19 vaccination and antirheumatic therapy. Rheumatology (Oxford) 2021;60:3496–502.
6. Houot R, Levy R, Cartron G, Armand P. Could anti-CD20 therapy jeopardise the efficacy of a SARS-CoV-2 vaccine? Eur J Cancer 2020;136:4–6.
7. Arad U, Tzadok S, Amir S, Mandelboim M, Mendelson E, Wigler I, et al. The cellular immune response to influenza vaccination is preserved in rheumatoid arthritis patients treated with rituximab. Vaccine 2011;29:1643–8.
8. Spiera R, Jinich S, Jannat-Khah D. Rituximab, but not other antirheumatic therapies, is associated with impaired serological response to SARS- CoV-2 vaccination in patients with rheumatic diseases. Ann Rheum Dis 2021;80:1357–9.
9. Moor MB, Suter-Riniker F, Horn MP, Aeberli DD, Amsler J, Möller B, et al. Humoral and cellular responses to mRNA vaccines against SARS-CoV-2 in patients with a history of CD20 B-cell-depleting therapy (RituxiVac): an investigator-initiated, single-centre, open-label study. Lancet Rheumatol 2021;3:e789–97.
10. Furer V, Eviatar T, Zisman D, Peleg H, Paran D, Levartovsky D, et al. Immunogenicity and safety of the BNT162b2 mRNA COVID-19 vaccine in adult patients with autoimmune inflammatory rheumatic diseases and in the general population: a multicentre study. Ann Rheum Dis 2021;80:1330–8.
11. Connolly CM, Boyarsky BJ, Ruddy JA, Werbel WA, Christopher-Stine L, Garonzik-Wang J, et al. Absence of humoral response after two-dose SARS-CoV-2 messenger RNA vaccination in patients with rheumatic and musculoskeletal diseases: a case series. Ann Intern Med 2021;174:1332–4.
12. Bonelli MM, Mrak D, Perkmann T, Haslacher H, Aletaha D. SARS-CoV-2 vaccination in rituximab-treated patients: evidence for impaired humoral but inducible cellular immune response. Ann Rheum Dis 2021;80:1355–6.
13. Ammitzbøll C, Bartels LE, Andersen JB, Vils SR, Mistegård CE, Johannsen AD, et al. Impaired antibody response to the BNT162b2 messenger RNA coronavirus disease 2019 vaccine in patients with systemic lupus erythematosus and rheumatoid arthritis. ACR Open Rheumatol 2021;3:622–8.
14. Furer V, Eviatar T, Zisman D, Peleg H, Paran D, Levartovsky D, et al. Factors associated with reduced immunogenicity of the BNT162b2 mRNA COVID-19 vaccine in patients with autoimmune inflammatory rheumatic diseases (AIIRD) treated with rituximab [abstract]. Arthritis Rheumatol 2021;73 Suppl 10.
15. Stone JH, Merkel PA, Spiera R, Seo P, Langford CA, Hoffman GS, et al. Rituximab versus cyclophosphamide for ANCA-associated vasculitis. N Engl J Med 2010;363:221–32.
16. Iacobucci G. Covid-19: most UK adults had antibodies after one dose of AstraZeneca or Pfizer vaccine, data suggest. BMJ 2021; 373:1274.

Arthritis & Rheumatology
Vol. 74, No. 5, May 2022, pp 783–790
DOI 10.1002/art.42035

AMERICAN COLLEGE of RHEUMATOLOGY
Empowering Rheumatology Professionals

BRIEF REPORT

Impact of Cytokine Inhibitor Therapy on the Prevalence, Seroconversion Rate, and Longevity of the Humoral Immune Response Against SARS–CoV-2 in an Unvaccinated Cohort

David Simon,[1] Koray Tascilar,[1] Arnd Kleyer,[1] Filippo Fagni,[1] Gerhard Krönke,[1] Christine Meder,[1] Peter Dietrich,[1] Till Orlemann,[1] Thorsten Kliem,[1] Johanna Mößner,[1] Anna-Maria Liphardt,[1] Verena Schönau,[1] Daniela Bohr,[1] Louis Schuster,[1] Fabian Hartmann,[1] Moritz Leppkes,[1] Andreas Ramming,[1] Milena Pachowsky,[1] Florian Schuch,[2] Monika Ronneberger,[2] Stefan Kleinert,[2] Axel J. Hueber,[3] Karin Manger,[4] Bernhard Manger,[1] Raja Atreya,[1] Carola Berking,[1] Michael Sticherling,[1] Markus F. Neurath,[1] and Georg Schett[1]

Objective. To investigate the impact of biologic disease-modifying antirheumatic drug (bDMARD) treatment on the prevalence, seroconversion rate, and longevity of the humoral immune response against SARS–CoV-2 in patients with immune-mediated inflammatory diseases (IMIDs).

Methods. Anti–SARS–CoV-2 IgG antibodies were measured in a prospective cohort of health care professional controls and non–health care controls and IMID patients receiving no treatment or receiving treatment with conventional or biologic DMARDs during the first and second COVID-19 waves. Regression models adjusting for age, sex, sampling time, and exposure risk behavior were used to calculate relative risks (RRs) of seropositivity. Seroconversion rates were assessed in participants with polymerase chain reaction (PCR)–positive SARS–CoV-2 infection. Antibody response longevity was evaluated by reassessing participants who tested positive during the first wave.

Results. In this study, 4,508 participants (2,869 IMID patients and 1,639 controls) were analyzed. The unadjusted RR (0.44 [95% confidence interval (95% CI) 0.31–0.62]) and adjusted RR (0.50 [95% CI 0.34–0.73]) for SARS–CoV-2 IgG antibodies were significantly lower in IMID patients treated with bDMARDs compared to non–health care controls ($P < 0.001$), primarily driven by treatment with tumor necrosis factor inhibitors, interleukin-17 (IL-17) inhibitors, and IL-23 inhibitors. Adjusted RRs for untreated IMID patients (1.12 [95% CI 0.75–1.67]) and IMID patients receiving conventional synthetic DMARDs (0.70 [95% CI 0.45–1.08]) were not significantly different from non–health care controls. Lack of seroconversion in PCR-positive participants was more common among bDMARD-treated patients (38.7%) than in non–health care controls (16%). Overall, 44% of positive participants lost SARS–CoV-2 antibodies by follow-up, with higher rates in IMID patients treated with bDMARDs (RR 2.86 [95% CI 1.43–5.74]).

Conclusion. IMID patients treated with bDMARDs have a lower prevalence of SARS–CoV-2 antibodies, seroconvert less frequently after SARS–CoV-2 infection, and may exhibit a reduced longevity of their humoral immune response.

INTRODUCTION

SARS–CoV-2 poses a considerable threat to patients with immune-mediated inflammatory diseases (IMIDs). Due to their immune dysfunction, the consequence of immunomodulatory treatment, and the large burden of comorbidities, IMID patients are of particular interest in the current COVID-19 pandemic (1). Initially, there were concerns that IMID patients, particularly those receiving cytokine inhibitors, may be at an increased susceptibility for SARS–CoV-2 infection and may develop a more severe

Supported by the DFG (FOR 2886, PANDORA, and the CRC1181 Checkpoints for Resolution of Inflammation). Supported in part by the BMBF (project MASCARA), the Bayerisches Staatsministerium für Wissenschaft und Kunst, the ERC Synergy grant 4D Nanoscope, the IMI-funded projects RTCure and HIPPOCRATES, the Emerging Fields Initiative MIRACLE of the Friedrich-Alexander University Erlangen-Nuremberg, the Schreiber Stiftung, and the Else Kröner-Memorial Scholarship (grant no. 2019_EKMS.27 to Dr. Simon).

disease course if infected. However, more recent data suggest that IMID patients, especially those treated with cytokine inhibitors, are not at increased risk for severe COVID-19 (2).

SARS–CoV-2 encounters a different immune system in IMID patients treated with cytokine inhibitors. Respective drugs target key mediators that mount adaptive immune responses to infections, such as interleukin-23 (IL-23) and IL-17, but also those with inflammatory effector function, such as tumor necrosis factor (TNF) and IL-6 (3). Therefore, the immune response against SARS–CoV-2 may be altered in IMID patients. This situation may have advantages, as impaired inflammatory responses could explain the observed milder course of COVID-19 in patients treated with cytokine inhibitors (2,4,5). Alternatively, cytokine inhibitors may influence the mounting of a protective immunity against the virus.

SARS–CoV-2 triggers the formation of specific antibodies, which are related to the severity of the infection (6). IMID patients, especially those treated with cytokine inhibitors, may have an altered prevalence, seroconversion rate, and longevity of the anti–SARS–CoV-2 immune response. Large studies assessing these parameters in IMID patients are lacking to date. It has previously been shown that the majority of IMID patients are capable of developing protective immunity after SARS–CoV-2 infection (7,8) as well as after messenger RNA vaccination (9,10). However, a study conducted during the first wave of the COVID-19 pandemic showed that the prevalence of anti–SARS–CoV-2 antibody positivity was significantly lower in IMID patients treated with cytokine inhibitors compared to patients receiving no such treatments and compared to healthy controls (11). This finding suggests that anticytokine treatment may dampen the adaptive immune responses to SARS–CoV-2 vaccines, which has been described for conventional synthetic disease-modifying antirheumatic drugs (csDMARDs), such as methotrexate (12), but that could not yet be confirmed for biologic DMARDS (bDMARDs) (i.e., cytokine inhibitors) (13,14). Furthermore, studies on the humoral response to SARS–CoV-2 and other coronaviruses in healthy individuals indicated that humoral immunity is not permanent but declines over time, rendering individuals susceptible for reinfection with coronaviruses (15).

Based on these data, we investigated whether IMID patients and healthy controls differ in their humoral immune response to SARS–CoV-2 infection and especially if individual cytokine inhibitors may affect this process. In order to test the influence of individual cytokine inhibitors on the prevalence of SARS–CoV-2 infection, large and well-controlled data sets that allow for adjustment for social exposure are needed. Furthermore, information on polymerase chain reaction–confirmed SARS–CoV-2 infection helps to test for true seroconversion rates, while prospectively collected longitudinal data allow testing for the longevity of humoral immune responses in IMID patients and controls. To address these points, we analyzed a large prospective cohort of IMID patients and controls and investigated the prevalence, seroconversion rate, and longevity of humoral SARS–CoV-2 immune responses in IMID patients and healthy controls.

PATIENTS AND METHODS

Participants. IMID patients and healthy controls were recruited from a large longitudinal COVID-19 study at the Deutsche Zentrum fuer Immuntherapie, which was initiated in February 2020 and monitors respiratory infections including COVID-19, anti–SARS–CoV-2 antibody responses, and social exposure. Exact details of the recruitment have been described elsewhere (11). The study had 2 sample collection waves (i.e., from March 1, 2020 to June 1, 2020 during the first wave of COVID-19 and from December 1, 2020 to March 1, 2021 during the second wave). For the cross-sectional analysis, we included all subjects who provided samples during the second wave of sample collection. For the longitudinal analysis, participants were included if they had a positive anti–SARS–CoV-2 antibody test in the first wave and were also evaluated in the second wave of the sample collection. Accordingly, patients who had already been enrolled in a first cross-sectional analysis (11) were included in the cross-sectional analysis performed for the second wave and the longitudinal analysis.

Briefly, the study recruited IMID patients receiving either no treatment or treatment with csDMARDs, bDMARDS, or targeted synthetic DMARDs (tsDMARDs). In addition, 2 healthy control groups were recruited: non–health care controls from the general population as well as health care professionals (physicians, nurses, and technicians). Healthy controls did not have any IMIDs. Subjects who already had received a SARS–CoV-2 vaccination

[1]David Simon, MD, Koray Tascilar, MD, Arnd Kleyer, MD, Filippo Fagni, MD, Gerhard Krönke, MD, Christine Meder, MD, Peter Dietrich, MD, Till Orlemann, MD, Thorsten Kliem, MD, Johanna Mößner, MD, Anna-Maria Liphardt, PhD, Verena Schönau, MD, Daniela Bohr, MD, Louis Schuster, PhD, Fabian Hartmann, PhD, Moritz Leppkes, MD, Andreas Ramming, MD, Milena Pachowsky, MD, Bernhard Manger, MD, Raja Atreya, MD, Carola Berking, MD, Michael Sticherling, MD, Markus F. Neurath, MD, Georg Schett, MD: Friedrich-Alexander University Erlangen-Nuremberg and Universitätsklinikum Erlangen, Erlangen, Germany; [2]Florian Schuch, MD, Monika Ronneberger, MD, Stefan Kleinert, MD: Rheumatology Clinical Practice Erlangen, Germany; [3]Axel J. Hueber, MD, PhD: Friedrich-Alexander University Erlangen-Nuremberg and Universitätsklinikum Erlangen, Erlangen, Germany, and Rheumatology Section, Sozialstiftung Bamberg, Bamberg, Germany; [4]Karin Manger, MD: Rheumatology Practice Bamberg, Bamberg, Germany.

Drs. Simon and Tascilar contributed equally to this work.

Author disclosures are available at https://onlinelibrary.wiley.com/action/downloadSupplement?doi=10.1002%2Fart.42035&file=art42035-sup-0001-Disclosureform.pdf.

Address correspondence to Georg Schett, MD, Department of Internal Medicine 3 - Rheumatology and Immunology, Friedrich-Alexander University Erlangen-Nuremberg and Universitätsklinikum Erlangen, Ulmenweg 18, 91054 Erlangen, Germany. Email: georg.schett@uk-erlangen.de.

Submitted for publication September 21, 2021; accepted in revised form November 24, 2021.

Table 1. Baseline characteristics of the study subjects*

	IMID (n = 2,869)	Health care professional controls (n = 455)	Non–health care controls (n = 1,184)	Overall (n = 4,508)
Age, mean ± SD years	55.1 ± 15.2	40.0 ± 12.9	43.5 ± 14.7	50.5 ± 16.1
Sex				
Male	1,180 (41.1)	133 (29.2)	820 (69.3)	2,133 (47.3)
Female	1,687 (58.8)	321 (70.5)	362 (30.6)	2,370 (52.6)
Smoking status				
Current	508 (17.7)	59 (13.0)	197 (16.6)	764 (16.9)
Past	738 (25.7)	70 (15.4)	219 (18.5)	1,027 (22.8)
Never	1,339 (46.7)	301 (66.2)	690 (58.3)	2,330 (51.7)
Missing	284 (9.9)	25 (5.5)	78 (6.6)	387 (8.6)
BMI, mean ± SD kg/m^2	27.3 ± 5.9	24.0 ± 4.3	26.6 ± 4.9	26.8 ± 5.6
Diagnosis				
No IMID	–	455 (100.0)	1,184 (100.0)	1,639 (36.4)
RA	979 (34.1)	–	–	979 (21.7)
SpA†	794 (27.7)	–	–	794 (17.6)
CTD	307 (10.7)	–	–	307 (6.8)
IBD	223 (7.8)	–	–	223 (4.9)
Other‡	207 (7.2)	–	–	207 (4.6)
Systemic vasculitis	180 (6.3)	–	–	180 (4.0)
Psoriasis	136 (4.7)	–	–	136 (3.0)
Autoinflammatory disease	43 (1.5)	–	–	43 (1.0)
Comorbidities				
Diabetes mellitus	271 (9.5)	5 (1.1)	33 (2.9)	309 (7.0)
Hypertension	1,094 (38.4)	27 (6.2)	184 (16.3)	1,305 (29.6)
Ischemic heart disease	71 (2.5)	-	6 (0.5)	77 (1.7)
DVT	54 (1.9)	1 (0.2)	8 (0.7)	63 (1.4)
Cancer	231 (8.1)	12 (2.7)	46 (4.1)	289 (6.5)
Lung disease	252 (8.8)	24 (5.5)	44 (3.9)	320 (7.3)
Treatment				
bDMARDs	1,344 (46.8)	–	–	1,344 (29.8)
csDMARDs	742 (25.9)	–	–	742 (16.5)
tsDMARDs	176 (6.1)	–	–	176 (3.9)
Blockade type				
TNFi	666 (23.2)	–	–	666 (14.8)
IL-17 inhibitors	202 (7.0)	–	–	202 (4.5)
IL-12/23 inhibitors	117 (4.1)	–	–	117 (2.6)
IL-6 inhibitors	109 (3.8)	–	–	109 (2.4)
CD20 depletion	101 (3.5)	–	–	101 (2.2)
IL-23 inhibitors	47 (1.6)	–	–	47 (1.0)
CD80/86 inhibitors	35 (1.2)	–	–	35 (0.8)
Integrin α4β7	27 (0.9)	–	–	27 (0.6)
Other§	40 (1.4)	–	–	40 (0.9)
PCR test results				
Total tested	1,109 (38.7)	273 (60.0)	575 (48.6)	1,957 (43.4)
Positive¶	57 (5.1)	45 (16.5)	50 (8.7)	152 (7.8)
Negative¶	1,040 (93.8)	227 (83.2)	523 (91.0)	1,790 (91.5)
Risk behavior				
Home office	1,120 (39.0)	26 (5.7)	370 (31.2)	1,516 (33.6)
Contact with infected	262 (9.1)	199 (43.7)	231 (19.5)	692 (15.4)
Visit to risk area	87 (3.0)	62 (13.6)	73 (6.2)	222 (4.9)
Social distancing	2,244 (78.2)	391 (85.9)	1,020 (86.1)	3,655 (81.1)

* Except where indicated otherwise, values are the number (%) of subjects. IMID = immune-mediated inflammatory disease; BMI = body mass index; RA = rheumatoid arthritis; SpA = spondyloarthritis; CTD = connective tissue disease; IBD = inflammatory bowel disease; DVT = deep vein thrombosis; bDMARDs = biologic disease-modifying antirheumatic drugs; csDMARDs = conventional synthetic DMARDs; tsDMARDs = targeted synthetic DMARDs; TNFi = tumor necrosis factor inhibitors; PCR = polymerase chain reaction.
† Including psoriatic arthritis.
‡ Including autoimmune hepatitis, uveitis, eosinophilic fasciitis, IgG4 disease, juvenile idiopathic arthritis, polymyalgia rheumatica, recurrent polychondritis, sarcoidosis, and undifferentiated arthritis.
§ Including neutralizing antibodies against interleukin-1 (IL-1), IL-4, IL-5, and B lymphocyte stimulator.
¶ Percentages among subjects tested.

were excluded from the study. In all participants, a structured questionnaire was used to collect data on age, sex, body mass index, and risk factors for severe COVID-19 (smoking status, arterial hypertension, diabetes mellitus, and chronic lung diseases). Recent history of COVID-19–related symptoms was also recorded. Data about exposure risk–related behavior, including compliance with social distancing, avoidance of the workplace, contact with infected individuals, and travel to respective risk areas designated by the German federal government agency for disease control and prevention (the Robert Koch Institute [RKI]) at the time of data collection were documented. In addition, the results from all the conducted mucosal swabs for SARS–CoV-2 PCR testing were documented, as reported by participants. Ethical approval (no. 157_20 B) to conduct this analysis was granted by the institutional review board of the University Clinic of Erlangen. Written informed consent was obtained from all study participants.

Anti–SARS–CoV-2 antibody testing. IgG antibodies against the S1 domain of the spike protein of SARS–CoV-2 were tested by enzyme–linked immunosorbent assay (recent CE version [April 2020]) (Euroimmun) using the Euroimmun Analyzer I platform and according to manufacturer protocols. Optical density (OD) was determined at 450 nm with reference wavelength at 630 nm. A cutoff of ≥0.8 (OD at 450 nm) was considered as positive. Assays were performed according to the guidelines of the German Medical Association (RiliBAK) with stipulated internal and external quality controls.

Statistical analysis. Participant characteristics are described using the mean ± SD, median and interquartile range (IQR), and percentages, as appropriate. We calculated the crude proportions of seropositivity for anti–SARS–CoV-2 IgG (≥0.8, OD at 450 nm) and estimated exact 95% confidence intervals (95% CIs) based on the binomial distribution for each study group. Relative risks (RRs) of seropositivity in study groups were estimated using a Poisson regression model with robust sandwich SEs using the non–health care control group as the reference. This method enables estimation of adjusted RRs; therefore, in addition to crude RRs, we estimated RRs adjusted for age, sex, sampling time, and participant-reported exposure risk behavior (16). Adjustment for sampling time was achieved using the mean cumulative incidences of COVID-19 in the administrative districts of Erlangen and Erlangen-Höchstadt per 100,000 population as reported by the RKI for the date of serum sampling, to approximate the overall risk of exposure to SARS–CoV-2. Case count data was acquired from the RKI using the R package covid19germany (version 0.0.2; https://github.com/nevrome/covid19germany).

Exposure risk behavior was included in models as a count of favorable responses to 4 questions about compliance with social distancing, avoidance of the workplace, contact with infected individuals, and travel to risk areas. Finally, we used a similar regression to estimate the RR of losing naturally acquired SARS–CoV-2 spike IgG antibodies among initially seropositive participants during follow-up, in which we adjusted for age, sex, OD value at baseline, and number of days between baseline and follow-up samples. We used R version 4.0.1 for the analyses. Two-sided *P* values less than 0.05 or 95% CIs for RRs excluding unity were considered significant.

RESULTS

Patient characteristics. A total of 4,508 participants provided samples for SARS–CoV-2 spike protein S1 IgG antibody analysis between December, 2020 and March, 2021 (Table 1). Of these subjects, 2,869 were patients with IMIDs and 1,639 were healthy controls (455 health care professional controls and 1,184 non–health care controls). The most common IMIDs in the cohort were rheumatoid arthritis (n = 979), spondyloarthritis (SpA; n = 794, including psoriatic arthritis), connective tissue diseases (n = 307), and inflammatory bowel disease (n = 223). Among patients with IMIDs, 1,344 (47%) were treated with bDMARDs, 742 (26%) with csDMARDs, and 176 (6%) with tsDMARDs. Among bDMARDs, TNF inhibitors (n = 666), IL-17 inhibitors (n = 202), IL-23 inhibitors (n = 117), IL-6 inhibitors (n = 109), and B cell–depleting agents (n = 109) were the most frequently used drugs. Of those receiving bDMARDs, 394 patients (29%) were receiving combination treatment with csDMARDs. Overall, 1,957 participants (43%) had a history of a SARS–CoV-2 PCR test, with 152 participants (8%) having had a positive PCR test.

Seroprevalence of anti–SARS–CoV-2 antibodies in IMID patients and controls. Among the 4,508 participants, 256 (5.7%) had SARS–CoV-2 spike protein S1 IgG antibodies. Similar crude prevalence rates of humoral immune responses against SARS–CoV-2 occurred in healthy non–health care controls (84 of 1,184; 7.1%) and IMID patients without DMARD treatment (42 of 607; 6.9%). In contrast, IMID patients treated with bDMARDs (42 of 1,344; 3.1%) or csDMARDs (29 of 742; 3.9%) showed the lowest point prevalence estimate for anti–SARS–CoV-2 antibodies. Health care professional controls had a substantially higher prevalence (51 of 455; 11.2%) of anti–SARS–CoV-2 antibodies. Crude seroprevalence rates and the corresponding 95% CIs are summarized in Table 2.

Unadjusted RRs for SARS–CoV-2 IgG antibodies were significantly lower in IMID patients treated with bDMARDs (RR 0.44 [95% CI 0.31–0.62]) ($P < 0.001$) compared to non–health care controls (Table 2). These differences between healthy non–health care controls and bDMARD-treated IMID patients remained significant after adjusting for age, sex, sampling time, and participant-reported exposure risk behavior (RR 0.50 [95% CI 0.34–0.73]) ($P < 0.001$). Furthermore, the adjusted RR was numerically lower when bDMARDs were combined with csDMARDs (adjusted RR

Table 2. Unadjusted and adjusted relative risks (RRs) for SARS–CoV-2 spike IgG antibodies in IMID patients compared to non–health care controls*

Group	Total no.	No. of positive subjects	Prevalence, % (95% CI)	Unadjusted RR (95% CI)	Crude *P*	Adjusted RR (95% CI)†	Adjusted *P*
Controls							
Non–health care professionals	1,184	84	7.09 (5.70–8.71)	1 (reference)	–	1 (reference)	–
Health care professionals	455	51	11.21 (8.46–14.47)	1.58 (1.14–2.20)	0.007	1.77 (1.19–2.64)	0.005
IMID patients							
bDMARD-treated	1,344	42	3.12 (2.26–4.20)	0.44 (0.31–0.63)	<0.001	0.50 (0.34–0.73)	<0.001
csDMARD-treated	742	29	3.91 (2.63–5.57)	0.55 (0.36–0.83)	0.005	0.70 (0.45–1.08)	0.107
tsDMARD-treated	176	8	4.55 (1.98–8.76)	0.64 (0.32–1.30)	0.218	0.82 (0.39–1.72)	0.607
Untreated	607	42	6.92 (5.03–9.24)	0.98 (0.68–1.39)	0.891	1.12 (0.75–1.67)	0.591

* 95% CI = 95% confidence interval (see Table 1 for other definitions).
† Adjusted using Poisson regression for age, sex, sampling time, and participant-reported exposure risk behavior. Non–health care controls are the reference group.

0.34 [95% CI 0.16–0.71]) as opposed to bDMARD monotherapy (adjusted RR 0.55 [95% CI 0.37–0.82]), whereas a formal interaction was not detected (*P* for interaction = 0.45).

Unadjusted RRs for SARS–CoV-2 IgG antibodies were also significantly lower in IMID patients treated with csDMARDs (RR 0.55 [95% CI 0.36–0.83]) (*P* = 0.005), but after adjusting for age, sex, sampling time, and participant-reported exposure risk behavior, the point estimate shifted toward unity (RR 0.70 [95% CI 0.45–1.08]) (*P* = 0.107). Furthermore, in untreated IMID patients, there was no RR difference for developing SARS–CoV-2 IgG antibodies (RR 1.12 [95% CI 0.75–1.67]) (*P* = 0.591). As expected, the unadjusted and adjusted RRs for SARS–CoV-2 IgG antibodies were significantly higher in health care professional controls than in non–health care controls.

Seroprevalence according to diagnosis and type of treatment. In further analyses, we explored whether individual IMID groups and types of treatments influenced the RR of SARS–CoV-2 IgG antibody development. In the analyses for diagnoses, point estimates for the RR of antibody development were below unity with considerable lack of precision (Figure 1A). Patients with SpA and psoriasis showed the highest and lowest point estimates respectively, but none of them were significant. In contrast, 3 particular types of cytokine inhibitors seemed to drive the overall negative association with bDMARD treatment and antibody development. These included TNF inhibitors (adjusted RR 0.60 [95% CI 0.38–0.94]), IL-17 inhibitors (adjusted RR 0.40 [95% CI 0.16–0.98]), and IL-23 inhibitors (adjusted RR 0.28 [95% CI 0.09–0.89]) (Figure 1B).

Seroconversion in the subset of patients with positive SARS–CoV-2 PCR test results. A total of 152 among the 1,109 tested participants had a history of positive SARS–CoV-2 PCR test. When these individuals were analyzed for SARS–CoV2 IgG antibodies, we could observe that most but not all developed antibodies (120 of 152; 78%). Notably, seroconversion rates were dependent on treatment. Therefore, lack of seroconversion was found in only 16% and 15.5% in non–health care and health care controls, respectively. Additionally, only 13.3% of untreated IMID patients did not seroconvert. In contrast, the likelihood of a lack of seroconversion was numerically higher in IMID patients treated with csDMARDs (27.3%) and those receiving either bDMARDs or tsDMARDs (38.7%) (Supplementary Figure 1, available on the *Arthritis & Rheumatology* website at https://onlinelibrary.wiley.com/doi/10.1002/art.42035). Of note, the time period between positive PCR tests and analysis of antibody levels was not different between IMID patients treated with bDMARDs (median 49.5 days [IQR 35.5–82.0]), IMID patients treated with csDMARDs (median 52.0 days [IQR 46.5–75.5]), and controls (median 59.0 days [IQR 35.0–282.0]).

Longevity of the humoral immune response to SARS–CoV-2. Among the 4,508 participants, 1,812 (40.2%) had previously donated a blood sample between March 1 and June 1, 2020. The median time interval between first-wave and second-wave samples was 270 days (IQR 261–281). Among participants with available longitudinal data, there were 48 seropositive participants (2.6%) in the first wave and 81 seropositive participants (4.5%) in the second wave, which is depicted in the spaghetti plot in Supplementary Figure 2 (https://onlinelibrary.wiley.com/doi/10.1002/art.42035) and reflects the impact of the second SARS–CoV-2 wave in autumn/winter 2020. Conversely, we observed uniformly decreasing antibody levels over time among initially seropositive participants. Among 48 participants who were initially positive, 21 tested negative during the second wave, indicating a high proportion of loss (43.8%) in SARS–CoV-2 infection–induced antibodies over a 9-month period. The number and proportion of participants losing initial antibodies per study group are summarized in Supplementary Table 1 (https://onlinelibrary.wiley.com/doi/10.1002/art.42035). Of note, all 4 participants receiving bDMARDs (all anticytokine treatments) lost the initial antibody response in the second wave, corresponding to an adjusted RR of 2.86 (95% CI 1.43–5.74) compared to non–health care controls.

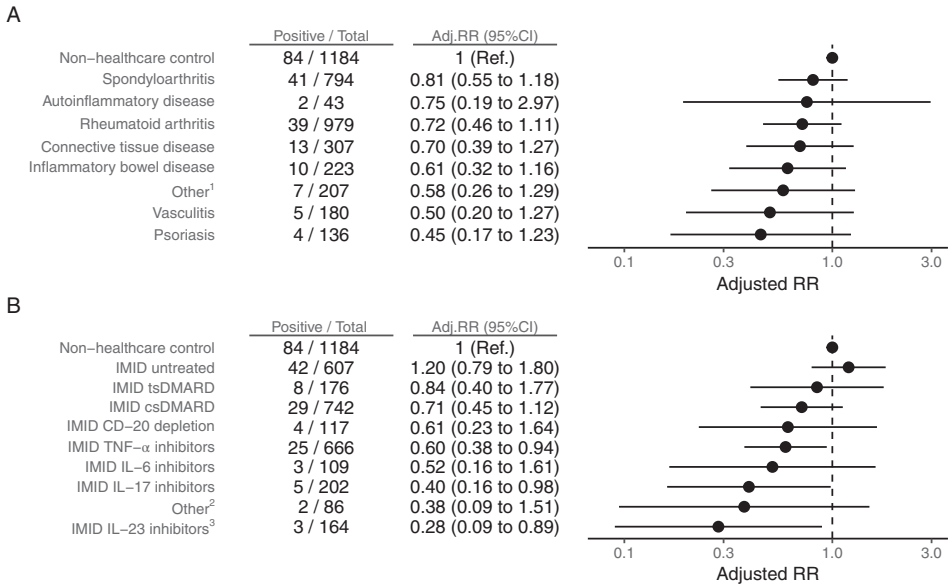

Figure 1. Relative risk (RR) of SARS–CoV-2 IgG antibody prevalence according to type of disease and type of treatment. **A**, RRs with 95% confidence intervals (95% CIs) of positive IgG antibodies against SARS–CoV-2 according to type of disease, compared to non–health care controls as the reference (Ref.). **B**, RRs with 95% CIs of positive IgG antibodies against SARS–CoV-2 according to type of treatment, compared to non–health care controls as the reference. [1] Other diagnoses include autoimmune hepatitis, uveitis, eosinophilic fasciitis, IgG4 disease, juvenile idiopathic arthritis, polymyalgia rheumatica, recurrent polychondritis, sarcoidosis, and undifferentiated arthritis. [2] Other types of blockades include neutralizing antibodies against interleukin-1 (IL-1), IL-4, IL-5, and B lymphocyte stimulator. [3] IL-23 inhibitors include IL-12/23 inhibitors as well as IL-23 inhibitors. IMID = immune-mediated inflammatory disease; tsDMARD = targeted synthetic disease-modifying antirheumatic drug; bDMARD = biologic DMARD; csDMARD = conventional synthetic DMARD; TNF = tumor necrosis factor.

DISCUSSION

This large prospective cohort study shows that IMID patients receiving bDMARDs, most of them treated with cytokine inhibitors, have lower seroprevalence rates for SARS–CoV-2 infection than healthy controls. This "protective" effect in bDMARD-treated IMID patients remained robust after adjustment for age, sex, and participant-reported exposure risk behavior and was not observed in IMID patients receiving no treatment or conventional drug treatment. The data support the concept that IMID patients treated with bDMARDs are not at particular risk during the SARS–CoV-2 pandemic, supporting statements in favor of the continuation of treatment. One exception is B cell–depleting treatment, which shows more severe courses of COVID-19 (17,18).

Based on the mere size of the cohort (>1,300 patients treated with bDMARDs and tsDMARDs) this study also allowed for assessment of the influence of different agents, in particular cytokine inhibitors, on the SARS–CoV-2 immune response. Hence, IL-23 inhibitors, IL-17 inhibitors, and TNF inhibitors were associated with significantly lower seroconversion rates. These cytokines are released upon SARS–CoV-2–induced alveolar tissue damage, mount systemic adaptive immunity to the virus, and trigger inflammation and tissue damage (19). Therefore, SARS–CoV-2 infection may not be able to induce full-blown inflammation and adaptive immune responses in hosts, in whom these mediators are neutralized by respective drugs. Targeted inhibition of these cytokines may thus not only mitigate the risk for severe COVID-19, as previously shown (2,4,5), but also attenuate the formation of anti–SARS–CoV-2 antibodies. This concept is supported by the observation that among participants with a history of SARS–CoV-2 PCR positivity, those treated with cytokine inhibitors had the lowest seroconversion rates. Supporting this notion, the time period between positive PCR tests and analysis of antibody levels was not different between IMID patients and controls.

The prospective part of this study, in which participants who were assessed in the first COVID-19 wave were reassessed during the second wave, provided insights into the persistence of the humoral response in IMID patients after SARS–CoV-2 infection. It is known from previous work that the level of humoral response corresponds with protection from COVID-19 (20). Notably, 44% of the participants lost protective SARS–CoV-2 antibody responses between the 2 sampling periods. An increased tendency toward losing protective anti–SARS–CoV-2 IgG responses was noted in initially seropositive IMID patients receiving stable anticytokine treatment. Although observed in a very small subset of patients, it is important that this finding also aligns with a lower rate of seroconversion in bDMARD-treated patients with PCR-confirmed SARS–CoV-2 infection. Consequently, protective

humoral responses against SARS–CoV-2 seem to be comparatively short-lived in IMID patients, potentially putting patients at risk for reinfection earlier and identifying a need for booster vaccination.

Our study has some limitations. IMID patients who were receiving bDMARDs not blocking cytokines, i.e., those affecting B/T lymphocytes and cell migration, constituted a minority of our study population, and thus, the analyses had less power for these subgroups in comparison to those receiving cytokine-blocking bDMARDs. Furthermore, we were able to longitudinally assess only a limited number of participants who showed positive antibodies in the first wave, among whom only a few were receiving bDMARD treatment. Therefore, the risk of losing antibodies over time needs to be confirmed in a larger group of seropositive patients. Another limitation is that the PCR test results were participant-reported and therefore potentially subject to reporting error; however, we expect such error to be evenly distributed and only bias the findings toward the null. Nonetheless, we observed a lower proportion of seroconversion among PCR-positive IMID patients who received bDMARDs. Finally, our study did not analyze the clinical manifestations in patients who were PCR-positive. However, very few study participants reported to have been hospitalized due to COVID-19. This is consistent with reported hospitalization rates for SARS–CoV-2 infection ranging between 0.06% and 1.5% (21) and reflects that studies on hospitalization rates require cohorts of infected patients, as has been done previously (17,18).

In conclusion, these data show that IMID patients receiving bDMARDs, i.e., those receiving cytokine inhibitors, have a lower prevalence rate of SARS–CoV-2 seropositivity, exhibit a blunted seroconversion rate, and lose their anti–SARS–CoV-2 antibodies faster than healthy controls or IMID patients not receiving bDMARDs. While it is highly unlikely that cytokine inhibitors lower the susceptibility to SARS–CoV-2 infection, it seems that they mitigate the overshooting inflammatory response to the virus and, consequently, the severity of SARS–CoV-2 infection. While this effect appears to be an advantage in the case of SARS–CoV-2 infection, it presents some challenges in maintaining protective immunity against the virus.

ACKNOWLEDGMENT

Open access funding enabled and organized by Projekt DEAL.

AUTHOR CONTRIBUTIONS

All authors were involved in drafting the article or revising it critically for important intellectual content, and all authors approved the final version to be published. Dr. Schett had full access to all of the data in the study and takes responsibility for the integrity of the data and the accuracy of the data analysis.

Study conception and design. Simon, Tascilar, Kleyer, Krönke, Neurath, Schett.

Acquisition of data. Simon, Tascilar, Kleyer, Fagni, Krönke, Meder, Dietrich, Orlemann, Kliem, Mößner, Liphardt, Schönau, Bohr, Schuster, Hartmann, Leppkes, Ramming, Pachowsky, Schuch, Ronneberger, Kleinert, Hueber, K. Manger, B. Manger, Atreya, Berking, Sticherling, Neurath, Schett.

Analysis and interpretation of data. Simon, Tascilar, Kleyer, Fagni, Berking, Sticherling, Neurath, Schett.

REFERENCES

1. Williamson EJ, Walker AJ, Bhaskaran K, Bacon S, Bates C, Morton CE, et al. Factors associated with COVID-19-related death using OpenSAFELY. Nature 2020;584:430–6.
2. Fagni F, Simon D, Tascilar K, Schoenau V, Sticherling M, Neurath MF, et al. COVID-19 and immune-mediated inflammatory diseases: effect of disease and treatment on COVID-19 outcomes and vaccine responses. Lancet Rheumatol 2021;3:e724–36.
3. Schett G, Sticherling M, Neurath MF. COVID-19: risk for cytokine targeting in chronic inflammatory diseases? Nat Rev Immunol 2020;20: 271–2.
4. Haberman R, Axelrad J, Chen A, Castillo R, Yan D, Izmirly P, et al. Covid-19 in immune-mediated inflammatory diseases—case series from New York. N Engl J Med 2020;383:85–8.
5. Haberman RH, Castillo R, Chen A, Yan D, Ramirez D, Sekar V, et al. COVID-19 in patients with inflammatory arthritis: a prospective study on the effects of comorbidities and disease-modifying antirheumatic drugs on clinical outcomes. Arthritis Rheumatol 2020; 72:1981–9.
6. Zhao J, Yuan Q, Wang H, Liu W, Liao X, Su Y, et al. Antibody responses to SARS-CoV-2 in patients of novel coronavirus disease 2019. Clin Infect Dis 2020;71:2233–5.
7. D'Silva KM, Serling-Boyd N, Hsu TY, Sparks JA, Wallace ZS. SARS-CoV-2 antibody response after COVID-19 in patients with rheumatic disease. Ann Rheum Dis 2021;80:817.
8. Saxena A, Guttmann A, Masson M, Kim MY, Haberman RH, Castillo R, et al. Evaluation of SARS-CoV-2 IgG antibody reactivity in patients with systemic lupus erythematosus: analysis of a multiracial and multi-ethnic cohort. Lancet Rheumatol 2021;3: e585–94.
9. Geisen UM, Berner DK, Tran F, Sümbül M, Vullriede L, Ciripoi M, et al. Immunogenicity and safety of anti-SARS-CoV-2 mRNA vaccines in patients with chronic inflammatory conditions and immunosuppressive therapy in a monocentric cohort. Ann Rheum Dis 2021;80: 1306–11.
10. Simon D, Tascilar K, Fagni F, Krönke G, Kleyer A, Meder C, et al. SARS-CoV-2 vaccination responses in untreated, conventionally treated and anticytokine-treated patients with immune-mediated inflammatory diseases. Ann Rheum Dis 2021;80:1312–6.
11. Simon D, Tascilar K, Krönke G, Kleyer A, Zaiss MM, Heppt F, et al. Patients with immune-mediated inflammatory diseases receiving cytokine inhibitors have low prevalence of SARS-CoV-2 seroconversion. Nat Commun 2020;11:3774.
12. Haberman RH, Herati R, Simon D, Samanovic M, Blank RB, Tuen M, et al. Methotrexate hampers immunogenicity to BNT162b2 mRNA COVID-19 vaccine in immune-mediated inflammatory disease. Ann Rheum Dis 2021;80:1339–44.
13. Furer V, Eviatar T, Zisman D, Peleg H, Paran S, Levartovsku D, et al. Immunogenicity and safety of the BNT162b2 mRNA COVID-19 vaccine in adult patients with autoimmune inflammatory rheumatic diseases and in the general population: a multicentre study. Ann Rheum Dis 2021;80:1330–8.
14. Deepak P, Kim W, Paley MA, Yang M, Carvidi AB, Demissie EG, et al. Effect of immunosuppression on the immunogenicity of mRNA vaccines to SARS-CoV-2: a prospective cohort study. Ann Intern Med 2021;147:1572–85.

15. Edridge AW, Kaczorowska J, Hoste AC, Bakker M, Klein M, Loens K, et al. Seasonal coronavirus protective immunity is short-lasting. Nat Med 2020;26:1691–3.
16. Chen W, Qian L, Shi J, Franklin M. Comparing performance between log-binomial and robust Poisson regression models for estimating risk ratios under model misspecification. BMC Med Res Methodol 2018;18:63.
17. Sparks JA, Wallace ZS, Seet AM, Gianfrancesco MA, Izadi Z, Hyrich KL, et al. Associations of baseline use of biologic or targeted synthetic DMARDs with COVID-19 severity in rheumatoid arthritis: results from the COVID-19 Global Rheumatology Alliance physician registry. Ann Rheum Dis 2021;80:1137–46.
18. Strangfeld A, Schäfer M, Gianfrancesco MA, Lawson-Tovey S, Liew JW, Ljung L, et al. Factors associated with COVID-19-related death in people with rheumatic diseases: results from the COVID-19 Global Rheumatology Alliance physician-reported registry. Ann Rheum Dis 2021;80:930–42.
19. Pedersen SF, Ho YC. SARS-CoV-2: a storm is raging. J Clin Invest 2020;30:2202–5.
20. Lumley SF, O'Donnell D, Stoesser NE, Matthews PC, Howarth A, Hatch SB, et al. Antibody status and incidence of SARS-CoV-2 infection in health care workers. N Engl J Med 2020;384:533–40.
21. Subramanian R, He Q, Pascual M. Quantifying asymptomatic infection and transmission of COVID-19 in New York City using observed cases, serology, and testing capacity. Proc Natl Acad Sci U S A 2021;118:e2019716118.

Arthritis & Rheumatology
Vol. 74, No. 5, May 2022, pp 791–800
DOI 10.1002/art.42051

American College of Rheumatology
Empowering Rheumatology Professionals

Association of Polygenic Risk Scores With Radiographic Progression in Patients With Rheumatoid Arthritis

Suguru Honda,[1] Katsunori Ikari,[1] Koichiro Yano,[1] Chikashi Terao,[2] Eiichi Tanaka,[1] Masayoshi Harigai,[1] and Yuta Kochi[3]

Objective. To investigate whether polygenic risk scores obtained using data from a genome-wide association study (GWAS) of rheumatoid arthritis (RA) susceptibility can be predictors of radiographic progression.

Methods. We constructed polygenic risk scores using GWAS summary data on associations of single-nucleotide polymorphisms with RA susceptibility. The polygenic risk scores were stratified into quintiles based on levels of significance (ranging from top quintile of polygenic risk scores to bottom quintile). In addition, change in the Sharp/van der Heijde score (SHS) of radiographic progression over the first 5 years after onset of RA was assessed. The change in SHS over 5 years was stratified according to quartiles, with the top quartile of change in SHS defined as severe radiographic progression (score change of >35 points) and the remaining 3 quartiles defined as nonsevere radiographic progression. Polygenic risk scores were assessed for their ability to predict the SHS status over 5 years in a training set (n = 500 RA patients) for selection of the best model, and in a testing set (n = 740 RA patients) for validation of the data. We evaluated the performance of the polygenic risk score as a predictor of severe radiographic progression in univariable and multivariable analyses with inclusion of other factors.

Results. Polygenic risk scores constructed from 43,784 single-nucleotide polymorphisms significantly differed between patients who experienced severe radiographic progression and those with nonsevere radiographic progression in both the training set ($P = 0.0064$) and the testing set ($P = 0.017$). Patients with polygenic risk scores in the top quintile had a higher risk of severe progression compared to those with polygenic risk scores in the bottom quintile (odds ratio [OR] 1.90, $P = 0.0022$), and the risk of severe radiographic progression was even higher when restricted to patients who were younger at disease onset (OR 5.06, $P = 0.00038$). The group with polygenic risk scores in the top quintile and the anti–citrullinated protein antibody (ACPA)–positive group had significantly higher proportions of patients with severe radiographic progression ($P = 0.00052$ and $P = 0.0022$, respectively) compared to the remaining groups. Multivariable analysis showed that polygenic risk score ($P = 0.00019$) as well as female sex ($P = 0.0033$), ACPA positivity ($P = 0.0023$), and body mass index ($P = 0.024$) were independent risk factors for severe radiographic progression.

Conclusion. A polygenic risk score that is derived from GWAS data on RA susceptibility is associated with the level of severity of radiographic progression in patients with RA.

INTRODUCTION

Rheumatoid arthritis (RA) is a chronic autoimmune inflammatory disease that leads to joint destruction and reduction in quality of life. The goal of treatment is to suppress bone destruction and improve physical activity. The number of patients with severe radiographic progression has decreased over the last decades due to younger age at diagnosis and the development of several therapeutic agents. However, in a percentage of patients, prevention of severe radiographic progression remains a challenge due

Supported by the Japan Society for the Promotion of Science (Kakenhi Grant-in-Aid JP19K09583 and JP20H03722) and the Medical Research Institute of Tokyo Medical and Dental University Joint Usage/Research Program.

[1]Suguru Honda, MD, Katsunori Ikari, MD, PhD, Koichiro Yano, MD, PhD, Eiichi Tanaka, MD, PhD, Masayoshi Harigai, MD, PhD: Tokyo Women's Medical University School of Medicine and Tokyo Women's Medical University Hospital, Tokyo, Japan; [2]Chikashi Terao, MD, PhD: RIKEN Center for Integrative Medical Sciences, Yokohama, Japan, and Shizuoka General Hospital and University of Shizuoka, Shizuoka, Japan; [3]Yuta Kochi, MD, PhD: Tokyo Medical and Dental University, Tokyo, Japan.

Author disclosures are available at https://onlinelibrary.wiley.com/action/downloadSupplement?doi=10.1002%2Fart.42051&file=art42051-sup-0001-Disclosureform.pdf.

Address correspondence to Yuta Kochi, MD, PhD, Department of Genomic Function and Diversity, Medical Research Institute, Tokyo Medical and Dental University, Yushima, 1-5-45, Bunkyo-ku, Tokyo 113-8510, Japan. Email: y-kochi.gfd@mri.tmd.ac.jp.

Submitted for publication July 29, 2021; accepted in revised form December 9, 2021.

to inadequate treatment response or adverse events associated with therapeutic agents (1,2). Furthermore, previous studies demonstrated that anti–citrullinated protein antibodies (ACPAs) and the presence of HLA-region genes were associated with bone destruction, but their predictive accuracy was not sufficient (3–6). Therefore, identifying additional factors associated with radiographic progression in RA is an important step in developing more accurate predictive models for precision medicine.

In addition to HLA–DRB1 alleles, which have a strong impact on RA, previous genome-wide association studies (GWAS) have identified >100 genetic regions and single-nucleotide polymorphisms (SNPs) associated with RA susceptibility (7–9). These SNPs associated with RA susceptibility may have the potential to predict disease progression. In fact, several studies of RA have demonstrated that HLA–DRB1 alleles and non-HLA gene alleles, such as those of *PADI4* and *C5orf3*, are also associated with radiographic progression (5,10). However, when the cumulative effects of alleles associated with RA susceptibility were evaluated with the use of a genetic risk score (GRS)—a method of scoring the risk of RA susceptibility associated with non-HLA alleles in loci previously determined to be significant by GWAS—it was observed that the GRS was not significantly associated with radiographic progression of RA (11). These results indicate that loci found to have genome-wide significance in RA may not be sufficiently informative by themselves, and that incorporation of nonsignificant GWAS alleles might improve predictability.

Polygenic risk scores are useful tools that estimate the propensity to develop or display a certain phenotype, with the scores represented by a single value that is calculated as the sum of the variant alleles present, weighted by the effect size of each allele based on prior GWAS data on significance. The strength of a polygenic risk score is that it can capture the missing heritability derived from the loss of small-effect SNPs without significant GWAS signals by setting a proper threshold for selecting SNPs. In the present study, we constructed polygenic risk scores using the summary statistics from a large GWAS meta-analysis of RA susceptibility, assessed the risk of severe radiographic progression based on polygenic risk score, and compared the predictive capacity of the polygenic risk score to that of presence of ACPAs and the HLA region in terms of predicting the risk of radiographic progression of RA. We confirmed that the polygenic risk score was an independent risk factor for radiographic progression in patients with RA and that its discriminatory power in predicting severe radiographic progression is comparable to that of ACPAs.

PATIENTS AND METHODS

Study population. The study design is shown in Figure 1. Participants' clinical information was obtained from the Institute of Rheumatology, Rheumatoid Arthritis (IORRA) cohort, which was established in 2000 and began collecting genotype data in 2002. The IORRA cohort is a large, institute-based, single observational cohort of Japanese patients with RA, and includes ~1%

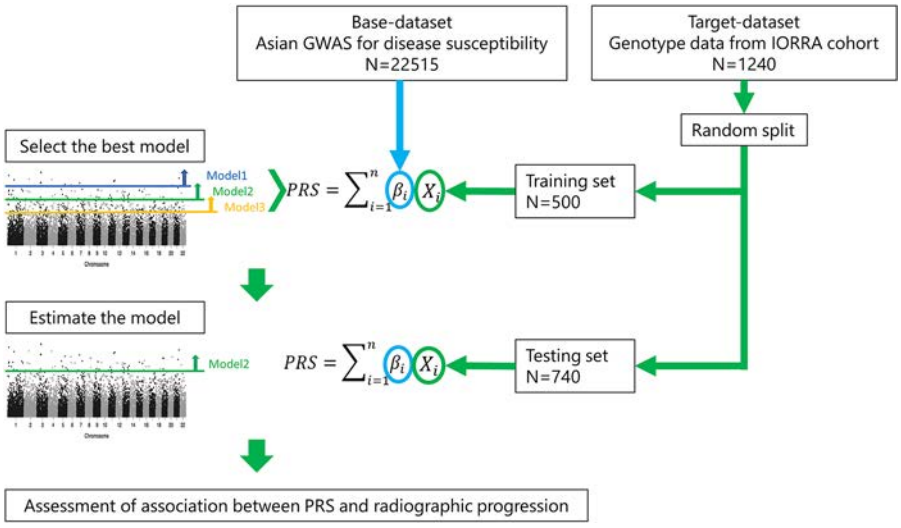

Figure 1. Flow diagram showing the study design. Polygenic risk scores (PRS) were constructed using a base data set containing genome-wide association study (GWAS) data on associations of single-nucleotide polymorphisms with rheumatoid arthritis (RA) susceptibility in Asian patients, and a target data set of GWAS data from the Institute of Rheumatology, Rheumatoid Arthritis (IORRA) cohort. Polygenic risk scores were calculated for each individual in the target data set by summing the number of effect alleles (X) weighted by the effect size (β) obtained from the base data set. Patients were randomly stratified into a training set (n = 500) and a testing set (n = 740). The best model that yielded the largest Nagelkerke's pseudo R^2 in the training set was selected. The same *P* value threshold and r^2 were applied to the testing set. The performance of polygenic risk scores in univariable as well as multivariable analyses was then assessed.

of all Japanese RA patients (12). Patients were classified as having no history of periodontitis if there was no evidence of periodontitis in the clinical record, or if they indicated by questionnaire that they had never been diagnosed as having periodontitis. Body mass index (BMI) was extracted from the cohort record of each patient at the closest time point to the age at onset of RA.

Ethics approval. The IORRA cohort studies (2952-R and 2922-R16) and their genetic study (217C) were approved by the ethics committee of the Tokyo Women's Medical University, and informed consent was obtained from all patients before each survey. The genetic analysis was also approved by the ethics committee of the Medical Research Institute, Tokyo Medical and Dental University (02019-005-04).

Genotype data. Genotyping and quality control were performed using the Illumina HumanCoreExome and HumanOmniExpress BeadChip, as previously described (13). Identity by descent similarity was determined using Plink (14), and individuals shown to have familial relationships (PI_HAT >0.25) were excluded from the study. Genotype data were further imputed with the 1000 Genomes Project database (phase 3 release) using Minimac4 version 1.0.0 software. After imputation, we excluded variants with an imputation quality of Rsq <0.7 or those with a minor allele frequency of <1% or those in Hardy–Weinberg equilibrium ($P < 1.0 \times 10^{-7}$) as determined using the Plink program. In total, 1,240 patients were included in the study.

Evaluation of radiographic joint damage. Radiographic findings from 5 years after onset of RA were collected from the patients' medical records. The Sharp/van der Heijde score (SHS), which was determined by a single experienced evaluator (KY) using anteroposterior radiographs of the hands, was used to evaluate radiographic joint damage. Change in the SHS over the first 5 years after the onset of RA was stratified into quartiles. The top quartile was defined as severe radiographic progression (change in SHS of >35 points) and the remaining quartiles were defined as nonsevere radiographic progression.

Construction of polygenic risk scores. Individual polygenic risk scores were calculated using the sum of the number of effect alleles (X) from genotype data of the IORRA cohort, weighted by the effect size (β) from the GWAS meta-analysis calculated using the following formula:

$$PRS = \sum_{i=1}^{n} \beta_i X_i$$

where n denotes the number of variants, β_i denotes the effect size of i-th SNP, and X_i denotes the genotype dosage of the i-th SNP in an individual. We selected SNPs with the pruning and thresholding method (15) by using summary data on RA susceptibility in Asian patients in a GWAS meta-analysis (9) combined with data on RA susceptibility in Japanese and Chinese populations from the 1000 Genomes Project (phase 3 release) as the linkage disequilibrium reference panel.

Polygenic risk scores for individuals in the IORRA cohort were constructed using PRSice-2 software (16) with the following flags: --clump-kb 250kb, --clump-p 1.0, and --clump-r^2 0.1, 0.2, 0.3, 0.5, 0.7, and 0.9. For the *P* value threshold, we used the default parameters of the PRSice program (lower threshold $P = 5 \times 10^{-8}$, upper threshold $P = 0.5$, interval $P = 5 \times 10^{-5}$). We performed a holdout validation by randomly dividing the patients into 2 groups: the training set (n = 500) and the testing set (n = 740) (Figure 1). We selected the best model that yielded the largest R^2 in the training set. We applied the same *P* value threshold and R^2 to the testing set and evaluated the performance of the model.

Statistical analysis to assess association between polygenic risk score and SHS progression. We compared polygenic risk scores between the severe radiographic progression group and the nonsevere radiographic progression group using Welch's *t*-test. The capacity of the polygenic risk score to predict radiographic progression was evaluated using the area under the curve (AUC). In addition, using logistic regression analysis, we constructed quantile plots to examine the risk of radiographic progression among patients with RA according to quintiles of polygenic risk score. The quintiles were based on levels of significance, with the top quintile indicating the highest polygenic risk scores, and the bottom quintile indicating the lowest polygenic risk scores. In these analyses stratified by SHS progression group and polygenic risk score, patients were assigned a binary SHS status and a binary polygenic risk score status for regression. For binary polygenic risk score status, a code of 0 was assigned to patients in the bottom quintile for polygenic risk score and a code of 1 was assigned to those in the remaining quintiles. For binary SHS status, a code of 0 was assigned to patients in the nonsevere radiographic progression group and a code of 1 to those in the severe radiographic progression group.

A logistic regression model was applied to analyze the association between SHS status and a combination of polygenic risk score, the presence of serine at position 11 (Ser^{11}) in *HLA–DRB1*, and clinical characteristics including age at onset, sex, smoking status, BMI at the time of initial registration, rheumatoid factor and ACPA positivity, periodontitis, and treatment with methotrexate (MTX) and/or biologic disease-modifying antirheumatic drugs (bDMARDs) during a follow-up period of 5 years. Quantitative variables (age, BMI, and polygenic risk score) were normalized before applying the model. Variance inflation factor (VIF) was used to check for multicollinearity among the covariates using R version 3.4.2 and its package car. The Nagelkerke's pseudo-R^2 and AUC were generated using the R packages BaylorEdPsych and pROC. Finally, we performed 10-fold cross-validation (training to testing ratio 9:1) to evaluate the performance of the logistic regression model while reducing overfitting using scikit-learn from Python.

Data from the GWAS meta-analysis of Asian patients with RA are available on the Japanese ENcyclopedia of GEnetic associations (JENGER) website by Riken (see http://jenger.riken.jp/en/result). The list of SNPs used in the polygenic risk scores is available upon request from the corresponding author.

RESULTS

Patient characteristics. Patients were randomly divided into 2 groups: the training set and the testing set (Figure 1). The mean age at disease onset in the training and testing sets was 48.7 years and 48.5 years, respectively, the proportion of female patients was 85.8% and 85.6%, respectively, and the median SHS was 16 in both groups (see Supplementary Table 1, available on the *Arthritis & Rheumatology* website at http://onlinelibrary.wiley.com/doi/10.1002/art.42051). The percentages of patients treated with MTX and/or bDMARDs were low because radiographs of the joints were obtained from the majority of patients who participated in this cohort before the introduction of MTX and bDMARDs into clinical use in the Japanese health care system.

Construction of polygenic risk scores and their classification accuracy for prediction of radiographic disease progression. To construct a polygenic risk score model that would explain and predict an individual's SHS status, we first determined the *P* and r^2 value thresholds to construct the best polygenic risk score model using the training set. In the training set (n = 500), the best polygenic risk score model for binary SHS status consisted of 43,784 SNPs, at a *P* value threshold of 0.13 (*P* = 0.0026) and R^2 value threshold of 0.1 (Nagelkerke's pseudo-R^2 = 0.027) (see Supplementary Figure 1, available on

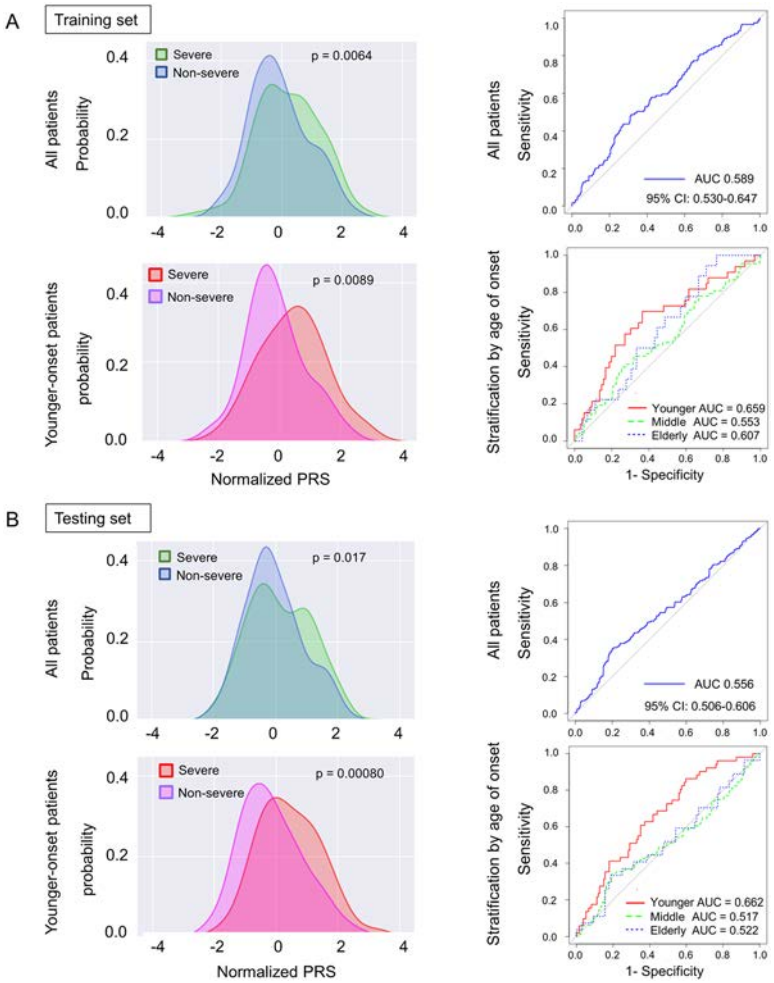

Figure 2. Classification accuracy of polygenic risk scores in predicting the severity of radiographic progression in patients with rheumatoid arthritis (RA) in the training and testing sets. Left, Probability density plots of normalized polygenic risk scores (PRS) with kernel density estimation using Gaussian distributions in all patients with RA and in patients according to the age at onset of RA, in the training set (**A**) and the testing set (**B**). Right, Area under the curve (AUC) analyses for assessment of accuracy of the model in predicting severe radiographic progression in all patients and in patients according to the age at onset of RA, in the training set (**A**) and the testing set (**B**). Age groups were defined as follows: younger age at onset ≤40 years, middle age at onset >40 but ≤60 years, and elderly age at onset >60 years.

the *Arthritis & Rheumatology* website at http://onlinelibrary.wiley.com/doi/10.1002/art.42051). In the testing set (n = 740), the polygenic risk score with the same SNPs was significantly associated with the binary SHS status ($P = 0.012$). A significant association was also shown when polygenic risk scores were constructed for quantitative SHS ($P = 0.013$ for the training set and $P = 0.018$ for the testing set) (Supplementary Figure 1).

We then compared the polygenic risk scores between the severe and nonsevere radiographic progression groups, and a significant difference was observed in the training set (mean ± SD normalized polygenic risk score 0.22 ± 1.03 in the severe radiographic progression group versus –0.07 ± 0.98 in the nonsevere radiographic progression group; $P = 0.0064$) (Figure 2A). A significant difference was replicated in the testing set (mean ± SD normalized polygenic risk score 0.16 ± 1.04 in the severe radiographic progression group versus –0.05 ± 0.98 in the nonsevere radiographic progression group; $P = 0.017$) (Figure 2B), demonstrating that our polygenic risk score model was robust in its ability to distinguish SHS status.

We used AUC analysis to assess the classification accuracy of polygenic risk scores. The ability of the model to discriminate between severe and nonsevere radiographic progression was shown by an AUC of 0.589 for the training set (Figure 2A) and 0.556 for the testing set (Figure 2B).

Based on the findings of a previous study on systemic lupus erythematosus which showed that the prediction accuracy of polygenic risk scores improved as the age at onset of RA decreased (17), patients were stratified into 3 groups according to their ages at the onset of RA: younger age at onset (≤40 years), middle age at onset (>40 but ≤60 years), and elderly age at onset (>60 years). In the training and testing sets, the difference in polygenic risk scores between the severe and nonsevere radiographic progression groups was significant in the group of patients who were younger at onset of RA ($P = 0.0089$ for those in the training set and $P = 0.00080$ for those in the testing set) (Figures 2A and B), whereas there was no significant difference between the severe and nonsevere radiographic progression groups among patients with onset of RA in middle age ($P = 0.27$ in the training set and $P = 0.54$ in the testing set) or in patients with onset of RA in elderly age ($P = 0.15$ in the training set and $P = 0.81$ in the testing set). We calculated the AUC to assess the ability of the model to discriminate between those with severe radiographic progression and those with nonsevere radiographic progression according to age at RA onset. Compared with the middle age and elderly age at onset groups, the AUC was highest in the younger age at onset group, with an AUC of 0.659 in the training set (Figure 2A) and an AUC of 0.662 in the testing set (Figure 2B).

Assessment of the risk of severe radiographic progression based on polygenic risk score quintiles. We next compared the risk of being classified into the severe radiographic progression group according to quintiles of polygenic risk scores, assessed among all 1,240 patients with RA. The patients in the top quintile for polygenic risk score had approximately twice the risk of being classified into the severe progression group compared with patients in the bottom quintile ($P = 0.0022$, odds ratio [OR] 1.90 [95% confidence interval (95% CI) 1.26–2.86]) (Figure 3A). When we restricted the analysis to the group of patients with younger age at RA onset, patients in the top quintile and the second quintile of polygenic risk scores had a significant risk of being classified into the severe progression group ($P = 0.00038$, OR 5.06 [95% CI 2.07–12.4] and $P = 0.0087$, OR 3.38 [95% CI 1.36–8.37], respectively) (Figure 3B).

Similar results were obtained from analysis of the testing set, in which those in the top quintile of polygenic risk scores had a greater risk of being classified into the severe progression group compared with those in the bottom quintile ($P = 0.019$, OR 1.87 [95% CI 1.11–3.15]), and those in the top quintile of polygenic risk scores who had a younger age at onset of RA also had a greater risk of severe radiographic progression compared with those in the bottom quintile ($P = 0.003$, OR 6.29 [95% CI 1.85–21.4] (see Supplementary Figure 2, available on the *Arthritis &*

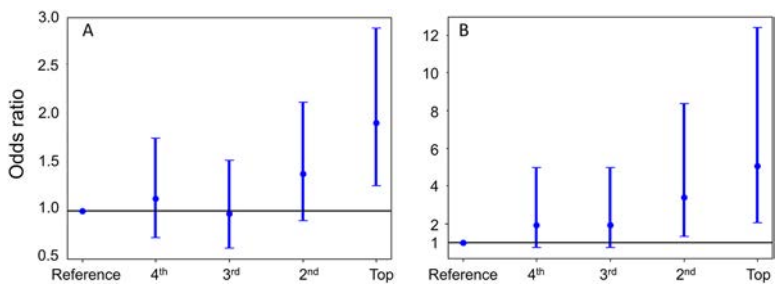

Figure 3. Quantile plots for polygenic risk scores in all patients and in patients with younger age at onset of rheumatoid arthritis (RA). All patients (n = 1,240) (**A**) and patients with younger age at RA onset (n = 314) (**B**) were separated into quintiles according to polygenic risk score, and odds ratios for the likelihood of an association between quintile of polygenic risk score and severe radiographic progression were generated using logistic regression analysis. The top quintile in all patients showed significantly higher risks for severe radiographic progression ($P = 0.0022$) compared with the reference quintile (**A**), as did the top and second quintiles in the younger age at onset group ($P = 0.00038$ and $P = 0.0087$, respectively) (**B**). Values are the odds ratios with 95% confidence intervals.

Rheumatology website at http://onlinelibrary.wiley.com/doi/10.1002/art.42051). Conversely, patients in the middle and elderly age at onset groups had no significant increase in risk of being classified into the severe progression group, including those patients with polygenic risk scores within the top quintile.

Comparison of the discriminatory power of polygenic risk scores, ACPAs, and Ser^{11} for identifying severe radiographic progression. We compared the predictive capacity of polygenic risk scores to ACPAs and variants in the HLA region, which are known factors associated with radiographic progression (3,18,19). Multiple genes, including *HLA–DRB1* and *HLA–DPB1*, and their amino acid residues have been associated with disease susceptibility as well as with radiographic progression. We performed association analyses based on the classic shared epitope status of *HLA–DRB1*, amino acid residues/positions of *HLA–DRB1/HLA–DPB1* (20,21), and haplotypes of *HLA–DRB1* (22). Only the presence of Ser^{11} in *HLA–DRB1* was significantly associated with radiographic progression ($P = 0.046$) (see Supplementary Figures 3 and 4, available on the *Arthritis & Rheumatology* website at http://onlinelibrary.wiley.com/doi/10.1002/art.42051). Therefore, we decided to use Ser^{11} to represent the HLA region in the subsequent analyses.

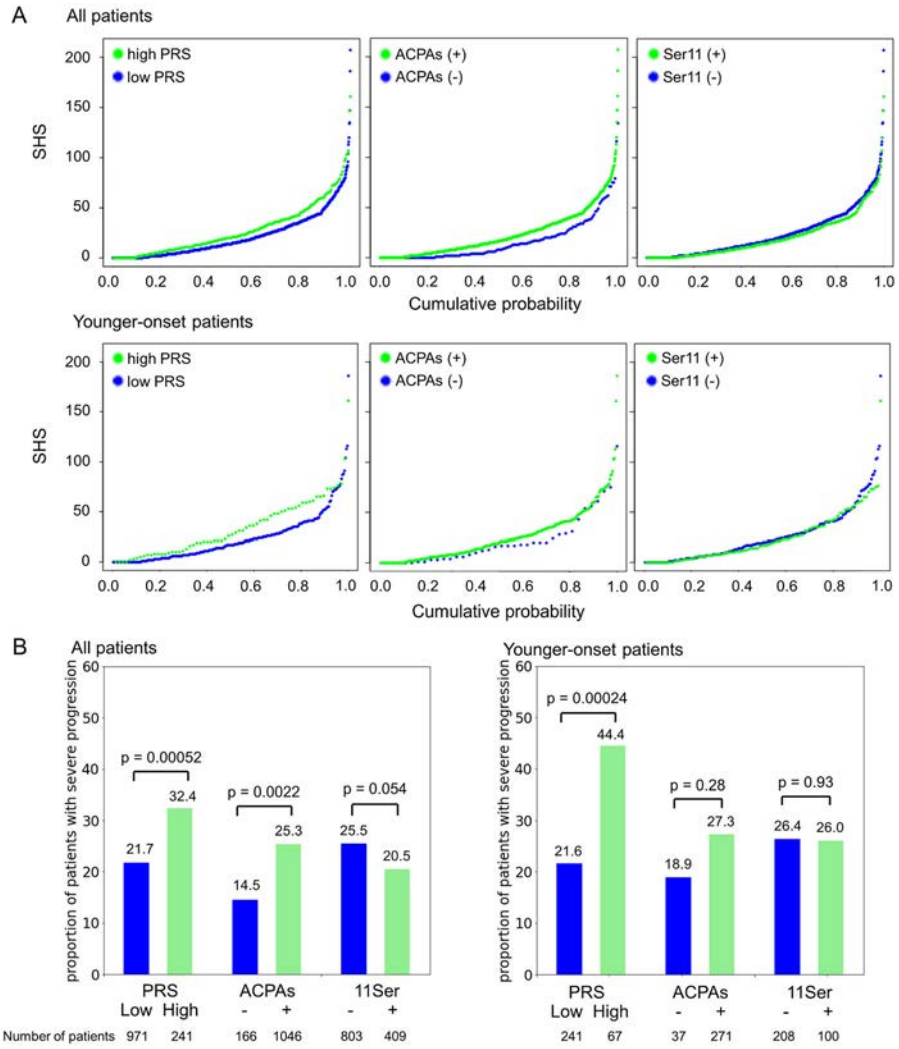

Figure 4. Discriminatory power of polygenic risk scores (PRS) (high versus low), anti–citrullinated protein antibody (ACPA) positivity (versus ACPA negativity), and presence (versus absence) of serine at position 11 (Ser11) in *HLA–DRB1* with regard to predicting changes in the Sharp/van der Heijde score (SHS) of radiographic progression in the first 5 years after the onset of rheumatoid arthritis (RA). **A**, Cumulative probability plots of association of each factor with change in the SHS over the first 5 years after disease onset are shown for all patients (top) and for patients with younger age at onset of RA (bottom). Each point in the plot represents an individual patient. **B**, Bar plots show the proportions of patients in whom an association of each factor with severe radiographic progression was observed, assessed in all patients (left) and in patients with younger age at onset of RA (right). Numbers over the bars are the percentage of patients.

Table 1. Multivariable analysis of risk factors for radiographic progression in RA using a logistic regression model*

Variable	Referent	OR (95% CI)	*P*
Sex (female)	Male	2.02 (1.26–3.23)	0.0033
Age at RA onset†	–	0.96 (0.84–1.11)	0.61
Ever smoker (yes)	No	0.84 (0.63–1.13)	0.25
ACPA positive	Negative	2.60 (1.41–4.80)	0.0023
Rheumatoid factor positive	Negative	0.68 (0.43–1.08)	0.10
Ser^{11} (1 or 2 amino acids)	0	0.72 (0.53–0.96)	0.027
BMI†	–	0.86 (0.76–0.98)	0.024
Periodontitis (yes)	No	1.19 (0.82–1.74)	0.36
MTX treatment (yes)	No	1.32 (0.99–1.76)	0.055
bDMARD treatment (yes)	No	0.46 (0.27–0.82)	0.0082
PRS†	–	1.30 (1.13–1.50)	0.00019

* RA = rheumatoid arthritis; 95% CI = 95% confidence interval; ACPA = anti–citrullinated protein antibody; Ser^{11} = serine at position 11 in *HLA–DRB1*; BMI = body mass index; MTX = methotrexate; bDMARD = biologic disease-modifying antirheumatic drug; PRS = polygenic risk score.
† Normalized continuous variable. The corresponding odds ratio (OR) represents the likelihood of a 1-unit increase in that variable.

We created cumulative probability plots to visualize the discriminatory power of 3 factors (polygenic risk scores, ACPAs, and Ser^{11}) for radiographic progression after excluding 28 patients without *HLA–DRB*1 data (n = 1,212). Based on the findings shown in the quantile plot for polygenic risk scores in all patients (Figure 3A), we divided patients into 2 groups: the top quintile (high polygenic risk scores) versus the remaining quintiles (low polygenic risk scores). Cumulative probability plots for all patients suggested that polygenic risk scores and ACPAs had comparable discriminatory power for distinguishing between the severe and nonsevere radiographic progression groups (Figure 4A), with significant differences in the proportion of patients with severe radiographic progression based on these factors (Figure 4B). However, analysis of patients who were younger at RA onset showed a significant difference in SHS status only in the comparison between high and low polygenic risk score ($P = 0.00024$) (Figures 4A and B). This indicates that polygenic risk scores had greater discriminatory power than Ser^{11} in predicting severe radiographic progression of RA in patients with younger age at onset. Similar results were obtained when analysis was restricted to the testing set (see Supplementary Figure 5, available on the *Arthritis & Rheumatology* website at http://onlinelibrary.wiley.com/doi/10.1002/art.42051).

Confirmation of the association between polygenic risk scores and radiographic progression in multivariable analysis. We conducted multivariable analysis using a logistic regression model to investigate the associations between SHS status and a combination of polygenic risk scores and age at RA onset, sex, smoking status, ACPA positivity, rheumatoid factor positivity, BMI, periodontitis, treatment with methotrexate, treatment with bDMARDs, and the presence of Ser^{11} in *HLA–DRB1*. We evaluated the VIF of each variable to check for multicollinearity, but none of the VIFs exceeded 10, indicating negligible collinearity in the model. Multivariable analysis showed that polygenic risk score ($P = 0.00019$), female sex ($P = 0.0033$), ACPA positivity ($P = 0.0023$), treatment with bDMARDs ($P = 0.0082$), presence of Ser^{11} ($P = 0.027$), and BMI ($P = 0.024$) were independent risk factors for severe radiographic progression (Table 1). Nagel-kerke's pseudo R^2 of the multivariable model was 0.072, and the AUC was 0.648 (Figure 5A).

We also performed a multivariable analysis for quantitative SHS using SHS score as a continuous value in multiple regression analysis and obtained similar results (see Supplementary Table 2, available on the *Arthritis & Rheumatology* website at http://onlinelibrary.wiley.com/doi/10.1002/art.42051). In analyzing the sensitivity and specificity of the model with patients stratified according to age at RA onset, the accuracy for prediction of severe versus nonsevere radiographic progression in the multivariable model with polygenic risk scores was higher in the younger age at onset of RA group (AUC 0.711) than in the middle and elderly age at onset groups (AUC 0.648 and AUC 0.688, respectively) although the difference was not statistically significant ($P = 0.12$ for younger age at onset versus middle age at onset and $P = 0.69$ for younger onset versus elderly onset). Similar results were obtained in the analysis limited to the testing set (see Supplementary Figure 6, available on the *Arthritis & Rheumatology* website at http://onlinelibrary.wiley.com/doi/10.1002/art.42051).

To estimate the generalizability of the model and reduce the risk of overfitting, we divided the patients into a training set and a validation set in a ratio of 9:1 and performed 10-fold cross-validation. The mean ± SD AUC for prediction of severe radiographic progression was 0.628 ± 0.047 among all patients and 0.682 ± 0.060 among the group of patients who were younger at the onset of RA.

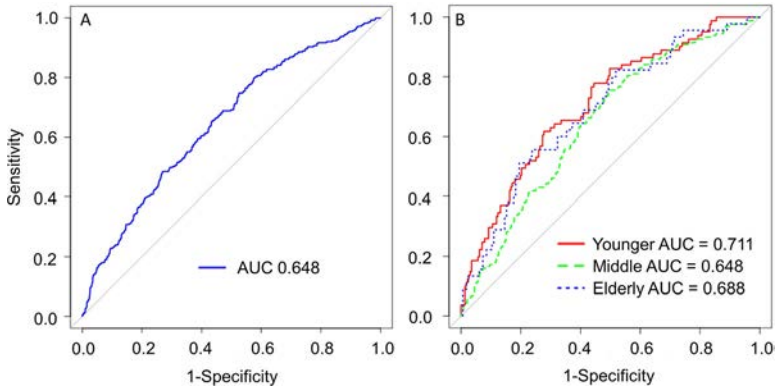

Figure 5. The classification accuracy of the multivariable model for predicting the severity of radiographic progression in patients with rheumatoid arthritis (RA), assessed using area under the curve (AUC) analyses in all patients (**A**) and in patients stratified according to age at onset of RA (**B**). The younger, middle, and elderly age groups are defined in Figure 2.

DISCUSSION

To our knowledge, this is the first study to show that polygenic risk scores constructed with the use of alleles associated with RA susceptibility, including those in loci considered not to have genome-wide significance, are associated with the severity of radiographic progression of RA. After patients were stratified according to age at onset of RA, the capacity of polygenic risk scores to accurately predict the severity of radiographic progression improved in patients who were younger at the time of disease onset. The discriminatory power of polygenic risk scores to distinguish between severe and nonsevere radiographic progression was comparable to that of ACPAs and was significantly greater than HLA–DRB1 alleles (Ser^{11}) when restricted to patients who were younger at the onset of RA.

Furthermore, our multivariable model, which used a combination of polygenic risk scores and other clinical characteristics, revealed that polygenic risk scores were an independent risk factor for severe radiographic progression in patients with RA. This finding is in contrast to previous research in which it was found that a GRS using only non-HLA alleles with genome-wide significance was not significantly associated with radiographic progression (11). This indicates that in order to increase the capacity of polygenic risk scores to predict the severity of radiographic progression, it is essential to incorporate small-effect SNPs not previously shown to have significant genome-wide significance.

Additionally, our findings in a model constructed with polygenic risk scores and disease onset (equivalent to disease susceptibility) as factors indicate that polygenic risk scores are associated with the disease phenotype in patients with RA, which is similar to the findings with regard to varying phenotypes in other diseases (23,24). In the setting of RA, non-HLA alleles associated with disease susceptibility, such as variants in *PADI4* and *C5orf3*, have also been associated with radiographic progression (5,10). Because *PADI4* generates citrullinated autoantigenic proteins (the targets of ACPAs), the consistent presence of self antigens may also be important for the persistence of arthritis (5). *C5orf3*, which is highly expressed in RA synovial fibroblasts, could suppress proinflammatory cytokines via the regulation of cell migration and the cell cycle (10). These pieces of evidence suggest that a substantial proportion of genes that are involved in the onset of RA are also involved in the progression of the disease.

In this study, the accuracy with which polygenic risk scores predicted the severity of radiographic progression was shown to be greater in patients who were younger at the time of RA onset compared to patients who were of middle or elderly age. A similar observation has been reported in the setting of systemic lupus erythematosus; polygenic risk scores had the best predictive accuracy for disease onset in patients age <20 years compared to patients age ≥20 years (17). These observations related to age at disease onset may be attributable to the biased distribution of age at onset among those patients recruited in the GWAS analyses whose data were used to construct the polygenic risk scores in this model (17). Because the demographic group most prevalent in GWAS conducted in Asia is middle-aged women, the loci determined to be significant may represent the genetic factors of this population but not of other populations, such as elderly men. In our study, a higher proportion of patients who were elderly at the onset of RA were male compared to those who were younger at RA onset (20.7% versus 12.1%, respectively), which may have decreased the accuracy with which the severity of radiographic progression was predicted by the polygenic risk scores. Thus, large-scale or stratified GWAS are needed to improve the performance of polygenic risk scores in predicting severe radiographic progression in male patients with RA whose disease onset occurred at an elderly age.

In this study, low BMI was associated with radiographic progression in patients with RA. To investigate whether low BMI is the cause of bone destruction or the result of inflammation, we assessed changes in BMI over 5 years. However, there was no significant change in BMI in either the severe or nonsevere radiographic progression groups. In patients with severe radiographic progression, BMI was 20.8 kg/m^2 at the time of registration

versus 21.0 kg/m^2 after 5 years ($P = 0.28$), and in patients with nonsevere radiographic progression, BMI was 21.5 kg/m^2 at the time of registration versus 21.6 kg/m^2 after 5 years ($P = 0.42$). These results indicate that a low BMI may be an independent risk factor for radiographic progression in RA. In fact, recent studies demonstrated that obesity in patients with RA was associated with a lower rate of radiographic progression (25–28). However, because this population of patients with obesity showed low treatment response (27,28), further research is needed to determine whether low body weight is a direct cause of bone destruction or a confounding factor.

This study has some limitations. The proportion of patients being treated with MTX and/or bDMARDs in the present study (76.4% with MTX and 29.5% with bDMARDs) was lower than the proportions currently being treated with MTX and/or bDMARDs in an ongoing study of the IORRA cohort (12), which could result in an overestimation of the capacity of polygenic risk scores to predict the severity of radiographic progression. Therefore, we cannot directly apply the results of our polygenic risk score model to current clinical practice. However, it would be useful to reevaluate our polygenic risk score model using data from patients who received the current standard treatment, because there is a population of patients who experience severe radiographic progression of RA despite treatment with MTX and/or bDMARDs. Moreover, we did not validate these results using another independent cohort due to the lack of available data sets. Instead, our data set was randomly divided into a training set to select the best polygenic risk score model and a testing set to evaluate the ability of the model to accurately predict the severity of radiographic progression in RA. However, as previously discussed (29), the possibility of overfitting remains in our prediction model due to the similar stratification of the populations in the training and testing sets. Although we tried to avoid this issue by performing additional analyses, including 10 principal components analysis using genotypes as covariates, our model needs to be tested using an external cohort to confirm the predictive accuracy.

In conclusion, the polygenic risk scores we constructed using summary data from a GWAS meta-analysis of RA susceptibility were associated with radiographic progression in patients with RA, particularly in patients who were younger at the onset of RA. Furthermore, the association of polygenic risk scores with radiographic progression was independent of other clinical factors. Our study demonstrates that, in the setting of polygenic rheumatic diseases, genetic profiling has potential applications in precision medicine, which should be validated and improved in future studies.

ACKNOWLEDGMENTS

We thank all of the patients in the IORRA database and all of the members of the Institute of Rheumatology, Tokyo Women's Medical University Hospital for the successful management of the IORRA study cohort.

AUTHOR CONTRIBUTIONS

All authors were involved in drafting the article or revising it critically for important intellectual content, and all authors approved the final version to be published. Dr. Kochi had full access to all of the data in the study and takes responsibility for the integrity of the data and the accuracy of the data analysis.

Study conception and design. Ikari, Kochi.

Acquisition of data. Honda, Ikari, Yano, Terao, Tanaka, Harigai, Kochi.

Analysis and interpretation of data. Honda, Ikari, Harigai, Kochi.

REFERENCES

1. Aletaha D, Smolen JS. Diagnosis and management of rheumatoid arthritis. JAMA 2018;320:1360.
2. Okazaki M, Kobayashi H, Shimizu H, Ishii Y, Yajima T, Kanbori M. Safety, effectiveness, and treatment persistence of golimumab in elderly patients with rheumatoid arthritis in real-world clinical practice in Japan. Rheumatol Ther 2018;5:135–48.
3. Syversen SW, Gaarder PI, Goll GL, Ødegård S, Haavardsholm EA, Mowinckel P, et al. High anti-cyclic citrullinated peptide levels and an algorithm of four variables predict radiographic progression in patients with rheumatoid arthritis: results from a 10-year longitudinal study. Ann Rheum Dis 2008;67:212–7.
4. Traylor M, Knevel R, Cui J, Taylor J, Harm-Jan W, Conaghan PG, et al. Genetic associations with radiological damage in rheumatoid arthritis: meta-analysis of seven genome-wide association studies of 2,775 cases. PLoS One 2019;14:e0223246.
5. Suzuki T, Ikari K, Yano K, Inoue E, Toyama Y, Taniguchi A, et al. PADI4 and HLA-DRB1 are genetic risks for radiographic progression in RA patients, independent of ACPA status: results from the IORRA cohort study. PLoS One 2013;8:e61045.
6. Hetland ML, Ejbjerg B, Hørslev-Petersen K, Jacobsen S, Vestergaard A, Jurik AG, et al. MRI bone oedema is the strongest predictor of subsequent radiographic progression in early rheumatoid arthritis: results from a 2-year randomised controlled trial (CIMESTRA). Ann Rheum Dis 2009;68:384–90.
7. Okada Y, Terao C, Ikari K, Kochi Y, Ohmura K, Suzuki A, et al. Meta-analysis identifies nine new loci associated with rheumatoid arthritis in the Japanese population. Nat Genet 2012;44:511–6.
8. Eyre S, Bowes J, Diogo D, Lee A, Barton A, Martin P, et al. High-density genetic mapping identifies new susceptibility loci for rheumatoid arthritis. Nat Genet 2012;44:1336–40.
9. Okada Y, Wu D, Trynka G, Raj T, Terao C, Ikari K, et al. Genetics of rheumatoid arthritis contributes to biology and drug discovery. Nature 2014;506:376–81.
10. Muthana M, Hawtree S, Wilshaw A, Linehan E, Roberts H, Khetan S, et al. C5orf30 is a negative regulator of tissue damage in rheumatoid arthritis. Proc Natl Acad Sci U S A 2015;112:11618–23.
11. Scott IC, Rijsdijk F, Walker J, Quist J, Spain SL, Tan R, et al. Do genetic susceptibility variants associate with disease severity in early active rheumatoid arthritis? J Rheumatol 2015;42:1131–40.
12. Yamanaka H, Tanaka E, Nakajima A, Furuya T, Ikari K, Taniguchi A, et al. A large observational cohort study of rheumatoid arthritis, IORRA: providing context for today's treatment options. Mod Rheumatol 2020;30:1–6.
13. Ishigaki K, Kochi Y, Suzuki A, Tsuchida Y, Tsuchiya H, Sumitomo S, et al. Polygenic burdens on cell-specific pathways underlie the risk of rheumatoid arthritis. Nat Genet 2017;49:1120–5.
14. Purcell S, Neale B, Todd-Brown K, Thomas L, Ferreira MA, Bender D, et al. PLINK: a tool set for whole-genome association and population-based linkage analyses. Am J Hum Genet 2007;81:559–75.
15. Choi SW, Mak TS, O'Reilly PF. Tutorial: a guide to performing polygenic risk score analyses. Nat Protoc 2020;15:2759–72.

16. Choi SW, O'Reilly PF. PRSice-2: polygenic risk score software for biobank-scale data. Gigascience 2019;8:giz082.
17. Reid S, Alexsson A, Frodlund M, Morris D, Sandling JK, Bolin K, et al. High genetic risk score is associated with early disease onset, damage accrual and decreased survival in systemic lupus erythematosus. Ann Rheum Dis 2020;79:363–9.
18. Terao C, Yano K, Ikari K, Furu M, Yamakawa N, Yoshida S, et al. Main contribution of DRB1*04:05 among the shared epitope alleles and involvement of DRB1 amino acid position 57 in association with joint destruction in anti–citrullinated protein antibody–positive rheumatoid arthritis. Arthritis Rheumatol 2015;67:1744–50.
19. Visser K, Goekoop-Ruiterman YP, de Vries-Bouwstra JK, Ronday HK, Seys PE, Kerstens PJ, et al. A matrix risk model for the prediction of rapid radiographic progression in patients with rheumatoid arthritis receiving different dynamic treatment strategies: post hoc analyses from the BeSt study. Ann Rheum Dis 2010;69:1333–7.
20. Raychaudhuri S, Sandor C, Stahl EA, Freudenberg J, Lee HS, Jia X, et al. Five amino acids in three HLA proteins explain most of the association between MHC and seropositive rheumatoid arthritis. Nat Genet 2012;44:291–6.
21. Okada Y, Kim K, Han B, Pillai NE, Ong RT, Saw WY, et al. Risk for ACPA-positive rheumatoid arthritis is driven by shared HLA amino acid polymorphisms in Asian and European populations. Hum Mol Genet 2014;23:6916–26.
22. Ling SF, Viatte S, Lunt M, Van Sijl AM, Silva-Fernandez L, Symmons DP, et al. HLA–DRB1 amino acid positions 11/13, 71, and 74 are associated with inflammation level, disease activity, and the Health Assessment Questionnaire score in patients with inflammatory polyarthritis. Arthritis Rheumatol 2016;68:2618–28.
23. Axelrud LK, Santoro ML, Pine DS, Talarico F, Gadelha A, Manfro GG, et al. Polygenic risk score for Alzheimer's disease: implications for memory performance and hippocampal volumes in early life. Am J Psychiatry 2018;175:555–63.
24. Chaudhury S, Patel T, Barber IS, Guetta-Baranes T, Brookes KJ, Chappell S, et al. Polygenic risk score in postmortem diagnosed sporadic early-onset Alzheimer's disease. Neurobiol Aging 2018;62:244. e1-244.
25. Poudel D, George MD, Baker JF. The impact of obesity on disease activity and treatment response in rheumatoid arthritis. Curr Rheumatol Rep 2020;22:56.
26. Rydell E, Forslind K, Nilsson JÅ, Jacobsson LT, Turesson C. Smoking, body mass index, disease activity, and the risk of rapid radiographic progression in patients with early rheumatoid arthritis. Arthritis Res Ther 2018;20:82.
27. Vidal C, Barnetche T, Morel J, Combe B, Daïen C. Association of body mass index categories with disease activity and radiographic joint damage in rheumatoid arthritis: a systematic review and metaanalysis. J Rheumatol 2015;42:2261–9.
28. Baker JF, Østergaard M, George M, Shults J, Emery P, Baker DG, et al. Greater body mass independently predicts less radiographic progression on X-ray and MRI over 1–2 years. Ann Rheum Dis 2014;73:1923–8.
29. Wray NR, Yang J, Hayes BJ, Price AL, Goddard ME, Visscher PM. Pitfalls of predicting complex traits from SNPs. Nat Rev Genet 2013;14:507–15.

Arthritis & Rheumatology
Vol. 74, No. 5, May 2022, pp 801–809
DOI 10.1002/art.42044

American College of Rheumatology
Empowering Rheumatology Professionals

Extramucosal Formation and Prognostic Value of Secretory Antibodies in Rheumatoid Arthritis

Klara Martinsson,[1] Lovisa Lyttbacka Kling,[1] Karin Roos-Ljungberg,[1] Irina Griazeva,[2] Marina Samoylovich,[2] Stephane Paul,[3] Johan Rönnelid,[4] Tomas Weitoft,[5] Jonas Wetterö,[1] and Alf Kastbom[6]

Objective. To investigate levels and possible extramucosal formation of secretory Ig, including anti–citrullinated protein antibodies (ACPAs), in rheumatoid arthritis (RA).

Methods. Three patient groups were studied: 1) ACPA-positive patients with musculoskeletal pain without clinical arthritis, 2) patients with recent-onset RA, and 3) patients with established RA. In baseline serum samples (groups 1 and 2) and paired synovial fluid samples (group 3), we analyzed total secretory IgA, total secretory IgM, free secretory component (SC), and SC-containing ACPA. Extramucosal formation of SC-containing ACPA was investigated by preincubating RA sera and affinity-purified ACPA with recombinant free SC.

Results. Compared to healthy controls, serum levels of total secretory IgA and total secretory IgM were increased both in patients with early RA and at-risk patients ($P < 0.05$). Patients with early RA with elevated total secretory Ig had significantly higher disease activity during the 3-year follow-up period compared to those without increased levels. At-risk patients who developed arthritis during follow-up (39 of 82) had higher baseline total secretory IgA levels compared to those who did not ($P = 0.041$). In established RA, total secretory IgA and total secretory IgM levels were higher in serum than in synovial fluid ($P < 0.0001$), but SC-containing ACPAs adjusted for total secretory Ig concentration were higher in synovial fluid ($P < 0.0001$). Preincubation with recombinant free SC yielded increased SC-containing ACPA reactivity in sera as well as in affinity-purified IgA and IgM ACPA preparations.

Conclusion. Circulating secretory Ig are elevated before and at RA onset. In the presence of free SC, secretory Ig may form outside the mucosa, and SC-containing ACPAs are enriched in RA joints. These findings shed important new light on the mucosal connection in RA development.

INTRODUCTION

The mechanisms by which rheumatoid arthritis (RA) is induced remain incompletely understood. Autoantibodies against citrullinated proteins (ACPAs) are highly specific for RA and may be detected in serum several years before diagnosis and are prognostic for arthritis development (1,2). Although ACPAs can be generated locally within the joint in manifest RA (3,4), this was not evident in ACPA-positive patients with arthralgia prior to arthritis development (5). Thus, triggering events in RA development may occur outside the joints.

Recent advances suggest that mucosal surfaces are important early in the development of RA, particularly in ACPA-positive disease (6,7). Mucosal antibody production predominately involves IgA subjected to transcellular transport via the polymeric Ig receptor located at the basolateral surface of epithelial cells. As the polymeric Ig receptor–antibody complex is released at the luminal side, a part of the polymeric Ig receptor remains attached and is then denoted as secretory component (SC). Antibodies with SC attached are defined as secretory Ig, and occur as both IgA and IgM classes (8). We previously identified SC-containing ACPAs in the circulation of patients with early RA (9).

Supported by the Swedish Society of Medicine (grant SLS-682741), King Gustaf V's 80-year foundation (grant FAI-2017-0420), the Swedish Rheumatism Association (grant R-754141), and the Östergötland County Council (grant LIO-700501).

[1]Klara Martinsson, PhD, Lovisa Lyttbacka Kling, MSc, Karin Roos Ljungberg, MSc, Jonas Wetterö, PhD: Linköping University, Linköping, Sweden; [2]Irina Griazeva, PhD, Marina Samoylovich, PhD: Russian Research Center for Radiology and Surgical Technologies, St. Petersburg, Russia; [3]Stephane Paul, MD, PhD: Centre International de Recherche en Infectiologie, Team GIMAP, U1111, CNRS, UMR530, University Lyon, Université Claude Bernard Lyon 1, CIC 1408 Vaccinology, Saint-Etienne, France; [4]Johan Rönnelid, MD, PhD: Uppsala University, Uppsala, Sweden; [5]Tomas Weitoft, MD, PhD: Uppsala University/Region of Gävleborg, Gävle, Sweden; [6]Alf Kastbom, MD, PhD: Linköping University and Linköping University Hospital, Linköping, Sweden.

Author disclosures are available at https://onlinelibrary.wiley.com/action/downloadSupplement?doi=10.1002%2Fart.42044&file=art42044-sup-0001-Disclosureform.pdf.

Address correspondence to Klara Martinsson, PhD, II, Building 420, Floor 12, Linköping University, Campus US 581 85, Linköping, Sweden. Email: klara.martinsson@liu.se.

Submitted for publication December 7, 2020; accepted in revised form December 7, 2021.

Later work showed that these antibodies were mainly of the IgM class and not IgA (10). Since secretory IgA normally predominate over secretory IgM at mucosal surfaces (11), the IgM dominance in serum SC-containing ACPAs may thus imply that these antibodies do not originate from the mucosa. Furthermore, support for extramucosal formation of SC-containing antibodies has been previously shown in vitro (12,13). Therefore, one can speculate that secretory ACPAs in the circulation may have been formed outside the mucosa.

We recently reported that free SC is elevated in RA sera prior to the onset of arthritis and that levels correlate with circulating ACPA (14). Thus, we wished to expand these findings by investigating whether circulating secretory Ig are altered and of prognostic value in different phases and phenotypes of RA, and whether they are enriched in joint fluid. We also aimed to test the hypothesis that SC-containing ACPAs can be formed in serum in the presence of free SC. Such knowledge would improve our understanding of the connections between mucosa and RA development.

PATIENTS AND METHODS

This study included 3 patient cohorts: 1) ACPA-positive at-risk patients, 2) patients with recent-onset RA, and 3) patients with established RA. In addition, 100 healthy blood donors (50% women, median age 54.5 years) were included as controls.

At-risk patients. Eighty-two patients with a positive IgG ACPA test performed in a clinical setting who had musculoskeletal pain of any sort and duration, but no baseline arthritis, were followed up prospectively for the development of clinical arthritis as part of the Extra Early Rheumatology Follow-up Study (TIRx) (14,15). Baseline characteristics are shown in Table 1. Patients were recruited between 2010 and 2013 from the rheumatology unit at Linköping University Hospital (Linköping, Sweden). Exclusion criteria included previous rheumatic disease or treatment with oral glucocorticoids within 6 weeks. Follow-up visits were scheduled regularly, and arthritis development was assessed upon clinical examination by an experienced rheumatologist. We analyzed follow-up data until September 1, 2017, resulting in a median follow-up time of 69 months (interquartile range [IQR] 57–77). Progression to arthritis occurred in 39 of 82 patients (48%) after a median of 6 months (IQR 3–24).

Patients with early RA. We studied 445 patients with recent-onset RA from the Timely Intervention in RA (TIRA-2) prospective observational cohort, recruited between 2006 and 2009 from 7 rheumatology clinics in southeast and central Sweden (Table 1). Inclusion criteria were either fulfilment of the American College of Rheumatology 1987 classification criteria for RA (n = 429) (16), or the presence of morning stiffness ≥60 minutes, symmetrical arthritis, and arthritis of hands or feet (n = 23). Symptom duration was <12 months. Follow-up procedures in TIRA-2 have been detailed previously (9,17). Radiographic damage was graded according to the Larsen method (18).

Patients with established RA. We studied paired sera and synovial fluid samples from 59 RA patients (76% women, mean ± SD age 60 ± 16 years) previously described in a clinical study investigating factors predicting the response to intraarticular glucocorticoids (19). The mean ± SD disease duration was 10.4 ± 10.4 years, and the mean ± SD Disease Activity Score in 28 joints (DAS28) (20) was 4.52 ± 1.13 at the time of sampling. Among these patients, 56% currently or previously smoked. Sixty-nine percent of patients were positive for anti–cyclic citrullinated peptide 2 (anti–CCP-2), and 68% were positive for IgM rheumatoid factor (RF). At the time of sampling, 47 patients were treated with conventional synthetic disease-modifying antirheumatic drugs (csDMARDs) (5 in combination with biologic DMARDs [bDMARDs]), and 4 were treated with bDMARDs in monotherapy. Eight patients did not receive any DMARD treatment.

Ethics approval. All participants provided written informed consent, and the study protocol was approved by the Ethics Review Boards in Linköping and Uppsala, Sweden (decision nos. M168-05, M220-09, 2015/236-32, and 2007/047).

Secretory Ig analyses. An in-house sandwich enzyme-linked immunosorbent assay (ELISA) (21) was modified to detect total secretory IgA and total secretory IgM, respectively, in serum and synovial fluid. Half-area 96-well plates were coated with a monoclonal anti-SC antibody (Sigma-Aldrich), diluted 1:1,000 in phosphate buffered saline (PBS) at pH 7.4 (Medicago AB), and incubated in a moist chamber at 37°C for 2 hours, followed by incubation for 3 hours at 4°C. The plates were washed and blocked with 0.5% bovine serum albumin (BSA) (Sigma-Aldrich) in PBS, incubated 2 hours in a moist chamber at 37°C, and subsequently incubated at 4°C overnight. Thereafter, serum samples were diluted 1:100 in PBS–Tween–0.5% BSA and incubated 1 hour in a moist chamber at 37°C.

Following washing, detection using antibodies for either total secretory IgA (polyclonal goat anti-human IgA alfa-chain–specific peroxidase–conjugated antibody, diluted 1:25,000) or total secretory IgM (horseradish peroxidase [HRP]–conjugated polyclonal goat anti-human IgM antibody Fc 5μ, diluted 1:20,000) (both from Sigma-Aldrich) and incubation for 1 hour in a moist chamber at 37°C were performed. After washing, tetramethylbenzidine (TMB; Sigma-Aldrich) was added to the plates and incubated in the dark at room temperature for 30 minutes, stopped using 1.8*M* sulfuric acid, and read at an optical density (OD) of 450 nm (Tecan). Standard curves were set up using serial dilutions of purified IgA from human colostrum (containing secretory IgA; Sigma-Aldrich) or

Table 1. Baseline characteristics of the study participants*

	Early RA (TIRA-2) (n = 445)	At-risk (TIRx) (n = 82)	Established RA (n = 59)
Women	296 (67)	66 (81)	45 (76)
Age, mean ± SD years	59 ± 14	52 ± 14	60 ± 16
RF-positive	264 (59)	25 (31)	40 (68)
IgG ACPA–positive	303 (68)†	82 (100)	41 (69)
IgA ACPA–positive	193 (57)‡	NA	–
SC-containing ACPA–positive	81 (19)§	NA	–
IgM ACPA–positive	136 (40)¶	NA	–
Free SC–positive	114 (25)#	9 (11)	–
Elevated total secretory IgA	122 (27)	17 (21)	–
Elevated total secretory IgM	186 (42)	12 (15)	–
Current smoker	56 (24)**	13 (16)	33 (56)††

* Except where indicated otherwise, values are the number (%) of subjects. RA = rheumatoid arthritis; TIRA-2 = Timely Intervention in RA cohort; TIRx = Extra Early Rheumatology Follow-up Study; RF = rheumatoid factor; ACPA = anti–citrullinated protein antibody; NA = not analyzed; SC = secretory component.
† Data available for 443 subjects.
‡ Data available for 338 subjects.
§ Data available for 439 subjects.
¶ Data available for 337 subjects.
# Data available for 438 subjects.
** Data available for 238 subjects.
†† Current and former smokers.

IgM from human serum (containing secretory IgM; Sigma-Aldrich), respectively. The cutoff value was set at the 95th percentile among controls (total secretory IgA 13.6 μg/ml and total secretory IgM 4.9 μg/ml).

Free SC and autoantibody analyses. Free SC was analyzed using an in-house sandwich ELISA (14,22). Serum samples were diluted 1:25, added in duplicate to microtiter plates precoated with 10 μg/ml monoclonal antibody (mAb) anti–free SC 6B3 and incubated at 37°C. Following washing, HRP-conjugated mAb anti-SC 5D8, diluted 1:100, were added and incubated at 37°C. TMB (Merck) was added as the substrate, and the reaction was stopped with 1*M* sulfuric acid and read at $OD_{450\ nm}$. A 7-step serial diluted standard curve was used to calculate the concentrations. The cutoff for positivity was set at the 99th percentile among the 100 healthy controls (32 ng/ml). The intraassay and interassay variations were 2% and 9%, respectively. Secretory IgA and samples high in secretory IgM added to the wells yielded free SC levels similar to the buffer ($OD_{450\ nm}$ of 0.223–0.346 versus 0.218), verifying that Ig-bound SC was not detected in the free SC ELISA.

Serum SC-containing ACPAs and IgM ACPAs were measured by modifying anti-CCP ELISA kits (Euro-Diagnostica) (23). Serum samples were diluted 1:25, added to precoated CCP microtiter plates, and incubated at room temperature. Following washing, HRP-conjugated polyclonal goat anti-human SC or IgM antibodies (Nordic Biosite) were used to detect SC-containing ACPAs (dilution 1:2,000) or IgM (dilution 1:10,000). Incubation was stopped and read at $OD_{450\ nm}$. The intraassay and interassay variations in the SC-containing ACPA ELISA were 5% and 10%, respectively. For the IgM ACPAs, the intraassay and interassay variations were 2% and 17%, respectively. A 7-step serial dilution was used for standard curve calculations using patient sera with high levels of SC-containing ACPA and IgM ACPA, respectively. The cutoff level for positivity was set at the 99th percentile among healthy controls (SC-containing ACPA 124 AU/ml and IgM 241 AU/ml).

Serum IgA and IgG ACPA were analyzed by a fluoroenzyme immunoassay (EliA Phadia AB; ThermoFisher Scientific) as described previously (24). The cutoff level for IgA ACPA test was set at the 99th percentile among healthy blood donors (2 μg/liter). For IgG ACPA analyses, the manufacturer's cutoff level was used (7 units/ml, in accordance with the standard protocol in Swedish clinical immunology laboratories). RF tests were performed in a clinical setting at each local laboratory associated with the participating rheumatology unit.

Purification of ACPAs. Anti-CCP antibodies were isolated from a highly positive serum sample by affinity chromatography using a CCP column (Euro Diagnostica AB). The sample was filtered through a Millex GV 0.2-μm pore-size filter (Merck) and then added to the column. Bound antibodies were eluted using 0.1*M* glycine (pH 2.7) and immediately neutralized with 1*M* Tris (pH 9.0). CCP-specific antibodies were then added to a Peptide M column (InvivoGen), and IgA class anti-CCP antibodies were eluted (in 0.3-ml aliquots) using 0.1*M* sodium acetate (pH 4.0). The flowthrough was added to a Capture Select IgM Affinity Resin (ThermoFisher Scientific), and IgM class anti-CCP antibodies were eluted in 0.3 ml aliquots using 0.1*M* glycine (pH 3.0). Immediately after elution, both IgA and IgM class anti-CCP antibodies were neutralized with 1*M* Tris HCl (pH 8.3). The purified antibodies were stored at –20°C until further use.

In vitro generation of SC-containing ACPAs. Ten microliters (1 mg/ml) of recombinant human SC (25) were added to 10 μl ACPA-positive serum, to affinity-purified ACPA (IgA, IgM, or IgG), and to affinity-purified non-ACPA preparations (IgA or IgM; Sigma-Aldrich). After incubation at 37°C for 30 minutes, the samples were diluted 1:10 and analyzed for SC-containing ACPA reactivity by the previously described ELISA.

Statistical analysis. The Mann–Whitney U test was used to test differences in levels between groups, and Fisher's exact test was used for dichotomous variables. Correlation analyses were carried out using Spearman's correlation test. Cox regression analysis was used to test differences in arthritis-free survival in the TIRx cohort. DAS28 scores over time were compared between groups using the general linear model for repeated measures. For missing DAS28 values beyond month 3 (12% of values), we applied the last observation carried forward method. Wilcoxon's test was used to test differences in serum versus synovial fluid and to evaluate SC-containing ACPA reactivity after preincubation with free SC. Statistical calculations were performed using IBM SPSS Statistics, version 25. Two-sided *P* values less than 0.05 were considered significant.

RESULTS

Serum levels of secretory Ig in patients and controls. Patients with early RA showed the highest levels of total secretory IgA and total secretory IgM compared to both at-risk patients ($P < 0.01$ for total secretory IgA; $P < 0.0001$ for total secretory IgM) and healthy controls ($P < 0.0001$ for both) (Figures 1A and B). At-risk patients showed significantly increased levels of both total secretory IgA and total secretory IgM compared to healthy controls, but the difference was more pronounced for total secretory IgA ($P < 0.001$ versus $P = 0.04$) (Figures 1A and B). Total secretory IgA did not differ between men and women among controls ($P = 0.78$), but women had higher levels of total secretory IgM ($P = 0.009$). To adjust for this, total secretory IgM levels were also compared between female patients and female controls. The difference remained significant for early RA ($P < 0.0001$) but was lost for at-risk patients ($P = 0.90$). Patients with early RA who were positive for IgG ACPA had significantly higher serum total secretory IgM levels compared to IgG ACPA–negative patients (4.9 μg/ml [IQR 8.5–3.2] versus 2.9 μg/ml [IQR 4.9–1.7]; $P < 0.001$), but not total secretory IgA (10.4 μg/ml [IQR 15.6–7.0] versus 9.3 μg/ml [IQR 13.3–6.5]; $P = 0.09$).

Correlation of smoking habits with serum secretory Ig. Among both patients with early RA and at-risk patients, current smokers had higher total secretory IgA levels ($P < 0.0001$) and total secretory IgM levels ($P < 0.0001$) compared to those who were not current smokers. Smoking data were not available for the controls, but to account for possible differences in smoking habits, we also compared nonsmoker patients to the controls. Among those with early RA, nonsmokers had increased levels of both total secretory IgA and total secretory IgM compared to controls ($P < 0.0001$ for both). Among the at-risk patients, levels of total secretory IgA remained significantly elevated among nonsmokers compared to controls ($P = 0.007$), while total secretory IgM did not ($P = 0.33$). Finally, total secretory IgA levels were higher among nonsmoker TIRx patients who developed arthritis during follow-up compared to patients who did not progress ($P = 0.016$), while no such difference was detected for total secretory IgM levels ($P = 0.45$).

Correlation of autoantibodies and free SC with serum secretory Ig. There were weak correlations of serum total secretory IgA levels with ACPA isotypes and free SC in early RA ($\rho = 0.142–0.363$, $P < 0.01$). Total secretory IgM levels correlated significantly with serum levels of all analyzed ACPA isotypes

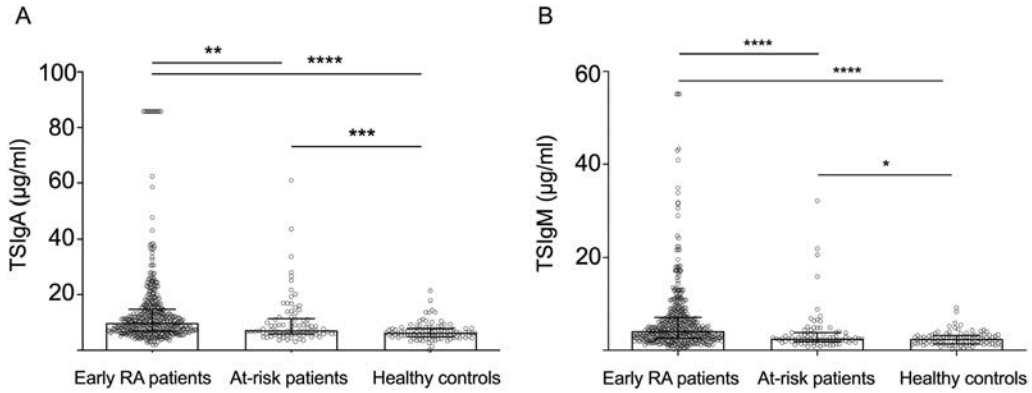

Figure 1. Levels of total secretory IgA (TSIgA) (**A**) and total secretory IgM (TSIgM) (**B**) in patients with early rheumatoid arthritis (RA) (from the Timely Intervention in RA cohort), at-risk patients (from the Extra Early Rheumatology Follow-up Study), and healthy controls. Symbols represent individual subjects. Bars show the median and interquartile range. * = $P < 0.05$; ** = $P < 0.01$; *** = $P < 0.001$; **** = $P < 0.0001$, by Mann-Whitney U test.

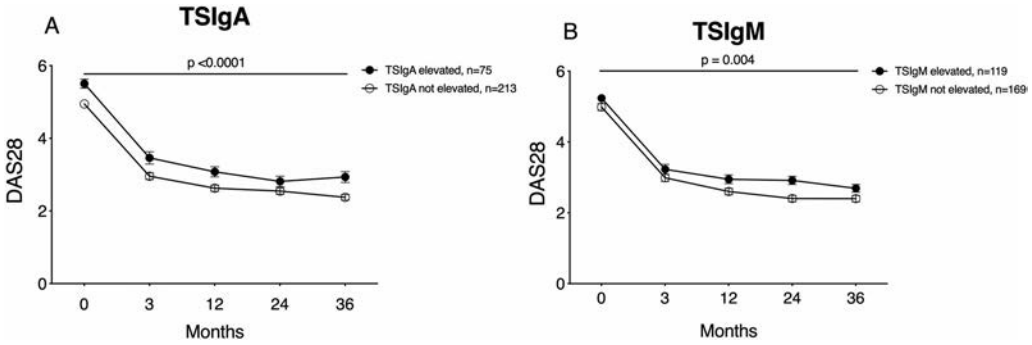

Figure 2. Disease Activity Score in 28 joints (DAS28) over time in early RA (Timely Intervention in RA cohort) versus baseline status of total secretory IgA (**A**) and total secretory IgM (**B**), analyzed with general linear model for repeated measures. Lines show the mean ± SEM. See Figure 1 for other definitions.

and free SC, although correlation coefficients were low to moderate (ρ = 0.174–0.432, $P < 0.001$).

Correlation of arthritis development and disease course with serum secretory Ig. At-risk patients who subsequently developed arthritis (n = 39) had significantly higher baseline levels of total secretory IgA compared to patients who remained free of arthritis during follow-up (median 8.9 μg/ml [IQR 14.6–6.0] versus 6.6 μg/ml [IQR 9.1–5.5]; $P = 0.041$). This was not apparent for total secretory IgM (median 2.6 μg/ml [IQR 3.9–2.0] versus 2.5 μg/ml [IQR 3.8–1.7]; $P = 0.37$). In Cox regression analyses, neither total secretory IgA nor total secretory IgM levels were prognostic for progression to arthritis ($P = 0.96$ and $P = 0.25$, respectively).

During 3 years of follow-up, patients with early RA with elevated serum total secretory IgA had significantly higher DAS28 scores compared to those with total secretory IgA levels below the cutoff (P < 0.0001) (Figure 2A). Similar findings were made regarding total secretory IgM ($P = 0.004$) (Figure 2B). This remained significant after adjustment for age, sex, IgG ACPA status, csDMARD initiation at baseline, and bDMARD treatment during follow-up ($P = 0.008$ for total secretory IgA; $P = 0.025$ for total secretory IgM). We also adjusted for smoking in a separate analysis due to missing data, where both elevated total secretory IgA and total secretory IgM remained associated with increased DAS28 scores over time ($P = 0.038$ and $P = 0.012$, respectively). Radiographic joint damage in early RA did not differ significantly according to total secretory IgA status either at baseline (median

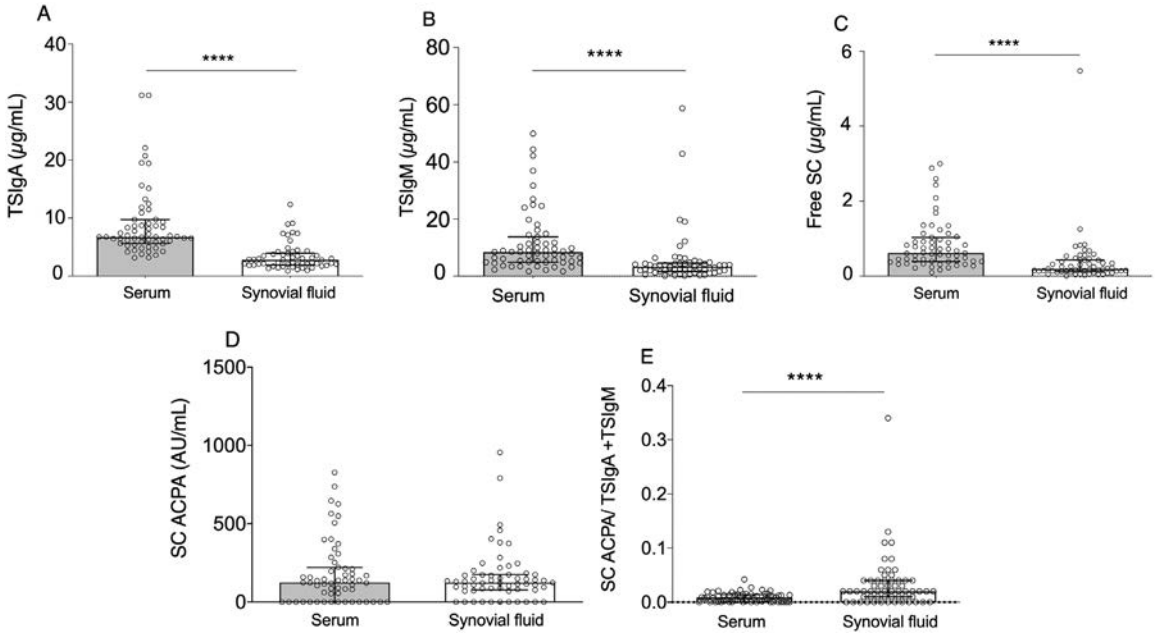

Figure 3. Secretory Ig in serum and synovial fluid. **A–D**, Levels of total secretory IgA (**A**), total secretory IgM (**B**), free secretory component (SC) (**C**), and SC-containing anti–citrullinated protein antibodies (ACPAs) (**D**) in paired samples of serum and synovial fluid from RA patients. **E**, The ratio between SC-containing ACPAs and total secretory IgA and IgM levels in paired samples of serum and synovial fluid. Symbols represent individual subjects. Bars show the median and interquartile range. **** = $P < 0.0001$ by Wilcoxon's test. See Figure 1 for other definitions.

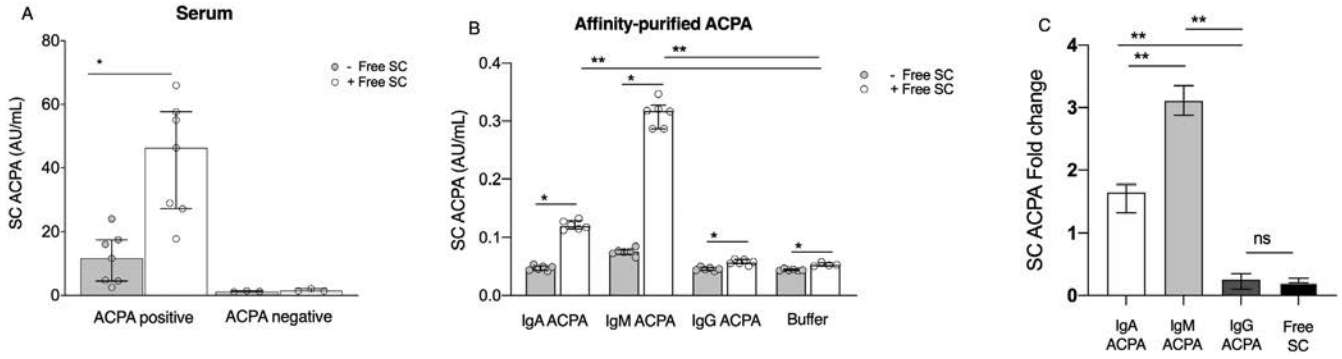

Figure 4. Levels of SC-containing ACPA before and after preincubation with 1 mg/ml human recombinant free SC. **A**, Levels of SC-containing ACPA in serum samples from patients with early rheumatoid arthritis who were positive for IgA and IgM ACPA (n = 7) and patients who were negative for IgA and IgM ACPA (n = 3). **B**, Levels of affinity-purified fractions of IgA ACPA (n = 6), IgM ACPA (n = 6), IgG ACPA (n = 6), and free SC in buffer only. **C**, Fold change in SC-containing ACPA reactivity following free SC preincubation. Symbols represent individual subjects. Bars show the median and interquartile range. * = $P < 0.05$; ** = $P < 0.01$, by Wilcoxon's test. See Figure 3 for definitions.

Larsen score 2.0 [IQR 4.0–0.0] versus 2.0 [IQR 4.0–0.0]; $P = 0.55$) or at 3 years (median Larsen score 3.0 [IQR 7–1] versus 3.0 [IQR 7.0–1.0]; $P = 1.0$). Total secretory IgM level was also unrelated to baseline radiographic damage (median Larsen score 1.0 [IQR 5.0–0.0] versus 2.0 [IQR 4.0–0.0]; $P = 0.75$) and at 3 years (median Larsen score 2.5 [IQR 7.3–1.0] versus 3.0 [IQR 7.0–1.0]; $P = 0.50$).

Secretory Ig in serum and synovial fluid. Levels of total secretory IgA, free SC, and total secretory IgM were significantly higher in serum compared to synovial fluid ($P < 0.0001$) (Figures 3A–C). Since total Ig levels are higher in serum than in joint fluid, we calculated ratios between SC-containing ACPA levels and the sum of total secretory IgA and total secretory IgM concentrations in order to adjust for this difference when comparing SC-containing ACPA reactivity between compartments. This ratio was significantly higher in synovial fluids compared to serum ($P < 0.0001$) (Figure 3E). SC-containing ACPAs showed moderate to strong correlations with total secretory IgA and total secretory IgM levels in serum (ρ = 0.352–0.812, $P < 0.01$). Free SC showed moderate to strong correlations with total secretory IgA and total secretory IgM levels in serum (ρ = 0.487–0.693, $P < 0.001$) and synovial fluid (ρ = 0.436–0.672, $P < 0.001$).

Extramucosal formation of secretory IgA and secretory IgM ACPAs. We incubated sera (n = 7) from TIRA-2 patients with recombinant free SC, whereafter SC-containing ACPA reactivity increased 3–5-fold ($P = 0.016$) among those positive for IgA and IgM ACPAs (Figure 4A). There was no substantial change in SC-containing ACPA reactivity in serum samples negative for IgA and IgM ACPAs (1.3-fold; $P = 0.5$). When incubating affinity-purified ACPA fractions (n = 6) with recombinant free SC, the SC reactivity increased in both IgA ACPA and IgM ACPA fractions (Figure 4B). The slight increase in SC reactivity in IgG ACPA

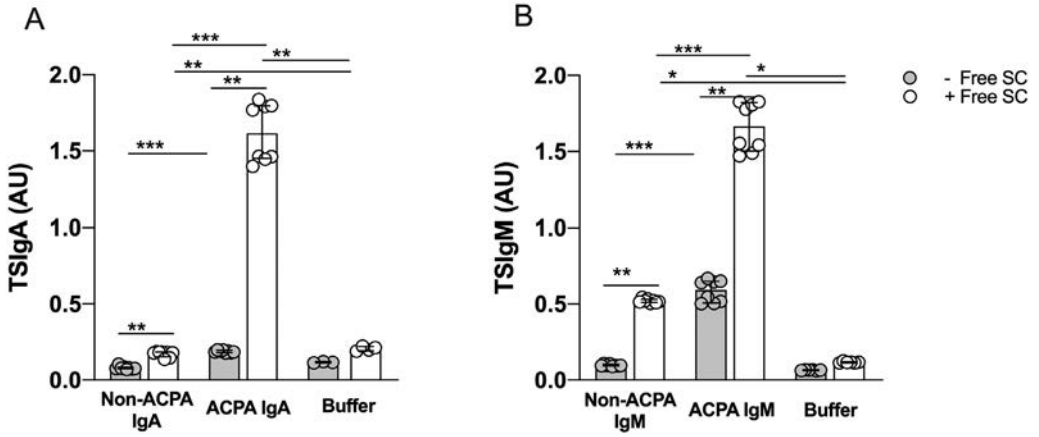

Figure 5. Levels of total secretory IgA (TSIgA) (**A**) and total secretory IgM (TSIgM) (**B**) in ACPA and non-ACPA fractions before and after preincubation with 1 mg/ml human recombinant free SC. Samples contained equal protein concentrations of secretory IgA from colostrum, IgM, and affinity-purified fractions of IgA ACPA (n = 6) and IgM ACPA (n = 6). Symbols represent individual subjects. Bars show the median and interquartile range. * = $P < 0.05$; ** = $P < 0.01$; *** = $P < 0.001$, by Wilcoxon's test. See Figure 3 for other definitions.

was not different from that of free SC only ($P = 0.89$) (Figure 4C). IgA and IgM ACPAs showed greater fold changes in SC-containing ACPA reactivity following free SC incubation compared to IgG ACPAs ($P = 0.002$), and IgM ACPAs showed greater free SC binding ($P = 0.002$ for fold change) compared to IgA ACPAs (Figure 4C).

Comparisons of SC content between ACPA and non-ACPA preparations showed that for IgA, IgA ACPA had higher baseline SC content compared to IgA non-ACPA ($P = 0.0002$) and also showed a higher fold change following preincubation with recombinant free SC ($P = 0.0002$) (Figure 5A). For IgM, the ACPA preparation had higher SC content than non-IgM ACPA ($P = 0.0002$), and although the latter showed a larger fold change following SC preincubation ($P = 0.0002$ for fold change), it still did not reach baseline levels for IgM ACPA (Figure 5B).

DISCUSSION

This is the first study to show that secretory Ig are elevated in the circulation prior to RA onset. We also present in vitro data supporting possible extramucosal formation of SC-containing ACPAs, as well as evidence of SC-containing ACPA enrichment in joint fluid.

It has previously been described that circulating secretory Ig are elevated in established RA (26), and we now expand this knowledge by showing that levels are increased even prior to arthritis and in recent-onset RA. Elevated secretory Ig serum concentration is not, however, a unique feature of RA but has been reported in several different conditions such as spondyloarthropathies (26,27), Sjögren's syndrome (28), and alcoholic liver disease (29). This contrasts to free SC, which we previously found specifically elevated in RA and its pre-phases (14).

In the present study, total secretory IgA levels were increased among at-risk patients who subsequently developed arthritis compared to those who did not, but there was no clear prognostic value in this at-risk population. In early RA, however, there was a clear association between elevated secretory Ig at baseline and increased disease activity over time, including after adjustment for possible confounders. Thus, secretory Ig in serum should be further evaluated as possible prognostic markers to improve identification of patients in need of early potent pharmacotherapy.

The mechanism by which secretory Ig appear in the circulation remains elusive. Serum levels were higher among smokers, which may suggest pulmonary origin, but we also present evidence that secretory autoantibodies can be formed in vitro in the presence of free SC. Therefore, we propose that this mechanism may occur in vivo in RA patients, since levels of free SC in the circulation are clearly and specifically elevated before arthritis onset and further increase in early manifest disease in a pattern very similar to secretory Ig (14). However, further studies are warranted to firmly establish the occurrence and extent of secretory Ig formation in the circulation in RA. Van Delft et al recently showed that circulating secretory ACPA is predominately of the IgM class (10). In agreement with this, we found that SC-containing ACPA reactivity increased more readily when an IgM ACPA fraction was preincubated with free SC, compared to IgA ACPA. It should be pointed out, however, that binding of free SC to IgA requires dimeric antibodies, and the dimeric IgA:monomeric IgA ratio was not specifically addressed in our study. Interestingly, we find that ACPA fractions are more prone to contain SC compared to non-ACPA isotype controls. This was most prominent for IgA, which possibly implies that the proportion of dimeric antibodies is increased in the IgA ACPA fraction.

Given the possible extramucosal formation of secretory Ig, we also investigated several mucosal markers locally in RA joints. Indeed, secretory Ig as well as free SC were readily identified in joint fluids in correlation with serum levels, and after considering the background differences in secretory Ig between compartments, SC-containing ACPAs were increased in joint fluid compared to serum. Since previous work has shown joint fluid enrichment of IgG ACPA (3), and free SC is present, we speculate that SC-containing ACPAs could assemble locally in the joint and not necessarily originate from mucosal surfaces. If secretory autoantibodies can be formed distant from mucosal epithelia, e.g., in the circulation and in joints, their relevance as markers of mucosal involvement in RA could at a glance appear limited. However, their formation requires free SC which, to our knowledge, is produced by epithelial cells only (25), and therefore, their origin most likely remains related to the mucosa. Given that SC-containing ACPAs occur in joint fluid and may be formed in serum, where they predict arthritis onset among at-risk patients (30), we believe that these autoantibodies may be involved in triggering arthritis. Therefore, functional characterization of SC-containing ACPAs should be addressed in future work, facilitated by the methods of in vitro SC-containing ACPA formation described here.

Although we show a prognostic value of baseline total secretory IgA and total secretory IgM in early RA, a limitation of this study is that we cannot establish whether these Ig are formed at mucosal sites or in the circulation. Both mechanisms are likely to be relevant in vivo, but the proportional contribution of each is difficult to delineate. Data on smoking were lacking in the control group, and the sex distribution differed from that of the patient groups. In sensitivity analyses addressing this, the role of total secretory IgM among at-risk patients became less clear, while all findings remained virtually unaltered concerning total secretory IgA. Other limitations of the current study include the lack of mucosal fluid and joint fluid samples from patients with early RA.

In summary, secretory Ig are increased in the circulation both at RA onset and prior to arthritis development in ACPA-positive patients. At RA onset, elevated levels were associated with increased disease activity over time, suggesting that secretory Ig should be further evaluated as a prognostic biomarker in early

RA. In addition, we show that SC-containing ACPAs can be formed in the presence of free SC, and that SC-containing ACPAs are enriched in RA joint fluid. This is essential information for future studies to assess the mucosal contributions in RA development.

ACKNOWLEDGMENTS

We are grateful to all TIRA and TIRx colleagues and participating patients. We thank the Epidemiological Investigation of RA (EIRA) Study Group for providing data on smoking habits in the TIRA-2 cohort. The Clinical Immunology Laboratory at Linköping University Hospital is acknowledged for excellent technical assistance.

AUTHOR CONTRIBUTIONS

All authors were involved in drafting the article or revising it critically for important intellectual content, and all authors approved the final version to be published. Dr. Martinsson had full access to all of the data in the study and takes responsibility for the integrity of the data and the accuracy of the data analysis.

Study conception and design. Kastbom.

Acquisition of data. Martinsson, Kling, Roos-Ljungberg, Griazeva, Samoylovich, Paul, Rönnelid, Weitoft.

Analysis and interpretation of data. Martinsson, Wetterö, Kastbom.

REFERENCES

1. Rantapää-Dahlqvist S, de Jong BA, Berglin E, Hallmans G, Wadell G, Stenlund H, et al. Antibodies against cyclic citrullinated peptide and IgA rheumatoid factor predict the development of rheumatoid arthritis. Arthritis Rheum 2003;48:2741–9.
2. Nielen MM, van Schaardenburg D, Reesink HW, van de Stadt RJ, van der Horst-Bruinsma IE, de Koning MH, et al. Specific autoantibodies precede the symptoms of rheumatoid arthritis: a study of serial measurements in blood donors. Arthritis Rheum 2004;50:380–6.
3. Sohrabian A, Mathsson-Alm L, Hansson M, Knight A, Lysholm J, Cornillet M, et al. Number of individual ACPA reactivities in synovial fluid immune complexes, but not serum anti-CCP2 levels, associate with inflammation and joint destruction in rheumatoid arthritis. Ann Rheum Dis 2018;77:1345–53.
4. Snir O, Widhe M, Hermansson M, von Spee C, Lindberg J, Hensen S, et al. Antibodies to several citrullinated antigens are enriched in the joints of rheumatoid arthritis patients. Arthritis Rheum 2010;62:44–52.
5. De Hair MJ, van de Sande MG, Ramwadhdoebe TH, Hansson M, Landewé R, van der Leij C, et al. Features of the synovium of individuals at risk of developing rheumatoid arthritis: implications for understanding preclinical rheumatoid arthritis. Arthritis Rheumatol 2014;66:513–22.
6. Pentony P, Duquenne L, Dutton K, Mankia K, Gul H, Vital E, et al. The initiation of autoimmunity at epithelial surfaces: a focus on rheumatoid arthritis and systemic lupus erythematosus. Discov Med 2017;24:191–200.
7. Malmström V, Catrina AI, Klareskog L. The immunopathogenesis of seropositive rheumatoid arthritis: from triggering to targeting. Nat Rev Immunol 2017;17:60–75.
8. Brandtzaeg P. Mucosal immunity: induction, dissemination, and effector functions. Scand J Immunol 2009;70:505–15.
9. Roos K, Martinsson K, Ziegelasch M, Sommarin Y, Svärd A, Skogh T, et al. Circulating secretory IgA antibodies against cyclic citrullinated peptides in early rheumatoid arthritis associate with inflammatory activity and smoking. Arthritis Res Ther 2016;18:119.
10. Van Delft MA, van der Woude D, Toes RE, Trouw LA. Secretory form of rheumatoid arthritis-associated autoantibodies in serum are mainly of the IgM isotype, suggesting a continuous reactivation of autoantibody responses at mucosal surfaces. Ann Rheum Dis 2019;78:146–48.
11. Horton RE, Vidarsson G. Antibodies and their receptors: different potential roles in mucosal defense. Front Immunol 2013;4:200.
12. Crottet P, Cottet S, Corthesy B. Expression, purification and biochemical characterization of recombinant murine secretory component: a novel tool in mucosal immunology. Biochem J 1999;341:299–306.
13. Phalipon A, Cardona A, Kraehenbuhl JP, Edelman L, Sansonetti PJ, Corthesy B. Secretory component: a new role in secretory IgA-mediated immune exclusion in vivo. Immunity 2002;17:107–15.
14. Martinsson K, Ljungberg KR, Ziegelasch M, Cedergren J, Eriksson P, Klimovich V, et al. Elevated free secretory component in early rheumatoid arthritis and prior to arthritis development in patients at increased risk. Rheumatology (Oxford) 2020;59:979–87.
15. Eloff E, Martinsson K, Ziegelasch M, Cedergren J, Reckner A, Skogh T, et al. Autoantibodies are major predictors of arthritis development in patients with anti-citrullinated protein antibodies and musculoskeletal pain. Scand J Rheumatol 2021;50:189–97.
16. Arnett FC, Edworthy SM, Bloch DA, McShane DJ, Fries JF, Cooper NS, et al. The American Rheumatism Association 1987 revised criteria for the classification of rheumatoid arthritis. Arthritis Rheum 1988;31:315–24.
17. Hallert E, Husberg M, Kalkan A, Rahmqvist M, Skogh T, Bernfort L. Changes in sociodemographic characteristics at baseline in two Swedish cohorts of patients with early rheumatoid arthritis diagnosed 1996-98 and 2006-09. Scand J Rheumatol 2015;44:100–5.
18. Larsen A. How to apply Larsen score in evaluating radiographs of rheumatoid arthritis in long-term studies. J Rheumatol 1995;22:1974–5.
19. Weitoft T, Ronnelid J, Knight A, Lysholm J, Saxne T, Larsson A. Outcome predictors of intra-articular glucocorticoid treatment for knee synovitis in patients with rheumatoid arthritis: a prospective cohort study. Arthritis Res Ther 2014;16:R129.
20. Prevoo ML, van't Hof MA, Kuper HH, van Leeuwen MA, van de Putte LB, van Riel PL. Modified disease activity scores that include twenty-eight–joint counts: development and validation in a prospective longitudinal study of patients with rheumatoid arthritis. Arthritis Rheum 1995;38:44–8.
21. Böttcher MF, Haggström P, Björksten B, Jenmalm MC. Total and allergen-specific immunoglobulin A levels in saliva in relation to the development of allergy in infants up to 2 years of age. Clin Exp Allergy 2002;32:1293–8.
22. Griazeva IV, Samoilovich MP, Klimovich BV, Pavlova MS, Vartanian NL, Kirienko AN, et al. Monoclonal antibodies against human secretory component: epitope specificity and utility for immunoanalysis. Zh Mikrobiol Epidemiol Immunobiol 2010:54–9. In Russian.
23. Kastbom A, Roos Ljungberg K, Ziegelasch M, Wetterö J, Skogh T, Martinsson K. Changes in anti-citrullinated protein antibody isotype levels in relation to disease activity and response to treatment in early rheumatoid arthritis. Clin Exp Immunol 2018;194:391–9.
24. Svärd A, Skogh T, Alfredsson L, Ilar A, Klareskog L, Bengtsson C, et al. Associations with smoking and shared epitope differ between IgA- and IgG-class antibodies to cyclic citrullinated peptides in early rheumatoid arthritis. Arthritis Rheumatol 2015;67:2032–7.
25. Rindisbacher L, Cottet S, Wittek R, Kraehenbuhl JP, Corthesy B. Production of human secretory component with dimeric IgA binding capacity using viral expression systems. J Biol Chem 1995;270:14220–8.
26. Wendling D, Didier JM, Seilles E. Serum secretory immunoglobulins in ankylosing spondylitis. Clin Rheumatol 1996;15:590–3.

27. Salas-Cuestas F, Bautista-Molano W, Bello-Gualtero JM, Arias I, Castillo DM, Chila-Moreno L, et al. Higher levels of secretory IgA are associated with low disease activity index in patients with reactive arthritis and undifferentiated spondyloarthritis. Front Immunol 2017;8:476.
28. Wehmeyer A, Das PK, Swaak T, Gebhart W, Kijlstra A. Sjogren syndrome: comparative studies in local ocular and serum immunoglobulin concentrations with special reference to secretory IgA. Int Ophthalmol 1991;15:147–51.
29. Seilles E, Rossel M, Vuitton DA, Mercier M, Njoya O, Capron JP, et al. Serum secretory IgA and secretory component in patients with non-cirrhotic alcoholic liver diseases. J Hepatol 1995;22:278–85.
30. Roos Ljungberg K, Martinsson K, Wettero J, Svard A, Kastbom A. Circulating anti-citrullinated protein antibodies containing secretory component are prognostic for arthritis onset in at-risk patients. Clin Exp Immunol 2021;204:344–51.

DOI 10.1002/art.42069

Clinical Images: Giant cell arteritis with positive temporal artery biopsy findings but without ultrasound halo sign

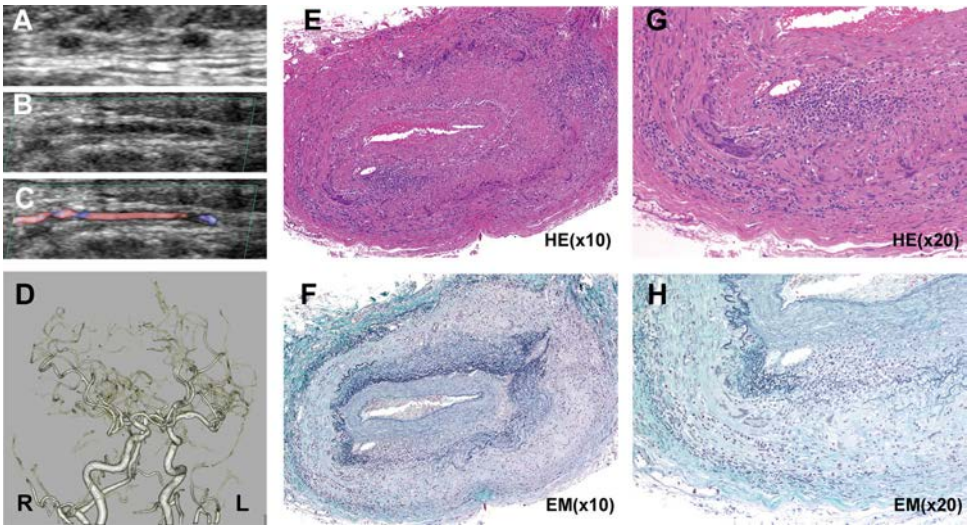

The patient, a 66-year-old woman, had been experiencing chronic pain in the shoulder and hip girdle for 8 months. She had also experienced transient visual disturbance 3 months prior to presentation. A fundus examination revealed some cotton-wool spots in the right eye. Her C-reactive protein level was elevated (4.2 mg/dl). Ultrasound of the temporal artery showed narrowing of the temporal arteries bilaterally. The intima-media thickening that could be measured was 0.2–0.4 mm. No halo sign (**A**–**C**) or compression sign was detected. The patient's right temporal artery was not detected on computed tomographic (CT) angiography, while the left was partially narrowed (**D**). Based on the clinical history and CT findings, giant cell arteritis (GCA) was strongly suspected, and a temporal artery biopsy was performed, which showed diffuse intimal thickening and fibrotic change. Multinucleated giant cells and lymphocytic infiltration were observed, mainly in the smooth muscle layer of the media, forming a granuloma. Partial tearing of the internal elastic lamina was also seen (**E**–**H**; HE = hematoxylin and eosin; EM = Elastica-Masson stain). These changes were observed throughout the collected samples. A recent systematic review showed that, in the setting of GCA, the specificity of the appearance of halo sign on ultrasound is as high as 95% (95% confidence interval 89–98%) when the clinical diagnosis is used as a reference (1); however, this is especially true in the acute phase (2) and not in all phases (e.g., in the late phase as in the present case). Thus, in addition to ultrasound, a comprehensive examination, especially at the time of symptom onset, should be considered for the accurate diagnosis of GCA.

Author disclosures are available at https://onlinelibrary.wiley.com/action/downloadSupplement?doi=10.1002%2Fart.42069&file=art42069-sup-0001-Disclosureform.pdf.

1. Sebastian A, Coath F, Innes S, Jackson J, van der Geest KS, Dasgupta B. Role of the halo sign in the assessment of giant cell arteritis: a systematic review and meta-analysis. Rheumatol Adv Pract 2021;5:rkab059.
2. Schmidt WA. Ultrasound in the diagnosis and management of giant cell arteritis [review]. Rheumatology (Oxford) 2018;57 Suppl 2:ii22–31.

Takeshi Suzuki, MD, PhD
Sumiyo Ando, MD, PhD
Miho Ohshima, MD, PhD
Akitake Suzuki, MD, PhD
Mitsui Memorial Hospital
Tokyo, Japan

Arthritis & Rheumatology
Vol. 74, No. 5, May 2022, pp 810–817
DOI 10.1002/art.42056

American College of Rheumatology
Empowering Rheumatology Professionals

Associations of Body Mass Index With Pain and the Mediating Role of Inflammatory Biomarkers in People With Hand Osteoarthritis

Marthe Gløersen,[1] Pernille Steen Pettersen,[1] Tuhina Neogi,[2] S. Reza Jafarzadeh,[2] Maria Vistnes,[3] Christian S. Thudium,[4] Anne-Christine Bay-Jensen,[4] Joe Sexton,[5] Tore K. Kvien,[1] Hilde B. Hammer,[1] and Ida K. Haugen[5]

Objective. To examine the association of body mass index (BMI) with pain in people with hand osteoarthritis (OA), and explore whether this association, if causal, is mediated by systemic inflammatory biomarkers.

Methods. In 281 Nor-Hand study participants, we estimated associations between BMI and hand pain, as measured by the Australian/Canadian Osteoarthritis Hand Index (AUSCAN; range 0–20) and Numerical Rating Scale (NRS; range 0–10); foot pain, as measured by NRS (range 0–10); knee/hip pain, as measured by the Western Ontario and McMaster Universities Osteoarthritis Index (WOMAC; range 0–20); painful total body joint count; and pain sensitization. We fit natural-effects models to estimate natural direct and natural indirect effects of BMI on pain through inflammatory biomarkers.

Results. Each 5-unit increase in BMI was associated with more severe hand pain (on average increased AUSCAN by 0.64 [95% confidence interval (95% CI) 0.23, 1.08]), foot pain (on average increased NRS by 0.65 [95% CI 0.36, 0.92]), knee/hip pain (on average increased WOMAC by 1.31 [95% CI 0.87, 1.73]), generalized pain, and pain sensitization. Mediation analyses suggested that the effects of BMI on hand pain and painful total body joint count were partially mediated by leptin and high-sensitivity C-reactive protein (hsCRP), respectively. Effect sizes for mediation by leptin were larger for the hands than for the lower extremities, and were statistically significant for the hands only.

Conclusion. In people with hand OA, higher BMI is associated with greater pain severity in the hands, feet, and knees/hips. Systemic effects of obesity, measured by leptin, may play a larger mediating role for pain in the hands than in the lower extremities. Low-grade inflammation, measured by hsCRP, may contribute to generalized pain in overweight/obese individuals.

INTRODUCTION

Osteoarthritis (OA) is the most common joint disease, with pain as the primary symptom. Body weight is a potential modifiable risk factor for OA pain (1), and weight loss may reduce pain, mechanical loading, and systemic inflammation in people with knee OA (2). Since mechanical loading caused by obesity does not have the same effects on hand joints as on the weight-bearing joints in the lower extremities, hand joints are well suited to study the possible systemic effects of obesity on pain.

Overweight and obesity induce a low-grade inflammatory state as adipose tissue produces inflammatory biomarkers, which

Supported by Major and Lawyer Eivind Eckbo's Foundation. Data collection in the Nor-Hand study was supported by the South-Eastern Norway Regional Health Authority, Dr. Trygve Gythfeldt and wife's Research Foundation, Pahle's Foundation, and Simon Fougner Hartmann's Family Foundation. Dr. Neogi's work was supported by the NIH (award P30-AR-072571). Dr. Jafarzadeh's work was supported by the National Institute on Aging, NIH (award R03-AG-060272) and the National Institute of Arthritis and Musculoskeletal and Skin Diseases, NIH (awards R21-AR-074578 and P30-AR-072571).

[1]Marthe Gløersen, MD, Pernille Steen Pettersen, MD, Tore K. Kvien, MD, PhD, Hilde B. Hammer, MD, PhD: Diakonhjemmet Hospital and University of Oslo, Oslo, Norway; [2]Tuhina Neogi, MD, PhD, S. Reza Jafarzadeh, MPVM, PhD: Boston University School of Medicine, Boston, Massachusetts; [3]Maria Vistnes, MD, PhD: Diakonhjemmet Hospital, Oslo University Hospital Ullevål, and University of Oslo, Oslo, Norway; [4]Christian S. Thudium, MSc, PhD, Anne-Christine Bay-Jensen, MSc, PhD: Nordic Bioscience A/S, Herlev, Denmark; [5]Joe Sexton, PhD, Ida K. Haugen, MD, PhD: Diakonhjemmet Hospital, Oslo, Norway.

Author disclosures are available at https://onlinelibrary.wiley.com/action/downloadSupplement?doi=10.1002%2Fart.42056&file=art42056-sup-0001-Disclosureform.pdf.

Address correspondence to Marthe Gløersen, MD, Division of Rheumatology and Research, Diakonhjemmet Hospital, Box 23 Vinderen, NO-0319 Oslo, Norway. E-mail: marthe.gl@hotmail.com.

Submitted for publication March 15, 2021; accepted in revised form December 16, 2021.

may affect pain mechanisms. Cytokines such as interleukin-1β (IL-1β), IL-6, and tumor necrosis factor (TNF) may act directly on nociceptive neurons through their receptors or indirectly through induction of prostaglandin production, which may activate or sensitize nociceptive neurons, leading to increased pain (3). Cytokines are also proposed to be involved in central pain mechanisms (3). A few clinical studies have indicated that cytokines may be involved in the induction of OA pain, but their findings were inconsistent, and the majority of studies were conducted on people with knee OA (3). Some studies, with conflicting results, have investigated associations between adipokines, such as leptin, adiponectin, and resistin, and symptomatic hand OA or hand OA pain (4–6).

Recent reviews have suggested that central pain sensitization, a phenomenon characterized by increased neural signaling in the central nervous system, contributes to chronic OA pain (7,8). Results from a study of persons undergoing bariatric surgery have suggested that reduced pain sensitization can partly explain the observed improvement in knee pain after weight loss (9). Other studies have investigated pain thresholds before and after weight loss or in persons with higher versus lower body mass index (BMI) and showed conflicting results (10–13).

Previous hand OA studies have presented conflicting results on the associations between BMI and symptomatic hand OA or hand pain (5,6,14–20). Only one of those studies investigated whether adipokines can mediate this possible association (6). That study did not examine pain intensity and did not assess mediation by other inflammatory biomarkers (6). We hypothesized that overweight/obesity is associated with joint pain in both the hands and lower extremities as well as pain sensitization, mediated through the inflammatory state that is affected by the overweight/obesity status. Hence, our aim was to examine whether higher BMI is associated with more severe pain and more central pain sensitization in people with hand OA. Further, using a causal inference-based mediation analysis, we explored whether any associations between BMI and pain, if causal, might be mediated by inflammatory biomarkers measured in serum/plasma.

PATIENTS AND METHODS

Study design and population. We used cross-sectional data from the baseline examination of the Nor-Hand study (2016–2017) in the current analyses. The Nor-Hand study is an observational cohort study of people with hand OA. Participants were recruited to the study through the outpatient clinic or a multidisciplinary course organized by the Division of Rheumatology and Research at Diakonhjemmet Hospital. All participants were between 40 and 70 years of age and had hand OA diagnosed by ultrasound and/or clinical examination performed by a rheumatologist. A detailed description of the inclusion and exclusion criteria has been published previously (21). The study has been approved by the Norwegian Regional Committee for Medical and Health Research Ethics (Ref. no: 2014/2057), and all participants provided written informed consent to participate. The study has been registered at ClinicalTrials.gov (identifier: NCT03083548).

Physical examination. For all participants, height in a standing position without shoes was measured to the nearest millimeter, and weight in light indoor clothing was measured in kilograms, with accuracy to one decimal place, to calculate the BMI as kg/m^2. Waist circumference was measured to the nearest millimeter midway between the iliac crest and the lowest rib after the participant took a deep breath and exhaled. We assessed whether participants fulfilled the American College of Rheumatology (ACR) criteria for hand OA and the ACR clinical criteria for knee OA (22,23).

Pain questionnaires. Pain in the hands and feet during the last 24 hours was rated on a Numerical Rating Scale (NRS) (range 0–10, where 0 = no pain and 10 = worst imaginable pain). The Australian/Canadian Osteoarthritis Hand Index (AUSCAN) pain subscale (range 0–20) and the Western Ontario and McMaster Universities Osteoarthritis Index (WOMAC) pain subscale (range 0–20) were used to assess hand pain and knee/hip pain, respectively, during the last 48 hours (24,25). Persistent joint pain during the prior 6 weeks was marked on a homunculus illustrating the neck; the upper, middle, and lower back; and bilateral shoulders, elbows, wrists, hips, knees, and ankles. Pain in at least one joint in each hand, marked on a hand diagram depicting the bilateral distal and proximal interphalangeal, metacarpophalangeal, and thumb base joints, counted as a painful hand in the painful total body joint count (range 0–18). The same homunculus was used to identify the presence of widespread pain for the last 6 weeks, which was defined according to the ACR 1990 criteria as the presence of axial skeletal pain, pain on both the left and right side of the body, and pain both above and below the waist (26). However, in contrast to the definition in the ACR criteria, low back pain was not considered lower segment pain.

Quantitative sensory testing (QST). Pressure pain threshold (PPT) was assessed by applying pressure with a digital algometer (FPIX25; Wagner) at mid-portions of the anterior tibialis muscle. The pressure of the algometer was gradually increased by 0.5 kg/second until the participant first reported it to be slightly painful. This examination was performed 3 times with 30-second intervals between the measurements, and the average of the 3 values was used for analyses. Low PPTs, i.e., higher pain sensitivity, at distant nonpainful sites were considered to reflect manifestations of central pain sensitization.

Temporal summation (TS) is another manifestation of central pain sensitization, which can be measured as increased pain ratings after repetitive stimuli (27). TS was assessed with 7 weighted punctuate probes (8–512 mN), which were tapped against the left distal radioulnar joint with increasing weight. The probe that

caused a pain rating of ≥4 on the NRS (or alternatively the 512 mN probe if none of the probes caused a pain intensity rating of ≥4), was tapped 10 times with a rate of once per second at the same site. Pain intensity at the first, fifth, and tenth tap was rated on the NRS. TS was calculated by subtracting the pain rating at the first tap from the pain rating at either the fifth or tenth tap, whichever was higher.

The QST protocol was performed by 2 medical students who were trained according to a detailed predefined protocol. Interassessor reliability was determined by examination of 9 participants by both medical students on the same afternoon. The intraclass correlation coefficient (2-way mixed-effects model, absolute agreement, individual measure) was 0.43 for PPT at the anterior tibialis and 0.56 for TS.

Inflammatory biomarkers. Plasma was collected in containers with EDTA and was centrifuged immediately (maximum of 30 minutes) after collection. Serum was collected in containers without additives and was left to coagulate 30 minutes before centrifugation. The samples were stored at –20°C until all samples from participants assessed on the same day were collected (maximum of 5 hours). Plasma and serum were thereafter stored at –80°C.

Serum was analyzed for high-sensitivity C-reactive protein (hsCRP) and matrix metalloproteinase–dependent degradation of C-reactive protein (CRPM). High-sensitivity CRP was measured on an ADVIA 1800 platform using a CardioPhase hsCRP assay (Siemens Medical Solutions) according to the manufacturer's instructions. The hsCRP measurements were performed in singlet. CRPM measurements were performed in duplicate using a handheld competitive enzyme-linked immunosorbent assay (Nordic Bioscience). Briefly, 96-well streptavidin-coated plates were coated with 0.4 ng/ml of KAFVFPKESDK-biotin and left for 30 minutes at 20°C. After washing, calibrators, controls, and serum samples (diluted 1:4 in incubation buffer) were added, followed by peroxidase-conjugated antibody. The sample/antibody mixture was incubated at 20°C for 60 minutes. Tetramethylbenzidine was added after washing off the plates, incubated at 20°C, and stopped with sulfuric acid after 15 minutes. The colorimetric reaction was measured at 450 nm with reference at 650 nm using SoftMax Pro, version 5 software (Molecular Devices).

Plasma was analyzed for inflammatory biomarkers using a Luminex assay (Bio-Techne) according to the manufacturer's protocol. The samples were evenly distributed across plates based on the pain severity and BMI of the individuals they were obtained from. The following biomarkers were selected to represent Th1, Th17, and M1 inflammatory responses, based on previously identified associations with obesity and/or OA: IL-1β, IL-1 receptor antagonist (IL-1Ra), IL-4, IL-6, IL-10, IL-12, IL-17, IL-18, IL-21, interferon-γ, TNF, vascular endothelial growth factor, granulocyte–macrophage colony-stimulating factor (GM-CSF), CCL2, CCL3, CCL4, CXCL10, leptin, and resistin. These measurements were performed in singlet. Values below the detection limit were estimated as half of the lower limit of detection or the lowest estimated value, depending on which was the lowest. Biomarkers for which >50% of the values were estimated (CCL3, IL-12, and GM-CSF) were excluded from the statistical analyses. The intraassay and interassay coefficients of variation for leptin were acceptable (4.6% and 12.0%, respectively).

Potential confounders. Data regarding age and sex were collected from patient journals. Participants answered questions about potential confounders, such as their highest degree of completed education (7 levels), physical exercise (4 levels, dichotomized into "at least one time weekly" and "less than one time weekly"), sleep (5 levels, from normal sleep to extreme sleep disturbances), smoking (dichotomized into "current regular or occasional smoker" and "previous smoker or non-smoker"), anxiety and depression, measured by the Hospital Anxiety and Depression Scale (HADS; range 0–42) (28), and pain catastrophizing, measured by the Pain Catastrophizing Scale (PCS; range 0–52) (29).

Statistical analysis. In all analyses, the inflammatory biomarkers were log-transformed to decrease skewness. First, we wanted to examine whether BMI was associated with inflammatory biomarkers in our data, and linear regression analyses were therefore conducted. In our main analyses, a causal inference–based mediation analysis was performed by fitting natural-effects models to decompose the effect of BMI on pain into a natural indirect effect, which is potentially mediated by an inflammatory biomarker, and a natural direct effect that is not mediated by the biomarker. The natural-effects decomposition is used to formally assess mediation and is estimated based on the counterfactual framework for causal inference (30). The natural-effects model enables a nonparametric (i.e., model-free) decomposition of the effect of an exposure on an outcome. This causal inference–based mediation analysis does not rely on assessing whether the association between levels of exposure and mediators/outcomes reach statistical significance. Rather, it relies on the counterfactual framework to infer whether mediating effects exist. Natural effects were fitted using the imputation-based approach for mediation analysis (31). Estimates for the total, natural direct, and natural indirect effects are presented per SD increase in BMI with corresponding 95% confidence intervals (95% CIs) estimated by the bootstrapping technique.

We further assessed mediated interaction, that is, whether BMI and the inflammatory biomarker interact in their effects on the pain outcomes, whenever estimates of indirect effects suggest that mediation by the inflammatory biomarker is present. Sensitivity analyses were performed per SD increase in waist circumference to assess the relationship between abdominal obesity and pain. The potential mediating role of leptin was analyzed

with mediation analyses that were stratified by sex because of known sex differences in leptin levels. Analyses were performed with Stata version 14 and R software version 4.0.2 with the *medflex* package.

All analyses were adjusted for confounding by age, sex, and education (in parsimonious models). We repeated the analyses with additional adjustment for physical exercise, smoking, sleep, HADS, and PCS (in comprehensive models), because of uncertainty about the directions of the relationships between these factors and the exposure, mediator, and outcome. We did not adjust for structural OA changes because the association between BMI and radiographic hand OA is a subject of controversy, and because structural OA changes may be in the causal pathway between BMI and pain. We were interested in the effects of BMI on pain through inflammatory biomarkers, irrespective of whether the associations were partially mediated through structural OA changes. No correlations were found between BMI and Kellgren/Lawrence sum score in the hands in our study (Spearman's correlation coefficient 0.008; $P = 0.89$), suggesting that the effects of BMI on pain were not mediated by structural changes. Missing values in potential confounders were imputed and replaced with the mean of all available scores.

The validity of the mediation analysis rests on the assumption that the exposure (BMI) is a potential cause of the mediator (inflammatory biomarkers) and the mediator a potential cause of the outcome (pain). Due to the use of cross-sectional data, we made the assumption that the exposure preceded the mediator, and similarly that the mediator preceded the outcome.

Table 1. Characteristics of the study population (n = 281)*

Age, median (IQR) years	61 (57–66)
Sex, no. (%) women	249 (89)
Fulfilled ACR hand OA criteria, no. (%)	261 (93)
Fulfilled ACR clinical knee OA criteria, no. (%)†	172 (63)
Body mass index, mean ± SD kg/m^2	26.5 ± 5.0
Waist circumference, mean ± SD cm	88.8 ± 13.1
AUSCAN hand pain, mean ± SD (range 0–20)	8.1 ± 4.0
NRS hand pain, mean ± SD (range 0–10)	3.8 ± 2.3
NRS foot pain, median (IQR) (range 0–10)	2 (0–4)
WOMAC knee/hip pain, median (IQR) (range 0–20)‡	4.5 (1.0–8.5)
Painful total body joint count, median (IQR) (range 0–18)	4 (2–8)
Presence of widespread pain, no. (%)	99 (35.2)
PPT at the anterior tibialis muscle, mean ± SD kg/cm^2†	5.5 ± 2.6
Temporal summation, median (IQR)§	1 (0–2)
Leptin, median (IQR) μg/liter	12.8 (5.6–24.4)
hsCRP, median (IQR) mg/liter	1.5 (0.8–4.1)
Physical exercise at least 1 time weekly, no. (%)¶	192 (70)
University or other higher education, no. (%)‡	163 (58)
Moderate to extreme sleep disturbances, no. (%)‡	113 (40)
Current regular or occasional smoker, no. (%)	44 (16)
HADS total score, median (IQR) (range 0–42)†	6 (3–10)
PCS total score, median (IQR) (range 0–52)#	9 (5–15)

* IQR = interquartile range; ACR = American College of Rheumatology; OA = osteoarthritis; AUSCAN = Australian/Canadian Osteoarthritis Hand Index; NRS = Numerical Rating Scale; WOMAC = Western Ontario and McMaster Universities Osteoarthritis Index; PPT = pressure pain threshold; hsCRP = high-sensitivity C-reactive protein; HADS = Hospital Anxiety and Depression Scale; PCS = Pain Catastrophizing Scale.
† Data were missing for 9 participants.
‡ Data were missing for 1 participant.
§ Data were missing for 2 participants.
¶ Data were missing for 5 participants.
# Data were missing for 4 participants.

RESULTS

Participant characteristics and inflammatory biomarkers. The Nor-Hand study includes 300 participants, of whom 19 had missing plasma/serum samples. Characteristics of the 281 participants who were included are listed in Table 1. The participants demonstrated a wide range of pain intensity in the hands, feet, and knees/hips, with the highest pain intensity in the hands. Ninety-five (34%) of the participants were overweight, and 60 (21%) were obese. Higher BMI was associated with higher levels of 6 of the inflammatory biomarkers, namely, TNF, IL-6, IL-1Ra, resistin, leptin, and hsCRP (data not shown).

BMI and pain outcomes. Participants with a higher BMI reported more severe pain in their hands, feet, and knees/hips, as well as a higher painful total body joint count during the prior 6 weeks (total effects in Table 2). Further, participants with a higher BMI had more central pain sensitization (i.e., lower PPTs at the anterior tibialis and greater TS) (Table 3). The odds of widespread pain were higher in participants with a higher BMI, such that for every 5-unit increase in BMI, widespread pain experience increased by 54% (total effects odds ratio 1.54 [95% CI 1.17, 1.96] in the parsimonious model).

Mediating role of inflammatory biomarkers. In these exploratory analyses, estimates of the natural indirect effects suggested that the effect of BMI on hand pain was partially mediated through plasma levels of leptin. Effect sizes for mediation by leptin were larger for hand pain than for pain in the lower extremities and for painful total body joint count, and reached statistical significance for hand pain only (Table 2 and Supplementary Figure 1, available on the *Arthritis & Rheumatology* website at http://onlinelibrary.wiley.com/doi/10.1002/art.42056). The effects of BMI on measures of central pain sensitization did not appear to be mediated through leptin (Table 3). Similar results were found after additional adjustment for other potential confounders in the comprehensive model (Supplementary Table 1, available on the *Arthritis & Rheumatology* website at http://onlinelibrary.wiley.com/doi/10.1002/art.42056).

A borderline statistically significant mediating effect of hsCRP was found on the effect of BMI on the painful total body joint count in the parsimonious model, whereas the mediating effect in the comprehensive model was statistically significant (Supplementary Table 2, available on the *Arthritis & Rheumatology* website at http://onlinelibrary.wiley.com/doi/10.1002/art.42056).

Table 2. Estimates of the total effect of a 5-unit increase in BMI on pain and the corresponding natural direct effects and natural indirect effects mediated by plasma levels of leptin*

	AUSCAN hand pain (range 0–20)	NRS hand pain (range 0–10)	NRS foot pain (range 0–10)	WOMAC knee/hip pain (range 0–20)	Painful total body joint count (range 0–18)
Total effect	0.64 (0.23, 1.08)†	0.46 (0.20, 0.72)†	0.65 (0.36, 0.92)†	1.31 (0.87, 1.73)†	1.15 (0.68, 1.60)†
Direct effect	0.26 (−0.34, 0.85)	0.24 (−0.09, 0.56)	0.57 (0.13, 0.96)†	1.13 (0.52, 1.75)†	0.87 (0.25, 1.47)†
Indirect effect	0.39 (0.02, 0.78)†	0.22 (−0.00, 0.44)	0.09 (−0.14, 0.34)	0.18 (−0.23, 0.56)	0.28 (−0.11, 0.66)

* The effect estimates (95% confidence intervals) shown in the table represent the estimated average increase in the pain outcomes per SD (5.0 kg/m^2) increase in body mass index (BMI). Analyses were adjusted for age, sex, and education. AUSCAN = Australian/Canadian Osteoarthritis Hand Index; NRS = Numerical Rating Scale; WOMAC = Western Ontario and McMaster Universities Osteoarthritis Index.
† Significant.

Weak and not statistically significant mediating effects of hsCRP were found on the effects of BMI on pain in the hands, feet, and knees/hips. Estimates of natural indirect effects suggested that none of the inflammatory biomarkers mediated the association between BMI and the presence of widespread pain, although small effect sizes were observed for hsCRP and leptin (natural indirect effect odds ratio 1.08 [95% CI 0.96, 1.19] and 1.12 [95% CI 0.90, 1.40], respectively, in the parsimonious model).

Natural indirect effect estimates for the other inflammatory biomarkers measured in plasma/serum did not suggest a mediating role in the effect of BMI on pain outcomes (data not shown). Estimates of the mediated interaction suggested no interaction between BMI and leptin or hsCRP on the BMI effects on pain outcomes.

Sensitivity analyses. Participants with a larger waist circumference reported more pain. Estimates of the total effects per SD (13.1 cm) increase in waist circumference on pain, and the estimated natural direct and natural indirect effects of plasma levels of leptin were of similar magnitude as the estimates reported for BMI (Supplementary Table 3, available on the *Arthritis & Rheumatology* website at http://onlinelibrary.wiley.com/doi/10.1002/art.42056). The effect of waist circumference on painful total body joint count was partially mediated through hsCRP, although it was only borderline statistically significant in the parsimonious model (data not shown).

In sex-stratified mediation analyses, similar estimates for the total effects, natural direct effects, and natural indirect effects of plasma levels of leptin were observed in women as in the main analyses (data not shown). Weak and not statistically significant associations between BMI and pain were observed in men (n = 32). Due to the small number of men in the study, natural direct and natural indirect effects were not estimated for men separately.

Table 3. Estimates of the total effect of a 5-unit increase in BMI on pain sensitization and the corresponding natural direct and natural indirect effects mediated by plasma levels of leptin*

	PPT at the anterior tibialis	Temporal summation of pain
Total effect	−0.38 (−0.64, −0.12)†	0.27 (0.09, 0.45)†
Direct effect	−0.34 (−0.70, 0.01)	0.23 (0.02, 0.45)†
Indirect effect	−0.04 (−0.31, 0.24)	0.04 (−0.10, 0.18)

* The effect estimates (95% confidence intervals) shown in the table represent the estimated average change in the pain sensitization outcomes per SD (5.0 kg/m^2) increase in body mass index (BMI). Analyses were adjusted for age, sex, and education. PPT = pressure pain threshold.
† Significant.

DISCUSSION

In the Nor-Hand study, participants with a higher BMI reported greater pain severity in their hands, feet, and knees/hips, a higher painful total body joint count, a more frequent presence of widespread pain, and more central pain sensitization. If these associations express a causal effect of BMI on pain, our analysis suggests that leptin and hsCRP might play the role of mediators on hand pain and painful total body joint count, respectively. Effect sizes for mediation by leptin were larger for the hands than for the lower extremities.

As expected, due to increased loading of joints in the lower extremities, a higher BMI was associated with more pain in the feet and knees/hips. Interestingly, a higher BMI was also related to greater pain severity in the hands, although the strength of association was modest. A difference of 1 point on the NRS for pain is the minimal clinically important difference (32). According to our model, 2 persons would need to have a difference of ~10 units in their BMI to have a clinically meaningful difference in hand pain. Positive associations between BMI and hand pain have been shown in previous cross-sectional studies (5,15,18), whereas longitudinal studies have not been able to demonstrate that baseline BMI or changes in BMI are associated with pain outcomes (16,17). The lack of significant associations in longitudinal studies may be related to small changes in exposure and/or outcome.

Our results suggest that plasma levels of leptin may partially mediate the association between BMI and hand pain. Leptin is an adipokine mainly secreted by adipose tissue, with proinflammatory effects. Findings from previous studies are inconsistent with regard to the association between leptin and pain, which may be due to the inclusion of BMI as a covariate in most, but not all, studies. Since BMI and leptin are highly correlated, collinearity may be a problem in these analyses. In contrast to our

findings, a small pilot study suggested a negative association between serum leptin levels and hand pain in people with hand OA (5). In the Third National Health and Nutrition Examination Survey cohort, no differences in serum leptin levels between people with symptomatic hand OA, those with asymptomatic hand OA, and those without hand OA were found (4). A recent cross-sectional study, however, found a positive association between serum leptin levels and symptomatic hand OA, and the relationship between adiposity and symptomatic hand OA was partially mediated by leptin (6). Conflicting results have been found in people with knee and hip OA with regard to the association between serum/plasma levels of leptin or leptin/adiponectin ratio and pain (33–36). Higher leptin levels were associated with a higher self-reported intensity of general body pain in the Women's Health Initiative (37).

Several mechanisms for how leptin may influence pain and pain sensitivity have been proposed. Leptin may contribute to the development of allodynia by stimulating the production of pronociceptive factors in macrophages (38). Further, leptin has been shown to modulate and exert structural changes in microglia (39), and microglia are increasingly recognized as important for the induction and maintenance of chronic pain (40). Glial cell dysfunction in the peripheral and central nervous system may cause chronic pain (40). A preclinical study has suggested that leptin may decrease pain thresholds in mice (41). However, this finding is not supported by our results, as we found no mediating effect of leptin on the association between BMI and pain sensitization. Our results are consistent with the findings of 2 other studies demonstrating no correlation between pain thresholds and leptin in patients with fibromyalgia or obese individuals (12,42). The lack of a mediating effect in our study may be related to the modest reliability of the QST. Furthermore, assessment of sensitization should preferably include various pain mechanisms (e.g., pain thresholds, tolerance thresholds, temporal and spatial summation, and conditioned pain modulation), and several different modalities (e.g., mechanical, electrical, and chemical stimuli) (43). In the present study, we assessed only PPTs and mechanical TS summation due to feasibility reasons.

We found that the association between BMI and painful total body joint count may be partially mediated by hsCRP. There was also a tendency toward a mediating effect of hsCRP on the association between BMI and the presence of widespread pain, although it was not statistically significant. These results may suggest that low-grade inflammation in overweight/obese individuals, reflected by increased levels of hsCRP, contribute to more generalized pain. It is well-known that overweight and obese individuals are more likely to have elevated CRP levels compared with persons of normal weight (44), and this is consistent with our results. Our results are also consistent with those of a meta-analysis that found a significant correlation between levels of hsCRP and joint pain (45). However, the meta-analysis included mainly studies on knee and hip OA, and only one study of OA in several joints. In contrast to these results, associations between BMI and pain in the hands, feet, and knees/hips were not mediated through hsCRP in our study. Our result may be due to involvement of other joints and/or fibromyalgia-like symptoms in the painful total body joint count. CRP levels above the reference value have been found in fibromyalgia patients (46).

Except for leptin and hsCRP, the inflammatory biomarkers in serum/plasma did not seem to mediate the association between BMI and pain, although there is increasing evidence that cytokines like IL-1β, IL-6, and TNF play a role in the development of chronic pain (47). Future studies should explore whether combinations of inflammatory biomarkers, rather than one biomarker alone, influence pain to a larger extent than what we found for the individual inflammatory biomarkers.

There are some limitations to this study that should be considered. Due to the cross-sectional study design, we cannot answer questions about causality, and reverse causation cannot be excluded. Longitudinal studies are needed to confirm the mediating role of inflammatory biomarkers on pain. We made the assumption that the exposure preceded the mediator, and that the mediator preceded the outcome. The first of these assumptions is based on the fact that adipose tissue produces inflammatory adipokines and obesity is associated with a low-grade inflammatory state (48). Longitudinal studies have suggested that a higher BMI predicts development of chronic pain (49). We cannot exclude the possibility that pain might also influence BMI through, e.g., a more sedentary lifestyle, but we consider this to be less likely for hand pain. Although we adjusted for several potential confounders, residual confounding by unmeasured variables may be present. This may have led to biased results. Furthermore, we have no information about the use of analgesics on the same day participants answered pain questionnaires and underwent QST. The interassessor reliability of the QST was moderate. The reliability could possibly have been improved by the inclusion of more participants in the exercise, more extensive training of the examiners, and increased emphasis on the cooperation, focus, and concentration of the participants in the QST protocol.

The generalizability of the results may be limited, since OA patients from secondary care may have more pain than patients seeking primary care. However, we did not require participants to fulfill the ACR hand OA criteria or a certain level of pain at inclusion, so that participants with a wide range of symptoms could be included in our study. This may increase the generalizability of the results to people with milder disease severity. We have limited information about OA in joints other than the hands and knees. Joint pain and biomarker levels may fluctuate throughout the day. All blood samples were collected between 4:00 PM and 9:00 PM, and it was thus not feasible to draw fasting blood samples. This may have introduced variation, although the variation between fasting and postprandial adipokine levels is usually small (50). Our relatively

small sample size (n = 281) contributed to a lack of sufficient precision in the CIs, so that CIs for some of the mediating effects slightly overlapped with the null despite sizable effect sizes. Because a lot of inflammatory biomarkers were tested, false-positive results cannot be ruled out, especially for hsCRP.

In conclusion, our results support a relationship between increased BMI and pain severity in both the hands and the lower extremities in a population with hand OA. Effect sizes for mediation by leptin were larger for the hands than for the lower extremities, which may suggest that the systemic effects of obesity on pain are more important in the hands than in the lower extremities, where the biomechanical effects of obesity may play a more important role. Most of the inflammatory biomarkers assessed in this study did not mediate the relationship between BMI and pain, suggesting that there are more specific pathways by which specific mediators may contribute to pain or that systemic low-grade inflammation mediates the relationship to a lesser extent than what we hypothesized. Despite modest strengths of associations, our results suggest that weight loss may be a strategy to prevent or treat pain in people with hand OA, which should be further explored in future studies.

ACKNOWLEDGMENTS

We would like to thank the participants; the project coordinators Karin Magnusson, Elisabeth Mulrooney, and Janicke Magnus; and the physicians and research assistants who contributed to the Nor-Hand study; as well as Siri Beisvåg Rom and Gro Jensen at the Department of Medical Biochemistry at Diakonhjemmet Hospital for analyzing the plasma inflammatory biomarkers.

AUTHOR CONTRIBUTIONS

All authors were involved in drafting the article or revising it critically for important intellectual content, and all authors approved the final version to be published. Dr. Gløersen had full access to all of the data in the study and takes responsibility for the integrity of the data and the accuracy of the data analysis.

Study conception and design. Neogi, Kvien, Hammer, Haugen.
Acquisition of data. Gløersen, Vistnes, Thudium, Bay-Jensen, Haugen.
Analysis and interpretation of data. Gløersen, Steen Pettersen, Neogi, Jafarzadeh, Vistnes, Sexton, Kvien, Hammer, Haugen.

ADDITIONAL DISCLOSURES

Authors Thudium and Bay-Jensen are employees of Nordic Bioscience A/S.

REFERENCES

1. Neogi T. The epidemiology and impact of pain in osteoarthritis. Osteoarthritis Cartilage 2013;21:1145–53.
2. Messier SP, Mihalko SL, Legault C, Miller GD, Nicklas BJ, DeVita P, et al. Effects of intensive diet and exercise on knee joint loads, inflammation, and clinical outcomes among overweight and obese adults with knee osteoarthritis: the IDEA randomized clinical trial. JAMA 2013;310:1263–73.
3. Eitner A, Hofmann GO, Schaible HG. Mechanisms of osteoarthritic pain. Studies in humans and experimental models. Front Mol Neurosci 2017;10:349.
4. Massengale M, Reichmann WM, Losina E, Solomon DH, Katz JN. The relationship between hand osteoarthritis and serum leptin concentration in participants of the Third National Health and Nutrition Examination Survey. Arthritis Res Ther 2012;14:R132.
5. Massengale M, Lu B, Pan JJ, Katz JN, Solomon DH. Adipokine hormones and hand osteoarthritis: radiographic severity and pain. PLoS One 2012;7:e47860.
6. Kroon FP, Veenbrink AI, de Mutsert R, Visser AW, van Dijk KW, le Cessie S, et al. The role of leptin and adiponectin as mediators in the relationship between adiposity and hand and knee osteoarthritis. Osteoarthritis Cartilage 2019;27:1761–7.
7. Fu K, Robbins SR, McDougall JJ. Osteoarthritis: the genesis of pain. Rheumatology (Oxford) 2018;57 Suppl:iv43–50.
8. Arendt-Nielsen L. Pain sensitisation in osteoarthritis. Clin Exp Rheumatol 2017;35 Suppl:68–74.
9. Stefanik JJ, Felson DT, Apovian CM, Niu J, Margaret Clancy M, LaValley MP, et al. Changes in pain sensitization after bariatric surgery. Arthritis Care Res (Hoboken) 2018;70:1525–8.
10. Tashani OA, Astita R, Sharp D, Johnson MI. Body mass index and distribution of body fat can influence sensory detection and pain sensitivity. Eur J Pain 2017;21:1186–96.
11. Price RC, Asenjo JF, Christou NV, Backman SB, Schweinhardt P. The role of excess subcutaneous fat in pain and sensory sensitivity in obesity. Eur J Pain 2013;17:1316–26.
12. Dodet P, Perrot S, Auvergne L, Hajj A, Simoneau G, Decleves X, et al. Sensory impairment in obese patients? Sensitivity and pain detection thresholds for electrical stimulation after surgery-induced weight loss, and comparison with a nonobese population. Clin J Pain 2013;29:43–9.
13. Zhang Y, Zhang S, Gao Y, Tan A, Yang X, Zhang H, et al. Factors associated with the pressure pain threshold in healthy Chinese men. Pain Med 2013;14:1291–300.
14. Magnusson K, Osteras N, Haugen IK, Mowinckel P, Nordsletten L, Natvig B, et al. No strong relationship between body mass index and clinical hand osteoarthritis: results from a population-based case-control study. Scand J Rheumatol 2014;43:409–15.
15. Cimmino MA, Scarpa R, Caporali R, Parazzini F, Zaninelli A, Sarzi-Puttini P. Body mass and osteoarthritic pain: results from a study in general practice. Clin Exp Rheumatol 2013;31:843–9.
16. Ding H, Solovieva S, Leino-Arjas P. Determinants of incident and persistent finger joint pain during a five-year followup among female dentists and teachers. Arthritis Care Res (Hoboken) 2011;63:702–10.
17. Magnusson K, Slatkowsky-Christensen B, van der Heijde D, Kvien TK, Hagen KB, Haugen IK. Body mass index and progressive hand osteoarthritis: data from the Oslo hand osteoarthritis cohort. Scand J Rheumatol 2015;44:331–6.
18. Damman W, Liu R, Kroon FP, Reijnierse M, Huizinga TW, Rosendaal FR, et al. Do comorbidities play a role in hand osteoarthritis disease burden? Data from the Hand Osteoarthritis in Secondary Care Cohort. J Rheumatol 2017;44:1659–66.
19. Visser AW, Ioan-Facsinay A, de Mutsert R, Widya RL, Loef M, de Roos A, et al. Adiposity and hand osteoarthritis: the Netherlands Epidemiology of Obesity study. Arthritis Res Ther 2014;16:R19.
20. Andrianakos AA, Kontelis LK, Karamitsos DG, Aslanidis SI, Georgountzos AI, Kaziolas GO, et al. Prevalence of symptomatic knee, hand, and hip osteoarthritis in Greece. The ESORDIG study. J Rheumatol 2006;33:2507–13.
21. Gløersen M, Mulrooney E, Mathiessen A, Hammer HB, Slatkowsky-Christensen B, Faraj K, et al. A hospital-based observational cohort study exploring pain and biomarkers in patients with hand osteoarthritis in Norway: the Nor-Hand protocol. BMJ Open 2017;7:e016938.
22. Altman R, Alarcón G, Appelrouth D, Bloch D, Borenstein D, Brandt K, et al. The American College of Rheumatology criteria for the classification and reporting of osteoarthritis of the hand. Arthritis Rheum 1990; 33:1601–10.

23. Altman R, Asch E, Bloch D, Bole G, Borenstein D, Brandt K, et al. Development of criteria for the classification and reporting of osteoarthritis: classification of osteoarthritis of the knee. Arthritis Rheum 1986;29:1039–49.
24. Bellamy N, Campbell J, Haraoui B, Buchbinder R, Hobby K, Roth JH, et al. Dimensionality and clinical importance of pain and disability in hand osteoarthritis: development of the Australian/Canadian (AUSCAN) Osteoarthritis Hand Index. Osteoarthritis Cartilage 2002; 10:855–62.
25. Bellamy N, Buchanan WW, Goldsmith CH, Campbell J, Stitt LW. Validation study of WOMAC: a health status instrument for measuring clinically important patient relevant outcomes to antirheumatic drug therapy in patients with osteoarthritis of the hip or knee. J Rheumatol 1988;15:1833–40.
26. Wolfe F, Smythe HA, Yunus MB, Bennett RM, Bombardier C, Goldenberg DL, et al. The American College of Rheumatology 1990 criteria for the classification of fibromyalgia: report of the Multicenter Criteria Committee. Arthritis Rheum 1990;33:160–72.
27. Curatolo M, Petersen-Felix S, Arendt-Nielsen L. Sensory assessment of regional analgesia in humans: a review of methods and applications. Anesthesiology 2000;93:1517–30.
28. Zigmond AS, Snaith RP. The hospital anxiety and depression scale. Acta Psychiatr Scand 1983;67:361–70.
29. Sullivan MJ, Bishop SR, Pivik J. The pain catastrophizing scale: development and validation. Psychol Assess 1995;7:524–32.
30. Lange T, Vansteelandt S, Bekaert M. A simple unified approach for estimating natural direct and indirect effects. Am J Epidemiol 2012; 176:190–5.
31. Vansteelandt S, Bekaert M, Lange T. Imputation strategies for the estimation of natural direct and indirect effects. Epidemiologic Methods 2012;1:131–58.
32. Salaffi F, Stancati A, Silvestri CA, Ciapetti A, Grassi W. Minimal clinically important changes in chronic musculoskeletal pain intensity measured on a numerical rating scale. Eur J Pain 2004;8:283–91.
33. Martel-Pelletier J, Tardif G, Trépanier JR, Abram F, Dorais M, Raynauld JP, et al. The ratio adipsin/MCP-1 is strongly associated with structural changes and CRP/MCP-1 with symptoms in obese knee osteoarthritis subjects: data from the Osteoarthritis Initiative. Osteoarthritis Cartilage 2019;27:1163–73.
34. Orellana C, Calvet J, Berenguer-Llergo A, Albinana N, Garcia Manrique M, Galisteo Lencastre C, et al. Synovial adiponectin was more associated with clinical severity than synovial leptin in women with knee osteoarthritis. Cartilage 2020:1947603520904776.
35. Perruccio AV, Mahomed NN, Chandran V, Gandhi R. Plasma adipokine levels and their association with overall burden of painful joints among individuals with hip and knee osteoarthritis. J Rheumatol 2014;41:334–7.
36. Sellam J, Rat AC, Fellahi S, Bastard JP, Ngueyon Sime W, Ea HK, et al. Pain in women with knee and/or hip osteoarthritis is related to systemic inflammation and to adipose tissue dysfunction: cross-sectional results of the KHOALA cohort. Semin Arthritis Rheum 2021;51:129–36.
37. Younger J, Kapphahn K, Brennan K, Sullivan SD, Stefanick ML. Association of leptin with body pain in women. J Womens Health (Larchmt) 2016;25:752–60.
38. Maeda T, Kiguchi N, Kobayashi Y, Ikuta T, Ozaki M, Kishioka S. Leptin derived from adipocytes in injured peripheral nerves facilitates development of neuropathic pain via macrophage stimulation. Proc Natl Acad Sci U S A 2009;106:13076–81.
39. Lafrance V, Inoue W, Kan B, Luheshi GN. Leptin modulates cell morphology and cytokine release in microglia. Brain Behav Immun 2010; 24:358–65.
40. Ji RR, Berta T, Nedergaard M. Glia and pain: is chronic pain a gliopathy? Pain 2013;154 Suppl:S10–28.
41. Kutlu S, Canpolat S, Sandal S, Ozcan M, Sarsilmaz M, Kelestimur H. Effects of central and peripheral administration of leptin on pain threshold in rats and mice. Neuro Endocrinol Lett 2003;24:193–6.
42. Paiva ES, Andretta A, Batista ED, Lobo M, Miranda RC, Nisihara R, et al. Serum levels of leptin and adiponectin and clinical parameters in women with fibromyalgia and overweight/obesity. Arch Endocrinol Metab 2017;61:249–56.
43. Arendt-Nielsen L, Skou ST, Nielsen TA, Petersen KK. Altered central sensitization and pain modulation in the CNS in chronic joint pain. Curr Osteoporos Rep 2015;13:225–34.
44. Visser M, Bouter LM, McQuillan GM, Wener MH, Harris TB. Elevated C-reactive protein levels in overweight and obese adults. JAMA 1999;282:2131–5.
45. Jin X, Beguerie JR, Zhang W, Blizzard L, Otahal P, Jones G, et al. Circulating C reactive protein in osteoarthritis: a systematic review and meta-analysis. Ann Rheum Dis 2015;74:703–10.
46. Sanada K, Diez MA, Valero MS, Perez-Yus MC, Demarzo MM, Garcia-Toro M, et al. Effects of non-pharmacological interventions on inflammatory biomarker expression in patients with fibromyalgia: a systematic review. Arthritis Res Ther 2015;17:272.
47. Zhang JM, An J. Cytokines, inflammation, and pain. Int Anesthesiol Clin 2007;45:27–37.
48. Berenbaum F, Eymard F, Houard X. Osteoarthritis, inflammation and obesity. Curr Opin Rheumatol 2013;25:114–8.
49. Okifuji A, Hare BD. The association between chronic pain and obesity. J Pain Res 2015;8:399–408.
50. Finucane FM, Luan J, Wareham NJ, Sharp SJ, O'Rahilly S, Balkau B, et al. Correlation of the leptin:adiponectin ratio with measures of insulin resistance in non-diabetic individuals. Diabetologia 2009;52: 2345–9.

Arthritis & Rheumatology
Vol. 74, No. 5, May 2022, pp 818–828
DOI 10.1002/art.42040

American College of Rheumatology
Empowering Rheumatology Professionals

No Added Value of Duloxetine in Patients With Chronic Pain due to Hip or Knee Osteoarthritis: A Cluster-Randomized Trial

Jacoline J. van den Driest,[1] Dieuwke Schiphof,[1] Aafke R. Koffeman,[2] Marc A. Koopmanschap,[3] Patrick J. E. Bindels,[1] and Sita M. A. Bierma-Zeinstra[1]

Objective. To assess the effectiveness of duloxetine in addition to usual care in patients with chronic osteoarthritis (OA) pain. The cost-effectiveness and whether the presence of symptoms of centralized pain alters the response to duloxetine were secondary objectives.

Methods. We conducted an open-label, cluster-randomized trial. Patients with chronic hip or knee OA pain who had an insufficient response to acetaminophen and nonsteroidal antiinflammatory drugs were included. Randomization took place at the general practice level, and patients received duloxetine (60 mg/day) in addition to usual care or usual care alone. The presence of centralized pain was defined as a modified PainDETECT Questionnaire score >12. The primary outcome measure was Western Ontario and McMaster Universities Osteoarthritis Index (WOMAC) pain scores (scale 0–20) at 3 months after the initiation of treatment. Our aim was to detect a difference between the groups of a clinically relevant effect of 1.9 points (effect size 0.4). We used a linear mixed model with repeated measurements to analyze the data.

Results. In total, 133 patients were included, and 132 patients were randomized into treatment groups. A total of 66 patients (at 31 practices) were randomized to receive duloxetine in addition to usual care, and 66 patients (at 35 practices) were randomized to receive usual care alone. We found no differences in WOMAC pain scores between the groups at 3 months (adjusted difference –0.58 [95% confidence interval (95% CI) –1.80, 0.63]) or at 12 months (adjusted difference –0.26 [95% CI –1.86, 1.34]). In the subgroup of patients with centralized pain symptoms, we also found no effect of duloxetine compared to usual care alone (adjusted difference –0.32 [95% CI –2.32, 1.67]).

Conclusion. We found no effect of duloxetine added to usual care compared to usual care alone in patients with chronic knee or hip OA pain. Another trial including patients with centralized pain symptoms should be conducted to validate our results.

INTRODUCTION

Osteoarthritis (OA) is one of the major chronic pain conditions involving the musculoskeletal system, and it affects ~15% of the population (1,2). Persistent pain and loss of function are 2 important problems for patients with OA. Treatment is symptomatic and consists of education, exercise, physiotherapy, and analgesics.

In OA, analgesics are prescribed in a stepwise approach. The first step is acetaminophen, which has a small therapeutic effect, but is often well tolerated and has few contraindications (3). Besides acetaminophen, topical nonsteroidal antiinflammatory drugs (NSAIDs) can be prescribed. The next step is the prescription of oral NSAIDs, which have a moderate effect on OA pain (4). Oral NSAIDs especially are often contraindicated and are associated with side effects. As a third step, opioids can be considered, but they often lack effectiveness for OA pain, and serious side effects are common (5,6). Finally, glucocorticoid injections can be administered when signs of inflammation are present (7), but there is ongoing debate regarding whether the injections may accelerate the progression of OA (8,9). Therefore, other treatment options are needed.

One option may be duloxetine, a serotonin and norepinephrine reuptake inhibitor. It is hypothesized that duloxetine reduces

Dutch trial registry no. NTR4798.
Supported by the Netherlands Organisation for Health Research and Development (award 80-83600-98-3141).
[1]Jacoline J. van den Driest, MD, Dieuwke Schiphof, PhD, Patrick J. E. Bindels, MD, PhD, Sita M. A. Bierma-Zeinstra, PhD: Erasmus University Medical Center, Rotterdam, The Netherlands; [2]Aafke R. Koffeman, MD, PhD: Leiden University Medical Center, Leiden, The Netherlands; [3]Marc A. Koopmanschap, PhD: Erasmus University Rotterdam, Rotterdam, The Netherlands.

Author disclosures are available at https://onlinelibrary.wiley.com/action/downloadSupplement?doi=10.1002%2Fart.42040&file=art42040-sup-0001-Disclosureform.pdf.
Address correspondence to Jacoline J. van den Driest, MD, Department of General Practice, Erasmus Medical Center, Wytemaweg 80, PO Box 2040, 3000 CA Rotterdam, The Netherlands. Email: j.vandendriest@erasmusmc.nl.
Submitted for publication April 21, 2021; accepted in revised form December 2, 2021.

chronic pain through the central inhibition of pain and acts by modulating descending (inhibitory) pain pathways in the central nervous system (10). In OA, pain can refer to nociceptive pain in the joint, peripheral sensitized pain resulting from inflammatory factors, and centrally sensitized pain (11,12). This centrally sensitized pain can occur after intense, repeated, or prolonged nociceptive input (11,13) and is present in ~23% of patients with chronic pain due to OA (14).

Several placebo-controlled trials have examined the efficacy of duloxetine in patients with OA and demonstrated effect sizes of 0.4–0.5 for pain and 0.6 for disability (15–20). Based on these trials, the Osteoarthritis Research Society International (OARSI) recommends duloxetine in patients with knee OA who have depression and/or widespread pain (7) and the American College of Rheumatology (ACR) conditionally recommends duloxetine for OA (21).

The placebo-controlled trials mentioned above investigated the short-term use of duloxetine in highly controlled secondary care settings (15–20). In a primary care setting, the effectiveness of duloxetine in addition to usual care compared to usual care alone is not known; however, most OA patients receive treatment in this setting for many years. It is also not known whether the presence of symptoms of centrally sensitized pain alters the response to duloxetine.

Therefore, we conducted a cluster-randomized controlled trial with a 12-month follow-up period to examine the effectiveness and cost-effectiveness of duloxetine in a primary care setting in patients with OA and to assess whether a beneficial effect of duloxetine is seen predominantly in patients with symptoms of centrally sensitized pain.

PATIENTS AND METHODS

Study design. A pragmatic open-label cluster-randomized trial with 2 parallel arms was conducted in general practices. A cluster design was chosen because this type of design is particularly useful in effectiveness and implementation studies, since the cluster design has the advantage of preventing treatment group contamination and reflects general practice more closely (22). The study was approved by the Local Medical Ethics Committee at the Erasmus Medical Center (approval no. MEC 2015-293). The trial is registered in the Dutch Trial Registry (identifier: NTR4798) and EudractCT (database no. 2015-001669-16). Detailed information regarding the study design is published elsewhere (23).

Data availability. Relevant anonymized patient-level data are available upon reasonable request.

Setting and participants. General practices in the southwestern region of The Netherlands were asked to participate in the study. Participating general practices identified all possible eligible patients in their patient registries and sent these patients an invitation. If they were interested, patients provided written informed consent and were screened for eligibility by the research team.

Patients were eligible if they were age ≥18 years, had hip and/or knee OA according to the ACR clinical criteria (24), had chronic pain, defined as pain on most days of the last 3 months, and had shown an insufficient response to treatment with NSAIDs, had contraindications for NSAIDs, or had previous adverse reactions to NSAIDs (e.g., were eligible for third choice pain medication).

Patients were excluded if they were scheduled for total hip replacement (THR) or total knee replacement (TKR), were currently receiving antidepressants or neuropathic pain medication (gabapentin, pregabalin, carbamazepine, capsaicin cream, or lidocaine cream), had rheumatoid arthritis, were unable to sign the informed consent, or had contraindications for the use of duloxetine (current use of monoamine oxidase inhibitors, uncontrolled narrow-angle glaucoma, receiving a combination treatment with other central nervous system–acting drugs [e.g., benzodiazepines], hypersensitivity to duloxetine, liver disease resulting in hepatic impairment, severe renal impairment [creatinine clearance <30 ml/minute], current use of *CYP1A2* inhibitors, current use of *CYP2D6* inhibitors and substrates, uncontrolled hypertension, pregnancy, or lactation).

Intervention. The participating general practices were randomized to prescibe duloxetine in addition to usual care (intervention group) or provide usual care alone to the patients (control group). In the intervention group, patients were prescribed duloxetine at 60 mg/day. In the first week of treatment, patients were prescribed a duloxetine dose of 30 mg/day to minimize potential adverse events. If the dose was well tolerated, it was increased to 60 mg/day in the second week. The therapeutic effect was regularly assessed by the treating general practitioner (at week 2 and months 1, 3, 6, 9, and 12). Duloxetine was gradually discontinued after 3 months when patients experienced no effect and/or when patients had intolerable side effects.

Usual care was provided according to the Dutch general practice guidelines (25) and consists of education, lifestyle advice, diet, physiotherapy, and analgesics. Intraarticular injection of glucocorticoids and referral to secondary care were also allowed.

Randomization. Randomization of patients to a treatment group was performed at the practice level (cluster-randomized design). An independent data manager of the department provided a computer-generated, blinded randomization list (allocation ratio 1:1). Block randomization was used with blocks varying between 2, 4, and 6 numbers. Since care provided by the general practitioner can differ based on practice characteristics, randomization at the practice level was stratified according to 1) socioeconomic status of the practice location based on the registration of The Netherlands Institute for Social Research (low

versus normal and high socioeconomic status) (26), 2) the number of general practitioners working at the practice (≤1 full-time employee versus >1 full-time employee), and the mean age of the general practitioners (<50 years versus ≥50 years) (27,28).

Researchers were blinded with regard to the randomization procedure. The research team performed the randomization after all eligible patients were identified and the first patient had provided signed informed consent. Patients were informed about the outcome of randomization after filling in the baseline questionnaire. The study was open label; patients, general practitioners, and the research team were not blinded with regard to the treatment.

Outcome measures. Patients received questionnaires at baseline, at week 6, and at months 3, 6, 9, and 12. The primary outcome measure was the pain score at month 3, measured using the Western Ontario and McMaster Universities Osteoarthritis Index (WOMAC) scores (29). The WOMAC consists of 3 domains: pain (scale 0–20), stiffness (scale 0–8), and function (scale 0–68), with higher scores indicating more problems.

The secondary outcome measures were the WOMAC scores for pain and function at 1 year. At baseline, the modified PainDETECT Questionnaire was administered to assess the presence of centralized pain (30,31). The 5-level EuroQol 5-domain questionnaire was administered to assess the cost-effectiveness of the intervention (32). Cointerventions (medication use, visits to health care professionals, THR or TKR) and patient-reported adverse events were recorded. Also, patient satisfaction with the treatment of pain was measured using an 11-point numerical rating scale (with a score of 0 indicating completely dissatisfied with treatment to a score of 10 indicating completely satisfied), and patient improvement (presence of symptoms) was measured using a 7-point Likert scale (with a score of 0 indicating total improvement of symptoms to a score of 7 indicating "worse than ever"). Patients were asked what they regarded as their most painful activity, with each designated activity rated on an 11-point numerical visual analog scale (33). Patients could choose this activity from the WOMAC function items and were able to mention another activity.

The percentage of responders was also evaluated using the Outcome Measures in Rheumatology (OMERACT)–Osteoarthritis Research Society International (OARSI) response criteria (34). Response was defined as 1) high improvement in pain or function (≥50%) and an absolute change in the pain or function score of ≥20 points (scale 0–100) or 2) improvement in at least 2 of the following 3 criteria: change in pain score ≥20% and absolute change ≥10 points; change in function score ≥20% and absolute change ≥10 points; and change in patient's global assessment of disease activity ≥20% and absolute change ≥10 points.

Sample size. A total of 102 patients per treatment group was required to detect a clinically relevant difference in WOMAC pain score of 1.9 points (pooled SD 4.8) (15) between the 2 groups with an effect size of 0.4 (80% power to detect a significant difference at a significance threshold of $P \leq 0.05$). This is taking into account the cluster randomization with the assumption of equal cluster sizes with 3 patients per practice and an intracluster correlation coefficient of 0.01. We expected ~10% loss to follow-up (35) and we therefore needed to include 224 patients (2×112). In order to detect a larger effect in patients with symptoms of centrally sensitized pain, we needed to include 44 patients per group (effect size 0.6, a difference in WOMAC pain score of 2.9 points [pooled SD 4.8] with the same power and cluster assumptions). In advance, we estimated that 37% of included patients would have symptoms of centrally sensitized pain (30), and 47% of patients in the trial had symptoms of centrally sensitized pain. Therefore, no sample size adjustments had to be made for this subgroup analysis.

Statistical analysis. Analyses were performed according to the intent-to-treat principle. Descriptive statistics were used to describe baseline characteristics of the general practices and patients.

A linear mixed-effects model with repeated measurements was used to assess the differences between the 2 groups. The general practices were included as a random effect to account for clustering. The change in all WOMAC scores over time was nonlinear and therefore a natural spline was added at week 26.

Generalized estimating equation (GEE) analyses with an autoregressive correlation structure were performed for analyses of dichotomous outcomes. Analyses were adjusted for prognostic factors at baseline when they differed ≥10% between the 2 groups.

Additional per-protocol analyses were conducted. Patients were included if they received duloxetine for ≥4 weeks or if they did not receive neuropathic pain medication in the usual care group. Furthermore, a predefined subgroup analysis was performed in which the analysis was limited to patients who had symptoms of centrally sensitized pain. Patients were included in this subgroup analysis if they scored >12 on the modified PainDETECT questionnaire. Scores >12 on this questionnaire are associated with the presence of symptoms of centralized pain in OA (30).

According to the protocol, a cost-utility analysis would only be performed if the intervention was found effective. Mixed-effects model analyses and GEE analyses were performed using R package version 3.6.3. All other analyses were performed using SPSS version 25 (IBM).

RESULTS

Participants. Patient recruitment took place between January 2016 and February 2019, and the follow-up period was completed in February 2020. A total of 231 general practitioners

at 110 general practices participated in the study. In total, 4,748 patients were classified as having knee or hip OA in general practice records, and 3,258 patients were excluded based on the presence of exclusion criteria in their medical records (Figure 1). A total of 1,490 patients were potentially eligible for inclusion and were invited to participate; 768 patients declined the study invitation, 295 patients were interested but not eligible, and 72 patients were interested and eligible but declined to participate. The most frequently mentioned reason for eligible patients declining was fear of side effects. Finally, 133 patients were included in the study, but 1 patient was lost to follow-up before randomization occurred. Therefore, 66 patients (at 31 general practices) were randomized to receive duloxetine and usual care, and 66 patients (at 35 general practices) were randomized to receive usual care alone. A total of 53 patients in each treatment arm completed the 12-month follow-up period (80.3%).

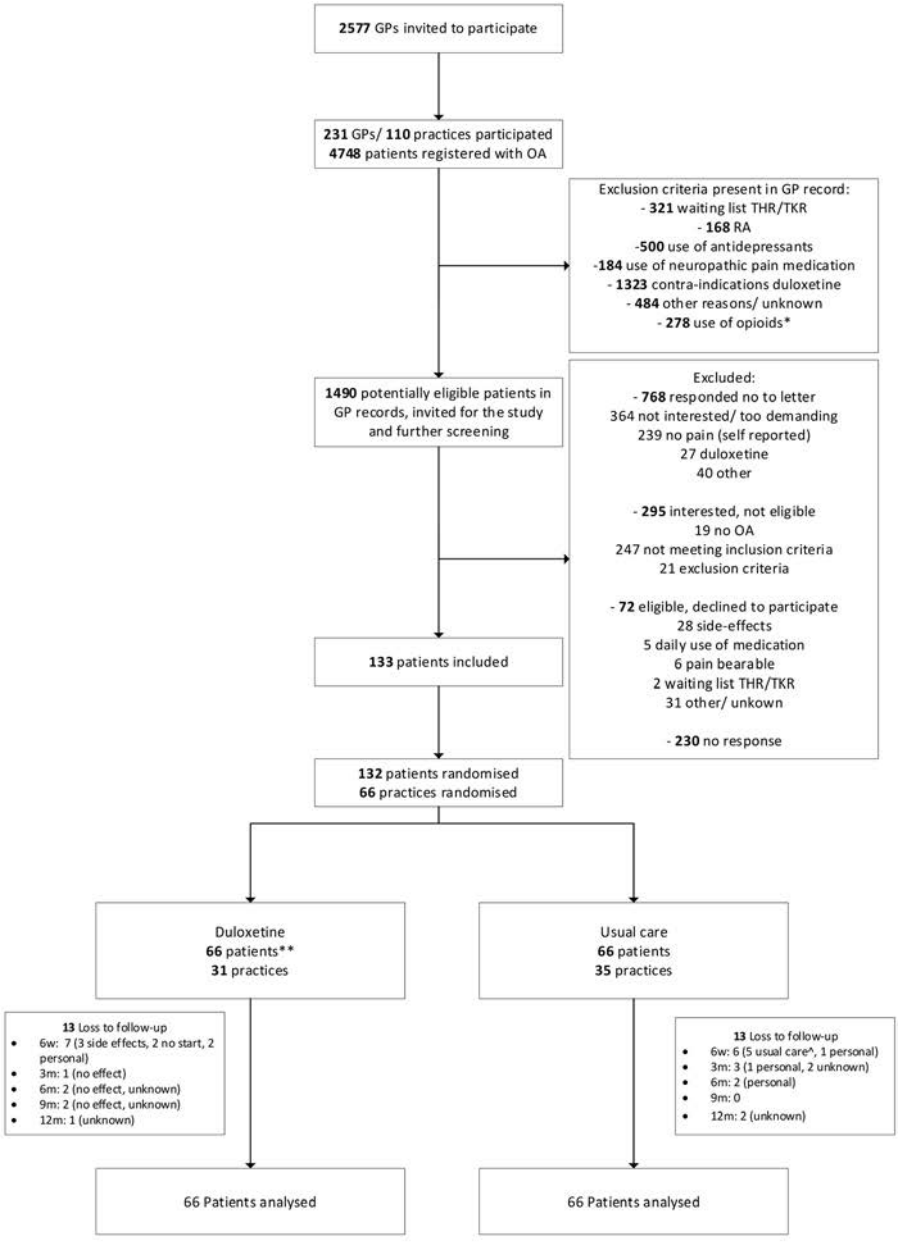

Figure 1. Flow chart of the study design showing that general practitioners were invited to participate and either declined or accepted. General practice records of patients with knee or hip OA were reviewed for exclusion criteria, and included patients were randomized to receive either duloxetine in addition to usual care or usual care alone.

Table 1. Baseline characteristics of the general practices and the OA patients in each practice randomized to receive treatment with either duloxetine in addition to usual care or usual care alone*

	Randomization to duloxetine	Randomization to usual care alone
General practices		
No. of general practices	31	35
No. of general practitioners, median	2	2
No. of days general practitioners worked in the practice, mean ± SD	1.7 ± 1.1	1.9 ± 1.0
High SES vs. low SES	23 (74.2)	27 (77.1)
Age of general practitioners, mean ± SD years	48.7 ± 8.2	48.3 ± 8.8
No. of patients included, median (range)	2 (1–6)	2 (1–4)
Patients		
No. of patients randomized	66	66
Sex, female	39 (59.1)	50 (75.8)
Age, mean ± SD years	63.2 ± 10.5	65.4 ± 11.2
BMI, mean ± SD kg/mg^2	30.6 ± 6.6	30.9 ± 6.2
Self-reported comorbidities		
CVDs	4 (6.1)	9 (13.6)
Lung diseases	4 (6.1)	15 (22.7)
Diabetes mellitus	10 (15.2)	8 (12.1)
Neurologic disorders	4 (6.1)	1 (1.5)
Lower back pain	41 (62.5)	34 (51.5)
Other musculoskeletal disorders	32 (48.5)	38 (57.5)
≥2 comorbidities	10 (15.2)	22 (33.3)
Employed at baseline	31 (47.0)	23 (34.8)
Duration of symptoms, mean ± SD years	7.8 ± 6.5	9.2 ± 8.2
Affected joints†		
Hip	15 (22.7)	9 (13.6)
Also knee OA	9 (60.0)	5 (55.6)
OA in both hips	4 (26.7)	5 (55.6)
Knee	51 (77.3)	57 (86.4)
Also hip OA	8 (15.7)	19 (33.3)
OA in both knees	35 (68.8)	34 (59.6)
WOMAC score, mean ± SD		
Pain (scale 0–20)	9.8 ± 4.2	10.5 ± 3.6
Stiffness (scale 0–8)	4.5 ± 1.8	5.0 ± 1.5
Function (scale 0–68)	34.8 ± 13.3	36.2 ± 11.1
Modified PainDETECT score (scale 0–35)		
Mean ± SD	11.4 ± 6.8	13.5 ± 7.0
No. (%)		
≤12	39 (59.1)	32 (48.5)
13–18	14 (21.2)	13 (19.7)
>18	13 (19.7)	19 (28.8)
Most painful activity score, mean ± SD (scale 0–10)‡	7.0 ± 1.3	7.4 ± 1.4
HADS score, mean ± SD		
Depression (scale 0–21)	4.2 ± 3.5	3.6 ± 3.1
Anxiety (scale 0–21)	4.5 ± 3.8	4.0 ± 3.3
EQ-5D-5L score, mean ± SD (scale –0.446, 1)	0.628 ± 0.168	0.613 ± 0.161
Treatment		
None	18 (27.3)	20 (30.3)
Acetaminophen	28 (42.4)	25 (37.9)
Topical NSAIDs	1 (1.5)	0 (0.0)
NSAIDs	30 (45.5)	28 (42.4)
Opioids	6 (9.1)	10 (15.2)

* Except where indicated otherwise, values are the number (%). OA = osteoarthritis; SES = socioeconomic status; BMI = body mass index; CVDs = cardiovascular diseases; WOMAC = Western Ontario and McMaster Universities Osteoarthritis Index; HADS = Hospital Anxiety and Depression Scale; EQ-5D-5L = 5-level EuroQol 5-domain questionnaire; NSAIDs = nonsteroidal antiinflammatory drugs.
† When patients reported pain in both hips and both knees, questions were asked about the most painful joint. The denominator for the subgroups is the total number of patients in whom the knee or hip was affected.
‡ Patients were asked what they regarded as their most painful activity; activities are listed in Supplementary Table 4 (http://onlinelibrary.wiley.com/doi/10.1002/art.42040/abstract).

Table 1 shows the baseline clinical and demographic characteristics of the patients at the general practices (for baseline clinical and demographic characteristics of the patients with symptoms of centrally sensitized pain, see Supplementary Table 1, available on the *Arthritis & Rheumatology* website at http://onlinelibrary.wiley.com/doi/10.1002/art.42040/abstract). In

Table 2. Results for primary and secondary outcomes in patients receiving duloxetine in addition to usual care compared to those receiving usual care alone*

			Unadjusted model		Adjusted model†	
	Duloxetine (n = 66)	Usual care alone (n = 66)	Difference (95% CI)	Effect size	Difference (95% CI)	Effect size
WOMAC pain score (scale 0–20)						
Week 6	8.5 ± 4.9	9.2 ± 4.1	−0.87 (−2.17, 0.42)	0.22	−0.49 (−1.62, 0.65)	0.14
Month 3	8.0 ± 4.3	9.3 ± 3.7	−0.84 (−2.18, 0.49)	0.21	−0.58 (−1.80, 0.63)	0.16
Month 6	8.4 ± 3.9	9.1 ± 3.8	−0.80 (−2.32, 0.70)	0.18	−0.66 (−2.09, 0.78)	0.15
Month 9	8.5 ± 4.6	8.9 ± 3.8	−0.79 (−2.28, 0.71)	0.18	−0.52 (−1.93, 0.89)	0.12
Month 12	8.5 ± 4.8	9.6 ± 4.2	−0.78 (−2.46, 0.91)	0.15	−0.26 (−1.86, 1.34)	0.05
WOMAC function score (scale 0–68)						
Week 6	29.4 ± 15.6	34.4 ± 12.6	−3.95 (−8.03, 0.13)	0.32	−1.42 (−5.31, 2.47)	0.12
Month 3	28.2 ± 15.1	33.3 ± 13.4	−4.19 (−8.61, 0.23)	0.32	−2.10 (−6.39, 2.20)	0.16
Month 6	30.1 ± 16.1	31.9 ± 13.2	−4.49 (−9.70, 0.71)	0.29	−2.84 (−8.00, 2.33)	0.18
Month 9	29.2 ± 14.8	32.3 ± 13.8	−4.52 (−9.57, 0.53)	0.30	−2.61 (−7.52, 2.31)	0.18
Month 12	29.8 ± 16.2	34.1 ± 13.8	−4.38 (−9.84, 1.09)	0.27	−1.79 (−7.22, 3.64)	0.11
WOMAC stiffness score (scale 0–8)						
Week 6	4.1 ± 2.0	4.5 ± 1.7	−0.56 (−1.07, −0.05)	0.37	−0.58 (−1.10, −0.06)	0.37
Month 3	4.0 ± 1.8	4.7 ± 1.7	−0.54 (−1.06, −0.01)	0.34	−0.57 (−1.11, −0.03)	0.35
Month 6	4.2 ± 1.6	4.5 ± 1.7	−0.48 (−1.07, 0.11)	0.27	−0.51 (−1.13, 0.11)	0.27
Month 9	4.0 ± 1.6	4.4 ± 1.6	−0.38 (−0.93, 0.17)	0.23	−0.37 (−0.94, 0.20)	0.22
Month 12	4.0 ± 1.8	4.3 ± 1.7	−0.26 (−0.92, 0.41)	0.13	−0.18 (−0.87, 0.50)	0.09
Most painful activity score (scale 0–10)						
Month 3	6.1 ± 2.3	6.8 ± 1.8	−0.45 (−0.98, 0.06)	0.29	−0.52 (−1.05, 0.02)	0.32
Month 12	6.2 ± 2.6	6.8 ± 1.8	−0.46 (−0.98, 0.05)	0.30	−0.52 (−1.05, 0.01)	0.33
Quality of Life score (scale −0.446, 1)						
Month 3	0.678 ± 0.157	0.641 ± 0.144	0.01 (−0.01, 0.03)	0.17	0.02 (−0.04, 0.07)	0.12
Month 6	0.642 ± 0.171	0.623 ± 0.180	0.01 (−0.02, 0.05)	0.10	0.02 (−0.04, 0.09)	0.10
Month 9	0.656 ± 0.172	0.617 ± 0.187	0.01 (−0.03, 0.05)	0.08	0.02 (−0.04, 0.08)	0.11
Month 12	0.652 ± 0.221	0.638 ± 0.177	0.00 (−0.05, 0.05)	0.00	0.01 (−0.06, 0.08)	0.05
Patient satisfaction score (scale 0–10)						
Month 3	6.0 ± 2.8	5.6 ± 2.7	0.56 (−0.66, 1.78)	0.15	0.62 (−0.67, 1.91)	0.16
Month 6	5.9 ± 2.7	5.6 ± 2.3	0.56 (−0.66, 1.78)	0.33	0.63 (−0.66, 1.93)	0.16
Month 9	5.9 ± 2.8	5.7 ± 2.3	0.56 (−0.66, 1.77)	0.15	0.63 (−0.66, 1.92)	0.16
Month 12	5.8 ± 2.7	5.5 ± 2.5	0.55 (−0.65, 1.75)	0.15	0.61 (−0.66, 1.88)	0.16
Perceived improvement, no. (%)						
Month 3	16 (28.6)	3 (6.0)	6.38 (1.68, 24.21)‡	–	17.40 (2.85, 106.18)‡	–
Month 12	15 (29.4)	4 (7.8)	4.65 (1.39, 15.45)‡	–	5.33 (1.57, 19.29)‡	–
OMERACT–OARSI criteria responder, no. (%)§						
Month 3	21 (37.5)	13 (25.0)	1.74 (0.75, 4.01)‡	–	1.95 (0.78, 4.84)‡	–
Month 12	17 (32.1)	13 (24.5)	1.69 (0.70, 4.04)‡	–	1.33 (0.51, 3.50)‡	–

* Except where indicated otherwise, values are the mean ± SD. WOMAC = Western Ontario and McMaster Universities Osteoarthritis Index; 95% CI = 95% confidence interval; OMERACT–OARSI = Outcome Measures in Rheumatology–Osteoarthritis Research Society International.
† Adjusted for age, sex, modified PainDETECT score, Hospital Anxiety and Depression Scale score, and the presence of ≥2 comorbidities.
‡ Values are the odds ratio (95% confidence interval [95% CI]).
§ At month 3, 56 patients in the duloxetine group and 52 patients in the usual care group filled out the questionnaire. At month 12, 53 patients filled out the questionnaire in each group.

both groups, baseline characteristics of the general practices were similar. Some clinical characteristics of the patients differed between the 2 groups. The duloxetine group consisted of fewer women (59.1% versus 75.8%) and patients were slightly younger (mean 63.2 years versus 65.4 years) and had fewer comorbidities (15.2% versus 33.3% had ≥2 comorbidities). Most of the patients who were included had knee OA (77.3% in the duloxetine group and 86.4% in the usual care group) and 40% of patients had symptoms of centralized pain. On average, patients with symptoms of centralized pain were 2 years younger and had higher WOMAC pain scores.

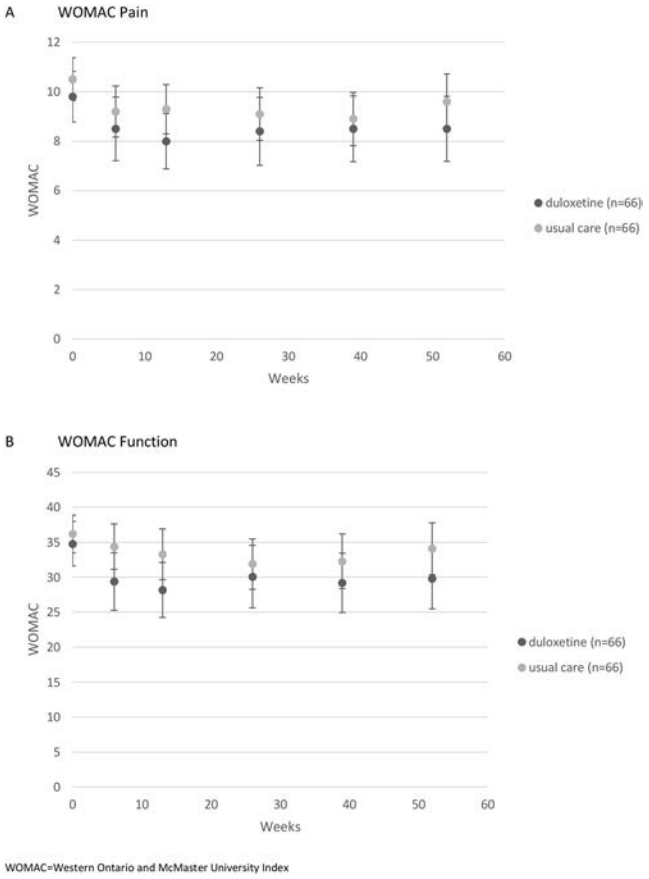

Figure 2. Course of WOMAC scores for for pain (**A**) and function (**B**) over time in OA patients receiving duloxetine in addition to usual care compared to those receiving usual care alone. Results are the mean ± SD, in which circles represent the mean for the indicated group and bars represent the SD.

Primary outcome measure. The primary outcome measure was the WOMAC pain score at month 3. Patients in the duloxetine group reported slightly less pain than patients in the usual care group (adjusted difference –0.58 [95% confidence interval (95% CI) –1.80, 0.63]), which was not clinically relevant or statistically significant. The 95% CI ruled out a clinically relevant effect size of 1.9 points. Our analyses were adjusted for age, sex, modified PainDETECT Questionnaire score, Hospital Anxiety and Depression Scale score, and the presence of ≥2 comorbidities. The intraclass correlation coefficient for the adjusted analysis for WOMAC pain scores was 0.18 (Table 2 and Figure 2).

Secondary outcome measures. The WOMAC pain scores at month 12 also showed a small difference in favor of the duloxetine group compared to the usual care group (adjusted difference –0.26 [95% CI –1.86, 1.34]). There was also a small between-group difference in WOMAC function scores at month 3 (adjusted difference –2.10 [95% CI –6.39, 2.20]) and at month 12 (adjusted difference –1.79 [95% CI –7.22, 3.64]). There were small differences in the other secondary outcome measures: quality of life, patient satisfaction, and the OMERACT–OARSI responder criteria. None of the differences between the 2 groups were clinically relevant or statistically significant. Patient improvement scores (based on patients' ratings of symptom improvement versus worsening) were significantly different between the 2 groups, with an increased likelihood of greater improvement in the duloxetine group relative to the usual care group (odds ratio 17.40 [95% CI 2.85, 106.18]); however, the numbers of patients assessed were small, and the CIs were broad. An additional per-protocol analysis yielded similar results (Supplementary Table 2, http://onlinelibrary.wiley.com/doi/10.1002/art.42040/abstract). In the subgroup analysis of patients with symptoms of central sensitization of pain, there was a small, but not statistically significant, difference in WOMAC pain scores at months 3 and 12 (adjusted difference –0.32 [95% CI –2.32, 1.67] at month 3; adjusted difference 1.02 [95% CI –1.22, 3.27] at month 12) (Supplementary Table 3, http://onlinelibrary.wiley.com/doi/10.1002/art.42040/abstract). Based on the 95% CI, we ruled out a larger effect of duloxetine (difference of 2.9 points in WOMAC pain scale scores, effect size 0.6), but based on the 95% CI, the possibility that duloxetine had a smaller effect size (difference in WOMAC pain score 1.9 points, effect size 0.4) cannot be excluded.

Duloxetine use. Of the 66 patients in the duloxetine group, 56 patients (85%) initiated treatment with duloxetine (Figure 3). The most frequently mentioned reason for not initiating treatment with duloxetine was fear of side effects (7 patients). After 3 months, 61% of patients were still receiving duloxetine, and at 1 year, 35% of patients were still receiving duloxetine. In total, 33 patients (59%) discontinued treatment with duloxetine. Patient-reported reasons for stopping were a lack of effect (24%), side effects (49%), and a lack of effect in addition to side effects (18%) (data were missing for 10% of patients).

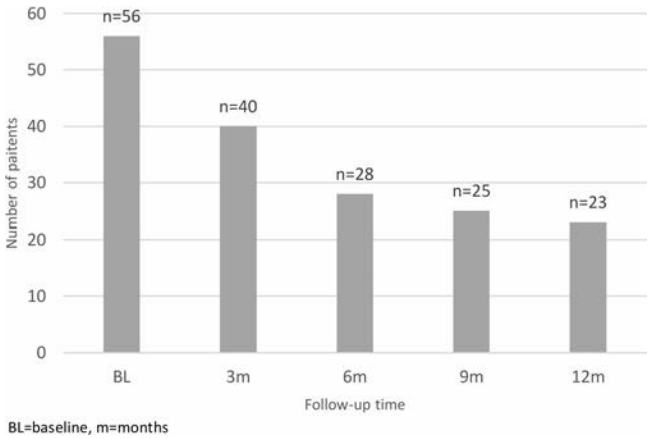

Figure 3. Number of patients with chronic hip or knee osteoarthritis pain who were receiving treatment with duloxetine at baseline (BL) and at months 3, 6, 9, and 12 of follow-up.

Table 3. Cointerventions at week 6 and months 3, 6, 9, and 12 of follow-up in patients receiving treatment with duloxetine in addition to usual care compared to those receiving usual care alone*

	Week 6	Month 3	Month 6	Month 9	Month 12
Medication					
Acetaminophen					
Duloxetine	24 (43.6)	31 (55.4)	30 (60.0)	28 (59.6)	30 (56.6)
Usual care	29 (50.0)	34 (51.5)	31 (60.8)	27 (56.3)	31 (58.5)
NSAIDs†					
Duloxetine	10 (18.2)	16 (28.6)	25 (50.0)	18 (38.3)	19 (35.8)
Usual care	18 (31.0)	25 (48.1)	28 (54.9)	24 (50.0)	29 (54.7)
Opioids					
Duloxetine	1 (1.8)	2 (3.6)	5 (10.0)	4 (8.5)	5 (9.4)
Usual care	3 (5.2)	6 (11.5)	5 (9.8)	4 (8.3)	6 (11.3)
None					
Duloxetine	25 (45.5)	17 (30.4)	7 (14.0)	11 (23.4)	13 (24.5)
Usual care	17 (29.3)	8 (15.4)	4 (7.8)	9 (18.7)	12 (22.6)
Cumulative visits to a general practitioner					
Duloxetine	NA	29 (51.8)	36 (54.5)	40 (60.6)	42 (63.6)
Usual care	NA	16 (24.2)	18 (35.3)	22 (45.8)	26 (49.1)
Cumulative visits for physiotherapy					
Duloxetine	NA	11 (19.6)	12 (24.0)	14 (29.8)	15 (28.3)
Usual care	NA	9 (17.3)	14 (27.4)	16 (33.3)	16 (30.2)
Cumulative visits to an orthopedic surgeon					
Duloxetine	NA	6 (10.7)	9 (18.0)	10 (21.2)	11 (20.8)
Usual care	NA	2 (3.8)	5 (9.8)	6 (12.5)	7 (13.2)
Cumulative glucocorticoid injections					
Duloxetine	1 (1.8)	1 (1.8)	3 (6.0)	3 (6.4)	3 (5.7)
Usual care	4 (7.0)	6 (11.5)	7 (13.7)	9 (18.9)	9 (17.0)
Cumulative joint replacements					
Duloxetine	1 (1.8)	0 (0)	2 (4.0)	3 (6.3)	5 (9.4)
Usual care	0 (0)	0 (0)	0 (0)	0 (0)	0 (0)

* Except where indicated otherwise, values are the number (%) of patients. Values were missing for some patients at some time points. Visiting a general practitioner was not considered an applicable cointervention. NA = not applicable.
† Nonsteroidal antiinflammatory drugs (NSAIDs) refers to oral NSAIDs. One patient in the usual care group was receiving treatment with topical NSAIDs at month 9.

Adverse events. At month 3, 89.3% of patients in the duloxetine group reported having at least 1 side effect compared to 72.5% of patients in the usual care group (Supplementary Figure 1). Nausea, weight loss, constipation, yawning, and hyperhidrosis, which are well-known side effects of duloxetine, were significantly more frequently reported by patients in the duloxetine group.

Cointerventions. Patients in the duloxetine group contacted their general practitioner more frequently (51.8% versus 24.2% at month 3) (Table 3) and were more often referred to an orthopedic surgeon (10.7% versus 3.8% at month 3). Over the total follow-up period, 5 patients in the duloxetine group had a THR or TKR, while none of the patients receiving usual care had a THR or TKR. At month 3, more patients in the usual care group compared to the duloxetine group were receiving treatment with NSAIDs (48.1% versus 28.6%) and opioids (11.5% versus 3.6%), and patients in the usual care group were more likely to receive a glucocorticoid injection (11.5% versus 1.8% of patients in the duloxetine group at month 3).

DISCUSSION

In this study of patients with chronic OA pain, we examined the effectiveness of duloxetine when added to usual care compared to usual care alone. Furthermore, we assessed whether a beneficial effect of duloxetine is seen predominantly in patients with symptoms of centrally sensitized pain. We did not find a clinically relevant or statistically significant effect of duloxetine on WOMAC pain scores at month 3 or other time points, nor was there an effect for the other outcomes, and we can therefore rule out a clinically relevant effect in the overall group (1.9-point difference in WOMAC pain scores). Finally, we found no effect in the subgroup of patients with symptoms of centrally sensitized pain.

While other studies have identified a small-to-moderate effect of duloxetine (15–20), we did not find an effect of duloxetine in patients with OA pain. In our trial, patients' baseline pain scores were similar to the pain scores reported by patients in the other trials (15–20). This difference in outcome could be due to the fact that we studied the effectiveness of duloxetine in a primary care setting, while the other studies examined the efficacy in placebo-controlled trials in secondary care. Furthermore, the patients in our trial were older, reported OA pain for a longer time, and had more comorbidities than those in the other studies. It is established that smaller effects are found in these real-life primary care populations and in effectiveness studies rather than in highly controlled efficacy trials (22). We evaluated duloxetine as a third-choice analgesic, i.e., one used when treatment with acetaminophen and NSAIDs is unsuccessful. In most other studies this was not a prerequisite to participate in the study. The study by Frakes et al (17) is the only one in which treatment was first optimized with NSAIDs and patients were included in the trial when still in pain despite receiving optimal treatment with NSAIDs.

Finally, we had a follow-up period of 1 year and found that 35% of patients were still receiving treatment with duloxetine at the end of the follow-up period. The majority of the patients discontinued treatment with duloxetine around month 3 because of a lack of effect or the presence of side effects. The percentage of patients discontinuing treatment with duloxetine was higher in our study than in the 2 other studies that evaluated the long-term use of duloxetine in OA in an open-label extension phase of the trial. In one study, ~80% of patients continued to receive treatment with duloxetine until week 26 (36). In the second study, ~85% of patients continued treatment with duloxetine for up to 1 year (37). However, only 25% of patients entered the extension phase, and those who discontinued did not mention reasons for not continuing in the extension phase of the study, which could have resulted in the selection of patients who showed tolerance to treatment with duloxetine and whose condition improved with the treatment. In our trial, general practitioners were instructed to discontinue treatment with duloxetine after 3 months, when either treatment was unsuccessful or the patient had intolerable side effects. This may also have contributed to the higher percentage of patients who discontinued treatment with duloxetine in our trial.

Interestingly, during the follow-up period, patients in the duloxetine group more often underwent a THR or TKR than patients in the usual care group. At month 3, these patients were more frequently referred to an orthopedic surgeon, and afterward, more THR and TKR procedures were performed. We believe this is caused by the fact that patients in the duloxetine group visited their general practitioner more often, and when treatment with duloxetine was unsuccessful, this was the next step. To our knowledge, this has not been demonstrated in other pragmatic trials.

Furthermore, patients in the duloxetine group more often reported significant improvement in OA pain compared to patients in the usual care group, while none of the other outcome measures differed between the 2 groups. This may have been caused by the open-label nature of the trial. The number of patients reporting improvement was low, which resulted in a wide 95% CI.

We also found no effect in patients with symptoms of central sensitization of pain. Overall, these patients reported more pain at baseline and were slightly younger (but reported a similar duration of pain) compared to the overall group. Higher pain scores are associated with the presence of central sensitization of pain (38). Since the prognostic differences between the 2 groups were slightly different, a sensitivity analysis was performed, adjusting for these variables (age, sex, affected joint, and comorbidities). Results of this analysis were similar to those of the original analysis (data not shown). We also conducted a post hoc analysis with a higher threshold for the modified PainDETECT score (>18), which is indicative of neuropathic pain. We found no effect of duloxetine with similar estimates, but there were very large CIs because of low numbers (data not shown).

The presence of central sensitization of pain was defined as a score of >12 on the modified PainDETECT Questionnaire (30,31). The gold standard to identify the presence of central sensitization of pain is quantitative sensory testing (39). These tests are time consuming and expensive and therefore not feasible in daily clinical practice. When using a cutoff score of 12, the modified PainDETECT Questionnaire has a sensitivity of 50% and a specificity of 74% to detect symptoms of central sensitization of pain (30). Small-to-moderate correlations between PainDETECT scores and pressure pain thresholds have been found (40,41). Therefore, we might not have perfectly selected patients for the subgroup analyses.

One strength of the current trial is the pragmatic cluster design, which is suitable for evaluating an intervention in clinical practice and demonstrating the effectiveness of the intervention (22). Cluster randomized controlled trials can be prone to recruitment bias (42,43), but this was minimized by identifying all eligible patients before randomization. However, one general practice in the duloxetine group recruited 4 patients after the randomization period. Conducting a sensitivity analysis without those 4 patients did not alter the results (data not shown).

A limitation of the current trial is that we did not recruit the number of patients calculated in the sample size. However, even with the sample size, we can rule out the presence of a clinically relevant effect in the overall group, since the predefined clinically relevant difference of 1.9 points was not within the 95% CI and makes the presence of an effect highly unlikely (44,45). We cannot rule out the fact that there may be a clinically relevant effect in the subgroup analysis of patients with symptoms of centralized pain. We hypothesized that in this subgroup the effect of duloxetine would be greater (difference of 2.9 points in WOMAC pain scale score), and though this larger effect can be ruled out, the presence of a smaller difference of 1.9 points on the WOMAC pain score scale cannot be completely ruled out, though the point

estimates in this subgroup analysis were similar to the point estimates in the overall group.

We had a low number of both general practitioners and patients participating in the trial and therefore decided to stop recruiting after 3 years. The rate of participation by general practitioners was similar to previous trials in our department, and recruitment is difficult because general practitioners lack time (46,47). Furthermore, we interviewed general practitioners about their attitude toward duloxetine in patients with OA pain. General practitioners were relatively unfamiliar with duloxetine, since duloxetine is not often prescribed (48,49), and were concerned about the occurrence of side effects. Some general practitioners stated that duloxetine may be an option for patients in whom other therapies have proven unsuccessful. These factors may have also contributed to the participation rate of the general practitioners. The number of patients participating per general practice was lower than we expected beforehand. Patients were frequently excluded based on the presence of exclusion criteria in their medical records at the general practice or because pain was bearable or not present (when receiving acetaminophen or NSAIDs).

To conclude, there was no clinically relevant effect of duloxetine added to usual care compared to usual care alone for the treatment of chronic OA pain, and it should not be implemented. In patients with symptoms of centralized pain, a potential effect of duloxetine cannot be ruled out, so future studies in this subgroup including patients with centralized pain symptoms should be conducted to validate our results.

AUTHOR CONTRIBUTIONS

All authors were involved in drafting the article or revising it critically for important intellectual content, and all authors approved the final version to be published. Dr. van den Driest had full access to all of the data in the study and takes responsibility for the integrity of the data and the accuracy of the data analysis.

Study conception and design. Van den Driest, Schiphof, Koffeman, Koopmanschap, Bindels, Bierma-Zeinstra.

Acquisition of data. Van den Driest, Schiphof, Bierma-Zeinstra.

Analysis and interpretation of data. Van den Driest, Schiphof, Koopmanschap.

REFERENCES

1. Johnson VL, Hunter DJ. The epidemiology of osteoarthritis. Best Pract Res Clin Rheumatol 2014;28:5–15.
2. Cross M, Smith E, Hoy D, Nolte S, Ackerman I, Fransen M, et al. The global burden of hip and knee osteoarthritis: estimates from the global burden of disease 2010 study. Ann Rheum Dis 2014;73:1323–30.
3. Leopoldino AO, Machado GC, Ferreira PH, Pinheiro MB, Day R, McLachlan AJ, et al. Paracetamol versus placebo for knee and hip osteoarthritis. Cochrane Database Syst Rev 2019;2:CD013273.
4. Da Costa BR, Reichenbach S, Keller N, Nartey L, Wandel S, Juni P, et al. Effectiveness of non-steroidal anti-inflammatory drugs for the treatment of pain in knee and hip osteoarthritis: a network meta-analysis. Lancet 2017;390:e21–33.
5. Da Costa BR, Nuesch E, Kasteler R, Husni E, Welch V, Rutjes AW, et al. Oral or transdermal opioids for osteoarthritis of the knee or hip. Cochrane Database Syst Rev 2014:CD003115.
6. April KT, Bisaillon J, Welch V, Maxwell LJ, Juni P, Rutjes AW, et al. Tramadol for osteoarthritis. Cochrane Database Syst Rev 2019;5:CD005522.
7. Bannuru RR, Osani MC, Vaysbrot EE, Arden NK, Bennell K, Bierma-Zeinstra SM, et al. OARSI guidelines for the non-surgical management of knee, hip, and polyarticular osteoarthritis. Osteoarthritis Cartilage 2019;27:1578–89.
8. Zeng C, Lane NE, Hunter DJ, Wei J, Choi HK, McAlindon TE, et al. Intra-articular corticosteroids and the risk of knee osteoarthritis progression: results from the Osteoarthritis Initiative. Osteoarthritis Cartilage 2019;27:855–62.
9. Conaghan PG. Corticosteroids and osteoarthritis progression: a confounded issue. Osteoarthritis Cartilage 2019;27:e5–6.
10. Mease PJ, Hanna S, Frakes EP, Altman RD. Pain mechanisms in osteoarthritis: understanding the role of central pain and current approaches to its treatment. J Rheumatol 2011;38:1546–51.
11. Fu K, Robbins SR, McDougall JJ. Osteoarthritis: the genesis of pain. Rheumatology (Oxford) 2018;57 Suppl:iv43–50.
12. Clauw DJ, Hassett AL. The role of centralised pain in osteoarthritis. Clin Exp Rheumatol 2017;35 Suppl:79–84.
13. Fingleton C, Smart K, Moloney N, Fullen BM, Doody C. Pain sensitization in people with knee osteoarthritis: a systematic review and meta-analysis. Osteoarthritis Cartilage 2015;23:1043–56.
14. French HP, Smart KM, Doyle F. Prevalence of neuropathic pain in knee or hip osteoarthritis: a systematic review and meta-analysis. Semin Arthritis Rheum 2017;47:1–8.
15. Abou-Raya S, Abou-Raya A, Helmii M. Duloxetine for the management of pain in older adults with knee osteoarthritis: randomised placebo-controlled trial. Age Ageing 2012;41:646–52.
16. Chappell AS, Desaiah D, Liu-Seifert H, Zhang S, Skljarevski V, Belenkov Y, et al. A double-blind, randomized, placebo-controlled study of the efficacy and safety of duloxetine for the treatment of chronic pain due to osteoarthritis of the knee. Pain Pract 2011;11:33–41.
17. Frakes EP, Risser RC, Ball TD, Hochberg MC, Wohlreich MM. Duloxetine added to oral nonsteroidal anti-inflammatory drugs for treatment of knee pain due to osteoarthritis: results of a randomized, double-blind, placebo-controlled trial. Curr Med Res Opin 2011;27:2361–72.
18. Chappell AS, Ossanna MJ, Liu-Seifert H, Iyengar S, Skljarevski V, Li LC, et al. Duloxetine, a centrally acting analgesic, in the treatment of patients with osteoarthritis knee pain: a 13-week, randomized, placebo-controlled trial. Pain 2009;146:253–60.
19. Wang G, Bi L, Li X, Li Z, Zhao D, Chen J, et al. Efficacy and safety of duloxetine in Chinese patients with chronic pain due to osteoarthritis: a randomized, double-blind, placebo-controlled study. Osteoarthritis Cartilage 2017;25:832–8.
20. Uchio Y, Enomoto H, Alev L, Kato Y, Ishihara H, Tsuji T, et al. A randomized, double-blind, placebo-controlled phase III trial of duloxetine in Japanese patients with knee pain due to osteoarthritis. J Pain Res 2018;11:809–21.
21. Kolasinski SL, Neogi T, Hochberg MC, Oatis C, Guyatt G, Block J, et al. 2019 American College of Rheumatology/Arthritis Foundation Guideline for the management of osteoarthritis of the hand, hip, and knee. Arthritis Rheumatol 2020;72:220–33.
22. Allen KD, Bierma-Zeinstra SM, Foster NE, Golightly YM, Hawker G. OARSI Clinical Trials Recommendations: design and conduct of implementation trials of interventions for osteoarthritis. Osteoarthritis Cartilage 2015;23:826–38.
23. Van den Driest JJ, Schiphof D, Luijsterburg PA, Koffeman AR, Koopmanschap MA, Bindels PJ, et al. Effectiveness and cost-effectiveness of duloxetine added to usual care for patients with

chronic pain due to hip or knee osteoarthritis: protocol of a pragmatic open-label cluster randomised trial (the DUO trial). BMJ Open 2017;7: e018661.

24. Altman RD. Classification of disease: osteoarthritis. Semin Arthritis Rheum 1991;20 Suppl:40–7.
25. Dutch College of General Practitioners (NHG). NHG Standaard Niet-traumatische knieklachten. 2016. URL: https://www.nhg.org/standaarden/volledig/nhg-standaard-niet-traumatische-knieklachten#Richtlijnendiagnostiek.
26. The Netherlands Institute for Social Science. URL: https://www.cbs.nl/nl-nl/maatwerk/2021/45/berekenwijze-ses-score-per-wijk-buurt.
27. Smink AJ, Bierma-Zeinstra SM, Dekker J, Vliet Vlieland TP, Bijlsma JW, Swierstra BA, et al. Agreement of general practitioners with the guideline-based stepped-care strategy for patients with osteoarthritis of the hip or knee: a cross-sectional study. BMC Fam Pract 2013;14:33.
28. Landon BE, Reschovsky J, Reed M, Blumenthal D. Personal, organizational, and market level influences on physicians' practice patterns: results of a national survey of primary care physicians. Med Care 2001;39:889–905.
29. Bellamy N, Buchanan WW, Goldsmith CH, Campbell J, Stitt LW. Validation study of WOMAC: a health status instrument for measuring clinically important patient relevant outcomes to antirheumatic drug therapy in patients with osteoarthritis of the hip or knee. J Rheumatol 1988;15:1833–40.
30. Hochman JR, Davis AM, Elkayam J, Gagliese L, Hawker GA. Neuropathic pain symptoms on the modified painDETECT correlate with signs of central sensitization in knee osteoarthritis. Osteoarthritis Cartilage 2013;21:1236–42.
31. Hochman JR, Gagliese L, Davis AM, Hawker GA. Neuropathic pain symptoms in a community knee OA cohort. Osteoarthritis Cartilage 2011;19:647–54.
32. Brooks R. EuroQol: the current state of play. Health Policy 1996;37: 53–72.
33. Parkes MJ, Callaghan MJ, O'Neill TW, Forsythe LM, Lunt M, Felson DT. Sensitivity to change of patient-preference measures for pain in patients with knee osteoarthritis: data from two trials. Arthritis Care Res (Hoboken) 2016;68:1224–31.
34. Pham T, van der Heijde D, Altman RD, Anderson JJ, Bellamy N, Hochberg M, et al. OMERACT-OARSI initiative: Osteoarthritis Research Society International set of responder criteria for osteoarthritis clinical trials revisited. Osteoarthritis Cartilage 2004;12:389–99.
35. Rozendaal RM, Koes BW, van Osch GJ, Uitterlinden EJ, Garling EH, Willemsen SP, et al. Effect of glucosamine sulfate on hip osteoarthritis: a randomized trial. Ann Intern Med 2008;148:268–77.
36. Wang G, Bi L, Li X, Li Z, Zhao D, Chen J, et al. Maintenance of effect of duloxetine in Chinese patients with pain due to osteoarthritis: 13-week open-label extension data. BMC Musculoskelet Disord 2019;20:174.
37. Uchio Y, Enomoto H, Ishida M, Tsuji T, Ochiai T, Konno S. Safety and efficacy of duloxetine in Japanese patients with chronic knee pain due to osteoarthritis: an open-label, long-term, phase III extension study. J Pain Res 2018;11:1391–403.
38. Lluch E, Nijs J, Courtney CA, Rebbeck T, Wylde V, Baert I, et al. Clinical descriptors for the recognition of central sensitization pain in patients with knee osteoarthritis. Disabil Rehabil 2018;40:2836–45.
39. Uddin Z, MacDermid JC. Quantitative sensory testing in chronic musculoskeletal pain. Pain Med 2016;17:1694–703.
40. Moore RL, Clifford AM, Moloney N, Doody C, Smart KM, O'Leary H. The relationship between clinical and quantitative measures of pain sensitization in knee osteoarthritis. Clin J Pain 2020;36:336–43.
41. Moreton BJ, Tew V, das Nair R, Wheeler M, Walsh DA, Lincoln NB. Pain phenotype in patients with knee osteoarthritis: classification and measurement properties of painDETECT and self-report Leeds assessment of neuropathic symptoms and signs scale in a cross-sectional study. Arthritis Care Res (Hoboken) 2015;67: 519–28.
42. Brierley G, Brabyn S, Torgerson D, Watson J. Bias in recruitment to cluster randomized trials: a review of recent publications. J Eval Clin Pract 2012;18:878–86.
43. Eldridge S, Kerry S, Torgerson DJ. Bias in identifying and recruiting participants in cluster randomised trials: what can be done? BMJ 2009;339:b4006.
44. Goodman SN, Berlin JA. The use of predicted confidence intervals when planning experiments and the misuse of power when interpreting results. Ann Intern Med 1994;121:200–6.
45. Ranstam J. Why the P-value culture is bad and confidence intervals a better alternative. Osteoarthritis Cartilage 2012;20:805–8.
46. Schreijenberg M, Luijsterburg PA, Van Trier YD, Rizopoulos D, Koopmanschap MA, Voogt L, et al. Discontinuation of the PACE Plus trial: problems in patient recruitment in general practice. BMC Musculoskelet Disord 2018;19:146.
47. Wartna JB, Bohnen AM, Elshout G, Pijnenburg MW, Pols DH, Gerth van Wijk RR, et al. Symptomatic treatment of pollen-related allergic rhinoconjunctivitis in children: randomized controlled trial. Allergy 2017;72:636–44.
48. Aarts N, Noordam R, Hofman A, Tiemeier H, Stricker BH, Visser LE. Utilization patterns of antidepressants between 1991 and 2011 in a population-based cohort of middle-aged and elderly. Eur Psychiatry 2014;29:365–70.
49. Van den Driest JJ, Schiphof D, de Wilde M, Bindels PJ, van der Lei J, Bierma-Zeinstra SM. Antidepressant and anticonvulsant prescription rates in patients with osteoarthritis: a population-based cohort study. Rheumatology (Oxford) 2021;60:2206–16.

Arthritis & Rheumatology
Vol. 74, No. 5, May 2022, pp 829–839
DOI 10.1002/art.42023

American College of Rheumatology
Empowering Rheumatology Professionals

Urine Proteomics and Renal Single-Cell Transcriptomics Implicate Interleukin-16 in Lupus Nephritis

Andrea Fava,[1] Deepak A. Rao,[2] Chandra Mohan,[3] Ting Zhang,[3] Avi Rosenberg,[1] Paride Fenaroli,[4] H. Michael Belmont,[5] Peter Izmirly,[5] Robert Clancy,[5] Jose Monroy Trujillo,[1] Derek Fine,[1] Arnon Arazi,[6] Celine C. Berthier,[7] Anne Davidson,[8] Judith A. James,[9] Betty Diamond,[6] Nir Hacohen,[10] David Wofsy,[11] Soumya Raychaudhuri,[12] William Apruzzese,[2] the Accelerating Medicines Partnership in Rheumatoid Arthritis and Systemic Lupus Erythematosus Network, Jill Buyon,[5] and Michelle Petri[1]

Objective. Current lupus nephritis (LN) treatments are effective in only 30% of patients, emphasizing the need for novel therapeutic strategies. We undertook this study to develop mechanistic hypotheses and explore novel biomarkers by analyzing the longitudinal urinary proteomic profiles in LN patients undergoing treatment.

Methods. We quantified 1,000 urinary proteins in 30 patients with LN at the time of the diagnostic renal biopsy and after 3, 6, and 12 months. The proteins and molecular pathways detected in the urine proteome were then analyzed with respect to baseline clinical features and longitudinal trajectories. The intrarenal expression of candidate biomarkers was evaluated using single-cell transcriptomics of renal biopsy sections from LN patients.

Results. Our analysis revealed multiple biologic pathways, including chemotaxis, neutrophil activation, platelet degranulation, and extracellular matrix organization, which could be noninvasively quantified and monitored in the urine. We identified 237 urinary biomarkers associated with LN, as compared to controls without systemic lupus erythematosus. Interleukin-16 (IL-16), CD163, and transforming growth factor β mirrored intrarenal nephritis activity. Response to treatment was paralleled by a reduction in urinary IL-16, a CD4 ligand with proinflammatory and chemotactic properties. Single-cell RNA sequencing independently demonstrated that *IL16* is the second most expressed cytokine by most infiltrating immune cells in LN kidneys. IL-16–producing cells were found at key sites of kidney injury.

Conclusion. Urine proteomics may profoundly change the diagnosis and management of LN by noninvasively monitoring active intrarenal biologic pathways. These findings implicate IL-16 in LN pathogenesis, designating it as a potentially treatable target and biomarker.

Supported by the Accelerating Medicines Partnership (AMP) in Rheumatoid Arthritis and Systemic Lupus Erythematosus Network. AMP is a public-private partnership (AbbVie, the Arthritis Foundation, Bristol Myers Squibb, the Foundation for the National Institutes of Health, the Lupus Foundation of America, the Lupus Research Alliance, Merck Sharp & Dohme, the National Institute of Allergy and Infectious Diseases, the National Institute of Arthritis and Musculoskeletal and Skin Diseases, Pfizer, the Rheumatology Research Foundation, Sanofi, and Takeda Pharmaceuticals International) created to develop new ways of identifying and validating promising biological targets for diagnostics and drug development. Funding was provided by the NIH (grants UH2-AR-067676, UH2-AR-067677, UH2-AR-067679, UH2-AR-067681, UH2-AR-067685, UH2-AR-067688, UH2-AR-067689, UH2-AR-067690, UH2-AR-067691, UH2-AR-067694, UM2-AR-067678, and AR-074096). The Oklahoma Rheumatic Disease Research Cores Center is supported by NIH grant P30-AR-073750. The Hopkins Lupus Cohort is funded by NIH grant AR-69572. Dr Fava's work was supported by the Jerome L. Greene Foundation and the Cupid Foundation.

[1]Andrea Fava, MD, Avi Rosenberg, MD, PhD, Jose Monroy Trujillo, MD, Derek Fine, MD, Michelle Petri, MD, MPH: Johns Hopkins University, Baltimore, Maryland; [2]Deepak A. Rao, MD, PhD, William Apruzzese, MPH: Harvard Medical School, Boston, Massachusetts; [3]Chandra Mohan, MD, PhD, Ting Zhang, PhD: University of Houston, Houston, Texas; [4]Paride Fenaroli, MD: Johns Hopkins University, Baltimore, Maryland, and Parma University Hospital, Parma, Italy; [5]H. Michael Belmont, MD, Peter Izmirly, MD, Robert Clancy, MD, Jill Buyon, MD: New York University School of Medicine, New York, New York; [6]Arnon Arazi, PhD, Betty Diamond, MD: Feinstein Institutes for Medical Research, Manhasset, New York; [7]Celine C. Berthier, PhD: University of Michigan, Ann Arbor; [8]Anne Davidson, MBBS: Northwell Health, New York, New York; [9]Judith A. James, MD, PhD: Oklahoma Medical Research Foundation, Oklahoma City; [10]Nir Hacohen, PhD: Broad Institute, Boston, Massachusetts; [11]David Wofsy, MD: University of California, San Francisco; [12]Soumya Raychaudhuri, MD, PhD: Harvard Medical School, Boston, Massachusetts, Broad Institute of MIT and Harvard, Cambridge, Massachusetts, and The University of Manchester, Manchester, UK.

Author disclosures are available at https://onlinelibrary.wiley.com/action/downloadSupplement?doi=10.1002%2Fart.42023&file=art42023-sup-0001-Disclosureform.pdf.

Address correspondence to Andrea Fava, MD, 1830 East Monument Street, Suite 7500, Baltimore, MD 21205. Email: afava1@jh.edu.

Submitted for publication February 18, 2021; accepted in revised form November 9, 2021.

INTRODUCTION

Lupus nephritis (LN) is a severe manifestation of systemic lupus erythematosus (SLE) that frequently leads to end-stage kidney disease despite treatment (1). Diagnosis and treatment of LN rely on histopathologic features of kidney biopsy samples from patients with proteinuria. Kidney biopsies have an indispensable role in that they can distinguish active nephritis from chronic damage, both of which manifest with proteinuria. However, kidney biopsies have limitations. Most notably, histology does not capture patient-specific active biologic pathways. Further, the histologic class frequently changes on repeat kidney biopsies, suggesting that the histologic classification may artificially divide patients based on results from one point in time (2,3). Procedure-related complications may occur (4), and up to 35% of kidney biopsies may fail to obtain an adequate sample (5). Access to kidney biopsies may delay diagnosis and treatment, and can be limited by antithrombotic and anticoagulation treatments, severe thrombocytopenia, and resource-poor settings. Finally, because the presence of proteinuria implies that underlying kidney damage has already happened, kidney biopsy results are a lagging indicator. Thus, there is a pressing need for a noninvasive biomarker to probe in "real-time" the active molecular pathologic processes in the kidney and to monitor them over time in response to treatment.

Several available biomarkers correlate with histologic features, but none are currently used in clinical practice (6,7). These lack the sensitivity and specificity to detect active renal inflammation, predict flares, and reliably inform prognosis, and do not add actionable information in addition to proteinuria or renal function (6,7). Unbiased proteomic screenings carry a high potential for discovery, but these have been limited to the evaluation of proteins or peptides sufficiently abundant to be detectable by mass spectrometry (8,9). More sensitive aptamer-based arrays have identified candidate urinary biomarkers associated with proteinuria, but their ability to predict nephritis activity and clinical outcomes is still to be determined (10). Management of LN could be greatly enhanced by a resource that can identify candidate biomarkers that predict histologic features and clinical outcomes, as well as infer the renally active biologic pathways. Here, we used a glass slide–based protein microarray to screen and quantify 1,000 proteins covering a wide range of biologic processes in longitudinal urine samples from patients with LN (starting at the time of biopsy) to develop mechanistic hypotheses and explore novel biomarkers. This array allowed the unbiased, precise, and sensitive quantification of the concentration of each of the 1,000 proteins, as validated in previous studies (11–13). We found that protein expression patterns define distinct molecular pathways that are differentially expressed among LN patients. We also discovered that interleukin-16 (IL-16), a proinflammatory chemokine, is strongly associated with LN activity and may have role in LN pathogenesis, thus nominating IL-16 as a potentially treatable target.

PATIENTS AND METHODS

Patients and sample collection. This study enrolled SLE patients with a urine protein–to-creatinine ratio (UPr:Cr) of >0.5 who were undergoing clinically indicated renal biopsy. Only patients with a pathology report confirming LN were included in the study. Renal biopsy sections were scored by 1 renal pathologist at each of the 2 sites according to the International Society of Nephrology (ISN)/Renal Pathology Society guidelines and the National Institutes of Health (NIH) activity and chronicity indices (14). Clinical information, including serologies, were collected at the most recent visit before the biopsy. Response status at week 52 was defined as follows: complete response (UPr:Cr ≤0.5, normal serum creatinine or <25% increase from baseline if abnormal, and prednisone ≤10 mg daily), partial response (UPr:Cr >0.5 but ≤50% of baseline value, and identical serum creatinine and prednisone rules as complete response), or no response (UPr:Cr >50% of baseline value, new abnormal elevation of serum creatinine or ≥25% from baseline, or prednisone ≥10 mg daily). Urine samples from healthy volunteers (all women, median age 42 years [interquartile range 32–54], 3 identifying as Caucasian and 4 as African American) were included. Urine specimens were acquired on the day of the biopsy (before the procedure) at 2 clinical sites in the US (Johns Hopkins University [JHU] and New York University [NYU]). For the validation cohort (n = 101), urine samples were collected on the day of (73%) or within 3 weeks (27%) of the kidney biopsy. Serologic features and complement levels were assessed at the clinical visit preceding the biopsy. Proteinuria was measured on or near the day of the biopsy.

Study approval. Human study protocols were approved by the institutional review boards (IRBs) at JHU and NYU, and written informed consent was obtained from all participants. For healthy controls, IRB approval was obtained from the Oklahoma Medical Research Foundation. After informed consent, controls were recruited through the Oklahoma Rheumatic Disease Research Cores Center and were matched for sex, race, ethnicity, and age. Subjects were screened using a questionnaire and tested negative for the following antibodies: antinuclear, double-stranded DNA, chromatin, ribosomal P, Ro, La, Smith (Sm), SmRNP, RNP, centromere B, Scl-70, and Jo-1. Samples were processed, stored, and shipped using protocols from the Accelerating Medicines Partnership in Rheumatoid Arthritis and Systemic Lupus Erythematosus (AMP RA/SLE) Network to align with the patient samples. See Appendix A for a list of members of the AMP RA/SLE Network, and see Supplementary Acknowledgments (https://onlinelibrary.wiley.com/doi/10.1002/art.42023) for additional details.

Urine Quantibody assay. The Kiloplex Quantibody protein array platform (RayBiotech) was used to screen urine samples as previously described (12). Validation was performed

using an immunoquantitative (polymerase chain reaction [PCR]–based) IL-16 enzyme-linked immunosorbent assay (ELISA) (RayBiotech) to match and improve the sensitivity and dynamic range provided by the Kiloplex array. These are summarized in Supplementary Methods (https://onlinelibrary.wiley.com/doi/10.1002/art.42023).

Renal tissue single-cell RNA sequencing. Renal tissue was collected, stored, and processed as previously described (15). Briefly, research biopsy cores were collected from consenting subjects as an additional biopsy pass or tissue from routine clinical passes. Only biopsy samples with confirmed LN were included. Kidney tissue was frozen on site and shipped to a central processing location where it was thawed and disaggregated. Individual cells were retrieved and sorted by flow cytometry. For each sample, 10% of the sample was allocated to sort CD10+CD45– epithelial cells as single cells, and the remaining 90% was used to sort CD45+ leukocytes as single cells. For each single cell, the whole gene expression profile was sequenced using the CEL-Seq2 method.

Prevalence of cytokine-positive cells. Analysis of cytokine-positive cells was based on a compendium of 237 cytokines obtained from Gene Ontology (16) and manually extended using the Cytokine Registry (https://www.immport.org/resources/cytokineRegistry), the iTalk database (17), and the International Union of Basic and Clinical Pharmacology and British Pharmacological Society database. For each cytokine, we calculated the prevalence of the cells with ≥1 transcript over the total number of cells. For details on immunohistochemistry, see Supplementary Methods (https://onlinelibrary.wiley.com/doi/10.1002/art.42023).

Statistical analysis. Differential protein abundance was calculated using a moderated T statistic. To achieve normal distribution, the protein abundances were log-transformed after adding 10% (arbitrary constant empirically shown not to significantly alter distributions) of the lowest measured abundance to remove zeros. With 30 LN and 7 healthy donor samples, using a 2-sided test with a significance level of 0.05, adjusting for 1,000 comparisons (Bonferroni), there was 80% power to detect a difference in mean peptide magnitude of 1.2 SDs (i.e., an effect size of 1.2). Concentrations of all urinary proteins for all urine samples were available without missing data. Clustering was performed using the Ward's minimum variance method. Receiver operating characteristic (ROC) curves and areas under the curve (AUCs) were calculated using the function roc within the pROC R package. The impact of confounders on the association between the NIH activity index score and the urinary abundance of a biomarker was tested using 1 confounder at the time (given limited sample size), using a linear regression model as follows: *activity ~ biomarker_abundance + confounder*. The models were fitted

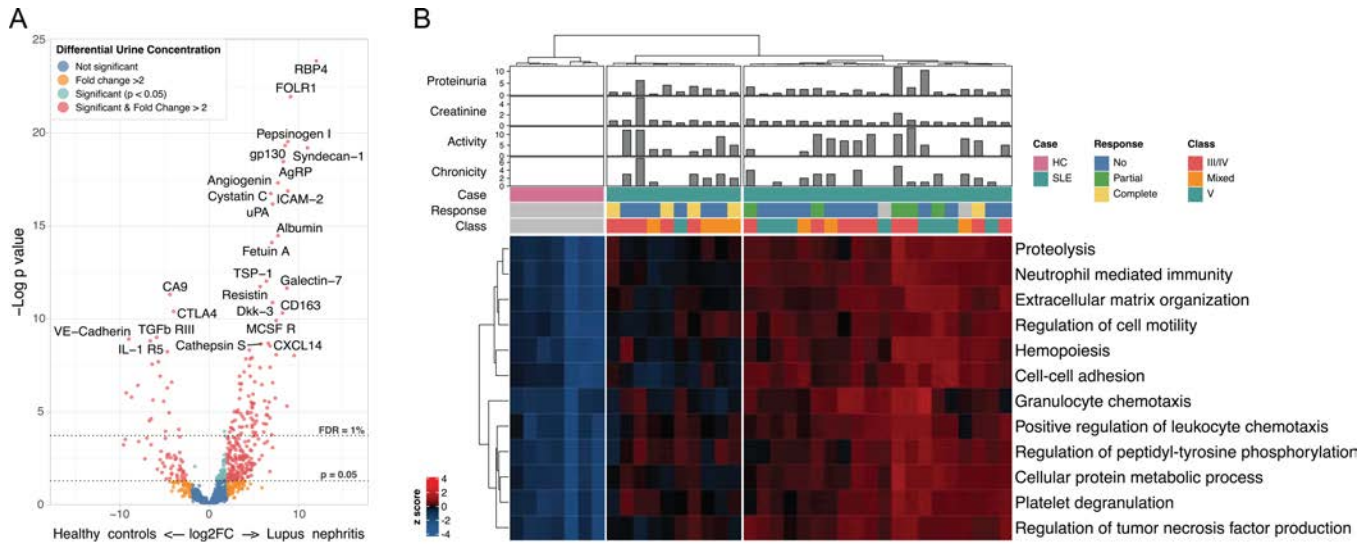

Figure 1. Identification of pathogenic pathways by urine proteomics. **A**, Volcano plot illustrating the differential abundance of 1,000 urinary proteins in patients with lupus nephritis (LN; n = 30) and healthy controls (HC; n = 7). There were 237 proteins that were significantly more abundant in LN (>2-fold change, false discovery rate [FDR] <10%, moderated *t*-test). **B**, Heatmap of the abundance of the 12 nonoverlapping pathways enriched in LN urine samples by pathway enrichment analysis (Gene Ontology biological process). Among the 30 patients, 20 displayed an LN cluster with higher abundance of all pathways, whereas the patients in the other cluster exhibited an intermediate abundance as compared to healthy controls. Clustering was otherwise not explained by other clinical variables such as proteinuria, renal function, nephritis activity, chronic damage, or class. Values were scaled by rows. Clustering was performed using Ward's minimum variance method. TGFβRIII = transforming growth factor β receptor III; IL-1R5 = interleukin-1 receptor 5; TSP-1 = thrombospondin 1; RBP-4 = retinol binding protein 4; FOLR-1 = folate receptor 1; ICAM-2 = intercellular adhesion molecule 2; uPA = urokinase plasminogen activator; $\log_2$ FC = $\log_2$ fold change; SLE = systemic lupus erythematosus. Color figure can be viewed in the online issue, which is available at http://onlinelibrary.wiley.com/doi/10.1002/art.42023/abstract.

using the *lm* function within the stats R package. See Supplementary Methods (https://onlinelibrary.wiley.com/doi/10.1002/art.42023) for pathway enrichment analysis. Pearson's correlation coefficients are used throughout the manuscript. All analyses were performed in R.

Data availability. The data reported in this publication, including the clinical and serologic data of the study participants, are deposited in the ImmPort repository (accession code SDY997). The raw single-cell RNA sequencing data are also deposited in dbGAP (accession code phs001457.v1.p1).

RESULTS

Urine proteomics identifies biologically relevant active pathways in LN. Urine samples from 30 patients with active LN were collected near or at the time of renal biopsy. Clinical and demographic characteristics are summarized in Supplementary Table 1 (https://onlinelibrary.wiley.com/doi/10.1002/art.42023). Compared to healthy donors, there were 237 proteins significantly elevated in the urine of patients with LN (false discovery rate [FDR] <10%), as shown in Figure 1A. This list includes both novel and previously described urinary biomarkers (Supplementary Data File 1, https://onlinelibrary.wiley.com/doi/10.1002/art.42023). Pathway enrichment analysis of the proteins that were significantly elevated in LN identified 12 enriched nonoverlapping pathways, including relevant biologic processes such as chemotaxis, neutrophil activation, platelet degranulation, and extracellular matrix organization (Supplementary Figure 1, https://onlinelibrary.wiley.com/doi/10.1002/art.42023). Hierarchical clustering using enriched pathways segregated LN patients into 2 groups, with 80% of those who later achieved a complete renal response being in the same group with overall less inflammatory pathways (odds ratio 12.6, $P = 0.03$) (Figure 1B). Baseline parameters such as proteinuria, creatinine level, histologic activity or chronicity scores, and ISN class were present in similar frequencies in both clusters, suggesting that urine proteomics may provide unique informative features (Figure 1B).

Identification of urinary biomarkers of renal histology. We sought to identify urinary proteins that could identify renal histology. LN can be classified in 2 broad categories based on the presence of a glomerular endocapillary immune infiltrate or "proliferation." Proliferative LN (ISN class III or IV) is a more aggressive phenotype associated with glomerular endocapillary hypercellularity, abundant immune cell infiltration, and higher risk of permanent renal damage. Compared to pure membranous LN (n = 9), patients with proliferative LN (n = 14) showed a higher concentration of several urine cytokines and molecules involved in immune activation and chemotaxis (Figures 2A and B). IL-16 was the most significantly enriched urinary protein in proliferative LN (Figure 2A). Pathway enrichment analysis revealed that the pattern of chemokines matched the chemokine released in response to interferon-γ (IFNγ), IL-1β, and tumor necrosis factor (TNF) (Figure 2B).

Many of the urinary proteins that were differentially abundant when comparing proliferative and membranous LN were not significantly more abundant when comparing all LN patients to healthy controls. In fact, although most of the proteins enriched in proliferative LN were generally more abundant in LN compared to healthy controls, these were not among the most abundant (>2 SDs) (Supplementary Figures 2A and B, https://onlinelibrary.wiley.com/doi/10.1002/art.42023). This is because the first comparison (LN patients versus healthy controls) is aimed to identify proteins that are generally more abundant in all LN patients, regardless of ISN class. Not surprisingly, the most abundant protein in all LN patients was retinol binding protein 4, a general marker of tubular impairment (18). These findings indicate that contrasting well-defined subgroups allowed for identification of relevant biomarkers that could have been missed by analyzing all LN patients together. Different pathogenic processes may underlie each histologic subgroup, and thus, these biomarkers may provide insight into the relative active pathways.

Urinary IL-16 reflects histologic activity. The degree of histologic activity is often used to inform clinical decisions, so we sought to identify noninvasive urinary biomarkers that reflect histologic activity. We studied the correlation of the urinary abundances of all 1,000 biomarkers in urine samples collected at the time of biopsy with the histologic NIH activity index score. We found that IL-16 was the urinary protein most strongly positively correlated with the NIH activity index ($r = 0.73$, $P = 1.2 \times 10^{-5}$, FDR <10%) (n = 28), followed by CD163 and transforming growth factor β (TGFβ) (FDR <10%) (Figures 3A–D). We validated the significant concurrent correlation between urinary IL-16 abundance and NIH activity index score in an independent cohort of 101 patients ($r = 0.59$, $P = 9.3 \times 10^{-11}$) (Supplementary Figure 3 and Supplementary Table 2, https://onlinelibrary.wiley.com/doi/10.1002/art.42023) and with a PCR-based ELISA (Supplementary Figure 4, https://onlinelibrary.wiley.com/doi/10.1002/art.42023). Notably, IL-16 was the only protein not associated with proteinuria (Figure 3H), suggesting the potential to provide actionable information in addition to classic biomarkers such as proteinuria. In multivariate models, IL-16, CD163, and TGFβ retained their association with histologic activity after adjustment for multiple confounders, including proteinuria (Supplementary Table 3, https://onlinelibrary.wiley.com/doi/10.1002/art.42023). The pathways associated with histologic activity are displayed in Supplementary Figure 4 (https://onlinelibrary.wiley.com/doi/10.1002/art.42023).

In addition to having the strongest correlation with histologic activity, IL-16 was the urinary protein most strongly associated with proliferative LN (Figure 2A). The ROC curve revealed that IL-16 was a promising urinary biomarker to identify patients with

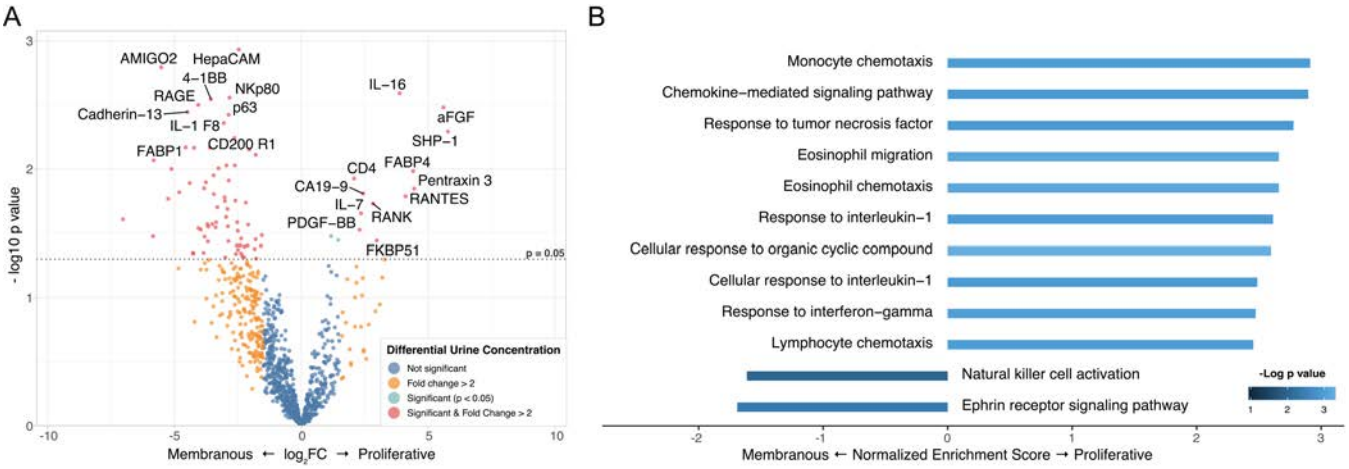

Figure 2. Proteomic profile of proliferative lupus nephritis. **A**, Volcano plot shows the differential abundance of 1,000 urinary proteins in proliferative LN (n = 14) and pure membranous LN (n = 9). **B**, Pathway enrichment analysis (Gene Ontology biological process) of the urinary proteomic profile revealed that chemotaxis was the process most enriched in proliferative LN. In particular, these were chemokines secreted in response to tumor necrosis factor, IL-1, and interferon-γ. The enrichment FDR (gene set enrichment analysis rank permutation) was <5% for all pathways except for "Natural killer cell activation" (16%). FABP-1 = fatty acid binding protein 1; PDGF-BB = platelet-derived growth factor BB; aFGF = acidic fibroblast growth factor; IGFBP-1 = insulin-like growth factor binding protein 1; FKBP51 = FK-506 binding protein 51; SHP-1 = SH2 domain–containing phosphatase 1 (see Figure 1 for other definitions). Color figure can be viewed in the online issue, which is available at http://onlinelibrary.wiley.com/doi/10.1002/art.42023/abstract.

proliferative LN, with AUCs of 0.85 ($P = 0.016$) and 0.89 ($P = 0.037$) in association with CD163 and TGFβ, respectively (Supplementary Figure 5, https://onlinelibrary.wiley.com/doi/10.1002/art.42023).

Correlation of urinary biomarkers with activity decrease, according to clinical response in longitudinal samples. A goal of immunosuppression in LN is to eradicate pathologic renal inflammation to ultimately prevent irreversible

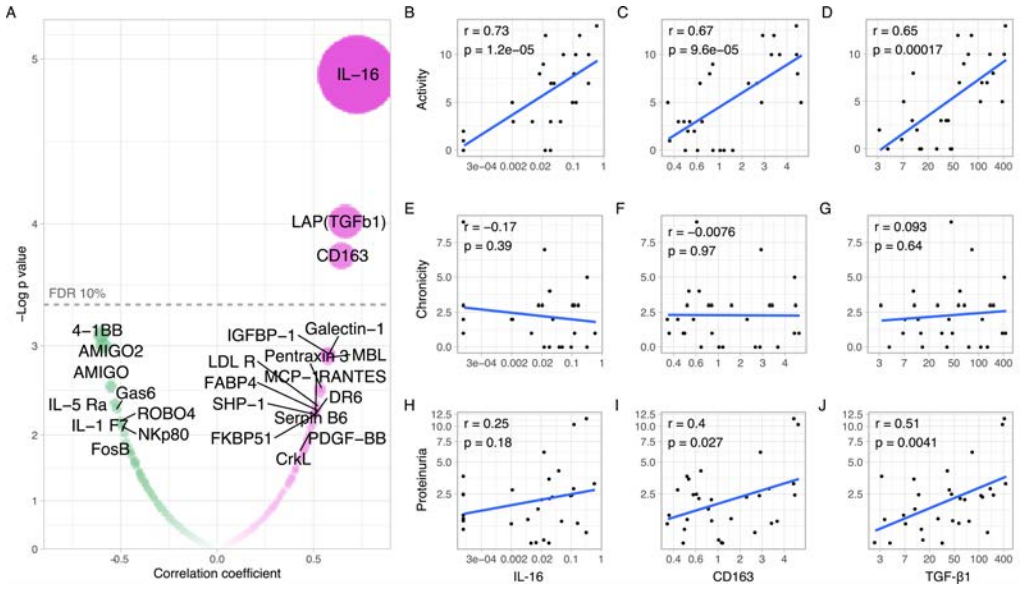

Figure 3. Urinary biomarkers of histologic nephritis activity. **A**, Pearson's correlation coefficients for the urinary abundance of 1,000 proteins and the histologic National Institutes of Health (NIH) activity index score in near or same-day renal biopsy samples. Each dot represents a protein within the array. The dashed line marks the significance threshold after correcting for multiple comparisons (FDR 10%). The area of the dot is proportional to the absolute of the correlation coefficient. Three proteins showed an FDR of <10%. The FDR of IL-16 was 1.2%. **B–J**, Scatterplots displaying the Pearson's correlation coefficient and *P* value for correlations of the urinary abundance of IL-16, CD163, and TGFβ1 with the NIH activity score (**B–D**), NIH chronicity score (**E–G**), and proteinuria (**H–J**). GAS-6 = growth arrest–specific protein 6; SHP-1 = SH2 domain–containing phosphatase 1; PDGF-BB platelet-derived growth factor BB (see Figure 1 for other definitions). Color figure can be viewed in the online issue, which is available at http://onlinelibrary.wiley.com/doi/10.1002/art.42023/abstract.

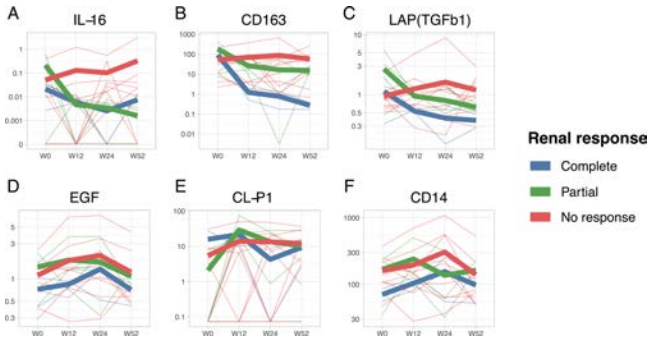

Figure 4. Biomarkers associated with nephritis activity decrease in responders. **A–F**, Urinary concentration of all biomarkers was measured at the time of biopsy (e.g., week 0 [W0]) and after 12, 24, and 52 weeks. Thin lines depict the trajectories of each patient categorized according to the response status determined at week 52. Thick lines represent the average for each group. The urinary concentration of the 3 biomarkers that significantly correlated with histologic activity declined in complete and partial responders but not in nonresponders (**A–C**). In contrast, 3 biomarkers that did not correlate with histologic activity (r values ranged from –0.0018 to 0.0015, *P* not significant) did not show a decline over time (**D–F**). IL-16 = interleukin-16; LAP = latency-associated peptide; TGFβ1 = transforming growth factor β type 1; EGF = endothelial growth factor; CL-P1 = collectin placenta 1. Color figure can be viewed in the online issue, which is available at http://onlinelibrary.wiley.com/doi/10.1002/art.42023/abstract.

renal damage and preserve function. The NIH activity index captures many renal inflammatory features, and, as a consequence, it improves with treatment in patients achieving renal remission (2,19). However, it is impractical to monitor in clinical practice as it requires frequent repeat renal biopsies. Thus, we hypothesized that the 3 urinary biomarkers associated with histologic activity would decline over time in patients responding to treatment and might serve as noninvasive biomarkers of response. The urinary concentration of all 3 candidate biomarkers declined in complete and partial responders but not in nonresponders (Figures 4A–C). The average decline was most striking in IL-16, with a decrease in partial and complete responders by week 12. CD163 concentration improved by week 12 in complete responders but not in partial responders. TGFβ showed a more modest decline.

Since response status is defined by reduction in proteinuria, we wanted to ensure that the observed biomarker trajectories were not simply a reflection of a decline in all urinary protein in responders. The trajectories of 3 urinary proteins that were selected among those that did not correlate with histologic activity demonstrated that there was not a nonspecific decline (Figures 4D–F). These findings indicate that IL-16, CD163, and TGFβ trajectories represent a specific decrease in the production and excretion of these molecules and, as they correlated with activity at baseline, likely reflect a corresponding improvement of intrarenal LN activity, supporting their value as biomarkers.

***IL16* is one of the most expressed cytokines in infiltrating immune cells in LN kidneys.** To determine whether the urinary concentration of the 3 candidate biomarkers reflects an active intrarenal process rather than passive filtration through

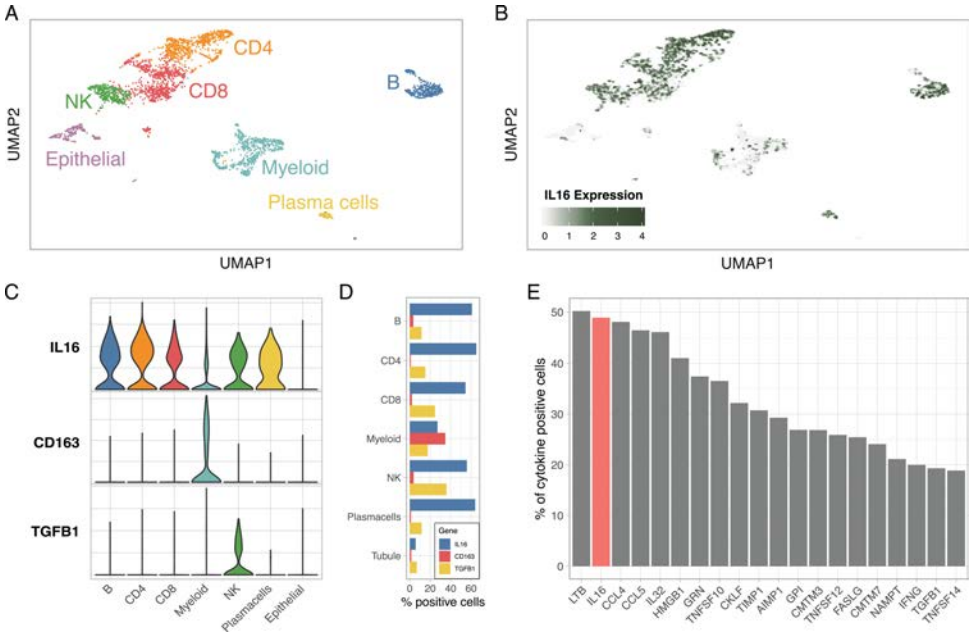

Figure 5. High expression of *IL16* in lupus nephritis (LN) kidneys. **A**, UMAP plot of single-cell RNA sequencing of renal biopsies (3131 cell) by lineage. **B**, Feature plot displaying *IL16* expression at the single-cell level. **C** and **D**, Violin plots (**C**) and bar plots (**D**) summarizing the expression of the genes coding for the urinary proteins associated with nephritis activity. *IL16* was abundantly expressed by most infiltrating immune cells in kidneys, *CD163* mostly by macrophages, and *TGFB1* by natural killer cells. **E**, Prevalence of cytokine positive cells out of a compendium of 237 cytokines ranked decreasingly (top 20 are shown). *IL16* (red) was the second most expressed cytokine in LN kidneys. Color figure can be viewed in the online issue, which is available at http://onlinelibrary.wiley.com/doi/10.1002/art.42023/abstract.

a damaged glomerular membrane, we evaluated the intrarenal relative gene expression using single-cell RNA sequencing of LN renal biopsies. *IL16* was abundantly expressed by most immune infiltrating cells, *CD163* by a subset of myeloid cells, and *TGFB1* mostly by natural killer (NK) cells (Figures 5A–D).

In LN, most of *IL16* expression was in immune infiltrating cells, especially the lymphoid lineage (Figures 5C and D). In renal allograft rejection, single-cell RNA sequencing showed that *IL16* was expressed by endothelial, epithelial, and immune cells, but immune cells were the main source (20) (Supplementary Figure 6A, https://onlinelibrary.wiley.com/doi/10.1002/art.42023). Conversely, in healthy kidneys, single nuclear RNA sequencing and ATAC-seq (Assay for Transposase-Accessible Chromatin using sequencing) revealed substantial *IL16* expression by podocytes, fibroblasts, endothelial cells, mesangial cells, and proximal tubular cells (21,22) (Supplementary Figures 5B and C, https://onlinelibrary.wiley.com/doi/10.1002/art.42023). These findings suggest that while immune cells are likely the major intrarenal source of IL-16 in LN, IL-16 secretion by endothelial and tubular cells may precede immune infiltration. It can be speculated that this initial event can then be amplified by infiltrating immune cells, as seen in LN and allograft rejection.

Finally, we explored whether *IL16* was disproportionally more expressed compared to other cytokines in LN. Out of a compendium of 237 cytokines, *IL16* was the second most commonly expressed cytokine (49% of all infiltrating immune cells) (Figure 5E). These findings independently suggest IL-16 as a major cytokine involved in LN.

Correlation of tissue expression of IL-16 with LN activity and urinary IL-16 abundance. To establish the location of IL-16–secreting cells in renal tissue, we performed immunohistochemical staining of human IL-16 in 7 LN kidney biopsy samples, with matching urine IL-16 collected at or near the time of biopsy. We observed abundant interstitial and glomerular IL-16 expression in proliferative LN (Figure 6 and Supplementary Figures 7A–C, https://onlinelibrary.wiley.com/doi/10.1002/art.42023), with the exception of 1 case (Supplementary Figure 7D), in which the activity index score was uncharacteristically low (score of 2) and IL-16 was not detectable in the urine. In contrast,

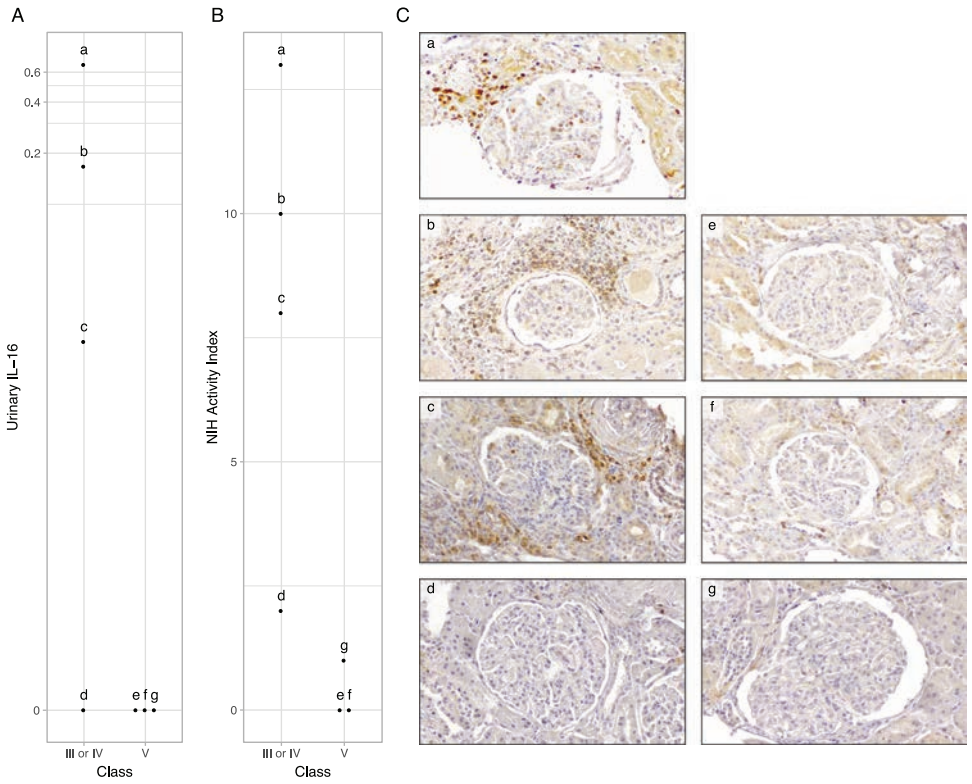

Figure 6. Interleukin-16 (IL-16)–positive cells are abundant in proliferative lupus nephritis (LN) and qualitatively correlate with urinary IL-16 and LN activity. Immunohistochemical staining for human IL-16 was performed in 7 LN kidney biopsy samples with matching urine IL-16 collected at or near the time of biopsy. **A** and **B**, The corresponding urinary abundance of IL-16 (**A**) and National Institutes of Health (NIH) activity index (**B**) of the patients whose biopsy results depicted in **C** are plotted according to the International Society of Nephrology class. Lower-case letters in **A–C** identify information from the same patients. **C**, Immunohistochemical staining of IL-16 in 4 proliferative LN biopsy sections (a–d) and 3 pure membranous LN biopsy sections (e–g). An abundance of IL-16–positive cells was noted in proliferative LN (**C**; a–d), with qualitatively more prominent intraglomerular IL-16 positivity in patients with higher urinary IL-16 levels and NIH activity index scores. Original magnification × 33.6. Lower-magnification images with larger representation of the interstitium are displayed in Supplementary Figure 6 (https://onlinelibrary.wiley.com/doi/10.1002/art.42023).

there was very scant IL-16 positivity in membranous LN (Figure 6 and Supplementary Figures 7E–G), and there was marginal IL-16 in a class I LN biopsy sample used as negative control (Supplementary Figure 7H). These findings were consistent with the urinary IL-16 profile. Furthermore, there was a qualitative correlation between the number of IL-16–positive cells and urinary IL-16 abundance as well as with the NIH activity index score (Figure 6). This was particularly evident for glomerular IL-16–positive cells. These findings indicate that IL-16 is intrarenally produced in proliferative LN, and urinary IL-16 reflects the abundance of intrarenal IL-16–positive cells and LN activity.

DISCUSSION

Leveraging urine proteomics in LN patients and healthy controls, the findings of this study confirmed that the pathologic processes in LN can be noninvasively captured and monitored over time. In the present study, we found the following: 1) 237 urinary proteins associated with LN that represented ≥12 distinct molecular pathways, 2) a strong chemokine signature characterizing the urine of patients with proliferative LN, and 3) several candidate biomarkers to detect active nephritis that can be monitored over time to assess response to treatment. Overall, IL-16 emerged as the most robust correlate of histologic activity, suggesting a role in LN pathogenesis and thus subsequent translation to clinical application both as a biomarker and treatable target.

Proteomic analysis revealed that the intrarenal activation of several pathogenic mechanisms contributing to LN can be quantified in the urine. These biologic processes were previously implicated in LN, including neutrophil immunity (23,24), platelet degranulation (25), extracellular matrix organization (26), and chemotaxis (27). Patients did not cluster based on the abundance of a single signature or a group of signatures. Rather, we observed 2 clusters characterized by high and intermediate abundance of all signatures, respectively. This is consistent with previous findings from an agnostic approach to urine proteomics in LN that showed that patients are stratified on a gradient (27). Importantly, 80% of complete responders were clustered in the intermediate abundance group. The predictive value of this approach needs to be validated in a larger cohort, given the small number of responders.

In this study, urinary abundance of proteomic signatures was independent from proteinuria, indicating that these signatures specifically reflect active biologic processes rather than a nonspecific increase or decrease of all urine proteins. In particular, pathway enrichment analysis revealed a strong chemokine signature in proliferative LN, suggesting active recruiting of immune cells in the kidney in these patients. This is biologically consistent with the abundant immune cell infiltration and more aggressive phenotype observed in class III and class IV LN, further supporting the ability of urine proteomics to infer intrarenal biologic processes.

Ideal biomarkers in LN should noninvasively infer nephritis activity, longitudinally track response to treatment, and capture the intrarenal biology. Based on feasibility, the current management of LN hinges on monitoring proteinuria to establish renal activity rather than frequent biopsies. However, proteinuria is a poor marker of nephritis activity. Six-month repeated biopsies after induction therapy revealed that ~50% of the patients with disease in complete clinical remission (proteinuria <0.5 gm/24 hours and no increase in serum creatinine) had persistent histologically active proliferative nephritis (28). Conversely, >50% of patients who achieved complete histologic remission had persistent proteinuria >0.5 gm/24 hours. Moreover, patients in clinical remission 3 years after induction treatment may show persistent nephritis activity on per-protocol biopsies, which is associated with flares of nephritis as immunosuppression is tapered (2).

Using an unbiased approach, we discovered a previously unrecognized biomarker of intrarenal activity, IL-16, in addition to 2 previously recognized LN biomarkers, CD163 (29) and TGFβ (30). IL-16 showed the strongest and most significant association with the renal activity index of any marker measured, and urinary abundance of IL-16 decreased over time in patients who ultimately responded to treatment after 1 year. IL-16, CD163, and TGFβ were selected based on their correlation with histologic activity; therefore, it is conceivable that their decreasing urinary abundance mirrored an improvement of intrarenal histologic activity. In fact, urinary proteins that did not correlate with activity did not decrease over time in responders.

Renal single-cell RNA sequencing revealed that *IL16*, *CD163*, and *TGFB1* are actively expressed by immune infiltrating cells in LN kidney biopsy samples, suggesting that their detection in the urine reflects intrarenal immune activity. Because their expression was observed in distinct immune cell types, their urinary abundance could identify the activity of distinct immune processes. We discovered that *IL16* was the second most expressed cytokine in LN kidneys (49% of all infiltrating immune cells). This striking concordant result was independent of the urine proteomics data set, thus demonstrating the relevance of IL-16 in LN in an orthogonal approach. Furthermore, we demonstrated prominent intraglomerular and interstitial renal production of IL-16 in proliferative LN by immunohistochemistry. Although we did not evaluate circulating cells or serum, IL-16 urinary abundance correlated with intrarenal IL-16–positive cells, indicating that urinary IL-16 is the direct consequence of intrarenal IL-16 secretion. Because urinary IL-16, intrarenal IL-16–positive cells, and histologic activity are positively co-correlated and *IL16* is one the most expressed cytokines in LN, our findings suggest that IL-16 may be implicated in LN pathogenesis, and this process can be noninvasively measured in urine.

IL-16 is a proinflammatory chemokine secreted by immune cells and nonimmune cells (endothelial cells, epithelial cells, fibroblasts, and neurons) in response to several stimuli, such as complement activation, antigen stimulation, IFN, hypoxia, and

cell injury (31–34). Because the release of bioactive IL-16 depends on caspase 3 activation (33), apoptosis and proapoptotic stimuli, including sublethal doses of granzymes, may also lead to its release. IL-16 can also be released upon cleavage by proteinase 3 (35), which suggests that urinary IL-16 may indicate neutrophil degranulation. IL-16 is the natural ligand for CD4 and CD9 and is a strong chemoattractant for CD4+ T cells (especially Th1 cells), as well as CD8 T cells, NK cells, B cells, monocytes, neutrophils, dendritic cells, and mast cells (31). IL-16 can activate CD4 T cells independently of T cell receptor activation (36) and may lead to the release of proinflammatory cytokines such as TNF, IL-1β, IL-6, IL-15, and IL-12 (31). *IL16* polymorphisms were associated with an increased risk of SLE (odds ratio 3.3–10.4), suggesting a potential causal role (37). Plasma IL-16 levels were associated with SLE severity, including renal involvement (38). Finally, IL-16 was mechanistically linked to lung disease in the pristane model of SLE (39). The role of IL-16 in LN is yet to be fully understood, but it has been implicated in several other immune-mediated diseases, such as multiple sclerosis, scleroderma, rheumatoid arthritis, and allograft rejection (31,40,41). Further studies are needed to address the efficacy of IL-16 blockade in LN.

Our study demonstrated the power of integrating urinary proteomic screening platforms with matching clinical and pathologic information and with tissue single-cell transcriptomics (42). In fact, in addition to a newly discovered biomarker, our approach detected that CD163 and TGFβ are proven biomarkers in LN. Similar to our findings, soluble CD163 was shown to correlate with LN nephritis activity and to improve with treatment (29). CD163 is a scavenger receptor expressed on phagocytic monocytes, especially in M2c-polarized macrophages that infiltrate tissue during the healing phase of inflammation and are implicated in fibrosis resolution (43). Notably, M2c macrophages are inducible by TGFβ (44). CD163+ cells are a dominant macrophage subtype in LN (44), once again supporting the notion of capability of urinary proteomic to infer intrarenal biology. CD163+ cells have been detected in proliferative glomerular lesions and in tubulointerstitial inflammation (45), and they constitute ~80% of the urinary cells in LN (46). Similarly consistent with our results, urinary TGFβ correlated with nephritis activity and response in previous studies (30,47,48), but sensitive immunoassays (such as the one used here) are required to reliably detect urinary TGFβ (48). TGFβ regulates inflammation and progression of renal fibrosis. Notably, TGFβ increased IL-16 release in synovial fibroblasts, suggesting a possible similar interplay between these 2 cytokines in LN (49). Here, we have shown that NK cells are the major immune cell type expressing *TGFB1* in LN; whether NK cells or tubular cells (50) are responsible for urinary TGFβ in LN is yet to be determined.

We acknowledge the limitations of our study. Since we did not analyze serum or plasma, we could not establish with definitive certainty whether the concentration of specific proteins in the urine was the consequence of extrarenal leakage from the circulation through a damaged glomerular basement membrane or of intrarenal production. For example, plasma IL-16 levels were associated with disease severity, including renal involvement, in a group of SLE patients (38), but whether the source IL-16 was intra- or extrarenal was not established. We have unequivocally demonstrated that there is high intrarenal production of IL-16 in LN, indicating that urinary IL-16 derives, at least in part, from active intrarenal secretion. Importantly, the association between urinary IL-16 and proliferative LN activity was independent of proteinuria and suggests that a change in urinary IL-16 abundance is an independent process rather than nonspecific leakage from plasma. Future studies will be needed to address the power of urinary IL-16 to discriminate "active" from "nonactive" proliferative LN. In addition, as there was a limited number of complete responders, we could not study biomarkers to predict future response with statistically robust confidence nor confidently evaluate whether the longitudinal trajectories were statistically significant. Ongoing studies as part of the AMP RA/SLE consortium will allow us to address these questions.

In summary, this study linked IL-16 release with LN activity, suggesting a possible role as a biomarker and in LN pathogenesis, thus nominating IL-16 as a potentially treatable target. Further, our study demonstrated the feasibility to detect novel and biologically relevant biomarkers in LN using a urine proteomic platform in a well-characterized longitudinal cohort. Further ongoing studies are required to confirm the clinical applicability of these findings. This unprecedented data set may further discovery by allowing investigators to research and validate new biomarkers, test new hypotheses, and complement mechanistic studies in LN.

AUTHOR CONTRIBUTIONS

All authors were involved in drafting the article or revising it critically for important intellectual content, and all authors approved the final version to be published. Dr. Fava had full access to all of the data in the study and takes responsibility for the integrity of the data and the accuracy of the data analysis.

Study conception and design. Fava, Mohan, James, Wofsy, the Accelerating Medicines Partnership in Rheumatoid Arthritis and Systemic Lupus Erythematosus Network, Buyon, Petri.

Acquisition of data. Fava, Mohan, Zhang, Rosenberg, Belmont, Izmirly, Clancy, Trujillo, Fine, Wofsy, Apruzzese, the Accelerating Medicines Partnership in Rheumatoid Arthritis and Systemic Lupus Erythematosus Network, Buyon, Petri.

Analysis and interpretation of data. Fava, Rao, Rosenberg, Fenaroli, Arazi, Berthier, Davidson, James, Diamond, Hacohen, Raychaudhuri, the Accelerating Medicines Partnership in Rheumatoid Arthritis and Systemic Lupus Erythematosus Network, Buyon, Petri.

REFERENCES

1. Fava A, Petri M. Systemic lupus erythematosus: diagnosis and clinical management. J Autoimmun 2018;96:0–1.
2. De Rosa M, Azzato F, Toblli JE, De Rosa G, Fuentes F, Nagaraja HN, et al. A prospective observational cohort study highlights kidney biopsy findings of lupus nephritis patients in remission who flare

following withdrawal of maintenance therapy. Kidney Int 2018;94: 788–94.
3. Greloni G, Scolnik M, Marin J, Lancioni E, Quiroz C, Zacariaz J, et al. Value of repeat biopsy in lupus nephritis flares. Lupus Sci Med 2014; 1:1–6.
4. Luciano RL, Moeckel GW. Update on the native kidney biopsy: core curriculum 2019. American J Kidney Dis 2019;73:404–15.
5. Geldenhuys L, Nicholson P, Sinha N, Dini A, Doucette S, Alfaadhel T, et al. Percutaneous native renal biopsy adequacy: a successful interdepartmental quality improvement activity. Can J Kidney Health Dis 2015;2:1–7.
6. Birmingham DJ, Merchant M, Waikar SS, Nagaraja H, Klein JB, Rovin BH. Biomarkers of lupus nephritis histology and flare: deciphering the relevant amidst the noise. Nephrol Dial Transplant 2017;32:i71–9.
7. Soliman S, Mohan C. Lupus nephritis biomarkers. Clin Immunol 2017; 185:10–20.
8. Pejchinovski M, Siwy J, Mullen W, Mischak H, Petri MA, Burkly LC, et al. Urine peptidomic biomarkers for diagnosis of patients with systematic lupus erythematosus. Lupus 2018;27:6–16.
9. Davidson A. What is damaging the kidney in lupus nephritis? Nat Rev Rheumatol 2016;12:143–53.
10. Stanley S, Vanarsa K, Soliman S, Habazi D, Pedroza C, Gidley G, et al. Comprehensive aptamer-based screening identifies a spectrum of urinary biomarkers of lupus nephritis across ethnicities. Nat Commun 2020;11:2197.
11. Zhang T, Duran V, Vanarsa K, Mohan C. Targeted urine proteomics in lupus nephritis — a meta-analysis. Expert Rev Proteomics 2020;17: 767–76.
12. Vanarsa K, Soomro S, Zhang T, Strachan B, Pedroza C, Nidhi M, et al. Quantitative planar array screen of 1000 proteins uncovers novel urinary protein biomarkers of lupus nephritis. Ann Rheum Dis 2020;79: 1349–61.
13. Platonov ME, Borovjagin AV, Kaverina N, Xiao T, Kadagidze Z, Lesniak M, et al. KISS1 tumor suppressor restricts angiogenesis of breast cancer brain metastases and sensitizes them to oncolytic virotherapy in vitro. Cancer Lett 2018;417:75–88.
14. Bajema IM, Wilhelmus S, Alpers CE, Bruijn JA, Colvin RB, Cook HT, et al. Revision of the International Society of Nephrology/Renal Pathology Society classification for lupus nephritis: clarification of definitions, and modified National Institutes of Health activity and chronicity indices. Kidney Int 2018;93:789–96.
15. Arazi A, Rao DA, Berthier CC, Davidson A, Liu Y, Hoover PJ, et al. The immune cell landscape in kidneys of patients with lupus nephritis. Nat Immunol 2019;20:902–14.
16. Kuleshov MV, Jones MR, Rouillard AD, Fernandez NF, Duan Q, Wang Z, et al. Enrichr: a comprehensive gene set enrichment analysis web server 2016 update. Nucleic Acids Res 2016;44:W90–7.
17. Wang Y, Wang R, Zhang S, Song S, Jiang C, Han G, et al. iTALK: an R package to characterize and illustrate intercellular communication. bioRxiv 2019:507871.
18. Norden AG, Lapsley M, Unwin RJ. Urine retinol-binding protein 4: a functional biomarker of the proximal renal tubule. Adv Clin Chem 2014;63:85–122.
19. Alvarado AS, Malvar A, Lococo B, Alberton V, Toniolo F, Nagaraja HN, et al. The value of repeat kidney biopsy in quiescent Argentinian lupus nephritis patients. Lupus 2014;23:840–7.
20. Wu H, Malone AF, Donnelly EL, Kirita Y, Uchimura K, Ramakrishnan SM, et al. Single-cell transcriptomics of a human kidney allograft biopsy specimen defines a diverse inflammatory response. J Am Soc Nephrol 2018;29:2069–80.
21. Wu H, Uchimura K, Donnelly EL, Kirita Y, Morris SA, Humphreys BD. Comparative analysis and refinement of human PSC-derived kidney organoid differentiation with single-cell transcriptomics. Cell Stem Cell 2018;23:869–81.
22. Muto Y, Wilson PC, Wu H, Waikar SS, Humphreys B. Single cell transcriptional and chromatin accessibility profiling redefine cellular heterogeneity in the adult human kidney. Nat Commun 2021;12: 2190.
23. Banchereau R, Hong S, Cantarel B, Baldwin N, Baisch J, Edens M, et al. Personalized immunomonitoring uncovers molecular networks that stratify Lupus patients. Cell 2016;165:551–65.
24. Villanueva E, Yalavarthi S, Berthier CC, Hodgin JB, Khandpur R, Lin AM, et al. Netting neutrophils induce endothelial damage, infiltrate tissues, and expose immunostimulatory molecules in systemic lupus erythematosus. J Immunol 2011;187:538–52.
25. Linge P, Fortin PR, Lood C, Bengtsson AA, Boilard E. The non-haemostatic role of platelets in systemic lupus erythematosus [review]. Nat Rev Rheumatol 2018;14:195–13.
26. Wei R, Gao B, Shih F, Ranger A, Dearth A, Mischak H, et al. Alterations in urinary collagen peptides in lupus nephritis subjects correlate with renal dysfunction and renal histopathology. Nephrol Dial Transplant 2017;32:1468–77.
27. Fava A, Buyon J, Mohan C, Zhang Y, Belmont H, Izmirly P, et al. Integration of urine proteomics and renal single-cell genomics identifies an interferon-γ response gradient in lupus nephritis. JCI Insight 2020;5: e138345.
28. Malvar A, Pirruccio P, Alberton V, Lococo B, Recalde C, Fazini B, et al. Histologic versus clinical remission in proliferative lupus nephritis. Nephrol Dial Transplant 2017;32:1338–44.
29. Mejia-Vilet JM, Zhang XL, Cruz C, Cano-Verduzco ML, Shapiro JP, Nagaraja HN, et al. Urinary soluble CD163: a novel noninvasive biomarker of activity for lupus nephritis. J Am Soc Nephrol 2020;31: 1335–47.
30. Torabinejad S, Mardani R, Habibagahi Z, Roozbeh J, Khajedehi P, Pakfetrat M, et al. Urinary monocyte chemotactic protein-1 and transforming growth factor-β in systemic lupus erythematosus. Indian J Nephrol 2012;22:5–12.
31. Glass WG, Sarisky RT, Del Vecchio AM. Not-so-sweet sixteen: the role of IL-16 in infectious and immune-mediated inflammatory diseases [review]. J Interferon Cytokine Res 2006;26:511–20.
32. Roth S, Agthe M, Eickhoff S, Möller S, Karsten CM, Borregaard N, et al. Secondary necrotic neutrophils release interleukin-16C and macrophage migration inhibitory factor from stores in the cytosol. Cell Death Discov 2015;1:1–9.
33. Zhang Y, Center DM, Wu DM, Cruikshank WW, Yuan J, Andrews DW, et al. Processing and activation of pro-interleukin-16 by caspase-3. J Biol Chem 1998;273:1144–9.
34. Cruikshank W, Little F. Interleukin-16: the ins and outs of regulating T-cell activation [review]. Crit Rev Immunol 2008;28:467–83.
35. Kerstein-Staehle A, Alarcin C, Luo J, Riemekasten G, Lamprecht P, Müller A. OP0054 new role for proteinase 3 in IL-16 bioactivity control in granulomatosis with polyangiitis. Ann Rheum Dis 2021;80:28–9.
36. Lun WH, Takeda A, Nakamura H, Kano M, Mori K, Sata T, et al. Loss of virus-specific CD4+ T cells with increases in viral loads in the chronic phase after vaccine-based partial control of primary simian immunodeficiency virus replication in macaques. J Gen Virol 2004; 85:1955–63.
37. Xue H, Gao L, Wu Y, Fang W, Wang L, Li C, et al. The IL-16 gene polymorphisms and the risk of the systemic lupus erythematosus. Clinica Chimica Acta 2009;403:223–5.
38. Lard LR, Roep BO, Verburgh CA, Zwinderman AH, Huizinga TW. Elevated IL-16 levels in patients with systemic lupus erythematosus are associated with disease severity but not with genetic susceptibility to lupus. Lupus 2002;11:181–5.

39. Mariani LH, Martini S, Barisoni L, Canetta PA, Troost JP, Hodgin JB, et al. Interstitial fibrosis scored on whole-slide digital imaging of kidney biopsies is a predictor of outcome in proteinuric glomerulopathies. Nephrol Dial Transplant 2018;33:310–8.
40. De Oliveira JG, Xavier PD, Sampaio SM, Tavares IS, Mendes AA. The synthesis by fine-needle aspiration biopsy cultures of IL-7, IL-16 and IL-18 is significantly associated with acute rejection in kidney transplants. Nephron 2002;92:622–8.
41. Kawabata K, Makino T, Makino K, Kajihara I, Fukushima S, Ihn H. IL-16 expression is increased in the skin and sera of patients with systemic sclerosis. Rheumatology (Oxford) 2020;59:519–23.
42. Fava A, Raychaudhuri S, Rao DA. The power of systems biology: insights on lupus nephritis from the Accelerating Medicines Partnership. Rheum Dis Clin North Am 2021;47:335–50.
43. Lu J, Cao Q, Zheng D, Sun Y, Wang C, Yu X, et al. Discrete functions of M2a and M2c macrophage subsets determine their relative efficacy in treating chronic kidney disease. Kidney Int 2013;84: 745–55.
44. Olmes G, Büttner-Herold M, Ferrazzi F, Distel L, Amann K, Daniel C. CD163+ M2c-like macrophages predominate in renal biopsies from patients with lupus nephritis. Arthritis Res Ther 2016;18:1–16.
45. Li YR, Li J, Zhao SD, Bradfield JP, Mentch FD, Maggadottir SM, et al. Meta-analysis of shared genetic architecture across ten pediatric autoimmune diseases. Nature Med 2015;21:1018–27.
46. Arazi A, Rao DA, Berthier CC, Davidson A, Liu Y, Hoover PJ, et al. The immune cell landscape in kidneys of patients with lupus nephritis. Nat Immunol 2019;20:902–14.
47. Avihingsanon Y, Phumesin P, Benjachat T, Akkasilpa S, Kittikowit V, Praditpornsilpa K, et al. Measurement of urinary chemokine and growth factor messenger RNAs: a noninvasive monitoring in lupus nephritis. Kidney Int 2006;69:747–53.
48. Tsakas S, Goumenos DS. Accurate measurement and clinical significance of urinary transforming growth factor-β. Am J Nephrol 2006; 26:186–93.
49. Warstat K, Hoberg M, Rudert M, Tsui S, Pap T, Angres B, et al. Transforming growth factor β1 and laminin-111 cooperate in the induction of interleukin-16 expression in synovial fibroblasts from patients with rheumatoid arthritis. Ann Rheum Dis 2010;69:270–5.
50. Lee JS, Lim JY, Kim J. Mechanical stretch induces angiotensinogen expression through PARP1 activation in kidney proximal tubular cells. In Vitro Cell Dev Biol Anim 2015;51:72–8.

APPENDIX A: THE ACCELERATING MEDICINES PARTNERSHIP IN RHEUMATOID ARTHRITIS AND SYSTEMIC LUPUS ERYTHEMATOSUS NETWORK

Members of the Accelerating Medicines Partnership in Rheumatoid Arthritis and Systemic Lupus Erythematosus Network include the following authors: Andrea Fava, Deepak A. Rao, Chandra Mohan, Ting Zhang, H. Michael Belmont, Peter Izmirly, Robert Clancy, Jose Monroy Trujillo, Derek Fine, Arnon Arazi, Celine C. Berthier, Anne Davidson, Judith A. James, Betty Diamond, Nir Hacohen, David Wofsy, Soumya Raychaudhuri, William Apruzzese, Jill Buyon, Michelle Petri, Yanyan Liu, Paul J. Hoover, Adam Chicoine, Thomas M. Eisenhaure, A. Helena Jonsson, Shuqiang Li, David J. Lieb, Fan Zhang, Ilya Korsunski, Joseph Mears, Kamil Slowikowski, Edward P. Browne, Akiko Noma, Danielle Sutherby, Scott Steelman, Dawn E. Smilek, Patti Tosta, Elena Massarotti, Maria Dall'Era, Meyeon Park, Diane L. Kamen, Richard A. Furie, Fernanda Payan-Schober, William F. Pendergraft III, Elizabeth A. McInnis, Chaim Putterman, Kenneth C. Kalunian, E. Steve Woodle, James A. Lederer, David A. Hildeman, Chad Nusbaum, Matthias Kretzler, Jennifer H. Anolik, Michael B. Brenner, Dia Waguespack, Sean M. Connery, Maureen A. McMahon, William J. McCune, Ruba B. Kado, Raymond Hsu, Melissa A. Cunningham, Paul J. Utz, Mina Pichavant, Holden T. Maecker, Rohit Gupta, Joel M. Guthridge, Chamith Fonseka, Evan Der, Thomas Tuschl, Hemant Suryawanshi, Daniel Goldman.

American College of Rheumatology
Empowering Rheumatology Professionals

Arthritis & Rheumatology
Vol. 74, No. 5, May 2022, pp 840–848
DOI 10.1002/art.42021

Identification of Shared and Asian-Specific Loci for Systemic Lupus Erythematosus and Evidence for Roles of Type III Interferon Signaling and Lysosomal Function in the Disease: A Multi-Ancestral Genome-Wide Association Study

Yong-Fei Wang,[1] Wei Wei,[2] Pattarin Tangtanatakul,[3] Lichuan Zheng,[4] Yao Lei,[4] Zhiming Lin,[5] Chengmin Qian,[4] Xiao Qin,[6] Fei Hou,[6] Xinyu Zhang,[4] Li Shao,[2] Nusara Satproedprai,[7] Surakameth Mahasirimongkol,[7] Prapaporn Pisitkun,[8] Qin Song,[2] Yu Lung Lau,[4] Yan Zhang,[9] Nattiya Hirankarn,[3] and Wanling Yang[4]

Objective. Systemic lupus erythematosus (SLE) is a prototypical autoimmune disease with differences in prevalence and severity among ancestral groups. This study was undertaken to identify novel genetic components, either shared by or distinct between Asian and European populations.

Methods. Both trans-ancestral and ancestry-specific meta-analyses of genome-wide association studies (GWAS) for SLE were performed, involving 30,604 participants of European, Chinese, or Thai origin. Using public epigenomic data and expression quantitative trait loci, fine-mapping analyses were conducted to identify putative causal variants and genes for the newly identified loci. Performance of polygenic risk scores for the Thai cohort was evaluated by comparing different training data.

Results. A 1-bp deletion upstream of *IFNLR1* was found to be associated with SLE, with the risk allele correlated with increased expression of *IFNLR1*. This gene encodes interferon-λ (IFNλ) receptor 1, providing evidence of a role of type III IFN signaling in SLE. An intronic variant in *SLC29A3* was found to be associated with SLE in Asians only. The putative risk variant may modulate *SLC29A3* expression in a monocyte-specific manner. *SLC29A3* encodes a lysosomal nucleoside transporter, and subsequent analyses suggested that reduced lysosomal function and phagocytosis might be the mechanism underlying this association. Ancestry-shared loci in or near *TAOK3*, *CHD9*, *CAMK1D*, *ATXN1*, and *TARBP1* and Asian-specific loci close to *PEX2*, *FCHSD2*, and *TMEM116* also reached the genome-wide significant association with SLE. In addition, trans-ancestral meta-analysis was shown to be valuable in risk prediction for individuals without ancestry-matched data.

Conclusion. In this study both shared and Asian-specific loci for SLE were identified, and functional annotation provided evidence of the involvement of increased type III IFN signaling and reduced lysosomal function in SLE.

Dr. Wang's work was supported by the National Natural Science Foundation of China (grant 81801636). Drs. Satproedprai and Mahasirimongkol's work was supported by Genomic Thailand (Department of Medical Science, Thailand Ministry of Public Health). Drs. Pisitkun's and Hirankarn's work was supported by the International Network for Lupus Research (grant IRN59W0004) and the Ratchadaphiseksomphot Matching Fund. Dr. Y. Zhang's work was supported by the National Natural Science Foundation of China (grant 81601423). Dr. Yang's work was supported by the Research Grant Council of Hong Kong (grants 17146616 and 17106320).

[1]Yong-Fei Wang, PhD: University of Hong Kong, Hong Kong, China, and Shenzhen Futian Hospital for Rheumatic Diseases, Shenzhen, China; [2]Wei Wei, MS, Li Shao, MS, Qin Song, MS: Affiliated Hospital of Jining Medical University, Shandong, China; [3]Pattarin Tangtanatakul, PhD, Nattiya Hirankarn, MD, PhD: Chulalongkorn University, Bangkok, Thailand; [4]Lichuan Zheng, MPhil, Yao Lei, BS, Chengmin Qian, PhD, Xinyu Zhang, BS, Yu Lung Lau, MD, Wanling Yang, PhD: University of Hong Kong, Hong Kong, China; [5]Zhiming Lin, MD: Third Affiliated Hospital of Sun Yat-Sen University, Guangzhou, China; [6]Xiao Qin, BS, Fei Hou, MS: Collaborative Innovation Center for Birth Defect Research and Transformation of Shandong Province and Jining Medical University, Shandong, China; [7]Nusara Satproedprai, PhD, Surakameth Mahasirimongkol, MD: Ministry of Public Health, Nonthaburi, Thailand; [8]Prapaporn Pisitkun, MD: Ramathibodi Hospital and Mahidol University, Bangkok, Thailand; [9]Yan Zhang, PhD: Guangzhou Institute of Pediatrics, Guangdong Provincial Key Laboratory of Research in Structural Birth Defect Disease, Guangzhou Women and Children's Medical Center, and Guangzhou Medical University, Guangzhou, China.

Drs. Wang and Wei contributed equally to this work.

Author disclosures are available at https://onlinelibrary.wiley.com/action/downloadSupplement?doi=10.1002%2Fart.42021&file=art42021-sup-0001-Disclosureform.pdf.

Address correspondence to Yan Zhang, PhD, 13F, 9 Jinsui Road, Guangzhou, China (email: yannizy@gmail.com); or to Nattiya Hirankarn, MD, PhD, 1873 RamaIV, Pathumwan, Bangkok 10330, Thailand (email: Nattiya.H@chula.ac.th); or to Wanling Yang, PhD, L7-55 FoM, 21 Sassoon Road, Pokfulam, Hong Kong (email: yangwl@hku.hk).

Submitted for publication June 28, 2021; accepted in revised form November 9, 2021.

INTRODUCTION

Systemic lupus erythematosus (SLE) is an autoimmune disease characterized by prominent heterogeneity across ancestral groups, with non-European populations having a much higher disease prevalence and patients of non-European ancestries being more likely to develop lupus nephritis (1–4). Despite great efforts toward elucidating the associated loci for SLE (5–8), the genetic basis underlying the ancestral heterogeneity is still poorly understood.

We recently demonstrated significant but incomplete sharing of genetic factors for SLE between Chinese and European populations and reported several genetic loci with evidence of association in Chinese but not in European populations (7). We further demonstrated that the ancestral genetic differences affected transferability of polygenic risk scores (PRS) among different populations (7). Additionally, in a study focusing on a Thai SLE cohort, we have shown that the *FBN2* locus was associated with SLE in the Thai population but not in either Chinese or European populations (9). Consistent with studies on other complex diseases (10–12), multi-ancestral genome-wide association studies (GWAS) in SLE have proven to be valuable in detecting genetic factors that underlie ancestral differences.

In this study, we incorporated SLE GWAS from European, Chinese, and Thai populations to investigate both shared and distinct genetic components among the ancestral groups. Through both trans-ancestral and Asian-specific meta-analyses involving a total of 10,145 SLE cases and 20,459 controls, we identified 10 novel loci associated with SLE. Four of these 10 loci were associated with the disease in Asian populations but were either nonpolymorphic or showed no evidence of association in Europeans.

Ancestral differences in the genetic architecture for SLE may affect the predictive performance of PRS, and our previous study showed that the PRS method performs better when trained on ancestry-matched data (7). The majority of GWAS in SLE have been conducted on either Chinese or European populations. In the present study, we used a Thai GWAS as a test case to evaluate the impact of training data when applying the PRS method on a population for which exactly matched ancestry data are not available.

PATIENTS AND METHODS

Ethics approval. This study was approved by the respective institutional review boards associated with each author, including the ethics committee of the University of Hong Kong, Hospital Authority Hong Kong West Cluster (UW 07-119), the Affiliated Hospital of Jining Medical University (2020C008), and the Faculty of Medicine, Chulalongkorn University (COA no.923/2017).

Overview of SLE GWAS data sets. GWAS data on European populations were retrieved from previous studies involving a total of 4,576 cases and 8,039 controls (7,13,14). GWAS data on Chinese populations were retrieved from our previous studies derived from Hong Kong, Guangzhou, Central China, and Jining populations (7,15), comprising 4,734 cases and 9,425 controls (7,15). The Thai GWAS was obtained from a recent study (9) and was reanalyzed to be consistent with the processes of imputation and quality control for the European and Chinese GWAS (7), resulting in a total of 835 cases and 2,995 controls. Sample information for each cohort is summarized in Supplementary Table 1, on the *Arthritis & Rheumatology* website at https://onlinelibrary.wiley.com/doi/10.1002/art.42021.

Principal components analysis (PCA) plots for the Hong Kong, Guangzhou, Central China, and Jining GWAS and for Europe GWAS 1–3 have been published by us previously (7,15). PCA plots to compare the population substructure between cases and controls in the Thai GWAS and combined analysis of samples from different cohorts are shown in Supplementary Figures 1 and 2, respectively (https://onlinelibrary.wiley.com/doi/10.1002/art.42021).

Quality control, imputation, and association analysis of Thai GWAS. Strands of variants in the Thai GWAS were aligned to the references of the 1,000 Genomes Project Phase 3 panel using Genotype Harmonizer (16). Variants that had a genotype call rate of <90%, had a minor allele frequency (MAF) of <0.5%, and were in violation of Hardy–Weinberg equilibrium ($P < 1.00 \times 10^{-4}$) were removed. Samples were excluded if they had a genotype-missing rate of ≥5%, an estimated identity-by-descent value of >12.5% with respect to another sample in the cohort, or an inbreeding coefficient with an absolute value of >0.05. PCA was performed using Plink, version 1.90 (17). After prephasing by ShapeIt (18), individual-level genotype data were imputed to the density of the 1,000 Genomes Project Phase 3 reference using Impute2 (19). SNPTest (20) was used for association testing, based on an additive model. The top 8 principal components, as determined by their prominent contribution to eigenvalues, using a cutoff at the point the effect levels off (based on the scree plot method) (Supplementary Figure 3, on the *Arthritis & Rheumatology* website at https://onlinelibrary.wiley.com/doi/10.1002/art.42021), were adjusted for in the association analyses.

Meta-analyses of SLE GWAS. The "Chinese GWAS" refers to the meta-analysis of GWAS data from Hong Kong, Guangzhou, Central China, and Jining cohorts. The "Asian GWAS" refers to the meta-analysis of the data from the Chinese GWAS and the Thai GWAS. Trans-ancestral meta-analysis was conducted using data from the European, the Chinese, and the Thai GWAS. We first performed the meta-analyses based on a fixed-effects model, weighted by the inverse of variance (21). Considering potential heterogeneous effects between ancestral groups for certain associated loci, the DerSimonian-Laird random-effects model was further applied, using Metal (21). In

addition, a modified random-effects model (RE2C), which has better power to detect associations when there are heterogeneous effects (22), was carried out for the trans-ancestral meta-analysis.

Fine-mapping analysis of newly identified SLE-associated loci. Paintor, version 3.0 (23), was used to estimate the posterior probability (PP) of causality for each variant at a given locus, which is a Bayesian approach that leverages differences in linkage disequilibrium (LD) patterns from different populations. Variants with a MAF of <1% were filtered out. For ancestry-shared loci, we performed Paintor analysis using results from the Asian meta-analysis as well as the European meta-analysis. The LD information for Asian and European populations was calculated using the control samples from the Hong Kong cohort and the Europe GWAS 2 cohort, respectively. For the Asian-specific loci, we performed Paintor analysis using the Chinese meta-analysis results and the Thai GWAS. The LD information for Chinese and Thai populations was computed using the control samples from the Hong Kong GWAS and the Thai GWAS, respectively.

Previous studies have shown that SLE-associated loci were significantly enriched in regions with H3K4me1 and H3K27ac modifications (which are associated with active enhancers) (7). To further narrow the list of putative causal variants, we fine-mapped the associated loci using public epigenomic data (24) on H3K4me1 and H3K27ac modifications in immune-related cells, including peripheral blood mononuclear cells (PBMCs), primary monocytes, and T and B lymphocytes. In addition, the epigenomic profile in a lung fibroblast cell line (IMR-90) was included as a baseline control. To identify target genes in the associated loci, information on expression quantitative trait loci (eQTL) in whole blood was downloaded from the eQTLGen consortium (25), which was derived from 31,684 individuals mainly of European origin. Specific immune cell–derived eQTL data were obtained from the Biobank Japan Project (26). Colocalization between SLE association signals and eQTL signals was analyzed with the R package coloc (27), which estimates the posterior probabilities of 5 configurations: no association in either group (PP0), disease association only (PP1), eQTL only (PP2), associations with both disease and expression but by different causal signals (PP3), and association with both disease and eQTL and by the same signals (PP4).

RNA-Seq data analysis. To examine whether genes of interest were differentially expressed between SLE cases and controls, RNA-Seq data derived from 62 SLE cases and 79 healthy controls of East Asian ancestry were retrieved from the ImmuNexUT project (28). Read count data were downloaded from the National Bioscience Database Center (accession ID E-GEAD-397). DESeq2 (29) was performed to examine differential gene expression between SLE cases and healthy controls; sex, age, and study phase were used as covariates. Using the Benjamini-Hochberg method (30), *P* values were adjusted for multiple testing by the number of expressed genes with a non-zero sum of read counts (30).

Calculation of polygenic risk scores. As most GWAS on SLE to date have been conducted on either Chinese or European populations, choice of the training data on the performance of PRS for individuals without ancestry-matched association data becomes a relevant question. The Thai GWAS was used as a test case for the performance of PRS trained by different data sets using lassosum (31), based on HapMap3 data on single-nucleotide polymorphisms (SNPs) from the Chinese GWAS, the European GWAS, and the meta-analysis of the Chinese and European GWAS. The performance of these predictors was evaluated by the area under the receiver operating characteristic curve (AUC). The R package pROC (32) was used to estimate the optimal PRS cutoff for classification as cases versus controls.

Data availability. Genome-wide association summary statistics on the Chinese populations can be accessed through the GWAS Catalog (GCST90011866) and https://drive.google.com/file/d/1OHvuLEBWgmuB-5UH0ReQ72qtDmRBHAoi/view. The data on Thai populations is publicly available at https://1drv.ms/u/s!AibDDBT3YJysgfxDznmEJthYleOKVQ?e=YySlEf. The data on the European populations can be downloaded through the GWAS Catalog (GCST003156).

RESULTS

Novel SLE susceptibility loci. Manhattan plots of the genetic associations with SLE identified in the European, Chinese, and Thai populations are shown in Supplementary Figure 4 (https://onlinelibrary.wiley.com/doi/10.1002/art.42021). We performed trans-ancestral meta-analysis of the data from the 3 ancestral groups, comprising a total of 10,145 SLE cases and 20,459 controls. Six novel SLE susceptibility loci surpassing the genome-wide significance threshold were identified (Table 1 and Supplementary Figure 5 [https://onlinelibrary.wiley.com/doi/10.1002/art.42021]), including rs113333331 (*IFNLR1* [$P = 4.32 \times 10^{-8}$]), rs6586391 (*TARBP1* [$P = 4.13 \times 10^{-8}$]), rs10807602 (*ATXN1* [$P = 1.99 \times 10^{-8}$]), rs10795956 (*CAMK1D* [$P = 2.87 \times 10^{-8}$]), rs428073 (*TAOK3* [$P = 2.52 \times 10^{-8}$]), and rs9934578 (*CHD9* [$P = 4.86 \times 10^{-8}$]). In addition, we carried out the meta-analyses using the DerSimonian-Laird and RE2C random-effects models (21,22). While there was no evidence of heterogeneity for 5 of the 6 loci, a heterogeneous effect was suggested for the association of rs6586391 with SLE ($\tau^2 = 2.71 \times 10^{-3}$) (Supplementary Table 2, https://onlinelibrary.wiley.com/doi/10.1002/art.42021). For this locus, a combined odds ratio (OR) estimate was slightly increased to 1.16, and the association *P* values were 3.28×10^{-6} from the conservative DerSimonian-Laird model and 3.36×10^{-8} for RE2C, an algorithm designed to increase power for detecting

Table 1. Summary statistics on newly identified SLE-associated loci*

	Loci found by trans-ancestral meta-analysis						Loci found by Asian-specific meta-analysis			
	rs113333331	rs6586391	rs10807602	rs10795956	rs428073	rs9934578	rs117821148	rs780669†	rs11235667	rs76596471
Chromosome	1	1	6	10	12	16	8	10	11	12
Position (hg19)	24516387	234634203	16968788	12488136	118682751	53129034	78108225	73112241	72863697	112412518
Allele A	TA	T	T	G	C	T	C	C	A	T
Allele B	T	C	C	A	T	C	T	T	G	C
Gene context	*IFNLR1*	*TARBP1*	*ATXN1*, *RP3-486B10.1*	*CAMK1D*	*TAOK3*	*CHD9*	*PEX2*	*SLC29A3*	*FCHSD2*	*TMEM116*
Annotation	Upstream	Intergenic	Intergenic	Intronic	Missense	Intronic	Intergenic	Intronic	Intergenic	Intronic
Asian GWAS (5,569 cases, 12,420 controls)										
Frequency of allele B	0.25	0.06	0.63	0.30	0.74	0.83	0.038	0.652	0.099	0.044
Odds ratio	1.11	1.25	1.10	1.13	1.14	1.18	1.46	1.16	0.76	1.45
Standard error	0.03	0.05	0.03	0.03	0.03	0.04	0.07	0.03	0.05	0.05
P	5.46×10^{-4}	4.81×10^{-6}	3.47×10^{-4}	9.89×10^{-7}	2.56×10^{-6}	5.97×10^{-5}	4.87×10^{-8}	4.83×10^{-9}	9.69×10^{-10}	6.60×10^{-12}
European GWAS (4,576 cases, 8,039 controls)										
Frequency of allele B	0.13	0.50	0.64	0.35	0.70	0.77	–	0.892	–	–
Odds ratio	1.19	1.10	1.14	1.09	1.10	1.13	–	1.04	–	–
Standard error	0.04	0.03	0.03	0.03	0.03	0.03	–	0.05	–	–
P	1.06×10^{-5}	3.92×10^{-4}	8.29×10^{-6}	4.49×10^{-3}	1.81×10^{-3}	1.97×10^{-4}	–	4.15×10^{-1}	–	–
Trans-ancestry meta-analysis (10,145 cases, 20,459 controls)										
Odds ratio	1.13	1.13	1.11	1.11	1.12	1.15	–	1.13	–	–
Standard error	0.02	0.02	0.02	0.02	0.02	0.03	–	0.02	–	–
P	4.32×10^{-8}	4.13×10^{-8}	1.99×10^{-8}	2.87×10^{-8}	2.52×10^{-8}	4.86×10^{-8}	–	3.86×10^{-8}	–	–

* Odds ratios are in relation to the B allele (allele B would be the risk allele when the odds ratio is >1). Details of the results for each data set are summarized in Supplementary Tables 3 and 4, and forest plots for each variant are shown in Supplementary Figures 5 and 6 (on the *Arthritis & Rheumatology* website at https://onlinelibrary.wiley.com/doi/10.1002/art.42021). GWAS = genome-wide association study.

† This locus was found to be significantly associated with systemic lupus erythematosus (SLE) in Asian populations but not in European populations, with significant heterogeneity between the 2 ancestral groups as assessed by Cochran's Q test ($P = 0.03$). Significant heterogeneity between the 2 ancestral groups was not found for any of the other loci.

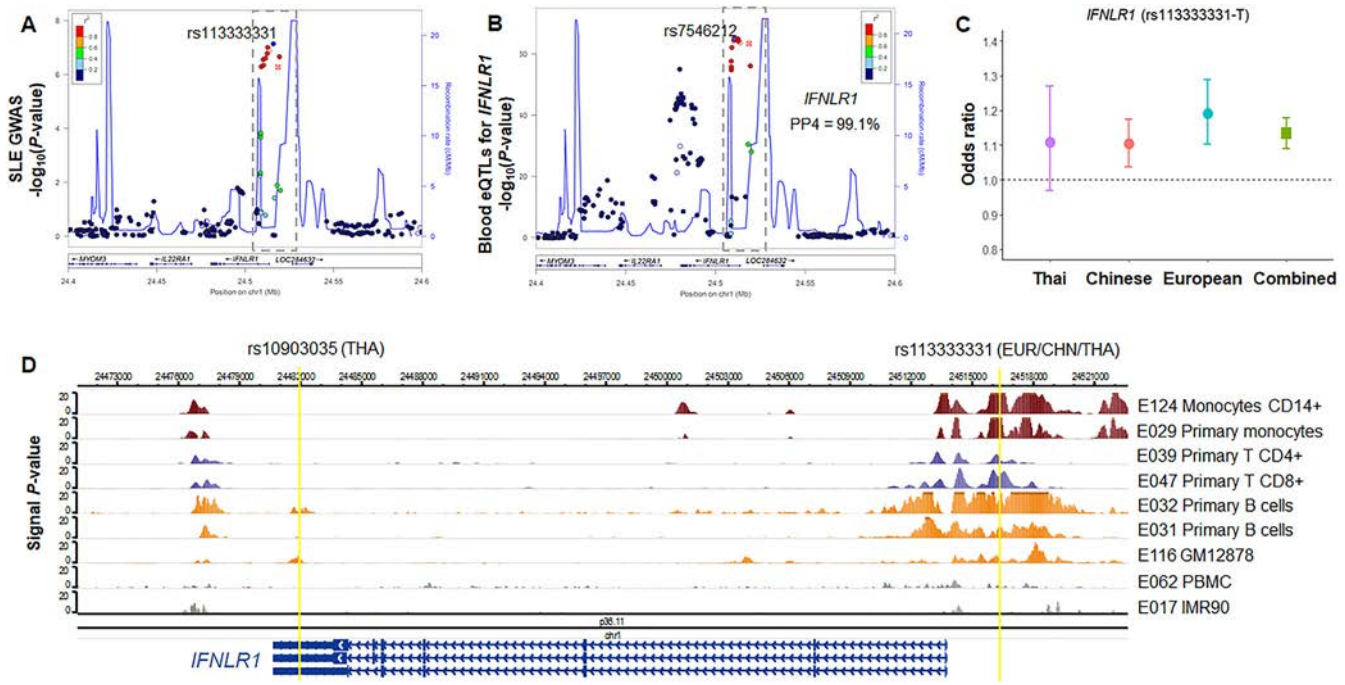

Figure 1. Fine-mapping analyses for systemic lupus erythematosus (SLE) association in the *IFNLR1* locus. **A,** SLE association profiles from the trans-ancestry meta-analysis. **B,** Colocalization of SLE genome-wide association study (GWAS) signals with blood expression quantitative trait loci (eQTLs) for *IFNLR1*. **C,** Forest plots of association results for the ancestry-shared variant. Bars show the 95% confidence interval. **D,** Epigenomic profiles for H3K4me1 modification in the *IFNLR1* locus across immune-related cells, including primary monocytes, subtypes of T and B cells, peripheral blood mononuclear cells (PBMCs), and the lung fibroblast cell line IMR-90. PP4 = posterior probability 4 (association with both disease and eQTL and by the same signals). THA = Thai population; EUR = European population; CHN = Chinese population.

association when there is evidence of heterogeneity among different populations.

An Asian-specific meta-analysis of the data from Chinese and Thai populations was also conducted, totaling 5,569 cases and 12,420 controls. Four novel SLE susceptibility loci reached genome-wide significance (Table 1 and Supplementary Figure 6 [https://onlinelibrary.wiley.com/doi/10.1002/art.42021]), 3 of which were monomorphic in European populations. These variants showed relatively large effect size on SLE in Asians (OR >1.30). Population specificity and relatively low MAF might explain why these loci were not identified in previous studies. The strongest signal was at rs117821148 (MAF 0.038; OR 1.46, $P = 4.87 \times 10^{-8}$), located in an intergenic region near *PEX2*. Another signal was at rs76596471 (MAF 0.044; OR 1.45, $P = 6.60 \times 10^{-12}$), an intronic SNP in *TMEM116*. Epigenetic data suggested that this region is highly active in T lymphocytes (Supplementary Figure 7 [https://onlinelibrary.wiley.com/doi/10.1002/art.42021]). Another signal, rs11235667 (MAF 0.099; OR 0.76, $P = 9.69 \times 10^{-10}$), was located upstream of *FCHSD2*, whose association with SLE was reported previously in Koreans (33). This locus was also found to be associated with Crohn's disease in the Korean population (34) but, interestingly, in an opposite direction from the association we found with SLE.

Association of *IFNLR1* locus links type III interferon (IFN) signaling to SLE. We performed fine-mapping analyses for each newly identified locus using Paintor, which makes use of LD information from the ancestral groups under study. The trans-ancestral lead variant, rs113333331, achieved the highest posterior probability of causality in this locus (PP 0.30) (Figures 1A and C). Through comparing the association profiles in different ancestral groups, we identified another association signal in the Thai GWAS (rs10903035 [$P = 1.70 \times 10^{-4}$]) (Supplementary Figures 8A–C [https://onlinelibrary.wiley.com/doi/10.1002/art.42021]), which was independent of rs113333331 and appeared to be Thai specific (P adjusted for the effect of rs113333331 = 4.51×10^{-4}, $r^2 = 0.003$, $D' = 0.11$ with rs113333331 in the Thai population).

Epigenomic profiling by H3K4me1, a marker for enhancers, showed that rs113333331, located upstream of *IFNLR1*, was in a highly active region across various immune cells, including primary monocytes and T and B lymphocytes (Figure 1D). SNP rs10903035, the Thai-specific variant, is located in the 3′-untranslated region of *IFNLR1*, which overlaps with the H3K4me1 modification in primary B cells. SNP rs113333331, which is an indel, is in intermediate LD with a psoriasis-associated SNP (rs4649203 [$r^2 = 0.40$ in Europeans]) (35) and in high LD with rs7546212 ($r^2 = 0.94$ in Europeans), whose risk allele correlates with increased expression of *IFNLR1* in whole blood ($P = 8.87 \times 10^{-66}$) (25). Colocalization analysis indicated a shared causal effect between the GWAS signals and the eQTLs for *IFNLR1* (PP4 99.1%) (Figure 1B), suggesting that

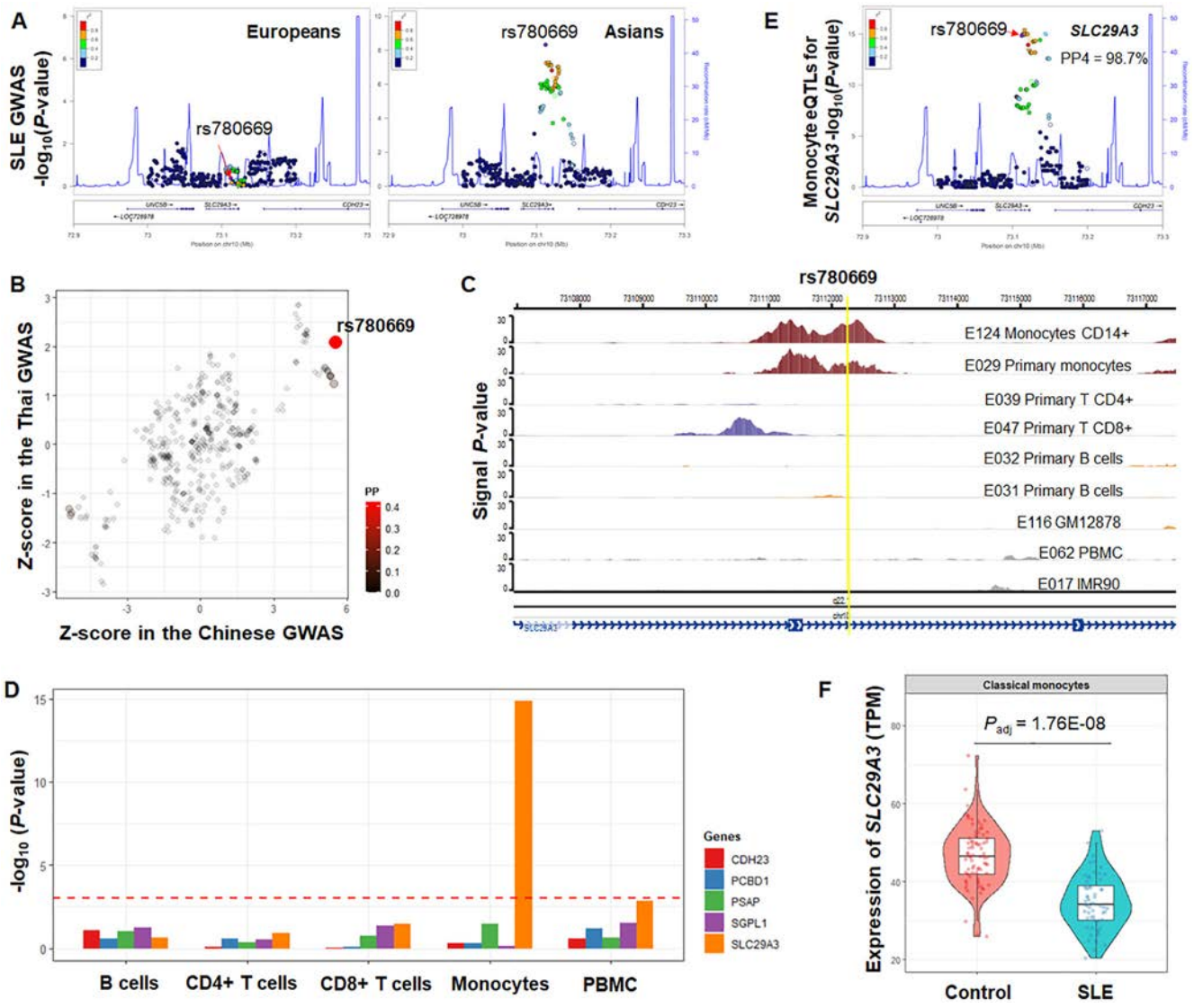

Figure 2. Fine-mapping analyses for SLE association in the *SLC29A3* locus. **A,** SLE association profiles of the *SLC29A3* locus in the European GWAS and the Asian GWAS. **B,** Comparison of association Z score (per-allele effect size divided by standard error) for each variant estimated in the Chinese and Thai GWAS populations. Dot color and size indicate posterior probability of causality estimated with Paintor. **C,** Demonstration that the lead single-nucleotide polymorphism (SNP) coincided with the peaks for H3K4me1 modification in primary monocytes but not in other cells. **D,** Association of the lead SNP with expression of its surrounding genes across various immune cells. **E,** Colocalization of SLE association signals in Asians with the monocyte-derived eQTL signals for *SLC29A3* (PP4 98.7%). **F,** Comparison of *SLC29A3* expression in classic monocytes from SLE cases and healthy controls. The upper and lower borders of the boxes represent the first and third quartiles, respectively. Horizontal lines within the boxes show the median. TPM = transcripts per million; P_{adj} = adjusted *P* (see Figure 1 for other definitions). Color figure can be viewed in the online issue, which is available at http://onlinelibrary.wiley.com/doi/10.1002/art.42021/abstract.

increased expression of *IFNLR1* is likely the mechanism underlying the SLE association of this locus. *IFNLR1* encodes IFNλ receptor 1, which binds IFNλ cytokines with high affinity and has an important role in type III IFN signaling (36).

Although the Thai-specific association variant (rs10903035) is also an eQTL for *IFNLR1* ($P = 3.11 \times 10^{-27}$) (25), the GWAS signals did not seem to colocalize with the eQTL signals for *IFNLR1*, with a low posterior probability (PP4 9.7%) (Supplementary Figure 8D). This Thai-specific association requires further validation in future studies.

Association of *SLC29A3* found in Asians may contribute to SLE through affecting lysosome function in monocyte/macrophages. Through comparing the results with those in the European GWAS, we found that the *SLC29A3* locus (rs780669) was associated with SLE in Asian populations but not in Europeans ($P = 4.83 \times 10^{-9}$ in the Asian GWAS meta-analysis, $P = 0.415$ in the meta-analysis of European GWAS) (Table 1), with significant heterogeneity between the 2 ancestral groups as detected by Cochran's Q test ($P = 0.03$) (Figure 2A). Analysis of the GWAS from Chinese and Thai populations by

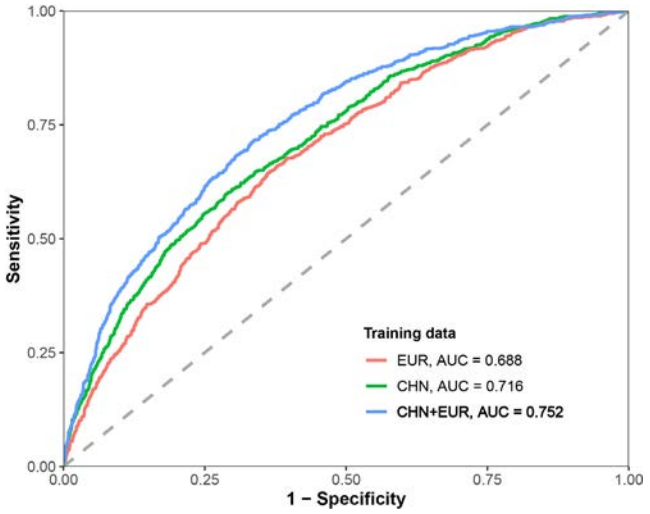

Figure 3. Evaluation of polygenic risk scores (PRS) for SLE in the Thai GWAS cohort. PRS were trained using data from the European and Chinese GWAS, as well as the association results from the meta-analysis of the 2 ancestral groups. PRS performance was evaluated using the area under the receiver operating characteristic curve (AUC). See Figure 1 for other definitions. Color figure can be viewed in the online issue, which is available at http://onlinelibrary.wiley.com/doi/10.1002/art.42021/abstract.

Paintor indicated that SNP rs780669 was a likely causal variant (PP 0.41) (Figure 2B). This variant was in a region with prominent H3K4me1 modification in primary monocytes but not T and B lymphocytes (Figure 2C). A similar pattern was also observed based on the profiles of H3K27ac modifications (Supplementary Figure 9, on the *Arthritis & Rheumatology* website at https://onlinelibrary.wiley.com/doi/10.1002/art.42021), suggesting a cell type–specific regulation mechanism.

We next investigated potential target(s) for this association by using immune cell–derived eQTL data (26) and examined correlations of rs780669 with expression levels of its surrounding genes (±500 kbp). The risk allele for SLE, rs780669-T, was found to be significantly associated with decreased expression of *SLC29A3* in monocytes ($\beta = -0.985$, $P = 1.41 \times 10^{-15}$), with little evidence of association in other immune cells (Figure 2D). Colocalization analysis supported the notion of a shared casual effect between the disease association and the eQTL for *SLC29A3* (PP4 98.7%) (Figure 2E). These results suggest that reduced expression of *SLC29A3* in monocytes may be involved in the development of SLE.

To further test this hypothesis, we compared *SLC29A3* expression levels between SLE cases and controls of Asian ancestry. The relevant RNA-Seq data were downloaded from the ImmuNexUT project, which consists of subjects of East Asian origin. We found that expression of *SLC29A3* in classic monocytes was significantly lower among SLE cases than among healthy controls (adjusted $P = 1.76 \times 10^{-8}$) (Figure 2F). Taken together, these findings strongly suggest that reduced expression of *SLC29A3* in monocytes is the likely mechanism for this association. *SLC29A3* encodes a lysosomal nucleoside transporter that plays a vital role in macrophage homeostasis (37).

Effect of training data on the performance of PRS in the Thai population. We have recently shown that PRS perform better when trained on ancestry-matched data (7). However, considering that most SLE GWAS have been conducted using data from either East Asian or European populations, choice of the training data for populations without available ancestry-matched data becomes a relevant question. In this study, using a Thai cohort as a test case, we examined the performance of PRS trained by data from either Chinese or European populations or by meta-analysis results using data from the 2 ancestral groups.

PRS trained by data from the Chinese populations (AUC 0.716) outperformed the model trained by data from the European GWAS (AUC 0.688) (Figure 3), which might be explained by higher genetic similarity between the Thai and Chinese populations, as the sample sizes for the 2 training data sets were comparable. PRS trained by meta-analysis results from Chinese and European GWAS achieved the best performance (AUC 0.752), which resulted in up to 71.5% sensitivity and 66.4% specificity in predicting disease status in the Thai data set, highlighting the benefit of both increased sample size and ancestry-shared effects in risk prediction.

DISCUSSION

The results of this study demonstrate the value of multi-ancestral GWAS in mapping novel disease genes, especially for the ancestry-specific genetic components that have remained mostly elusive after more than a decade of extensive effort in genome-wide association studies. Adding the Thai data to the available GWAS data sets allowed identification of 6 novel loci that are shared by Asians and Europeans. More importantly, meta-analysis of the Thai and Chinese GWAS data revealed 4 loci that are likely Asian specific, of which 3 are monomorphic in Europeans. They are also on the spectrum of lower MAF relative to previously reported associated variants, which explains why they can be detected only with increased sample size, especially in non-European populations.

Epigenomic and eQTL data, especially those derived from specific cell types, provide strong suggestions on association mechanisms for certain genetic loci. We showed that the ancestry-shared variant upstream of *IFNLR1* may contribute to SLE through increased expression of *IFNLR1*. *IFNLR1* encodes IFNλ receptor 1, which binds IFNλ with high affinity and recruits interleukin-10 receptor β, a partner receptor for IFNλ signaling (36). It has been shown that although type III IFNs share many features with type I IFNs, type III IFN signaling may play nonredundant roles in autoimmunity. Production of IFNλ is more abundant at mucosal sites in epithelial and myeloid cells in response to viral

infection. In mice with Toll-like receptor 7–induced lupus, IFNλ cytokines were increased, and *Ifnlr1* deficiency significantly reduced immune cell activation and organ damage, without affecting autoantibody production (38). Expression of *IFNLR1* was shown to be up-regulated in PBMCs from SLE patients (39). Serum levels of IFNλ were found to be elevated in SLE patients and positively correlated with lupus disease activity and anti–double-stranded DNA levels (40).

We found that the *SLC29A3* locus was associated with SLE in Asians but had little evidence of an association in Europeans. Fine-mapping analyses strongly suggest that this association with SLE may result from down-regulation of *SLC29A3* in monocytes. *SLC29A3* encodes a lysosomal transmembrane nucleoside transporter. Mice deficient in *SLC29A3* developed splenomegaly and defects in apoptotic cell clearance by macrophages (37). Impaired lysosomal function diminishes the ability of macrophages to degrade apoptotic debris–containing IgG immune complexes, prolonging the intracellular residency of nucleic acids (41). Accumulation of nucleoside in the lysosomes stimulates Toll-like receptors and promotes production of inflammatory cytokines (41,42). *SLC29A3* deficiency is known to cause H syndrome, which is a genodermatosis associated with autoinflammatory symptoms (43). Our present findings suggest that the aberrant genetic regulation of *SLC29A3* may be involved in SLE development through impairing lysosomal function in monocytes, especially in Asian populations.

We also identified a missense variant in *TAOK3* (the gene for tau kinase 3) as the top association signal in this locus. The risk allele (rs428073-T) substitutes the 47th amino acid of *TAOK3* from serine to asparagine (S47N), whose functional role remains unknown. S47 is located at the loop region between strands β2 and β3, and the substitution should not change the overall structure of the protein, despite being well conserved among orthologous proteins during evolutionary courses (Supplementary Figure 10, on the *Arthritis & Rheumatology* website at https://onlinelibrary.wiley.com/doi/10.1002/art.42021). Taok3 plays an important role in DNA damage–induced activation of the p38/MAPK14 stress-activated MAPK cascade. It enhances T cell receptor signaling by regulating its negative feedback by SH2 domain–containing phosphatase 1 (44), and *Taok3* deficiency in mice was found to cause defects in the development of marginal-zone B cells but not follicular B cells (45).

Another newly identified disease locus, rs6586391, is located upstream of AR (HIV-1) RNA binding protein 1 (*TARBP1*) and is a potential eQTL for the gene in whole blood ($P = 2.78 \times 10^{-40}$) (25). SNP rs9934578 is in the intronic region of *CHD9* and is a potential eQTL for this gene ($P = 1.63 \times 10^{-30}$). The functional mechanisms of other associations found in this study are not clear and require further investigation. We noted that the fine-mapping study could also be improved by using more functional annotations, such as cell state–specific regulatory elements inferred using Impact (46).

In addition, to evaluate the influence of ancestral differences on the predictive power of PRS, we used the Thai GWAS as a test case and showed that the PRS trained by the trans-ancestral meta-analysis results outperformed the model trained by either Chinese or European GWAS. These results highlight the value of increased sample size even if ancestry is not fully matched.

ACKNOWLEDGMENTS

We thank Professor Tim Vyse (King's College London, London, UK) and Professor Xuejun Zhang (Anhui Medical University, Anhui, China) for sharing SLE data.

AUTHOR CONTRIBUTIONS

All authors were involved in drafting the article or revising it critically for important intellectual content, and all authors approved the final version to be published. Dr. Yang had full access to all of the data in the study and takes responsibility for the integrity of the data and the accuracy of the data analysis.

Study conception and design. Wang, Yang.

Acquisition of data. Tangtanatakul, Lin, Qin, Hou, X. Zhang, Shao, Satproedprai, Mahasirimongkol, Pisitkun, Song, Lau, Y. Zhang, Hirankarn.

Analysis and interpretation of data. Wang, Wei, Zheng, Yao, Qian, Qin, Yang.

REFERENCES

1. Johnson AE, Gordon C, Palmer RG, Bacon PA. The prevalence and incidence of systemic lupus erythematosus in Birmingham, England: relationship to ethnicity and country of birth. Arthritis Rheum 1995;38:551–8.
2. Danchenko N, Satia JA, Anthony MS. Epidemiology of systemic lupus erythematosus: a comparison of worldwide disease burden [review]. Lupus 2006;15:308–18.
3. Costenbader KH, Desai A, Alarcón GS, Hiraki LT, Shaykevich T, Brookhart MA, et al. Trends in the incidence, demographics, and outcomes of end-stage renal disease due to lupus nephritis in the US from 1995 to 2006. Arthritis Rheum 2011;63:1681–8.
4. Ballou S P, Khan MA, Kushner I. Clinical features of systemic lupus erythematosus: differences related to race and age of onset. Arthritis Rheum 1982;25:55–60.
5. Morris DL, Sheng Y, Zhang Y, Wang YF, Zhu Z, Tombleson P, et al. Genome-wide association meta-analysis in Chinese and European individuals identifies ten new loci associated with systemic lupus erythematosus. Nat Genet 2016;48:940–6.
6. Yin X, Kim K, Suetsugu H, Bang SY, Wen L, Koido M, et al. Meta-analysis of 208370 East Asians identifies 113 susceptibility loci for systemic lupus erythematosus. Ann Rheum Dis 2021;80:632–40.
7. Wang YF, Zhang Y, Lin Z, Zhang H, Wang TY, Cao Y, et al. Identification of 38 novel loci for systemic lupus erythematosus and genetic heterogeneity between ancestral groups. Nat Commun 2021;12:772.
8. Wang YF, Zhang Y, Zhu Z, Wang TY, Morris DL, Shen JJ, et al. Identification of ST3AGL4, MFHAS1, CSNK2A2 and CD226 as loci associated with systemic lupus erythematosus (SLE) and evaluation of SLE genetics in drug repositioning. Ann Rheum Dis 2018;77:1078–84.
9. Tangtanatakul P, Thumarat C, Satproedpai N, Kunhapan P, Chaiyasung T, Klinchanhom S, et al. Meta-analysis of genome-wide association study identifies FBN2 as a novel locus associated with systemic lupus erythematosus in Thai population. Arthritis Res Ther 2020;22:185.

10. Wojcik GL, Graff M, Nishimura KK, Tao R, Haessler J, Gignoux CR, et al. Genetic analyses of diverse populations improves discovery for complex traits. Nature 2019:570:514–8.
11. Martin AR, Kanai M, Kamatani Y, Okada Y, Neale BM, Daly MJ. Clinical use of current polygenic risk scores may exacerbate health disparities [review]. Nat Genet 2019:51:584–91.
12. Lam M, Chen CY, Li Z, Martin AR, Bryois J, Ma X, et al. Comparative genetic architectures of schizophrenia in East Asian and European populations. Nat Genet 2019;51:1670–8.
13. Bentham J, Morris DL, Graham DS, Pinder CL, Tombleson P, Behrens TW, et al. Genetic association analyses implicate aberrant regulation of innate and adaptive immunity genes in the pathogenesis of systemic lupus erythematosus. Nat Genet 2015;47:1457–64.
14. Julià A, López-Longo FJ, Venegas JJ, Bonàs-Guarch S, Olivé A, Andreu JL, et al. Genome-wide association study meta-analysis identifies five new loci for systemic lupus erythematosus. Arthritis Res Ther 2018;20:100.
15. Song Q, Lei Y, Shao L, Li W, Kong Q, Lin Z, et al. Genome-wide association study on Northern Chinese identifies KLF2, DOT1L and STAB2 associated with systemic lupus erythematosus. Rheumatology 2021; 60:4407–17.
16. Deelen P, Bonder MJ, van der Velde KJ, Westra HJ, Winder E, Hendriksen D, et al. Genotype harmonizer: automatic strand alignment and format conversion for genotype data integration. BMC Res Notes 2014;7:901.
17. Chang CC, Chow CC, Tellier LC, Vattikuti S, Purcell SM, Lee JJ. Second-generation PLINK: rising to the challenge of larger and richer datasets. Gigascience 2015;4:7.
18. Delaneau O, Marchini J, on behalf of the 1000 Genomes Project. Integrating sequence and array data to create an improved 1000 Genomes Project haplotype reference panel. Nat Commun 2014;5:3934.
19. Howie B, Fuchsberger C, Stephens M, Marchini J, Abecasis GR. Fast and accurate genotype imputation in genome-wide association studies through pre-phasing. Nat Genet 2012;44:955–9.
20. Marchini J, Howie B, Myers S, McVean G, Donnelly P. A new multipoint method for genome-wide association studies by imputation of genotypes. Nat Genet 2007;39, 906–13.
21. Willer CJ, Li Y, Abecasis GR. METAL: fast and efficient meta-analysis of genomewide association scans. Bioinformatics 2010;26: 2190–1.
22. Lee CH, Eskin E, Han B. Increasing the power of meta-analysis of genome-wide association studies to detect heterogeneous effects. Bioinformatics 2017;33:i379–88.
23. Kichaev G, Pasaniuc B. Leveraging functional-annotation data in trans-ethnic fine-mapping studies. Am J Hum Genet 2015;97: 260–71.
24. Roadmap Epigenomics Consortium. Integrative analysis of 111 reference human epigenomes. Nature 2015:518:317–30.
25. Võsa U, Westra H, Bonder MJ, Deelen P, Zeng B, Kirsten H, et al. Unraveling the polygenic architecture of complex traits using blood eQTL metaanalysis [preprint]. bioRxiv 2018. doi:10.1101/447367.
26. Ishigaki K, Kochi Y, Suzuki A, Tsuchida Y, Tsuchiya H, Somitomo S, et al. Polygenic burdens on cell-specific pathways underlie the risk of rheumatoid arthritis. Nat Genet 2017;49:1120–5.
27. Giambartolomei C, Vukcevic D, Schadt EE, Franke L, Hingorani AD, Wallace C, et al. Bayesian test for colocalisation between pairs of genetic association studies using summary statistics. PLoS Genet 2014;10:e1004383.
28. Ota M, Nagafuchi Y, Hatano H, Ishigaki K, Terao C, Takeshima Y, et al. Dynamic landscape of immune cell-specific gene regulation in immune-mediated diseases. Cell 2021;184:3006–21.
29. Love MI, Huber W, Anders S. Moderated estimation of fold change and dispersion for RNA-seq data with DESeq2. Genome Biol 2014; 15:550.
30. Benjamini Y, Hochberg Y. Controlling the false discovery rate: a practical and powerful approach to multiple testing. J R Stat Soc Series B Stat Methodol 1995:57;289–300.
31. Mak TS, Porsch RM, Choi SW, Zhou X, Sham PC. Polygenic scores via penalized regression on summary statistics. Genet Epidemiol 2017;41:469–80.
32. Robin X, Turck N, Hainard A, Tiberti N, Lisacek F, Sanchez JC, et al. pROC: an open-source package for R and S+ to analyze and compare ROC curves. BMC Bioinformatics 2011;12:77.
33. Lessard CJ, Sajuthi S, Zhao J, Kim K, Ico JA, Li H. et al. Identification of a systemic lupus erythematosus risk locus spanning ATG16L2, FCHSD2, and P2RY2 in Koreans. Arthritis Rheumatol 2016;68:1197–209.
34. Yang SK, Hong M, Zhao W, Jung Y, Baek J, Tayebi N, et al. Genome-wide association study of Crohn's disease in Koreans revealed three new susceptibility loci and common attributes of genetic susceptibility across ethnic populations. Gut 2014;63:80–7.
35. Genetic Analysis of Psoriasis Consortium, the Wellcome Trust Case Control Consortium 2. A genome-wide association study identifies new psoriasis susceptibility loci and an interaction between HLA-C and ERAP1. Nat Genet 2010;42:985–90.
36. Lazear HM, Nice TJ, Diamond MS. Interferon-λ: immune functions at barrier surfaces and beyond [review]. Immunity 2015;43:15–28.
37. Hsu CL, et al. Equilibrative nucleoside transporter 3 deficiency perturbs lysosome function and macrophage homeostasis. Science 2012;335:89–92.
38. Goel RR, Wang X, O'Neil LJ, Nakabo S, Hasneen K, Gupta S, et al. Interferon λ promotes immune dysregulation and tissue inflammation in TLR7-induced lupus. Proc Natl Acad Sci U S A 2020;117:5409–19.
39. Cheng YY, Sheng YJ, Chang Y, Lin Y, Zhu ZW, Wen LL, et al. Increased expression of IL-28RA mRNA in peripheral blood mononuclear cells from patients with systemic lupus erythematosus. Clin Rheumatol 2015;34:1807–11.
40. Wu Q, Yang Q, Lourenco E, Sun H, Zhang Y. Interferon-λ1 induces peripheral blood mononuclear cell-derived chemokines secretion in patients with systemic lupus erythematosus: its correlation with disease activity. Arthritis Res Ther 2011;13:R88.
41. Monteith AJ, Kang S, Scott E, Hillman K, Rajfur Z, Jacobson K et al. Defects in lysosomal maturation facilitate the activation of innate sensors in systemic lupus erythematosus. Proc Natl Acad Sci U S A 2016;113:E2142–51.
42. Shibata T, et al. Nucleosides drive histiocytosis in SLC29A3 disorders by activating TLR7 [preprint]. bioRxiv 2019. doi:10.1101/ 2019.12.16.877357.
43. Molho-Pessach V, Agha Z, Aamar S, Glaser B, Doviner V, Hiller N, et al. The H syndrome: a genodermatosis characterized by indurated, hyperpigmented, and hypertrichotic skin with systemic manifestations. J Am Acad Dermatol 2008;59:79–85.
44. Ormonde JV, Li Z, Stegen C, Madrenas J. TAOK3 regulates canonical TCR signaling by preventing early SHP-1-mediated inactivation of LCK. J Immunol 2018;201:3431–42.
45. Hammad H, Vanderkerken M, Pouliot P, Deswarte K, Toussaint W, Vergote K, et al. Transitional B cells commit to marginal zone B cell fate by Taok3-mediated surface expression of ADAM10. Nat Immunol 2017;18:313–20.
46. Amariuta T, Luo Y, Gazal S, Davenport EE, van de Geijin B, Ishigaki K, et al. IMPACT: genomic annotation of cell-state-specific regulatory elements inferred from the epigenome of bound transcription factors. Am J Hum Genet 2019;104:879–95.

Arthritis & Rheumatology
Vol. 74, No. 5, May 2022, pp 849–859
DOI 10.1002/art.42054

American College of Rheumatology
Empowering Rheumatology Professionals

Diastolic Dysfunction in Systemic Sclerosis: Risk Factors and Impact on Mortality

Alicia M. Hinze,[1] Jamie Perin,[2] Adrianne Woods,[3] Laura K. Hummers,[3] Fredrick M. Wigley,[3] Monica Mukherjee,[3] and Ami A. Shah[3]

Objective. To determine the independent risk factors for diastolic dysfunction (DD) in patients with systemic sclerosis (SSc) and to evaluate the impact of DD on mortality.

Methods. SSc patients enrolled in the Johns Hopkins Scleroderma Center Cohort between November 1, 2006 and November 1, 2017 with ≥1 analyzable 2-dimensional (2-D) echocardiogram in our system were included (n = 806). DD risk factors and SSc disease characteristics were prospectively obtained, and the presence or absence of DD was determined using the most recent 2-D echocardiogram. Logistic regression models examined associations between clinical risk factors and DD, and Cox proportional hazards models were used to assess survival.

Results. DD was present in 18.6% of participants. The majority of participants were female (84%) with a median age of 58.4 years (interquartile range 48.8–68.1). Older age (odds ratio [OR] 1.12 [95% confidence interval (95% CI) 1.09–1.15], $P < 0.001$), coronary artery disease (OR 3.69 [95% CI 1.52–8.97], $P = 0.004$), obesity (OR 4.74 [95% CI 2.57–8.74], $P < 0.001$), longer SSc disease duration (OR 1.04 [95% CI 1.01–1.06], $P = 0.004$), diffusing capacity for carbon monoxide ≤60% of predicted (OR 2.41 [95% CI 1.40–4.16], $P = 0.002$), and history of scleroderma renal crisis (OR 3.18 [95% CI 1.12–9.07], $P = 0.031$) were all independently associated with an increased risk of DD. Anti–Scl-70 positivity (OR 0.49 [95% CI 0.26–0.93], $P = 0.03$) and severe gastrointestinal disease (OR 0.48 [95% CI 0.30–0.79], $P = 0.004$) were associated with a reduced risk of DD. The presence of DD was independently associated with an increase in the risk of mortality (hazard ratio 1.69 [95% CI 1.07–2.68], $P = 0.027$).

Conclusion. DD is independently associated with an increased risk of mortality in patients with SSc. Potentially modifiable risk factors, including coronary artery disease and obesity, should be addressed in patients with SSc to reduce mortality risk.

INTRODUCTION

Primary cardiac involvement in systemic sclerosis (SSc) accounts for one-third of SSc-related deaths and traditionally includes conduction blocks, arrhythmias, and non-ischemic cardiomyopathy (1,2). Recent studies show a prevalence of diastolic dysfunction (DD) ranging 18–62% in patients with SSc (3–6), compared with a prevalence of 1.4–38.1% in similarly aged community-dwelling adults without SSc (7,8). The higher prevalence of DD in SSc has been attributed to SSc myocardial involvement. However, the contributing risk factors across SSc and non-SSc conditions have been incompletely evaluated. Given the increased risk of mortality in SSc patients with DD (4,5,9), it is important to improve comprehensive identification of potentially modifiable risks.

DD is caused by progressive left ventricular (LV) stiffness leading to impaired compliance and is diagnosed using 2-dimensional (2-D) echocardiography. Over time, atrial enlargement, arrhythmia, and elevated LV filling pressures underlying the clinical syndrome of heart failure with preserved ejection

Supported by the NIH (awards T32-AR-048522 to Dr. Hinze, P30-AR-070254 to Dr. Perin, and R01-AR-073208 to Dr. Shah), the Chresanthe Staurulakis Memorial Discovery Fund, the Donald B. and Dorothy L. Stabler Foundation, the Johns Hopkins inHealth Precision Medicine Initiative, and the Scleroderma Research Foundation. Dr. Wigley's work was supported by a Martha McCrory Endowed Professorship. Dr. Mukherjee's work was supported by the Scleroderma Foundation and the Johns Hopkins Clinician Scientist Award.

[1]Alicia M. Hinze, MD, MHS: Mayo Clinic, Rochester, Minnesota; [2]Jamie Perin, PhD: Johns Hopkins Bloomberg School of Public Health, Baltimore, Maryland; [3]Adrianne Woods, BS, CCRP, Laura K. Hummers, MD, MSc, Fredrick M. Wigley, MD, Monica Mukherjee, MD, MPH, Ami A. Shah, MD, MHS: Johns Hopkins University, Baltimore, Maryland.

Drs. Shah and Mukherjee contributed equally to this work.

Author disclosures are available at https://onlinelibrary.wiley.com/action/downloadSupplement?doi=10.1002%2Fart.42054&file=art42054-sup-0001-Disclosureform.pdf.

Address correspondence to Ami A. Shah, MD, MHS, Johns Hopkins Scleroderma Center, 5200 Eastern Avenue, Mason F. Lord Building, Center Tower Suite 4100, Baltimore, MD 21224. Email: Ami.Shah@jhmi.edu.

Submitted for publication May 1, 2021; accepted in revised form December 16, 2021.

fraction can be observed. Risk factors for DD in the general population include older age, female sex, hypertension, coronary artery disease (CAD), diabetes mellitus (DM), obesity, chronic obstructive pulmonary disease (COPD), tobacco use, dyslipidemia, and chronic kidney disease (CKD) (7,10). In SSc-specific studies, longer disease duration (9,11) and the presence of pulmonary fibrosis (6) have been inconsistently associated with an increased risk of DD (5,12). A major limitation in these studies is the ascertainment of and adjustment for other traditional risk factors for DD, which requires a large cohort size (5,6,9). Additionally, the definition of DD has varied widely among studies and has not consistently applied echocardiographic guideline–based criteria, which further limits conclusions and generalizability of results.

In this study, we sought to overcome these limitations by prospectively ascertaining DD risk factors and SSc characteristics in a large, well-characterized SSc cohort. DD was rigorously defined using the most current guidelines from the American Society of Echocardiography (ASE)/European Society of Cardiovascular Imaging (ESCVI) (13). The primary goals of this study were to identify DD risk factors in SSc and to determine the independent impact of DD on mortality in SSc by controlling for other SSc specific risk factors and cardiovascular risk factors for mortality.

PATIENTS AND METHODS

Study population. All SSc patients enrolled in the Institutional Review Board–approved Johns Hopkins Scleroderma Center cohort who had ≥1 technically adequate 2-D echocardiogram performed within our institution between November 1, 2006 and November 1, 2017 were reviewed for inclusion.

All participants satisfied ≥1 of the following classification criteria for SSc: 1) 1980 or 2013 American College of Rheumatology criteria (14,15), 2) at least 3 of 5 features of CREST (calcinosis, Raynaud's phenomenon [RP], esophageal dysmotility, sclerodactyly, telangiectasias) syndrome, or 3) the combination of definite RP, abnormal nailfold capillaries, and SSc-specific antibodies (anticentromere, anti–topoisomerase I/Scl-70, or anti–RNA polymerase III).

Our center's standard practice includes obtaining an annual 2-D echocardiogram to screen for pulmonary hypertension (PH), regardless of clinical symptoms. The most recent 2-D echocardiogram for a participant was included if deemed technically adequate for diastology assessment. Two-dimensional echocardiograms were excluded for any of the following reasons: 1) they were performed in the setting of an acute myocardial infarction, shock, or while the patient was in the intensive care unit, 2) presence of moderate or severe aortic or mitral valvulopathy, 3) presence of moderate or severe mitral annular calcification which may underestimate tissue Doppler velocities, 4) presence of a moderate or large pericardial effusion, or 5) presence of a depressed LV ejection fraction of <50%. If the 2-D echocardiogram did not meet inclusion criteria or met exclusion criteria, the prior 2-D echocardiogram (if available) was assessed until the most recent 2-D echocardiogram meeting inclusion criteria was identified.

Study procedures and measurements. *Clinical procedures and measurements.* All demographic and clinical variables were collected prospectively for cohort participants during routine clinical appointments at ~6-month intervals. Patients were classified as having limited or diffuse cutaneous SSc by established criteria (16). Disease duration was defined as time from onset of the first SSc symptom, either RP or non-RP, to time of 2-D echocardiogram. Race was self-reported. Measurements of forced vital capacity (FVC) and diffusing capacity of the lung for carbon monoxide (DL_{CO}) from pulmonary function tests were standardized for sex and age (17,18). Organ involvement and clinical severity scores (19,20) are defined in the Supplementary Methods (available on the *Arthritis & Rheumatology* website at https://onlinelibrary.wiley.com/doi/10.1002/art.42054) and included maximum expression/severity between date of cohort enrollment and date of 2-D echocardiogram. Traditional DD risk factors (hypertension, CAD, DM, obesity, COPD, ever tobacco use, dyslipidemia, and CKD) were defined by established criteria and updated every 6 months (Supplementary Methods).

Autoantibodies were deemed positive if they were assessed as positive by clinical laboratory evaluation or if they were assessed as moderately or highly positive by laboratory-based immunoassay (EuroLine Systemic Sclerosis [Nucleoli] Profile; Euroimmun) (Supplementary Methods). Mortality data were obtained via medical record review, family notification of patient's death, and annual review of the US Social Security Death Index.

Two-dimensional echocardiogram procedures and measurements. DD classification and grade of severity were determined based on the 2016 ASE/ESCVI recommendations (13). Diastolic parameters, including the peak velocities of early and late filling waves, the E/A ratio, and the deceleration time of the mitral E-wave velocity, were obtained (13). Tissue Doppler mitral annular velocities of the septal and/or lateral annulus (e′ velocity) were obtained, and the ratio of early mitral inflow to early tissue Doppler e′ velocities was used to calculate the E/e′ velocity ratio, a noninvasive surrogate of LV end-diastolic filling pressures (13). Left atrial volumes (LAVs) were obtained utilizing the modified biplane method from the apical 4- and 2-chamber views and indexed by body surface area (LAVi) (21). If both the apical 4- and 2-chamber views were not available or did not have technically adequate quality, LAVs were determined based on a single view (13). Peak tricuspid regurgitant (TR) velocity was obtained and, using the modified Bernoulli equation, was used to calculate right ventricular systolic pressure (RVSP).

The diagnosis of DD was defined by the presence of ≥3 of the following abnormal cutoff values for the following 4 variables: septal

E′ velocity <7 cm/seconds, septal E/E′ ratio >15, LAVi >34 ml/m^2, and peak TR velocity >2.8 meters/second. Diastolic function was classified by how many of these 4 parameters were normal or abnormal: they were classified as normal if <50% were abnormal, classified as indeterminate if 50% were abnormal, and classified as DD if >50% were abnormal (13). In the event that 1 of the 4 variables were missing, DD classification was based on 3 instead of 4 parameters, as per recommendations (13). Diastology grade in those with DD was determined by evaluating the ratio of early and late transmitral velocities and deceleration time (13).

Statistical analysis. Differences in demographics, cardiovascular and pulmonary disease, SSc characteristics, and medications were assessed across normal, indeterminate, and DD categories using chi-square tests of proportions for categorical data, analysis of variance for parametric data, and Kruskal-Wallis tests for nonparametric data. These analyses were completed in Stata/IC, version 14.2.

Univariable and multivariable logistic regression analyses of DD versus normal diastolic function were performed to examine associations between DD and SSc clinical features. We decided a priori to include all known DD risk factors (age, sex, hypertension, CAD, obesity, dyslipidemia, CKD, DM, COPD, and ever tobacco use) in the multivariable models. The multivariable models were constructed based on significant variables in unadjusted or adjusted univariable analyses in which the 95% confidence intervals (95% CIs) of the odds ratios (ORs) did not cross 1.00 or in which the *P* value was lower than 0.10 (22). An ordinal polytomous logistic regression analysis framing indeterminate diastolic function as a step between normal diastolic function and DD, yielding 3 levels of diastolic function with increasing dysfunction (normal→indeterminate→dysfunction), was also performed.

Cox proportional hazards models compared mortality in patients with DD to that in patients with normal diastolic function (23). We adjusted this analysis for clinical features identified as being related to DD in the literature or in our above analyses, as well as clinical characteristics with known associations with mortality in SSc. Unadjusted and age-adjusted Kaplan-Meier curves evaluated the association between mortality and diastology groups. The time scale was years from 2-D echocardiogram, and patients were censored either at 1 year from last clinic visit date or at time of death.

Multiple imputation analyses were used to address missing clinical data, which were assumed to be missing at random, and are presented as the primary analyses. Missing measurements were imputed using predictive mean matching with 10 separate imputations in a chained imputation conditional on other factors of interest (24). Multivariable logistic regression models and Cox proportional hazards models were replicated in patients with complete information, excluding those who were imputed. All analyses were conducted in R, version 3.6.2 (25), unless otherwise noted.

RESULTS

Summary of overall cohort characteristics. A total of 1,405 2-D echocardiograms were screened, and 806 2-D echocardiograms from 806 individual participants met inclusion/exclusion criteria for final analysis. Demographic, clinical, and serologic characteristics of 806 participants with SSc are presented in Table 1, according to diastolic function group. A total of 538 participants (66.7%) had normal diastolic function, 118 had indeterminate diastolic function (14.6%), and 150 had DD (18.6%). Of those with DD, most had grade 2 DD (n = 108; 72%). Few patients had grade 1 DD (n = 2; 1.3%) or grade 3 DD (n = 14; 9.3%). DD grade was inconclusive in the remaining patients (n = 26; 17.3%). The majority of participants were female (84%), White (71%), and had limited/sine cutaneous disease (63%). The median age at the time of 2-D echocardiogram for the entire cohort was 58.4 years (interquartile range [IQR] 48.8–68.1), and the median disease duration was 10.6 years (IQR 5.1– 17.9). At least 1 traditional risk factor for DD was present in 97% of the participants with DD (n = 146).

Analyses of clinical and serologic features according to diastolic function group. Median age increased significantly between the normal diastolic function, indeterminate diastolic function, and DD groups (*P* = 0.0001) (Table 1). The frequency of CAD, obesity, COPD, CKD, dyslipidemia, and ever tobacco use was highest in the DD group compared with the indeterminate and normal diastolic function groups. Hypertension was more frequent in the indeterminate diastolic function group (66%) and DD group (62%) compared with the normal diastolic function group (39%) (*P* < 0.001). Percentages of female participants were equally distributed across groups.

Median disease duration increased significantly between the normal diastolic function, indeterminate diastolic function, and DD groups (*P* = 0.0001) (Table 1). Participants with DD had a higher frequency of limited cutaneous disease (*P* = 0.016) and a history of scleroderma renal crisis (SRC) (*P* = 0.040) compared with the other groups. Participants with indeterminate diastology or DD had higher frequencies of positivity for Ro/SSA antibodies (*P* = 0.026), restrictive lung disease (FVC ≤70%) (*P* = 0.022), DL_{CO} ≤60% (*P* < 0.001), or an elevated RVSP (ever ≥45 mm Hg) (*P* < 0.001) compared with participants with normal diastolic function. Participants with normal diastolic function had a higher frequency of positivity for Scl-70 antibodies compared with the indeterminate diastolic function and DD groups (*P* = 0.014). Other SSc clinical manifestations had no significant associations with diastolic function groups (Table 1).

Prior use of mycophenolate mofetil, methotrexate, or hydroxychloroquine was found more frequently in those who had normal diastolic function (Table 2). The frequency of ever receiving a cardiovascular medication prior to 2-D echocardiogram, with the exception of calcium channel blockers, was higher in either the indeterminate or DD group compared with the normal diastolic function group (Table 2). Treatment with a calcium channel

Table 1. Clinical and serologic characteristics of the SSc patients, according to diastolic function group*

	Normal diastolic function group (n = 538)	Indeterminate diastolic function group (n = 118)	DD group (n = 150)	*P*
Female sex, no. (%)	452 (84)	96 (81)	129 (86)	0.59
Age at time of echocardiogram, median (IQR) years	54.3 (45.0–62.6)	65.4 (54.7–72.1)	67.7 (60.4–74.2)	0.0001
Race, no. (%)				
White	382 (71)	74 (63)	109 (73)	0.028
Black	115 (21)	38 (32)	37 (25)	
Other†	41 (8)	6 (5)	4 (3)	
SSc duration at time of echocardiogram, from first RP or non-RP symptom, median (IQR) years‡	9.3 (4.6–16.6)	11.5 (5.5–18.8)	13.8 (7.7–22.8)	0.0001
SSc subtype, no. (%)				
Limited/sine	326 (61)	74 (63)	110 (73)	0.016
Diffuse	212 (39)	44 (37)	40 (27)	
Autoantibody, ever positivity				
ANA	515/529 (97)	113/116 (97)	140/146 (96)	0.63
Anticentromere	166/531 (31)	34/118 (29)	50/146 (34)	0.63
Anti–Scl-70/topo I	153/531 (29)	22/116 (19)	28/145 (19)	0.014
Anti–RNAP III	96/491 (20)	19/103 (18)	22/137 (16)	0.65
Anti-PM/Scl	31/403 (8)	5/93 (5)	6/110 (5)	0.58
Anti-Th/To	12/403 (3)	4/93 (4)	2/110 (2)	0.58
Anti-fibrillarin/U3 RNP	13/403 (3)	3/93 (3)	3/110 (3)	0.96
Anti-Ro/SSA	102/526 (19)	31/114 (27)	41/144 (28)	0.026
Traditional risk factors for DD				
Hypertension	207/532 (39)	77/117 (66)	90/145 (62)	<0.001
CAD	17/532 (3)	13/118 (11)	25/146 (17)	<0.001
DM	25/527 (5)	8/115 (7)	14/147 (10)	0.085
Obesity (BMI ≥30 kg/m^2)	86/538 (16)	27/118 (23)	38/150 (25)	0.016
COPD	46/531 (9)	15/117 (13)	26/141 (18)	0.004
CKD	72/530 (14)	24/115 (21)	41/148 (28)	<0.001
Dyslipidemia	190/505 (38)	43/110 (39)	71/137 (52)	0.010
Past/current tobacco use	208/538 (39)	57/118 (48)	80/150 (53)	0.002
Clinical characteristics§				
FVC ≤70%	256/528 (48)	72/118 (61)	82/145 (57)	0.022
DLco ≤60%	213/517 (41)	75/114 (66)	84/138 (61)	<0.001
PH by RHC				
None	22/59 (37)	9/44 (20)	10/56 (18)	0.24
Pre-capillary	30/59 (51)	28/44 (63)	38/56 (68)	
Post-capillary	4/59 (7)	2/44 (5)	4/56 (7)	
Combined	3/59 (5)	5/44 (11)	4/56 (7)	
Severe RP	305/537 (57)	73/118 (62)	86/148 (58)	0.60
Myopathy (≤4/5 MMT)	123/534 (23)	24/118 (20)	29/148 (20)	0.60
Severe GI disease	287/537 (53)	69/117 (59)	77/148 (52)	0.48
TFR	98/537 (18)	16/118 (14)	22/149 (15)	0.35
Synovitis	116/537 (22)	25/118 (21)	36/149 (24)	0.78
Telangiectasias	494/536 (92)	110/118 (93)	141/149 (95)	0.58
Calcinosis	182/536 (34)	48/118 (41)	58/149 (39)	0.27
SRC	21/538 (4)	4/117 (3)	13/150 (9)	0.040
Maximum MRSS, median (IQR)	6 (3–16)	6.5 (4–16)	6 (3–13.5)	0.67

* Except where indicated otherwise, values are the number of patients/total number of patients assessed (%). SSc = systemic sclerosis; IQR = interquartile range; ANA = antinuclear antibody; anti–topo I = anti– topoisomerase I; anti–RNAP III = anti–RNA polymerase III; CAD = coronary artery disease; DM = diabetes mellitus; BMI = body mass index; COPD = chronic obstructive pulmonary disease; CKD = chronic kidney disease; FVC = forced vital capacity; DLco = diffusing capacity of the lung for carbon monoxide; PH = pulmonary hypertension; RHC = right-sided heart catheterization; MMT = manual muscle testing; TFR = tendon friction rubs; SRC = scleroderma renal crisis; MRSS = modified Rodnan skin thickness score.

† Includes Asian, Indian, Middle Eastern, Native American, Native Alaskan, Native Hawaiian/Pacific Islander, and unknown/not reported ethnicities.

‡ Calculated using the following group counts: normal diastolic function (n = 536), indeterminate diastolic function (n = 166), diastolic dysfunction (DD) (n = 149).

§ Clinical characteristics are reported as the maximum expressed at any time point up until the time of echocardiogram. Severe Raynaud's phenomenon (RP) was defined as ever presence of digital pitting scars, digital tip ulceration, or digital gangrene. Severe gastrointestinal (GI) disease was defined as use of high-dose gastroesophageal reflux disease medications, use of antibiotics for bacterial overgrowth, malabsorption syndrome, episodes of pseudo-obstructions, or total parenteral nutrition requirement.

Table 2. Medication use at any time point prior to echocardiogram, according to diastolic function group*

	Normal diastolic function group (n = 538)	Indeterminate diastolic function group (n = 118)	DD group (n = 150)	*P*
Immune medication (ever use)				
MMF	160/537 (30)	27/116 (23)	20/148 (14)	<0.001
Methotrexate	96/537 (18)	9/118 (8)	18/148 (12)	0.010
Hydroxychloroquine	132/537 (25)	20/118 (17)	22/148 (15)	0.016
Cyclophosphamide	38/537 (7)	8/118 (7)	6/148 (4)	0.41
Azathioprine	21/536 (4)	7/117 (6)	6/148 (4)	0.60
Prednisone	168/536 (31)	53/118 (45)	49/148 (33)	0.018
Cardiovascular medication (ever use)				
Beta-blocker	57/461 (12)	19/103 (18)	36/118 (31)	<0.001
Calcium channel blocker	344/537 (64)	83/118 (70)	94/148 (64)	0.40
ACE inhibitor	93/524 (18)	32/115 (28)	46/144 (32)	<0.001
ARB	58/457 (13)	21/99 (21)	27/115 (23)	0.005
Diuretics	124/537 (23)	68/118 (58)	82/148 (55)	<0.001
Aspirin	226/537 (42)	56/118 (47)	79/148 (53)	0.042
PDE5 inhibitor	91/536 (17)	37/118 (31)	48/148 (32)	<0.001
ERA	26/537 (5)	19/118 (16)	24/148 (16)	<0.001
Prostacyclin analog	17/537 (3)	7/118 (6)	13/148 (9)	0.012

* Values are the number of patients/total number of patients assessed (%). DD = diastolic dysfunction; MMF = mycophenolate mofetil; ACE = angiotensin-converting enzyme; ARB = angiotensin receptor blocker; PDE5 = phosphodiesterase 5; ERA = endothelin receptor antagonist.

blocker was evenly distributed across groups. A summary of 2-D echocardiogram parameters for each of the diastolic function groups (normal, indeterminate, and DD) is provided in Supplementary Table 1 (available on the *Arthritis & Rheumatology* website at https://onlinelibrary.wiley.com/doi/10.1002/art.42054).

Association between traditional DD risk factors and DD in SSc. In univariable analyses of traditional DD risk factors (including age, sex, hypertension, CAD, obesity, dyslipidemia, CKD, DM, COPD, and tobacco use), all risk factors except female sex were associated with an increased risk of DD (Table 3). In multivariable analyses, only older age (OR 1.11 [95% CI 1.08–1.13]), CAD (OR 3.07 [95% CI 1.40–6.74]), and obesity (OR 3.31 [95% CI 1.92–5.71]) remained independently associated with an increased risk of DD. Logistic regression of complete cases only showed similar results (Supplementary Table 2, available on the *Arthritis & Rheumatology* website at https://onlinelibrary.wiley.com/doi/10.1002/art.42054). An ordinal regression analysis, permitting the inclusion of the indeterminate diastolic function group as an intermediate step between normal diastolic function and DD, showed similar associations (Supplementary Table 3, available on the *Arthritis & Rheumatology* website at https://onlinelibrary.wiley.com/doi/10.1002/art.42054). A sex-stratified analysis of traditional DD risk factors and SSc clinical characteristics was also performed, as described in the Supplementary Methods.

Association between SSc characteristics and DD, after adjustment for traditional DD risk factors. SSc characteristics were analyzed to evaluate associations between SSc-specific risk factors and DD (Table 4). Each SSc characteristic

Table 3. Association between traditional DD risk factors and the presence of DD versus normal diastolic function, by logistic regression (imputed cases)*

	Univariable analysis of association with DD		Multivariable analysis of association with DD	
	OR (95% CI)	*P*	OR (95% CI)	*P*
Age at time of echocardiogram	1.10 (1.08–1.13)	<0.001	1.11 (1.08–1.13)	<0.001
Female sex	1.17 (0.70–1.96)	0.55	1.20 (0.64–2.25)	0.57
Hypertension	2.46 (1.69–3.58)	<0.001	1.17 (0.75–1.83)	0.49
CAD	5.60 (2.94–10.67)	<0.001	3.07 (1.40–6.74)	0.005
Obesity	1.78 (1.16–2.75)	0.009	3.31 (1.92–5.71)	<0.001
Dyslipidemia	1.79 (1.23–2.60)	0.002	0.82 (0.52–1.30)	0.41
CKD	2.39 (1.55–3.70)	<0.001	1.68 (0.99–2.86)	0.057
DM	2.06 (1.04–4.06)	0.038	1.19 (0.54–2.64)	0.67
COPD	2.43 (1.44–4.08)	0.001	1.29 (0.70–2.35)	0.41
Tobacco use (ever vs. never)	1.81 (1.26–2.61)	0.001	1.32 (0.85–2.05)	0.21

* OR = odds ratio; 95% CI = 95% confidence interval (see Table 1 for other definitions).

was then individually adjusted for traditional DD risk factors (including age, female sex, hypertension, CAD, obesity, dyslipidemia, CKD, DM, COPD, and tobacco use) to evaluate independent associations. In adjusted univariable analyses, longer SSc disease duration (OR 1.03 [95% CI 1.01–1.05]), Black race (OR 2.02 [95% CI 1.15–3.53]), anti-Ro/SSA positivity (OR 1.91 [95% CI 1.09–3.33]), FVC ≤70% (OR 1.72 [95% CI 1.08–2.73]), and DL_{CO} ≤60% (OR 2.66 [95% CI 1.65–4.31]) were associated with an increased risk of DD (Table 4). Anticentromere antibody positivity (OR 0.59 [95% CI 0.36–0.98]) was associated with a reduced risk of DD. Given the association between anti-Ro/SSA and DD in the univariable analysis, and the possibility that anti-Ro/SSA can occur in conjunction with other SSc autoantibodies, interactions of anti-Ro/SSA with anticentromere, anti–Scl-70, and anti–RNA polymerase III were modeled. No statistically significant associations between the interaction terms and DD were found.

A multivariable model was then constructed with all covariates that were associated with DD on univariable or adjusted univariable models. The multivariable model was adjusted for all cardiovascular and pulmonary risk factors listed in Table 3. Longer SSc disease duration (OR 1.04 [95% CI 1.01–1.06]) and a reduced DL_{CO} ≤60% (OR 2.41 [95% CI 1.40–4.16]) remained independently associated with DD. Additionally, a history of SRC was associated with an increased risk of DD (OR 3.18 [95% CI 1.12–9.07]). Race, diffuse SSc subtype, anticentromere positivity, anti–RNA polymerase III positivity, anti-Ro/SSA positivity, and FVC ≤70% were no longer significantly associated with an increased or decreased risk of DD in the final adjusted multivariable model. Positivity for anti–Scl-70 was associated with a 51% reduction in the odds of developing DD (OR 0.49 [95% CI 0.26–0.93]). Additionally, a history of severe gastrointestinal (GI) disease was associated with a 52% reduction in risk of DD (OR 0.48 [95% CI 0.30–0.79]).

Table 4. Association between SSc characteristics and DD, unadjusted and adjusted for DD risk factors (imputed cases)*

	Univariable analyses of association with DD				Adjusted multivariable analysis of association with DD†	
	Unadjusted		Adjusted†			
	OR (95% CI)	*P*	OR (95% CI)	*P*	OR (95% CI)	*P*
SSc duration from first ever symptoms (per 1 year)	1.05 (1.03–1.07)	<0.001	1.03 (1.01–1.05)	0.013	1.04 (1.01–1.06)	0.004
Race‡						
Black	1.13 (0.74–1.73)	0.58	2.02 (1.15–3.53)	0.014	1.35 (0.73–2.50)	0.33
Other§	0.34 (0.12–0.98)	0.045	1.21 (0.37–3.97)	0.76	1.24 (0.36–4.21)	0.73
Diffuse SSc subtype	0.56 (0.37–0.84)	0.005	0.82 (0.49–1.35)	0.43	0.95 (0.52–1.73)	0.87
Autoantibody positivity						
Anticentromere	1.17 (0.79–1.72)	0.43	0.59 (0.36–0.98)	0.041	0.48 (0.23–1.00)	0.051
Anti–Scl-70/topo I	0.58 (0.37–0.91)	0.018	0.76 (0.44–1.33)	0.34	0.49 (0.26–0.93)	0.030
Anti–RNAP III	0.80 (0.48–1.34)	0.40	0.53 (0.28–1.00)	0.050	0.51 (0.25–1.03)	0.060
Anti- PM/Scl	0.72 (0.29–1.78)	0.48	0.48 (0.16–1.42)	0.19		
Anti-Th/To	0.62 (0.13–2.85)	0.54	0.22 (0.04–1.15)	0.073	0.21 (0.04–1.06)	0.060
Anti-fibrillarin/U3 RNP	0.89 (0.29–2.78)	0.85	1.78 (0.41–7.71)	0.44		
Anti-Ro/SSA	1.68 (1.07–2.63)	0.026	1.91 (1.09–3.33)	0.024	1.51 (0.70–3.25)	0.30
Autoantibody interaction						
Anti-Ro–anticentromere	1.85 (0.94–3.65)	0.079	1.18 (0.54–2.57)	0.69	0.95 (0.27–3.31)	0.94
Anti-Ro–anti–Scl-70/topo I	0.71 (0.24–2.13)	0.55	0.75 (0.19–2.86)	0.67		
Anti-Ro–anti–RNAP III	1.91 (0.85–3.65)	0.12	1.66 (0.61–4.52)	0.32		
Anti-Ro–anti-Th/To	1.71 (0.35–8.42)	0.51	0.79 (0.13–4.77)	0.80		
Clinical characteristics						
Severe RP	1.06 (0.73–1.53)	0.76	1.21 (0.77–1.91)	0.42		
FVC ≤70%	1.39 (0.96–2.01)	0.082	1.72 (1.08–2.73)	0.023	1.22 (0.69–2.16)	0.49
DL_{CO} ≤60%	2.20 (1.51–3.21)	<0.001	2.66 (1.65–4.31)	<0.001	2.41 (1.40–4.16)	0.002
Myopathy (MMT ≤4)	0.81 (0.51–1.27)	0.35	1.12 (0.64–1.94)	0.70		
Severe GI disease	0.94 (0.65–1.36)	0.75	0.68 (0.44–1.05)	0.084	0.48 (0.30–0.79)	0.004
TFR	0.77 (0.47–1.28)	0.31	0.84 (0.44–1.61)	0.61		
Synovitis	1.15 (0.75–1.76)	0.53	0.94 (0.55–1.59)	0.81		
Telangiectasias	1.51 (0.69–3.29)	0.30	0.91 (0.32–2.61)	0.86		
Calcinosis	1.24 (0.85–1.80)	0.26	1.24 (0.78–1.96)	0.36		
SRC	2.34 (1.14–4.78)	0.021	2.13 (0.75–6.08)	0.16	3.18 (1.12–9.07)	0.031
Maximum MRSS	0.99 (0.98–1.01)	0.37	0.99 (0.97–1.02)	0.61		

* Multivariable model was constructed based on significant variables in unadjusted or adjusted univariable analysis (95% confidence intervals [95% CIs] that do not cross 1.00; or $P < 0.10$). OR = odds ratio; (see Table 1 for other definitions).
† Adjusted for all DD risk factors including age, sex, hypertension, CAD, obesity, dyslipidemia, CKD, diabetes, COPD, and tobacco use.
‡ Compared to White patients.
§ Includes Asian, Indian, Middle Eastern, Native American, Native Alaskan, Native Hawaiian/Pacific Islander, unknown/not reported ethnicities.

Only the traditional risk factors for DD of older age (OR 1.12 [95% CI 1.09–1.15]), CAD (OR 3.69 [95% CI 1.52–8.97]), and obesity (OR 4.74 [95% CI 2.57–8.74]) were independently associated with DD in the final multivariable model (data not shown).

Analyses of complete cases only are presented in Supplementary Table 4 (available on the *Arthritis & Rheumatology* website at https://onlinelibrary.wiley.com/doi/10.1002/art.42054). An ordinal regression including indeterminate diastolic cases showed similar trends in risk factor associations as seen in the primary logistic regression model (Supplementary Table 5, available on the *Arthritis & Rheumatology* website at https://onlinelibrary.wiley.com/doi/10.1002/art.42054).

Association between medication exposure and the presence of DD in univariable and multivariable regression analyses. In univariable analyses, ever exposure to mycophenolate mofetil or hydroxychloroquine was associated with a 63% reduction (OR 0.37 [95% CI 0.22–0.61]) and 47% reduction (OR 0.53 [95% CI 0.33–0.88]) in risk of DD, respectively (Supplementary Table 6, available on the *Arthritis & Rheumatology* website at https://onlinelibrary.wiley.com/doi/10.1002/art.42054). These associations were no longer present after adjustment for traditional risk factors for DD or in the adjusted multivariable model. These medication analyses were considered hypothesis-generating and were not included in the final model, as dose and duration were not available and would be hypothesized to impact associations. Associations were seen between most cardiovascular medications (with the exception of calcium channel blockers and nitrates) and DD in univariable models, which were mildly attenuated when adjusting for DD risk factors (Supplementary Table 6).

Impact of DD on survival in SSc. There were 135 deaths among 672 SSc patients with either DD or normal diastolic function. SSc patients with DD had an almost 3-fold increase in risk

Table 5. Cox proportional hazards models evaluating the association between mortality risk and presence of DD, traditional DD risk factors, or DD risk factors and SSc clinical features in 672 patients (imputed cases)*

	Univariable analysis of association with mortality risk		Multivariable analyses of association with mortality risk			
			DD risk factors		DD risk factors and SSc features	
	HR (95% CI)	*P*	HR (95% CI)	*P*	HR (95% CI)	*P*
DD†	2.86 (2.03–4.01)	<0.001	2.38 (1.56–3.61)	<0.001	1.69 (1.07–2.68)	0.027
Age at time of echocardiogram			1.01 (0.99–1.03)	0.26	1.02 (1.00–1.04)	0.037
Female sex			0.59 (0.39–0.91)	0.018	0.70 (0.44–1.11)	0.13
Hypertension			1.30 (0.89–1.89)	0.18	1.35 (0.90–2.03)	0.15
CAD			0.65 (0.35–1.18)	0.16	0.62 (0.32–1.21)	0.16
Obesity			0.63 (0.38–1.04)	0.071	0.68 (0.40–1.16)	0.16
Dyslipidemia			0.91 (0.63–1.31)	0.62	0.88 (0.60–1.31)	0.54
CKD			1.64 (1.11–2.42)	0.015	1.42 (0.91–2.20)	0.13
DM			1.73 (0.99–3.02)	0.058	1.16 (0.64–2.10)	0.63
COPD			1.93 (1.09–2.96)	0.025	1.56 (0.90–2.69)	0.12
Tobacco (ever vs. never)			1.21 (0.85–1.73)	0.28	1.18 (0.81–1.72)	0.39
Race‡						
Black					1.02 (0.64–1.62)	0.94
Other§					1.35 (0.59–3.07)	0.48
SSc duration from first symptoms					0.99 (0.97–1.01)	0.23
Diffuse SSc subtype					0.95 (0.61–1.48)	0.83
Autoantibody positivity						
Anticentromere					1.32 (0.74–2.36)	0.34
Anti–Scl-70/topo I					1.09 (0.69–1.71)	0.72
Anti–RNAP III					1.24 (0.73–2.11)	0.43
Anti-Th/To					0.65 (0.24–1.74)	0.39
Anti-Ro/SSA					1.28 (0.75–2.20)	0.37
Anti-Ro–anticentromere					0.85 (0.35–2.05)	0.72
Clinical characteristics						
FVC ≤70%					1.34 (0.83–2.15)	0.24
DL_{CO} ≤60%					3.24 (2.00–5.25)	<0.001
Severe GI disease					1.10 (0.74–1.65)	0.63
SRC					1.78 (0.90–3.50)	0.10

* HR = hazard ratio; 95% CI = 95% confidence interval (see Table 1 for other definitions).
† Compared to patients with normal diastolic function.
‡ Compared to White patients.
§ Includes Asian, Indian, Middle Eastern, Native American, Native Alaskan, Native Hawaiian/Pacific Islander, unknown/not reported ethnicities.

of mortality in the univariable Cox proportional hazards analysis (hazard ratio [HR] 2.86 [95% CI 2.03–4.01]) (Table 5). After adjusting for traditional DD risk factors, DD conferred a >2-fold increase in the risk of mortality (HR 2.38 [95% CI 1.56–3.61]), with CKD (HR 1.64 [95% CI 1.11–2.42]) and COPD (HR 1.93 [95% CI 1.09–2.96]) also associated with an increased risk of mortality. Female sex was protective against mortality risk (OR 0.59 [95% CI 0.39–0.91]).

In the final multivariable model, Black race, diffuse disease, anticentromere positivity, anti–Scl-70 positivity, anti–RNA polymerase III positivity, anti-Th/To positivity, FVC ≤70%, DLCO ≤60%, and SRC were all included, given the known positive or negative associations with mortality in SSc (1,2). Anti-Ro/SSA, anti-Ro/SSA–anticentromere interaction, and severe GI disease were also included as variables in the final model, given demonstrated associations with DD ($P \leq 0.10$ in logistic regression analyses in Table 4). In the final multivariable model, DD remained independently associated with an increase in the risk of mortality in imputed cases (HR 1.69 [95% CI 1.07–2.68]) (Table 5). Only age (HR 1.02 [95% CI 1.00–1.04]) and DLCO ≤60% (HR 3.24 [95% CI 2.00–5.25]) were independently associated with risk of mortality in the multivariable model. The point estimate for the HR of association of mortality risk with DD was similar (HR 1.78 [95% CI 0.98–3.24]) for complete (nonimputed) cases (Supplementary Table 8, available on the *Arthritis & Rheumatology* website at https://onlinelibrary.wiley.com/doi/10.1002/art.42054).

Unadjusted (Figure 1A) and age-adjusted (Figure 1B) Kaplan-Meier curves are shown for the DD and normal diastolic function groups. The unadjusted median survival for SSc patients with DD from time of 2-D echocardiogram was 2.76 years and could not be calculated for those with normal diastolic function due to survival >50% during the time under observation. In participants with DD, the age-adjusted 5- and 10-year survival rates were 40.8% and 30.5%, respectively. In participants with normal diastolic function, the age-adjusted 5- and 10-year survival rates were 68.9% and 61.1%, respectively. Kaplan-Meier graphs including the indeterminate diastolic function group, which showed similar survival as that in the DD group, are shown in Supplementary Figure 1 (available on the *Arthritis & Rheumatology* website at https://onlinelibrary.wiley.com/doi/10.1002/art.42054).

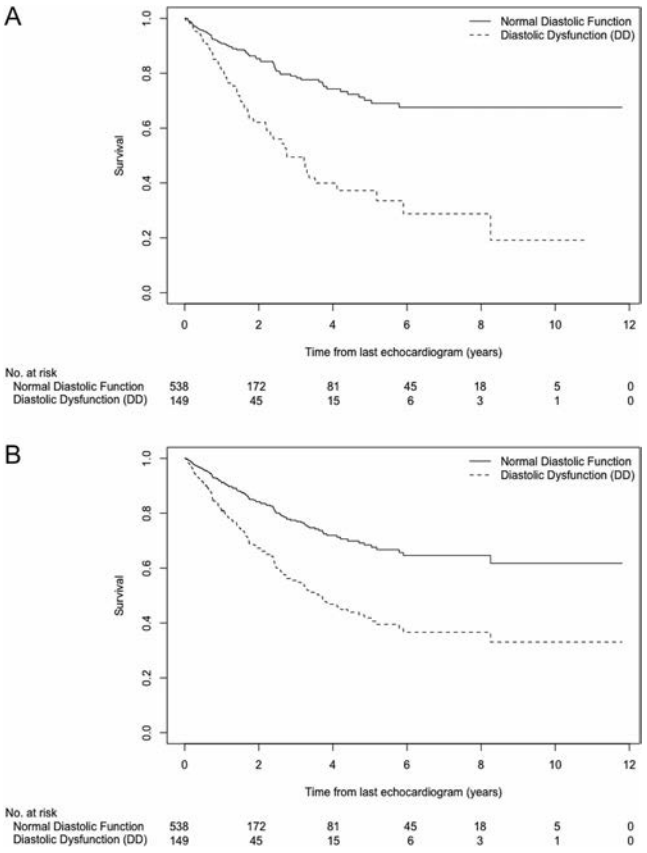

Figure 1. Association of normal diastolic function and diastolic dysfunction (DD) with risk of mortality in 672 systemic sclerosis patients in unadjusted (**A**) and age-adjusted (**B**) Kaplan-Meier analyses. Age-adjusted 5- and 10-year survival rates were 68.9% and 61.1%, respectively, for those with normal diastolic function. Age-adjusted 5- and 10-year survival rates were 40.8% and 30.5%, respectively, for those with DD.

DISCUSSION

We present the largest study to date examining risk factors for DD and the impact of DD on mortality in a well-characterized cohort of patients with SSc. Traditional risk factors for DD were ascertained prospectively, and CAD and obesity emerged as significant risk factors for DD in patients with SSc. We confirmed others' findings that age (5,9), SSc disease duration (9), and DLCO ≤60% (6,9) are associated with an increased risk of DD, and we are the first to identify an association between a history of SRC and an increased risk of DD. Interestingly, we also found that severe GI disease and anti–Scl-70 antibodies were associated with a decreased risk of DD. Importantly, DD independently conferred a 69% increase in risk of mortality in patients with SSc. Therefore, interventions targeting modifiable risk factors for DD, including CAD and obesity, may help reduce mortality in SSc.

A major strength of our study was the rigorous application of the most recent societal recommendations for the classification of diastolic function, which combines 4 parameters derived from 2-D echocardiograms to classify diastology. The aim of the 2016 ASE/ESCVI guidelines were to simplify the approach to diastology determination from the more complex, difficult to apply, and irregularly used 2009 guidelines, by selecting the most reproducible and feasible 2-D echocardiogram measurements (13). The use of these simplified yet rigorous guidelines improves generalizability of our study results and minimizes potential misclassification that occurs when using single parameters.

With application of these guidelines, we found a DD prevalence of 18.6% in our SSc cohort, which falls in the lower range of previous estimates of 18–62% (4,6,12,26). These prior studies, however, utilized older guidelines to classify diastology or used a

single 2-D echocardiogram parameter, which may lead to misclassification if used in isolation. Our prevalence estimate is similar, but slightly lower, than the prevalence estimate of 29% reported by Tennøe et al, who used the same 2016 ASE/ESCVI criteria to classify diastolic function (5). However, in contrast to that in the study by Tennøe et al, we excluded patients with moderate or severe valvular heart disease as we were focused on primary myocardial disease, which may account for this difference. Our prevalence estimate of 18.6% is higher than that of 1.4% in a population-based cohort with 1,000 non-SSc subjects of similar ages, in which the 2016 ASE/ESCVI guidelines were applied (8), which may suggest the existence of SSc-specific risk factors for DD. However, 2 other referral-based non-SSc cohorts (i.e., patients referred specifically for a 2-D echocardiogram) have shown prevalence estimates of 9.4–30% (27,28), which may indicate that underlying cardiovascular and pulmonary risks are most influential on DD risk. Further studies in which SSc patients and non-SSc patients are derived from the same population, and have similar demographics and comorbidities, are essential to evaluate the potential impact of SSc pathophysiology on DD risk.

With the potential increase in DD prevalence in SSc cohorts compared with non-SSc cohorts, we sought to identify SSc-specific risk factors for DD, which may provide further mechanistic insight into DD pathogenesis in this population. To robustly determine independent associations between SSc-specific risk factors and DD, 10 traditional risk factors for DD were examined. While all of these traditional risk factors (with the exception of sex) were significantly associated with DD in univariable analyses, only 3 of the 10 risk factors (age, CAD, obesity) were independently associated with DD in our final multivariable model. This is similar to the findings of Hinchcliff and colleagues, who reported an independent association of age and CAD with tissue Doppler lateral e′ velocity; however, obesity was not examined (9). Impressively, obesity was independently associated with a >4.5-fold increase in risk of DD in our population.

Interestingly, we did not find an independent association between hypertension and DD, which is similar to results presented by Maione and colleagues (11) but differs from findings of Hinchcliff et al (9). Given the known association between hypertension and obesity, as well as between hypertension and CAD, it is possible that the effect of hypertension on DD presence is mediated through obesity and/or CAD, which may explain the lack of association between hypertension and DD in the final multivariable model. We did not find an association between sex and DD, which may be due to differences in the prevalence of traditional risk factors in men compared with women (e.g., men had an increase in the frequency of CAD, CKD, and DLco ≤60%), which we accounted for in our models. Further study is required with general population controls to examine these sex-based differences.

We performed an in-depth examination of SSc-specific risk factors, adjusting for the 10 traditional risk factors for DD. We found an independent association between SSc disease duration and DD, as previously noted in some studies (6,9,26) but not others (5,11). This association between SSc disease duration and DD may suggest a relationship between SSc disease pathophysiology and DD pathophysiology, perhaps mediated by progressive endothelial dysfunction. We also identified a 2.4-fold increased risk of DD in participants who had a DLco ≤60%, even after controlling for restrictive lung disease, which suggests that the low DLco may represent concomitant pulmonary vascular disease. In the 159 participants who underwent a clinically indicated right-sided heart catheterization, the frequency of pre- and post-capillary pulmonary hypertension was evenly distributed among diastolic function groups (Table 1). It is possible that further provocative testing with exercise or fluid challenge may have identified elevated filling pressures in the groups with a DLco ≤60% and DD; however, that analysis was beyond the scope of this study. Other studies have also demonstrated lower DLco in SSc patients with DD (6,9).

We additionally report an independent association between SRC and DD in our final model, which adjusted for potential mediators including hypertension and CKD. An increased risk of DD in patients with a history of SRC is biologically plausible, as activation of the renin–angiotensin–aldosterone system underlies the pathophysiology of SRC (29) and is also known to promote myocardial fibrosis and stiffness (30). It is important to recognize that SRC may increase DD risk, highlighting the importance of addressing potentially modifiable DD risk factors such as CAD and obesity in SSc patients with a history of SRC.

Anti–Scl-70 was associated with a reduced risk of DD in our final model. Hinchcliff et al reported a reduction in the presence of DD in anti–Scl-70–positive patients and an increase in those with anticentromere antibodies, but these associations were not significant after controlling for age (9). A decrease in the frequency of anti–Scl-70 in patients with DD was also observed by Tennøe et al, although these results did not reach significance (5).

The association between severe GI disease and decreased risk of DD has not been previously examined. We hypothesize that this association may be mediated by a decrease in adipose tissue, with a resulting decrease in inflammatory mediators. Increase in adipose tissue is associated with an increase in inflammatory mediators that can lead to the endothelial dysfunction that underlies DD pathogenesis (31,32). The decreased risk of DD in those with severe GI disease may also be related to a decrease in left ventricular mass, as nutritional status has been shown to correlate with left ventricular mass in SSc (33). It is also possible that use of high-dose medications for gastroesophageal reflux disease in patients with severe GI disease may have protected against aspiration-induced lung damage with reduced DLco, thus decreasing risk.

Importantly, we show that DD is an independent risk factor for mortality in SSc, even after adjusting for cardiovascular, pulmonary, and SSc-specific risk factors for mortality. In fully adjusted models, only age and a DLco ≤60%, likely reflecting

pulmonary vascular disease, were also independently associated with a risk of mortality. These findings are consistent with those of other researchers, who have noted a similar association between DD and mortality in SSc in smaller cohorts (5,9).

Our study is limited by examination of a single 2-D echocardiogram per participant. Therefore, while important associations can be made regarding risk factors for prevalent DD, a cause and effect relationship should not be extrapolated. Strengths of this study include the utilization of classification criteria for DD, rigorous ascertainment of DD risk factors and SSc disease characteristics prospectively, and the large cohort size permitting robust multivariable analyses of risk factors.

In conclusion, we present the largest cohort study examining risk factors for DD in SSc and the impact of DD on mortality. CAD and obesity are comorbidities significantly associated with DD in SSc, which are also potentially modifiable risk factors. Given the strong association between DD and mortality, interventions targeting reduction in risk of CAD and obesity may also decrease mortality in SSc through a reduction in DD.

AUTHOR CONTRIBUTIONS

All authors were involved in drafting the article or revising it critically for important intellectual content, and all authors approved the final version to be published. Dr. Hinze had full access to all of the data in the study and takes responsibility for the integrity of the data and the accuracy of the data analysis.

Study conception and design. Hinze, Perin, Hummers, Wigley, Mukherjee, Shah.

Acquisition of data. Hinze, Woods, Hummers, Wigley, Mukherjee, Shah.

Analysis and interpretation of data. Hinze, Perin, Shah.

REFERENCES

1. Sampaio-Barros PD, Bortoluzzo AB, Marangoni RG, Rocha LF, Del Rio AP, Samara AM, et al. Survival, causes of death, and prognostic factors in systemic sclerosis: analysis of 947 Brazilian patients. J Rheumatol 2012;39:1971–8.
2. Tyndall AJ, Bannert B, Vonk M, Airò P, Cozzi F, Carreira PE, et al. Causes and risk factors for death in systemic sclerosis: a study from the EULAR Scleroderma Trials and Research (EUSTAR) database. Ann Rheum Dis 2010;69:1809–15.
3. Fernández-Codina A, Simeón-Aznar CP, Pinal-Fernandez I, Rodríguez-Palomares J, Pizzi MN, Hidalgo CE, et al. Cardiac involvement in systemic sclerosis: differences between clinical subsets and influence on survival. Rheumatol Int 2017;37:75–84.
4. Faludi R, Kolto G, Bartos B, Csima G, Czirjak L, Komocsi A. Five-year follow-up of left ventricular diastolic function in systemic sclerosis patients: determinants of mortality and disease progression. Semin Arthritis Rheum 2014;44:220–7.
5. Tennøe AH, Murbraech K, Andreassen JC, Fretheim H, Garen T, Gude E, et al. Left ventricular diastolic dysfunction predicts mortality in patients with systemic sclerosis. J Am Coll Cardiol 2018;72:1804–13.
6. Vemulapalli S, Cohen L, Hsu V. Prevalence and risk factors for left ventricular diastolic dysfunction in a scleroderma cohort. Scand J Rheumatol 2017;46:281–7.
7. Redfield MM, Jacobsen SJ, Burnett JC Jr, Mahoney DW, Bailey KR, Rodeheffer RJ. Burden of systolic and diastolic ventricular dysfunction in the community: appreciating the scope of the heart failure epidemic. JAMA 2003;289:194–202.
8. Almeida JG, Fontes-Carvalho R, Sampaio F, Ribero J, Bettencourt P, Flachkampf FA, et al. Impact of the 2016 ASE/EACVI recommendations on the prevalence of diastolic dysfunction in the general population. Eur Heart J Cardiovasc Imaging 2018;19:380–6.
9. Hinchcliff M, Desai CS, Varga J, Shah SJ. Prevalence, prognosis, and factors associated with left ventricular diastolic dysfunction in systemic sclerosis. Clin Exp Rheumatol 2012;30:S30–7.
10. Wan SH, Vogel MW, Chen HH. Pre-clinical diastolic dysfunction. J Am Coll Cardiol 2014;63:407–16.
11. Maione S, Cuomo G, Giunta A, de Horatio LT, La Montagna G, Manguso F, et al. Echocardiographic alterations in systemic sclerosis: a longitudinal study. Semin Arthritis Rheum 2005;34:721–7.
12. De Groote P, Gressin V, Hachulla E, Carpentier P, Guillevin L, Kahan A, et al. Evaluation of cardiac abnormalities by Doppler echocardiography in a large nationwide multicentric cohort of patients with systemic sclerosis. Ann Rheum Dis 2008;67:31–6.
13. Nagueh SF, Smiseth OA, Appleton CP, Byrd BF III, Dokainish H, Edvardsen T, et al. Recommendations for the evaluation of left ventricular diastolic function by echocardiography: an update from the American Society of Echocardiography and the European Association of Cardiovascular Imaging. Eur Heart J Cardiovasc Imaging 2016;17:1321–60.
14. Van den Hoogen F, Khanna D, Fransen J, Johnson SR, Baron M, Tyndall A, et al. 2013 classification criteria for systemic sclerosis: an American College of Rheumatology/European League against Rheumatism collaborative initiative. Arthritis Rheum 2013;65:2737–47.
15. Masi AT, Committee SFSCotARADaTC. Preliminary criteria for the classification of systemic sclerosis (scleroderma). Subcommittee for scleroderma criteria of the American Rheumatism Association Diagnostic and Therapeutic Criteria Committee. Arthritis Rheum 1980;23:581–90.
16. LeRoy EC, Black C, Fleischmajer R, Jablonska S, Krieg T, Medsger TA Jr, et al. Scleroderma (systemic sclerosis): classification, subsets and pathogenesis. J Rheumatol 1988;15:202–5.
17. Hankinson JL, Odencrantz JR, Fedan KB. Spirometric reference values from a sample of the general U.S. population. Am J Respir Crit Care Med 1999;159:179–87.
18. Crapo RO, Jensen RL, Wanger JS. Single-breath carbon monoxide diffusing capacity. Clin Chest Med 2001;22:637–49.
19. Medsger TA Jr, Bombardieri S, Czirjak L, Scorza R, Della Rossa A, Bencivelli W. Assessment of disease severity and prognosis. Clin Exp Rheumatol 2003;21:S42–6.
20. Medsger TA Jr, Silman AJ, Steen VD, Black CM, Akesson A, Bacon PA, et al. A disease severity scale for systemic sclerosis: development and testing. J Rheumatol 1999;26:2159–67.
21. Lang RM, Badano LP, Mor-Avi V, Afilalo J, Armstrong A, Ernande L, et al. Recommendations for cardiac chamber quantification by echocardiography in adults: an update from the American Society of Echocardiography and the European Association of Cardiovascular Imaging. J Am Soc Echocardiogr 2015;28:1–39.
22. Agresti A. Categorical Data. Second ed. Hoboken (NJ):Wiley; 2002.
23. Andersen P, Gill R. Cox's regression model for counting processes, a large sample study. Ann Stat 1982;10:1100–20.
24. Van Buuren S, Brand JP, Groothuis-Oudshoorn CG, Rubin DB. Fully conditional specification in multivariate imputation. J Stat Comput Simul 2006;76:1049–64.
25. R-Core-Team. R: a language and environment for statistical computing. Vienna (Austria): R Foundation for Statistical Computing; 2019.
26. Roque MC, Sampaio-Barros PD, Arruda AL, Barros-Gomes S, Becker D, de Andrade JL, et al. Evaluation of left ventricular diastolic

function by echocardiography with tissue doppler in systemic sclerosis. Arq Bras Cardiol 2017;109:410–5.

27. Sorrentino R, Esposito R, Santoro C, Vaccaro A, Cocozza S, Scalamogna M, et al. Practical impact of new diastolic recommendations on noninvasive estimation of left ventricular diastolic function and filling pressures. J Am Soc Echocardiogr 2020;33:171–81.
28. Kumar SS, Desai N, Gona OJ, Kumar V, Madhu B. Impact of updated 2016 ASE/EACVI VIS-A-VIS 2009 ASE recommendation on the prevalence of diastolic dysfunction and LV filling pressures in patients with preserved ejection fraction. J Cardiovasc Imaging 2021;29:31–43.
29. Denton CP, Hudson M. Renal crisis and other renal manifestations of scleroderma. In: Varga J, Denton CP, Wigley FM, Allanore Y, Kuwana M, eds. Scleroderma: from pathogenesis to comprehensive management. Second ed. New York: Springer; 2017.
30. Jia G, Aroor AR, Hill MA, Sowers JR. Role of renin-angiotensin-aldosterone system activation in promoting cardiovascular fibrosis and stiffness. Hypertension 2018;72:537–48.
31. Paulus WJ, Tschope C. A novel paradigm for heart failure with preserved ejection fraction: comorbidities drive myocardial dysfunction and remodeling through coronary microvascular endothelial inflammation. J Am Coll Cardiol 2013;62:263–71.
32. Shah SJ, Kitzman DW, Borlaug BA, van Heerebbeek L, Zile MR, Kass DA, et al. Phenotype-specific treatment of heart failure with preserved ejection fraction: a multiorgan roadmap. Circulation 2016;134:73–90.
33. Rosato E, Gigante A, Gasperini ML, Molinaro I, Giraldi GD, Afeltra A et al. Nutritional status measured by BMI is impaired and correlates with left ventricular mass in patients with systemic sclerosis. Nutrition 2014;30:204–9.

American College of Rheumatology
Empowering Rheumatology Professionals

Arthritis & Rheumatology
Vol. 74, No. 5, May 2022, pp 860–870
DOI 10.1002/art.42042

Therapeutic Effect of Cyclin-Dependent Kinase 4/6 Inhibitor on Dermal Fibrosis in Murine Models of Systemic Sclerosis

Akio Yamamoto,[1] Tetsuya Saito,[1] Tadashi Hosoya,[1] Kimito Kawahata,[1] Yoshihide Asano,[2] Shinichi Sato,[2] Fumitaka Mizoguchi,[†] Shinsuke Yasuda,[1] and Hitoshi Kohsaka[1]

Objective. One of the histologic characteristics of systemic sclerosis (SSc) is an increased number of dermal myofibroblasts, and transforming growth factor β (TGFβ) plays a crucial role in the promotion of myofibroblast differentiation from fibroblasts, leading to dermal fibrosis. This study was undertaken to 1) examine whether inhibition of the cell cycle with a cyclin-dependent kinase 4/6 (CDK4/6) inhibitor suppresses the proliferation of fibroblasts and their differentiation into myofibroblasts, and 2) assess the therapeutic effects of a CDK4/6 inhibitor, administered as monotherapy or in combination with a TGFβ receptor (TGFβR) inhibitor, on dermal fibrosis in murine models of SSc.

Methods. Fibroblasts obtained from the skin of patients with SSc were cultured in the presence or absence of TGFβ. The effects of palbociclib, a CDK4/6 inhibitor, on fibroblast proliferation and TGFβ-induced differentiation into myofibroblasts were examined using bromodeoxyuridine uptake assays as well as immunofluorescence and immunoblotting analyses. Murine models of HOCl- and bleomycin-induced dermal fibrosis were used to study the effect of a CDK4/6 inhibitor on dermal fibrosis, with the CDK4/6 inhibitor treatment administered as monotherapy or in combination with galunisertib, a TGFβR inhibitor.

Results. Addition of a CDK4/6 inhibitor to the cell cultures suppressed the proliferation of human dermal SSc fibroblasts and their TGFβ-induced differentiation into myofibroblasts, without inhibiting canonical and noncanonical TGFβ signals. In murine models of dermal fibrosis, treatment of mice with a CDK4/6 inhibitor decreased dermal thickness and collagen content, as well as dermal fibroblast proliferation and the numbers of myofibroblasts. Combination therapy with the CDK4/6 inhibitor and TGFβR inhibitor resulted in additive antifibrotic effects. Mechanistically, the CDK4/6 inhibitor suppressed the expression of cellular communication network 2 and cadherin-11, which are proteins that have important roles in the development and progression of fibrosis.

Conclusion. Results of this study demonstrate the therapeutic effect of a CDK4/6 inhibitor on dermal fibrosis when administered as monotherapy or in combination with a TGFβR inhibitor. CDK4/6 inhibitors, including palbociclib used in the present study, may represent novel agents for the treatment of SSc, which, if used in combination with a TGFβR inhibitor, might result in increased efficacy.

INTRODUCTION

Systemic sclerosis (SSc) is a complex autoimmune connective tissue disease that results in dermal and organ fibrosis (1). Immunosuppressive agents such as methotrexate, mycophenolate mofetil, cyclophosphamide, and rituximab are used for the treatment of progressive dermal fibrosis and interstitial lung disease. However, the therapeutic effects are limited (2,3).

In the pathogenesis of SSc, myofibroblasts play crucial roles by producing a variety of extracellular matrix (ECM) and inflammatory molecules to induce tissue fibrosis. Transforming growth factor β (TGFβ) is a major profibrotic cytokine that promotes myofibroblast differentiation from fibroblasts, and thus has been expected to represent a novel candidate target for therapy in patients with SSc (1,4). A clinical trial has shown that a neutralizing antibody that targets all 3 isoforms of TGFβ attenuated dermal fibrosis in patients with SSc (5). However, the therapeutic effects

[1]Akio Yamamoto, MD, Tetsuya Saito, MD, PhD, Tadashi Hosoya, MD, PhD, Kimito Kawahata, MD, PhD (current address: St. Marianna University School of Medicine, Kawasaki, Japan), Shinsuke Yasuda, MD, PhD, Hitoshi Kohsaka, MD, PhD (current address: Chiba-Nishi General Hospital, Chiba, Japan): Tokyo Medical and Dental University, Tokyo, Japan; [2]Yoshihide Asano, MD, PhD, Shinichi Sato, MD, PhD: The University of Tokyo, Tokyo, Japan.
[†]Fumitaka Mizoguchi, MD, PhD is deceased.

Author disclosures are available at https://onlinelibrary.wiley.com/action/downloadSupplement?doi=10.1002%2Fart.42042&file=art42042-sup-0001-Disclosureform.pdf.

Address correspondence to Shinsuke Yasuda, MD, PhD, 1-5-45 Yushima Bunkyo-ku, Tokyo, Japan 113-8519. Email: syasuda.rheu@tmd.ac.jp.

Submitted for publication October 19, 2021; accepted in revised form December 2, 2021.

are partial. In addition, the blockade of TGFβ could cause significant adverse events, including bleeding and anemia, because of the pleiotropic functions of TGFβ (5,6). In order to develop effective therapies targeting TGFβ signaling in SSc, it is necessary to employ strategies for increasing their efficacy while, at the same time, reducing the adverse effects of such therapies. One of the strategies to increase the therapeutic efficacy without increasing the adverse effects of these drugs is to use another agent with a different mode of action simultaneously. Combination therapy would enable a reduction in the dose of each drug, which potentially leads to a reduction in adverse effects. Thus, in addition to targeting TGFβ signaling, identifying other pathways involved in the promotion of tissue fibrosis is important.

The histologic features of SSc include an increased number of myofibroblasts as well as collagen deposition in the skin lesions (7,8). In addition, increased numbers of proliferating fibroblasts in the fibrotic skin lesions of patients with SSc have been reported, especially in those with early SSc (9). These findings suggest that the proliferation of fibroblasts is responsible for the increased number of myofibroblasts and subsequent tissue fibrosis in SSc.

Cell proliferation is regulated by the interaction of cyclins with cyclin-dependent kinases (CDKs). In response to mitogenic stimulation, cyclin D promotes the activation of CDK4 and CDK6 (CDK4/6), both of which are crucial regulators of the transition from G_1 to S phase in the cell cycle. The CDK4/6–cyclin D complexes inactivate the retinoblastoma (Rb) protein, which is an antiproliferative protein that limits the transcription of E2F target genes by catalyzing the phosphorylation of Rb (10).

Selective CDK4/6 inhibitors, including palbociclib, have been used for the treatment of advanced breast cancer. CDK4/6 inhibitors suppress cell cycle progression by binding to the ATP-binding pocket of CDK4 and CDK6 (10). The adverse effects of CDK4/6 inhibitors include the development of neutropenia, which is generally tolerable and reversible by reducing the dose (10). In preclinical studies, the CDK4/6 inhibitors have also been shown to be effective in the treatment of nonmalignant diseases, including autoimmune arthritis (11), pulmonary arterial hypertension (12), and acute kidney injury (13), in which the proliferation of synovial fibroblasts, smooth muscle cells, and tubular cells in each respective disease plays a crucial role in the pathogenesis. Of note, the required dose of CDK4/6 inhibitors for the treatment of these nonmalignant diseases is lower than that for cancers, suggesting that CDK4/6 inhibitors can be used safely in the treatment of these nonmalignant diseases (11).

Since the number of proliferating fibroblasts is increased in the skin lesions of patients with SSc, we hypothesized that CDK4/6 inhibitors should be effective in treating dermal fibrosis in SSc, and that a combination therapy involving a CDK4/6 inhibitor and a TGFβ receptor (TGFβR) inhibitor would provide an additive effect, considering their distinct modes of action. In this study, we examined the effects of a CDK4/6 inhibitor, administered as monotherapy or in combination with a TGFβR inhibitor, in the treatment of dermal fibrosis.

MATERIALS AND METHODS

Reagents. The following reagents and antibodies were used: palbociclib (PD0332991) and galunisertib (LY2157299) (both from Shanghai Sun-shine Chemical Technology), recombinant human TGFβ1 (240-B; R&D Systems), Alexa Fluor 555–conjugated rabbit IgG and Alexa Fluor 647–conjugated rabbit IgG (A32732 and A32733, respectively; Thermo Fisher Scientific), α-smooth muscle actin gene (ACTA2) (A2547) and Cy3-conjugated ACTA2 (C6198) (both from Sigma-Aldrich), horseradish peroxidase (HRP)–conjugated mouse IgG and HRP-conjugated rabbit IgG (7074 and 7076, respectively; both from Cell Signaling Technology), HRP-conjugated goat IgG (P0449; Dako North America), Alexa Fluor 488–conjugated phalloidin (A12379; Thermo Fisher Scientific), DAPI (0100-20; Southern Biotech), and antibodies targeted against phospho-Smad2/3 (ab52903) and Smad2/3 (ab63672) (both from Abcam), phospho-ERK (9101) and ERK (4695) (both from Cell Signaling Technology), phospho-p38 (4511) and p38 (8690) (both from Cell Signaling Technology), phospho-AKT (9271) and AKT (9272) (both from Cell Signaling Technology), cellular communication network (CCN) genes CCN1 (ab230987) and CCN2 (ab209780 and ab6992) (both from Abcam), procollagen-lysine, 2-oxoglutarate 5-dioxygenase 2 gene (PLOD2) (21214-1-AP; Proteintech), lysyl oxidase–like 2 gene (LOXL2) (NBP1-32954; Novus Biologicals), phospho-FAK (ab81298; Abcam), cadherin-11 gene (CDH11) (32-1700; Thermo Fisher Scientific), β-catenin (ab16051; Abcam), type I collagen (1310-01; Southern Biotech), phospho-Rb (8516; Cell Signaling Technology), β-actin (AC-15; Sigma-Aldrich), Alexa Fluor 647–conjugated CD45 (103123; BioLegend), Alexa Fluor 488–conjugated vimentin (ab154207; Abcam), and proliferating cell nuclear antigen (PCNA) (ab18197; Abcam).

Human skin biopsy samples. Human skin biopsy samples were obtained from the forearm of 5 patients with diffuse cutaneous SSc (2 women and 3 men, mean ± SD age 62.4 ± 8.1 years, mean ± SD modified Rodnan skin thickness score 14.8 ± 3.2 [scale 0–51]) with onset of skin sclerosis preceding the biopsy by 2 years. All of the patients were diagnosed as having diffuse cutaneous SSc based on clinical features and histologic findings, in accordance with the American College Rheumatology (ACR)/European League of Associations for Rheumatology (EULAR) criteria for SSc (14), and none of them had any other collagen diseases. In addition, skin biopsy samples were obtained from 3 healthy control subjects who were matched to the patients on the basis of sex and site and closely matched for age (1 woman and 2 men, mean ± SD age 58.3 ± 11.1 years).

Institutional approval was provided by the University of Tokyo, and written informed consent was obtained from all

subjects. The study protocols were approved by the institutional review board at Tokyo Medical and Dental University (approval no. M2016-168). Written informed consent was obtained from all patients.

Human dermal fibroblast cultures. Dermal fibroblasts from human skin biopsy specimens were analyzed in primary cultures using previously described methods (15). Briefly, fibroblasts were cultured in high-glucose Dulbecco's modified Eagle's medium (Sigma-Aldrich) supplemented with 10% fetal bovine serum (FBS), 100 units/ml penicillin, and 100 μg/ml streptomycin. Dermal fibroblasts were used between passages 3 and 6.

Bromodeoxyuridine (BrdU) proliferation assay in vitro. Human SSc fibroblasts were plated at 2,000 cells per well in 96-well plates. After serum starvation, fibroblasts were pretreated with palbociclib (a CDK4/6 inhibitor) or galunisertib (a TGFβR inhibitor) overnight, followed by treatment with 10 μ*M* BrdU for 24 hours. An enzyme-linked immunosorbent assay (ELISA) for measurement of BrdU uptake in the cells was performed in accordance with the manufacturer's instructions (11647229001 cell proliferation ELISA; Roche Applied Sciences).

Immunocytochemistry. Fibroblasts were fixed with 4% paraformaldehyde, permeabilized with 0.1% Triton X, blocked with 1% bovine serum albumin (BSA), and then stained with antibodies targeting ACTA2, followed by phalloidin and DAPI staining. For analysis of the ECM, fibroblasts were stained with antibodies targeting type I collagen or fibronectin, without permeabilization. Images were obtained using an FV10i confocal microscope (Olympus). Fluorescence intensity was quantified using ImageJ software (National Institutes of Health).

Western blotting. Protein samples (10 μg) were separated by sodium dodecyl sulfate–polyacrylamide gel electrophoresis and transferred onto a PVDF membrane. The blots were blocked with 5% BSA, and then incubated with primary antibodies, followed by secondary antibodies.

Mice. Mice were obtained from Charles River Japan. All animal experiments were approved by the Institutional Animal Care and Use Committee of Tokyo Medical and Dental University (approval no. A2019-281C) and were performed in accordance with institutional and national guidelines. Mice were housed 2–4 per cage in specific pathogen–free conditions on a 12-hour light/dark cycle at 20–26°C and 30–70% humidity. The mice were provided access to food and water ad libitum.

HOCl-induced dermal fibrosis in mice. Induction of dermal fibrosis with injections of HOCl in mice was performed as previously described (16). Six-week-old female BALB/c mice were injected intradermally with 250 μl of freshly prepared HOCl into 2 sites in the backs 5 days per week for 6 weeks. Phosphate buffered saline (PBS) was used as a control.

Bleomycin-induced fibrosis in mice. Bleomycin (Nippon Kayaku Co. Ltd.) was dissolved in PBS at a concentration of 0.5 mg/ml. Six-week-old C57BL/6 mice were injected intradermally with 100 μl of bleomycin into the back every day for 4 weeks, as previously described (17). PBS was used as a control.

In vivo administration of a CDK4/6 inhibitor and a TGFβR inhibitor in mice. Palbociclib (CDK4/6 inhibitor) was diluted in 0.5% methylcellulose. Galunisertib (TGFβR inhibitor) was diluted in 2% DMSO and 30% polyethylene glycol in deionized distilled water. Palbociclib (dosage of 20 mg/kg/day or 50 mg/kg/day) and/or galunisertib (dosage of 100 mg/kg/day) was orally administered to mice every day from day 0 in the concurrent treatment phase, and from day 21 onward in the early therapeutic treatment phase. In the late therapeutic (fibrosis reversal) treatment phase, palbociclib (dosage of 50 mg/kg/day) was orally administered to mice every day from day 42 onward for an additional 3 weeks. For the vehicle control group, the solvent without inhibitors, at the same dosages as used in the therapeutic groups, was administered orally.

The sample size was decided on the basis of our pilot experiments. Mice were randomly assigned to groups. The order of treatments was randomized. Mice were monitored for physical and behavioral abnormalities every day, to ensure that none of the animals surpassed the predefined humane end points, including development of respiratory distress, inability to eat, significant weight loss, and lying down. All of the mice were euthanized with an excess amount of pentobarbital. No mice were excluded from the analysis. Histologic analysis of skin tissue from the mice was conducted in a blinded manner.

Histologic analysis of dermal fibrosis in mice. Skin samples were collected from mice on day 21, day 42, or day 63 of HOCl-induced dermal fibrosis or on day 28 of bleomycin-induced fibrosis. The skin samples were fixed with 10% buffered formalin and embedded in paraffin. Hematoxylin and eosin–stained or Masson's trichrome–stained 5-μm sections of the skin tissue were examined (by AY and TS) in a blinded manner. Images were obtained using an Olympus BX50 microscope.

Immunohistochemistry. For immunohistochemical analyses of human skin biopsy samples obtained from patients with SSc, skin sections were stained with antibodies against phospho-Rb, followed by staining with secondary antibodies. In addition, skin sections were stained with antibodies targeting ACTA2 and CCN2, followed by staining with secondary antibodies. Images were obtained using an Olympus BX50 microscope. In addition, sections of the skin were stained with antibodies targeting CD45, vimentin, or PCNA, followed by staining with

secondary antibodies. Nuclei were stained with DAPI. Images were obtained using an Olympus FV10i confocal microscope.

Collagen measurement. Six-mm punch biopsy samples of skin from mice were hydrolyzed in 6*M* HCl at 95°C for 20 hours. Collagen content was quantified using a total collagen assay (QZBTOTCOL; QuickZyme) in accordance with the manufacturer's instructions.

Statistical analysis. Statistical analysis was conducted using GraphPad Prism version 5 software, with graphics created using Inkscape (https://inkscape.org). Results are expressed as the mean ± SD. Statistically significant differences were determined using one-way analysis of variance followed by Bonferroni's test for multiple comparisons. When only 2 groups were compared, the Mann–Whitney test was used. *P* values less than 0.05 were considered significant.

Data availability statement. The data that support the findings of this study are available upon request from the corresponding author.

RESULTS

Suppression of fibroblast proliferation and differentiation into myofibroblasts with a CDK4/6 inhibitor. To examine whether CDK4/6 activity is up-regulated in skin fibroblasts from SSc patients, we first determined the number of fibroblasts positive for phospho-Rb, a well-known indicator of CDK4/6 activity. In skin biopsy samples from patients with early SSc but not in those from healthy control subjects, increased numbers of phospho-Rb–positive spindle-shaped cells were detected (mean ± SD 6.9 ± 1.9 cells/high-power field [hpf] in SSc patients versus 0.6 ± 0.6 cells/hpf in healthy controls) (Figures 1A and B).

To examine whether CDK4/6 inhibition could suppress dermal fibrosis, we looked at the effects of a CDK4/6 inhibitor on human SSc dermal fibroblasts in vitro. The proliferation of SSc dermal fibroblasts in the presence of 10% FBS was suppressed by treatment with the CDK4/6 inhibitor palbociclib, in a dose-dependent manner, whereas in the presence of galunisertib, a TGFβR inhibitor, fibroblast proliferation was not altered (Figure 1C), similar to previously reported findings (18). Galunisertib was used as an inhibitor of TGFβR signaling because it is considered a safe, first-in-class small molecule that targets TGFβR,

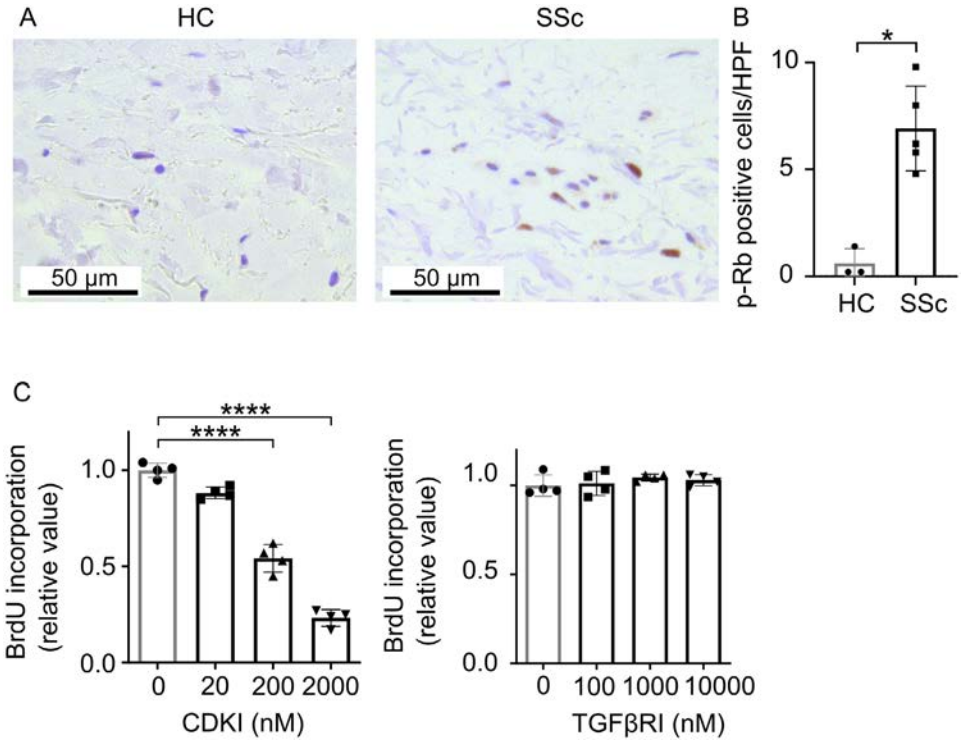

Figure 1. Suppressive effects of a cyclin-dependent kinase 4/6 inhibitor (CDKI) on proliferation of dermal fibroblasts from patients with systemic sclerosis (SSc). **A** and **B**, CDK4/6 activity was assessed using immunohistochemical staining of skin biopsy samples from healthy controls (HC) (n = 3) and patients with SSc (n = 5) (representative images shown) (**A**), with results expressed as the total number of phospho-Rb (p-Rb)–positive, spindle-shaped fibroblasts per high-power field (hpf) (**B**). * = $P < 0.05$. **C**, Bromodeoxyuridine (BrdU) uptake assays were performed to assess the proliferation of SSc fibroblasts following treatment with palbociclib, a CDK4/6 inhibitor, or galunisertib, a transforming growth factor β receptor inhibitor (TGFβRI). Cells were cultured in Dulbecco's modified Eagle's medium with 10% fetal bovine serum for 24 hours with or without overnight pretreatment with various doses of the CDK4/6 inhibitor or TGFβR inhibitor. Results are representative of 2 independent experiments. Bars show the mean ± SD of 4 samples per group. **** = $P < 0.0001$.

and clinical trials using galunisertib for the treatment of some cancers are ongoing.

We next examined the effect of CDK4/6 inhibition on the TGFβ-induced differentiation of fibroblasts into myofibroblasts in cultures of human SSc dermal fibroblasts. Immunocytochemical analyses revealed that the addition of TGFβ into the fibroblast cultures increased stress fiber formation, as evaluated with phalloidin staining, and also increased the expression of the α-smooth muscle actin gene ACTA2 and the production of extracellular type I collagen and fibronectin, indicating that the fibroblasts had differentiated into myofibroblasts (Supplementary Figure 1A, available on the *Arthritis & Rheumatology* website at https://onlinelibrary.wiley.com/doi/10.1002/art.42042). Treatment with the TGFβR inhibitor for 48 hours (early time point) suppressed the TGFβ-induced increase in stress fiber formation, ACTA2 expression, and production of extracellular type I collagen and fibronectin (Supplementary Figures 1A and C–F). However, treatment with the CDK4/6 inhibitor did not suppress the TGFβ-induced changes in differentiation of myofibroblasts from fibroblasts at this early time point.

Since we did not see any suppressive effect of the CDK4/6 inhibitor on the number of cells at the early time point, we next

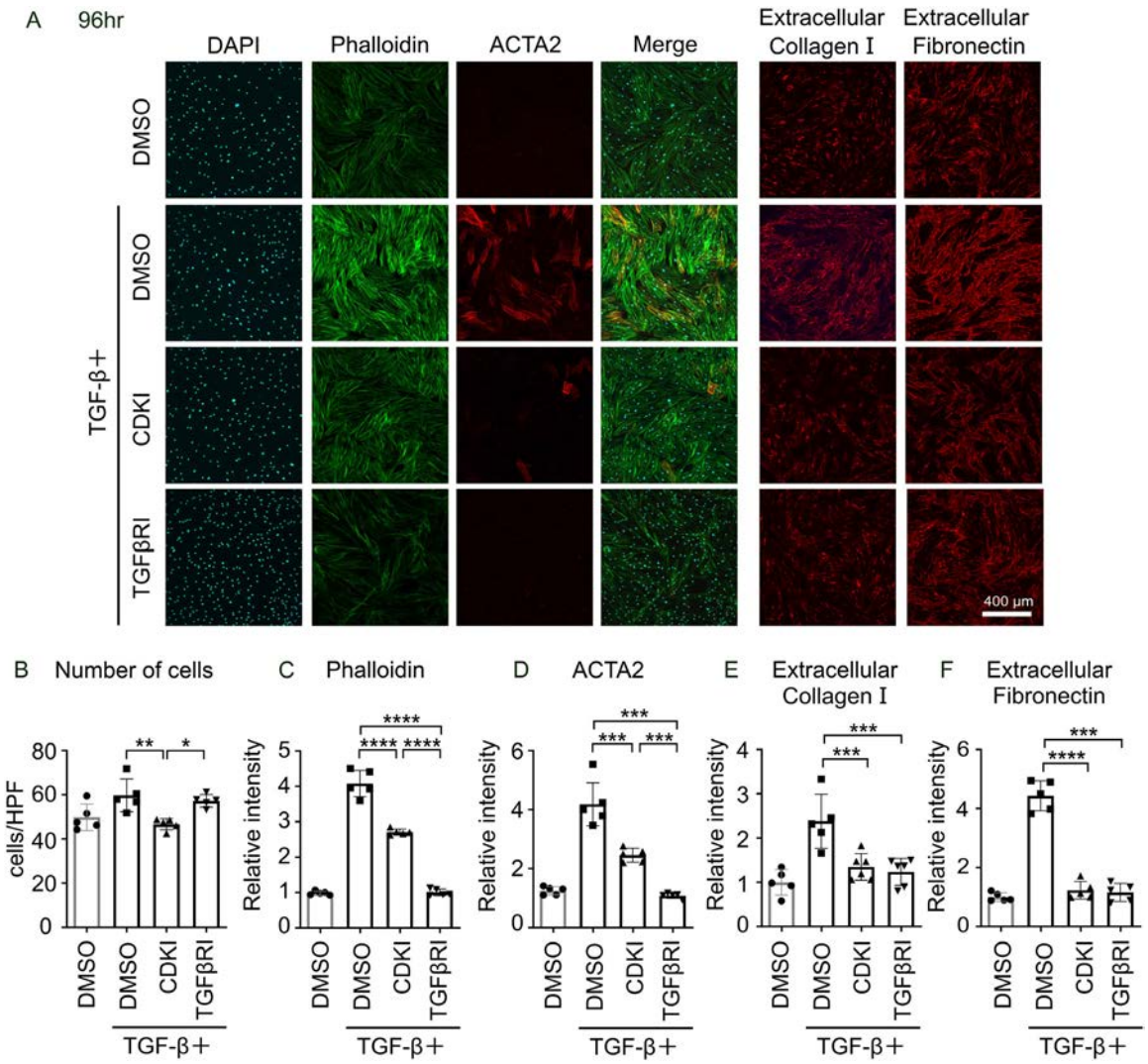

Figure 2. Suppressive effects of a CDK4/6 inhibitor on TGFβ-induced myofibroblast differentiation. **A**, Representative images show immunocytochemical staining for α-smooth muscle actin gene ACTA2, extracellular type I collagen, and extracellular fibronectin in cultures of human SSc dermal fibroblasts; nuclei were stained with DAPI, and stress-fiber staining was performed with phalloidin. SSc fibroblasts were cultured in the presence of 10 ng/ml TGFβ for 96 hours and then subjected to overnight pretreatment with 2 μ*M* CDK4/6 inhibitor or 10 μ*M* TGFβR inhibitor. DMSO was used as the vehicle control. **B–F**, The mean number of myofibroblasts per hpf (**B**) and the mean relative intensity of protein staining per area (**C–F**) were determined in cultures after 96 hours of stimulation with TGFβ and pretreatment with the CDK4/6 inhibitor or TGFβR inhibitor (n = 5 per group). Results are representative of >2 independent experiments. Bars show the mean ± SD. * = $P < 0.05$; ** = $P < 0.01$; *** = $P < 0.001$; **** = $P < 0.0001$. See Figure 1 for other definitions.

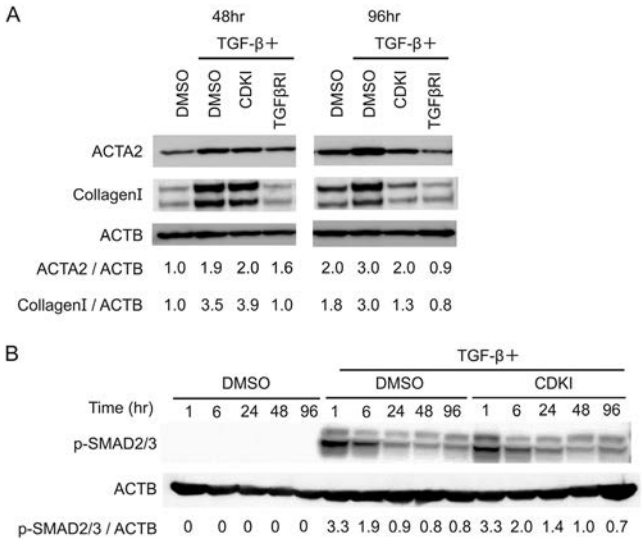

Figure 3. Effect of a CDK4/6 inhibitor on the expression of ACTA2 and type I collagen and the phosphorylation of Smad2/3 (p-Smad2/3). **A**, Western blots were analyzed for the expression of α-smooth muscle actin gene ACTA2 and type I collagen, relative to β-actin (ACTB), in TGFβ-treated SSc fibroblasts in the presence of 2 μ*M* CDK4/6 inhibitor or 10 μ*M* TGFβR inhibitor for 48 hours or 96 hours. **B**, Western blots were analyzed for the levels of p-Smad2/3 in TGFβ-treated SSc fibroblasts that were cultured in the presence of the CDK4/6 inhibitor for the indicated amounts of time. The band density of ACTB on the same blot was used as a loading control for densitometry analysis. DMSO was used as the vehicle control. Results are representative of >2 independent experiments. See Figure 1 for other definitions.

looked at the effect of the CDK4/6 inhibitor on the TGFβ-induced differentiation into myofibroblasts at a late time point (96 hours). At 96 hours, the number of differentiated cells per hpf was decreased in the presence of the CDK4/6 inhibitor (Figure 2B). In contrast to the results at the early time point, at the late time point, the CDK4/6 inhibitor suppressed the TGFβ-induced increase in stress fiber formation, ACTA2 expression, and production of extracellular type I collagen and fibronectin (Figures 2A and C–F).

We next examined whether the process of inhibition of TGFβ-induced myofibroblast differentiation differs in the presence of the CDK4/6 inhibitor when compared to the TGFβR inhibitor. Results of Western blot analysis revealed that, at both the early time point and the late time point, the TGFβR inhibitor suppressed the TGFβ-induced expression of ACTA2 and type I collagen (Figure 3A). At the early time point, the CDK4/6 inhibitor had no suppressive effect on the TGFβ-induced increase in expression of ACTA2 and type I collagen, whereas the phosphorylation of Rb was suppressed by the CDK4/6 inhibitor (Figure 3A; see also Supplementary Figure 2, available on the *Arthritis & Rheumatology* website at https://onlinelibrary.wiley.com/doi/10.1002/art.42042). At the late time point, the expression levels of ACTA2 and type I collagen were suppressed by treatment with the CDK4/6 inhibitor, though the level of the suppressive effect was milder with the CDK4/6 inhibitor than with the TGFβR inhibitor. These results suggest that the process of inhibition of myofibroblast differentiation differs between the CDK4/6 inhibitor and the TGFβR inhibitor.

We next investigated whether the suppressive effect of the CDK4/6 inhibitor on myofibroblast differentiation is mediated via inhibition of TGFβR signaling. Phosphorylation of Smad2/3 was observed within 1 hour after stimulation of the cells with TGFβ, and the amount of phosphorylated Smad2/3 declined over time (Figure 3B). Treatment with the CDK4/6 inhibitor did not suppress the TGFβ-induced Smad2/3 phosphorylation at any time point, ranging from 1 hour to 96 hours. These results suggest that the suppressive effects of the CDK4/6 inhibitor on myofibroblast differentiation are independent of TGFβ–Smad2/3 signaling.

Suppression of dermal fibrosis with a CDK4/6 inhibitor in mouse models of SSc. Given the compelling in vitro data demonstrating that a CDK4/6 inhibitor suppressed human dermal fibroblast proliferation and myofibroblast differentiation, we sought to determine whether CDK4/6 could be targeted in murine models of SSc. We chose to use the HOCl-induced dermal fibrosis model and bleomycin-induced dermal fibrosis model, since dermal fibroblast proliferation as well as collagen deposition is observed in both of these murine models, consistent with the characteristics of SSc in human patients (16,19).

In mice concurrently treated with a CDK4/6 inhibitor and injected subcutaneously with HOCl, we observed reductions in the HOCl-induced increase in dermal thickness (mean ± SD 246 ± 65 μm with 20 mg/kg and 218 ± 20 μm with 50 mg/kg CDK4/6 inhibitor versus 391 ± 120 μm with vehicle control). In addition, the amount of collagen in the fibrotic skin was reduced with the CDK4/6 inhibitor treatment (mean ± SD relative collagen amount 1.39 ± 0.13 with 20 mg/kg and 1.31 ± 0.12 with 50 mg/kg CDK4/6 inhibitor versus 1.86 ± 0.47 with vehicle control), though residual fibrosis was still evident (Figures 4A–D).

Immunohistochemical staining revealed that treatment with the CDK4/6 inhibitor suppressed the relative number of myofibroblasts (mean ± SD 2.82 ± 0.64 with 20 mg/kg and 2.09 ± 0.71 with 50 mg/kg CDK4/6 inhibitor versus 3.66 ± 0.55 with vehicle control) and the number of fibroblasts positive for CCN2 (a matricellular protein essential for skin fibrosis) (mean ± SD 7.33 ± 4.72 with 20 mg/kg and 5.90 ± 2.79 with 50 mg/kg CDK4/6 inhibitor versus 14.1 ± 2.24 with vehicle control). In addition, the CDK4/6 inhibitor suppressed the proportion of proliferating PCNA+ fibroblasts among total fibroblasts (mean ± SD 25.3 ± 13.7% with 20 mg/kg and 17.8 ± 7.7% with 50 mg/kg CDK4/6 inhibitor versus 46.2 ± 17.9% with vehicle control) and also suppressed the total number of fibroblasts (mean ± SD 49.8 ± 11.2 cells/hpf with 20 mg/kg and 34.0 ± 6.8 cells/hpf with 50 mg/kg CDK4/6 inhibitor versus 66.4 ± 19.3 cells/hpf with vehicle control) in the fibrotic skin lesions of mice (Figures 4E–I).

The suppressive effects of the CDK4/6 inhibitor on dermal fibrosis were also observed in the mouse model of bleomycin-induced dermal fibrosis, as demonstrated by a decrease in dermal thickness

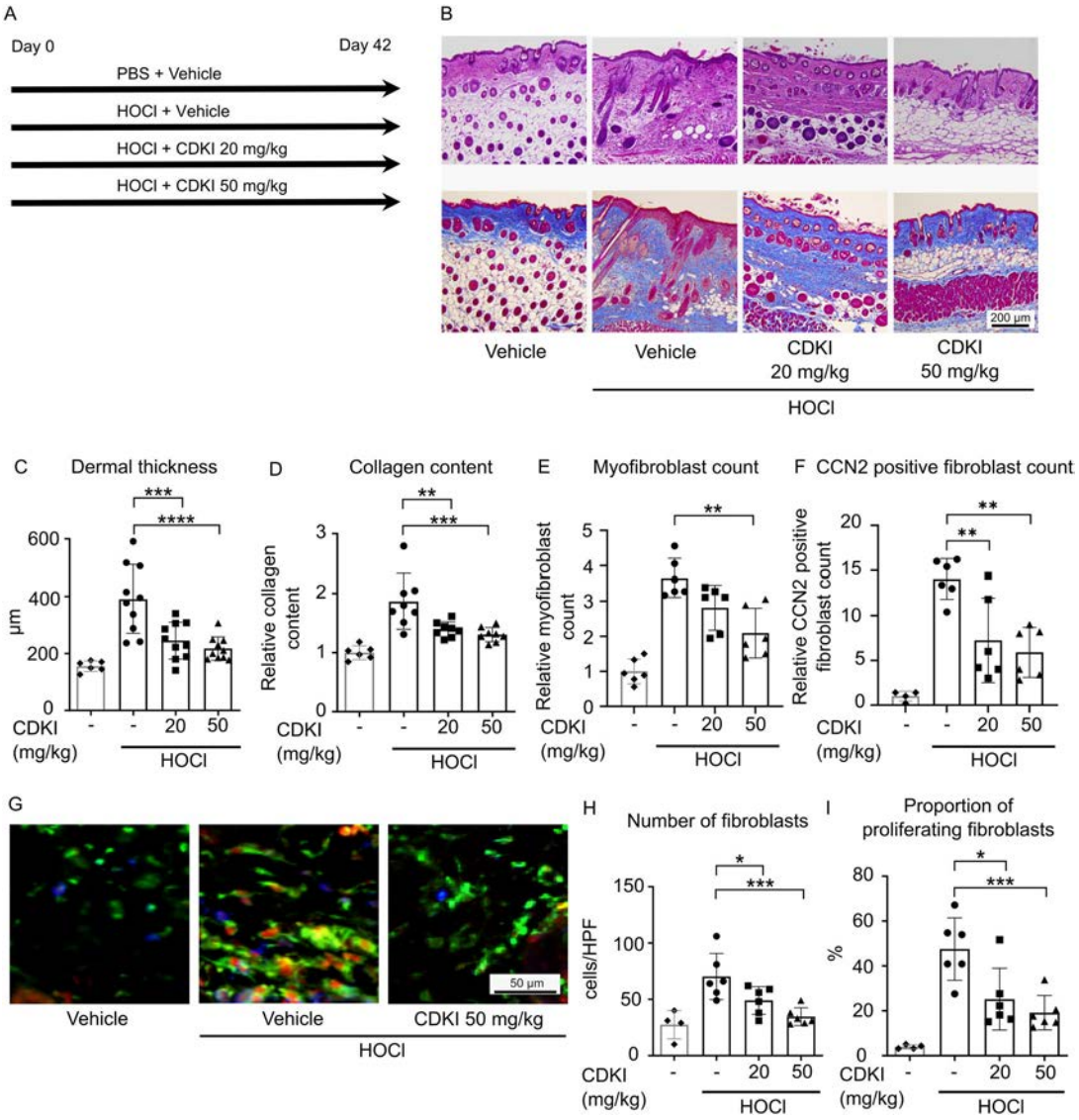

Figure 4. Amelioration of HOCl-induced dermal fibrosis by CDK4/6 inhibitor treatment in mice. **A**, Treatment scheme is shown for each CDK4/6 inhibitor–treated or vehicle-treated group of mice with HOCl-induced dermal fibrosis versus phosphate buffered saline (PBS)–injected, vehicle-treated mice as controls. **B–F**, Skin sections from mice were stained with hematoxylin and eosin (upper panels) or Masson's trichrome (lower panels) (representative images shown) (**B**) to assess dermal thickness (n = 10 per group in HOCl groups, n = 6 in no HOCl group) (**C**), collagen content (n = 8 per group in HOCl groups, n = 6 in no HOCl group) (**D**), the relative number of myofibroblasts (n = 6 per group) (**E**), and the relative number of cellular communication network 2 (CCN2)–positive, spindle-shaped cells (n = 6 per group) (**F**). Myofibroblasts were defined as α-smooth muscle actin gene ACTA2–positive, spindle-shaped cells. **G**, Representative images show immunohistologic staining of fibroblasts for proliferating cell nuclear antigen (PCNA) (red), CD45 (blue), and vimentin (green). **H** and **I**, The total number of fibroblasts per hpf (vimentin +CD45− cells) (n = 6 per group) (**I**) and the proportion of PCNA+ fibroblasts (PCNA+vimentin+CD45− cells) (n = 6 per group) were determined in skin sections from each group of mice. Results are representative of 2 independent experiments. Bars show the mean ± SD. * = $P < 0.05$; ** = $P < 0.01$; *** = $P < 0.001$; **** = $P < 0.0001$. See Figure 1 for other definitions.

with the CDK4/6 inhibitor at a dose of 50 mg/kg (mean ± SD 296 ± 44 μm with 20 mg/kg and 226 ± 44 μm with 50 mg/kg CDK4/6 inhibitor versus 284 ± 59 μm with vehicle control) and a decrease in collagen content with both doses of CDK4/6 inhibitor (mean ± SD relative collagen amount 1.58 ± 0.31 with 20 mg/kg and 1.47 ± 0.22 with 50 mg/kg CDK4/6 inhibitor versus 2.23 ± 0.29 with vehicle control) (Supplementary Figures 3A–D, available on the *Arthritis & Rheumatology* website at https://onlinelibrary.wiley.com/doi/10.1002/art.42042).

Consistent with these findings, in mice with bleomycin-induced dermal fibrosis, the CDK4/6 inhibitor suppressed the relative number of myofibroblasts in the 50 mg/kg group (mean ± SD 3.57 ± 1.06 with 20 mg/kg and 1.78 ± 0.73 with 50 mg/kg CDK4/6 inhibitor versus 3.52 ± 1.19 with vehicle

control), and also suppressed the number of fibroblasts positive for CCN2 (mean ± SD 4.23 ± 1.90 with 20 mg/kg and 2.66 ± 1.35 with 50 mg/kg CDK4/6 inhibitor versus 5.62 ± 1.67 with vehicle control), the total number of fibroblasts (mean ± SD 55.2 ± 10.2 cells/hpf with 20 mg/kg and 43.5 ± 15.3 cells/hpf with 50 mg/kg CDK4/6 inhibitor versus 68.0 ± 22.0 cells/hpf with vehicle control), and the proportion of proliferating PCNA+ fibroblasts (mean ± SD 13.9 ± 4.2% with 20 mg/kg and 6.6 ± 3.2% with 50 mg/kg CDK4/6 inhibitor versus 20.0 ± 7.5% with vehicle control) (Supplementary Figures 3E–I).

To address whether a CDK4/6 inhibitor would be effective in both the early and late phases of dermal fibrosis, we next tested 2 therapeutic treatment phases in the HOCl-induced dermal fibrosis model in mice (results in Supplementary Figure 4, available on the *Arthritis & Rheumatology* website at https://onlinelibrary.wiley.com/doi/10.1002/art.42042). For the early therapeutic treatment phase, the CDK4/6 inhibitor was started on day 21, when the dermal fibrosis had just started (Supplementary Figures 4A–E). For the late therapeutic treatment phase, mice were treated with the CDK4/6 inhibitor starting from day 42 and continuing for an additional 3 weeks, to evaluate the effects of reversal of fibrosis in established dermal fibrosis (Supplementary Figures 4F–J). Antifibrotic effects of the CDK4/6 inhibitor were demonstrated in the early therapeutic treatment phase, but not in the late therapeutic treatment phase, suggesting that the CDK4/6 inhibitor is effective in the early phase of dermal fibrosis.

Effectiveness of combination therapy with CDK4/6 inhibitor and TGFβR inhibitor in suppressing dermal fibrosis when compared to either monotherapy group. Since the therapeutic mode of action is different between CDK4/6 inhibitors and TGFβR inhibitors, we expected that the therapeutic effects of combination treatment with the 2 drugs would be additive. We chose to use a dose of 50 mg/kg for the CDK4/6 inhibitor in the combination regimen with the TGFβR inhibitor because the therapeutic effect on dermal fibrosis with a dose of 50 mg/kg of CDK4/6 inhibitor is only partial when administered as monotherapy and because we have shown that the adverse effects of CDK4/6 inhibitors, including development of neutropenia, are mild at a dose of 50 mg/kg (11). With regard to the TGFβR inhibitor, we chose a dose of 100 mg/kg; our preliminary data (20) suggested that the therapeutic effect on dermal fibrosis with a dose of 100 mg/kg of TGFβR inhibitor is only partial when administered as monotherapy (Supplementary Figures 5A and B, available on the *Arthritis & Rheumatology* website at https://onlinelibrary.wiley.com/doi/10.1002/art.42042). Moreover, the combination of the CDK4/6 inhibitor and TGFβR inhibitor at the concentrations used in vitro was not cytotoxic in human SSc dermal fibroblasts (Supplementary Figure 6, available on the *Arthritis & Rheumatology* website at https://onlinelibrary.wiley.com/doi/10.1002/art.42042).

When the mice with HOCl-induced dermal fibrosis were treated with the combination of the CDK4/6 inhibitor and TGFβR inhibitor, we observed further therapeutic effects in the combination group as compared to either monotherapy group or the vehicle control group, both in terms of a reduction in dermal thickness (mean ± SD 231 ± 47 μm with CDK4/6 inhibitor monotherapy, 227 ± 43 μm with TGFβR inhibitor monotherapy, and 330 ± 76 μm with vehicle control versus 164 ± 20 μm with the 2-drug combination) and a reduction in collagen content (mean ± SD relative collagen amount 1.39 ± 0.13 with CDK4/6 inhibitor monotherapy, 1.40 ± 0.10 with TGFβR inhibitor monotherapy, and 1.70 ± 0.31 with vehicle control versus 0.98 ± 0.23 with the 2-drug combination) in the fibrotic skin of mice (Supplementary Figures 7A–D, available on the *Arthritis & Rheumatology* website at https://onlinelibrary.wiley.com/doi/10.1002/art.42042). In addition, some values were lower in the combination therapy group compared to the CDK4/6 inhibitor monotherapy and TGFβR inhibitor monotherapy groups, including a decrease in the relative number of myofibroblasts (mean ± SD 2.42 ± 0.87 with CDK4/6 inhibitor monotherapy, 2.11 ± 0.63 with TGFβR inhibitor monotherapy, and 4.45 ± 0.67 with vehicle control versus 1.20 ± 0.35 with the 2-drug combination), the number of CCN2+ fibroblasts (mean ± SD 8.3 ± 3.2 with CDK4/6 inhibitor monotherapy, 10.8 ± 5.0 with TGFβR inhibitor monotherapy, and 23.4 ± 2.2 with vehicle control versus 5.2 ± 1.6 with the 2-drug combination), the total number of fibroblasts (mean ± SD 34.0 ± 6.6 cells/hpf with CDK4/6 inhibitor monotherapy, 63.4 ± 25.4 cells/hpf with TGFβR inhibitor monotherapy, and 76.6 ± 27.4 cells/hpf with vehicle control versus 33.3 ± 9.2 cells/hpf with the 2-drug combination), and the proportion of proliferating PCNA+ fibroblasts among total fibroblasts (mean ± SD 17.8 ± 4.2% with CDK4/6 inhibitor monotherapy, 20.6 ± 9.4% with TGFβR inhibitor monotherapy, and 40.3 ± 12.1% with vehicle control versus 7.5 ± 2.4% with the 2-drug combination) (Supplementary Figures 7E–I). These results indicate that the therapeutic effects of the CDK4/6 inhibitor and the TGFβR inhibitor on dermal fibroblasts were observed additively in vivo.

Suppression of TGFβ-induced expression of CCN2 and CDH11 with the CDK4/6 inhibitor. As a final experiment, we examined the effects of the CDK4/6 inhibitor on noncanonical TGFβ signaling, such as its effects on MAPKs and phosphatidylinositol 3-kinase (PI3K)/AKT. The CDK4/6 inhibitor did not suppress the TGFβ-induced phosphorylation of ERK, p38, and AKT (Figure 5A).

These results suggest that the suppressive effects of the CDK4/6 inhibitor on myofibroblast differentiation are independent of TGFβ canonical and noncanonical signaling and that the CDK4/6 inhibitor may inhibit secondary TGFβ signaling, such as mechanotransduction and cell–cell contact. Thus, we evaluated the effects of the CDK4/6 inhibitor on pathways of mechanotransduction, including phosphorylation of FAK (p-FAK) and expression of key molecules such as CCN1, CCN2, PLOD2, and LOXL2 (21). The CDK4/6 inhibitor suppressed the TGFβ-induced

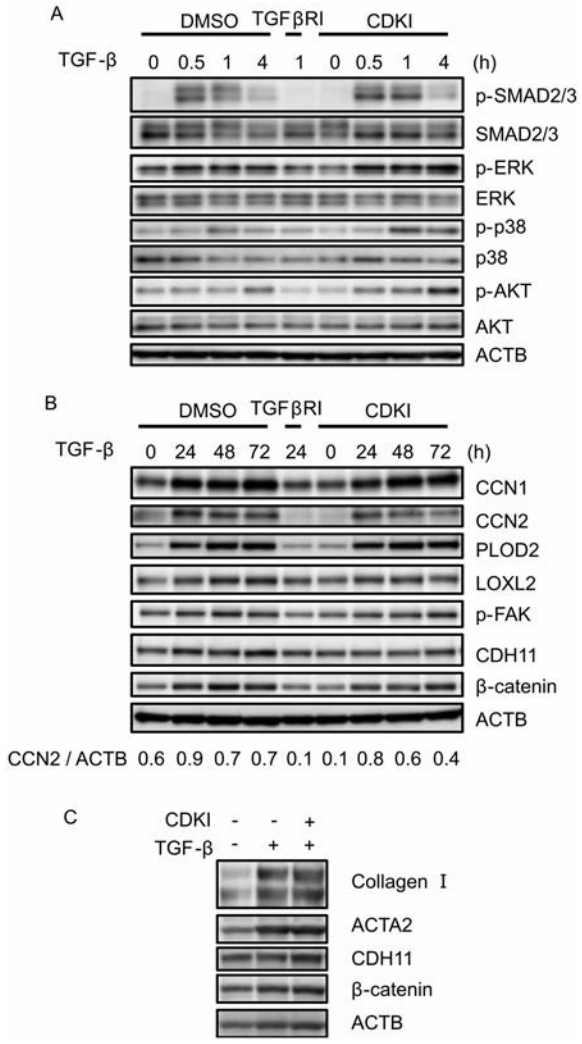

Figure 5. Effect of CDK4/6 inhibitor treatment on TGFβ canonical and noncanonical signals, and on molecules important for myofibroblast differentiation. **A**, Western blots were analyzed for TGFβ canonical and noncanonical signals in TGFβ-treated human SSc dermal fibroblasts in the presence of 2 μ*M* CDK4/6 inhibitor or 10 μ*M* TGFβR inhibitor for the indicated amounts of time. **B**, Western blots were analyzed for expression of molecules important for myofibroblast differentiation in TGFβ-treated SSc fibroblasts in the presence of 2 μ*M* CDK4/6 inhibitor or 10 μ*M* TGFβR inhibitor for the indicated amounts of time. **C**, Western blots were analyzed for expression of type I collagen, α-smooth muscle actin gene ACTA2, cadherin-11 gene CDH11, and β-catenin in TGFβ-treated SSc fibroblasts, with the cells plated at confluence density and cultured in the presence of 2 μ*M* CDK4/6 inhibitor for 96 hours. In all blots, β-actin (ACTB) was used as a loading control. Results are representative of >2 independent experiments. See Figure 1 for other definitions.

expression of CCN2 and LOXL2 but not CCN1, PLOD2, and p-FAK (Figure 5B; see also Supplementary Figure 8, available on the *Arthritis & Rheumatology* website at https://onlinelibrary.wiley.com/doi/10.1002/art.42042).

Cell density and cell–cell contact are important factors in the TGFβ-induced differentiation of myofibroblasts. We therefore investigated whether CDK4/6 inhibitor treatment suppresses myofibroblast differentiation via inhibition of cell proliferation, thereby affecting cell–cell contact. To achieve this, we examined the effects of the CDK4/6 inhibitor on the expression of CDH11, an important cadherin for myofibroblast differentiation, and its interacting partner, β-catenin. The CDK4/6 inhibitor suppressed the TGFβ-induced expression of both CDH11 and β-catenin (Figure 5B). Furthermore, the suppressive effects of the CDK4/6 inhibitor disappeared when the cells were plated at a confluence density that allowed for cell–cell contact (a threshold that had already been established before initiation of the CDK4/6 inhibitor treatment) (Figure 5C), indicating that this CDK4/6 inhibitor has an important effect on the differentiation of myofibroblasts, acting via its inhibition of cell proliferation, which thereby affects cell–cell contact.

DISCUSSION

In this study, we found that inhibition of the cell cycle could be a novel therapeutic strategy in SSc. CDK4/6 inhibitor treatment suppressed myofibroblast differentiation and ECM production as well as the proliferation of fibroblasts, without interfering with TGFβ canonical Smad2/3 and noncanonical signaling. In vivo, the CDK4/6 inhibitor suppressed dermal fibrosis when administered as monotherapy. In addition, the combination therapy with a TGFβR inhibitor resulted in further amelioration of dermal fibrosis compared to either monotherapy group. Mechanistically, the CDK4/6 inhibitor suppressed the expression of the matricellular protein CCN2 and the cell adhesion molecule CDH11, both of which are important for myofibroblast differentiation and fibrosis. These results indicate that CDK4/6 inhibitors could be novel agents for the treatment of SSc, and that CDK4/6 inhibitors may be used in combination with TGFβR inhibitors.

Our results indicate that the effect of the CDK4/6 inhibitor on myofibroblast differentiation was independent of Smad2/3 signaling, which is a major TGFβ pathway in the promotion of dermal fibrosis. The suppressive effect of the CDK4/6 inhibitor on TGFβ-induced myofibroblast differentiation was not observed in the cultures after 48 hours but was evident in the cultures at 96 hours, at which point cell–cell contact was increased. It has been reported that cell–cell contact plays a crucial role in dermal fibrosis. For example, expression of CDH11 in fibroblasts was found to be increased following their differentiation into myofibroblasts, and this contributed to myofibroblast adhesion and contractility (22). In in vivo mouse models of SSc, deficiency of CDH11 or blockade with monoclonal antibodies suppressed dermal fibrosis (23,24). Consistent with these results, our findings showed that the CDK4/6 inhibitor suppressed the TGFβ-induced expression of CDH11 and its interacting partner, β-catenin (Figure 5B). Furthermore, the CDK4/6 inhibitor was no more effective, at least in vitro, when the treatment was started in culture conditions in which the cells were allowed to reach confluence (when cell–cell contact

had already been established) (Figure 5C). The inhibition of cell–cell contact accompanied by the reduction in the number of fibroblasts might be one of the mechanisms by which the CDK4/6 inhibitor suppresses myofibroblast differentiation and dermal fibrosis in vivo.

The inhibition of noncanonical TGFβ pathways could also be a possible mechanism by which the CDK4/6 inhibitor suppresses myofibroblast differentiation and dermal fibrosis. While the major pathway of TGFβ involved in the promotion of tissue fibrosis is Smad2/3 signaling, non-Smad2/3 pathways, including ERK (25), p38 (24), JNK (26), PI3K/AKT/ mechanistic target of rapamycin (27), JAK/STAT (28), RhoA/Rho kinase (29), and AMP-activated protein kinase (30), have also been shown to be involved in fibrosis (31). We demonstrated that the CDK4/6 inhibitor did not interfere with ERK, p38, and PI3K/AKT signals.

Moreover, our data showed that the CDK4/6 inhibitor suppressed the TGFβ-induced expression of molecules important for mechanotransduction, such as CCN2 (32). CCN2 is a matricellular protein that coordinates the signaling among the ECM, secreted proteins, and cell surface receptors important for fibrosis (21). Recent studies using CCN2 gene–knockout and anti-CCN2 monoclonal antibodies in a mouse model of SSc revealed that CCN2 is essential for skin fibrosis and a promising drug target for the prevention of fibrosis (33,34). The inhibition of CCN2 by the CDK4/6 inhibitor may also contribute to the antifibrotic effects of the CDK4/6 inhibitor.

Our previous data have suggested that fibroblasts are more sensitive to CDK4/6 inhibitors than are immune cells, including neutrophils and lymphocytes (11). In a mouse model of rheumatoid arthritis, the decrease in numbers of peripheral neutrophils elicited by treatment with 50 mg/kg CDK4/6 inhibitor was mild, in contrast to the clear amelioration of arthritis. In vitro, the antigen-specific proliferation of lymph node–derived cells from mice with arthritis was not suppressed by treatment with a CDK4/6 inhibitor when used in a concentration that suppressed fibroblast proliferation. The decreased numbers of proliferating fibroblasts and myofibroblasts following treatment with a CDK4/6 inhibitor in our mouse model of SSc indicate that fibroblasts are the major targeted cells of CDK4/6 inhibitors in SSc.

We have demonstrated that palbociclib at a concentration of 2 μ*M* in vitro has antifibrotic effects. Moreover, in vivo, palbociclib was observed to exert prophylactic effects as well as early-phase therapeutic effects. Palbociclib could not reverse dermal fibrosis in the late phase of treatment, which is consistent with our observations in clinical practice. Although palbociclib is highly selective for CDK4/6, it may affect other CDKs at a higher concentration. Previously, in a study by Wei et al, the findings revealed that CDK5, an atypical CDK that interacts with p35 rather than cyclin, was activated in SSc and that one of the pan-CDK inhibitors, roscovitine, suppressed TGFβ-mediated fibrotic processes via inhibition of CDK5/p35 (35). The involvement of CDK5/p35 in the antifibrotic effects mediated by palbociclib is unlikely, since the inhibitory concentration of palbociclib against cell-free CDK5 is >10 μ*M*, compared to 0.26 μ*M* against CDK4/6 (36).

Limitations of this study include the inability of in vitro experiments that use human SSc dermal fibroblasts and in vivo experiments that use mouse models of SSc to fully recapitulate all aspects of the pathogenesis of human SSc. In addition, we cannot exclude the possible contribution of in vitro and in vivo off-target effects of palbociclib when used as a CDK4/6 inhibitor.

Considering the therapeutic effects observed in our preclinical study and the safety profile of CDK4/6 inhibitors in the treatment of breast cancer, a clinical trial of CDK4/6 inhibitors in patients with SSc would be warranted to confirm the effects of this therapeutic strategy in human SSc.

ACKNOWLEDGMENTS

We thank Dr. Frederic Batteux for providing the protocol for the HOCl mouse model. We thank Hidemi Kasahara, Katsuko Yamasaki, Naoko Fujita, Yoji Komiya, Yasuhiro Tagawa, Seiji Noda, and Junko Yagita for technical assistance.

AUTHOR CONTRIBUTIONS

All authors were involved in drafting the article or revising it critically for important intellectual content, and all authors approved the final version to be published. Dr. Yasuda had full access to all of the data in the study and takes responsibility for the integrity of the data and the accuracy of the data analysis.

Study conception and design. Mizoguchi, Yasuda, Kohsaka.
Acquisition of data. Yamamoto, Saito, Asano, Sato.
Analysis and interpretation of data. Yamamoto, Saito, Hosoya, Kawahata, Asano, Sato, Mizoguchi, Yasuda, Kohsaka.

REFERENCES

1. Ho YY, Lagares D, Tager AM, Kapoor M. Fibrosis—a lethal component of systemic sclerosis. Nat Rev Rheumatol 2014;10:390–402.
2. Kowal-Bielecka O, Fransen J, Avouac J, Becker M, Kulak A, Allanore Y, et al. Update of EULAR recommendations for the treatment of systemic sclerosis. Ann Rheum Dis 2017;76:1327–39.
3. Tashkin DP, Roth MD, Clements PJ, Furst DE, Khanna D, Kleerup EC, et al. Mycophenolate mofetil versus oral cyclophosphamide in scleroderma-related interstitial lung disease (SLS II): a randomised controlled, double-blind, parallel group trial. Lancet Respir Med 2016;4:708–19.
4. Lafyatis R. Transforming growth factor β—at the centre of systemic sclerosis. Nat Rev Rheumatol 2014;10:706–19.
5. Rice LM, Padilla CM, McLaughlin SR, Mathes A, Ziemek J, Goummih S, et al. Fresolimumab treatment decreases biomarkers and improves clinical symptoms in systemic sclerosis patients. J Clin Invest 2015;125:2795–807.
6. Denton CP, Merkel PA, Furst DE, Khanna D, Emery P, Hsu VM, et al. Recombinant human anti-transforming growth factor β1 antibody therapy in systemic sclerosis: a multicenter, randomized, placebo-controlled phase I/II trial of CAT-192. Arthritis Rheum 2007;56:323–33.
7. Sappino AP, Masouye I, Saurat JH, Gabbiani G. Smooth muscle differentiation in scleroderma fibroblastic cells. Am J Pathol 1990;137:585–91.

8. Van Caam A, Vonk M, van den Hoogen F, van Lent P, van der Kraan P. Unraveling SSc pathophysiology; the myofibroblast. Front Immunol 2018;9:1–22.
9. Rajkumar VS, Howell K, Csiszar K, Denton CP, Black CM, Abraham DJ. Shared expression of phenotypic markers in systemic sclerosis indicates a convergence of pericytes and fibroblasts to a myofibroblast lineage in fibrosis. Arthritis Res Ther 2005;7:R1113–23.
10. Thill M, Schmidt M. Management of adverse events during cyclin-dependent kinase 4/6 (CDK4/6) inhibitor-based treatment in breast cancer. Ther Adv Med Oncol 2018;10:1–12.
11. Hosoya T, Iwai H, Yamaguchi Y, Kawahata K, Miyasaka N, Kohsaka H. Cell cycle regulation therapy combined with cytokine blockade enhances antiarthritic effects without increasing immune suppression. Ann Rheum Dis 2016;75:253–9.
12. Weiss A, Neubauer MC, Yerabolu D, Kojonazarov B, Schlueter BC, Neubert L, et al. Targeting cyclin-dependent kinases for the treatment of pulmonary arterial hypertension. Nat Commun 2019;10:2204.
13. Pabla N, Gibson AA, Buege M, Ong SS, Li L, Hu S, et al. Mitigation of acute kidney injury by cell-cycle inhibitors that suppress both CDK4/6 and OCT2 functions. Proc Natl Acad Sci U S A 2015;112:5231–6.
14. Van den Hoogen F, Khanna D, Fransen J, Johnson SR, Baron M, Tyndall A, et al. 2013 classification criteria for systemic sclerosis: an American College of Rheumatology/European League Against Rheumatism collaborative initiative. Arthritis Rheum 2013;65:2737–47.
15. Asano Y, Ihn H, Yamane K, Kubo M, Tamaki K. Impaired Smad7-Smurf–mediated negative regulation of TGF-β signaling in scleroderma fibroblasts. J Clin Invest 2004;113:253–64.
16. Servettaz A, Goulvestre C, Kavian N, Nicco C, Guilpain P, Chereau C, et al. Selective oxidation of DNA topoisomerase 1 induces systemic sclerosis in the mouse. J Immunol 2009;182:5855–64.
17. Yamamoto T, Takagawa S, Katayama I, Yamazaki K, Hamazaki Y, Shinkai H, et al. Animal model of sclerotic skin. I: Local injections of bleomycin induce sclerotic skin mimicking scleroderma. J Invest Dermatol 1999;112:456–62.
18. Serova M, Tijeras-Raballand A, dos Santos C, Albuquerque M, Paradis V, Zeuzillet C, et al. Effects of TGF-β signalling inhibition with galunisertib (LY2157299) in hepatocellular carcinoma models and in ex vivo whole tumor tissue samples from patients. Oncotarget 2015; 6:21614–27.
19. Batteux F, Kavian N, Servettaz A. New insights on chemically induced animal models of systemic sclerosis. Curr Opin Rheumatol 2011;23: 511–8.
20. Yingling JM, McMillen WT, Yan L, Huang H, Sawyer JS, Graff J, et al. Preclinical assessment of galunisertib (LY2157299 monohydrate), a first-in-class transforming growth factor-β receptor type I inhibitor. Oncotarget 2018;9:6659–77.
21. Leask A. Conjunction junction, what's the function? CCN proteins as targets in fibrosis and cancers. Am J Physiol Cell Physiol 2020;318: C1046–54.
22. Hinz B, Pittet P, Smith-Clerc J, Chaponnier C, Meister JJ. Myofibroblast development is characterized by specific cell-cell adherens junctions. Mol Biol Cell 2004;15:4310–20.
23. Noss EH, Watts GF, Zocco D, Keller TL, Whitman M, Blobel CP, et al. Evidence for cadherin-11 cleavage in the synovium and partial characterization of its mechanism. Arthritis Res Ther 2015;17:126.
24. Pedroza M, Welschhans RL, Agarwal SK. Targeting of cadherin-11 decreases skin fibrosis in the tight skin-1 mouse model. PLoS One 2017;12:1–9.
25. Beyer C, Zenzmaier C, Palumbo-Zerr K, Mancuso R, Distler A, Dees C, et al. Stimulation of the soluble guanylate cyclase (sGC) inhibits fibrosis by blocking non-canonical TGFβ signalling. Ann Rheum Dis 2015;74:1408–16.
26. Reich N, Tomcik M, Zerr P, Lang V, Dees C, Avouac J, et al. Jun N-terminal kinase as a potential molecular target for prevention and treatment of dermal fibrosis. Ann Rheum Dis 2012;71:737–45.
27. Liang M, Lv J, Chu H, Wang J, Chen X, Zhu X, et al. Vertical inhibition of PI3K/Akt/mTOR signaling demonstrates in vitro and in vivo antifibrotic activity. J Dermatol Sci 2014;76:104–11.
28. Dees C, Tomcik M, Palumbo-Zerr K, Distler A, Beyer C, Lang V, et al. JAK-2 as a novel mediator of the profibrotic effects of transforming growth factor β in systemic sclerosis. Arthritis Rheum 2012;64: 3006–15.
29. Bei Y, Hua-Huy T, Nicco C, Duong-Quy S, Le-Dong NN, Tiev KP, et al. RhoA/Rho-kinase activation promotes lung fibrosis in an animal model of systemic sclerosis. Exp Lung Res 2016;42:44–55.
30. Rangarajan S, Bone NB, Zmijewska AA, Jiang S, Park DW, Bernard K, et al. Metformin reverses established lung fibrosis in a bleomycin model. Nat Med 2018;1:1.
31. Finnson KW, Almadani Y, Philip A. Non-canonical (non-SMAD2/3) TGF-β signaling in fibrosis: mechanisms and targets. Semin Cell Dev Biol 2020;101:115–22.
32. Gyftaki-Venieri DA, Abraham DJ, Ponticos M. Insights into myofibroblasts and their activation in scleroderma: opportunities for therapy? Curr Opin Rheumatol 2018;30:581–7.
33. Liu S, Shi-wen X, Abraham DJ, Leask A. CCN2 is required for bleomycin-induced skin fibrosis in mice. Arthritis Rheum 2011;63: 239–46.
34. Makino K, Makino T, Stawski L, Lipson KE, Leask A, Trojanowska M. Anti-connective tissue growth factor (CTGF/CCN2) monoclonal antibody attenuates skin fibrosis in mice models of systemic sclerosis. Arthritis Res Ther 2017;19:134.
35. Wei J, Marangoni RG, Fang F, Wang W, Huang J, Distler JH, et al. The non-neuronal cyclin-dependent kinase 5 is a fibrotic mediator potentially implicated in systemic sclerosis and a novel therapeutic target. Oncotarget 2018;9:10294–306.
36. Klein ME, Kovatcheva M, Davis LE, Tap WD, Koff A. CDK4/6 inhibitors: the mechanism of action may not be as simple as once thought. Cancer Cell 2018;34:9–20.

Arthritis & Rheumatology
Vol. 74, No. 5, May 2022, pp 871–881
DOI 10.1002/art.42033

American College of Rheumatology
Empowering Rheumatology Professionals

Impaired Mitochondrial Transcription Factor A Expression Promotes Mitochondrial Damage to Drive Fibroblast Activation and Fibrosis in Systemic Sclerosis

Xiang Zhou, Thuong Trinh-Minh, Cuong Tran-Manh, Andreas Gießl, Christina Bergmann, Andrea-Hermina Györfi, Georg Schett, and Jörg H. W. Distler

Objective. Mitochondrial transcription factor A (TFAM) controls the transcription of core proteins required for mitochondrial homeostasis. This study was undertaken to investigate changes in TFAM expression in systemic sclerosis (SSc), to analyze mitochondrial function, and to evaluate the consequences for fibroblast activation.

Methods. TFAM expression was analyzed by immunofluorescence and Western blotting. The effects of TFAM knockout were investigated in cultured fibroblasts and in murine models of bleomycin-induced skin fibrosis, bleomycin-induced lung fibrosis, and skin fibrosis induced by overexpression of constitutively active transforming growth factor β type I receptor (TGFβRI).

Results. TFAM expression was down-regulated in fibroblasts in SSc skin and in cultured SSc fibroblasts. The down-regulation of TFAM was associated with decreased mitochondrial number and accumulation of damaged mitochondria with release of mitochondrial DNA (mtDNA), accumulation of deletions in mtDNA, metabolic alterations with impaired oxidative phosphorylation, and release of the mitokine GDF15. Normal fibroblasts subjected to long-term, but not acute, exposure to TGFβ mimicked SSc fibroblasts, with down-regulation of TFAM and accumulation of mitochondrial damage. Down-regulation of TFAM promoted fibroblast activation with up-regulation of fibrosis-relevant Gene Ontology terms in RNA-Seq, partially in a reactive oxygen species–dependent manner. Mice with fibroblast-specific knockout of Tfam were prone to fibrotic tissue remodeling, with fibrotic responses even to NaCl instillation and enhanced sensitivity to bleomycin injection and overexpression of constitutively active TGFβRI. TFAM knockout fostered Smad3 signaling to promote fibroblast activation.

Conclusion. Alterations in the key mitochondrial transcription factor TFAM in response to prolonged activation of TGFβ and associated mitochondrial damage induce transcriptional programs that promote fibroblast-to-myofibroblast transition and drive tissue fibrosis.

INTRODUCTION

Systemic sclerosis (SSc) is a chronic fibrosing connective tissue disease of unknown etiology that affects the skin and various internal organs. A major hallmark of SSc is the aberrant activation of fibroblasts with uncontrolled release of collagens and other components of the extracellular matrix (1,2). The activated phenotype of fibroblasts from SSc patients is at least in part mediated by cell-intrinsic mechanisms, as SSc fibroblasts maintain their activated phenotype in the absence of exogenous stimuli under culture conditions (3–6). The activation of fibroblasts and the release of extracellular matrix are driven by a set of profibrotic cytokines and growth factors (7–10). The molecular mechanisms underlying this persistent activation of fibroblasts in SSc remain incompletely understood.

Mitochondria descend from ancient bacteria that have been internalized by eukaryotic cells to form an endosymbiotic

Supported by the German Research Foundation (grants DI 1537/12-1, DI 1537/13-1, DI 1537/14-1, DI 1537/17-1, and DI 1537/20-1, SFB CRC1181 project C01, and SFB TR221 project 324392634 [B04]), the IZKF in Erlangen (grant A79), ELAN (grant 21-07-23-1 to Dr. Györfi), the BMBF, the MASCARA program, TP 2 (award 01EC1903A), and a Career Support Award of Medicine of the Ernst Jung Foundation. Xiang Zhou's work was supported by the China Scholarship Council (CSC award 201708420139).

Xiang Zhou, MSc, Thuong Trinh-Minh, MSc, Cuong Tran-Manh, MSc, Andreas Gießl, PhD, Christina Bergmann, MD, Andrea-Hermina Györfi, MD, Georg Schett, MD, Jörg H. W. Distler, MD: Friedrich–Alexander University Erlangen–Nuremberg and University Hospital Erlangen, Erlangen, Germany.

Author disclosures are available at https://onlinelibrary.wiley.com/action/downloadSupplement?doi=10.1002%2Fart.42033&file=art42033-sup-0001-Disclosureform.pdf.

Address correspondence to Jörg H. W. Distler, MD, Department of Internal Medicine 3 - Rheumatology and Immunology, Friedrich–Alexander University Erlangen–Nuremberg (FAU) and University Hospital Erlangen, Erlangen, Germany. Email: joerg.distler@uk-erlangen.de.

Submitted for publication May 13, 2021; accepted in revised form November 18, 2021.

relationship (11). After billions of years of evolution, mitochondria has preserved an independent mitochondrial genome (mitochondrial DNA [mtDNA]), which encodes for proteins involved in oxidative phosphorylation (OXPHOS) (12). Mitochondria are multifunctional cellular organelles that are crucially required for multiple processes in all eukaryotic cells. Mitochondria are best known as the powerhouses of the cell (13). They generate ATP and acetyl-coenzyme A by aerobic respiration and by the citric acid cycle (14). Mitochondria also play an important role in reactive oxygen species (ROS) homeostasis. Dysfunction of mitochondria can result in leakage of free electrons from the electron transport chain and massive generation of ROS (15,16). Additional functions include regulation of calcium homeostasis, thermogenesis, and iron metabolism (17–19). Recent studies highlight the fact that mitochondria also release small peptides with endocrine effects, so-called mitokines, to exert regulatory metabolic and immunologic functions at distant sites of the body (20,21).

Many of these mitochondrial functions are at least in part regulated by mitochondrial transcription factor A (TFAM). TFAM regulates the transcription of core genes of mitochondrial biogenesis and mtDNA replication (22,23). TFAM is encoded by the nuclear genome and thereby serves as a gatekeeper of the nuclear genome for mitochondrial fate (22). Mitochondrial stress induces the expression of TFAM with enhanced translocation of TFAM from the nucleus to mitochondria to promote the transcription of the mitochondrial genome and restore mitochondrial homeostasis (24). Non-conditional knockout of TFAM is fatal to the embryo, and TFAM-deficient cells demonstrate signs of mitochondrial damage and metabolic stress (25,26).

Several factors implicated in the pathogenesis of SSc, such as hypoxia or cellular stress in response to chronic inflammation, can induce mitochondrial damage and metabolic reprogramming (27–31). Moreover, in situations of chronic stress, mitochondrial damage can be self-amplifying. Damaged mitochondria release ROS, which further aggravates the damage of mitochondria (32). In chronic diseases with persistent inflammation and hypoxia, the ongoing mitochondrial damage can overwhelm endogenous compensation mechanisms and may thus result in chronic and progressive accumulation of functionally impaired mitochondria. Indeed, mitochondrial damage has been reported in idiopathic pulmonary fibrosis and connective tissue disease–associated interstitial lung disease (ILD) as well as in experimental models of ILD (33,34). Mitochondrial damage not only profoundly affects cellular and systemic metabolism, but can also induce inflammation, e.g., via the release of mtDNA (35–39). However, the role of TFAM and associated mitochondrial damage with regard to fibroblast activation in SSc has not been investigated.

In the present study, we aimed to test the hypothesis that alterations in the key mitochondrial transcription factor TFAM and associated mitochondrial damage induce transcriptional programs that promote fibroblast-to-myofibroblast transition and drive the progression of tissue fibrosis.

MATERIALS AND METHODS

Study methods. Detailed information on materials and methods is provided in the Supplementary Methods, available on the *Arthritis & Rheumatology* website at https://onlinelibrary.wiley.com/doi/10.1002/art.42033. Briefly, experiments were conducted using both healthy and SSc human dermal fibroblasts and mouse models of fibrosis. Fibroblasts were analyzed by electron microscopy and Western blot analysis. For some experiments, fibroblasts were stimulated with 10 ng/ml of recombinant TGFβ. Mice with fibroblast-specific knockout of Tfam were generated in order to study the effects of Tfam deletion on tissue fibrosis. Three murine models of fibrosis were examined: bleomycin-induced skin fibrosis, skin fibrosis induced by overexpression of constitutively active TGFβ type I receptor (TGFβRI), and bleomycin-induced pulmonary fibrosis. For TFAM knockdown experiments, human dermal fibroblasts were transfected with TFAM siRNA or nontargeting siRNA in the presence of recombinant TGFβ. Data are presented as the median ± interquartile range. *P* values less than 0.05 were considered significant.

Ethics approval. The samples and the analysis of those samples have been approved by the ethical committee of the University of Erlangen–Nuremberg. Patients and/or the public were not involved in the design, conduct, reporting, or dissemination plans of this research. All patients and healthy volunteers signed a consent form approved by the local institutional review board. All mouse experiments were approved by the government of Mittelfranken or Unterfranken.

RESULTS

Mitochondrial damage in SSc fibroblasts. Given the presence of multiple factors that can cause mitochondrial stress in SSc, we analyzed the mitochondrial status of fibroblasts from SSc patients and matched healthy controls on several experimental levels. Staining with the mitochondrial membrane potential–dependent probe MitoTracker Deep Red demonstrated significantly reduced numbers of functional mitochondria per cell in SSc fibroblasts compared to controls (Figure 1A). Consistent with these findings, the levels of the mitochondrial outer membrane protein translocase of outer membrane 20 (TOM-20), which is commonly used to determine the mitochondrial mass (40), were also decreased in SSc fibroblasts (Figure 1B).

Fine structural analysis by electron microscopy demonstrated that the majority of the remaining mitochondria in SSc fibroblasts were damaged. Numeric increases were observed for severe type II or type III damage in SSc fibroblasts according to the classification by Scorrano et al (41), whereas mild class I changes were significantly less abundant (Figure 1C). Mitochondrial size and perimeter were increased in SSc fibroblasts

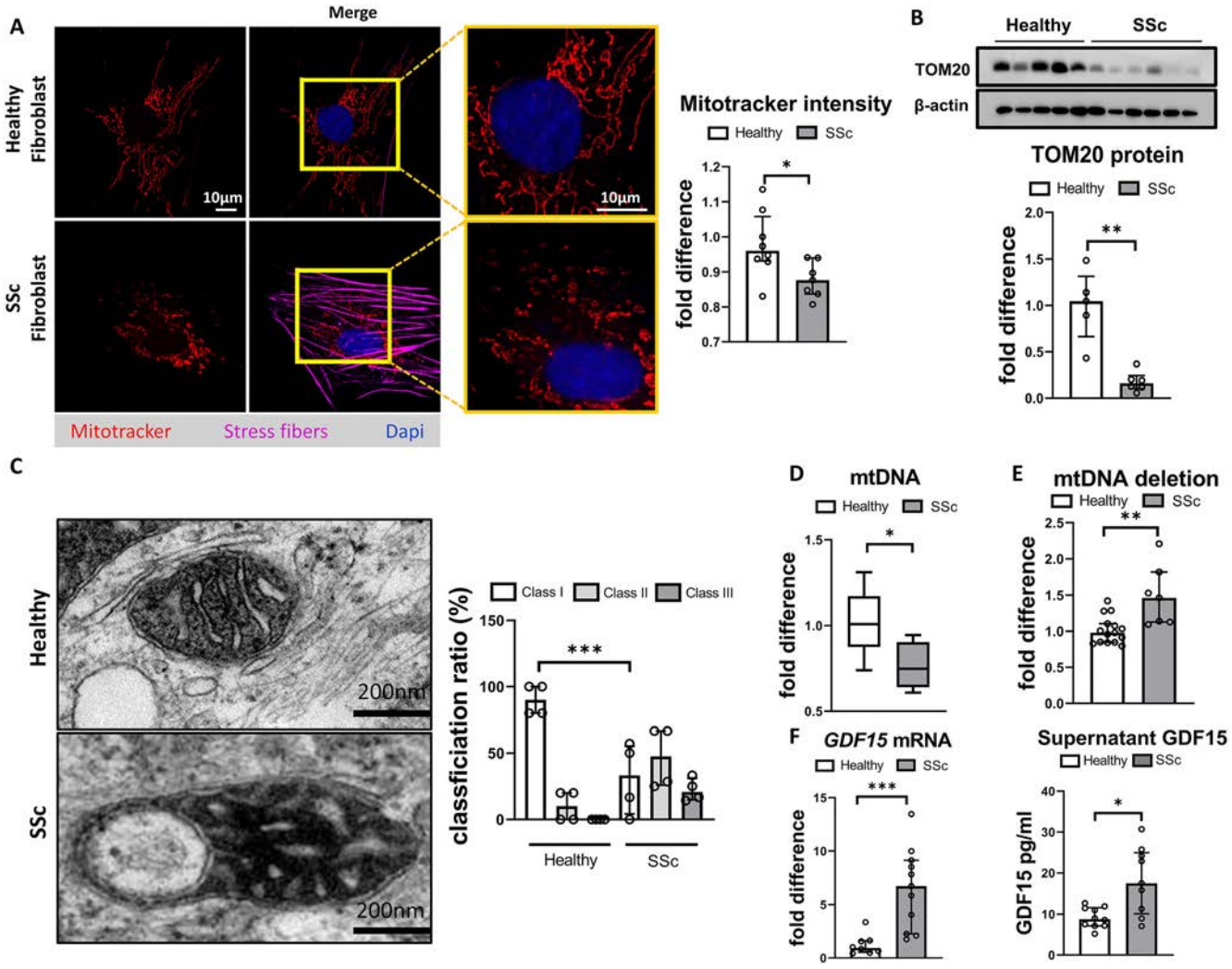

Figure 1. Mitochondrial damage in fibroblasts from patients with systemic sclerosis (SSc). **A**, Left, Representative confocal microscopy images of MitoTracker Deep Red staining for mitochondria (red), staining for stress fibers (magenta), and DAPI staining (blue) in cultured dermal fibroblasts from a healthy control and a patient with SSc. Right panels are higher-magnification views of the boxed areas in the merge panels. Bars = 10 μm. Right, Fold difference in MitoTracker staining intensity in dermal fibroblasts from healthy controls (n = 8) and SSc patients (n = 7; all diffuse cutaneous SSc). **B**, Western blot (top) and quantification (bottom) of the levels of the mitochondria outer membrane protein translocase of outer membrane 20 (TOM-20) in isolated dermal fibroblasts from healthy controls (n = 5) and SSc patients (n = 6). **C**, Left, Representative electron microscopy images of mitochondria in dermal fibroblasts from a healthy control and an SSc patient. Bars = 200 nm. Right, Quantification of mitochondrial damage in each group according to the criteria established by Scorrano et al (41) (n = 4 samples per group). **D**, Mitochondrial DNA (mtDNA) copy number in dermal fibroblasts from healthy controls (n = 8) and SSc patients (n = 9). **E**, Mitochondrial DNA deletion in dermal fibroblasts from healthy controls (n = 15) and SSc patients (n = 7). **F**, *GDF15* mRNA and protein levels in dermal fibroblasts from healthy controls (n = 8 for mRNA and n = 10 for protein levels) and SSc patients (n = 11 for mRNA and n = 9 for protein levels). In **A**–**C**, **E**, and **F**, circles represent individual subjects; bars show the median ± interquartile range (IQR). In **D**, data are shown as box plots. Each box represents the upper and lower IQR. Lines inside the boxes represent the median. Whiskers represent 1.5 times the upper and lower IQRs. * = $P \leq 0.05$; ** = $P \leq 0.01$; *** = $P \leq 0.001$, by 2-tailed Mann–Whitney U test in **A**, **B**, **D**, **E**, and **F**; by one-way analysis of variance with Tukey's post hoc multiple comparison test in **C**.

compared to healthy control fibroblasts (Supplementary Figure 1A, available on the *Arthritis & Rheumatology* website at https://onlinelibrary.wiley.com/doi/10.1002/art.42033). SSc fibroblasts also showed reduced mtDNA copy numbers (Figure 1D). In addition, mtDNA deletions were increased in SSc fibroblasts (Figure 1E). Also consistent with mitochondrial damage, SSc fibroblasts released increased amounts of mtDNA into the cell culture supernatant (Supplementary Figure 1B). The release of mtDNA was higher in fibroblasts from patients with diffuse cutaneous SSc (dcSSc) than in those from patients with limited cutaneous SSc (lcSSc). The messenger RNA (mRNA) and protein levels of GDF15, a mitokine that is released upon stress (42), were higher in SSc fibroblasts than in matched fibroblasts from healthy individuals (Figure 1F).

Impaired expression of TFAM in SSc. We next aimed to analyze the levels of TFAM, the key transcription factor of mitochondrial genes and central regulator of mitochondrial responses to stress and damage. Western blot analysis demonstrated decreased TFAM levels in fibroblasts from dcSSc patients (Figure 2A). Confocal staining and subsequent quantitative analysis confirmed the reduction in TFAM in dcSSc fibroblasts (Figures 2B and C). Further evaluation of the subcellular localization highlighted that TFAM was decreased not only in mitochondria, but also in the nucleus of dcSSc fibroblasts. The down-regulation of TFAM indicates that the physiologic repair mechanisms of mitochondria are exhausted or impaired in dcSSc. The impaired expression of TFAM in dcSSc may thus further augment mitochondria dysfunction and damage in SSc.

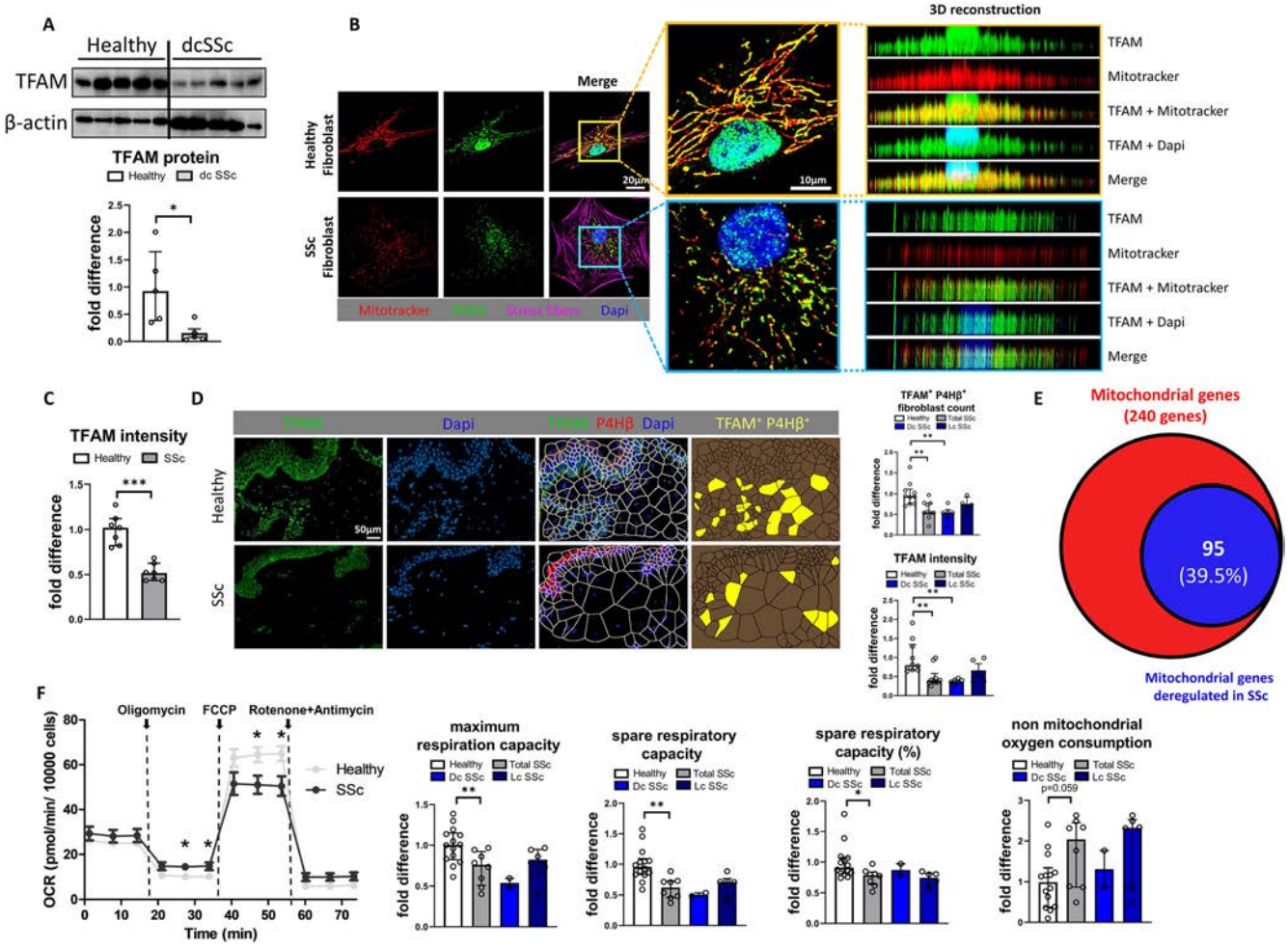

Figure 2. Decreased mitochondrial transcription factor A (TFAM) expression in systemic sclerosis (SSc). **A**, Western blot (top) and quantification (bottom) of protein levels of TFAM in cultured fibroblasts from healthy controls (n = 5) and patients with diffuse cutaneous SSc (dcSSc; n = 5). The lanes were run on the same gel but were noncontiguous. **B**, Representative confocal microscopy images of MitoTracker Deep Red staining for mitochondria (red), staining for TFAM (green), staining for stress fibers (magenta), and DAPI staining (blue) in dermal fibroblasts from a healthy control and a dcSSc patient. Middle panels show a higher-magnification view of the boxed areas in the merge panels. Right panels show 3-dimensional (3-D) reconstruction. Bars = 20 μm in the left panels and 10 μm in the middle panels. **C**, Fold difference in TFAM staining intensity in dermal fibroblasts from healthy controls (n = 7) and dcSSc patients (n = 7). **D**, Left, Representative images of staining for TFAM (green), DAPI staining (blue), and staining for the fibroblast marker P4Hβ (red) in skin sections from a healthy control and a dcSSc patient. Voronoi images illustrating P4Hβ and TFAM double-positive cells (P4Hβ+TFAM+) (yellow) in the dermis are shown. Bar = 50 μm. Right, Number of TFAM-positive fibroblasts (P4Hβ+TFAM+) and TFAM intensity in P4Hβ-positive fibroblasts in skin sections from healthy controls (n = 10), all SSc patients, (n = 10), dcSSc patients (n = 6), and limited cutaneous SSc (lcSSc) patients (n = 4). **E**, Number and percentage of down-regulated mitochondrial genes in SSc skin, retrieved from public data. **F**, Seahorse oxygen consumption rate (OCR) curves and quantification of maximum respiration capacity, spare respiratory capacity, relative spare respiratory capacity, and nonmitochondrial respiration in dermal fibroblasts from healthy controls (n = 14), all SSc patients (n = 8), dcSSc patients (n = 2), and lcSSc patients (n = 6). FCCP = carbonyl cyanide p-trifluoromethoxyphenylhydrazone. In **A**, **C**, **D**, and **F**, circles represent individual subjects; bars show the median ± interquartile range. * = $P \leq 0.05$; ** = $P \leq 0.01$; *** = $P \leq 0.001$, by 2-tailed Mann–Whitney U test in **A**, **C**, and **F**; by one-way analysis of variance with Tukey's post hoc multiple comparisons test in **D**.

We next aimed to demonstrate that these mechanisms are also operative in SSc skin. Staining of skin sections from patients with dcSSc demonstrated a pronounced reduction in the levels of TFAM in dermal fibroblasts from SSc patients (Figure 2D). Moreover, re-analysis of publicly available microarray data from a North American SSc cohort (NCBI GEO accession no. GSE59787) (43) demonstrated that 39.5% of the genes encoding for mitochondrial proteins were down-regulated in SSc skin (Figure 2E). The levels of TFAM were decreased by 4.16-fold in SSc patients compared to healthy individuals in this cohort (adjusted $P = 9.5 \times 10^{-11}$).

The impaired expression of TFAM and the associated mitochondrial damage translated into major metabolic changes in SSc fibroblasts. Real-time cell metabolic analysis highlighted profound decreases in maximal respiratory capacity, spare respiratory capacity, and relative spare respiratory capacity in SSc fibroblasts compared to healthy control fibroblasts (Figure 2F). The extracellular acidification rate did not differ between SSc fibroblasts and fibroblasts from healthy individuals (Supplementary Figure 2A, available on the *Arthritis & Rheumatology* website at https://onlinelibrary.wiley.com/doi/10.1002/art.42033). In contrast, non-mitochondrial, mitochondrial respiratory chain complex I (CI)–, CII-, or CIII-independent respiration was increased in a compensatory manner to counterbalance the decreases in respiratory capacity (Figure 2F).

Mitochondrial damage and down-regulation of TFAM in fibroblasts incubated with transforming growth factor β (TGFβ). We hypothesized that endogenous mechanisms may precipitate the mitochondrial phenotype of SSc fibroblasts. TGFβ signaling remains persistently activated in SSc fibroblasts in culture (44). We thus evaluated whether the aberrant activation of TGFβ signaling induces the defective mitochondrial phenotype and the down-regulation of TFAM in SSc fibroblasts. Long-term incubation of normal dermal fibroblasts with recombinant TGFβ for 7 days decreased the number of mitochondria (Figure 3A), whereas short-term exposure did not induce mitochondrial loss (data not shown).

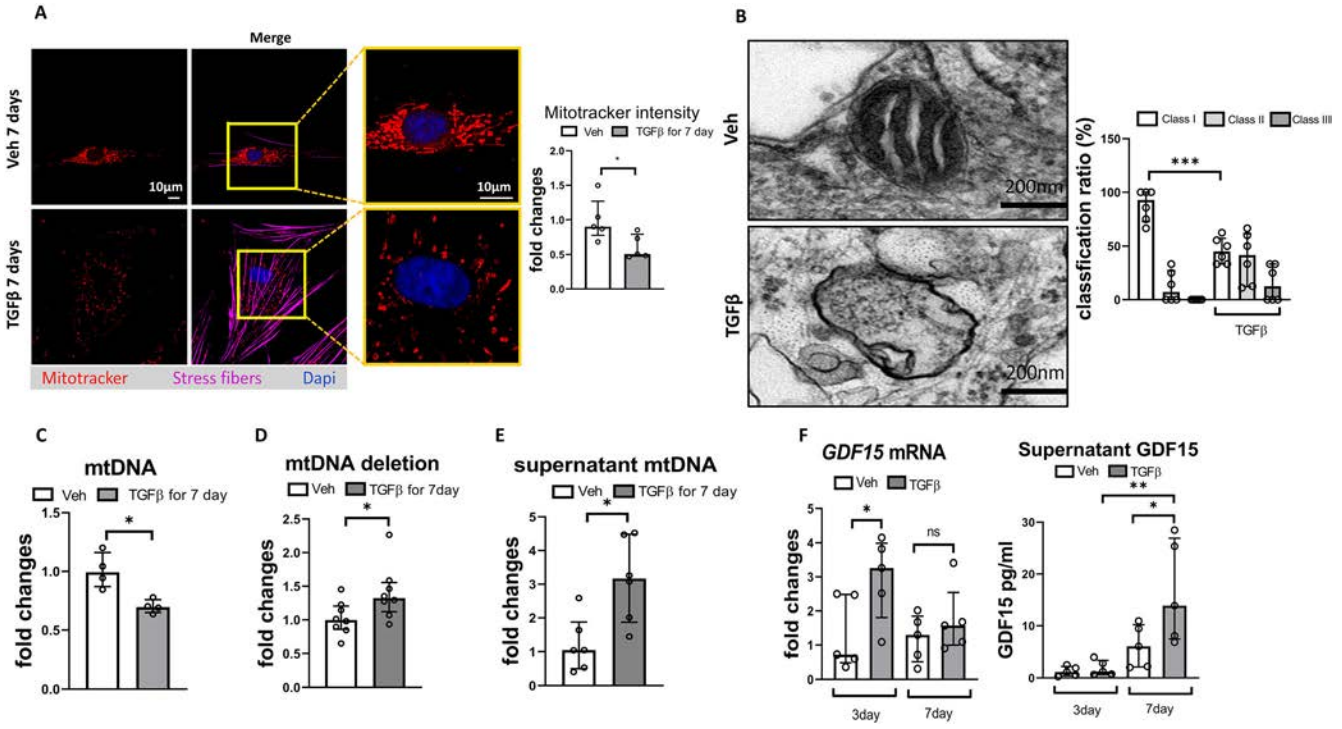

Figure 3. Mitochondrial damage and down-regulation of mitochondrial transcription factor A (TFAM) in healthy dermal fibroblasts stimulated with transforming growth factor β (TGFβ). **A**, Left, Representative confocal microscopy images of MitoTracker Deep Red staining for mitochondria (red), staining for stress fibers (magenta), and DAPI staining (blue) in human dermal fibroblasts incubated with vehicle (Veh) or TGFβ for 7 days. Bars = 10 μm. Right, Fold change in MitoTracker staining intensity in dermal fibroblasts incubated with vehicle (n = 5) and dermal fibroblasts incubated with TGFβ (n = 5). **B**, Left, Representative electron microscopy images of mitochondria in human dermal fibroblasts stimulated with vehicle or TGFβ. Bars = 200 nm. Right, Quantification of mitochondrial damage in each group according to the criteria established by Scorrano et al (41) (n = 6 samples per group). **C**, Fold change in mitochondrial DNA (mtDNA) copy number in human dermal fibroblasts stimulated with vehicle or TGFβ (n = 4 per group). **D**, Fold change in mtDNA deletion level in human dermal fibroblasts stimulated with vehicle or TGFβ (n = 8 per group). **E**, Fold change in mtDNA in the supernatant of human dermal fibroblasts stimulated with vehicle or TGFβ (n = 6 per group). **F**, *GDF15* mRNA and supernatant protein levels in cultured dermal fibroblasts stimulated with vehicle or TGFβ (n = 5 per group). Circles represent individual subjects; bars show the median ± interquartile range. * = $P \leq 0.05$; ** = $P \leq 0.01$; *** = $P \leq 0.001$, by 2-tailed Mann–Whitney U test in in **A**, **C**, **D**, **E**, and for GDF15 mRNA in **F**; by one-way analysis of variance with Tukey's post hoc multiple comparisons test in **B** and for GDF15 protein in **F**. NS = not significant. Color figure can be viewed in the online issue, which is available at http://onlinelibrary.wiley.com/doi/10.1002/art.42033/abstract.

Incubation of normal fibroblasts with TGFβ also induced fine structural changes in mitochondria reminiscent of those in SSc fibroblasts, with accumulation of damaged mitochondria, mitochondrial swelling, and disorganization as well as loss of cristae (Figure 3B). Similar to findings in SSc fibroblasts, the mitochondrial size and perimeters were increased in normal fibroblasts stimulated with TGFβ compared to those stimulated with vehicle control (Supplementary Figure 3A, available on the *Arthritis & Rheumatology* website at https://onlinelibrary.wiley.com/doi/10.1002/art.42033). Prolonged incubation with TGFβ for 7 days also decreased the mitochondrial copy number of normal fibroblasts to levels comparable to SSc fibroblasts (Figure 3C) and induced mtDNA deletions (Figure 3D). We also observed an increase in mtDNA in the cell culture supernatant of normal fibroblasts in response to TGFβ (Figure 3E). In contrast to long-term exposure, short-term stimulation with TGFβ had no effects on these markers of mitochondrial damage (data not shown). Stimulation with TGFβ also increased the mRNA and protein levels of the mitokine GDF15 (Figure 3F).

As in SSc fibroblasts, these changes might be coordinated by TFAM. Prolonged incubation of normal dermal fibroblasts with TGFβ decreased the expression of the transcription factor TFAM with reduced nuclear and mitochondrial levels of TFAM, as assessed by Western blotting and immunofluorescence with subsequent confocal microscopy (Figures 4A–C). Long-term exposure to TGFβ also phenocopied the metabolic changes in SSc fibroblasts, with decreases in maximal respiratory capacity and spare respiratory capacity (Figure 4D).

We next aimed to evaluate whether knockdown of TFAM can serve as a model for mitochondrial damage in SSc fibroblasts. Knockdown of TFAM significantly reduced TFAM mRNA and protein levels (Supplementary Figures 4A and B, available on the *Arthritis & Rheumatology* website at https://onlinelibrary.wiley.com/doi/10.1002/art.42033). Knockdown of TFAM rendered normal dermal fibroblasts more sensitive to the TGFβ-induced upregulation of GDF15 mRNA and supernatant protein levels (Supplementary Figure 4C). Loss of TFAM also enhanced the

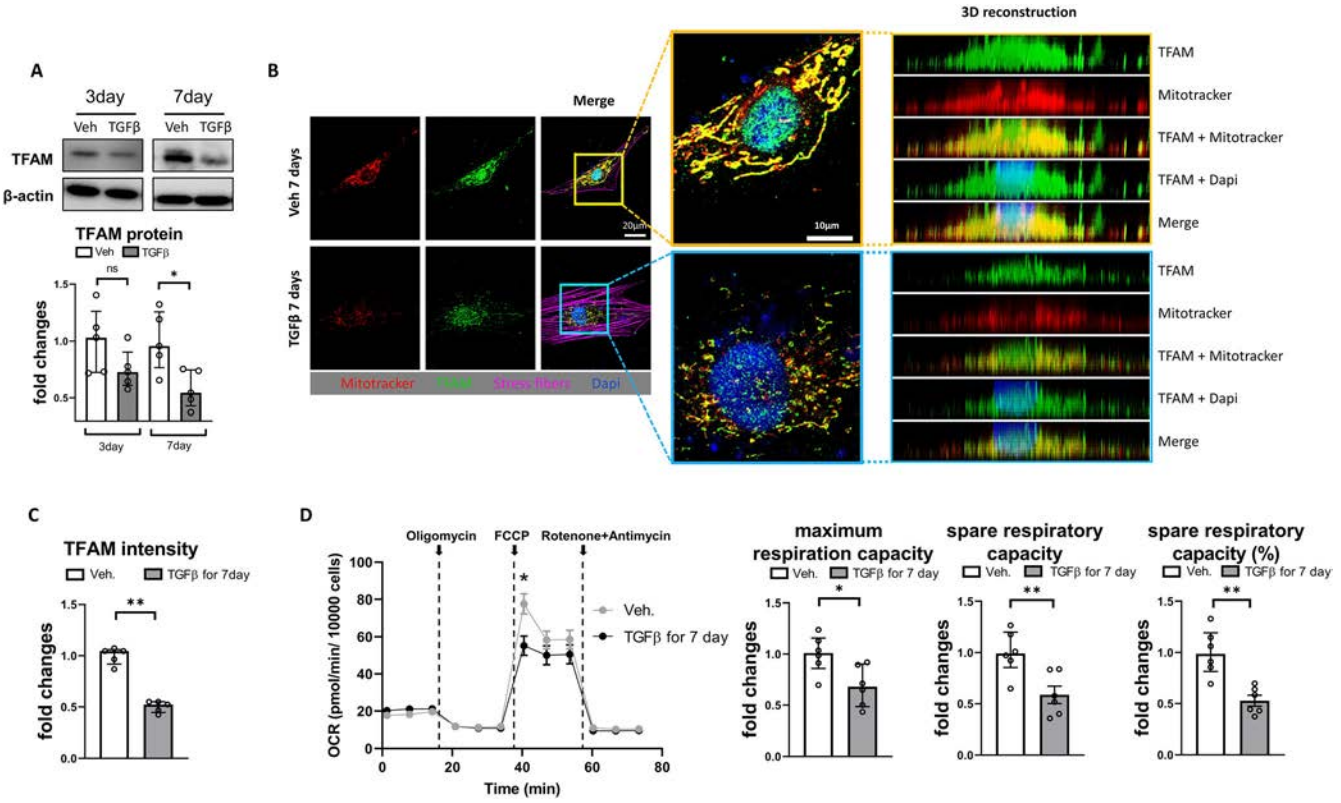

Figure 4. Transforming growth factor β (TGFβ) represses mitochondrial transcription factor A (TFAM) expression and induces systemic sclerosis (SSc)–like changes in mitochondrial respiration ability in normal dermal fibroblasts. **A**, Western blot (top) and quantification (bottom) of protein levels of TFAM in healthy dermal fibroblasts stimulated with vehicle (Veh) or TGFβ for 3 or 7 days (n = 5 per group). **B**, Representative confocal microscopy images of MitoTracker Deep Red staining for mitochondria (red), staining for TFAM (green), staining for stress fibers (magenta), and DAPI staining (blue) in dermal fibroblasts stimulated with vehicle or TGFβ for 7 days. Middle panels show a higher-magnification view of the boxed areas in the merge panels. Right panels show 3-dimensional (3-D) reconstruction. Bars = 20 μm in the left panels and 10 μm in the middle panels. **C**, Fold change in TFAM intensity in dermal fibroblasts stimulated with vehicle or TGFβ (n = 5 per group). **D**, Seahorse oxygen consumption rate (OCR) curves and quantification of maximum respiration capacity, spare respiratory capacity, and relative spare respiratory capacity in dermal fibroblasts stimulated with vehicle or TGFβ for 7 days (n = 6 per group). FCCP = carbonyl cyanide p-trifluoromethoxyphenylhydrazone. In **A**, **C**, and **D**, circles represent individual subjects; bars show the median ± interquartile range. * = $P \leq 0.05$; ** = $P \leq 0.01$, by 2-tailed Mann–Whitney U test. NS = not significant. Color figure can be viewed in the online issue, which is available at http://onlinelibrary.wiley.com/doi/10.1002/art.42033/abstract.

mtDNA deletion and supernatant mtDNA (Supplementary Figure 4D). Consistent with our previous results (Figure 3), shorter stimulation with TGFβ (48 hours in these experiments as the optimal time point to assess collagen release) was not sufficient to induce mtDNA deletion or mtDNA release. Of particular interest, small interfering RNA (siRNA)–mediated knockdown of TFAM stimulated the synthesis of extracellular matrix with increased mRNA levels of *COL1A1* (Supplementary Figure 4E) and increased deposition of type I collagen protein upon TGFβ stimulation (Supplementary Figure 4F). Furthermore, knockdown of TFAM increased the production of mitochondrial reactive oxygen species (MitoROS) upon TGFβ stimulation (Supplementary Figure 4G). Moreover, specific inhibition of MitoROS production by MitoQ partially reduced the increased sensitivity of fibroblasts with TFAM knockdown to TGFβ stimulation, resulting in decreased levels of mRNA for *COL1A1* (Supplementary Figure 4H).

Exacerbation of experimental skin fibrosis by fibroblast-specific knockout of TFAM in a mouse model. To analyze whether mitochondrial damage can also foster tissue fibrosis, we generated $Tfam^{fl/fl}$ × Col1a2-CreER mice with fibroblast-specific, inducible knockout of Tfam. Mice were challenged with tamoxifen (Tfam Fib^{KO} mice). $Tfam^{fl/fl}$ × Col1a2-CreER mice injected with corn oil (Tfam Fib^{WT} mice) were used as controls. We verified the depletion of Tfam by immunofluorescence staining of skin sections from tamoxifen-treated mice and controls. The number of Tfam-positive fibroblasts decreased significantly in skin sections from tamoxifen-challenged mice (Tfam Fib^{KO}) compared to mice injected with oil (Tfam Fib^{WT}) (Supplementary Figure 5A, available on the *Arthritis & Rheumatology* website at https://onlinelibrary.wiley.com/doi/10.1002/art.42033). We employed 3 complementary models of fibrosis: 1) bleomycin-induced skin fibrosis, 2) constitutively active TGFβRI ($TGFβRI^{CA}$)–induced skin fibrosis, and 3) bleomycin-induced pulmonary fibrosis.

Mice with selective depletion of Tfam in fibroblasts ($Tfam^{fl/fl}$ × Col1a2-CreER mice injected with tamoxifen; Tfam Fib^{KO} mice) did not show a phenotype in the absence of external manipulation (Figures 5A and C and Supplementary Figure 5B). However, even minor manipulations with intratracheal instillation of 0.9% NaCl induced a profibrotic response in the lungs. Tfam Fib^{KO} mice demonstrated subtle but significant increases in hydroxyproline content and in Ashcroft scores and a trend toward increased collagen-covered area compared to controls ($Tfam^{fl/fl}$ × Col1a2-CreER mice injected with the solvent corn oil; Tfam Fib^{WT} mice) (Figures 5A and B). These effects were more pronounced in the lungs than in the skin.

Moreover, Tfam Fib^{KO} mice were more sensitive to common profibrotic stimuli. Bleomycin-induced skin fibrosis was exacerbated in mice with fibroblast-specific knockout of Tfam, with increased dermal thickening, higher myofibroblast counts, and increased hydroxyproline content compared to controls (Supplementary Figures 5B and C). Tfam Fib^{KO} mice also demonstrated enhanced fibrotic responses to $TGFβRI^{CA}$ overexpression (Figures 5C and D). In addition to skin fibrosis, fibroblast-specific knockout of Tfam also increased the sensitivity to experimental pulmonary fibrosis. Tfam Fib^{KO} mice demonstrated more pronounced increases in modified Ashcroft scores, in fibrotic area, and in hydroxyproline content compared to controls (Figures 5A and B).

Smad3-dependent fibroblast activation upon knockdown of TFAM. To characterize the molecular mechanisms underlying the stimulatory effects of TFAM on fibroblasts, we performed RNA-Seq of human dermal fibroblasts transfected with TFAM siRNA or nontargeting siRNA in the presence of recombinant TGFβ (differentially expressed genes [DEGs] TFAM_TGFβ). We identified 1,048 DEGs (674 down-regulated and 374 up-regulated with a Hochberg false discovery rate [FDR] of ≤0.05 and fold change ≥1.5) between TGFβ-stimulated fibroblasts with and those without TFAM knockdown (DEGs TFAM_TGFβ) (Figure 6A and Supplementary Figure 6A and Supplementary Methods, available on the *Arthritis & Rheumatology* website at https://onlinelibrary.wiley.com/doi/10.1002/art.42033). The functional analysis of the DEGs TFAM_TGFβ by Gene Ontology (GO) highlighted enrichment of several biologic processes relevant to tissue fibrosis, including "extracellular matrix organization," "actin filament organization," "connective tissue development," "epithelial to mesenchymal transition," "positive regulation of cytoskeletal organization," and "regulation of wound healing" (Figure 6B).

Of particular interest, TFAM-associated GO terms also included several Smad-related pathways, including "pathway-restricted Smad protein phosphorylation," "Smad protein signal transduction," "regulation of pathway-restricted Smad protein phosphorylation," and "positive regulation of pathway-restricted Smad protein phosphorylation" (Figure 6B), indicating that TFAM may promote fibroblast activation in a Smad-dependent manner. We also compared the RNA-Seq data between human dermal fibroblasts transfected with TFAM siRNA and those transfected with nontargeting siRNA in the absence of TGFβ (DEGs TFAM_unstimulated). We identified 512 DEGs (396 down-regulated and 116 up-regulated with a Hochberg FDR of ≤0.05 and fold change ≥1.5) (Supplementary Methods). The functional analysis of the DEGs TFAM_unstimulated by GO showed that in the absence of TGFβ, knockdown of TFAM affected a different spectrum of biologic processes than in the presence of TGFβ. In particular, most processes related to fibroblast activation, fibrotic remodeling, and Smad-dependent signaling pathways were not represented among the differentially regulated GO processes in fibroblasts with TFAM knockdown without TGFβ stimulation (Supplementary Figure 6B).

To experimentally confirm the regulation of Smad signaling by TFAM, we first quantified the levels of phosphorylated Smad3 (pSmad3) and total Smad3 by Western blotting (Figure 6C).

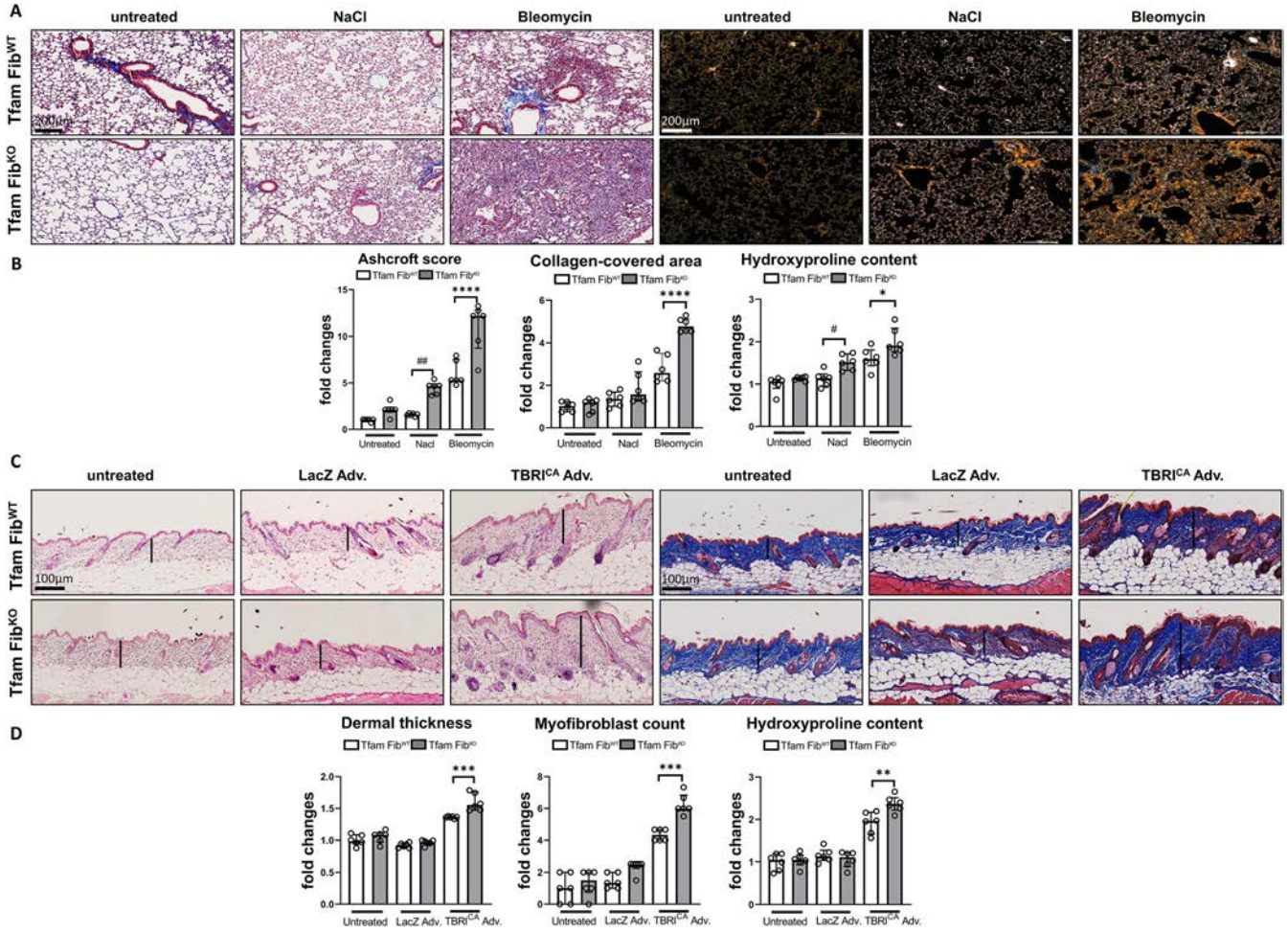

Figure 5. Exacerbation of experimental pulmonary and dermal fibrosis in mice with fibroblast-specific knockout of Tfam. **A**, Representative trichrome and sirius red staining of lung sections from Tfam$^{fl/fl}$ × Col1a2-CreER mice injected with corn oil (Tfam Fib^{WT} mice) and Tfam$^{fl/fl}$ × Col1a2-CreER mice injected with tamoxifen (Tfam Fib^{KO} mice) left untreated, treated with intratracheal instillation of NaCl, or treated with intratracheal instillation of bleomycin. Bars = 200 μm. **B**, Quantification of pulmonary changes using the Ashcroft score, quantification of the collagen-covered area, and assessment of hydroxyproline content in mice treated as indicated (n = 6 per group). **C**, Representative hematoxylin and eosin and trichrome staining of skin sections from Tfam Fib^{WT} and Tfam Fib^{KO} mice left untreated, subcutaneously injected with LacZ adenovirus (LacZ Adv), or subcutaneously injected with constitutively active transforming growth factor β type I receptor adenovirus (TGFβRI^{CA} Adv). Vertical lines indicate representative examples of the dermal thickness as quantified in **D**. Bars = 100 μm. **D**, Quantification of dermal thickness, myofibroblast counts, and hydroxyproline content in mice treated as indicated (n = 6 per group). In **B** and **D**, circles represent individual mice; bars show the median ± interquartile range. * = $P \leq 0.05$; ** = $P \leq 0.01$; *** = $P \leq 0.001$; **** = $P \leq 0.0001$, Tfam Fib^{WT} mice treated with bleomycin versus Tfam Fib^{KO} mice treated with bleomycin; # = $P \leq 0.05$; ## = $P \leq 0.01$, Tfam Fib^{WT} mice treated with NaCl versus Tfam Fib^{KO} mice treated with NaCl, by one-way analysis of variance with Tukey's post hoc multiple comparisons test. Color figure can be viewed in the online issue, which is available at http://onlinelibrary.wiley.com/doi/10.1002/art.42033/abstract.

Knockdown of TFAM in human dermal fibroblasts enhanced the accumulation of pSmad3 upon stimulation with TGFβ. Smad3-sensitive reporter assays confirmed the increased activation of Smad3-dependent transcription in TFAM-knockdown fibroblasts (Figure 6D). In addition, specific inhibition of Smad3 by specific inhibitor of Smad3 prevented the increased sensitivity of TFAM-knockdown fibroblasts to TGFβ stimulation and reduced the levels of *COL1A1* mRNA and type I collagen protein to that in unstimulated control fibroblasts (Figure 6E). Consistent with our in vitro findings, Tfam Fib^{KO} mice demonstrated enhanced activation of Smad3 signaling with accumulation of pSmad3 across all mouse models (Figure 6F and Supplementary Figure 6C, available on the *Arthritis & Rheumatology* website at https://onlinelibrary.wiley.com/doi/10.1002/art.42033).

DISCUSSION

In the present study, we demonstrate on multiple experimental levels that severe mitochondrial damage is a cardinal feature of SSc fibroblasts. The number of mitochondria is reduced in SSc fibroblasts as compared to fibroblasts from matched healthy individuals. The remaining mitochondria display reduced mtDNA

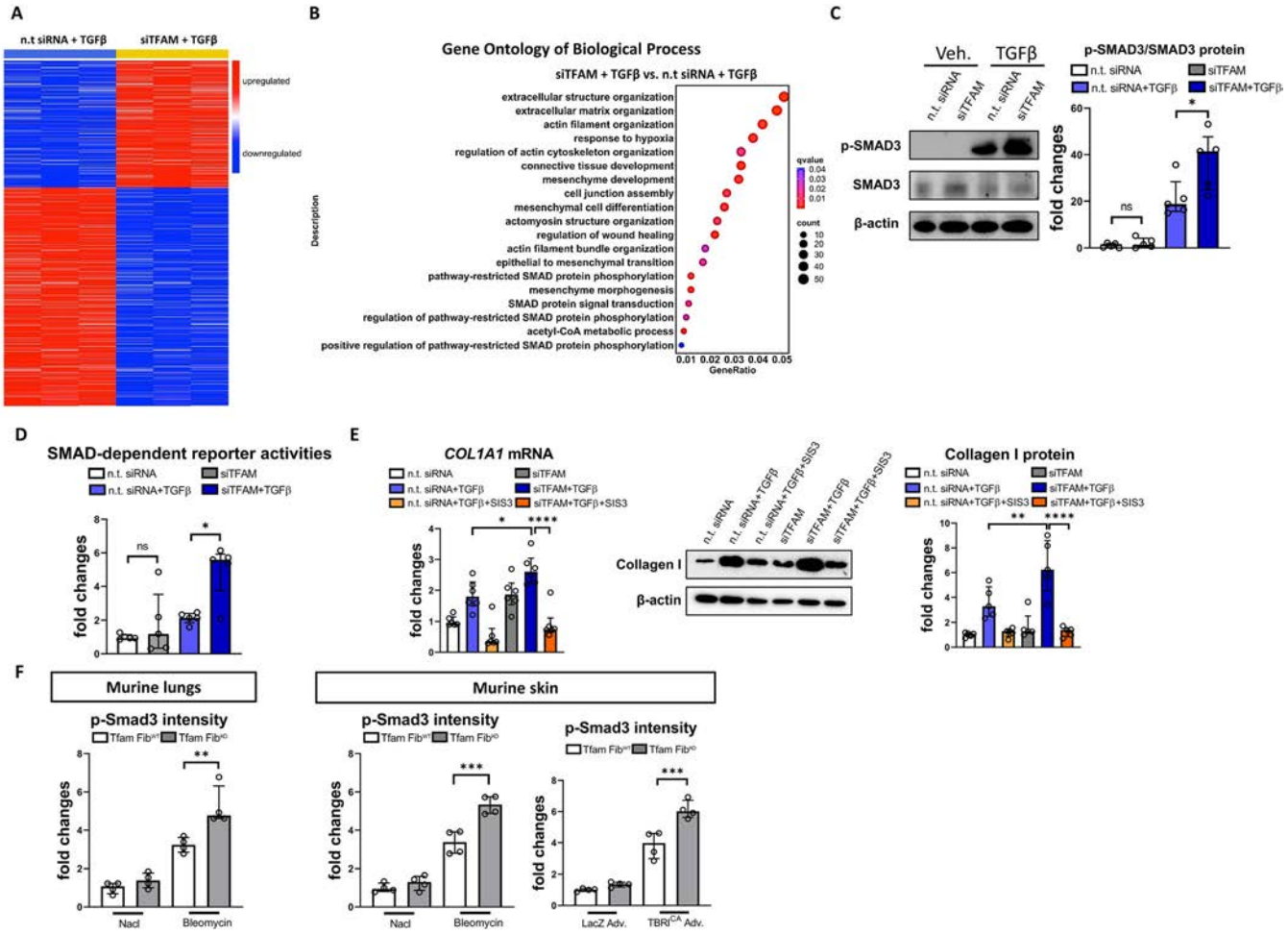

Figure 6. Knockdown of TFAM enhances fibroblast activation in a Smad3-dependent manner. **A**, Representative heatmap of differentially expressed genes (DEGs) between transforming growth factor β (TGFβ)–stimulated human dermal fibroblasts without TFAM knockdown (transfected with nontargeting small interfering RNA [nt siRNA]) and those with TFAM knockdown (transfected with TFAM siRNA [siTFAM]) (DEG TFAM_TGFβ). **B**, Gene Ontology functional analysis of the DEG TFAM_TGFβ. Acetyl-CoA = acetyl-coenzyme A. **C**, Western blot (left) and quantification (right) of protein levels of phosphorylated Smad3 (pSmad3) and total Smad3 in dermal fibroblasts transfected with nontargeting siRNA or TFAM siRNA and stimulated with vehicle (Veh) or TGFβ (n = 5 per group). **D**, Results of Smad-sensitive reporter assays in dermal fibroblasts transfected with nontargeting siRNA or TFAM siRNA with or without TGFβ stimulation (n = 5 per group). **E**, Quantification of *COL1A1* mRNA levels (n = 6 per group) (left), Western blot of intracellular type I collagen levels (middle), and quantification of intracellular type I collagen protein levels (n = 5 per group) (right) in dermal fibroblasts transfected with nontargeting siRNA or TFAM siRNA with or without TGFβ stimulation and specific inhibitor of Smad-3 (SIS-3; 6 μ*M*). **F**, Fold change in intensity of pSmad3 in mice with bleomycin-induced pulmonary fibrosis, mice with bleomycin-induced dermal fibrosis, and mice with constitutively active TGFβ type I receptor ($TGF\beta RI^{CA}$)–induced skin fibrosis and respective non-fibrotic control mice (n = 4 per group in each mouse model). In **C**–**F**, circles represent individual data points; bars show the median ± interquartile range. * = $P \leq 0.05$; ** = $P \leq 0.01$; *** = $P \leq 0.001$; **** = $P \leq 0.0001$, by one-way analysis of variance with Tukey's post hoc multiple comparisons test. NS = not significant. Color figure can be viewed in the online issue, which is available at http://onlinelibrary.wiley.com/doi/10.1002/art.42033/abstract.

content with accumulation of deletions as well as pronounced structural damage on electron microscopy. The mitochondrial damage is associated with profound changes in cellular metabolism with impaired capacity for OXPHOS and thus decreased ability to meet the metabolic demands of affected cells. Moreover, SSc fibroblasts with damaged mitochondria release mtDNA and secrete the mitokine GDF15, which act as paracrine factors to activate surrounding cells.

Mitochondrial damage in SSc fibroblasts might be precipitated, or at least aggravated, by deregulation of the transcription factor TFAM. TFAM is known to regulate the expression of multiple genes implicated in mitochondrial function and its expression increases with enhanced localization to the mitochondria in response to moderate mitochondrial damage to promote mitochondrial biogenesis (26,45). However, we demonstrate that the expression of TFAM is actually decreased in cultured SSc fibroblasts and in fibroblasts in SSc skin. Down-regulation of TFAM impairs repair of damaged mitochondria as well as neogenesis of mitochondria. Further studies on consecutive patient samples and larger cohorts are required to analyze whether the decrease

in TFAM precedes mitochondrial loss in SSc fibroblasts and might thus be causative or whether TFAM decreases over time as a potential indicator of exhausted repair mechanisms and driver of disease progression.

We present several lines of evidence that the down-regulation of TFAM as well as the damage and ultimately loss of mitochondria might be mediated by persistent, but not transient, activation of TGFβ signaling. We demonstrate that prolonged incubation of normal fibroblasts with TGFβ down-regulates the expression of TFAM and induces SSc-like mitochondrial changes with reduced mitochondrial mass, fine structural changes, accumulation of deletions within mtDNA, decreased intracellular mtDNA content, and increased release of mtDNA into the supernatant. Prolonged incubation with TGFβ induced the release of GDF15 and phenocopied the metabolic alterations of SSc fibroblasts with impaired capacity for OXPHOS. Impaired OXPHOS was also reported in patients with radiation-induced fibrosis (46), which is also characterized by enhanced activation of TGFβ signaling, highlighting that this regulation might be operative in different fibrotic diseases.

The reduction in TFAM and the associated mitochondrial damage translates into enhanced sensitivity of fibroblasts to profibrotic stimuli. Knockdown of TFAM in normal fibroblasts to levels comparable to those in SSc fibroblasts renders them more susceptible to the profibrotic effects of TGFβ, with enhanced fibroblast-to-myofibroblast transition and collagen release. Consistently, RNA-Seq of human dermal fibroblasts with knockdown of TFAM demonstrated a deregulation of multiple functional terms relevant to fibroblast activation and tissue fibrosis, confirming that the down-regulation of TFAM directly contributes to the activated, profibrotic phenotype of SSc fibroblasts. Of particular note, mice with fibroblast-specific knockout of Tfam were also more susceptible to fibrotic stimuli in 3 different mouse models resembling different aspects and manifestations of tissue fibrosis in SSc: bleomycin-induced skin and lung fibrosis as well as TGFβRI^{CA}-induced fibrosis. Of particular note, even instillation of 0.9% NaCl provoked a fibrotic response in the lungs of Tfam Fib^{KO} mice, highlighting a massively impaired tolerance for fibrotic tissue remodeling upon loss of Tfam.

Mechanistically, the enhanced sensitivity of TFAM-knockdown fibroblasts to profibrotic stimuli might arise from enhanced Smad3 signaling. Smad3 signaling is a core pathway of fibrosis and is hyperactive in fibrotic tissues of SSc patients. RNA-Seq demonstrated activation of GO terms related to Smad signaling, and TFAM-knockdown fibroblasts demonstrated increased levels of pSmad3 protein and enhanced Smad3-dependent transcription activity upon TGFβ stimulation. Phosphorylated Smad3 also accumulated at increased levels in Tfam Fib^{KO} mice compared to controls. Moreover, inhibition of Smad3 abrogated the enhanced sensitivity of TFAM-knockdown fibroblasts to the profibrotic effects of TGFβ and reduced the release of collagen to normal levels. In addition to Smad3 signaling, increased release of mitoROS may contribute to the activated phenotype (47,48).

In summary, we demonstrate here that impaired TFAM signaling and associated mitochondrial damage activate profibrotic transcriptional programs with enhanced Smad3 signaling in SSc fibroblasts. Down-regulation of TFAM occurs in response to chronic activation of TGFβ signaling and renders fibroblasts more susceptible to profibrotic stimuli, with exacerbation of dermal and pulmonary fibrosis in mice with fibroblast-specific knockout of Tfam. Impaired TFAM signaling thus causally links uncontrolled TGFβ signaling to mitochondrial damage and fibroblast activation in SSc. Breaking this link by interfering with the down-regulation of TFAM may offer potential for new venues for antifibrotic therapies.

ACKNOWLEDGMENTS

We thank Christoph Liebel, Regina Kleinlein, Lena Summa, Vladyslav Fedorchenko, Wolfgang Espach, Nadja Gießl, and Elke Meyer for excellent technical assistance.

AUTHOR CONTRIBUTIONS

All authors were involved in drafting the article or revising it critically for important intellectual content, and all authors approved the final version to be published. Dr. Distler had full access to all of the data in the study and takes responsibility for the integrity of the data and the accuracy of the data analysis.

Study conception and design. Zhou, Trinh-Minh, Distler.

Acquisition of data. Zhou, Trinh-Minh, Tran-Manh, Gießl, Bergmann, Györfi.

Analysis and interpretation of data. Zhou, Trinh-Minh, Tran-Manh, Gießl, Schett, Distler.

REFERENCES

1. Abraham DJ, Krieg T, Distler J, Distler O. Overview of pathogenesis of systemic sclerosis. Rheumatology (Oxford) 2009;48 suppl:iii3–7.
2. Distler JH, Feghali-Bostwick C, Soare A, Asano Y, Distler O, Abraham DJ. Frontiers of antifibrotic therapy in systemic sclerosis [review]. Arthritis Rheumatol 2017;69:257–67.
3. Leroy EC. Increased collagen synthesis by scleroderma skin fibroblasts in vitro. J Clin Invest 1974;54:880–9.
4. Distler JH, Gyorfi AH, Ramanujam M, Whitfield ML, Konigshoff M, Lafyatis R. Shared and distinct mechanisms of fibrosis. Nat Rev Rheumatol 2019;15:705–30.
5. Kendall RT, Feghali-Bostwick CA. Fibroblasts in fibrosis: novel roles and mediators. Front Pharmacol 2014;5:123.
6. Gillespie J, Ross RL, Corinaldesi C, Esteves F, Derrett-Smith E, McDermott MF, et al. Transforming growth factor β activation primes canonical Wnt signaling through down-regulation of axin-2. Arthritis Rheumatol 2018;70:932–42.
7. Shin JY, Beckett JD, Bagirzadeh R, Creamer TJ, Shah AA, McMahan Z, et al. Epigenetic activation and memory at a TGFB2 enhancer in systemic sclerosis. Sci Transl Med 2019;11: eaaw0790.
8. Lee YA, Wallace MC, Friedman SL. Pathobiology of liver fibrosis: a translational success story. Gut 2015;64:830–41.
9. Matucci-Cerinic M, Kahaleh B, Wigley FM. Evidence that systemic sclerosis is a vascular disease [review]. Arthritis Rheum 2013;65: 1953–62.
10. Barth AS, Tomaselli GF. Gene scanning and heart attack risk. Trends Cardiovasc Med 2016;26:260–5.

11. Roger AJ, Munoz-Gomez SA, Kamikawa R. The origin and diversification of mitochondria. Curr Biol 2017;27:R1177–92.
12. Yuan Y, Ju YS, Kim Y, Li J, Wang Y, Yoon CJ, et al. Comprehensive molecular characterization of mitochondrial genomes in human cancers. Nat Genet 2020;52:342–52.
13. Spinelli JB, Haigis MC. The multifaceted contributions of mitochondria to cellular metabolism. Nat Cell Biol 2018;20:745–54.
14. Martinez-Reyes I, Diebold LP, Kong H, Schieber M, Huang H, Hensley CT, et al. TCA cycle and mitochondrial membrane potential are necessary for diverse biological functions. Mol Cell 2016;61:199–209.
15. Shadel GS, Horvath TL. Mitochondrial ROS signaling in organismal homeostasis. Cell 2015;163:560–9.
16. Samanta D, Park Y, Andrabi SA, Shelton LM, Gilkes DM, Semenza GL. PHGDH expression is required for mitochondrial redox homeostasis, breast cancer stem cell maintenance, and lung metastasis. Cancer Res 2016;76:4430–42.
17. Oxenoid K, Dong Y, Cao C, Cui T, Sancak Y, Markhard AL, et al. Architecture of the mitochondrial calcium uniporter. Nature 2016; 533:269–73.
18. Sustarsic EG, Ma T, Lynes MD, Larsen M, Karavaeva I, Havelund JF, et al. Cardiolipin synthesis in brown and beige fat mitochondria is essential for systemic energy homeostasis. Cell Metab 2018;28: 159–74.
19. Lill R, Freibert SA. Mechanisms of mitochondrial iron-sulfur protein biogenesis. Annu Rev Biochem 2020;89:471–99.
20. Tsai VW, Husaini Y, Sainsbury A, Brown DA, Breit SN. The MIC-1/GDF15-GFRAL pathway in energy homeostasis: implications for obesity, cachexia, and other associated diseases. Cell Metab 2018; 28:353–68.
21. Duan J. Metabolic remodeling induced by mitokines in heart failure. Aging 2019;11:7307–27.
22. Hillen HS, Temiakov D, Cramer P. Structural basis of mitochondrial transcription. Nat Struct Mol Biol 2018;25:754–65.
23. Bernard K, Logsdon NJ, Miguel V, Benavides GA, Zhang J, Carter AB, et al. NADPH oxidase 4 (Nox4) suppresses mitochondrial biogenesis and bioenergetics in lung fibroblasts via a nuclear factor erythroid-derived 2-like 2 (Nrf2)-dependent pathway. J Biol Chem 2017;292:3029–38.
24. Uchiumi T, Kang D. The role of TFAM-associated proteins in mitochondrial RNA metabolism. Biochim Biophys Acta 2012;1820:565–70.
25. Larsson NG, Wang J, Wilhelmsson H, Oldfors A, Rustin P, Lewandoski M, et al. Mitochondrial transcription factor A is necessary for mtDNA maintenance and embryogenesis in mice. Nat Genet 1998;18:231–6.
26. Fu Z, Ye J, Dean JW, Bostick JW, Weinberg SE, Xiong L, et al. Requirement of mitochondrial transcription factor A in tissue-resident regulatory T cell maintenance and function. Cell Rep 2019;28: 159–71.
27. Nunnari J, Suomalainen A. Mitochondria: in sickness and in health. Cell 2012;148:1145–59.
28. Henderson J, Duffy L, Stratton R, Ford D, O'Reilly S. Metabolic reprogramming of glycolysis and glutamine metabolism are key events in myofibroblast transition in systemic sclerosis pathogenesis. J Cell Mol Med 2020;24:14026–38.
29. Yang C, Jiang L, Zhang H, Shimoda LA, DeBerardinis RJ, Semenza GL. Analysis of hypoxia-induced metabolic reprogramming. Methods Enzymol 2014;542:425–55.
30. Caporarello N, Meridew JA, Jones DL, Tan Q, Haak AJ, Choi KM, et al. PGC1α repression in IPF fibroblasts drives a pathologic metabolic, secretory and fibrogenic state. Thorax 2019;74:749–60.
31. Li X, Zhang W, Cao Q, Wang Z, Zhao M, Xu L, et al. Mitochondrial dysfunction in fibrotic diseases. Cell Death Discov 2020;6:80.
32. Quiros PM, Mottis A, Auwerx J. Mitonuclear communication in homeostasis and stress. Nat Rev Mol Cell Biol 2016;17:213–26.
33. Jaeger VK, Lebrecht D, Nicholson AG, Wells A, Bhayani H, Gazdhar A, et al. Mitochondrial DNA mutations and respiratory chain dysfunction in idiopathic and connective tissue disease-related lung fibrosis. Sci Rep 2019;9:5500.
34. Bueno M, Lai YC, Romero Y, Brands J, St Croix CM, Kamga C, et al. PINK1 deficiency impairs mitochondrial homeostasis and promotes lung fibrosis. J Clin Invest 2015;125:521–38.
35. Mills EL, Kelly B, O'Neill LA. Mitochondria are the powerhouses of immunity. Nat Immunol 2017;18:488–98.
36. Angelo A, Manfredi PR. The mitochondrion—a Trojan horse that kicks off inflammation? N Engl J Med 2010;362:2132–4.
37. Blanco LP, Pedersen HL, Wang X, Lightfoot YL, Seto N, Carmona-Rivera C, et al. Improved mitochondrial metabolism and reduced inflammation following attenuation of murine lupus with coenzyme Q10 analog idebenone. Arthritis Rheumatol 2020;72:454–64.
38. Lood C, Blanco LP, Purmalek MM, Carmona-Rivera C, De Ravin SS, Smith CK, et al. Neutrophil extracellular traps enriched in oxidized mitochondrial DNA are interferogenic and contribute to lupus-like disease. Nat Med 2016;22:146–53.
39. Lepelley A, Mina ED, Van Nieuwenhove E, Waumans L, Fraitag S, Rice GI, et al. Enhanced cGAS-STING-dependent interferon signaling associated with mutations in ATAD3A. J Exp Med 2021;218: e20201560.
40. Berthet A, Margolis EB, Zhang J, Hsieh I, Zhang J, Hnasko TS, et al. Loss of mitochondrial fission depletes axonal mitochondria in midbrain dopamine neurons. J Neurosci 2014;34:14304–17.
41. Scorrano L, Ashiya M, Buttle K, Weiler S, Oakes SA, Mannella CA, et al. A distinct pathway remodels mitochondrial cristae and mobilizes cytochrome c during apoptosis. Dev Cell 2002;2:55–67.
42. Patel S, Alvarez-Guaita A, Melvin A, Rimmington D, Dattilo A, Miedzybrodzka EL, et al. GDF15 provides an endocrine signal of nutritional stress in mice and humans. Cell Metab 2019;29:707–18.
43. Mahoney JM, Taroni J, Martyanov V, Wood TA, Greene CS, Pioli PA, et al. Systems level analysis of systemic sclerosis shows a network of immune and profibrotic pathways connected with genetic polymorphisms. PLoS Comput Biol 2015;11:e1004005.
44. Gyorfi AH, Matei AE, Distler JH. Targeting TGF-β signaling for the treatment of fibrosis. Matrix Biol 2018;68–69:8–27.
45. Chung KW, Dhillon P, Huang S, Sheng X, Shrestha R, Qiu C, et al. Mitochondrial damage and activation of the STING pathway lead to renal inflammation and fibrosis. Cell Metab 2019;30:784–99.
46. Zhao X, Psarianos P, Ghoraie LS, Yip K, Goldstein D, Gilbert R, et al. Metabolic regulation of dermal fibroblasts contributes to skin extracellular matrix homeostasis and fibrosis. Nat Metab 2019;1:147–57.
47. Sambo P, Baroni SS, Luchetti M, Paroncini P, Dusi S, Orlandini G, et al. Oxidative stress in scleroderma: maintenance of scleroderma fibroblast phenotype by the constitutive up-regulation of reactive oxygen species generation through the NADPH oxidase complex pathway. Arthritis Rheum 2001;44:2653–64.
48. Murphy-Marshman H, Quensel K, Shi-Wen X, Barnfield R, Kelly J, Peidl A, et al. Antioxidants and NOX1/NOX4 inhibition blocks TGFβ1-induced CCN2 and α-SMA expression in dermal and gingival fibroblasts. PLoS One 2017;12:e0186740.

American College of Rheumatology
Empowering Rheumatology Professionals

Arthritis & Rheumatology
Vol. 74, No. 5, May 2022, pp 882–891
DOI 10.1002/art.42050

Identification of Similarities Between Skin Lesions in Patients With Antisynthetase Syndrome and Skin Lesions in Patients With Dermatomyositis by Highly Multiplexed Imaging Mass Cytometry

Jay Patel, Adarsh Ravishankar, Spandana Maddukuri, Thomas Vazquez, Madison Grinnell, and Victoria P. Werth

Objective. Antisynthetase syndrome (ASyS) and dermatomyositis (DM) are autoimmune disorders that overlap clinically. Given the presence of DM-like skin lesions in ASyS patients, there is debate about whether ASyS is a distinct disease or a subclassification of DM. Recent studies identified differences in type I interferon (IFN) expression between ASyS and DM muscle and finger eruptions. This study was undertaken to elucidate similarities and differences in the pathogenesis of cutaneous disease in ASyS and DM at the single-cell level.

Methods. Five ASyS patients and 7 DM patients were recruited from a prospectively collected database of well-characterized DM patients. ASyS patients were clinically confirmed as having ASyS according to the Connors et al criteria and the Solomon et al criteria and the presence of aminoacyl–transfer RNA synthetase antibodies. Immunophenotyping was conducted using immunofluorescence (IF) and imaging mass cytometry (IMC).

Results. IF staining for MxA and IFNβ expression revealed up-regulation of type I IFN in ASyS and DM samples compared to healthy control samples ($P < 0.05$). IMC showed similar numbers of macrophages, T cells, B cells, and dendritic cells in ASyS and DM samples, with no differences in counts ($P > 0.05$), but an increase in myeloid dendritic cell percentage in DM samples ($P < 0.05$). Key type I IFN, cytokine, and JAK/STAT pathways were similarly expressed in both ASyS and DM ($P > 0.05$). At the single-cell level, macrophages positive for phosphorylated stimulator of IFN genes in ASyS samples expressed increased levels of tumor necrosis factor, interluekin-17 (IL-17), and IFNβ ($P < 0.001$).

Conclusion. IMC is a powerful tool that identifies a role for the type I IFN system in DM-like skin lesions in ASyS and DM with some differences at the cellular level, but overall significant overlap, supporting similar therapeutic decision making.

INTRODUCTION

Antisynthetase syndrome (ASyS) is a systemic autoimmune disorder characterized by the presence of autoantibodies against aminoacyl–transfer RNA synthetase (aaRS). Clinical features of ASyS include mechanic's hands, Raynaud's phenomenon (RP), interstitial lung disease (ILD), myositis, arthritis, and fever (1–3). Traditionally, ASyS is defined by the classic triad of arthritis, myositis, and ILD. Proposed diagnostic criteria by Connors et al (4) and Solomon et al (5) consist of anti-aaRS antibodies, ILD, dermatomyositis (DM) or polymyositis, arthritis, RP, and mechanic's hands. DM, similarly, is a systemic autoimmune disease that can occur with muscle weakness (classic DM) or without muscle weakness (amyopathic DM), both occurring with increased ILD risk and cutaneous manifestations including erythematous discoloration and papules over joints, erythema and scaling surrounding the eyelids, periungual telangiectasias, and cuticular dystrophy (6). DM is classically defined by a typical skin rash with

Supported by the NIH (grant R01-AA-R076766) and the Department of Veterans Affairs Veterans Health Administration, Office of Research and Development, Biomedical Laboratory Research.

Jay Patel, BS, Adarsh Ravishankar, MD, Spandana Maddukuri, MD, Thomas Vazquez, BS, Madison Grinnell, BA, Victoria P. Werth, MD: Corporal Michael J. Crescenz Veterans Affairs Medical Center and University of Pennsylvania, Philadelphia, Pennsylvania.

Author disclosures are available at https://onlinelibrary.wiley.com/action/downloadSupplement?doi=10.1002%2Fart.42050&file=art42050-sup-0001-Disclosureform.pdf.

Address correspondence to Victoria P. Werth, MD, Department of Dermatology, University of Pennsylvania, Perelman Center for Advanced Medicine, Suite 1-330A, 3400 Civic Center Boulevard, Philadelphia, PA 19104. Email: werth@pennmedicine.upenn.edu.

Submitted for publication April 25, 2021; accepted in revised form December 9, 2021.

or without evidence of muscle pathology determined by proximal muscle weakness, elevated muscle enzymes, electromyographic findings, or muscle biopsy abnormalities as proposed by Lundberg et al (7).

ASyS classification includes a serologic definition, ILD, arthritis, mechanic's hands, and RP, whereas DM classification focuses on objective skin or combined skin and muscle findings. The current criteria overlap significantly given the inclusion of DM criteria in ASyS criteria by Solomon et al (5) and given that ASyS criteria such as ILD, mechanic's hands, and RP are frequently present in patients with DM (3). Similarly, cutaneous DM manifestations are frequently observed in ASyS patients, with no differences found in erythema on the extensor surfaces of the extremities, periungual erythema, or poikiloderma (3). These similarities and differences may relate to specific aaRS antibodies, since Jo-1 and PL-7 are frequently associated with DM-specific skin manifestations and myositis, supporting the inclusion of Jo-1 in the European Alliance of Associations for Rheumatology (EULAR)/American College of Rheumatology (ACR) DM criteria (7,8).

Based on these criteria and other overlapping cutaneous manifestations of ASyS and DM, ASyS has traditionally been viewed clinically as a subset of DM (9). This continues to be a matter of debate among clinicians, with some describing the current ASyS criteria as poorly defined and requiring clinical judgement, ultimately leading to the current ongoing project of developing classification criteria for ASyS (1,10).

Recently, researchers have attempted to differentiate the pathogenesis of ASyS from that of DM to further separate the 2 entities. DM pathogenesis is thought to be a result of activation of the type I interferon system (IFN), in particular IFNβ (11–13). In light of this information, researchers have observed increased MxA protein expression in muscle and skin biopsy specimens from DM patients (14,15). Some evidence regarding reduced MxA expression in ASyS has emerged; muscle biopsy specimens from ASyS patients were shown to exhibit reduced MxA expression compared to samples from DM patients. Additionally, in finger eruptions in patients with anti-aaRS antibodies, there was decreased MxA expression. Moreover, on histopathologic examination, the lesions exhibited increased psoriasiform dermatitis and eczematous reaction when compared to melanoma differentiation–associated protein 5– and transcription intermediary factor 1γ–positive DM, which may be similar to the recently reported spongiotic dermatitis DM subset (3,15,16). Currently, most reported differences between ASyS and DM are observed on examination of biopsy specimens (17). This finding led to the suggestion of a unique myositis subtype at the European Neuromuscular Centre International Workshop (18).

With the current ongoing debate, we decided to investigate differences in the pathogenesis of skin lesions from areas other than the finger in ASyS and DM patients to see if we would observe similar differential expression of type I IFN using immunofluorescence (IF) and multiplexed imaging mass cytometry (IMC). This investigation on a multiplexed cellular level differs from traditional approaches and is capable of phenotyping single cells while preserving tissue architecture to identify similarities and differences between the immunopathogenesis of cutaneous lesions in DM patients and that of DM-like cutaneous lesions in ASyS patients. Ultimately, these findings will influence classification decisions made on holistic review of the syndrome and other manifestations of disease, but also importantly guide future treatment options for DM-like lesions in ASyS patients.

MATERIALS AND METHODS

Reagents and materials. All chemicals were diluted in Millipore filtered deionized water. Carrier-free antibodies were used, with vendor information provided in Supplementary Table 1, available on the *Arthritis & Rheumatology* website at http://onlinelibrary.wiley.com/doi/10.1002/art.42050. Conjugation of carrier-free antibodies to lanthanide series was performed using a Maxpar X8 antibody conjugation kit (Fluidigm). Blocking buffer consisted of phosphate buffered saline (PBS) with 5% bovine serum albumin (BSA), while staining buffer consisted of PBS with 1% BSA. Washing buffer consisted of PBS with 0.1% Tween 20 (Sigma-Aldrich).

Patients. Five ASyS patients and 7 DM patients were recruited from a prospectively collected database of well-characterized patients with DM according to the EULAR/ACR criteria (7). ASyS patients were referred to the clinic as DM patients, were clinically confirmed as having ASyS according to both the criteria of Connors et al (4) and the criteria of Solomon et al (5) and the presence of aaRS antibodies, and were subsequently included in this study with Institutional Review Board approval. All patients had to provide written informed consent to be included in the study. Lesional skin biopsy specimens were obtained before treatment at the time of diagnosis from sites that included the arm, neck, back, leg, chest, finger, and elbow (Supplementary Table 2, available on the *Arthritis & Rheumatology* website at http://onlinelibrary.wiley.com/doi/10.1002/art.42050). Information collected from chart review included demographic characteristics (age, sex, and race), DM subtype (classic or amyopathic), autoantibodies, presence of ILD, history of cancer-associated DM, and skin disease activity based on the Cutaneous Dermatomyositis Disease Area and Severity Index (19) closest to the time of biopsy.

Immunofluorescence. Biopsy specimens were obtained from the arm, leg, or chest of 3 ASyS patients and 3 matched DM patients and compared to biopsy specimens obtained from the arm, leg, or back of 3 healthy controls (Supplementary Table 2). IFNβ and MxA expression in biopsy specimens was evaluated by IF staining. Formalin-fixed paraffin-embedded (FFPE) biopsy specimens were cut into 4-μm sections and placed on glass slides. Slides were deparaffinized by heating overnight at

60°C followed by immersion in a xylene substitute (CitriSolv; Fisher Scientific). Subsequently, slides were rehydrated in 100%, 95%, 70%, and 50% ethanol followed by deionized water. Heat- and pressure-mediated antigen retrieval was performed using EDTA buffer at 95°C. Sections were blocked in 5% BSA for 1 hour at room temperature and then incubated with primary antibodies to the following antigens at 4°C overnight: IFNβ (Abcam) and MxA (GeneTex). Each section was then incubated with secondary goat anti-rabbit AF594 (ThermoFisher) for 1 hour at room temperature. Afterward, sections were treated with TrueView (Vector) for 2 minutes to reduce autofluorescence and mounted using antifade mounting medium containing DAPI (Vector). Sections were imaged using a Nikon Eclipse Ti microscope (Nikon Instruments). Three 20× objective magnification microscopic fields in the dermis were examined. ImageJ (National Institutes of Health) was used to measure the mean fluorescence intensity for each patient group.

Imaging mass cytometry. IMC was used to assess the composition of the immune cell population and the expression of inflammatory pathways at the single-cell level in FFPE sections as previously described (20). Tissue sections were collected and deparaffinized, and antigen was retrieved and blocked as described for IF staining. After blocking, sections were incubated in a cocktail of primary metal–conjugated antibodies at 4°C overnight (Supplementary Table 1). Slides were then washed in PBS–Tween 20 and counterstained using DNA intercalator (Fluidigm) for 30 minutes at room temperature. The slides were then washed with deionized water and air dried for 1 hour before imaging on a Hyperion Imaging System (Fluidigm). Two regions of interest at the dermal–epidermal junction of 2 mm × 1 mm spanning the entire immune infiltrate per tissue specimen were ablated at a frequency of 200 Hz.

Image processing and data analysis. An MCD Viewer (Fluidigm) was used to extract 32-bit TIFF images from each mass channel. All image composites generated for figures were passed through a 3 × 3 median filter in ImageJ software for visualization. Cell segmentation was performed using a nuclear-based algorithm designed in Visiopharm. The resulting segmentation image was imported into a CellProfiler pipeline to create an image mask. All images and corresponding masks were imported into histoCAT for single-cell mean pixel analysis. The PhenoGraph algorithm was implemented for user-guided unsupervised clustering of cell populations. Unresolved populations were further separated by another round of PhenoGraph analysis and subjected to gating when necessary to resolve cell populations, while unidentified populations were excluded from the analysis. The markers used for PhenoGraph analysis were selected based on cell markers displaying the best signal-to-noise ratio: phosphorylated stimulator of IFN genes (pSTING), CD14, CD16, CD31, FoxP3, CD4, CD68, blood dendritic cell antigen 2, CD8, CD56, CD3, CD20, CD11c, HLA–DR, and CD163 using the 30 nearest neighbors. Each cell cluster was overlaid with the respective cell marker TIFF images to confirm accurate identification of the cell type. Mean pixel intensities were used to assess the expression of inflammatory pathways in identified clusters, and t-distributed stochastic neighbor embedding (tSNE) plots were created to visualize the different clusters (histoCAT). Principal components analysis (PCA) of DM and ASyS patient samples utilizing cell counts and pathway expression was performed using the ClustVis web tool.

Deidentified data sets are available upon request from the corresponding author.

Statistical analysis. Statistical analysis was performed using GraphPad Prism version 8.3 (GraphPad Software). The nonparametric Kruskal-Wallis test controlled for false discovery rate was used to identify differences in IFNβ and MxA IF between healthy controls, DM patients, and ASyS patients. The Mann-Whitney test was used to identify differences in IMC cell populations and pathway expression between skin lesions from ASyS patients and skin lesions from DM patients. Values are presented as the median ± interquartile range. *P* values less than 0.05 were considered significant for all analyses except cellular pathway comparison, for which *P* values less than 0.001 were considered significant in order to correct for multiple hypothesis testing. Multiple hypothesis testing was not conducted for comparisons of IFNβ and MxA expression, immune cell distribution, or inflammatory pathway expression, given the

Table 1. Clinical characteristics of the patients*

	ASyS patients (n = 5)	DM controls (n = 7)
Anti-aaRS antibody positive, no.	5	0
ILD	5 (100)	1 (14.2)
Cancer-associated DM	1 (20)	0 (0)
CDASI activity score, median (IQR)	11 (7.5–14.5)	15 (3–27)
Gottron's sign	5 (100)	4 (57.1)
Gottron's papule	1 (20)	1 (14.2)
Heliotrope	3 (60)	6 (85.7)
V-neck erythema	3 (60)	5 (71.4)
Shawl sign	3 (60)	4 (57.1)
Mechanic's hands	3 (60)	3 (42.8)
Erosion/ulceration	1 (20)	1 (14.2)
Poikiloderma	2 (40)	6 (85.7)
Livedo	1 (20)	3 (42.8)
Oral ulceration	0 (0)	0 (0)
Arthritis	3 (60)	2 (28.5)
Myositis	4 (80)	4 (57.1)
Raynaud's phenomenon	1 (20)	4 (57.1)
Proximal nailfold changes	1 (20)	3 (42.8)

* Except where indicated otherwise, values are the number (%). Statistical comparisons were precluded by the small sample size. ASyS = antisynthetase syndrome; DM = dermatomyositis; anti-aaRS = anti–aminoacyl–transfer RNA synthetase; ILD = interstitial lung disease; CDASI = Cutaneous Dermatomyositis Disease Area and Severity Index; IQR = interquartile range.

small sample size, heterogeneity, limited tests, and statistically nonsignificant results.

RESULTS

Clinical characteristics of the ASyS and DM patients. A total of 5 antisynthetase antibody–positive patients and 7 DM controls without antisynthetase antibodies were enrolled. All patients in both cohorts were female and Caucasian (Supplementary Table 3, available on the *Arthritis & Rheumatology* website at http://onlinelibrary.wiley.com/doi/10.1002/art.42050). The clinical characteristics of the ASyS and DM patient groups are displayed in Table 1, and biopsy site locations are listed in Supplementary Table 2. In the ASyS group, 3 patients were positive for Jo-1, 1 was positive for PL-7, and 1 was positive for PL-12. All patients in the ASyS group had ILD, compared to only 14.2% of DM controls. All patients in both cohorts showed erythema over joints. ASyS patients had increased frequencies of mechanic's hands and erythema and papules over joints, while DM patients demonstrated increased frequencies of erythema and scaling on the eyelids and v of neck, and poikiloderma.

Similarly increased expression of IFNβ and MxA proteins in skin lesions from ASyS patients and DM patients. Skin lesions from ASyS patients showed increased IFNβ protein expression compared to skin from healthy controls ($P < 0.05$) (Figures 1A and C). These lesions also had elevated MxA protein expression compared to healthy control skin ($P < 0.05$)

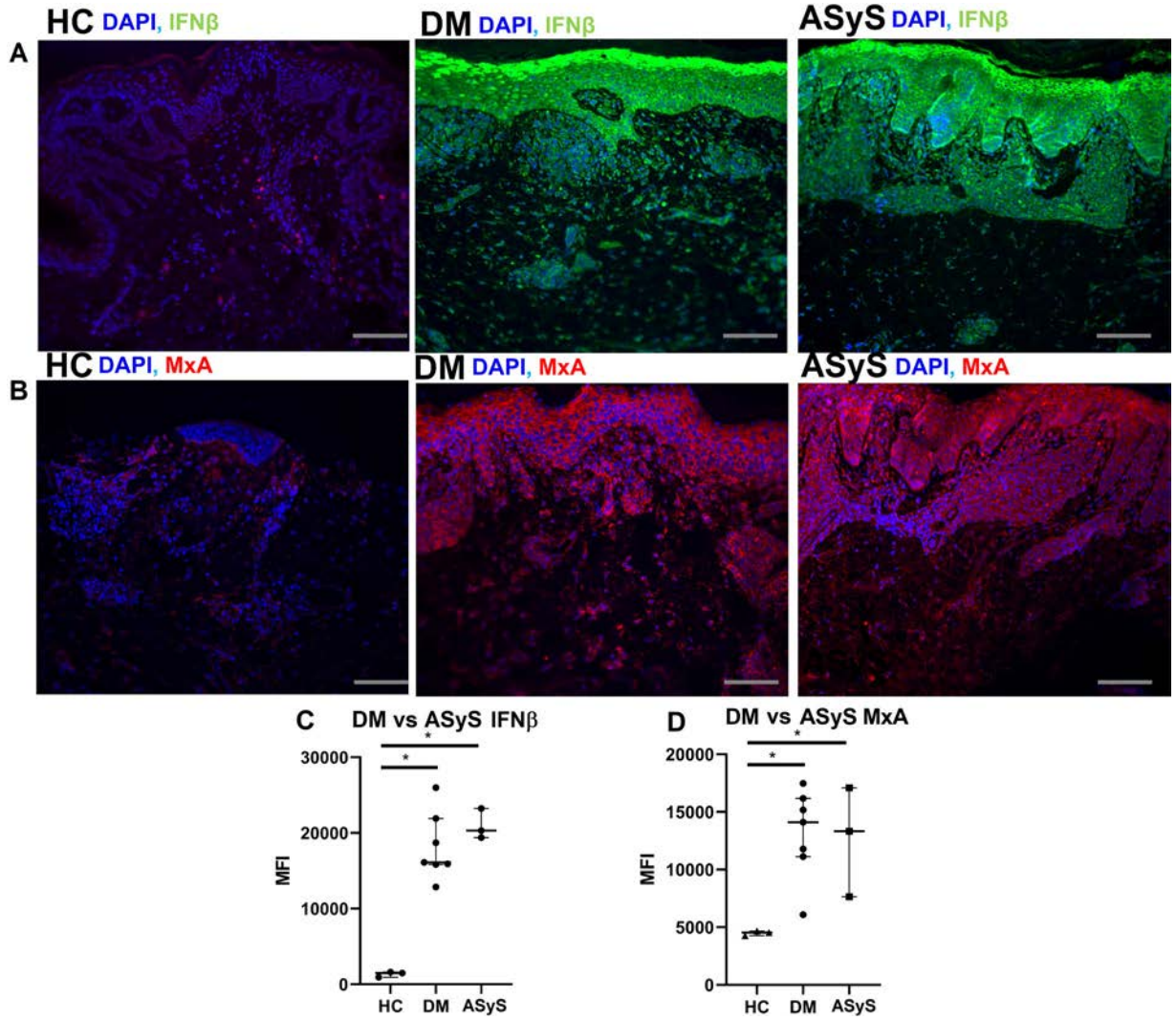

Figure 1. **A** and **B**, Immunofluorescence staining for interferon β (IFNβ) (**A**) and MxA (**B**) in skin samples from healthy controls (HCs), patients with dermatomyositis (DM), and patients with antisynthetase syndrome (ASyS). Staining showed decreased expression of IFNβ (green) and MxA (red) in skin samples from healthy controls compared to patients with DM and patients with ASyS. Nuclei were stained with DAPI (blue). Bars = 100 μm. **C** and **D**, Quantification of the mean fluorescence intensity (MFI) of IFNβ (**C**) and MxA (**D**) in skin samples from healthy controls, patients with DM, and patients with ASyS. IFNβ and MxA expression were significantly increased in lesional skin from DM patients and ASyS patients compared to skin samples from healthy controls. Symbols represent individual subjects; horizontal lines and error bars show the median and interquartile range. * = $P < 0.05$.

(Figures 1B and D). Similarly, DM patients had increased IFNβ and MxA protein expression compared to healthy controls ($P < 0.05$) (Figure 1). There was no difference in IFNβ or MxA protein expression between lesional skin from ASyS patients and lesional skin from DM patients ($P > 0.05$) (Figure 1).

Identification of cell clusters in skin lesions by IMC. We analyzed FFPE skin tissue from 5 ASyS patients and 7 DM patients by IMC to identify the different cell types present. Representative images from IMC are shown in Figure 2A, indicating a similar composition in skin from ASyS and DM patients. Utilizing a panel of immune cell markers, we used the PhenoGraph algorithm to independently cluster cells and identified 10 populations in skin lesions from both ASyS patients and DM patients. The cell populations were as follows: CD4+ T cells, Treg cells, CD8+ T cells, CD14+CD16+ macrophages, pSTING+ macrophages, myeloid dendritic cells (mDCs), plasmacytoid dendritic cells (pDCs), CD20+ B cells, endothelial cells, and CD56^{high} cells. A heatmap showing similar cell markers in ASyS and DM is displayed in Figure 2B. Plotting of the combined cell clusters in skin samples from ASyS patients and DM patients using the tSNE dimensionality reduction algorithm (Figure 2C) revealed similar spatial distribution of the cell clusters. The average relative composition of these cell populations in skin lesions from ASyS patients and DM patients is shown adjacent to tSNE plots via box plots (Figure 2C). Notably, on average, the mDC population was proportionally less in skin samples from ASyS patients compared to skin samples from DM patients. Despite similarities in the combined tSNE plot, there was significant intersample variability, which was subsequently addressed quantitatively using cell counts and pathway expression.

Similar absolute numbers of CD4+ T cells, CD8+ T cells, mDCs, Treg cells, CD56^{high} cells, CD14+CD16+ macrophages, pSTING+ macrophages, CD20+ B cells, and pDCs, but a higher percentage of mDCs, in skin lesions from DM patients compared to skin lesions from ASyS patients. To evaluate the contributions of each cell population in either ASyS or DM, we quantified each cell population as the absolute number of cells and as the percentage of total cells. Skin lesions from ASyS patients and skin lesions from DM patients, which had similar clusters of cells, also had similar absolute

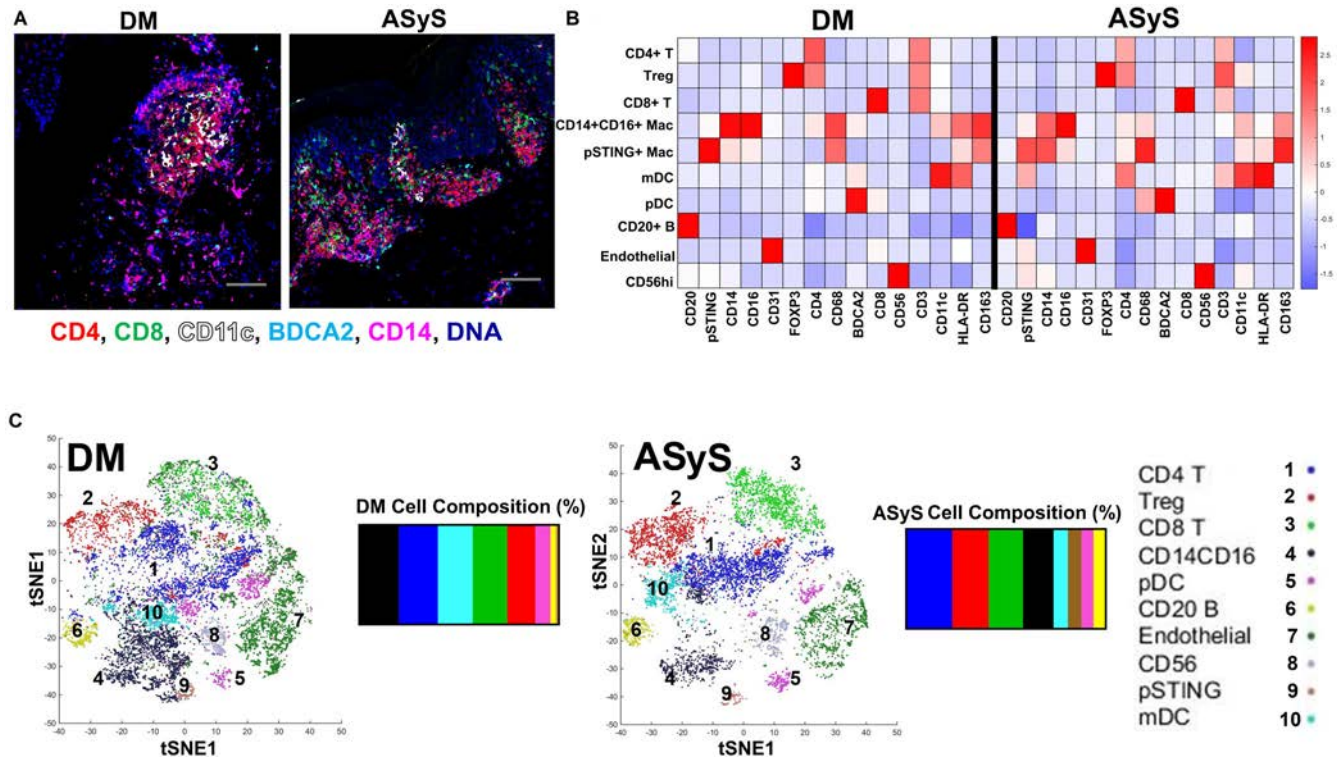

Figure 2. Identification of cell clusters in skin lesions from patients with dermatomyositis (DM) and patients with antisynthetase syndrome (ASyS), using imaging mass cytometry and the PhenoGraph algorithm for unsupervised clustering. **A**, Representative multiplexed images of lesional skin from a DM patient and lesional skin from an ASyS patient, showing similar proportions of CD4 cells (red), CD8 cells (green), CD11c cells (white), blood dendritic cell antigen (BDCA-2) cells (cyan), and CD14 cells (magenta). DNA was stained with Iridium Intercalator (blue). Bars = 100 μm. **B**, Heatmap generated from 10 PhenoGraph-derived clusters, showing similar cell surface expression in skin samples from DM patients and ASyS patients. **C**, Plots of t-distributed stochastic neighbor embedding (tSNE) of cell clusters in skin samples from ASyS patients and DM patients, and average composition of the cell population for the identified clusters. Mac = macrophage; pSTING = phosphorylated stimulator of interferon genes; mDC = myeloid dendritic cell; pDC = plasmacytoid dendritic cell.

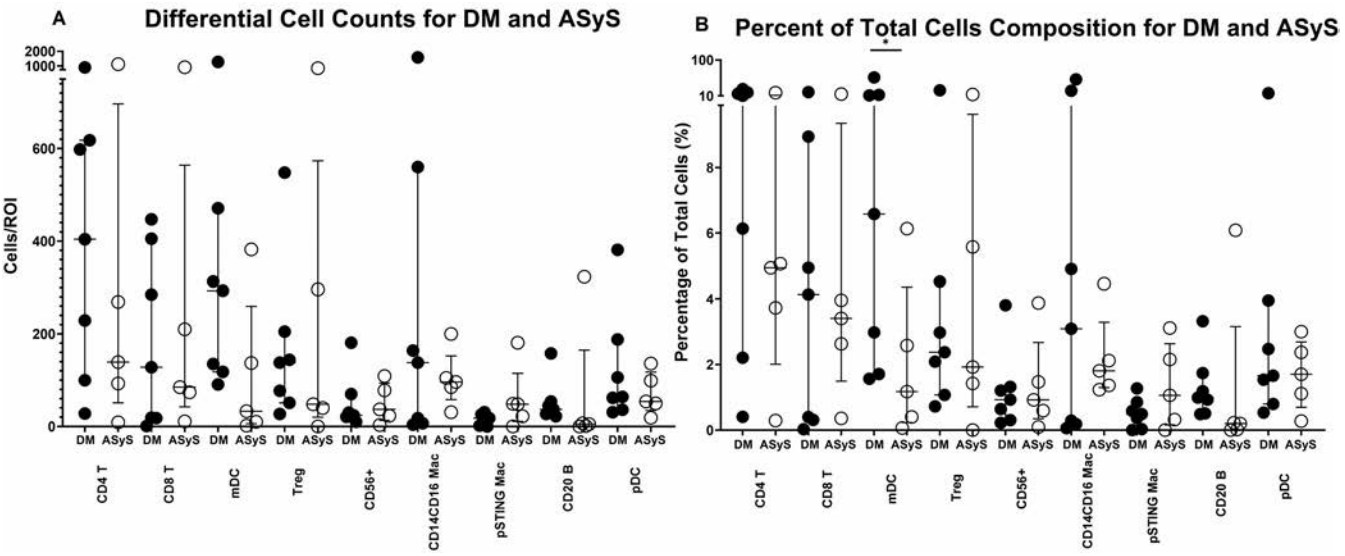

Figure 3. Distribution of immune cell subsets in skin samples from patients with DM and patients with ASyS. **A**, Absolute counts for each cell type. There were no differences between DM and ASyS ($P > 0.05$). **B**, Percentage of the total cell population for each cell type. There was an increased percentage of mDCs in DM compared to ASyS. Symbols represent individual patients; horizontal lines and error bars show the median and interquartile range. * = $P < 0.05$. ROI = region of interest (see Figure 2 for other definitions).

numbers of all 9 immune cell populations ($P > 0.05$) (Figure 3A). We also compared the cell clusters using percentage of total cells, which revealed an increase in the percentage of mDCs in skin lesions from DM patients compared to skin lesions from ASyS patients ($P < 0.05$) (Figure 3B).

Similar expression of key inflammatory pathways in skin lesions from ASyS patients and skin lesions from DM patients. To evaluate the expression of various phosphorylated inflammatory pathways and their contributions in each disease, the mean pixel intensity per cell was calculated and

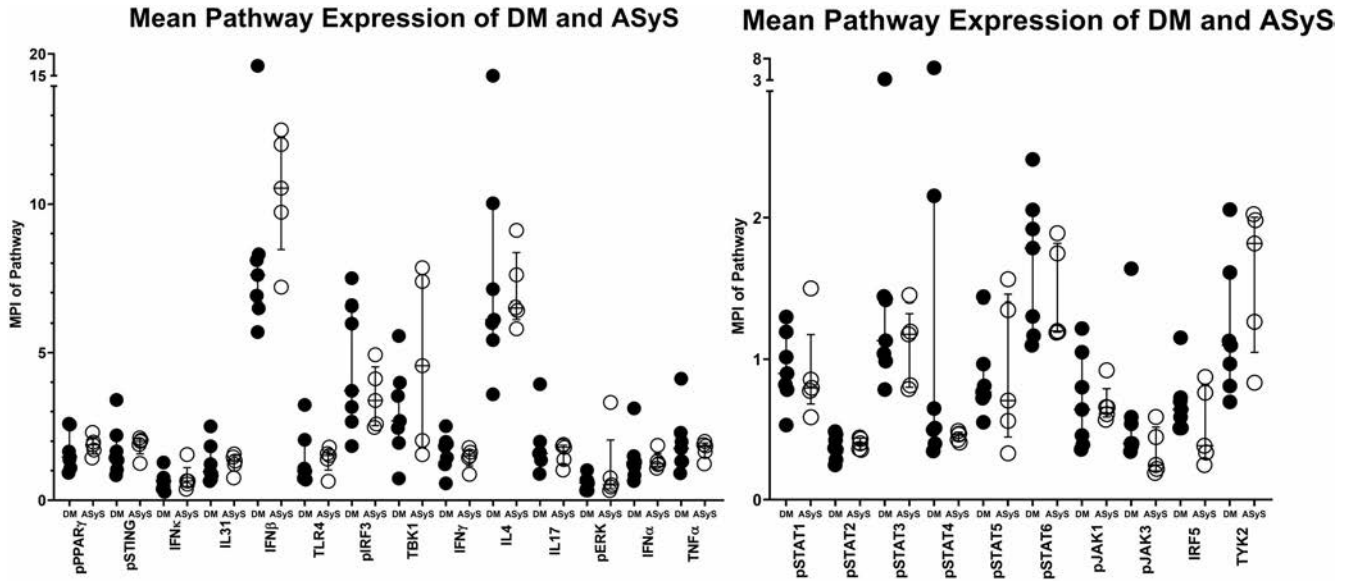

Figure 4. Key inflammatory pathway expression in skin samples from patients with dermatomyositis (DM) and patients with antisynthetase syndrome (ASyS). Inflammatory pathway expression was calculated as mean pixel intensity (MPI) per sample. No differences were found between DM and ASyS in the expression of the following pathways: phosphorylated peroxisome proliferator–activated receptor γ (pPPARγ), phosphorylated stimulator of interferon genes (pSTING), interferon-κ (IFNκ), interleukin-31 (IL-31), IFNβ, Toll-like receptor 4 (TLR-4), IFN regulatory factor 3 (IRF-3), TANK-binding kinase 1 (TBK1), IFNγ, IL-4, IL-17, pERK, IFNα, tumor necrosis factor (TNF), pSTAT1, pSTAT2, pSTAT3, pSTAT4, pSTAT5, pSTAT6, pJAK1, pJAK3, IRF-5, and TYK2 ($P > 0.05$). Symbols represent individual patients; horizontal lines and error bars show the median and interquartile range.

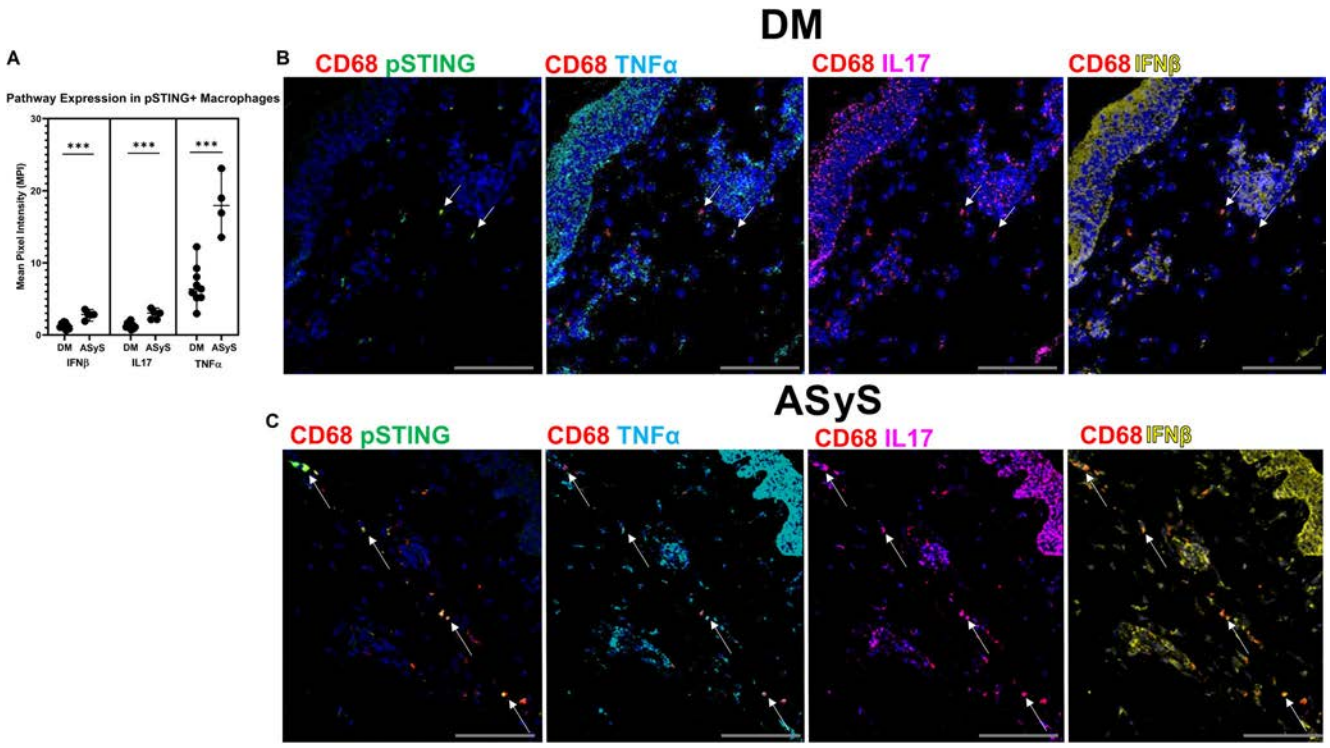

Figure 5. Higher expression of IFNβ, IL-17, and TNF by pSTING+ macrophages in skin samples from patients with ASyS than in skin samples from patients with DM. **A**, Mean pixel intensity of IFNβ, IL-17, and TNF expression by pSTING+ macrophages in skin samples from patients with DM and patients with ASyS. Expression of all 3 cytokines was higher in skin samples from ASyS patients. *** = $P < 0.001$. **B** and **C**, Representative images of pSTING+ (green) CD68+ (red) macrophages in skin samples from a DM patient and an ASyS patient, showing expression of TNF (teal), IL-17 (purple), and IFNβ (yellow). Nuclei were stained with intercalator Ir (blue). **Arrows** indicate representative cells. Bars = 100 μm. See Figure 4 for definitions.

compared. There was no difference in inflammatory pathway expression (mean pixel intensity) of the following between ASyS and DM: p–peroxisome proliferator–activated receptor γ, pSTING, IFNκ, interleukin-31 (IL-31), IFNβ, Toll-like receptor 4, IFN regulatory factor 3 (IRF-3), TANK-binding kinase 1 (TBK1), IFNγ, IL-4, IL-17, pERK, IFNα, tumor necrosis factor (TNF), pSTAT1, pSTAT2, pSTAT3, pSTAT4, pSTAT5, pSTAT6, pJAK1, pJAK3, IRF-5, and TYK2 ($P > 0.05$) (Figure 4). PCA of ASyS patient samples and DM patient samples revealed clustering of the 3 anti–Jo-1–positive ASyS patients (ASyS patients 2–4), the anti–PL-12–positive ASyS patient (ASyS patient 1), and a majority of the DM patients, with separation of the anti–PL-7–positive ASyS patient (ASyS patient 5) (Supplementary Figure 1, available on the *Arthritis & Rheumatology* website at http://onlinelibrary.wiley.com/doi/10.1002/art.42050).

Increased production of TNF, IL-17, and IFNβ by pSTING+ macrophages in skin samples from ASyS patients compared to skin samples from DM patients. Visual inspection of a heatmap of intracellular cytokines and phosphorylated pathways revealed potentially increased inflammatory cytokine production by pSTING+ macrophages in skin samples from ASyS patients relative to skin samples from DM patients. Comparison of cellular cytokine expression by pSTING+ macrophages between skin samples from ASyS patients and skin samples from DM patients showed increased production of IFNβ, TNF, and IL-17 in ASyS ($P < 0.001$) (Figure 5A). Representative images of pSTING+ macrophages in skin samples from DM patients and ASyS patients, demonstrating colocalization of CD68, pSTING, IFNβ, TNF, and IL-17, are shown in Figures 5B and C.

DISCUSSION

Recently, researchers have attempted to differentiate the pathogenesis of ASyS from that of DM to further separate the 2 entities and aid classification by contrasting the contribution of the type I IFN system in ASyS and DM (11–13). Given the presence of DM-like skin lesions in ASyS patients with anti–Jo-1, anti-EJ, and anti–PL-7, we sought to investigate differences between the cells, cytokines, and activated pathways in these DM-like lesions in ASyS patients and traditional DM lesions (3). By doing so we were able to observe pathologic similarities and differences to better classify such cutaneous manifestations as being consistent with DM and amenable to DM-targeted therapies, or as being a separate entity more consistent with ASyS.

With regard to type I IFN contribution, we observed increased IFNβ and MxA expression in skin samples from both ASyS patients and DM patients, with no differences between the 2 diseases, conflicting with previous findings of decreased MxA expression in finger eruptions and muscle biopsy specimens from ASyS patients (14,15). The increased levels of these 2 type I IFN proteins may suggest a role for type I IFNs in the pathogenesis of DM-like skin lesions seen in certain ASyS patients.

Given the similar type I IFN expression in skin samples from DM patients and ASyS patients, we decided to implement IMC to further analyze pathologic differences at the single-cell level. Use of a Hyperion imaging system allows for the identification of multiple antigens in tissue using a panel of metal-conjugated antibodies. Subsequent images may be processed using tools such as Visiopharm and CellProfiler to segment cellular outlines and create masks. These masks are ultimately imported into histoCAT along with original images to gather single-cell antigen data based on mask outlining. PhenoGraph was used as a tool that independently clusters cells based on identification of communities using higher-dimensional proximity. Conventional immunostaining would require an endless array of combinations to identify various populations of immune cells and their expression of markers of inflammation. Flow cytometry or mass cytometry techniques may similarly provide multiplexed data; however, these techniques require ex vivo processing of tissue and stimulation practices that undoubtedly alter cellular phenotype and ultimate conclusions. This novel unbiased approach of simultaneously staining different cell markers allows for identification of cell types and their similarities and differences between the 2 diseases while preserving tissue architecture and in vivo phenotypes.

Skin samples from both ASyS patients and DM patients exhibited similar cell clusters, as seen on the heatmap, IMC images, and tSNE dimensionality reduction plots for the 2 diseases. To examine differences in cell type prevalence, we quantified known infiltrating immune cells in DM and corresponding immune cells in ASyS. Monocyte/macrophages have been implicated in DM disease, as increased serum concentrations of monocyte-derived particles have been noted in DM patients (21). A recent study has identified significant differences in monocyte-derived macrophage migration in DM (22). We found similar numbers of CD14+CD16+ and pSTING+ macrophages in skin samples from both ASyS patients and DM patients, suggesting similar cell recruitment; however, there were differences with regard to pathway expression with pSTING+ macrophages when phenotypes were compared.

In terms of the T cell compartment, we investigated differences between CD4 T cells, CD8 T cells, and Treg cells. CD4 T cells have been known to be present in DM, and are thought to contribute to skin manifestations (23). CD8 T cells have been noted in DM muscle with decreased CD28 expression (24). Treg cells have been reported in DM and response/impairment may modulate the immunoregulatory environment (25). No differences in CD4 cells, CD8 cells, or Treg cells were observed between lesional skin from ASyS patients and lesional skin from DM patients, suggesting a similar distribution of the T lymphocytic infiltrate.

Plasmacytoid DCs have also been implicated in DM, with increased presence in the skin. The contribution of pDCs may be similar in each disease, since no difference was observed between skin samples from ASyS patients and skin samples from DM patients. Most recently, IFNβ+ mDCs have also been identified in DM (20,26); in the present study we found no difference in absolute mDC numbers between skin samples from ASyS patients and skin samples from DM patients. However, there was an increased percentage of mDCs in DM, suggesting their importance in type I IFN pathogenesis in DM compared to ASyS. Despite this finding, the large variability of the dermal counts of these cells in DM should be noted, as some patients have very few. Importantly, for all the other immune cells identified, there were no significant differences in absolute count or percentages, other than for mDCs, between ASyS and DM. This suggests a similar overall immune cell composition between DM-like lesions in ASyS and DM lesions, with the possibility of some differences with regard to mDCs.

When comparing pathway expression between ASyS and DM on IMC, we identified similar expression of key inflammatory pathways. Of these pathways, pSTING, pIRF-3, IFNβ, IFNκ, IFNα, IRF-5, TYK2, and TBK1 relate to the type I IFN system. The cGAS/STING pathway has gained attention due to its implications in systemic lupus erythematous and other autoimmune diseases as a stimulator of type I IFN (27). The IRF-3 and TBK1 pathways are downstream of STING, upstream of type I IFN transcription, and have been identified as possible therapeutic targets for certain autoimmune diseases such as DM, lupus, and "interferonopathies" (28). ASyS did not differ from DM in expression of these 3 pathways at the total biopsy level, and ASyS patients may therefore also benefit from type I IFN–guided therapy. The other cytokines and JAK/STAT pathways were identified based on their associations with DM pathogenesis and autoimmunity in general. These pathways did not differ in activation between skin samples from ASyS patients and skin samples from DM patients, suggesting they are not important differentiators of pathogenesis.

At the single-cell level, expression was compared between ASyS and DM within the cell populations identified. Further inspection of pSTING+ macrophages revealed increased production of IFNβ, IL-17, and TNF in ASyS compared to DM, with a trend toward increased pSTING+ macrophage counts in ASyS compared to DM. In combination with the decreased mDC percentages in ASyS, there may be a shift in IFNβ production toward pSTING+ macrophages and away from mDCs in ASyS compared to DM. Macrophage IL-17 increases may be related to profibrotic

differences between ASyS and DM, since IL-17 has been implicated in ILD and fibroblast response (29). Increased macrophage TNF may serve as a mechanism for regulation of type I IFN in ASyS since it is known to oppose IFN production at times. However, such observations are largely context dependent and require follow-up as overall type I IFN expression did not differ between the diseases (30).

Further research is needed, since ASyS is still poorly defined. Some of our findings conflict with the findings seen in muscle biopsy specimens and cutaneous finger eruptions in ASyS patients; however, we compared DM-like lesions in ASyS to lesions in DM. There may be some differences in mDCs and pSTING+ macrophages, although these findings are limited due to multiple hypothesis testing. Our study is limited by the inclusion of only 5 ASyS patients and 7 DM patients, limiting the power of each individual finding, and the need for matched locations of lesions in ASyS and DM. Larger studies may be needed to identify differences between the diseases and different site-specific cutaneous manifestations. There are also a variety of rare immune cell subsets that we did not investigate, such as other granulocytes, T cell subsets, and B cell subsets. Other pathways also exist that may aid in the resolution of their respective diseases.

Nonetheless, despite previous differences seen in finger eruptions, our examination of DM-like skin lesions in ASyS and skin lesions in DM revealed no major differences with regard to type I IFN pathways. We identified similar expression of IFNβ and MxA in skin samples from both DM patients and ASyS patients, the majority of immune cells in skin samples from DM patients and ASyS patients did not differ in cell number, and the expression of most selected inflammatory pathways did not differ. This suggests that the pathogenesis of DM-like skin lesions in ASyS may be closely related to DM and the type I IFN system. However, with the use of IMC we were able to further investigate cellular pathway differences, highlighting a potential shift in pSTING+ macrophage pathways in ASyS compared to DM. This novel technology augments overall understanding of pathogenesis in vivo as these differences are easily overlooked with traditional global staining methods. Despite differences among pSTING+ macrophages, DM-like lesions in ASyS patients notably have similar pathology to lesions in DM patients, and this study provides insight into the pathogenesis of both ASyS and DM to inform holistic classification goals while guiding treatment selection for skin disease.

AUTHOR CONTRIBUTIONS

All authors were involved in drafting the article or revising it critically for important intellectual content, and all authors approved the final version to be published. Dr. Werth had full access to all of the data in the study and takes responsibility for the integrity of the data and the accuracy of the data analysis.

Study conception and design. Patel, Ravishankar, Werth.

Acquisition of data. Patel, Ravishankar, Maddukuri, Vazquez, Grinnell, Werth.

Analysis and interpretation of data. Patel, Ravishankar, Maddukuri, Vazquez, Grinnell, Werth.

REFERENCES

1. Witt LJ, Curran JJ, Strek ME. The diagnosis and treatment of antisynthetase syndrome. Clin Pulm Med 2016;23:218–26.
2. Love LA, Leff RL, Fraser DD, Targoff IN, Dalakas M, Plotz PH, et al. A new approach to the classification of idiopathic inflammatory myopathy: myositis-specific autoantibodies define useful homogeneous patient groups. Medicine (Baltimore) 1991;70:360–74.
3. Fukamatsu H, Hirai Y, Miyake T, Kaji T, Morizane S, Yokoyama E, et al. Clinical manifestations of skin, lung and muscle diseases in dermatomyositis positive for anti-aminoacyl tRNA synthetase antibodies. J Dermatol 2019;46:886–97.
4. Connors GR, Christopher-Stine L, Oddis CV, Danoff SK. Interstitial lung disease associated with the idiopathic inflammatory myopathies: what progress has been made in the past 35 years? Chest 2010;138:1464–74.
5. Solomon J, Swigris JJ, Brown KK. Myositis-related interstitial lung disease and antisynthetase syndrome. J Bras Pneumol 2011;37:100–9.
6. Krathen M, Fiorentino D, Werth V. Dermatomyositis. Curr Dir Autoimmun 2008;10:313–32.
7. Lundberg IE, Tjärnlund A, Bottai M, Werth VP, Pilkington C, de Visser M, et al. 2017 European League Against Rheumatism/American College of Rheumatology classification criteria for adult and juvenile idiopathic inflammatory myopathies and their major subgroups. Arthritis Rheumatol 2017;69:2271–82.
8. Hamaguchi Y, Fujimoto M, Matsushita T, Kaji K, Komura K, Hasegawa M, et al. Common and distinct clinical features in adult patients with anti-aminoacyl-tRNA synthetase antibodies: heterogeneity within the syndrome. PLoS One 2013;8:60442.
9. Matsushita T, Hasegawa M, Fujimoto M, Hamaguchi Y, Komura K, Hirano T, et al. Clinical evaluation of anti-aminoacyl tRNA synthetase antibodies in Japanese patients with dermatomyositis. J Rheumatol 2007;34:1012–8.
10. Castañeda S, Cavagna L, González-Gay MA. New criteria needed for antisynthetase syndrome. JAMA Neurol 2018;75:258–9.
11. Baechler EC, Bilgic H, Reed AM. Type I interferon pathway in adult and juvenile dermatomyositis. Arthritis Res Ther 2011;13:249.
12. Liao AP, Salajegheh M, Nazareno R, Kagan JC, Jubin RG, Greenberg SA. Interferon β is associated with type 1 interferon-inducible gene expression in dermatomyositis. Ann Rheum Dis 2011;70:831–6.
13. Wong D, Kea B, Pesich R, Higgs BW, Zhu W, Brown P, et al. Interferon and biologic signatures in dermatomyositis skin: specificity and heterogeneity across diseases. PLoS One 2012;7:e29161.
14. Uruha A, Allenbach Y, Charuel JL, Musset L, Aussy A, Boyer O, et al. Diagnostic potential of sarcoplasmic myxovirus resistance protein A expression in subsets of dermatomyositis. Neuropathol Appl Neurobiol 2019;45:513–22.
15. Okiyama N, Yamaguchi Y, Kodera M, Hamaguchi Y, Yokozeki H, Ishiguro N, et al. Distinct histopathologic patterns of finger eruptions in dermatomyositis based on myositis-specific autoantibody profiles. JAMA Dermatology 2019;155:1080–2.
16. Zeidi M, Chen KL, Patel B, Ravishankar A, Lim R, Werth VP. Increased MxA protein expression and dendritic cells in spongiotic dermatitis differentiates dermatomyositis from eczema in a single-center case-control study. J Cutan Pathol 2020;48:364–73.
17. Aouizerate J, Amer YB, Bazzez G, Gherardi R, Rigoloet M, Authier F. Myofiber HLA-DR expression is a distinctive biomarker for overlap myositis and inclusion body myositis. Neuromuscul Disord 2015;2:154.

18. De Bleecker JL, De Paepe B, Aronica E, de Visser M, Amato A, Benveniste O, et al. 205th ENMC International Workshop: pathology diagnosis of idiopathic inflammatory myopathies part II 28-30 March 2014, Naarden, The Netherlands. Neuromuscul Disord 2015;25: 268–72.
19. Anyanwu CO, Fiorentino DF, Chung L, Dzuong C, Wang Y, Okawa J, et al. Validation of the Cutaneous Dermatomyositis Disease Area and Severity Index (CDASI): characterizing disease severity and assessing responsiveness to clinical change. Br J Dermatol 2015; 173:969–974.
20. Patel J, Maddukuri S, Li Y, Bax C, Werth VP. Highly multiplexed mass cytometry identifies the immunophenotype in the skin of dermatomyositis. J Invest Dermatol 2021;141:2151–60.
21. Baka Z, Senolt L, Vencovsky J, Mann H, Simon PS, Kittel Á, et al. Increased serum concentration of immune cell derived microparticles in polymyositis/dermatomyositis. Immunol Lett 2010;128: 124–30.
22. Jiang T, Huang Y, Liu H, Xu Q, Gong Y, Chen Y, et al. Reduced miR-146a promotes REG3A expression and macrophage migration in polymyositis and dermatomyositis. Front Immunol 2020;11:37.
23. Malmström V, Venalis P, Albrecht I. T cells in myositis. Arthritis Res Ther 2012;14:230.
24. Fasth AE, Dastmalchi M, Rahbar A, Salomonsson S, Pandya JM, Lindroos E, et al. T cell infiltrates in the muscles of patients with dermatomyositis and polymyositis are dominated by CD28 null T cells. J Immunol 2009;183:4792–9.
25. Antiga E, Kretz CC, Klembt R, Massi D, Ruland V, Stumpf C, et al. Characterization of regulatory T cells in patients with dermatomyositis. J Autoimmun 2010;35:342–50.
26. Chen KL, Patel J, Zeidi M, Wysocka M, Bashir MM, Patel B, et al. Myeloid dendritic cells are major producers of IFN-β in dermatomyositis and may contribute to hydroxychloroquine refractoriness. J Invest Dermatol 2021;141:1906–14.
27. Zhou R, Xie X, Li X, Qin Z, Wei C, Liu J, et al. The triggers of the cGAS-STING pathway and the connection with inflammatory and autoimmune diseases. Infect Genet Evol 2020;77:104094.
28. Gitiaux C, Bondet V, Bekaddour N, Nusbaum P, Hubas A, Melki I, et al. Inhibition of IFNα secretion in cells from patients with juvenile dermatomyositis under TBK1 inhibitor treatment revealed by single-molecular assay technology. Rheumatology 2020;59:1171–74.
29. Zhang J, Wang D, Wang L, Wang S, Roden AC, Zhao H, et al. Profibrotic effect of IL-17A and elevated IL-17RA in idiopathic pulmonary fibrosis and rheumatoid arthritis-associated lung disease support a direct role for IL-17A/IL-17RA in human fibrotic interstitial lung disease. Am J Physiol Lung Cell Mol Physiol 2019;316:L487–97.
30. Cantaert T, Baeten D, Tak PP, van Baarsen LG. Type I IFN and TNFα cross-regulation in immune-mediated inflammatory disease: basic concepts and clinical relevance. Arthritis Res Ther 2010;12:219.

American College of Rheumatology
Empowering Rheumatology Professionals

Arthritis & Rheumatology
Vol. 74, No. 5, May 2022, pp 902–907
DOI 10.1002/art.42017

BRIEF REPORT

Defibrotide Inhibits Antiphospholipid Antibody–Mediated Neutrophil Extracellular Trap Formation and Venous Thrombosis

Ramadan A. Ali,[1] Shanea K. Estes,[1] Alex A. Gandhi,[1] Srilakshmi Yalavarthi,[1] Claire K. Hoy,[1] Hui Shi,[1] Yu Zuo,[1] Doruk Erkan,[2] and Jason S. Knight[1]

Objective. Defibrotide is a heterogenous mixture of polyanionic oligonucleotides currently approved for treatment of transplant-associated venoocclusive disease. While defibrotide has a known role in limiting endothelial cell activation, some studies have also demonstrated anti-leukocyte properties. In a recent study, we found that neutrophil extracellular traps (NETs) play a role in the thrombotic complications of antiphospholipid syndrome (APS). In the present study, we investigated the hypothesis that defibrotide might act to mitigate APS-relevant NET formation in vitro and in mouse models.

Methods. We used in vitro assays and a mouse model to determine the mechanisms by which defibrotide inhibits NET formation and venous thrombosis in APS.

Results. At doses ranging from 1 to 10 μg/ml, defibrotide significantly suppressed NET formation from control neutrophils stimulated with IgG isolated from patients with APS. Defibrotide increased levels of intracellular cyclic AMP in neutrophils, and its suppressive effects on NET formation were mitigated by blocking adenosine A_{2A} receptor or by inhibiting the cyclic AMP–dependent kinase protein kinase A. Defibrotide at doses ranging from 15 to 150 mg/kg/day inhibited NET formation and venous thrombosis in a model of antiphospholipid antibody–accelerated thrombosis—an effect that was reduced in adenosine A_{2A} receptor–knockout mice.

Conclusion. This study is the first to demonstrate mechanisms by which defibrotide counteracts neutrophil-mediated thrombotic inflammation inherent to APS.

INTRODUCTION

Antiphospholipid syndrome (APS) is a thromboinflammatory disease characterized by circulating antiphospholipid antibodies, classically anticardiolipin and anti–β_2-glycoprotein I (anti-β_2GPI). Meanwhile, additional relevant antibodies such as anti–phosphatidylserine/prothrombin can be detected by a functional screen called the lupus anticoagulant assay (1). APS is a leading acquired cause of both thrombotic events and pregnancy morbidity. Treatment of APS typically focuses on suppressing thrombosis with anticoagulation. However, anticoagulation does not fully protect against thrombotic events, conveys an increased risk of bleeding, and in many cases fails to restrain microvascular complications of APS such as diffuse alveolar hemorrhage, nephropathy, and livedoid vasculopathy.

Neutrophil extracellular traps (NETs) are web-like tangles of DNA, chromatin, and granule proteins released into the extracellular space by neutrophils in response to both infectious and sterile stimuli (2,3). NETs have been revealed as pathogenic actors in numerous autoimmune and thromboinflammatory diseases ranging from lupus to sepsis to COVID-19. To this end, recent work has pointed to a multifaceted (and generally deleterious) intersection between NETs and the vasculature. The proteases and histones of NETs kill endothelial cells (4). NETs stimulate type

Supported by Jazz Pharmaceuticals. Dr. Zuo's work was supported by career development grants from the Rheumatology Research Foundation, Arthritis National Research Foundation, and AntiPhospholipid Syndrome Alliance for Clinical Trials and International Networking (APS ACTION). Dr. Knight's work was supported by grants from the NIH (R01-HL-115138), the Lupus Research Alliance, the Rheumatology Research Foundation, and the Burroughs Wellcome Fund.

[1]Ramadan A. Ali, PhD, Shanea K. Estes, MLI, Alex A. Gandhi, BS, Srilakshmi Yalavarthi, MS, Claire K. Hoy, BS, Hui Shi, MD, PhD, Yu Zuo, MD, Jason S. Knight, MD, PhD: University of Michigan, Ann Arbor; [2]Doruk Erkan, MD: Hospital for Special Surgery, Weill Cornell Medicine, New York, New York.

Author disclosures are available at https://onlinelibrary.wiley.com/action/downloadSupplement?doi=10.1002%2Fart.42017&file=art42017-sup-0001-Disclosureform.pdf.

Address correspondence to Jason S. Knight, MD, PhD, 1150 West Medical Center Drive, Ann Arbor, MI 48109. Email: jsknight@umich.edu.

Submitted for publication March 25, 2021; accepted in revised form October 28, 2021.

I interferon production, which reduces the numbers and function of restorative endothelial progenitors (5). Furthermore, NET-derived DNA triggers coagulation, while histones activate platelets (6).

In studies from our group and others, NETs have been observed to play a role in the thrombotic complications of APS. Neutrophils isolated from patients with APS have a diminished threshold for spontaneous NET formation, while neutrophils from healthy volunteers can be activated to release NETs by exposure to APS serum or purified antiphospholipid antibodies (7). In mouse models of antiphospholipid antibody–accelerated large vein thrombosis, treatments that counteract NETs such as neutrophil depletion (8), administration of intravenous deoxyribonuclease (8), agonism of neutrophil adenosine A_{2A} receptors (9), boosting neutrophil cyclic AMP (cAMP) levels (10), and interfering with adhesive interactions between neutrophils and the endothelium (11) are all protective.

Defibrotide is a mixture of polyanionic phosphodiester oligonucleotides isolated from porcine intestinal mucosa cells. Defibrotide is approved for the treatment of patients who have venooclusive disease (VOD) with hepatic, renal, or pulmonary dysfunction complications developing following hematopoietic stem cell transplantation (HSCT) (12,13). Defibrotide is considered a multitarget compound, and is best known for its ability to limit endothelial cell activation (14). At the same time, some older literature demonstrates anti-leukocyte and anti-neutrophil properties of defibrotide (15), with that research mostly completed prior to the first descriptions of NETs in 2004 (2). Almost 20 years ago, defibrotide was first suggested as a possible treatment for APS, especially the life-threatening microangiopathic variant known as catastrophic APS (CAPS) (16). However, this possibility has not been investigated in trials, nor have possible mechanisms been explored in the laboratory. Here, we hypothesized that defibrotide might act to mitigate APS-relevant NET formation in vitro and in mouse models.

MATERIALS AND METHODS

Isolation of human IgG. A protein G agarose kit (Pierce) was used to isolate IgG from the sera of patients with APS and healthy controls. This was done according to the manufacturer's instructions (Pierce) as we have reported previously (7,9).

Human neutrophil isolation and NET formation assays. Neutrophils were isolated from human blood as previously described by our group (7,9). NET formation was monitored using an assay that quantifies nuclease-liberated myeloperoxidase (MPO) activity. Neutrophils were cultured in RPMI medium (Gibco) supplemented with 0.5% heat-inactivated fetal bovine serum (Gibco) and 0.5% bovine serum albumin (Sigma) at 37°C. Neutrophils were seeded into 96-well plates at a density of 1×10^5/well. Stimulation was for 3 hours with 100 n*M* of phorbol 12-myristate 13-acetate (PMA; Sigma) or 10 μg/ml of IgG isolated from patients with APS (which was pooled from 5 primary APS patients). In some cases, cultures were also supplemented with different concentrations (1–40 μg/ml) of defibrotide (Jazz Pharmaceuticals), 10 μ*M* KT5720 (protein kinase A [PKA] inhibitor; Tocris), 10 μ*M* 8-cyclopentyltheophylline (adenosine A_1 receptor antagonist; Tocris), or 10 μ*M* SCH442416 (adenosine A_{2A} receptor antagonist; Tocris).

After stimulation, the culture medium was discarded, and the plate was gently emptied over a paper towel (to remove residual culture medium containing soluble MPO). Discarded medium was immediately replaced with RPMI medium alone or RPMI medium + 10 units/ml micrococcal nuclease (Thermo Fischer Scientific). The samples incubated with RPMI medium alone (without nuclease) were used to account for any NET-independent background signal. EDTA (10 m*M*) was used to stop the digestion of NETs after 10 minutes at 37°C. Supernatants were next transferred into a V-shaped 96-well plate, which was centrifuged at 350*g* to remove debris. MPO activity was then measured in a fresh plate by adding an equal volume of 3,3′,5,5′-tetramethylbenzidine (TMB) substrate (1 mg/ml; Thermo Fischer Scientific). The reaction was stopped 10 minutes later by the addition of 1 m*M* sulfuric acid (50 μl). Finally, a Cytation 5 Cell Imaging Multi-Mode Reader was used to measure absorbance at 450 nm.

Qualitative immunofluorescence microscopy. Neutrophils were seeded onto poly-L-lysine–(Sigma) coated coverslips. After fixing with 4% paraformaldehyde for 15 minutes, blocking was done with 1% bovine serum albumin overnight. Neutrophil elastase was labeled with a primary antibody (Abcam product no. 21595, diluted 1:100). The primary antibody was detected with a fluorescein isothiocyanate (FITC)–conjugated secondary antibody (SouthernBiotech product no. 4052-02, diluted 1:250). Hoechst 33342 (Invitrogen) was used to stain DNA. A Cytation 5 Cell Imaging Multi-Mode Reader was used to capture images.

Measurement of intracellular cAMP. Neutrophils were incubated for 30 minutes at room temperature with 1 μg/ml of defibrotide or 1 μ*M* CGS21680 (adenosine A_{2A} receptor agonist; Tocris). Other neutrophils were incubated for 10 minutes with 100 μ*M* forskolin (adenylyl cyclase activator; Tocris). Levels of cAMP were then measured using the Bridge-It cAMP Designer fluorescence assay kit (Mediomics catalog no. 122934) as instructed by the manufacturer and as we have done previously (10).

Animal housing and treatment. Mice were fed standard chow and housed in a specific pathogen–free facility. The

University of Michigan Institutional Animal Care and Use Committee approved all protocols. Male C57BL/6 mice were obtained from The Jackson Laboratory.

Adenosine A_{2A} receptor–knockout mice. We introduced a conditional knockout of the adenosine A_{2A} receptor in murine neutrophils (and other myeloid-lineage cells such as macrophages) using the Cre/loxP system. Mice with a "floxed" adenosine A_{2A} receptor gene (Adora2a$^{+/fl}$) on the C57BL/6 genetic background were purchased from The Jackson Laboratory (product no. 010687). Adora2a$^{+/fl}$ mice were bred to obtain homozygous Adora2a$^{fl/fl}$ mice. The Adora2a$^{fl/fl}$ mice were then crossed with hemizygote MRP8-Cre^{+} mice (purchased from The Jackson Laboratory; product no. 021614). The offspring (Adora2a$^{+/fl}$ MRP8-Cre^{+}) were then crossed with Adora2a$^{fl/fl}$ mice to obtain the experimental mice of interest: Adora2a$^{fl/fl}$ MRP8-Cre^{+} and Adora2a$^{fl/fl}$ MRP8-Cre^{-} (for the description of the breeding scheme see Supplementary Figure 1, available on the *Arthritis & Rheumatology* website at http://onlinelibrary.wiley.com/doi/10.1002/art.42017/abstract).

In vivo induction of venous thrombosis in mice. We used an electrolytic inferior vena cava (IVC) model that has been used previously by our group (9,10). After exposure of the IVC of mice, any lateral branches were ligated using 7-0 Prolene sutures. These side branches remained ligated for the duration of the experiment. Most animals had 1 or 2 side branches, but some animals had none (in which case no ligatures were placed). A 30-gauge silver-coated copper wire (KY-30-1-GRN; Electrospec) was placed inside a 25-gauge needle and inserted into the IVC. The wire was positioned against the anterior wall of the IVC where exposed copper wire at its end functioned as the anode. Meanwhile, a needle implanted subcutaneously completed the circuit and functioned as the cathode. For 15 minutes, a constant current of 250 μA was applied. The needle was then removed, and the abdomen was closed. Before recovery from the anesthetized state, the mice were intravenously injected with IgG from either healthy controls or patients with APS (500 μg); the IgG from APS patients was pooled from 3 patients experiencing an episode of CAPS. After 24 hours, mice were euthanized, and thrombus length was determined. Defibrotide sodium was diluted in saline and administered by retroorbital intravenous injection. Two injections were given; the first 24 hours prior to surgery and the second at the time of thrombus induction.

Quantification of MPO–DNA complexes. Serum was collected from the mice for MPO–DNA testing at the time of venous thrombus harvesting. MPO–DNA complexes were quantified as described previously (9,10). The protocol uses reagents from the Cell Death Detection ELISA kit (Roche) as well as an anti-MPO antibody (Bio-Rad0400-0002) that reacts with both human and mouse MPO.

RESULTS

Inhibition of NET formation by defibrotide in cultures of neutrophils with PMA or APS patient antibodies. We first tested the ability of defibrotide to suppress NET formation when control neutrophils were activated with PMA. We found that defibrotide significantly reduced PMA-triggered NET formation at concentrations as low as 1 μg/ml (Figure 1A). Beyond PMA stimulation, we reasoned that defibrotide might also prevent antiphospholipid antibody–mediated NET formation. Indeed, at concentrations as low as 1 μg/ml, defibrotide suppressed NET formation elicited from control neutrophils stimulated with IgG isolated from APS patients (pooled from 5 patients with primary APS) (Figure 1B). Defibrotide also suppressed NET formation by neutrophils isolated from patients with clinical features of APS who were "triple positive" for anticardiolipin antibodies, anti-β_2GPI antibodies, and lupus anticoagulant (Supplementary Figure 2, available at http://onlinelibrary.wiley.com/doi/10.1002/art.42017/abstract).

The impact of defibrotide on APS IgG–mediated NET formation was also assessed by immunofluorescence microscopy, with similar results (Figure 1C). In contrast to IgG from APS patients, IgG isolated from heterologous healthy controls did not increase NET formation by control neutrophils (Supplementary Figure 3, available at http://onlinelibrary.wiley.com/doi/10.1002/art.42017/abstract).

Elevation of cAMP levels and mitigation of antiphospholipid antibody–mediated NET formation by defibrotide through adenosine A_{2A} receptor agonism. Defibrotide has been reported to act as an adenosine receptor agonist in some settings (17–19), and we recently found that adenosine receptor agonism protects against both NET formation and venous thrombosis in APS (9). We therefore hypothesized that the inhibitory activity of defibrotide might be mediated through activation of adenosine A_{2A} receptors. In neutrophils, we found that defibrotide increased the level of intracellular cAMP in a manner similar to the synthetic adenosine A_{2A} receptor agonist CGS21680 and the adenylate cyclase activator forskolin (Figure 1D); defibrotide did not significantly increase cAMP levels in peripheral blood mononuclear cells (Supplementary Figure 4, available at http://onlinelibrary.wiley.com/doi/10.1002/art.42017/abstract).

We next considered that inhibiting the key cAMP-dependent kinase PKA might reverse the effects of defibrotide. Indeed, the ability of defibrotide to suppress NET formation was neutralized by a PKA inhibitor (Figure 1E). Finally, we also found that the ability of defibrotide to suppress NET formation could be partially

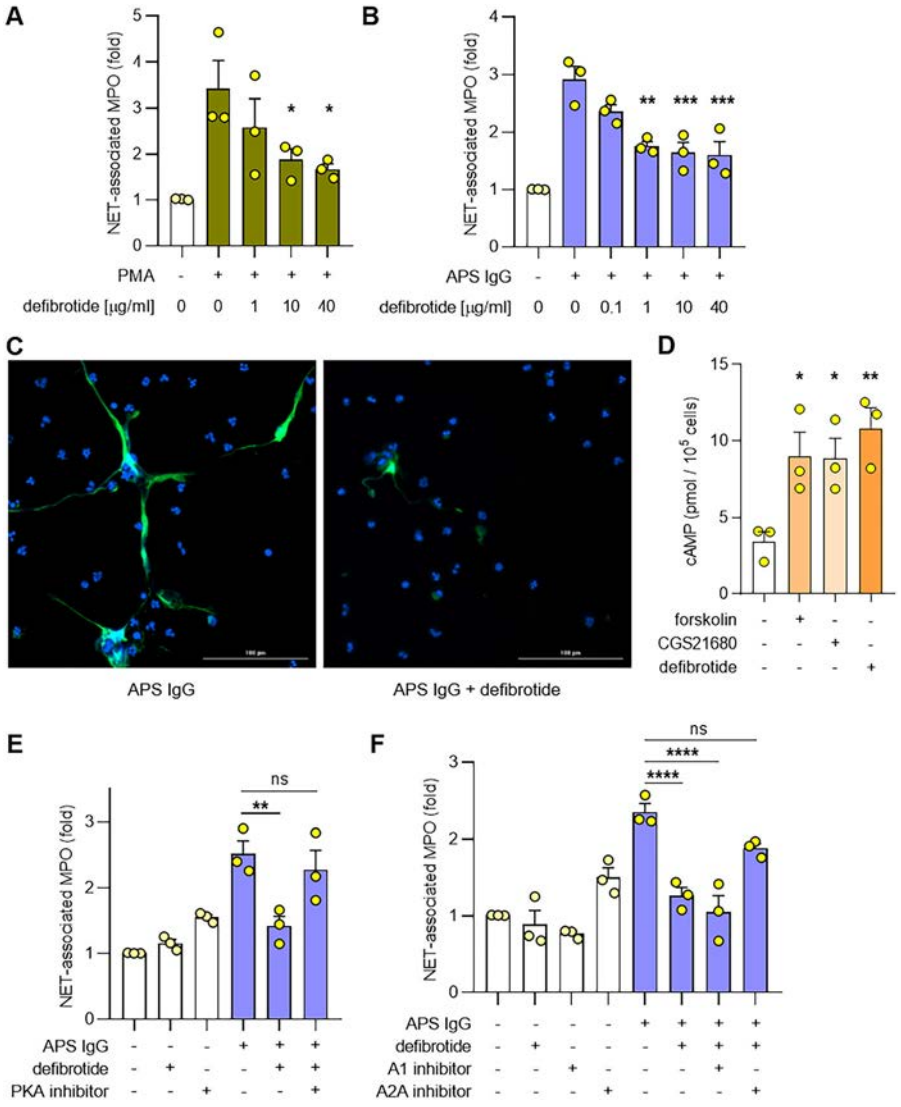

Figure 1. Defibrotide suppresses neutrophil extracellular trap (NET) formation in response to various stimuli through adenosine A_{2A} receptor agonism. **A** and **B**, Human neutrophils were isolated from healthy volunteers and then treated without or with phorbol 12-myristate 13-acetate (PMA) (**A**) or IgG from the sera of patients with antiphospholipid syndrome (APS) (**B**) for 3 hours in the presence or absence of different concentrations of defibrotide. NET formation was quantified by measuring the enzymatic activity of nuclease-liberated myeloperoxidase (MPO). **C**, NET formation in cultures of neutrophils treated with APS IgG in the presence or absence of defibrotide (1 μg/ml) was assessed qualitatively by immunofluorescence microscopy. Representative images are shown. Green = extracellular neutrophil elastase; blue = DNA. **D**, Human neutrophils were treated without or with forskolin (10 minutes), CGS21680 (30 minutes), or defibrotide (30 minutes), and cyclic AMP (cAMP) levels were measured. **E** and **F**, Neutrophils were treated with APS IgG in the presence or absence of defibrotide (1 μg/ml). Some samples were additionally treated with a protein kinase A (PKA) inhibitor (10 μ*M*), an adenosine A_1 receptor antagonist (10 μ*M*), or an adenosine A_{2A} receptor antagonist (10 μ*M*). NET formation was quantified by measuring the enzymatic activity of nuclease-liberated MPO. In **A**, **B**, **D**, **E**, and **F**, values are relative to untreated controls. Circles represent 1 of 3 independent experiments; bars show the mean ± SEM. * = $P < 0.05$; ** = $P < 0.01$; *** = $P < 0.001$; **** = $P < 0.0001$ by one-way analysis of variance, corrected with Dunnett's test. NS = not significant.

reversed by blocking adenosine A_{2A} (but not adenosine A_1) receptors (Figure 1F). Notably, adenosine receptor antagonists had no effect on APS IgG–mediated NET formation in the absence of defibrotide (Supplementary Figure 5). Taken together, these data demonstrate that defibrotide can suppress NET formation and that this suppression is at least in part attributable to the activation of adenosine A_{2A} receptors.

Attenuation of antiphospholipid antibody–mediated venous thrombosis by defibrotide in wild-type mice but not adenosine A_{2A} receptor–knockout mice. Since defibrotide suppressed antiphospholipid antibody–mediated NET formation in vitro, we were interested in whether it might also mitigate antiphospholipid antibody–accelerated NET formation and thrombosis in mice. To test this, we utilized an electrolytic IVC

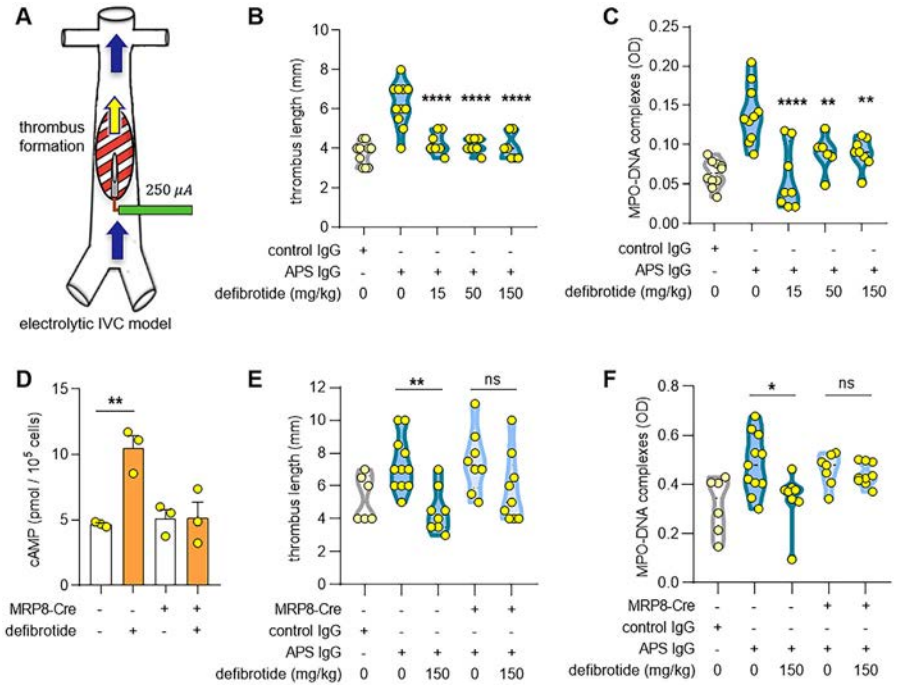

Figure 2. Defibrotide prevents antiphospholipid antibody–mediated venous thrombosis in wild-type mice but not in adenosine A_{2A} receptor–knockout mice. **A**, Schematic diagram depicting the electrolytic inferior vena cava (IVC) model of venous thrombosis. The application of direct current to a copper wire results in the release of free radicals. This activates endothelial cells and triggers a thrombogenic environment. Blood flow remains constant. **B** and **C**, C57BL/6J mice were treated without or with control IgG or APS IgG in the presence or absence of defibrotide. Thrombus formation was determined at 24 hours. Thrombus length (**B**) and MPO–DNA complexes (**C**) were quantified in the mouse serum. **D**, Cyclic AMP levels were determined in neutrophils isolated from Adora2a$^{fl/fl}$ MRP8-Cre^{+} mice compared with Adora2a$^{fl/fl}$ MRP8-Cre^{-} mice in the presence or absence of defibrotide (1 μg/ml) for 30 minutes. Circles represent 1 of 3 independent experiments; bars show the mean ± SEM. **E** and **F**, Adora2a$^{fl/fl}$ MRP8-Cre^{+} or Adora2a$^{fl/fl}$ MRP8-Cre^{-} mice were treated without or with control IgG or APS IgG in the presence or absence of defibrotide. Thrombus formation was assessed at 24 hours. Thrombus length (**E**) and MPO–DNA complexes (**F**) were quantified in the mouse serum. Circles in **B**, **C**, **E**, and **F** represent individual mice. * = $P < 0.05$; ** = $P < 0.01$; **** = $P < 0.0001$ by one-way analysis of variance, corrected with Dunnett's test. See Figure 1 for other definitions. Color figure can be viewed in the online issue, which is available at http://onlinelibrary.wiley.com/doi/10.1002/art.42017/abstract.

model to induce large-vein thrombosis (Figure 2A) (9,10). Administration of IgG isolated from patients with APS (pooled from 3 patients with CAPS), but not control IgG, increased thrombus length in C57BL/6 mice, which returned to baseline levels when defibrotide was administered at doses as low as 15 mg/kg (Figure 2B). As expected, administration of antiphospholipid antibodies increased a surrogate marker of NETs in serum (MPO–DNA complexes), which again returned to baseline when mice were treated with defibrotide (Figure 2C).

Having demonstrated in vitro that the suppressive effects of defibrotide on NET formation could be partially reversed by blocking adenosine A_{2A} receptors, we considered that the suppressive effects of defibrotide on venous thrombosis might be reversed in myeloid-specific adenosine A_{2A} receptor–knockout mice. We first confirmed that neutrophils isolated from these mice were resistant to the ability of defibrotide to boost intracellular cAMP levels (Figure 2D). We then found that defibrotide was not able to prevent venous thrombosis (Figure 2E) or NET formation (Figure 2F) in adenosine A_{2A} receptor–knockout mice. Taken together, these data suggest that defibrotide mediates its antithrombotic effects at least partially through adenosine A_{2A} receptors.

DISCUSSION

This study is the first to demonstrate a mechanism by which defibrotide prevents disease-relevant NET formation. Defibrotide is indicated for the treatment of patients who have VOD associated with hepatic, renal, or pulmonary dysfunction following HSCT. In those settings, the therapeutic dosage of defibrotide is 6.25 mg/kg given intravenously every 6 hours (for a total dosage of 25 mg/kg/day). The drug is typically infused over several weeks and may continue up to a maximum of 60 days. Given that the role of neutrophils in VOD has yet to receive significant attention, we can speculate that the anti-neutrophil properties of defibrotide may play a protective role in VOD. This is certainly an area that we hope will be investigated in the coming years by our group and others.

The data presented here suggest that adenosine A_{2A} receptor agonism is at least part of the mechanism by which defibrotide reduces NET formation. Several reports suggest that defibrotide mediates its effects by targeting multiple adenosine receptors (for example, both A_1 and A_2) (17–19). In the present study,

blocking adenosine A_1 receptors did not interfere with the ability of defibrotide to suppress NET formation. These findings are similar to those of a previous study in which the effects of defibrotide were abolished by a dual adenosine A_1/A_2 receptor antagonist, but not by a selective adenosine A_1 receptor antagonist (18). It is worth noting that adenosine A_{2A} receptors are more abundantly expressed by neutrophils than are adenosine A_1 receptors (20). The extent to which complementary defibrotide-mediated mechanisms may be at play in mitigating NET formation and thrombosis is certainly an area deserving of future research.

In conclusion, these preclinical data support the possibility of defibrotide as a repurposed drug candidate for APS. Given a dearth of effective therapies for patients with the microvascular variant of APS, one can consider whether defibrotide warrants systematic study in such individuals, who in many cases will be receiving therapy in the inpatient setting where administration of defibrotide would be quite feasible.

AUTHOR CONTRIBUTIONS

All authors were involved in drafting the article or revising it critically for important intellectual content, and all authors approved the final version to be published. Dr. Knight had full access to all of the data in the study and takes responsibility for the integrity of the data and the accuracy of the data analysis.

Study conception and design. Ali, Erkan, Knight.
Acquisition of data. Ali, Estes, Gandhi, Yalavarthi, Hoy, Shi, Zuo.
Analysis and interpretation of data. Ali, Estes, Gandhi, Yalavarthi, Hoy, Shi, Zuo, Erkan, Knight.

ROLE OF THE STUDY SPONSOR

Jazz Pharmaceuticals provided funding for these investigator-initiated preclinical experiments but did not have input regarding the experimental design, nor did they participate in the data analysis. The authors independently collected the data, interpreted the results, and had the final decision to submit the manuscript for publication. Publication of this article was not contingent upon approval by Jazz Pharmaceuticals.

REFERENCES

1. Bertolaccini ML, Amengual O, Andreoli L, Atsumi T, Chighizola CB, Forastiero R, et al. 14th International Congress on Antiphospholipid Antibodies Task Force. Report on antiphospholipid syndrome laboratory diagnostics and trends. Autoimmun Rev 2014;13:917–30.
2. Brinkmann V, Reichard U, Goosmann C, Fauler B, Uhlemann Y, Weiss DS, et al. Neutrophil extracellular traps kill bacteria. Science 2004;303:1532–5.
3. Kenny EF, Herzig A, Kruger R, Muth A, Mondal S, Thompson PR, et al. Diverse stimuli engage different neutrophil extracellular trap pathways. Elife 2017;6.
4. Saffarzadeh M, Juenemann C, Queisser MA, Lochnit G, Barreto G, Galuska SP, et al. Neutrophil extracellular traps directly induce epithelial and endothelial cell death: a predominant role of histones. PLoS One 2012;7:e32366.
5. Grenn RC, Yalavarthi S, Gandhi AA, Kazzaz NM, Nunez-Alvarez C, Hernandez-Ramirez D, et al. Endothelial progenitor dysfunction associates with a type I interferon signature in primary antiphospholipid syndrome. Ann Rheum Dis 2017;76:450–7.
6. Fuchs TA, Brill A, Duerschmied D, Schatzberg D, Monestier M, Myers DD Jr, et al. Extracellular DNA traps promote thrombosis. Proc Natl Acad Sci U S A 2010;107:15880–5.
7. Yalavarthi S, Gould TJ, Rao AN, Mazza LF, Morris AE, Núñez-Álvarez C, et al. Release of neutrophil extracellular traps by neutrophils stimulated with antiphospholipid antibodies: a newly identified mechanism of thrombosis in the antiphospholipid syndrome. Arthritis Rheumatol 2015;67:2990–3003.
8. Meng H, Yalavarthi S, Kanthi Y, Mazza LF, Elfline MA, Luke CE, et al. In vivo role of neutrophil extracellular traps in antiphospholipid antibody–mediated venous thrombosis. Arthritis Rheumatol 2017;69:655–67.
9. Ali RA, Gandhi AA, Meng H, Yalavarthi S, Vreede AP, Estes SK, et al. Adenosine receptor agonism protects against NETosis and thrombosis in antiphospholipid syndrome. Nat Commun 2019;10:1916.
10. Ali RA, Gandhi AA, Dai L, Weiner J, Estes SK, Yalavarthi S, et al. Antineutrophil properties of natural gingerols in models of lupus. JCI Insight 2021;6.
11. Sule G, Kelley WJ, Gockman K, Yalavarthi S, Vreede AP, Banka AL, et al. Increased adhesive potential of antiphospholipid syndrome neutrophils mediated by β2 integrin mac-1. Arthritis Rheumatol 2020;72:114–24.
12. Richardson PG, Elias AD, Krishnan A, Wheeler C, Nath R, Hoppensteadt D, et al. Treatment of severe veno-occlusive disease with defibrotide: compassionate use results in response without significant toxicity in a high-risk population. Blood 1998;92:737–44.
13. Ho VT, Revta C, Richardson PG. Hepatic veno-occlusive disease after hematopoietic stem cell transplantation: update on defibrotide and other current investigational therapies [review]. Bone Marrow Transplant 2008;41:229–37.
14. Pescador R, Capuzzi L, Mantovani M, Fulgenzi A, Ferrero ME. Defibrotide: properties and clinical use of an old/new drug. Vascul Pharmacol 2013;59:1–10.
15. Di Perri T, Pasini FL, Capecchi PL, Ceccatelli L, Pasqui AL, Orrico A. Defibrotide in vitro inhibits neutrophil activation by a Ca++-involving mechanism. Int J Tissue React 1987;9:399–406.
16. Burcoglu-O'Ral A, Erkan D, Asherson R. Treatment of catastrophic antiphospholipid syndrome with defibrotide, a proposed vascular endothelial cell modulator. J Rheumatol 2002;29:2006–11.
17. Bianchi G, Calvani AB, Mantovani M, Prino G. Enhancement by defibrotide of prostanoid neosynthesis from arachidonic acid: an adenosine receptor-mediated effect? Semin Thromb Hemost 1991;17:399–403.
18. Bianchi G, Barone D, Lanzarotti E, Tettamanti R, Porta R, Moltrasio D, et al. Defibrotide, a single-stranded polydeoxyribonucleotide acting as an adenosine receptor agonist. Eur J Pharmacol 1993;238:327–34.
19. Pasini FL, Frigerio C, Capecchi PL, Ceccatelli L, Messa GL, Franchi M, et al. Modulation of venous endothelial activity and transcellular calcium transport by defibrotide: the adenosine hypothesis. Semin Thromb Hemost 1996;22 Suppl:15–20.
20. Van der Hoeven D, Wan TC, Auchampach JA. Activation of the A adenosine receptor suppresses superoxide production and chemotaxis of mouse bone marrow neutrophils. Mol Pharmacol 2008;74:685–96.

American College of Rheumatology
Empowering Rheumatology Professionals

Arthritis & Rheumatology
Vol. 74, No. 5, May 2022, pp 908–914

LETTERS

DOI 10.1002/art.42011

Low levels of anti–SARS–CoV-2 antibodies after vaccination in rituximab-treated patients: comment on the article by Simon et al

To the Editor:

We read with great interest the report of the study by Dr. Simon and colleagues, in which impaired humoral immune responses, but not T cell immune responses, were observed after vaccination against SARS–CoV-2 in patients with immune-mediated inflammatory diseases (IMIDs) treated with rituximab (RTX) (1). The authors reported that none of the 8 vaccinated RTX-treated patients developed IgG antibodies against the spike S1 and nucleocapsid proteins of SARS–CoV-2. Moreover, Boyarsky et al recently reported increased rates of undetectable titers of anti–SARS–CoV-2 antibodies in patients treated with RTX (P = 0.04) (2). In patients with hematologic malignancies treated with RTX, only 0–14% developed a serologic response to the BNT162b2 messenger RNA (mRNA) vaccine when RTX was administered within the 12 months before vaccination (3).

On this basis, we examined antibody responses after 2 doses of the SARS–CoV-2 vaccine in 11 patients treated with RTX. Seven patients (63.6%) were female, 9 had a diagnosis of rheumatoid arthritis, 1 had a diagnosis of dermatomyositis, and 1 had a diagnosis of cryoglobulinemic vasculitis. Patients with a history of SARS–CoV-2 infection or low IgG levels were excluded. Patients had received a mean ± SD of 5.5 ± 3.9 RTX cycles before SARS–CoV-2 vaccination, and the first dose of the vaccine was administered a mean ± SD of 20.4 ± 13.4 weeks after the last RTX cycle. All patients except 1 were vaccinated with the BNT162b2 mRNA SARS–CoV-2 vaccine. We used a quantitative chemiluminescence microparticle immunoassay (Abbott) to detect IgG antibodies against the SARS–CoV-2 spike protein. Consistent with the aforementioned studies, only 2 (18.2%) of 11 patients had antibody levels above the cutoff value of 50 arbitrary units (AU)/ml; the median level of anti–SARS–CoV-2 antibodies was 21.3 AU/ml (interquartile range 4–28).

Our results confirm those from earlier studies showing reduced antibody response after COVID-19 vaccination in patients with IMIDs receiving RTX therapy (1,2,4). RTX treatment has been associated with worse COVID-19 outcomes, such as more severe disease and increased duration of hospitalization (5). Given that vaccination against SARS–CoV-2 has been highly effective in preventing the development of pneumonia associated with COVID-19 (6), it is considered essential for patients treated with RTX to be vaccinated. Nevertheless, RTX treatment has been associated with reduced antibody response after flu and pneumococcal vaccination (7). Based on these data, the American College of Rheumatology recommends that patients being treated with RTX should optimally be vaccinated against COVID-19 4 weeks before the next scheduled cycle and that RTX administration should be withheld for 2–4 weeks after the second vaccine dose (8).

However, we observed low levels of anti–SARS–CoV-2 antibodies even though the first vaccine dose was administered a mean of 5 months after the last RTX cycle. Mrak et al also reported inadequate antibody development when the first vaccine dose was administered ~6.9 months after the last RTX cycle (4). Indeed, the time from the last RTX cycle correlated with peripheral B cell counts and anti–SARS–CoV-2 antibody levels, and the percentage of peripheral B cells was associated with antibody development in vaccinated patients (4). These data imply that the time interval between the last RTX administration and the first vaccine dose should possibly be reconsidered. As RTX-treated patients seem to exhibit T cell immune responses to SARS–CoV-2 vaccination (1,4), the clinical significance of impaired humoral responses after vaccination in these patients remains unclear.

Author disclosures are available at https://onlinelibrary.wiley.com/action/downloadSupplement?doi=10.1002%2Fart.42011&file=art42011-sup-0001-Disclosureform.pdf.

Gerasimos Evangelatos, MD, MSc
First Department of Propaedeutic Internal Medicine
National and Kapodistrian University of Athens
Konstantina Kouna, MD, MSc
417 Army Share Fund Hospital (NIMTS)
George E. Fragoulis, MD, PhD
First Department of Propaedeutic Internal Medicine
National and Kapodistrian University of Athens
Melina Moschopoulou, BSc
Faculty of Pharmacy
National and Kapodistrian University of Athens
Maria Triantafylli, MD
Antigoni Lekka, MD, MPH
Alexios Iliopoulos, MD
417 Army Share Fund Hospital (NIMTS)
Athens, Greece

1. Simon D, Tascilar K, Schmidt K, Manger B, Weckwerth L, Sokolova M, et al. Humoral and cellular immune responses to SARS–CoV-2 infection and vaccination in autoimmune disease patients with B cell depletion. Arthritis Rheumatol 2022;74:33–7.
2. Boyarsky BJ, Ruddy JA, Connolly CM, Ou MT, Werbel WA, Garonzik-Wang JM, et al. Antibody response to a single dose of SARS–CoV-2 mRNA vaccine in patients with rheumatic and musculoskeletal diseases. Ann Rheum Dis 2021. doi: 10.1136/annrheumdis-2021-220289. E-pub ahead of print.

3. Teh BW, Tam CS. Between a rock and a hard place: COVID-19 vaccination and patients on rituximab therapy. Leuk Lymphoma 2021;62:2820–2.
4. Mrak D, Tobudic S, Koblischke M, Graninger M, Radner H, Sieghart D, et al. SARS–CoV-2 vaccination in rituximab-treated patients: B cells promote humoral immune responses in the presence of T-cell-mediated immunity. Ann Rheum Dis 2021;80:1345–50.
5. Avouac J, Drumez E, Hachulla E, Seror R, Georgin-Lavialle S, El Mahou S, et al. COVID-19 outcomes in patients with inflammatory rheumatic and musculoskeletal diseases treated with rituximab: a cohort study. Lancet Rheumatol 2021;3:e419–26.
6. McDonald I, Murray SM, Reynolds CJ, Altmann DM, Boyton RJ. Comparative systematic review and meta-analysis of reactogenicity, immunogenicity and efficacy of vaccines against SARS–CoV-2 [review]. NPJ Vaccines 2021;6:74.
7. Furer V, Rondaan C, Heijstek MW, Agmon-Levin N, van Assen S, Bijl M, et al. 2019 update of EULAR recommendations for vaccination in adult patients with autoimmune inflammatory rheumatic diseases. Ann Rheum Dis 2020;79:39–52.
8. Curtis JR, Johnson SR, Anthony DD, Arasaratnam RJ, Baden LR, Bass AR, et al. American College of Rheumatology guidance for COVID-19 vaccination in patients with rheumatic and musculoskeletal diseases: version 2. Arthritis Rheumatol 2021;73:e30–45.

DOI 10.1002/art.42012

Reply

To the Editor:

We appreciate the comments from Dr. Evangelatos and colleagues on our study of SARS–CoV-2 vaccine responses in RTX-treated patients. The authors briefly reviewed current evidence on the reduced rates of response to SARS–CoV-2 vaccines among patients undergoing B cell depletion therapy with RTX and provided novel data on this topic. In a series of 11 patients with immune-mediated inflammatory diseases treated with RTX, only 2 patients developed detectable levels of IgG antibodies against SARS–CoV-2 spike protein after vaccination with the BNT162b2 mRNA SARS–CoV-2 vaccine. This finding supports observations from other studies (1,2), including our own, in which we showed that humoral but not T cell–mediated responses to SARS–CoV-2 vaccination are reduced in patients treated with RTX.

These findings are highly relevant to the estimated 700,000 patients with hematologic malignancies (3) and 900,000 patients with immune-mediated inflammatory diseases (4) treated with RTX worldwide. Of note, RTX-treated patients show an increased risk of severe COVID-19 (5). Therefore, in light of the impaired humoral immune response to SARS–CoV-2 vaccination, new vaccination strategies and careful monitoring of vaccine efficacy are needed for this patient population, as urged by Evangelatos et al. For RTX-treated patients who have not been vaccinated, RTX therapy and vaccination regimens should be aligned. Thus, RTX administration can be time-adjusted, as also recommended in the American College of Rheumatology guidelines (vaccination 4 weeks before RTX administration [6]), or it could be administered depending on the grade of repopulation of peripheral B cells. The latter approach is reasonable, since adequate humoral immune responses are more likely if at least some B cells are detectable in the peripheral blood (1). However, further studies are needed to determine the effect of B cell repopulation and the best timing of vaccination.

Of note, T cell responses to SARS–CoV-2 vaccination have been shown to be intact in RTX-treated patients, and they have also been shown to support defense against infection and the development of severe COVID-19 (1). Therefore, patients treated with RTX should receive SARS–CoV-2 vaccination even in the absence of B cells. Furthermore, humoral immune responses should be assessed in RTX-treated patients who have received a full SARS–CoV-2 vaccination regimen. Fully vaccinated individuals who do not respond could benefit from additional boosters to achieve a protective humoral response (7). In this context, the observation that SARS–CoV-2 infection can mobilize tissue B cells and trigger protective antibody formation in RTX-treated patients without peripheral B cells is interesting and may support the use of booster vaccinations. When the standard vaccination regimen has failed, a humoral immune response may be mobilized by the timely administration of booster vaccines and by cross-vaccinating with different vaccine agents.

David Simon, MD
Filippo Fagni, MD
Koray Tascilar, MD
Georg Schett, MD
Friedrich-Alexander University Erlangen-Nürnberg
Universitätsklinikum Erlangen
and Deutsches Zentrum fuer Immuntherapie
Erlangen, Germany

1. Mrak D, Tobudic S, Koblischke M, Graninger M, Radner H, Sieghart D, et al. SARS–CoV-2 vaccination in rituximab-treated patients: B cells promote humoral immune responses in the presence of T-cell-mediated immunity. Ann Rheum Dis 2021;80:1345–50.
2. Spiera R, Jinich S, Jannat-Khah D. Rituximab, but not other antirheumatic therapies, is associated with impaired serological response to SARS–CoV-2 vaccination in patients with rheumatic diseases [letter]. Ann Rheum Dis 2021;80:1357–9.
3. Hoffmann-La Roche. MabThera recommended for approval in rheumatoid arthritis in Europe [press release]. June 2006. URL: https://www.sec.gov/Archives/edgar/vprr/0601/06014080.pdf.
4. Roche. FDA approves Roche's Rituxan (rituximab) in children with two rare blood vessel disorders [press release]. September 2019. URL: https://www.roche.com/media/releases/med-cor-2019-09-30b.htm.
5. Schulze-Koops H, Krueger K, Vallbracht I, Hasseli R, Skapenko A. Increased risk for severe COVID-19 in patients with inflammatory rheumatic diseases treated with rituximab [letter]. Ann Rheum Dis 2020;80:e67.
6. Curtis JR, Johnson SR, Anthony DD, Arasaratnam RJ, Baden LR, Bass AR, et al. American College of Rheumatology guidance for COVID-19 vaccination in patients with rheumatic and musculoskeletal diseases: version 1. Arthritis Rheumatol 2021;73:1093–107.

7. Albach FN, Burmester GR, Biesen R. Successful BNT162b2 booster vaccinations in a patient with rheumatoid arthritis and initially negative antibody response [letter]. Ann Rheum Dis 2021. doi: 10.1136/annrheumdis-2021-220834. E-pub ahead of print.

DOI 10.1002/art.42053

Extensive bone marrow capillary network masquerading as fungal hyphae in a patient with systemic lupus erythematosus

To the Editor:

Hypocellularity of the bone marrow (BM) is a common finding in systemic lupus erythematosus (SLE). Other pathologic abnormalities in the BM of SLE patients have been reported less frequently. Herein we describe a patient with newly diagnosed SLE in whom examination of a BM aspirate initially suggested the presence of mycosis, but with neovascularization identified upon further investigation.

The patient, a previously healthy 79-year-old Chinese woman, was admitted to our hospital with unintentional weight loss, diffuse alopecia, and Jaccoud's arthropathy. Laboratory investigations revealed leukopenia (total leukocyte count 1.68×10^9/liter), neutropenia (neutrophil count 0.53×10^9/liter), normocytic anemia (hemoglobin value 8.6 gm/dl), hypocomplementemia, antinuclear antibody positivity, anti–double-stranded DNA antibodies, and direct Coombs-positive reaction. There was no active hemolysis or renal dysfunction. Other than a small unilateral pleural effusion, findings on computed tomography of the thorax, abdomen, and pelvis and gastrointestinal endoscopy were unremarkable. A diagnosis of systemic lupus erythematosus (SLE) was made.

Examination of a BM aspirate revealed severe marrow hypoplasia with reduced hematopoiesis (Figure 1A). Squash preparation showed multiple fine elongated structures with varied configurations in marrow areas, sparing the intervening regions (Figure 1B). Higher magnification demonstrated individual cells with elongated, strand-like cytoplasm and fusiform nuclei (Figure 1C), occasionally aggregated in a fan-like array (Figure 1D).

The patient became febrile during her hospital stay. Because invasive mycosis was suspected based on examination of the BM aspirate, intravenous amphotericin was initiated. However, periodic acid–Schiff (PAS) and Grocott-Gomori methenamine silver (GMS) staining of the BM trephine did not reveal fungal hyphae. Closer examination of the BM aspirate showed intraluminal erythrocytes within these filamentous structures (Figure 1E), and CD31 immunohistochemical staining confirmed the latter as endothelial capillary networks (Figure 1F). Treatment with amphotericin was stopped and low-dose glucocorticoids and hydroxychloroquine were initiated, which led to swift resolution of her SLE-related symptoms and cytopenia.

Visualization of extensive intact capillary networks within marrow specimens is unusual, and the networks may be mistaken for fungal hyphae. Fungal hyphae are characterized by the presence of cell walls, septa, surrounding florid histiocytic reaction, and positive PAS and GMS staining. In our patient, the dense capillary network was suggestive of neovascularization resulting from marrow injury associated with hypoplasia.

BM hypocellularity has been reported in >50% of SLE patients (1,2). Other pathologic BM findings include necrotic alterations, stromal edema, variable reticulin fibrosis, dilated sinuses, and endothelial destruction (1). BM neovascularization is an uncommon finding although it is reported in hematologic malignancies and myeloproliferative disorders (3,4). In the setting of SLE, BM hypocellularity, dysplasia, fibrosis, and necrosis suggest

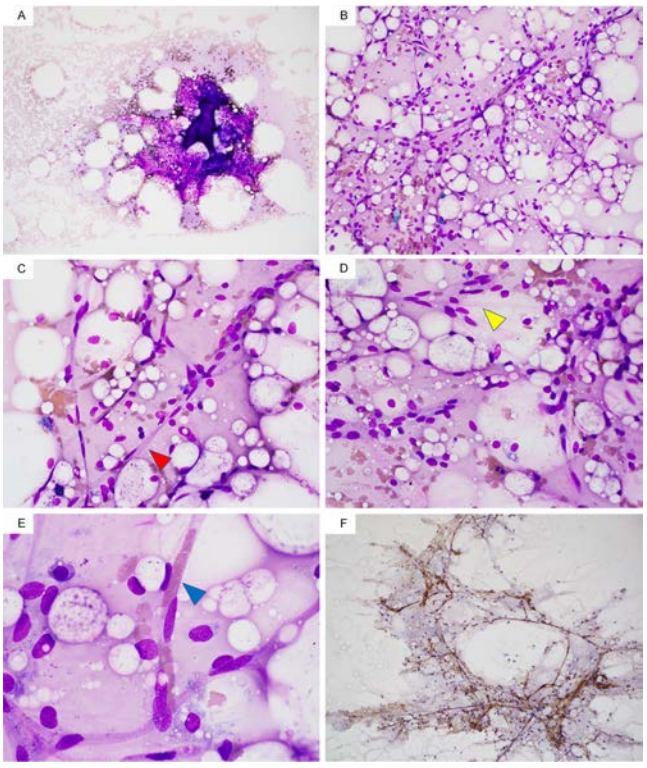

Figure 1. Stains of a bone marrow aspirate showing an extensive capillary network in a patient with systemic lupus erythematosus. **A**, Markedly hypocellular bone marrow with reduced numbers of hematopoietic cells. May-Grünwald-Giemsa stained; original magnification × 5. **B**, Squash preparation showing the presence of elongated structures in branched, curved, looped, and intersecting configurations. May-Grünwald-Giemsa stained; original magnification × 20. **C**, Individual cells composed of strand-like cytoplasm and fusiform nuclei (**arrowhead**). May-Grünwald-Giemsa stained; original magnification × 40. **D**, Aggregation of nuclei and cytoplasm in a fan-like array (**arrowhead**). May-Grünwald-Giemsa stained; original magnification × 40. **E**, Red blood cells visible inside the lumen of the capillaries (**arrowhead**). May-Grünwald-Giemsa stained; original magnification × 100. **F**, CD31 immunohistochemical staining of the endothelial cells of the capillary network. Original magnification × 5.

that the marrow may be a target of immune-mediated damage, with neovascularization seen in this case as a possible compensatory phenomenon (5). Our finding of BM neovascularization mimicking invasive mycosis in a patient with SLE illustrates the importance of taking the overall clinical picture into account when assessing pathologic findings.

Author disclosures are available at https://onlinelibrary.wiley.com/action/downloadSupplement?doi=10.1002%2Fart.42053&file=art42053-sup-0001-Disclosureform.pdf.

Dominic Seet, MBBS, MMed, MRCP
National University Health System
Shir Ying Lee, MBBS, MRCP, FRCPath
National University Cancer Institute and National University Hospital
Melissa Ooi, MB, BCh, PhD, MRCP, FRCPath
National University Cancer Institute and National University of Singapore
Ju Ee Seet, MB, BCh, MRCPath
National University Hospital
Jiacai Cho, MBBS, MMed, MRCP
Anselm Mak, MD, PhD, FRCP, FRCPI
National University Health System and National University of Singapore
Singapore, Singapore

1. Voulgarelis M, Giannouli S, Tasidou A, Anagnostou D, Ziakas PD, Tzioufas AG. Bone marrow histological findings in systemic lupus erythematosus with hematologic abnormalities: a clinicopathological study. Am J Hematol 2006;81:590–7.
2. Wanitpongpun C, Teawtrakul N, Mahakkanukrauh A, Siritunyaporn S, Sirijerachai C, Chansung K. Bone marrow abnormalities in systemic lupus erythematosus with peripheral cytopenia. Clin Exp Rheumatol 2012;30:825–9.
3. Vacca A, Ribatti D, Presta M, Minischetti M, Iurlaro M, Ria R, et al. Bone marrow neovascularization, plasma cell angiogenic potential, and matrix metalloproteinase-2 secretion parallel progression of human multiple myeloma. Blood 1999;93:3064–73.
4. Baglin TP, Crocker J, Timmins A, Chandler S, Boughton BJ. Bone marrow hypervascularity in patients with myelofibrosis identified by infrared thermography. Clin Lab Haematol 1991;13:341–8.
5. Monrad SU, Kaplan MJ. Cellular hematology. In: Lahita RG, editor. Systemic lupus erythematosus. 5th ed. San Diego (CA): Academic Press; 2011. p. 905–20.

DOI 10.1002/art.42059

Conflicting reports of anti–cytosolic 5′-nucleotidase 1A autoantibodies in juvenile dermatomyositis: comment on the article by Rietveld et al

To the Editor:

We read with interest the report by Dr. Rietveld and colleagues (1) describing their study in which serum from patients with juvenile dermatomyositis (DM) was tested for anti–cytosolic 5′-nucleotidase 1A (anti–cN-1A) autoantibodies using both an enzyme-linked immunosorbent assay (ELISA) and immunoblotting. In that study, no sample tested positive for anti–cN-1A autoantibodies by either method. These findings are consistent with those of Amlani et al (2), who showed that anti–cN-1A autoantibodies were not detected in any of the 40 juvenile DM serum samples tested using an addressable laser bead immunoassay. In contrast, Muro et al (3) found that 2 (16.7%) of 12 patients with juvenile DM were positive for anti–cN-1A by both ELISA and immunoprecipitation. Similarly, our group found that 83 (27%) of 307 juvenile DM patients had anti–cN-1A autoantibodies when tested by immunoblotting (4).

It is noteworthy that the percentages of positive test results in the 2 studies in which immunoblotting was used to detect anti–cN-1A autoantibodies in juvenile DM patients were so discordant (0% versus 27%) (1,4). In the assays used in both studies, lysates from HEK 293 cells expressing cN-1A protein and lysates from HEK 293 cells not expressing cN-1A protein were subjected to sodium dodecyl sulfate–polyacrylamide gel electrophoresis, transferred to nitrocellulose membranes, and incubated with patient sera.

One explanation for the discrepant results could be that the juvenile DM patient populations tested by each group may have marked differences in the prevalence of anti–cN-1A autoantibodies, possibly related to disease activity levels, presence of other myositis autoantibodies (which were less frequent in the cohorts studied by Rietveld et al), or other disease features. A more likely possibility is that subtle methodologic issues account for the observed differences. For example, while anti–cN-1A autoantibodies can be of the IgG, IgA, or IgM isotype (5), the secondary antibody used by Rietveld et al recognizes IgG only. In contrast, our group used a secondary antibody that also detects IgA and IgM antibodies (4). This relatively minor difference in methodology could account for the discrepant results if juvenile DM patients have significant levels of IgA and/or IgM but not IgG antibodies recognizing cN-1A protein.

We suggest that an international collaborative effort, in which multiple research groups test the same samples, should be initiated to identify a gold-standard test for anti–cN-1A autoantibodies. Such an approach could also help to develop gold-standard testing methods for other myositis autoantibodies, for which results can differ significantly depending on the assay.

Supported in part by the Intramural Research Program of the National Institute of Arthritis and Musculoskeletal and Skin Diseases, NIH, and by the National Institute of Environmental Health Sciences, NIH, Author disclosures are available at https://onlinelibrary.wiley.com/action/downloadSupplement?doi=10.1002%2Fart.42059&file=art42059-sup-0001-Disclosureform.pdf.

Andrew L. Mammen, MD, PhD
Iago Pinal-Fernandez, MD, PhD
National Institute of Arthritis and Musculoskeletal and Skin Diseases
Lisa G. Rider, MD
National Institute of Environmental Health Sciences
NIH
Bethesda, MD

1. Rietveld A, Wienke J, Visser E, Vree Egberts W, Schlumberger W, van Engelen B, et al. Anti–cytosolic 5′-nucleotidase 1A autoantibodies are absent in juvenile dermatomyositis. Arthritis Rheumatol 2021;73: 1329–33.
2. Amlani A, Choi MY, Tarnopolsky M, Brady L, Clarke AE, Garcia-De La Torre I, et al. Anti-NT5C1A autoantibodies as biomarkers in inclusion body myositis. Front Immunol 2019;10:745.
3. Muro Y, Nakanishi H, Katsuno M, Kono M, Akiyama M. Prevalence of anti-NT5C1A antibodies in Japanese patients with autoimmune rheumatic diseases in comparison with other patient cohorts. Clin Chim Acta 2017;472:1–4.
4. Yeker RM, Pinal-Fernandez I, Kishi T, Pak K, Targoff IN, Miller FW, et al. Anti-NT5C1A autoantibodies are associated with more severe disease in patients with juvenile myositis. Ann Rheum Dis 2018;77: 714–9.
5. Greenberg SA. Cytoplasmic 5′-nucleotidase autoantibodies in inclusion body myositis: isotypes and diagnostic utility. Muscle Nerve 2014;50:488–92.

DOI 10.1002/art.42047

The importance of rigorous methods in observational comparative effectiveness studies of rare diseases: comment on the article by Ruperto et al

To the Editor:

We read with interest the editorial by Dr. Ruperto and colleagues (1), which addresses the significance of our 2 recently published articles on optimizing treatment plans in polyarticular juvenile idiopathic arthritis (JIA) (2,3) and also raises the question about the necessity of randomized controlled trials (RCTs). While we believe this is a reasonable question to pose, the conclusions arrived at by the authors do not appreciate the powerful utility of state-of-the-art methods for trial design and analysis using real-world data. Particularly in the field of pediatric rheumatology, an informed understanding and application of modern study design methodology is essential to proving clinical effectiveness of therapies in real-world situations. In our opinion and experience, the answer to the question of randomization posed by Ruperto et al is not dichotomous. Furthermore, insisting upon RCTs when they are infeasible or impossible promotes an inefficient and even harmful precedent.

While traditionally considered the gold standard for questions of clinical effectiveness, RCTs are not feasible in many situations. Feasibility is particularly an issue when trials involve rare diseases (as is the case for all pediatric rheumatic diseases). Moreover, RCTs are often limited in real-world applicability (4). Recent advancements in clinical trial design and methodology allow prospective observational trials to provide an unbiased understanding of the real-world effectiveness of interventions. These methodologic advancements utilize the power of causal inference or causal methods (5). We employed propensity scoring, a widely accepted method, in our study.

We certainly agree that there is a need for international collaborations to successfully answer important questions related to JIA and pediatric rheumatology in general. However, we believe many questions can be answered by leveraging the rigorous approaches used in Start Time Optimization of Biologics in Polyarticular JIA (STOP-JIA) and remain doubtful that a much larger, open-label, randomized trial is a feasible or necessary solution.

Ruperto et al also made several errors in characterizing our studies that directly impact the validity of the conclusions they have reached. First, based on the *P* value, Ruperto et al propose that our study had inadequate statistical power. Calculating power post hoc is widely understood as "…not only conceptually flawed but also analytically misleading" (6,7). We maintain that the 95% confidence intervals as presented in the primary report (2) remain the most informative statistics, as they bound the plausible magnitude of the percentage differences in patients in whom clinically inactive disease (CID) was attained. When the STOP-JIA study was designed, the power calculation included an assumption that CID would be achieved in 20% of patients started on the step-up consensus treatment plan (CTP) and 60% of patients on the early combination CTP. This represented our informed opinion of the real-world level of difference that would justify initial use of early combination therapy. For this level of difference, with 257 patients in the step-up group and 100 patients in the early combination group (putting aside dropout and confounding), the power of the STOP-JIA study is nearly 100%. If, instead, a smaller difference was considered clinically important, a correspondingly greater number of participants would have been needed for the study.

Second, the intent-to-treat principle dictates that all participants assigned to a CTP be included in the between-group comparison of outcomes. In fact, we used a widely accepted method, multiple imputation (8), to ensure adherence to this principle. The problem of missing data arises in both prospective observational studies and RCTs, and the solutions are the same for both study types.

Third, the authors appear to confuse the importance of the imbalance in the numbers of participants in each CTP group with the imbalance in data on baseline characteristics. There is imbalance in the numbers per group because CTP choice reflects patient and physician preferences and the underlying inherent uncertainty. This is important as it allows the use of powerful causal methods, enabling us to obtain unbiased estimates. As Ruperto et al correctly note, nonrandom assignment to CTPs led to imbalances in baseline data, which is precisely why we used propensity score weighting (9).

Fourth, Ruperto et al propose that glucocorticoid (GC) use could have been a key determinant in the rapid improvement in disease activity. In fact, our trajectory analysis (3) demonstrated that the rates of GC use at baseline and 3 months did not significantly differ according to the latent classes (i.e., disease activity trajectories). From 6 to 12 months of follow-up, GC use varied significantly across the latent classes, with the rapid improvement group having a substantially reduced rate of GC use compared with slow and moderate improvement groups.

Finally, regarding our article on the use of trajectory analysis to determine treatment efficacy in JIA (3), Ruperto et al

mischaracterize our objective, the numbers of patients included, and how patient data were analyzed using current Childhood Arthritis and Rheumatology Research Alliance registry data (we did not use the "Legacy Registry" [closed in 2012] as was stated in the editorial). We did not have an a priori hypothesis that early introduction of biologic disease-modifying antirheumatic drugs (bDMARDs) would be associated with improved disease trajectories. Instead, our finding that the introduction of bDMARDs within 3 months from baseline is associated with early attainment of inactive disease was the result of an unbiased, data-driven analysis. Furthermore, the finding that, in a subgroup of patients, achievement of CID without bDMARD treatment demonstrates a heterogeneity of the population that needs to be explored, rather than a lack of generalizability of our findings.

We believe our studies demonstrated that carefully collected and rigorously analyzed prospective observational data can provide valid answers to consequential comparative effectiveness questions that are otherwise not feasible to address.

Author disclosures are available at https://onlinelibrary.wiley.com/action/downloadSupplement?doi=10.1002%2Fart.42047&file=art42047-sup-0001-Disclosureform.pdf.

Yukiko Kimura, MD
Joseph M. Sanzari Children's Hospital and Hackensack Meridian School of Medicine
Hackensack, NJ
Mei-Sing Ong, PhD
Harvard Medical School and Harvard Pilgrim Health Care Institute
Boston, MA
George Tomlinson, PhD
University of Toronto
Toronto, Ontario, Canada
Sarah Ringold, MD, MS
Seattle Children's Hospital
Seattle, WA
Laura E. Schanberg, MD
Duke University Medical Center and Childhood Arthritis and Rheumatology Research Alliance
Durham, NC
Brian M. Feldman, MD, MSc
The Hospital for Sick Children
Toronto, Ontario, Canada
Anne Dennos, MSPH
Duke Clinical Research Institute
Durham, NC
Vincent Del Gaizo, BS
Childhood Arthritis and Rheumatology Research Alliance
Milwaukee, WI
Katherine L. Murphy, MPH
Louisiana State Department of Health
New Orleans, LA
Marc Natter, MD
Boston Children's Hospital Massachusetts General Hospital and Harvard Medical School
Boston, MA

1. Ruperto N, Martini A, Pistorio A, for the Paediatric Rheumatology International Trials Organisation. To randomize, or not to randomize, that is the question. Arthritis Rheumatol 2021;73:1776–9.
2. Kimura Y, Schanberg LE, Tomlinson GA, Riordan ME, Dennos AC, Del Gaizo V, et al, and the CARRA STOP-JIA Investigators. Optimizing the start time of biologics in polyarticular juvenile idiopathic arthritis: a comparative effectiveness study of Childhood Arthritis and Rheumatology Research Alliance consensus treatment plans. Arthritis Rheumatol 2021;73:1898–909.
3. Ong MS, Ringold S, Kimura Y, Schanberg LE, Tomlinson GA, Natter MD, and the CARRA Registry Investigators. Improved disease course associated with early initiation of biologics in polyarticular juvenile idiopathic arthritis: trajectory analysis of a Childhood Arthritis and Rheumatology Research Alliance consensus treatment plans study. Arthritis Rheumatol 2021;73:1910–20.
4. Cartwright N. What are randomized controlled trials good for? Philos Stud 2009;147:59.
5. Pearl J, Glymour M, Jewell NP. Causal inference in statistics: a primer. Chichester (UK): John Wiley & Sons; 2016.
6. Zhang Y, Hedo R, Rivera A, Rull R, Richardson S, Tu XM. Post hoc power analysis: is it an informative and meaningful analysis? Gen Psychiatr 2019;32:e100069.
7. Hoenig JM, Heisey DM. The abuse of power: the pervasive fallacy of power calculations for data analysis. Am Statistician 2001;55:19–24.
8. Van Buuren, S. Flexible imputation of missing data. 2nd ed. Boca Raton (FL): Chapman & Hall/CRC; 2016.
9. Austin PC. An introduction to propensity score methods for reducing the effects of confounding in observational studies. Multivariate Behav Res 2011;46:399–424.

DOI 10.1002/art.42046

Reply

To the Editor:

We thank Dr. Kimura and colleagues for their comments on our article. The studies by Ringold et al (1) and Kimura et al (2) are extremely important for the pediatric rheumatology community. The aim of our editorial that accompanied the STOP-JIA articles was not to undermine the great scientific power of registries such as that of the Childhood Arthritis and Rheumatology Research Alliance (CARRA). Studies of this kind are essential to answer important clinical and research-related questions, many of which are not part of randomized clinical trials.

As clinicians and researchers, we support the underlying hypothesis of the 2 studies: in JIA, more aggressive therapies combined with treat-to-target approaches (3) could change long-term outcomes. The literature concerning adult patients clearly supports the validity of this hypothesis, allowing evidence-based treat-to-target recommendations (4,5) for patients with rheumatoid arthritis. However, in pediatrics, conflicting results (6–9) do not prove the validity of the

hypothesis, potentially raising doubts about a treat-to-target approach in JIA (3).

With regard to the points raised by Kimura et al in their letter, we do agree that 95% confidence intervals are an alternative and more informative source for interpretation of the results of a study rather than *P* values and post hoc power calculation. As the authors noted in their article, "the confidence intervals were wide, and the differences between groups were not significant" (2).

Further, we agree with Kimura et al that the intent-to-treat principle dictates that all participants assigned to a CTP should be included in the between-group comparison. However, 328 (82%) of 400 patients were available for the unadjusted model, and the analysis after propensity score weighting and multiple imputation did not change the reported outcome.

The observed important imbalance in the numbers of participants in each of the 3 CTP groups may pose a selection bias in favor of more aggressive therapies, since it likely reflects the preferences of caregivers and study participants. The authors equalize such differences with causal inference methods instead of randomization techniques. While these methods can be useful, they can only balance measured confounders, while randomization can balance known and unknown confounders.

The principal finding of the study by Ringold et al (1) is consistent with the underlying hypothesis even in the absence of the evaluation of the possible effect of intraarticular steroid injections that are now used often in clinical practice. The CARRA investigators should be commended for their important logistical efforts and sophisticated analytical framework, which resulted in promising findings with regard to secondary end points, even though the results for the primary outcome measure were not statistically significant.

Our editorial is a call for future international collaboration between CARRA and others. We hope that the current available evidence can be used to generate and test important hypotheses in pediatric rheumatology.

Author disclosures are available at https://onlinelibrary.wiley.com/action/downloadSupplement?doi=10.1002%2Fart.42046&file=art42046-sup-0001-Disclosureform.pdf.

Nicolino Ruperto, MD, MPH
Istituto G. Gaslini, IRCCS
UOSID Centro Trial
and PRINTO
Alberto Martini, MD
Università di Genova
and PRINTO
Angela Pistorio, MD, PhD
Istituto G. Gaslini, IRCCS
Genoa, Italy
for the Paediatric Rheumatology
International Trials Organisation

1. Ringold S, Weiss PF, Colbert RA, DeWitt EM, Lee T, Onel K, et al. Childhood Arthritis and Rheumatology Research Alliance consensus treatment plans for new-onset polyarticular juvenile idiopathic arthritis. Arthritis Care Res (Hoboken) 2014;66:1063–72.
2. Kimura Y, Schanberg LE, Tomlinson GA, Riordan ME, Dennos AC, Del Gaizo V, et al. Optimizing the start time of biologics in polyarticular juvenile idiopathic arthritis: a comparative effectiveness study of Childhood Arthritis and Rheumatology Research Alliance consensus treatment plans. Arthritis Rheumatol 2021;73:1898–909.
3. Ravelli A, Consolaro A, Horneff G, Laxer RM, Lovell DJ, Wulffraat NM, et al. Treating juvenile idiopathic arthritis to target: recommendations of an international task force. Ann Rheum Dis 2018;77:819–28.
4. Smolen JS, Breedveld FC, Burmester GR, Bykerk V, Dougados M, Emery P, et al. Treating rheumatoid arthritis to target: 2014 update of the recommendations of an international task force. Ann Rheum Dis 2016;75:3–15.
5. Smolen JS. Treat to target in rheumatology: a historical account on occasion of the 10th anniversary [review]. Rheum Dis Clin North Am 2019;45:477–85.
6. Wallace CA, Giannini EH, Spalding SJ, Hashkes PJ, O'Neil KM, Zeft AS, et al. Trial of early aggressive therapy in polyarticular juvenile idiopathic arthritis. Arthritis Rheum 2012;64:2012–21.
7. Tynjala P, Vahasalo P, Tarkiainen M, Kroger L, Aalto K, Malin M, et al. Aggressive combination drug therapy in very early polyarticular juvenile idiopathic arthritis (ACUTE-JIA): a multicentre randomised open-label clinical trial. Ann Rheum Dis 2011;70:1605–12.
8. Klein A, Minden K, Hospach A, Foeldvari I, Weller-Heinemann F, Trauzeddel R, et al. Treat-to-target study for improved outcome in polyarticular juvenile idiopathic arthritis. Ann Rheum Dis 2020;79:969–74.
9. Muller PH, Brinkman DM, Schonenberg-Meinema D, van den Bosch WB, Koopman-Keemink Y, Brederije IC, et al. Treat to target (drug-free) inactive disease in DMARD-naive juvenile idiopathic arthritis: 24-month clinical outcomes of a three-armed randomised trial. Ann Rheum Dis 2019;78:51–9.

Arthritis & Rheumatology
Vol. 74, No. 5, May 2022, pp e21–e36
DOI 10.1002/art.42109

American College of Rheumatology
Empowering Rheumatology Professionals

American College of Rheumatology Guidance for COVID-19 Vaccination in Patients With Rheumatic and Musculoskeletal Diseases: Version 4

Jeffrey R. Curtis,[1] Sindhu R. Johnson,[2] Donald D. Anthony,[3] Reuben J. Arasaratnam,[4] Lindsey R. Baden,[5] Anne R. Bass,[6] Cassandra Calabrese,[7] Ellen M. Gravallese,[5] Rafael Harpaz,[8] Andrew Kroger,[9] Rebecca E. Sadun,[10] Amy S. Turner,[11] Eleanor Anderson Williams,[12] and Ted R. Mikuls[13]

Due to the rapidly expanding information and evolving evidence related to COVID-19, which may lead to modification of some guidance statements over time, it is anticipated that updated versions of this article will be published, with the version number included in the title. Readers should ensure that they are consulting the most current version.

However, because of publication timelines, there may be more updated recommendations online at the ACR website that are pending journal peer review and full manuscript publication. Readers should check the ACR website at https://www.rheumatology.org/Practice-Quality/Clinical-Support/COVID-19-Guidance to confirm the ACR's most recent recommendations. The online version of the tables as they were originally published, as well as a summary of revisions over time and their location, are included in Supplementary Tables 2–6.

Guidance developed and/or endorsed by the American College of Rheumatology (ACR) is intended to inform particular patterns of practice and not to dictate the care of a particular patient. The ACR considers adherence to this guidance to be voluntary, with the ultimate determination regarding its application to be made by the physician in light of each patient's individual circumstances. Guidance statements are intended to promote beneficial or desirable outcomes but cannot guarantee any specific outcome. Guidance developed or endorsed by the ACR is subject to periodic revision as warranted by the evolution of medical knowledge, technology, and practice.

The American College of Rheumatology is an independent, professional, medical and scientific society which does not guarantee, warrant, or endorse any commercial product or service.

Objective. To provide guidance to rheumatology providers on the use of COVID-19 vaccines for patients with rheumatic and musculoskeletal diseases (RMDs).

Methods. A task force was assembled that included 9 rheumatologists/immunologists, 2 infectious disease specialists, and 2 public health physicians. After agreeing on scoping questions, an evidence report was created that summarized the published literature and publicly available data regarding COVID-19 vaccine efficacy and safety, as well as literature for other vaccines in RMD patients. Task force members rated their agreement with draft consensus statements on a 9-point numerical scoring system, using a modified Delphi process and the RAND/University of California Los Angeles Appropriateness Method, with refinement and iteration over 2 sessions. Consensus was determined based on the distribution of ratings.

Results. Despite a paucity of direct evidence, statements were developed by the task force and agreed upon with consensus to provide guidance for use of the COVID-19 vaccines, including supplemental/booster dosing, in RMD patients and to offer recommendations regarding the use and timing of immunomodulatory therapies around the time of vaccination.

Conclusion. These guidance statements are intended to provide direction to rheumatology health care providers on how to best use COVID-19 vaccines and to facilitate implementation of vaccination strategies for RMD patients.

INTRODUCTION

The global pandemic caused by SARS–CoV-2 has caused untold disruption to nearly all aspects of human health globally. The substantial morbidity and excess mortality attributed to COVID-19 has had a major impact on health and the delivery of health care. Given the role that rheumatology providers have in serving patients with rheumatic and musculoskeletal diseases (RMDs) (1), particularly those with autoimmune and inflammatory rheumatic diseases (AIIRDs), there is an urgent need to optimize strategies to curb the incidence of COVID-19. In addition to preventive measures such as physical distancing, mask-wearing, handwashing, and shelter-in-place orders, available COVID-19 vaccines provide a powerful tool to mitigate the burgeoning growth of adverse outcomes resulting from COVID-19.

Given the leadership role of the American College of Rheumatology (ACR) in facilitating dissemination of high-quality evidence and promoting best practices for the care of RMD patients, the ACR periodically convenes task forces charged with developing methodologically rigorous clinical practice guidelines and guidance documents. Previous ACR guidelines developed for the management of rheumatoid arthritis (RA) and psoriatic arthritis (PsA) have included some information regarding optimal use of vaccines for patients with those conditions. However, because the immunologic principles related to the use of vaccines and the impact of vaccine-preventable illnesses on patients cross a broad range of RMDs, the ACR altered its approach in 2020 and convened a new guideline development group to focus exclusively on vaccination. This cross-cutting team was charged with developing encompassing vaccination considerations for all disease and treatment-related areas within rheumatology, rather than embedding them into narrower, disease-specific clinical practice guidelines.

The development process of ACR guidelines follows a rigorous and formal methodology, is based on a reproducible and transparent systematic literature review, incorporates panelist expertise from rheumatology health care professionals and input from related medical experts in other disciplines (e.g., infectious disease, epidemiology), includes direct participation by patients that reflects their values and preferences, and is typically conducted over an extended time frame (e.g., 1 year or longer). In contrast, the ACR develops "guidance" documents when the components needed to develop a formal guideline are not present, e.g., if the need to provide guidance is more urgent than a longer guideline timeline would allow, there is not enough peer-reviewed evidence available to conduct a formal literature review, or when there is very limited expertise and experience, particularly on the part of patients, to help inform the development of recommendations. In these situations, an expert task force is formed to provide the best guidance possible based on the limited information available. The ACR expects that guidance documents will need to be updated with some frequency as new data become available and greater experience is acquired.

Responding to the need to provide timely guidance to practicing clinicians, the ACR COVID-19 Vaccine Guidance Task Force was created as a branch of the ACR Vaccine Guideline effort, to summarize the available evidence for newly available COVID-19 vaccines and to make timely clinical recommendations to rheumatology providers for their optimal use. It relied on a limited evidence base derived from clinical trials evaluating the COVID-19 vaccines in non-RMD populations and also included indirect evidence regarding the immunogenicity, clinical effectiveness, and safety of other vaccines administered to RMD patients receiving various immunomodulatory therapies. Armed with this information, task force members were asked to extrapolate across diseases and integrate relevant basic science and immunologic principles to inform the use, timing, and prioritization of

---

The findings and conclusions in this report are those of the authors and do not necessarily represent the views of the Centers for Disease Control and Prevention/the Agency for Toxic Substances and Disease Registry.

Supported by the American College of Rheumatology. The effort of some individual authors was supported in part by the NIH (National Institute of Arthritis and Musculoskeletal and Skin Diseases grant P30-AR072583).

[1]Jeffrey R. Curtis, MD, MS, MPH: University of Alabama at Birmingham; [2]Sindhu R. Johnson, MD, PhD: Toronto Western Hospital, Mount Sinai Hospital, and University of Toronto, Toronto, Ontario, Canada; [3]Donald D. Anthony, MD, PhD: Louis Stokes Cleveland VA Medical Center, MetroHealth Medical Center, and Case Western Reserve University, Cleveland, Ohio; [4]Reuben J. Arasaratnam, MD: VA North Texas Health Care System and University of Texas Southwestern Medical Center, Dallas; [5]Lindsey R. Baden, MD, MSc, Ellen M. Gravallese, MD: Brigham and Women's Hospital, Boston, Massachusetts; [6]Anne R. Bass, MD: Hospital for Special Surgery and Weill Cornell Medicine, New York, New York; [7]Cassandra Calabrese, DO: Cleveland Clinic, Cleveland, Ohio; [8]Rafael Harpaz, MD: Harpaz Herman Consultants, Atlanta, Georgia; [9]Andrew Kroger, MD, MPH: CDC, Atlanta, Georgia; [10]Rebecca E. Sadun, MD, PhD: Duke University, Durham, North Carolina; [11]Amy S. Turner: American College of Rheumatology, Atlanta, Georgia; [12]Eleanor Anderson Williams, MD: The Permanente Medical Group, Union City, California; [13]Ted R. Mikuls, MD, MSPH: University of Nebraska Medical Center and VA Nebraska–Western Iowa Health Care System, Omaha.

Dr. Curtis has received consulting fees, speaking fees, and/or honoraria from AbbVie, Bristol Myers Squibb, GlaxoSmithKline, Eli Lilly, and Novartis (less than $10,000 each) and from Amgen, Janssen, Pfizer, Myriad, and Sanofi (more than $10,000 each) and research grants from Genentech, Gilead, AbbVie, Bristol Myers Squibb, GlaxoSmithKline, Eli Lilly, Amgen, Janssen, Pfizer, Myriad, and Sanofi. Dr. Johnson has received consulting fees, speaking fees, and/or honoraria from Ikarai and Boehringer Ingelheim (less than $10,000 each) and research grants from Bayer, Boehringer Ingelheim, Corbus, and GlaxoSmithKline. Dr. Baden has received salary support form the *New England Journal of Medicine* (less than $10,000). Dr. Calabrese has received consulting fees, speaking fees, and/or honoriaria from AbbVie and Sanofi Genzyme (less than $10,000 each). Dr. Gravallese has received salary support from the *New England Journal of Medicine* (more than $10,000). Dr. Mikuls has received consulting fees, speaking fees, and/or honoraria from Sanofi, Horizon, Pfizer, and Gilead (less than $10,000 each) and research support from Bristol Myers Squibb and Horizon. No other disclosures relevant to this article were reported.

Address correspondence to Jeffrey R. Curtis, MD, MS, MPH, University of Alabama at Birmingham, FOT 802, 510 20th Street South, Birmingham, AL 35294. Email: jrcurtis@uabmc.edu.

Submitted for publication February 16, 2022; accepted in revised form March 2, 2022.

the COVID-19 vaccines available in the US and apply them to the care of RMD patients.

METHODS

Convening the ACR COVID-19 Vaccine Guidance Task Force and defining the scope of the clinical guidance. In October 2020, the ACR began assembling the ACR COVID-19 Vaccination Guidance Task Force. Invitations were made following a general solicitation sent to the broad ACR membership seeking interested volunteers. The task force consisted of 13 members from North America and included 9 rheumatologists, 2 infectious disease specialists, and 2 public health experts. Rheumatology task force members were chosen to represent various areas of specialty expertise within the field and to achieve diversity in geographic region, career stage, practice setting, sex, and race/ethnicity, while also ensuring that the majority of task force members had no conflicts of interest. The task force defined the intended scope of the guidance based on input from individual members, and external input was obtained informally from various stakeholders. The process was informed by the previously published ACR Guidance for the Management of Rheumatic Disease in Adult Patients During the COVID-19 Pandemic (2). The scope of this guidance includes clinically relevant questions that were intended to inform rheumatology patient care related to COVID-19 vaccination and treatment considerations around the time of vaccination. The scoping questions were agreed upon by all panel members at an initial teleconference conducted on December 14, 2020.

Developing the evidence summary. The task force was divided into teams that worked in parallel, each charged with summarizing the published literature and other available evidence spanning 4 topics: 1) the efficacy, immunogenicity, and safety data derived from clinical trials of late-stage (i.e., phase III) COVID-19 vaccines ongoing within the US or COVID-19 vaccines already available under the US Food and Drug Administration (FDA) Emergency Use Authorization (EUA) act; 2) the epidemiology of COVID-19 risk and outcomes in RMD patients; 3) the attenuation of immunogenicity to other vaccines (e.g., influenza, pneumococcal) associated with certain immunomodulatory therapies; and 4) the safety profile (e.g., disease flare, new-onset autoimmune conditions) of non–COVID-19 vaccines in RMD populations. The scoping questions were grouped into these domains and distributed to the teams, which were tasked with gathering and summarizing evidence that addressed the questions within their assigned domains.

The task force agreed that the intended audience for the guidance was rheumatology health care providers managing their individual patients, but they felt that some attention should be directed to a societal perspective, when relevant, around the availability of COVID-19 vaccines and prioritization for individuals with RMDs. The task force took the perspective of developing guidance for a US audience, particularly in view of the fact that the review of COVID-19 vaccine clinical trials was US-focused. Recognizing that RMD patients exhibit high variability with respect to their underlying health conditions, disease severity, treatments, and degree of multimorbidity, these considerations were noted as important facets of individualizing care. Therefore, this guidance was not intended to supersede the judgment of rheumatology care providers nor override the values and perspectives of their patients. Foundational principles, guiding assumptions, and acknowledged limitations were discussed and agreed upon throughout the process (Table 1) and are discussed in this document where most relevant.

Table 1. Foundational principles, assumptions, and considerations for the guidance statements*

ACR guidance statements are not intended to supersede the judgment of rheumatology care providers nor override the values and perspectives of their patients. Guidance was, in some cases, based on weak and/or indirect evidence and required substantial extrapolation by an expert task force. All statements, therefore, should be considered conditional or provisional. The ACR is committed to updating this guidance document as new evidence emerges.
The rheumatology community lacks important knowledge on how to best maximize vaccine-related benefits. RMD patients exhibit high variability with respect to their underlying health condition, disease severity, treatments, degree of multimorbidity, and relationship with their specialist provider. These considerations must be considered when individualizing care.
There is limited direct evidence about mRNA COVID-19 vaccine safety and efficacy in RMD patients. There is no reason to expect vaccine harms will trump expected COVID-19 vaccine benefits in RMD patients.
Evidence about the mRNA COVID-19 vaccine suggests that the benefits outweigh the risks in RMD patients.
The risk of deferring vaccination and thus failing to mitigate COVID-19 risk should be weighed against a possible blunted response to the vaccine if given under suboptimal circumstances. As a practical matter, this tension must be resolved in the context of imperfect prediction as to whether those circumstances may be transient as well as a paucity of scientific evidence.
Both individual and societal considerations related to a limited vaccine supply should be considered in issuing vaccine guidance and making policy decisions. Given that context, simplicity should be the touchstone: to avoid confusion, improve implementation, and maintain scientific credibility.
In the future, the ability to give vaccine boosters will no longer be constrained by limited supplies. Any vaccination strategy is a reasonable starting point, and decisions about implementation details reflect tradeoffs in the allocation of scarce vaccine resources.

* ACR = American College of Rheumatology; RMD = rheumatic and musculoskeletal disease.

Development of the evidence review summary document. Given the accelerated time frame for guidance development, a nonsystematic evidence review was completed and included serial PubMed searches supplemented by postings from the Centers for Disease Control and Prevention (CDC); briefings and other documents available from the FDA, such as dossiers

submitted by vaccine manufacturers and transcripts of data presented at the FDA's Vaccines and Related Biological Products Advisory Committee meetings (3,4); and other electronic media sources. References and original articles related to vaccination were culled from the systematic literature reviews developed for ACR guidelines for the management of RA in 2012, 2015, and 2021 (5–7), PsA in 2018 (8), and vaccination guidelines for RMD patients published by European Alliance of Associations for Rheumatology (9–11). Articles were dated 1994 through January 2021 (English language, domestic and international).

The scoping questions and the relevant evidence reviews contributed by team members were collated into a single evidence summary document, which was disseminated by email to the entire task force for review 2 days prior to initial ratings. Following the development of the evidence summary, regular PubMed searches were undertaken, and new evidence was shared with the task force prior to follow-up webinars. As limited direct evidence was anticipated to be immediately available for use of the COVID-19 vaccine in RMD patients, no formal assessment of evidence quality (e.g., using Grading of Recommendations Assessment, Development and Evaluation methodology [12]) was attempted, and all evidence was assumed to be indirect. For this reason, all guidance statements should be considered as provisional, or "conditional," until further evidence becomes available.

Initial ratings. The standard guideline development processes currently used by the ACR (13) were deemed to be too time-intensive to be feasible, given the immediate need for the guidance document. Therefore, following distribution of the evidence review document, the scoping questions were transformed into proposed positive statements for which task force members were asked to rate their initial agreement or disagreement. These statements were grouped into 4 broad categories: 1) general medical considerations that provided foundational information for the guidance document; 2) specific recommendations related to COVID-19 vaccination in RMD patients; 3) treatment-specific considerations regarding the timing of COVID-19 vaccination; and 4) the timing of RMD treatments in relation to vaccine administration.

A modified Delphi approach conducted as part of the RAND/University of California at Los Angeles Appropriateness Method (14) was used for guidance development. This method has been used for some past ACR guidelines and the more recent ACR COVID-19 guidance (15); it has been shown to be reproducible and to have content, construct, and predictive validity. Using this method, an initial round of rating was conducted anonymously by email. Task force members were asked to rate their level of agreement, and all votes were weighted equally. Voting was completed using a numerical rating scale of 1–9 for all items. Ratings of 9 corresponded to "complete agreement," 5 to "uncertain," and 1 to "complete disagreement." Median ratings for each statement falling into intervals of 1–3, 4–6, and 7–9 were interpreted as disagreement, uncertainty, and agreement, respectively. Agreement with each of the proposed guidance statements submitted by individual panel members was tabulated for the entire panel and used to classify consensus. Consensus was deemed "strong" when all 13 panel members' ratings fell within a single tertile (e.g., 7–9, indicative of agreement); all other combinations were considered to reflect "moderate" consensus. A lack of consensus was identified when the median rating fell into the uncertain range (4–6 interval), or more than one-quarter of the ratings fell into the opposite extreme tertile from the median (e.g., ≥4 panelists rated 1–3 [disagree] when the overall median rating was in the 7–9 [agree] range) (14).

Review and iteration for the ratings of the proposed guidance statements by the task force. Results from the first round of rating were reviewed and discussed in a task force webinar on January 15, 2021. Discussion was focused on statements for which there was no consensus. Individuals were given the opportunity to comment on all items presented in the initial rating process. Informed by voting results and the group discussion, the task force members refined the wording of several of the rated statements.

Revised statements were sent back to task force members and agreement was again assessed by email, using the same scoring approach described above. Results from the second round of voting were presented to the task force via webinar on January 22, 2021, and minor text revisions were made iteratively in real time until consensus was achieved. A draft manuscript was developed describing the results of the rating process, and all coauthors were given an opportunity to provide direct edits to the document. The ACR Guidance Subcommittee and ACR Quality of Care Committee were given the document in order to provide feedback. It was subsequently sent to the ACR Board of Directors, which approved these recommendations on February 8, 2021. Public vetting of the guidance document was held via an electronic and widely publicized "town hall" held on February 16, 2021 that was open to ACR members and the public, with questions solicited in advance and during the town hall webinar. Finally, given the multitude of uncertainties and evidence gaps considered by the task force, the panel proposed a research agenda of high-impact topics that would advance the science and inform the optimal use of COVID-19 vaccines in RMD patients treated with immunomodulatory therapies. After publication, an ACR project librarian will refresh the specified literature search on a regular basis and submit new articles to the task force for review, and this document will be updated through a similar process as new evidence emerges.

RESULTS

Of the guidance statements considered across the 2 rounds of ratings, the majority were rated with a median score of 7, 8, or

Table 2. General considerations related to COVID-19 vaccination in patients with RMD*

Statement domain	Guidance statement	Level of task force consensus
Clinical practice	The rheumatology health care provider is responsible for engaging the RMD patient in a discussion to assess COVID-19 vaccination status.	Strong
Clinical practice	The rheumatology health care provider is responsible for engaging the RMD patient in a shared decision-making process to discuss receiving the COVID-19 vaccine.	Moderate
Epidemiology	AIIRD patients are at higher risk for incident viral infections compared to the general population.	Moderate
Epidemiology	After considering the influence of age and sex, AIIRD patients are at higher risk for COVID-19 hospitalization compared to the general population.	Moderate
Epidemiology	Acknowledging heterogeneity due to disease- and treatment-related factors, AIIRD patients have worse outcomes associated with COVID-19 compared to the general population of similar age and sex.	Moderate
Epidemiology	Across AIIRD conditions, and within any specific disease, there is substantial variability in disease- and treatment-related risk factors for COVID-19 that may put some patients at higher risk than others.†	Moderate
Public health	Based on increased risk for COVID-19, AIIRD patients should be prioritized for vaccination before the nonprioritized general population of similar age and sex.	Moderate
Vaccine safety	Beyond known allergies to vaccine components, there are no known additional contraindications to COVID-19 vaccination for AIIRD patients.	Moderate
Vaccine effectiveness	The expected response to COVID-19 vaccination for many AIIRD patients receiving systemic immunomodulatory therapies is blunted in its magnitude and duration compared to the general population.	Moderate
Disease-related	As a general principle, vaccination should optimally occur in the setting of well-controlled AIIRD.	Moderate
Disease-related	A potential risk exists for AIIRD flare or disease worsening following COVID-19 vaccination.	Moderate
Vaccine safety	The benefit of COVID-19 vaccination for RMD patients outweighs the potential risk for new-onset autoimmunity.	Moderate

* RMD = rheumatic and musculoskeletal disease.
† For examples of these autoimmune and inflammatory rheumatic disease (AIIRD) conditions, see Supplementary Table 1, on the *Arthritis & Rheumatology* website at http://onlinelibrary.wiley.com/doi/10.1002/art.42109.

9 (i.e., agreement), and 3 of them were not agreed upon. Among the statements achieving agreement, consensus was strong for 9 and moderate for the remainder. One guidance statement related to COVID-19 vaccination in children was rated with a median value of 5 (uncertain) by the task force, in part reflecting the desire to obtain more feedback from pediatric rheumatology providers. Additional input was therefore sought from the ACR Pediatric Rheumatology Clinical Guidance Task Force. This task force has acknowledged ongoing clinical trials of COVID-19 vaccines in children and evolving FDA EUAs for the COVID-19 vaccine in children younger than age 16 years, although it recognized that ≥1 COVID-19 vaccine clinical trial has enrolled patients as young as age 5 years (ClinicalTrials.gov identifiers: NCT04649151 and NCT04368728) (16–19). On this basis, our task force and the Pediatric Task Force have consistently recommended to await appropriate evidence from clinical trials regarding the safety and effectiveness of COVID-19 vaccination in children and align our guidance with FDA EUAs. The second statement for which the task force was unable to reach consensus relates to vaccination in the context of ongoing treatment with high-dose glucocorticoids, discussed in detail below.

General considerations related to vaccination against COVID-19 in patients with RMDs. Twelve guidance statements related to general considerations of COVID-19 vaccination in RMD patients achieved consensus (Table 2). Statements were descriptively categorized into ≥1 domain to facilitate ease of reference. The panel concurred that rheumatology health care providers were responsible for engaging RMD patients in discussions to assess whether they had been vaccinated against COVID-19 and to document related details (e.g., which vaccine had been administered, timing of vaccination, whether the series had been completed). For those not vaccinated, and similar to other vaccination guidelines for immunocompromised patients such as those from the Infectious Diseases Society of America (20,21), it was thought that the rheumatology provider should share responsibility with the patients' primary care provider (when available) to ensure appropriate vaccinations are administered. Rheumatology providers should also engage patients in a shared decision-making process to discuss the following: their attitudes, intent, and concerns related to vaccination; local incidence of COVID-19; individual circumstances (e.g., disease activity, medications, comorbidities) that may affect risk; ability to adhere to nonpharmacologic public health interventions; and vaccine efficacy and potential safety concerns (e.g., local or systemic reactogenicity, potential for disease worsening or flare).

The epidemiology of viral infection risk in RMD patients, and specifically, the risk for infection due to SARS–CoV-2, was then discussed. For this topic, the task force elected to narrow the scope of the patient population under consideration and define a presumably higher-risk subgroup of patients with RMDs. Some RMD conditions would include those managed by rheumatology

providers but not generally associated with high levels of systemic inflammation (e.g., osteoarthritis, fibromyalgia, osteoporosis) and for which conventional, biologic, or targeted synthetic disease-modifying antirheumatic drugs (DMARDs) or other therapies with immunosuppressive effects are typically not indicated. The patient population was thus restricted to those with AIIRDs (see Supplementary Table 1 for definitions, available on the *Arthritis & Rheumatology* website at http://onlinelibrary.wiley.com/doi/10.1002/art.42109). Among these individuals, the risk for incident viral infections (e.g., herpes zoster) was rated as being higher than in the general population (22–24). There was also agreement that AIIRD patients are likely to be at increased risk for hospitalized SARS–CoV-2 infection (25–29) and that age, race/ethnicity (especially for underrepresented minorities), and sex were important risk factors that needed to be considered (30–33) in evaluating risk at the individual patient level.

Multimorbidity was felt to likewise play an important role in the risk for developing COVID-19. While some population-based epidemiologic studies of COVID-19 incidence and outcomes in AIIRD patients have controlled for general multimorbidity or specific comorbidities (25,26,34), the panel recognized that some comorbidities that increase infection risk were shared risk factors for development of AIIRDs (e.g., smoking and related pulmonary conditions associated with incident RA). These may represent direct manifestations such as interstitial lung disease associated with some AIIRDs, or they could be downstream sequelae causally related to the underlying inflammatory processes of AIIRDs or their treatment (e.g., premature and advanced atherosclerotic vascular disease in systemic lupus erythematosus (SLE) patients; obesity, diabetes, and features of the metabolic syndrome in PsA patients or those receiving long-term glucocorticoids). For that reason, adjustment for these comorbidities might be inappropriate and would underestimate the risk of COVID-19 infection in patients with AIIRDs. Therefore, age- and sex-adjusted risk estimates were preferred by some task force members when comparing risk and outcomes of COVID-19 in AIIRD patients to the general population.

The few large population-based studies of COVID-19 incidence and outcomes in AIIRD patients had minimal demographic diversity, and therefore race/ethnicity could not be easily evaluated as an independent risk factor. Finally, the panel acknowledged challenges in being able to disentangle the independent role of the disease activity and severity of various AIIRDs from the medications used to treat them (e.g., higher-dose glucocorticoids [35]), so-called confounding by severity, as risk factors for worse COVID-19 outcomes.

Despite these important methodologic caveats and acknowledged limitations in the evidence base, AIIRD patients were rated as having worse outcomes (e.g., need for intensive care unit [ICU] treatment, mechanical ventilation, persistent infection, death) following COVID-19 compared to patients of similar age and sex without such conditions (25–29,36). In terms of the policy implications of this reasoning, the task force agreed that in general, AIIRD patients should be prioritized to be allocated to receive vaccination before the nonprioritized general population of similar age and sex (37). The panel recognized important heterogeneity across AIIRD conditions, such that (for example) an RA patient with quiescent disease treated only with hydroxychloroquine likely has a lower risk for COVID-19 and adverse outcomes compared to a patient with very active vasculitis treated with intravenous (IV) cyclophosphamide or rituximab (RTX) and high-dose glucocorticoids (33), although the protection conferred by COVID-19 vaccination may also differ greatly.

Turning attention to vaccination of individual patients, the task force felt that there were no additional known contraindications to receipt of the COVID-19 vaccine other than known allergies to vaccine components as stipulated by guidance from the CDC (38). Extrapolating evidence derived from studies of other vaccines, the expected response to vaccination in many AIIRD patients receiving certain systemic immunomodulatory therapies was deemed likely to be blunted, albeit with uncertain diminution in either the magnitude or duration of response compared to the general population (38,39). The task force acknowledged a paucity of direct evidence supporting this assertion and placed great importance on prioritizing this topic as part of a future research agenda. The timing of vaccination was considered more ideal in the setting of well-controlled disease, yet the task force noted that patients and their providers should not be dissuaded from vaccination under less-than-ideal conditions, with additional timing considerations as discussed below.

Based on data derived from the published literature, a potential risk for a flare of the patient's underlying AIIRD following vaccination was acknowledged. For example, based on randomized controlled trial data (40), the frequency of flare was higher in RA patients randomized to have methotrexate (MTX) withheld at the time of influenza vaccination compared to those randomized to continue (10.6% versus 5.1%, respectively), with flare defined as an increase in the Disease Activity Score in 28 joints (DAS28) of >1.2, or >0.6 if the baseline DAS28 was ≥3.2 (41). A subsequent pooled analysis that included that trial and another showed that while the mean change in DAS28 did not differ between groups, the adjusted flare rate in the 2-week withhold group (MTX withhold) was 2.90-fold higher (95% confidence interval 0.96–4.56, $P = 0.063$) compared to the group that continued MTX (MTX continue), with a difference in proportions experiencing flare of 10.8% (MTX withhold group) versus 5.8% (MTX continue group) (40,42–44). This risk of flare or disease worsening was catalogued as an important topic slated for the future research agenda. Finally, although some new-onset AIIRDs (e.g., RA, vasculitis) or flares of preexisting AIIRDs have been reported after COVID-19 in published case reports (45,46), the expected benefit of vaccination for AIIRD patients was thought to outweigh any theoretical risk for the development of new-onset autoimmune conditions or

Table 3. Recommendations for primary and supplemental dosing of the COVID-19 vaccine in RMD patients*

Statement domain	Guidance statement	Level of task force consensus
Clinical practice	RMD patients should receive COVID-19 vaccination, consistent with the age restriction of the EUA and/or FDA approval.†	Strong
Clinical practice	RMD patients without an AIIRD who are receiving immunomodulatory therapy should be vaccinated in a similar manner as described in this guidance as AIIRD patients receiving those same treatments.	Moderate
Vaccine effectiveness/ safety	**For AIIRD patients who are not yet vaccinated, either of the mRNA vaccines is recommended over the Johnson & Johnson vaccine. There is no recommendation for one mRNA vaccine over another.**	**Moderate**
Vaccine effectiveness	For a multidose vaccine, AIIRD patients should receive the second dose of the same vaccine, even if there are nonserious adverse events associated with receipt of the first dose, consistent with timing described in CDC guidelines (32).	Strong
Clinical practice	**For patients who previously completed the 2-dose mRNA series, an additional COVID-19 vaccine dose is recommended ≥28 days after the completion of the vaccine series for AIIRD patients receiving any immunosuppressive or immunomodulatory therapy other than hydroxychloroquine monotherapy.**	**Moderate**
Clinical practice	**For patients who previously completed the mRNA COVID-19 vaccine series or 1-dose J&J COVID-19 vaccine, and who are receiving a booster dose, an mRNA vaccine supplemental dose of either type (Pfizer or Moderna) is preferred.**	**Moderate**
Clinical practice	Health care providers should not routinely order any laboratory testing (e.g., antibody tests for IgM and/or IgG to spike or nucleocapsid proteins) to assess immunity to COVID-19 postvaccination, nor to assess the need for vaccination in an as-yet-unvaccinated person.‡	Strong
Public health	Following COVID-19 vaccination, RMD patients should continue to follow all public health guidelines regarding physical distancing and other preventive measures.§	Strong
Clinical practice	**AIIRD patients at high risk for poor outcomes related to COVID-19 should receive monoclonal antibody therapy, either as prevention (i.e., post-exposure prophylaxis for asymptomatic, recently exposed patients) or as treatment for newly symptomatic patients, if licensed or approved under FDA EUA.**	**Moderate**
Clinical practice/public health	Household members and other frequent close contacts of AIIRD patients should undergo COVID-19 vaccination when available to them to facilitate a "cocooning effect" that may help protect the AIIRD patient. No priority for early vaccination is recommended for household members.	Moderate
Vaccine effectiveness/ disease-related	While vaccination would ideally occur in the setting of well-controlled AIIRD, except for AIIRD patients with life-threatening disease (e.g., in the ICU for any reason), COVID-19 vaccination should occur as soon as possible for those for whom it is being recommended, irrespective of disease activity and severity.	Strong
Vaccine effectiveness/ disease-related	In AIIRD patients with life-threatening disease (e.g., in the ICU for any reason), COVID-19 vaccination should be deferred until their disease is better controlled.	Moderate
Vaccine effectiveness/ disease-related	AIIRD patients with active but non–life-threatening disease should receive COVID-19 vaccination.	Strong
Vaccine effectiveness/ disease-related	AIIRD patients with stable or low disease activity AIIRDs should receive COVID-19 vaccination.	Strong
Vaccine effectiveness/ disease-related	AIIRD patients not receiving immunomodulatory treatments should receive the first dose of the COVID-19 vaccine prior to initiation of immunomodulatory therapy when feasible.	Moderate

* Boldface text indicates updates that were added to the version 4 summary document at the end of 2021. RMD = rheumatic and musculoskeletal disease; EUA = Emergency Use Authorization; FDA = US Food and Drug Administration; AAIRD = autoimmune and inflammatory rheumatic disease; CDC = Centers for Disease Control and Prevention; ICU = intensive care unit.
† Age ≥5 years as of October 29, 2021.
‡ Given uncertainties in the interpretation of laboratory testing following vaccination as it would impact clinical decision-making, the panel reaffirmed this statement in Version 4 of this guidance document.
§ The task force discussed the possibility of recommending additional and more sustained public health measures for patients with AIIRD. After deliberation, they did not elect to exceed current public health authority guidance given uncertainties about the clinical effectiveness of vaccination in such patients. The appropriateness for continued preventive measures (e.g., masking, physical distancing) should be discussed with patients as their rheumatology providers deem appropriate.

other potentially immune-mediated manifestations or abnormalities (e.g., Bell's palsy, Guillain-Barré syndrome, anti-RNA antibodies in SLE patients, immune thrombocytopenic purpura) following vaccination.

Indications for vaccination and timing considerations. As summarized in Table 3, and consistent with guidance from the CDC for the general US population, the panel recommended that RMD and AIIRD patients be offered and receive vaccination against SARS–CoV-2. Discussion was held regarding the age cutoff for vaccination, and the panel agreed that guidance should be made consistent with the EUA of available vaccines (i.e., age ≥5 years as of October 29, 2021), with the potential for that cutoff to change in the future based on future revisions to EUAs for existing vaccines, forthcoming EUAs for new vaccines, or age restrictions applicable to FDA licensure.

Recommendations on which patients should be vaccinated were extended to patients with RMDs who did not have conditions typically considered to be AIIRDs but for which immunomodulatory or DMARD therapies might be used off-label. For example, patients with erosive osteoarthritis might receive MTX, or gout patients treated with pegloticase might be concomitantly treated with MTX to reduce pegloticase immunogenicity. These circumstances, in which MTX or another immunomodulatory therapy is being used for a non-AIIRD condition, would be treated synonymously with the guidance for MTX offered in this document. However, within the category of patients with AIIRDs and/or those receiving immunomodulatory therapies, substantial heterogeneity of disease- and treatment-related risk factors was noted. Some AIIRD patients were expected to be at higher risk for infection and morbidity than others, and thus the impetus for COVID-19 vaccination might be stronger for some individual patients or patient groups (e.g., patients with SLE receiving cytotoxic therapy and higher-dose glucocorticoids, or patients receiving RTX therapy), although the vaccine might be less effective in these same individuals.

Extensive discussion was held regarding whether consideration for a particular vaccine or vaccine platform (e.g., messenger RNA [mRNA] versus adenoviral vector) might be preferred in general, or for select patients, based on potential differences in effectiveness or safety. Based on the task force members' ratings and the vaccine options in the US, the expert panel reached consensus on the guidance that RMD patients undergoing vaccination are recommended to receive whichever SARS–CoV-2 mRNA vaccine is available to them. Either of the mRNA vaccines is recommended over the single-dose Johnson & Johnson vaccine. The task force noted that none of the other SARS–CoV-2 vaccine candidates in development would be classified as a canonical live virus vaccine, including the adenoviral vector–based vaccines which are replication deficient (47). Thus, the usual prohibitions against the use of live virus vaccines in immunosuppressed patients do not apply.

Following receipt of the first dose in a vaccine series, patients were recommended to receive the second dose of the same type of vaccine, assuming no contraindication to the second dose per CDC guidance (e.g., a severe allergic reaction, or an immediate allergic reaction of any severity to the vaccine or any of its components, including polyethylene glycol) (37,48). Persons who develop SARS–CoV-2 infection between the first and second dose of a 2-dose vaccine series should delay the second dose until they have recovered from the acute illness (if symptomatic) and discontinued isolation, and then they should receive the second dose without delay (37,48). Consistent with CDC guidance (48), SARS–CoV-2–infected patients who received monoclonal antibodies (e.g., bamlanivimab, casirivimab, imdevimab) or convalescent plasma as part of treatment for COVID-19 are no longer recommended to defer vaccination following receipt of antibody products (anti–SARS–CoV-2 monoclonal antibodies or convalescent plasma). Also consistent with CDC guidance (48), providers may co-administer other vaccines at the same time as COVID-19 vaccines, and without regard to the timing of other vaccines.

For patients who previously completed the 2-dose mRNA series or received the 1-dose Johnson & Johnson COVID-19 vaccine, a supplemental/booster COVID-19 vaccine dose is recommended ≥28 days after the completion of the vaccine series. This guidance applies to AIIRD patients receiving any immunosuppressive or immunomodulatory therapy other than hydroxychloroquine monotherapy. In making this statement, the task force recognized the high potential for confusion related to nomenclature between an additional primary dose and a booster dose. A "third dose" is the term typically used to refer to an additional primary dose of a vaccine given to patients who previously completed the primary vaccine series (i.e., the 2-dose mRNA vaccine series) and who may have mounted a suboptimal response due to immunosuppressive medications or an immunocompromised medical condition (48–53). In contrast, a "booster dose" refers to an additional dose given to patients who are expected to have mounted an adequate response but in whom the response may have waned over time (e.g., ≥6 months) (48,53–59). For patients who already received a third dose, the booster may be a "fourth dose" (48). The timing of an additional primary/third dose might occur as early as 28 days after completion of the primary vaccine series, whereas a booster dose likely would be given ≥6 months later (48).

While these are distinct scenarios, the task force sought to simplify the nomenclature in relation to its guidance statements and therefore adopted a composite term "supplemental/booster dose" throughout the remainder of this document. The task force reviewed the evidence for homologous versus heterologous (i.e., "mix and match" supplemental/booster dosing) (60–67). After consideration, and similar to the preference for an mRNA vaccine for primary vaccination, patients who previously completed the mRNA COVID-19 vaccine series or 1-dose Johnson & Johnson COVID-19 vaccine are recommended to receive an mRNA vaccine supplemental/booster dose, either Pfizer or Moderna (68–70).

Thus far, there is no proven laboratory-based immune correlate of protection against SARS–CoV-2 following natural infection or vaccination. Moreover, some commercially available SARS–CoV-2 serologic assays do not detect antibody responses to spike protein generated by the currently available mRNA vaccines, but rather measure antibodies to nucleocapsid protein. Therefore, the task force recommended that health care providers not do any of the following: routinely order laboratory testing to assess the need for vaccination in an unvaccinated person, screen for asymptomatic SARS–CoV-2 shedding, or assess SARS–CoV-2 immunity following vaccination. The task force expressed strong interest in modifying this guidance once additional data evolve regarding the potential utility of laboratory-based testing that might be helpful in select patients.

AIIRD patients at high risk for poor outcomes related to COVID-19 were recommended to receive monoclonal antibody therapy with casirivimab and imdevimab (Regeneron) if available, either as prevention (i.e., post-exposure prophylaxis for asymptomatic, recently exposed patients) or as treatment for newly symptomatic patients. Household members and other frequent close contacts of AIIRD patients were recommended to undergo COVID-19 vaccination when available, in order to facilitate a "cocooning effect" that may help protect at-risk AIIRD patients. However, the priority for vaccination for these close contacts should not be elevated for this reason.

A series of statements were rated by the panel with respect to the general timing of COVID-19 vaccination in relation to AIIRD disease activity, again acknowledging a dearth of direct evidence. Except for those with severe and life-threatening illness (e.g., a hospitalized patient receiving treatment in the ICU for any condition), vaccination was recommended irrespective of disease activity and severity. Even for ICU-treated patients for whom vaccination was recommended to be deferred for a short time, the task force felt that when the patient was well enough to be discharged from the hospital, vaccination would likely be appropriate. Acknowledging a balance between vaccinating and obtaining a blunted but still modest response, and the duty to allocate vaccine resources toward the settings in which they are likely to have the greatest benefit, the panel identified this scenario as an important evidence gap. For AIIRD patients in other settings, including those with either active but non–life-threatening disease, and certainly for patients with stable and/or low disease activity, vaccination was recommended. Finally, patients naive to or not currently receiving immunomodulatory therapies were recommended to receive their first dose of vaccine without delay. Additional considerations for medication timing are subsequently discussed.

Treatment-specific timing of primary vaccination. There was recognition that the ability to carefully time COVID-19 vaccination is sometimes limited in a real-world setting, and the overarching view was that COVID-19 vaccination should be given rather than not given if timing in relation to immunomodulatory drugs is not under the provider's or patient's control.

Strong consensus was achieved regarding the statement to not delay COVID-19 vaccination for patients receiving hydroxychloroquine, sulfasalazine, leflunomide, apremilast, or IV immunoglobulin (10,71). A similar recommendation with moderate consensus was achieved for most of the remaining immunomodulatory therapies considered (72–83).

One exception was RTX (10,11,84–88), for which the panel recommended to schedule vaccination such that the vaccine series would be initiated ~4 weeks prior to the next scheduled RTX dose. For example, a patient receiving RTX as a 2-dose cycle (spaced 2 weeks apart), with cycles repeating every 6 months, would be recommended to initiate vaccination ~5 months after the start of the prior RTX cycle. RTX dosing could then be resumed 2–4 weeks after the second COVID-19 vaccination, as discussed in the next section. Those receiving RTX cycles at 4-month intervals would initiate vaccination 3 months after the prior RTX cycle. In order to follow this recommendation, the task force invoked the assumption that a patient's COVID-19 risk was low or able to be mitigated by preventive health measures. The rationale for this recommendation comes from a study demonstrating minimal response to influenza vaccination in 11 patients vaccinated 4–8 weeks after RTX treatment, with modestly restored responses in patients vaccinated 6–10 months after their last RTX dose (89), as well as data demonstrating that B cell–depleting therapy greatly attenuates the response to COVID-19 vaccination (90).

As the second statement for which consensus was not achieved, the panel was uncertain about whether to delay vaccination if an AIIRD patient was receiving glucocorticoids at a prednisone-equivalent dose of ≥20 mg per day. Controversy stemmed as to whether vaccine response might be blunted in this circumstance, which may relate to the glucocorticoids themselves or to the presumably high disease activity and severity (91,92). Other factors discussed included the disease being treated and the medical management considerations if the patient were to manifest systemic reactogenicity (e.g., persistent high fever). Concern regarding an attenuated response to the vaccine in this circumstance would be partially mitigated if there was a possibility to later order serologies or other laboratory tests, and clinicians were able to assess vaccine-induced immunity and administer a booster or revaccinate if needed. However, such laboratory-based correlates of protection are not currently available.

Use and timing of immunomodulatory therapies in relation to COVID-19 vaccination administration. The task force continued to update its literature review through October 2021, including published information regarding the immunogenicity and safety of primary vaccination in RMD patients (68,69,93) and the literature on supplemental/booster vaccine dosing in non-RMD patients (94,95). Considering the goal to align guidance for recommendations related to primary vaccination, additional primary vaccination, and booster dosing to facilitate ease of implementation, the task force harmonized their recommendations for the use and timing of immunomodulatory therapies related to all vaccine administrations. Updated recommendations are shown in Table 4.

Based on some evidence that immunosuppressive therapies may attenuate vaccine response (68,96–98), for abatacept, belimumab, and most conventional (e.g., mycophenolate mofetil, MTX, azathioprine) and targeted (e.g., JAK inhibitor) immunomodulatory therapies, the task force recommended to withhold these for 1–2 weeks after each COVID-19 vaccine dose, assuming disease activity allows. For biologics that inhibit certain cytokines (e.g., tumor necrosis factor, interleukin-6 receptor [IL-6R],

Table 4. Guidance related to the use and timing of immunomodulatory therapies in relation to COVID-19 vaccination administration in RMD patients*

Medication(s)	Timing considerations for immunomodulatory therapy and vaccination	Level of task force consensus
Abatacept (IV)	**Time vaccination to occur 1 week prior to the next dose of abatacept (IV).**	**Moderate**
Abatacept (SC)	**Withhold for 1–2 weeks (as disease activity allows) after each COVID-19 vaccine dose.**	**Moderate**
Acetaminophen, NSAIDs	Assuming that disease is stable, withhold for 24 hours prior to vaccination. No restrictions on use postvaccination if symptoms develop.	Moderate
Belimumab (SC)	**Withhold for 1–2 weeks (as disease activity allows) after each COVID-19 vaccine dose.**	**Moderate**
TNFi, IL-6R, IL-1Ra, IL-17, IL-12/23, IL-23, and other cytokine inhibitors†	**The task force failed to reach consensus on whether or not to temporarily interrupt these following each COVID-19 vaccine dose, including both primary vaccination and supplemental/ booster dosing.**	**Moderate**
Cyclophosphamide (IV)	**Time cyclophosphamide administration so that it will occur ~1 week after each vaccine dose, when feasible.**	**Moderate**
Hydroxychloroquine	**No modifications to either immunomodulatory therapy or vaccination timing.**	**Strong**
Rituximab or other anti-CD20 B cell–depleting agents	**Discuss the optimal timing of dosing and vaccination with rheumatology provider before proceeding.‡**	**Moderate**
All other conventional and targeted immunomodulatory or immunosuppressive medications (e.g., JAK inhibitors, MMF) except for those listed above§	**Withhold for 1–2 weeks (as disease activity allows) after each COVID-19 vaccine dose.**	**Moderate**

* This guidance applies to both primary vaccination and supplemental/booster dosing. Boldface text indicates updates that were added to the version 4 summary document at the end of 2021. For details on the history of updates to these guidance statements, see Supplementary Table 6, on the *Arthritis & Rheumatology* website at http://onlinelibrary.wiley.com/doi/10.1002/art.42109. RMD = rheumatic and musculoskeletal disease; IV = intravenous; SC = subcutaneous; NSAIDs = nonsteroidal antiinflammatory drugs; TNFi = tumor necrosis factor inhibitor.
† Examples of cytokine inhibitors include the following: for interleukin-6 receptor (IL-6R), sarilumab and tocilizumab; for IL-1 receptor antagonist (IL-1Ra), anakinra and canakinumab; for IL-17, ixekizumab and secukinumab; for IL-12/IL-23, ustekinumab; for IL-23, guselkumab and rizankizumab.
‡ Some practitioners measure CD19 B cells as a tool with which to time the booster and subsequent rituximab dosing. For those who elect to dose without such information, or for whom such measurement is not available or feasible, a supplemental vaccine dose 2–4 weeks should be provided before next anticipated rituximab dose (e.g., at month 5.0 or 5.5 in patients being administered rituximab every 6 months).
§ Includes apremilast, azathioprine, calcineurin inhibitors, cyclophosphamide (oral), IV immunoglobulin, leflunomide, methotrexate, JAK inhibitors (tofacitinib, upadacitinib, baricitinib), mycophenolate mofetil (MMF), and sulfasalazine.

IL-1R, IL-17, IL-12/23, IL-23), the task force failed to reach consensus on whether or not to temporarily interrupt these following each COVID-19 vaccine dose. Some panel members felt that withholding treatment for 1–2 weeks was unnecessary, had minimal effect on vaccine response (68,99), and could put the patient at greater increased risk for disease to worsen. In contrast, other task force members felt that even limited evidence suggesting the possibility that these therapies could attenuate vaccine response should result in a recommendation of a temporary interruption of therapy (100,101). For that reason, no consensus was reached, and decision-making was deferred to the discretion of individual providers and patients.

Hydroxychloroquine was a notable exception, as the task force recommended that this therapy not be interrupted. Given the complexities of RTX dosing for RA, vasculitis, and other potential off-label uses (e.g., SLE), as well as the substantial literature suggesting that vaccine response is attenuated by B cell–depleting therapies (68,96,102,103), the task force recommended that patients discuss the optimal timing of RTX and other B cell–depleting therapies and vaccination timing with their rheumatology provider before proceeding. While some clinicians measure CD19 B cells and use the information to time the vaccine booster and subsequent RTX dosing, this option may not be available in community practice settings. For those who elect to dose B cell–depleting therapies without such information, or for whom such measurement is not available or feasible, additional doses of the vaccine were recommended 2–4 weeks before the next anticipated dose (e.g., at month 5.0 or 5.5 for patients on an recurring 6-month RTX dosing schedule).

Finally, based on the literature suggesting that acetaminophen and/or nonsteroidal antiinflammatory drugs may somewhat impair vaccine response (104), the task force recommended withholding these for 24 hours prior to vaccination, assuming that disease is stable. There was no prohibition against their use in patients who experience local or systematic symptoms postvaccination (48).

Table 5. Research agenda for future COVID-19 vaccine studies in RMD patients proposed by the task force*

Conduct clinical efficacy and laboratory-based immunogenicity studies in RMD patients following vaccination, especially for AIIRD patients receiving certain immunomodulatory therapies (e.g., methotrexate, abatacept, JAK inhibitors, rituximab, mycophenolate, GCs).
Optimize response to primary vaccination and supplemental/booster dose by considering timing related to intentional short-term cessation of certain immunomodulatory therapies (e.g., methotrexate, subcutaneous abatacept, JAK inhibitors, mycophenolate mofetil) to optimize vaccine response.
Evaluate risk of disease flare, disease worsening, and systemic reactogenicity following COVID-19 vaccination in RMD patients, by disease and in relation to background immunomodulatory therapies.
Directly compare vaccines and vaccine platforms for the above efficacy, immunogenicity, and safety outcomes: notable given the potential for some COVID-19 vaccines to achieve the minimum threshold for the FDA's EUA yet have seemingly lower vaccine efficacy based on large clinical trials in non-RMD patients.
Long-term follow-up for durability and magnitude of vaccine protection in relation to various immunomodulatory medications, and as new SARS–CoV-2 strains emerge.
Assess benefits and timing of additional COVID-19 vaccine administration (i.e., booster doses).
Generate real-world evidence (e.g., large pragmatic trial or observational studies) embedded in routine clinical practice to study the above topics, especially to promote large-scale safety surveillance.
Establish a biorepository with associated clinical data infrastructure to facilitate future COVID-19 (and possibly other) vaccine-related research in RMD patients, considering the future potential to identify laboratory-based correlates of protection relevant for individual patients.
Identify laboratory-based serologic testing to identify patients with a suboptimal response to COVID-19 vaccination who might be candidates for a booster dose or need to repeat the vaccination series.
Evaluate the impact of coadministration of the COVID-19 vaccine given concurrently with other, non–live-virus vaccines (e.g., shingles, influenza, pneumococcal) on vaccine immunogenicity and tolerability.
Optimize approaches to address vaccine hesitancy for high-risk RMD patients who are reticent or unwilling to undergo vaccination, with particular attention to vulnerable populations (e.g., underrepresented racial/ethnic groups).
Identify COVID-19 vaccine–induced immune parameters (immunogen-specific neutralizing antibody levels, total immunogen-specific antibody levels or isotypes, T cell immunity, innate immunity) or host determinants that are predictive of successful host response to vaccine, as reflected by protection from infection or mitigation of morbidity during subsequent infection.
Conduct large epidemiology studies of COVID-19 outcomes (e.g., using large administrative databases of health plans, electronic health record data [e.g., the ACR RISE registry], or other data sources or methods) and examine the role of AIIRD disease features, treatments, and vaccination. While risk factors for incident disease may be shaped by confounding and unmeasured variability in exposure, examining outcomes conditioning on incident COVID-19 diagnosis may be more fruitful.

* RMD = rheumatic and musculoskeletal disease; AIIRD = autoimmune and inflammatory rheumatic disease; GCs = glucocorticoids; FDA = US Food and Drug Administration; EUA = Emergency Use Authorization; ACR = American College of Rheumatology; RISE = Rheumatology Informatics System for Effectiveness.

As an outgrowth of the evidence report, the task force assembled a research agenda where evidence was lacking (Table 5). Given that there was little direct evidence in any RMD population, the topics were broad and spanned domains related to clinical effectiveness, safety, flare, reactogenicity, study design, immunogenicity, and laboratory-based correlates of protection. With the relatively small size of the task force, no attempt was made to prioritize these topics given the expectation that they would evolve over time and as new science in non-RMD populations was forthcoming.

DISCUSSION

This ACR guidance encompasses the optimal use of COVID-19 vaccines, including supplemental/booster dosing, for patients with rheumatic and musculoskeletal diseases. It is intended to aid in the care of individual patients but not to supplant personalized care or constrain shared decision-making with patients. The mRNA vaccine platform is novel, and considerations for vaccines developed on this platform may differ from those relevant to other vaccines. The guidance regarding the use and timing of immunomodulatory medications was often based on extrapolation of the available evidence of their immunologic effects as they relate to other vaccines and vaccine platforms. As such, all of these recommendations are considered conditional. Finally, the task force advised health care providers to avoid being overly dogmatic in following these recommendations. The attempt to optimize vaccine response in relation to the use and timing of immunosuppressive medications should not compromise a willing patient's ability to undergo vaccination in a timely manner and risk a missed vaccination opportunity.

As an overarching principle, the sparsity of information regarding COVID-19 vaccination in RMD patients yielded a need for extrapolation based on the literature published for other vaccines. The evidence base was, therefore, of low or very low quality and suffered from indirectness (12) in almost all respects. The guidance provided herein represents a balance between evidence regarding efficacy, effectiveness, safety, feasibility (e.g., withholding a therapy with a long half-life or extended recirculation like leflunomide may be unrealistic), expected vaccine availability, and tradeoffs in resource utilization. For example, vigorous debate was held about whether it was preferable to vaccinate a high-risk patient in a suboptimal circumstance (e.g., active disease, receiving high-dose glucocorticoids, receiving cytotoxic therapy), under the assumption that the vaccine would confer at least some protection to a patient at high risk for a poor outcome if they contract COVID-19. Or rather, might it be preferable to wait until a more optimal circumstance presented itself? However, given the uncertainty in most medical settings to predict the future course of a patient's AIIRD or the need for additional immunomodulatory treatments, a more salutary setting to optimize vaccine response might never

materialize. Thus, the task force typically favored proceeding more immediately with vaccination.

If a laboratory-based correlate of protection existed that could serve as a proxy for immunity, and if a booster dose could be administered or the vaccine series repeated at a later time, there would be greater certainty to recommend vaccinating all patients immediately, regardless of setting or underlying treatment. These societal considerations regarding vaccine allocation in light of constrained vaccine supply and regional resource limitations to revaccinate posed important tradeoffs for the panel. Given tradeoffs like these, the extant uncertainties posed by the scoping questions informed by imperfect evidence, and the highly dynamic environment of vaccination implementation, the task force recommended as it did.

The strengths of this effort are notable given the urgent need presented by the availability of new COVID-19 vaccines and critical questions about how to best use those vaccines for RMD patients. The task force generated an evidence summary over a very compressed time frame and leveraged a well-established consensus methodology process used previously by the ACR. Of high importance, the task force's composition included experts in rheumatology, infectious disease, and public health, representing a plurality of different stakeholder perspectives.

Regarding important limitations, our ability to generalize from the literature for other vaccines and vaccine platforms in RMD patients to the novel COVID-19 vaccines now available in the US is limited. Vaccination against SARS–CoV-2 raises different issues than those for other vaccine-preventable illnesses, given the potential for ongoing public health measures to partially mitigate exposure. This guidance therefore must be interpreted by clinicians and patients in light of underlying principles rather than considering them either prescriptive or proscriptive. For example, an AIIRD patient with minimal public contact who is able to strongly adhere to all preventive health measures might choose to withhold RMD treatments or briefly defer vaccination in accordance with this guidance, whereas this same decision may not be possible for a patient employed in a high-risk setting (e.g., front-line health care, or long-term care facility). From a vaccine policy and recommendation context, the task force prioritized simplicity, noting that this guidance would be expected to apply to the care of most RMD patients in most settings.

Finally, the procedures used to develop this guidance did not follow the rigorous methodology routinely used by the ACR when formal clinical practice guidelines are created, although they were adherent to the ACR standardized operating procedures for guidance documents (13). This was an expected limitation given the accelerated time frame desired by the ACR to issue practical and timely recommendations both to its membership and to the rheumatology community. Once the urgency of the pandemic has passed, the work of this task force will eventually be folded back under the aegis of the broader ACR vaccine guideline development group, charged with covering this and all other vaccines in the context of RMDs, and the more typical guideline development process favored by the ACR will be applied. Additional and important input from other stakeholders, including patients and patient advocates, will also be sought, as the ACR has done for past clinical practice guidelines (6).

As new safety and efficacy evidence becomes available for COVID-19 vaccines in patients with RMDs and AIIRDs, the ACR's guidance document will continue to be updated and expanded, consistent with the notion of a "living document." The need for future updates will be routinely assessed by the ACR, this task force, and the larger ACR guideline development group. The ACR is committed to maintaining this process throughout the pandemic to facilitate evidence-based practice and promote optimal outcomes for all patients with RMDs and AIIRDs with respect to mitigating COVID-19 risk.

ACKNOWLEDGMENT

The task force would like to thank Regina Parker (ACR) for her role in coordinating the activities of the Task Force.

AUTHOR CONTRIBUTIONS

All authors were involved in drafting the article or revising it critically for important intellectual content, and all authors approved the final version to be published. Dr. Curtis had full access to all of the data in the study and takes responsibility for the integrity of the data and the accuracy of the data analysis.

Study conception and design. Curtis, Johnson, Anthony, Arasaratnam, Baden, Bass, Calabrese, Gravallese, Harpaz, Kroger, Sadun, Turner, Williams, Mikuls.

Acquisition of data. Curtis, Johnson, Anthony, Arasaratnam, Baden, Bass, Calabrese, Gravallese, Harpaz, Kroger, Sadun, Turner, Williams, Mikuls.

Analysis and interpretation of data. Curtis, Johnson, Anthony, Arasaratnam, Baden, Bass, Calabrese, Gravallese, Harpaz, Kroger, Sadun, Turner, Williams, Mikuls.

REFERENCES

1. Van der Heijde D, Daikh DI, Betteridge N, Burmester GR, Hassett AL, Matteson EL, et al. Common language description of the term rheumatic and musculoskeletal diseases (RMDs) for use in communication with the lay public, healthcare providers, and other stakeholders endorsed by the European League Against Rheumatism (EULAR) and the American College of Rheumatology (ACR). Arthritis Rheumatol 2018;70:826–31.
2. Mikuls TR, Johnson SR, Fraenkel L, Arasaratnam RJ, Baden LR, Bermas BL, et al. American College of Rheumatology guidance for the management of rheumatic disease in adult patients during the COVID-19 pandemic: version 3. Arthritis Rheumatol 2021;73:e1–12.
3. US Food and Drug Administration. Vaccines and Related Biological Products Advisory Committee meeting: FDA briefing document Pfizer-BioNTech COVID-19 vaccine. December 2020. URL: https://www.fda.gov/media/144245/download.
4. US Food and Drug Administration. Vaccines and Related Biological Products Advisory Committee meeting: FDA briefing document Moderna COVID-19 vaccine. December 2020. URL: https://www.fda.gov/media/144434/download.

5. Singh JA, Furst DE, Bharat A, Curtis JR, Kavanaugh AF, Kremer JM, et al. 2012 update of the 2008 American College of Rheumatology recommendations for the use of disease-modifying antirheumatic drugs and biologic agents in the treatment of rheumatoid arthritis. Arthritis Care Res (Hoboken) 2012;64:625–39.
6. Singh JA, Saag KG, Bridges SL Jr, Akl EA, Bannuru RR, Sullivan MC, et al. 2015 American College of Rheumatology guideline for the treatment of rheumatoid arthritis. Arthritis Rheumatol 2016;68:1–26.
7. Fraenkel L, Bathon JM, England BR, St.Clair EW, Arayssi T, Carandang K, et al. 2021 American College of Rheumatology guideline for the treatment of rheumatoid arthritis. Arthritis Rheumatol 2021;73:1108–23.
8. Singh JA, Guyatt G, Ogdie A, Gladman DD, Deal C, Deodhar A, et al. 2018 American College of Rheumatology/National Psoriasis Foundation guideline for the treatment of psoriatic arthritis. Arthritis Rheumatol 2019;71:5–32.
9. Furer V, Rondaan C, Heijstek MW, Agmon-Levin N, van Assen S, Bijl M, et al. 2019 update of EULAR recommendations for vaccination in adult patients with autoimmune inflammatory rheumatic diseases. Ann Rheum Dis 2020;79:39–52.
10. Rondaan C, Furer V, Heijstek MW, Agmon-Levin N, Bijl M, Breedveld FC, et al. Efficacy, immunogenicity and safety of vaccination in adult patients with autoimmune inflammatory rheumatic diseases: a systematic literature review for the 2019 update of EULAR recommendations. RMD Open 2019;5:e001035.
11. Van Assen S, Agmon-Levin N, Elkayam O, Cervera R, Doran MF, Dougados M, et al. EULAR recommendations for vaccination in adult patients with autoimmune inflammatory rheumatic diseases. Ann Rheum Dis 2011;70:414–22.
12. Guyatt GH, Oxman AD, Kunz R, Woodcock J, Brozek J, Helfand M, et al. GRADE guidelines: 8. Rating the quality of evidence–indirectness. J Clin Epidemiol 2011;64:1303–10.
13. American College of Rheumatology. American College of Rheumatology Guidance Subcommittee and Endorsement of Guidance Documents, 2020. URL: https://www.rheumatology.org/Portals/0/Files/ACR-Guidance-Subcommittee-Processes-Framework.pdf.
14. Fitch K, Bernstein SJ, Aguilar MD, Burnand B, LaCalle JR, Lazaro P, et al. The RAND/UCLA appropriateness method user's manual. Santa Monica (CA): RAND; 2001.
15. American College of Rheumatology. COVID-19 guidance. URL: https://www.rheumatology.org/Practice-Quality/Clinical-Support/COVID-19-Guidance.
16. Moderna TX, sponsor. A study to evaluate the safety, reactogenicity, and effectiveness of mRNA-1273 vaccine in adolescents 12 to <18 years old to prevent COVID-19 (TeenCove). ClinicalTrials.gov identifier: NCT04649151.
17. BioNTech SE and Pfizer, sponsors. Study to describe the safety, tolerability, immunogenicity, and efficacy of RNA vaccine candidates against COVID-19 in healthy individuals. ClinicalTrials.gov identifier: NCT04368728.
18. Centers for Disease Control and Prevention. Pfizer-BioNTech COVID-19 vaccine (5 through 11 years of age). February 2022. https://www.cdc.gov/vaccines/covid-19/info-by-product/pfizer/pfizer-bioNTech-children-adolescents.html.
19. Walter E, Talaat K, Sabharwal C, Gurtman A, Lockhart S, Paulsen G, et al. Evaluation of the BNT162b2 COVID-19 vaccine in children 5 to 11 years of age. N Engl J Med 2022;386:35–46.
20. Rubin LG, Levin MJ, Ljungman P, Davies EG, Avery R, Tomblyn M, et al. 2013 IDSA clinical practice guideline for vaccination of the immunocompromised host. Clin Infect Dis 2014;58:e44–100.
21. Rubin LG, Levin MJ, Ljungman P, Davies EG, Avery R, Tomblyn M, et al. 2013 IDSA clinical practice guideline for vaccination of the immunocompromised host. Clin Infect Dis 2014;58:309–18.
22. Blumentals WA, Arreglado A, Napalkov P, Toovey S. Rheumatoid arthritis and the incidence of influenza and influenza-related complications: a retrospective cohort study. BMC Musculoskelet Disord 2012;13:158.
23. Van Assen S, Elkayam O, Agmon-Levin N, Cervera R, Doran MF, Dougados M, et al. Vaccination in adult patients with auto-immune inflammatory rheumatic diseases: a systematic literature review for the European League Against Rheumatism evidence-based recommendations for vaccination in adult patients with auto-immune inflammatory rheumatic diseases [review]. Autoimmun Rev 2011;10:341–52.
24. Yun H, Yang S, Chen L, Xie F, Winthrop K, Baddley JW, et al. Risk of herpes zoster in autoimmune and inflammatory diseases: implications for vaccination. Arthritis Rheumatol 2016;68:2328–37.
25. Cordtz R, Lindhardsen J, Soussi BG, Vela J, Uhrenholt L, Westermann R, et al. Incidence and severeness of COVID-19 hospitalisation in patients with inflammatory rheumatic disease: a nationwide cohort study from Denmark. Rheumatology (Oxford) 2020. doi: https://doi.org/10.1093/rheumatology/keaa897. E-pub ahead of print.
26. Williamson EJ, Walker AJ, Bhaskaran K, Bacon S, Bates C, Morton CE, et al. Factors associated with COVID-19-related death using OpenSAFELY. Nature 2020;584:430–6.
27. D'Silva KM, Jorge A, Cohen A, McCormick N, Zhang Y, Wallace ZS, et al. COVID-19 outcomes in patients with systemic autoimmune rheumatic diseases compared to the general population: a US multicenter, comparative cohort study. Arthritis Rheumatol 2021;73:914–20.
28. Topless R, Phipps-Green A, Leask M, Dalbeth N, Stamp LK, Robinson P, et al. Gout, rheumatoid arthritis and the risk of death from COVID-19: an analysis of the UK Biobank. ACR Open Rheumatol 2021;3:333–40.
29. Eder L, Croxford R, Drucker A, Mendel A, Kuriya B, Touma Z, et al. COVID-19 hospitalizations, ICU admission, and death among patients with immune mediated inflammatory diseases (IMID) - a population based study [abstract]. Ann Rheum Dis 2021;80 Suppl 1:173.
30. Zhou F, Yu T, Du R, Fan G, Liu Y, Liu Z, et al. Clinical course and risk factors for mortality of adult inpatients with COVID-19 in Wuhan, China: a retrospective cohort study. Lancet 2020;395:1054–62.
31. Wu C, Chen X, Cai Y, Xia J, Zhou X, Xu S, et al. Risk factors associated with acute respiratory distress syndrome and death in patients with coronavirus disease 2019 pneumonia in Wuhan, China. JAMA Intern Med 2020;180:934–43.
32. Gianfrancesco MA, Leykina LA, Izadi Z, Taylor T, Sparks JA, Harrison C, et al. Association of race and ethnicity with COVID-19 outcomes in rheumatic disease: data from the COVID-19 Global Rheumatology Alliance physician registry. Arthritis Rheumatol 2021;73:374–80.
33. Strangfeld A, Schäfer M, Gianfrancesco MA, Lawson-Tovey S, Liew JW, Ljung L, et al. Factors associated with COVID-19-related death in people with rheumatic diseases: results from the COVID-19 Global Rheumatology Alliance physician-reported registry. Ann Rheum Dis 2021;80:930–42.
34. Gianfrancesco M, Hyrich KL, Al-Adely S, Carmona L, Danila MI, Gossec L, et al. Characteristics associated with hospitalisation for COVID-19 in people with rheumatic disease: data from the COVID-19 Global Rheumatology Alliance physician-reported registry. Ann Rheum Dis 2020;79:859–66.
35. Ungaro RC, Agrawal M, Park S, Hirten R, Colombel JF, Twyman K, et al. Autoimmune and chronic inflammatory disease patients with COVID-19. ACR Open Rheumatol 2021;3:111–5.

36. Choi B, Choudhary MC, Regan J, Sparks JA, Padera RF, Qiu X, et al. Persistence and evolution of SARS-CoV-2 in an immunocompromised host [letter]. N Engl J Med 2020;383:2291–3.
37. Centers for Disease Control and Prevention. Vaccine recommendations and guidelines of the ACIP: COVID-19 vaccine recommendations. March 2021. URL: https://www.cdc.gov/vaccines/hcp/acip-recs/vacc-specific/covid-19.html.
38. Centers for Disease Control and Prevention. Vaccines and immunizations: interim considerations—preparing for the potential management of anaphylaxis after COVID-19. vaccination. March 2021. URL: https://www.cdc.gov/vaccines/covid-19/clinical-considerations/managing-anaphylaxis.html?CDC_AA_refVal=https%3A%2F%2Fwww.cdc.gov%2Fvaccines%2Fcovid-19%2Finfo-by-product%2Fpfizer%2Fanaphylaxis-management.html.
39. Yun H, Xie F, Baddley JW, Winthrop K, Saag KG, Curtis JR. Long-term effectiveness of herpes zoster vaccine among patients with autoimmune and inflammatory diseases. J Rheumatol 2017;44:1083–7.
40. Park JK, Lee YJ, Shin K, Ha YJ, Lee EY, Song YW, et al. Impact of temporary methotrexate discontinuation for 2 weeks on immunogenicity of seasonal influenza vaccination in patients with rheumatoid arthritis: a randomised clinical trial. Ann Rheum Dis 2018;77:898–904.
41. Van der Maas A, Lie E, Christensen R, Choy E, de Man YA, van Riel P, et al. Construct and criterion validity of several proposed DAS28-based rheumatoid arthritis flare criteria: an OMERACT cohort validation study. Ann Rheum Dis 2013;72:1800–5.
42. Park JK, Kim MJ, Choi Y, Winthrop K, Song YW, Lee EB. Effect of short-term methotrexate discontinuation on rheumatoid arthritis disease activity: post-hoc analysis of two randomized trials. Clin Rheumatol 2020;39:375–9.
43. Park JK, Choi Y, Winthrop KL, Song YW, Lee EB. Optimal time between the last methotrexate administration and seasonal influenza vaccination in rheumatoid arthritis: post hoc analysis of a randomised clinical trial [letter]. Ann Rheum Dis 2019;78:1283–4.
44. Park JK, Lee MA, Lee EY, Song YW, Choi Y, Winthrop KL, et al. Effect of methotrexate discontinuation on efficacy of seasonal influenza vaccination in patients with rheumatoid arthritis: a randomised clinical trial. Ann Rheum Dis 2017;76:1559–65.
45. Oda R, Inagaki T, Ishikane M, Hotta M, Shimomura A, Sato M, et al. Case of adult large vessel vasculitis after SARS-CoV-2 infection [letter]. Ann Rheum Dis 2020. doi: https://doi.org/10.1136/annrheumdis-2020-218440. E-pub ahead of print.
46. Perrot L, Hemon M, Busnel JM, Muis-Pistor O, Picard C, Zandotti C, et al. First flare of ACPA-positive rheumatoid arthritis after SARS-CoV-2 infection. Lancet Rheumatol 2021;3:e6–8.
47. Baden LR, Walsh SR, Seaman MS, Tucker RP, Krause KH, Patel A, et al. First-in-human evaluation of the safety and immunogenicity of a recombinant adenovirus serotype 26 HIV-1 Env vaccine (IPCAVD 001). J Infect Dis 2013;207:240–7.
48. Centers for Disease Control and Prevention. Vaccines and immunizations: interim clinical considerations for use of COVID-19 vaccines currently authorized in the United States. July 16, 2021. URL: https://www.cdc.gov/vaccines/covid-19/info-by-product/clinical-considerations.html.
49. Khan N, Mahmud N. Effectiveness of SARS-CoV-2 vaccination in a Veterans Affairs cohort of patients with inflammatory bowel disease with diverse exposure to immunosuppressive medications. Gastroenterology 2021;161:827–36.
50. Boyarsky BJ, Werbel WA, Avery RK, Tobian AAR, Massie AB, Segev DL, et al. Antibody response to 2-dose SARS-CoV-2 mRNA vaccine series in solid organ transplant recipients. JAMA 2021;325:2204–6.
51. Boyarsky BJ, Ruddy JA, Connolly CM, Ou MT, Werbel WA, Garonzik-Wang JM, et al. Antibody response to a single dose of SARS-CoV-2 mRNA vaccine in patients with rheumatic and musculoskeletal diseases. Ann Rheum Dis 2021. doi: 10.1136/annrheumdis-2021-220289. E-pub of print.
52. Hall VG, Ferreira VH, Ku T, Ierullo M, Majchrzak-Kita B, Chaparro C, et al. Randomized trial of a third dose of mRNA-1273 vaccine in transplant recipients. N Engl J Med 2021;385:1244–6.
53. Centers for Disease Control and Prevention. Science brief: COVID-19 vaccines and vaccination 2021. September 2021. URL: https://www.cdc.gov/coronavirus/2019-ncov/science/science-briefs/fully-vaccinated-people.html.
54. Pegu A, O'Connell SE, Schmidt SD, O'Dell S, Talana CA, Lai L, et al. Durability of mRNA-1273 vaccine-induced antibodies against SARS–CoV-2 variants. Science 2021;373:1372–7.
55. Wu K, Choi A, Koch M, LingZhi M, Hill A, Nunna N, et al. Preliminary analysis of safety and immunogenicity of a SARS–CoV-2 variant vaccine booster [preprint]. medRxiv 2021.
56. Tenforde MW, Self WH, Naioti EA, Ginde AA, Douin DJ, Olson SM, et al. Sustained effectiveness of Pfizer-BioNTech and Moderna vaccines against COVID-19 associated hospitalizations among adults - United States, March-July 2021. MMWR Morb Mortal Wkly Rep 2021;70:1156–62.
57. Mizrahi B, Lotan R, Kalkstein N, Peretz A, Perez G, Ben-Tov A, et al. Correlation of SARS-CoV-2-breakthrough infections to time-from-vaccine. Nat Commun 2021;12:6379.
58. Thompson MG, Burgess JL, Naleway AL, Tyner H, Yoon SK, Meece J, et al. Prevention and attenuation of Covid-19 with the BNT162b2 and mRNA-1273 vaccines. N Engl J Med 2021;385:320–9.
59. Kustin T, Harel N, Finkel U, Perchik S, Harari S, Tahor M, et al. Evidence for increased breakthrough rates of SARS-CoV-2 variants of concern in BNT162b2-mRNA-vaccinated individuals. Nat Med 2021;27:1379–84.
60. Atmar RL, Lyke KE, Deming ME, Jackson LA, Branche AR, El Sahly HM, et al. Heterologous SARS-CoV-2 booster vaccinations - preliminary report [preprint]. medRxiv 2021.
61. Behrens GM, Cossmann A, Stankov MV, Nehlmeier I, Kempf A, Hoffmann M, et al. SARS-CoV-2 delta variant neutralisation after heterologous ChAdOx1-S/BNT162b2 vaccination. Lancet 2021;398:1041–2.
62. Borobia AM, Carcas AJ, Pérez-Olmeda M, Castaño L, Bertran MJ, García-Pérez J, et al. Immunogenicity and reactogenicity of BNT162b2 booster in ChAdOx1-S-primed participants (Com-VacS): a multicentre, open-label, randomised, controlled, phase 2 trial. Lancet 2021;398:121–30.
63. Normark J, Vikström L, Gwon YD, Persson IL, Edin A, Björsell T, et al. Heterologous ChAdOx1 nCoV-19 and mRNA-1273 vaccination. N Engl J Med 2021;385:1049–51.
64. Rose R, Neumann F, Grobe N, Lorentz T, Fickenscher H, Krumbholz A. Heterologous immunisation with vector vaccine as prime followed by mRNA vaccine as boost leads to humoral immune response against SARS-CoV-2, which is comparable to that according to a homologous mRNA vaccination scheme [preprint]. medRxiv 2021.
65. Groß R, Zanoni M, Seidel A, Conzelmann C, Gilg A, Krnavek D, et al. Heterologous ChAdOx1 nCoV-19 and BNT162b2 prime-boost vaccination elicits potent neutralizing antibody responses and T cell reactivity against prevalent SARS–CoV-2 variants. EBioMedicine 2022;75:103761.
66. Schmidt T, Klemis V, Schub D, Mihm J, Hielscher F, Marx S, et al. Immunogenicity and reactogenicity of heterologous ChAdOx1 nCoV-19/mRNA vaccination. Nat Med 2021;27:1530–5.
67. Barros-Martins J, Hammerschmidt SI, Cossmann A, Odak I, Stankov MV, Morillas Ramos G, et al. Immune responses against SARS-CoV-2 variants after heterologous and homologous ChAdOx1 nCoV-19/BNT162b2 vaccination. Nat Med 2021;27:1525–9.

68. Furer V, Eviatar T, Zisman D, Peleg H, Paran D, Levartovsky D, et al. Immunogenicity and safety of the BNT162b2 mRNA COVID-19 vaccine in adult patients with autoimmune inflammatory rheumatic diseases and in the general population: a multicentre study. Ann Rheum Dis 2021;80:1330–8.
69. Felten R, Kawka L, Dubois M, Ugarte-Gil MF, Fuentes-Silva Y, Piga M, et al. Tolerance of COVID-19 vaccination in patients with systemic lupus erythematosus: the international VACOLUP study. Lancet Rheumatol 2021;3:e613–5.
70. Papagoras C, Fragoulis GE, Zioga N, Simopoulou T, Deftereou K, Kalavri E, et al. Better outcomes of COVID-19 in vaccinated compared to unvaccinated patients with systemic rheumatic diseases. Ann Rheum Dis 2021 doi:10.1136/annrheumdis-2021-221539. E-pub ahead of print.
71. Elkayam O, Amir S, Mendelson E, Schwaber M, Grotto I, Wollman J, et al. Efficacy and safety of vaccination against pandemic 2009 influenza A (H1N1) virus among patients with rheumatic diseases. Arthritis Care Res (Hoboken) 2011;63:1062–7.
72. Battafarano DF, Battafarano NJ, Larsen L, Dyer PD, Older SA, Muehlbauer S, et al. Antigen-specific antibody responses in lupus patients following immunization. Arthritis Rheum 1998;41:1828–34.
73. Mok CC, Ho LY, Fong LS, To CH. Immunogenicity and safety of a quadrivalent human papillomavirus vaccine in patients with systemic lupus erythematosus: a case–control study. Ann Rheum Dis 2013; 72:659–64.
74. Bingham CO III, Rizzo W, Kivitz A, Hassanali A, Upmanyu R, Klearman M. Humoral immune response to vaccines in patients with rheumatoid arthritis treated with tocilizumab: results of a randomised controlled trial (VISARA). Ann Rheum Dis 2015;74:818–22.
75. Mori S, Ueki Y, Akeda Y, Hirakata N, Oribe M, Shiohira Y, et al. Pneumococcal polysaccharide vaccination in rheumatoid arthritis patients receiving tocilizumab therapy. Ann Rheum Dis 2013;72:1362–6.
76. Mori S, Ueki Y, Hirakata N, Oribe M, Hidaka T, Oishi K. Impact of tocilizumab therapy on antibody response to influenza vaccine in patients with rheumatoid arthritis. Ann Rheum Dis 2012;71: 2006–10.
77. Sahin U, Muik A, Derhovanessian E, Vogler I, Kranz LM, Vormehr M, et al. COVID-19 vaccine BNT162b1 elicits human antibody and TH1 T cell responses. Nature 2020;586:594–9.
78. Tsuru T, Terao K, Murakami M, Matsutani T, Suzaki M, Amamoto T, et al. Immune response to influenza vaccine and pneumococcal polysaccharide vaccine under IL-6 signal inhibition therapy with tocilizumab. Mod Rheumatol 2014;24:511–6.
79. Migita K, Akeda Y, Akazawa M, Tohma S, Hirano F, Ideguchi H, et al. Pneumococcal polysaccharide vaccination in rheumatoid arthritis patients receiving tacrolimus. Arthritis Res Ther 2015;17:149.
80. Doornekamp L, Goetgebuer RL, Schmitz KS, Goeijenbier M, van der Woude CJ, Fouchier R, et al. High immunogenicity to influenza vaccination in Crohn's disease patients treated with ustekinumab. Vaccines (Basel) 2020;8:455.
81. Furer V, Rondaan C, Heijstek M, van Assen S, Bijl M, Agmon-Levin N, et al. Incidence and prevalence of vaccine preventable infections in adult patients with autoimmune inflammatory rheumatic diseases (AIIRD): a systemic literature review informing the 2019 update of the EULAR recommendations for vaccination in adult patients with AIIRD. RMD Open 2019;5:e001041.
82. Furer V, Zisman D, Kaufman I, Arad U, Berman M, Sarbagil-Maman H, et al. Immunogenicity and safety of vaccination against seasonal influenza vaccine in patients with psoriatic arthritis treated with secukinumab. Vaccine 2020;38:847–51.
83. Richi P, Martín MD, de Ory F, Gutiérrez-Larraya R, Casas I, Jiménez-Díaz AM, et al. Secukinumab does not impair the immunogenic response to the influenza vaccine in patients. RMD Open 2019;5: e001018.
84. Bar-Or A, Calkwood JC, Chognot C, Evershed J, Fox EJ, Herman A, et al. Effect of ocrelizumab on vaccine responses in patients with multiple sclerosis: the VELOCE study. Neurology 2020;95:e1999–2008.
85. Nazi I, Kelton JG, Larche M, Snider DP, Heddle NM, Crowther MA, et al. The effect of rituximab on vaccine responses in patients with immune thrombocytopenia. Blood 2013;122:1946–53.
86. Houot R, Levy R, Cartron G, Armand P. Could anti-CD20 therapy jeopardise the efficacy of a SARS-CoV-2 vaccine? Eur J Cancer 2020;136:4–6.
87. Baker D, Roberts CA, Pryce G, Kang AS, Marta M, Reyes S, et al. COVID-19 vaccine-readiness for anti-CD20-depleting therapy in autoimmune diseases [review]. Clin Exp Immunol 2020;202:149–61.
88. Hua C, Barnetche T, Combe B, Morel J. Effect of methotrexate, anti–tumor necrosis factor α, and rituximab on the immune response to influenza and pneumococcal vaccines in patients with rheumatoid arthritis: a systematic review and meta-analysis. Arthritis Care Res (Hoboken) 2014;66:1016–26.
89. Van Assen S, Holvast A, Benne CA, Posthumus MD, van Leeuwen MA, Voskuyl AE, et al. Humoral responses after influenza vaccination are severely reduced in patients with rheumatoid arthritis treated with rituximab. Arthritis Rheum 2010;62:75–81.
90. Paley MA, Deepak P, Kim W, Yang M, Carividi A, Demissie EG, et al. Immunosuppression attenuates antibody and neutralization titers in patients with chronic inflammatory disease following SARS-CoV-2 vaccination [abstract]. Arthritis Rheumatol 2021;73 Suppl:S945–7.
91. Aikawa NE, Campos LM, Silva CA, Carvalho JF, Saad CG, Trudes G, et al. Glucocorticoid: major factor for reduced immunogenicity of 2009 influenza A (H1N1) vaccine in patients with juvenile autoimmune rheumatic disease. J Rheumatol 2012;39:167–73.
92. Kim EY, Lim JE, Jung JY, Son JY, Lee KJ, Yoon YW, et al. Performance of the tuberculin skin test and interferon-γ release assay for detection of tuberculosis infection in immunocompromised patients in a BCG-vaccinated population. BMC Infect Dis 2009;9:207.
93. Li X, Tong X, Yeung WW, Kuan P, Yum SH, Chui CS, et al. Two-dose COVID-19 vaccination and possible arthritis flare among patients with rheumatoid arthritis in Hong Kong. Ann Rheum Dis 2022;81:564–8.
94. Levin EG, Lustig Y, Cohen C, Fluss R, Indenbaum V, Amit S, et al. Waning immune humoral response to BNT162b2 Covid-19 vaccine over 6 months. N Engl J Med 2021;385:e84.
95. Bar-On YM, Goldberg Y, Mandel M, Bodenheimer O, Freedman L, Kalkstein N, et al. Protection of BNT162b2 vaccine booster against Covid-19 in Israel. N Engl J Med 2021;385:1393–1400.
96. Deepak P, Kim W, Paley MA, Yang M, Carvidi AB, Demissie EG, et al. Effect of immunosuppression on the immunogenicity of mRNA vaccines to SARS-CoV-2: a prospective cohort study. Ann Intern Med 2021;174:1572–85.
97. Prendecki M, Clarke C, Edwards H, McIntyre S, Mortimer P, Gleeson S, et al. Humoral and T-cell responses to SARS-CoV-2 vaccination in patients receiving immunosuppression. Ann Rheum Dis 2021;80: 1322–9.
98. Kearns P, Siebert S, Willicombe M, Gaskell C, Kirkham A, Pirrie S, et al. Examining the immunological effects of COVID-19 vaccination in patients with conditions potentially leading to diminished immune response capacity – The OCTAVE Trial [preprint]. SSRN 2021.
99. Venerito V, Stefanizzi P, Fornaro M, Cacciapaglia F, Tafuri S, Perniola S, et al. Immunogenicity of BNT162b2 mRNA SARS-CoV-2 vaccine in patients with psoriatic arthritis on TNF inhibitors. RMD Open 2022; 8:e001847.
100. Connolly CM, Chiang TP, Boyarsky BJ, Ruddy JA, Teles M, Alejo JL, et al. Temporary hold of mycophenolate augments humoral response to SARS-CoV-2 vaccination in patients with rheumatic

and musculoskeletal diseases: a case series. Ann Rheum Dis 2022; 81:293–5.

101. Park JK, Lee YJ, Shin K, Ha YJ, Lee EY, Song YW, et al. Impact of temporary methotrexate discontinuation for 2 weeks on immunogenicity of seasonal influenza vaccination in patients with rheumatoid arthritis: a randomised clinical trial. Ann Rheum Dis 2018;77:898–904.
102. Moor MB, Suter-Riniker F, Horn MP, Aeberli D, Amsler J, Möller B, et al. Humoral and cellular responses to mRNA vaccines against SARS-CoV-2 in patients with a history of CD20 B-cell-depleting therapy (RituxiVac): an investigator-initiated, single-centre, open-label study. Lancet Rheumatol 2021;3:e789–97.
103. Felten R, Gallais F, Schleiss C, Chatelus E, Javier RM, Pijnenburg L, et al. Cellular and humoral immunity after the third dose of SARS-CoV-2 vaccine in patients treated with rituximab. Lancet Rheumatol 2022;4:e13–6.
104. Saleh E, Moody MA, Walter EB. Effect of antipyretic analgesics on immune responses to vaccination. Hum Vaccin Immunother 2016; 12:2391–402.